Aalborg Universitet

AALBORG UNIVERSITY
DENMARK

The Effects of Time on Soil Behaviour and Pile Capacity

PhD Thesis defended public at Aalborg University (17 November 2006)

Augustesen, Anders

Publication date:
2006

Document Version
Publisher's PDF, also known as Version of record

Link to publication from Aalborg University

Citation for published version (APA):
Augustesen, A. (2006). *The Effects of Time on Soil Behaviour and Pile Capacity: PhD Thesis defended public at Aalborg University (17 November 2006)*. Department of Civil Engineering, Aalborg University. DCE Thesis No. 4

General rights
Copyright and moral rights for the publications made accessible in the public portal are retained by the authors and/or other copyright owners and it is a condition of accessing publications that users recognise and abide by the legal requirements associated with these rights.

- Users may download and print one copy of any publication from the public portal for the purpose of private study or research.
- You may not further distribute the material or use it for any profit-making activity or commercial gain
- You may freely distribute the URL identifying the publication in the public portal -

Take down policy
If you believe that this document breaches copyright please contact us at vbn@aub.aau.dk providing details, and we will remove access to the work immediately and investigate your claim.

Downloaded from vbn.aau.dk on: May 05, 2023

The Effects of Time on Soil Behaviour and Pile Capacity

PhD Thesis

Anders Hust Augustesen

ISSN 1901-7294
DCE Thesis No. 4

AALBORG UNIVERSITY
Department of Civil Engineering

Aalborg University
Department of Civil Engineering
Division of Water & Soil

DCE Thesis No. 4

The Effects of Time on Soil Behaviour and Pile Capacity

PhD Thesis defended public at Aalborg University (17 November 2006)

by

Anders Hust Augustesen

2006

© Aalborg University

Scientific Publications at the Department of Civil Engineering

Technical Reports are published for timely dissemination of research results and scientific work carried out at the Department of Civil Engineering (DCE) at Aalborg University. This medium allows publication of more detailed explanations and results than typically allowed in scientific journals.

Technical Memoranda are produced to enable the preliminary dissemination of scientific work by the personnel of the DCE where such release is deemed to be appropriate. Documents of this kind may be incomplete or temporary versions of papers—or part of continuing work. This should be kept in mind when references are given to publications of this kind.

Contract Reports are produced to report scientific work carried out under contract. Publications of this kind contain confidential matter and are reserved for the sponsors and the DCE. Therefore, Contract Reports are generally not available for public circulation.

Lecture Notes contain material produced by the lecturers at the DCE for educational purposes. This may be scientific notes, lecture books, example problems or manuals for laboratory work, or computer programs developed at the DCE.

Theses are monograms or collections of papers published to report the scientific work carried out at the DCE to obtain a degree as either PhD or Doctor of Technology. The thesis is publicly available after the defence of the degree.

Latest News is published to enable rapid communication of information about scientific work carried out at the DCE. This includes the status of research projects, developments in the laboratories, information about collaborative work and recent research results.

Published 2006 by
Aalborg University
Department of Civil Engineering
Sohngaardsholmsvej 57,
DK-9000 Aalborg, Denmark

Printed in Denmark at Aalborg University

ISSN 1901-7294
DCE Thesis No. 4

PREFACE

This thesis "The Effects of Time on Soil Behaviour and Pile Capacity" is submitted as one of the requirements for obtaining the degree of Ph.D. according to the regulations put forward by The European Doctoral School of Technology and Science at Aalborg University.

The thesis consists of two parts:

- **Part I** deals with piles. The influence of engineering time on pile capacity is in focus as well as the reliability of different calculation procedures used to predict pile capacities. Chapter 1 states the important conclusions related to Part I.

- **Part II** deals with time effects in soils in general. A review of the various observed time- and rate-dependent phenomena, that are known to exist for both clay and sand, is presented. Further, models developed to capture the observed time-dependent behaviour have been studied. Chapter 2 states the important conclusions related to Part II.

Part I has been carried out under supervision of the Associated Professors Carsten S. Sørensen and Lars Andersen, Aalborg University. Part II has been done in cooperation with Professor Poul V. Lade, Catholic University of America in Washington, and Ph.D. student Morten Liingaard, Aalborg University. It was the author's hope to relate the two parts but in the present form they should be looked upon as steps forward towards a more reliable pile design and towards a better understanding of time effects in soil in general. Further, suggestions for future work within the two areas will be outlined and it is the author's hope that the thesis will form the basis for future research.

Part I and Part II are based on the following collection of scientific papers and reports written by the author and in cooperation with other authors:

- Augustesen, A., Liingaard, M. and Lade, P.V. (2004), Evaluation of Time-Dependent Behavior of Soils, *International Journal of Geomechanics*, 4(3), pp.137-156.

- Liingaard, M., Augustesen, A. and Lade, P.V. (2004), Characterization of Models for Time-Dependent Behavior of Soils, *International Journal of Geomechanics*, 4(3), pp.157-177.

- * Augustesen, A., Liingaard, M. and Lade, P.V. (2002), Time Effects in Soils, *15th European Young Geotechnical Engineers' Conference, XV EYGEC*, 12-14 September, 2002, Dublin, Ireland.

- * Augustesen, A., Liingaard, M. and Lade, P.V. (2002), Examination of Models for Time Dependent Behavior of Soils, *Symposium On Computational Inelasticity, 15th ASCE Engineering Mechanics Conference (EMD 2002)*, 2-5 June, 2002, New York City, USA.

- * Liingaard, M., Augustesen, A. and Lade, P.V. (2002), Observed Time Dependent Behavior of Soils, *Symposium On Computational Inelasticity, 15th ASCE Engineering Mechanics Conference (EMD 2002)*, 2-5 June, 2002, New York City, USA.

- Augustesen, A.H., Andersen, L., and Sørensen, C.S. (2006), Assessment of Time Functions for Piles Driven in Clay, *Available from the Department of Civil Engineering, Aalborg University, Denmark, DCE Technical Memorandum No.1*, ISSN: 1901-7278. To be submitted for publication in an international journal.

- Augustesen, A., Andersen, L., and Sørensen, C.S. (2005), Time Function for Driven Piles in Clay, *Available from the Department of Civil Engineering, Aalborg University, Denmark, Internal report*, ISSN: 1398-6465 R0501.

- Jensen, J.L., Augustesen, A. and Sørensen, C.S. (2004), The Influence of Time on the Bearing Capacity of Driven Piles, *In proceedings: NGM-2004 (Nordic Geotechnical Meeting), XIVth Nordiska Geoteknikermötet*, Ystad, 19.-21. May 2004, Sweden, pp.D103-D111.

- Augustesen, A., Andersen, L., and Sørensen, C.S. (2005), Capacity of Piles in Clay, *Available from the Department of Civil Engineering, Aalborg University, Denmark, Internal report*, ISSN: 1398-6465 R0502. To be submitted for publication in an international journal in a shorter version.

- Augustesen, A., Andersen, L., and Sørensen, C.S. (2005), Capacity of Piles in Sand, *Available from the Department of Civil Engineering, Aalborg University, Denmark, Internal report*, ISSN: 1398-6465 R0519.

Copies of all publications, except for the three conference papers marked with asterisk, are enclosed in the back of the thesis. The conference papers are omitted because they are fragments of the two published journal papers.

The Ph.D. thesis has only been published in a limited number of issues due to copyright restrictions and cannot be reprinted without authorization from the author, co-authors and from the publishers of the scientific papers. However, most papers can be aquired through public libraries, whereas the reports can be aquired through the Department of Civil Engineering, Aalborg University.

I would like to thank my supervisors, Associated Professors Carsten S. Sørensen and Lars Andersen. Their guidance during the study is greatly appreciated. Further, gratitude is also expressed for CP Test A/S, COWI A/S, Carl Bro A/S, and Per Aarsleff A/S for kindly providing pile test data. Especially, I would like to thank Rikard Skov, CP Test A/S, for fruitful discussions in the early stages of the project.

Special thanks should be directed to Per Magne Aas and C.J.F. Clausen for giving me inspiration to the project during the five months stay at the Norwegian Geotechnical Institute in Oslo, Norway, and for providing the FORTRAN code PILCAP and numereous pile test data. Further, I would like to thank the Norwegian Geotechnical Institute in general for making my time in Oslo pleasant.

I would also like to thank my friend and colleague Morten Liingaard and Professor Poul V. Lade for the cooperation regarding the studies associated with Part II.

Finally, I thank my colleagues, friends and family for fruitful discussions, moral support and helpfulness during the course of the project. Most importantly, I express my greatest appreciation to my fantastic wife Sofie for her great patience, love and support.

Aalborg, September 2006

Anders Hust Augustesen

Summary in English

When designing pile foundations, static design equations, pile driving formulae, static loading tests or stress wave analyses can be employed to estimate the axial capacity of single piles. Both laboratory and field tests show that soil exhibits time-dependent behaviour. An important result is that soil gains additional strength and stiffness with time due to time-dependent processes such as ageing. Similarly, results show that the capacity of piles increases, to a certain extent, with time after installation due to time-dependent processes in the soil. However, most design methods do not take this into account. This implies that the design methods used today do not in general make use of the full capacity of piles.

This thesis is based on a number of scientific papers and reports that deal with elements of pile design and time effects in soils in general. With regard to pile design, focus is placed on estimation of the axial pile capacity by static design equations and especially the influence of time on pile capacity. In respect of time effects in soils in general focus is placed on observed time-dependent behaviour of soils and models developed to capture this behaviour. The thesis consists of two parts. Part I deals with pile design, whereas Part II deals with time effects in soils in general. The two parts should be looked upon as steps forward towards a more reliable pile design and towards a better understanding of time effects in soil in general.

An increase in pile capacity with time after installation is denoted “set-up”. It is important to quantify set-up because time effects offer potential practical benefits if piles have been, or can be, driven months or even years before any critical loading events can occur – as in carefully staged construction, or when reusing pre-installed aged foundations. Further, design methods that take no account of time will be subject to considerable error unless they consider a tightly specified age range. Time functions (relation between time after installation and capacity), which have been offered for quantifying set-up for piles in clay, are investigated based on a set of static loading tests. In the literature it is suggested that the pile capacity increases with the logarithm to time after installation which is confirmed in this thesis. In continuation of this, it is analysed whether the magnitude of the set-up is related to the properties of the clay surrounding a pile. Statistical analyses show that the rate of set-up is constant and thereby independent of clay properties. The devised time functions are compared to existing time functions. Set-up for piles in clay is in Denmark quantified by employing a so-called regeneration factor in the static design equations. The possibility of introducing a regeneration factor dependent on time elapsed since driving and undrained shear strength is investigated.

Design methods for piles in clay and sand have been a controversial matter within geotechnical engineering for many years due to their empirical nature. Therefore, the design of piles has remained a constant source of attention, especially with regard to the methodology for predicting the capacity. Three very different design methods for piles in both clay and sand are assessed by comparing predicted capacities with measured capacities from established databases of static loading tests. The three calculation procedures in consideration are proposed by the Norwegian Geotechnical Institute, the Imperial College in London and the American Petroleum Institute, respectively. Guidelines are given for the choice of design method to be used in different circumstances (e.g. load specifications, length of pile, pile material). In order to evaluate the design methods for piles in clay, it is necessary to correct for time between pile driving and pile testing. Results of testing the calculation procedures against the available data by employing different time functions are presented.

In respect of time effects in soils in general, the purpose of the study is twofold. Firstly, a concise review of time-related phenomena (creep, stress relaxation, rate effects and accumulated effects such as ageing) observed in connection with laboratory tests on clay and sand is presented. These phenomena are present in both clay and sand. However, they are more pronounced in clay than sand. The review reveals essential characteristic situations for different types of soils, i.e. whether the time-dependent behaviour can be characterised as isotach or non-isotach. Apparently, isotach behaviour is adequate for describing time effects in clays in many situations. In contrast, sand exhibits non-isotach behaviour. Secondly, a concise review which categorizes and describes the basic features of existing models as well as their advantages and limitations is presented. Existing models can be used for modelling isotach behaviour. Thus, existing models and concepts can in principle be used to model time-dependent behaviour of clay whereas this is not the case when considering sand.

Resumé (Summary in Danish)

I forbindelse med design af pælefundamenter kan geostatiske formler, rammeformler, statiske belastningsforsøg eller stødbølgeanalyser anvendes ved estimering af en enkeltpæls lodrette bæreevne. Både laboratorie- og markforsøg viser, at jord udviser tidsafhængig opførsel. Et vigtigt resultat i den forbindelse er, at jord opnår større styrke og stivhed over tid på grund af de tidsafhængige processer, der foregår i jorden. Tilsvarende viser resultater, at pæles bæreevne i nogen grad stiger med tiden efter indramning. De fleste beregningsmetoder tager imidlertid ikke højde for dette.

Afhandlingen er baseret på en række videnskabelige artikler og rapporter, der beskæftiger sig med forskellige elementer vedrørende design af pæle og tidseffekter i jord generelt. Med hensyn til design af pæle fokuseres der på estimering af den lodrette bæreevne ved hjælp af geostatiske formler og specielt tidens indflydelse på bæreevnen. Med hensyn til tidseffekter i jord generelt fokuseres der på observeret tidsafhængig opførsel af jord og på modeller, som er udviklet med henblik på at beskrive denne opførsel. Afhandlingen består af to dele. Del I omhandler design af pæle, og del II omhandler tidseffekter i jord. De to dele skal opfattes som skridt i retningen af et mere pålideligt design af pæle og en bedre forståelse for tidseffekter i jord.

En forøgelse af bæreevnen over tid betegnes ”set-up”. Det er vigtigt at angive størrelsen af set-up, da tidseffekter kan have potentielle praktiske fordele, hvis pæle har været eller kan blive rammet måneder eller endda år før eventuelle kritiske belastningssituationer. Beregningsmetoder, der ikke tager højde for tid, vil endvidere være genstand for usikkerhed. Eksisterende tidsfunktioner (relation mellem tid efter indramning samt bæreevnen), som angiver størrelsen af set-up for pæle i ler, undersøges på baggrund af en række statiske belastningsforsøg. I litteraturen antydes det, at bæreevnen stiger med logaritmen til tiden efter installation. Dette bekræftes i denne afhandling. I forlængelse heraf undersøges det, hvorvidt størrelsen af set-up er relateret til lers egenskaber. Statistiske undersøgelser viser, at hastigheden, hvormed set-up foregår, er konstant. Dermed er set-up ikke afhængig af lers egenskaber. De udviklede tidsfunktioner sammenlignes med eksisterende tidsfunktioner. Størrelsen af set-up for pæle i ler angives i Danmark ved at anvende en såkaldt regenerationsfaktor i de geostatiske formler. Muligheden for at indføre en regenerationsfaktor, som er afhængig af tiden og den udrænede forskydningsstyrke, undersøges.

Beregningsmetoder for pæle i ler og sand har i mange år været genstand for megen diskussion på grund af deres empiriske natur. Derfor har design af pæle konstant været i fokus, specielt med hensyn til de metoder der bruges til estimering af bæreevnen. Tre meget forskellige beregningsmetoder for pæle i ler og sand evalueres ved at sammenligne estimerede bæreevner med målte. Dette gøres på baggrund af til lejligheden etablerede databaser omfattende statiske belastningsforsøg. De tre metoder er udviklet af henholdsvis Norsk Geoteknisk Institutt, Imperial College i London og the American Petroleum Institute. Der gives retningslinjer i forbindelse med valg af beregningsmetode alt afhængigt af for eksempel belastningspåførslen, pælelængden og pælematerialet. For at kunne vurdere anvendeligheden af metoderne for pæle i ler, er det nødvendigt at korrigere for tiden mellem indramning og forsøg. Pålideligheden af de tre metoder er undersøgt i forbindelse med brug af forskellige tidsfunktioner.

Der er to formål med studiet af tidseffekter i jord. Først præsenteres en kort og præcis opsummering af fænomener relateret til tid (krybning, relaksation, hastighedseffekter og akkumulerede effekter såsom ”ageing”), som er observeret i forbindelse med laboratorieforsøg. Disse fænomener optræder både i sand og ler, men de er dog mere udbredte i ler end i sand. Undersøgelser viser, at jordarter har forskellige karakteristika, som for eksempel hvorvidt de udviser isotach eller non-isotach opførsel. Tilsyneladende udviser ler isotach opførsel, hvorimod sand har tendens til non-isotach opførsel. Herefter præsenteres en kort og præcis opsummering, som kategoriserer og beskriver de karakteristiske træk ved eksisterende modeller, inklusive en vurdering af deres anvendelighed. Eksisterende modeller kan anvendes ved modellering af isotach opførsel. Det kan derved konkluderes, at eksisterende modeller i princippet kan bruges til modellering af den tidsafhængige opførsel observeret i ler, hvorimod dette ikke er gældende for sand.

TABLE OF CONTENTS

1 CAPACITY OF PILES - PART I

Foundation solutions depend on the soil, the ground water table, and the loads to which a structure is subjected. There are numerous types of foundation concepts but two of the more common are spread footings and piles. This thesis focuses on piles, which are columnar elements of timber, concrete, and/or steel that are driven, pushed or otherwise installed in the ground (see Figure 1). The function of piles is to transfer load from the superstructure through weak compressible strata or water onto stiffer or more compact or less compressible soils or rock (Tomlinson, 1995). Both lateral and vertical loads may be involved. Piles may also be required to carry uplift loads when supporting tall structures subjected to overturning forces from, for example, wind and waves, or to control the settlements when spread footings are underlain by a highly compressible stratum. Piles can be used to compact loose, cohesionsless deposits through a combination of pile volume displacement and driving vibrations. In addition to this, piles can be required to stiffen the soil beneath machine foundations to control both amplitudes of vibration and the natural frequency of the system (Bowles, 1996). As indicated, piles are widely employed in various disciplines within foundation engineering.

1.1.1 Types of Piles

Piles may be classified as end-bearing piles and friction piles. This distinction is purely one of convenience since almost all piles carry load as a combination of side resistance and end-bearing. There are other ways to classify piles, e.g. by installation method, material type, loading conditions, or by the amount of soil displaced when installed. A simple classification is proposed by Tomlinson (1995) based on the British Standard Code of Practice for Foundations (BS 8004):

- *Large displacement piles* comprise solid-section piles or hollow-section piles with a closed-end, which are driven or jacked into the ground and thus displace the soil. Steel tubes (driven closed-ended), precasted or

Figure 1 Examples of pile types. Steel monopile (a.) and driving of a monopile (b.) associated with Horns Rev Offshore Wind Farm, Denmark. Typical concrete piles (c. and d.) used in Danish geotechnical engineering practice.

prestressed solid concrete piles (Figure 1), and timber piles with round or squared sections are examples of pile types belonging to this category.

- *Small-displacement piles* are also driven or jacked into the ground but have a relatively small cross-section area. They include rolled steel H- or I-sections, and pipe or box sections installed with an open end such that soil enters the hollow section. Where these piles types plug with soil during installation they become large displacement piles. Steel tubes driven open-ended (Figure 1), steel piles with H-section, tubular precast or prestressed concrete piles driven open-ended are examples of pile types belonging to this category.

- *Replacement piles* are formed by first removing the soil by boring using a wide range of drilling techniques. Concrete may be placed into an unlined or lined hole, or the lining may be withdrawn as the concrete is placed. Preformed elements of timber, concrete, or steel may be placed in the drilled hole.

It should be mentioned that numerous types of piles of composite construction may be performed by combining units in each of the above categories (Tomlinson, 1995). Further, advantages and disadvantages, depending on material type, of the different pile categories when it comes to foundation practice have been reported extensively in the literature and will not be repeated here. Bowles (1996), West (1972) and Tomlinson (1995), for example, present consistent reviews regarding this subject.

Delimitations of the study
Focus is entirely paid to driven large and small-displacement piles.

1.1.2 History of driven piles

The driving of piles to support structures is one of the earliest examples of the art and science of the civil engineer (Tomlinson, 1995). As early as 200 BC, timber piling was used in China by the bridge builders of the Han Dynasty. In the Roman world piles have also been known BC. Until the end of the nineteenth century piles were exclusive timber piles driven by drop hammers on small wooden rigs (Pile Buck, 2006). The nineteenth century saw real progress on several fronts for driven piles. Steam hammers, concrete piles and a dynamic pile driving formula saw the light for the first time. In 1897, the French engineer Francois Hennebique introduced the use of reinforced concrete piles. They largely replaced timber piles for high-capacity piling for works on land (Tomlinson, 1995). The U.S. was not far behind and in 1901, A.A. Raymond was the first to use concrete piles in a building foundation in Chicago (Pile Buck, 2006). The beginning of the twentieth century also saw the start of the use of steel piling, both H-piles and pipe piles. Both of these steel shapes existed for structural use and were adapted to piles. During the last century, advantages in pile driving rigs and hammers (for hammers in the period from 1950 to the 1970s) have also taken place. Especially, the advent of large mobile cranes, with their greater manoeuvrability, led to a new era in pile driving (Pile Buck, 2006). Today, several types of hammers exist; see, for example, Tomlinson (1995) for more information.

1.1.3 Estimation of capacity

Pile foundations are normally one of the more economically expensive parts of structures such as houses, bridges or wind turbines. For design purposes the accuracy in the estimation of pile capacities is of extreme importance since it, besides safe structures, leads to economic savings through fewer, shorter, or smaller piles. In this thesis, the term capacity is only related to the capacity of the supporting soil and not to the structural strength of the pile shaft. Generally, the capacity can be established by:

1. *Testing*, e.g. static and dynamic pile load tests.

2. *Calculation*, e.g. pile driving formulae or static design equations based on soil and other relevant parameters.

The two ways of estimating the capacity have been extensively studied and reported in the literature. The present study is aimed at calculating the axial capacity of piles by static design equations. Thus, problems related to testing, pile driving formulae, installation and pile engineering practice in general are not the primary goals even though they are of major concern. Nevertheless, results of static tests will be employed in order to fulfil the stated objectives presented in Section 1.1.4.

Figure 2 Factors that plausibly affect the axial capacity of a pile.

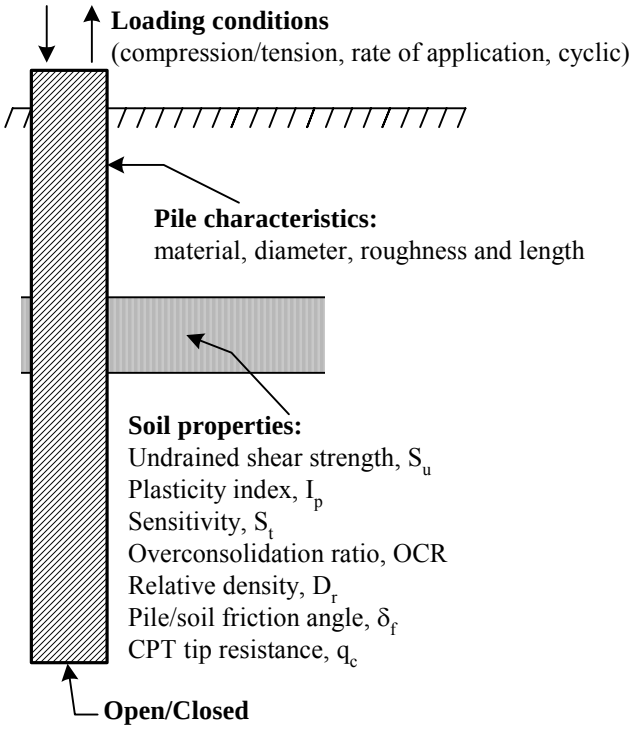

Important factors that plausibly affect the axial capacity of a pile, and thereby elements that should be incorporated in a consistent design method, are (cf. Figure 2):

- *The media in which the pile is installed*
  a. Soil and rock conditions.
  b. Presence of water.

- *The physical properties of the pile*
  c. Material.
  d. Length.
  e. Diameter.

- *The way the pile is installed*
  f. Installation method, e.g. driving, jacking, vibrating.
  g. Pile tip condition during installation, i.e. open-ended (small-displacement pile) or closed-ended (large-displacement pile). In addition to this, a pile driven open-ended can plug and thereby become a large-displacement pile.

- *The loading conditions*
  h. Piles loaded vertically and statically in either compression or tension.
  i. Rate of load application.
  j. Cyclic loading.
  k. Dynamic loads resulting from for example earthquakes.

- *The time elapsed since the end of installation*.

As indicated, the calculation of piles capacity must be of complex matter and at present time it is based partly on theoretical concepts from sciences of soil and rock mechanics, but mainly on empirical methods based on experience (Tomlinson, 1995). This is due to the fact that during driving the soil is remoulded (the degree of remoulding depends

on the installation conditions) and the stresses acting against the pile and the mechanical properties of the disturbed pile/soil contact zone are not known (Clausen and Aas, 2001a). Thus, since calculation is often based on the physical properties of the soil in the undisturbed state and since the soil parameters associated with the disturbed state govern the capacity as well as changes with time, correlations and fitting must be an integrated part of developing calculation procedures. In general, in the author's opinion a design method must be based on a semi-empirical approach and calibrated against a database containing a representative set of, for example, static loading tests. Not only calibration but also assessing existing calculation procedures and evaluating the effects of the listed factors on capacity must be based on a database of pile tests.

1.1.4 Aim and scope

The objectives of Part I, which all are related to the estimation of pile capacities, are three-fold:

1. *Time and its effect on pile capacity*, see Section 1.2, Augustesen et al. (2005c, 2006), and Jensen et al. (2004). This section deals with the effects of time on the axial capacity. An increase in pile capacity with time is denoted "set-up" whereas a decrease is referred to as "relaxation". It is important to quantify set-up because calculation procedures that take no account of time will be subject to considerable error unless they consider a tightly specified age range. Further, time effects offer potential practical benefits if piles have been, or can be, driven months or even years before any critical loading events can occur – as in carefully staged construction, or when reusing pre-installed aged foundations. Focus is paid to empirical relations, relating time since installation and capacity, which have been offered for quantifying set-up. Such empirical relations are denoted time functions. Existing time functions, proposed by Skov and Denver (1988), Bullock et al. (2005a,b), and Clausen and Aas (2000), have been assessed and the possibilities of introducing an alternative time function is investigated based on a set of pile tests. Further, set-up is in Denmark quantified by employing a so-called regeneration factor in the static design equations. If not measured, the regeneration factor is chosen to be 0.4 in the ultimate limit-state. The possibility of introducing a regeneration factor dependent on time elapsed since driving and undrained shear strength have been investigated. In summary, the idea of this part of the thesis is to suggest a practicable way in which consulting engineers and contractors can consider the additional capacity when designing piles in clay.

2. *Assessment of design methods for piles in clay*, see Section 1.3 and Augustesen et al. (2005a). The reliability of three well-known design methods, proposed by the Norwegian Geotechnical Institute, the Imperial College in London and the American Petroleum Institute, respectively, is studied by comparing predicted capacities with measured capacities from an established database. Guidelines are given for the choice of design method to be used in different circumstances (load specifications, length of pile, pile material etc.). Further, in order to evaluate the design methods in consideration, it is necessary to correct for time between pile driving and pile testing. Results of testing the calculation procedures against the available data by employing an alternative time function, instead of one of the existing time functions, are presented.

3. *Assessment of design methods for piles in sand*, see Section 1.4 and Augustesen et al. (2005b). The objective is similar to the intention of assessing design methods for piles in clay.

To the best of the author's belief, the following aspects of this part of the thesis contribute to the area of pile design:

- Validation of the linear relationship between the logarithmic to time after installation and the axial capacity of piles in clay, cf. Augustesen et al. (2006) and Section 1.2.1.

- Evaluation of existing time functions used to quantify set-up for axial loaded piles, cf. Augustesen et al. (2006) and Section 1.2.1.

- Formulations of new and more reliable time functions, which can be employed by consulting engineers and contractors, in order to take the effects of time on the capacity into consideration, when designing piles, cf. Augustesen et al. (2005a, 2006) and Section 1.2.1.

- Step-by-step procedure which can be applied in the calibration of time functions, cf. Augustesen et al. (2005c).

- Calibration of the regeneration factor employed (to quantify set-up) in the static design equations associated with Danish geotechnical engineering pratice, cf. Jensen et al. (2004) and Section 1.2.2.

- Expansion of existing databases with relatively well-documented pile tests. The databases, one for piles in clay and one for piles in sand, can be used to develop or re-assess design methods for piles in clay and sand, respectively, cf. Augustesen et al. (2005a,b), Sections 1.3 to 1.4 and this section.

- A consistent and an impartial assessment of three well-known design methods, Augustesen et al. (2005a). Both piles in clay and sand have been examined.

In the rest of this section general deliminations and considerations regarding the stated objectives will be presented.

Design methods in consideration

Design methods for piles in clay and sand have been a controversial matter within geotechnical engineering in many years due to their empirical nature. Therefore, the design of piles has remained a constant source of attention, especially with regard to the methodology for predicting the capacity. As a result numerous calculation procedures are proposed in the literature, see for example De Cock and Legrand (1997), Jardine and Chow (1996), API (1993), Clausen and Aas (2000), and the references given in Lacasse and Nadim (1996) and Augustesen et al. (2005a,b). The design methods can, for piles in clay, be categorized as an α-method, a β-method or a λ-method depending on the way the skin friction is determined:

- α-*method*. Characteristic for the α-approach is that the skin friction is related to the undrained shear strength by the factor α.

- β-*method*. The β-approach is an effective-stress-based method and the skin friction is related to the vertical effective free field stress by the factor β.

- λ-*method*. The λ-approach is a so-called α-β-approach and it is a combination of the two other approaches. α and β can be very complicated functions if they include all the factors affecting the capacity as described in Section 1.1.3. Further, α and β can be highly interrelated.

For piles in sand a similar categorization of design methods does not exist.

It is outside the scope of this thesis to evaluate all existing calculation procedures. Therefore, focus is here paid to three models when considering either piles in clay and sand, namely NGI-99, ICM-96, and API-RP2A. The methods are described in some details in Augustesen et al. (2005a,b) for piles in clay and sand, respectively. API-RP2A is a part of the existing API (American Petroleum Institute) procedure (API, 1993). ICM-96 has been developed at Imperial College in London by Jardine and his co-workers (Jardine and Chow, 1996, 1997), whereas NGI-99 is proposed by Clausen and Aas (2000) at the Norwegian Geotechnical Institute (NGI). Reasons for focusing on NGI-99, ICM-96 and API-RP2A are:

- NGI-99, ICM-96, and API-2 are of high standard and their approaches to capacity predictions are very different. NGI-99 is a λ-approach, ICM-96 is a β-method whereas the current version of API-RP2A is an α-approach.

- ICM-96 and NGI-99 include many of the factors affecting the capacity, cf. Section 1.1.3. Exceptions are piles installed by jacking or vibration and piles subjected to cyclic or dynamic loads resulting from, for example, earthquakes, i.e. these factors are left out of consideration in the rest of this thesis.

- Norwegian Geotechnical Institute has done a comprehensive research on comparison of API-RP2A with ICM-96 and NGI-99 for piles in clay and sand. During the study period abroad at NGI the author was introduced to this research and some of the work presented here is supplementary to the work performed by NGI (Clausen and Aas, 2000, 2001a,b).

- API-RP2A has been recognised internationally and many civil engineers follow the API procedures when designing large driven piles for major structures such as bridges and harbours (Jardine and Chow, 1997). Further, many offshore piles have been designed based on the API recommendations.

- The history of API-RP2A goes back to 1969 and it is the reference method when evaluating other design methods. The historical development is well-described in Pelletier et al. (1993).

The design methods in consideration are primarily minded on the offshore industry. However, they are derived predominantly from onshore load tests on short piles. Therefore, it is the author's hope that the conclusions drawn and the principal structure of the methods eventually can be applied in future development of calculation procedures for onshore piles, for example in connection with the Danish national code.

Established database

In order to evaluate the above-mentioned design methods and to explore the effects of time on pile capacity, databases (one for piles in clay and one for piles in sand) of relatively well-documented pile tests have been established. The tests have been found in the literature and provided by Danish and Norwegian companies. Especially, the Norwegian Geotechnical Institute has provided numerous pile tests. When considering piles in clay, the number of relevant pile tests are 268 and they are distributed on 111 sites, see Augustesen et al. (2005a). For piles located primarily in sand the number of relevant pile tests are 152 distributed on 59 sites, see Augustesen et al. (2005b).

Focus is placed on the static capacity of piles. Since the most reliable method to measure the static capacity is pile loading tests (Bowles, 1996), the databases are entirely based on such tests. Cases including stress-wave measurements could advantageously be incorporated if capacities obtained from dynamic and static loading tests are strictly comparable. By focusing on static tests uncertainty regarding this subject is neglected and the data are thereby treated in a consistent manner. However, there is not differentiated between CRP (Constant Rate of Penetration) and ML (Maintained Load) tests when considering "static" loading tests. For CRP tests it is assumed that the loading rate is very low, compared to dynamic tests, and the capacity obtained expresses the static capacity.

When interpreting loading tests, the failure condition can be interpreted in several different ways. Tomlinson (1995) lists some of the recognized criteria and Pile Buck (2006) list disadvantages and advantages of pile tests in general. In this study interpreted failure loads correspond to settlements equal to $0.1d$, where d is the equivalent pile diameter referring to an equivalent circle diameter for square and hexagonal piles. For example, for a closed-ended square concrete pile the equivalent diameter $d = 4b/\pi$ where b is the side length, i.e. the determination of d is based on the perimeter (surface area), which is reasonably for friction piles. Alternatively, the determination of d could be based on the cross-sectional area (in that case $d^2 = 4b^2/\pi$), which is reasonably for end-bearing piles. In this study, the calculation of d is preferably based on the perimeter since the majority of the piles associated with this study are friction piles. The above-mentioned failure criterion is employed in this study because it is then most likely that both the toe and shaft resistance are fully mobilised (Vijayvergiya, 1977; API, 2000). Further, the failure criterion is very easy to apply in practice.

Miscellaneous

Uncertainty is introduced in several ways when exploring the stated objectives. For example, uncertainty is related to the determination of the measured capacities even though the same failure criterion and testing technique have been employed in all cases. Further, determination of soil characteristics due to spatial variation of soil properties, limited site exploration, and testing methods can be subjected to uncertainty. The majority of the cases have been found in the literature, i.e. limited or insufficient information regarding pile, soil and testing conditions leads to incorrect conclusions. The above-mentioned uncertainties and randomness related to determination of soil properties and measured capacities have not explicitly been quantified when assessing the design methods or evaluating the effects of time on axial capacity, i.e. reliability theory is not employed when establishing soil profiles and interpreting loading tests. The guidelines given are therefore not based on conservative reasons for design but instead sober facts concerning which model that provides the better description of the available data. However, randomness and uncertainty associated with the recommended calculation procedures, the time functions, the estimation of soil parameters, and the loads to which the structure in consideration is subjected, should be taken into consideration when employing a probabilistic approach for pile design, see for example Lacasse and Nadim (1996), and Horsnell and Toolan (1996). Further, in deterministic pile design safeties in terms of partial coefficients or a total factor of safety should be employed.

It should be mentioned that focus is paid to single piles, i.e. effects of group action is omitted though it results in greater capacities for piles in clay (Bullock et al. 2005a,b). In this thesis the term capacity is not defined according to the structural strength of the pile shaft or pile settlements. It is exclusively related to the capacity of the supporting soil.

1.2 Time and its effect on pile capacity

An increase in pile capacity with time is denoted set-up. Time is in this case simply the time elapsed since the end of driving. Thus, time is not associated with cyclic loading, loading rate and inertia. It is commonly believed that set-up is caused by two different effects (Augustesen et al., 2005c):

1. *Dissipation of excess pore water pressures due to driving*. This leads to increased horizontal effective stresses acting against the pile shaft implying increased mobilised skin friction with time.

2. *Ageing*. Capacity increases with time due to changes in the characteristics of the soil skeleton, changes in the pile-soil interaction and/or changes in stress regime in the soil surrounding a given pile. For piles in clays thixotropy, cementation or bonding of clay particles with time also play a role.

Up to present, several studies concerning the influence of time on the capacity of piles have been reported in the literature. Bullock et al. (2005a,b), Long et al. (1999), Augustesen et al. (2005b) and recently Jardine et al. (2006) present reviews concerning magnitudes of observed set-up, causes of set-up (effects of dissipation of excess pore pressures and ageing) and empirical relations, also denoted time functions, that have been offered for quantifying set-up. It is important to quantify set-up because calculation procedures that take no account of time will be subject to considerable error unless they consider a tightly specified age range. Further, time effects offer potential practical benefits if piles have been, or can be, driven months or even years before any critical loading events can occur – as in carefully staged construction, or when reusing pre-installed aged foundations.

1.2.1 Time function

A semi-logarithmic linear relation (Skov and Denver, 1988) is often used to describe the relation between time, t, and bearing capacity, Q:

$$Q = Q_0 \left\{ 1 + \Delta_{10} \log_{10} \left(\frac{t}{t_0} \right) \right\} \tag{1}$$

where Q is the vertical bearing capacity at time t after the end of installation, Q_0 is the reference capacity determined according to the reference time t_0. Δ_{10} is the set-up factor, i.e. the capacity increase corresponding to a ten-fold increase in time. It can be a function of relevant soil parameters or even constant. In this thesis, focus has been paid to the form and magnitude of Δ_{10}. A relation between t and Q as expressed in eq.(1) is denoted a time function. It should be noted that the determination of the reference time, t_0, affects the value of Δ_{10} by changing the reference capacity, Q_0, cf. eq.(1). t_0 can in principle be chosen freely but once chosen t_0 is assumed constant and should be used together with the corresponding Δ_{10} and Q_0. The choice of reference time is further discussed in Augustesen et al. (2005c, 2006) and it is similar to the problem of similitude when quantifying the magnitude of creep strains. The problem of similitude is discussed in Augustesen et al. (2004).

The semi-logarithmic relation between Q and t has been investigated for piles in clay based on a special subset of loading tests from the AAU database (see Section 1.3), namely piles subjected to staged loading, i.e. piles tested at least two times. 18 cases including 27 piles and in total 88 loading tests have been included in the investigations. The time elapsed to the final static test on each pile varied from 22 to 9778 days after the end of installation. Further, the number of tests on each pile ranged from two to six. Based on the available data, Augustesen et al. (2006) confirm/validate the linear relationship between Q and $\log_{10}(t)$ as expressed by eq.(1) for piles in clay.

The set-up factor Δ_{10} for piles in clay

Three existing time functions have been re-assessed; namely the models proposed by Skov and Denver (1988), Bullock et al. (2005b), and Clausen and Aas (2000). Skov and Denver (1988) recommend using $\Delta_{10} = 0.60$ for $t_0 = 1$day whereas Bullock et al. (2005b) suggest using $\Delta_{10} = 0.1$ and $t_0 = 1$day for design purposes if predictor tests have not been performed, and higher values when supported by dynamic and static tests. $\Delta_{10} = 0.1$ is valid for piles, which are not subjected to staged loading. In contrast, $\Delta_{10} = 0.25$ is proposed for piles undergoing staged loading. Last, Clausen and Aas (2000) postulate that Δ_{10} describing long-term effects is a function of plasticity index, I_p, and overconsolidation ratio, *OCR*, as follows:

$$\Delta_{10} = 0.1 + 0.4\left(1 - \frac{I_p}{50}\right) OCR^{-0.8}, \quad 0.1 \le \Delta_{10} \le 0.5 \tag{2}$$

The reference time, t_0, is chosen to be 100 days. Information on the model can also be found in Karlsrud et al. (2005).

Augustesen et al. (2006) conclude that the time function proposed by Skov and Denver (1988) provides the better fit of the available data whereas the model suggested by Clausen and Aas (2000) provides the least suitable fit in spite of the fact that it includes a dependency on soil properties.

The possibilities of introducing an alternative time function to the models proposed by Skov and Denver (1988), Bullock et al. (2005a,b) and Clausen and Aas (2000) have been investigated. The starting point was to assume that Δ_{10} = constant. It turns out that the time function based on $\Delta_{10} = 0.24$ (the reference time, t_0, is chosen to be 100 days) provides the better estimate of the measured capacities (Augustesen et al., 2006). It has also been investigated whether it is advantageously to make Δ_{10} more sophisticated in terms of introducing relevant soil parameters, i.e. plasticity index I_p, overconsolidation ratio *OCR*, and undrained shear strength S_u, in the expression of Δ_{10}. Augustesen et al. (2005c) found that

$$\Delta_{10} = 1.24 - \left(\frac{S_{uu}}{S_{uu}^0}\right)^{0.03}, \quad S_{uu}^0 = 60\text{kPa} \tag{3}$$

provides the better estimate of the available data. S_{uu} is the average unconsolidated undrained shear strength in kPa along the pile shaft. By introducing a reference strength (S^0_{uu} = 60 kPa) Δ_{10} becomes dimensionless since the constants 1.24 and 0.03 are dimensionless. Again, the reference time, t_0, is chosen to be 100 days. For the S_{uu} range examined, Δ_{10} varies between 0.22 and 0.29. Considering the scatter and the power of 0.03, Augustesen et al. (2006) concluded that there is no "distinctive" correlation between S_{uu} and the set-up factor.

In case of staged loading, Augustesen et al. (2006) recommend to make use of the time function based on $\Delta_{10} = 0.24$ when estimating the development of capacity with time. The corresponding reference time, t_0, is 100 days. The upper and lower limits of a two-sided 95% confidence level on Δ_{10} are with caution estimated to 0.20 and 0.29, respectively. Further, Δ_{10} equals 0.13 for unstaged loading and t_0 = 100 days whereas Δ_{10} equals 0.46 and 0.18 for staged and unstaged loading, respectively, when t_0 = 1 day.

Improvements and future work

The following improvements and suggestions for future work regarding the effects of time on pile capacity in general could be considered:

- *Establish more well-described pile tests of high quality*. Existing time functions can thereby be re-assessed or new time functions can be developed. According to Bullock et al. (2005b), almost all research on the influence of time on pile capacity come from static or dynamic tests "staged" successively on the same pile at increasing times after installation, thus including a pre-shearing effect that might increase or decrease the capacity measured during subsequent stages. A study that isolates the effects of time and pre-shearing is needed for piles in clay; the author is only aware of three studies (Karlsrud and Haugen, 1986; Miller, 1994; Bullock et al., 2005b) related to staged and unstaged testing. Last, heavily instrumented pile loading tests are also needed because they provide detailed information regarding the variation of set-up with depth, set-up of well-defined

strata instead of the pile as a whole, set-up related to end-bearing and side shear, and set-up related to for example soil state, installation method, and pile conditions, respectively.

- *Separation of the effects of pore pressure dissipation and ageing*.

- Employ *stress-wave measurements*, interpreted by either the CASE or CAPWAP-method, in the development of time functions, see for example Skov and Denver (1988). If using the CAPWAP-method information regarding variation of set-up with depth, set-up of well-defined strata, and set-up related to end-bearing and side shear, respectively, is also obtained.

- *Ageing mechanisms causing set-up*. The mechanisms are complicated and not yet fully understood. To the author's knowledge, limited information on ageing mechanisms describing set-up of piles in clay have been reported (Augustesen et al., 2005c). However, during the last decade several studies on ageing of piles in sand have been elucidated, see Chow et al. (1998), Axelsson (1998, 2002), Schmertmann (1991), and recently Bowman and Soga (2005) as well as Jardine et al. (2006). One of the dominant processes is thought to be gains in the radial effective stresses acting on the pile shafts resulting from the relaxation, through creep, of circumferential arching established around the pile shafts during installation (Chow et al., 1998 and reproduced in Augustesen et al., 2005b). Karlsrud et al. (1992) also give this as a plausible reason for the mechanism controlling set-up for piles in clay. According to Axelsson (1998, 2002) another dominant process is the increase in dilatancy and stiffness of the soil with time, i.e. changes in soil properties with time. Bowman and Soga (2005) propose a hypothesis, involving kinematically restrained dilation of the soil close to the pile shaft and soil ageing, to explain pile set-up. Initially, creep volume changes are contractant but gradually the creep straining become dilatant. As the kinematic restraint provided by the pile would inhibit expansion of the soil, any such dilation would lead to increased horizontal stresses and thereby capacity. The starting point of further investigations into ageing mechanisms for both piles in sand and clay should be the above-mentioned references eventually coupled with some of the observations regarding ageing effects (additional stiffness and strength due to periods of creep) and some of the suggestions for future work (see Section 2.4) discussed in Part II.

- *Make to a greater extent use of commercial FE programmes* to obtain a better understanding of the ageing mechanisms controlling set-up. This implies among other factors that 1) it is possible to model a driving process numerically, 2) the material model implemented in the FE codes consider inviscid and time-dependent behaviour of soils, and 3) the model describing the pile/soil interface accounts for time-dependency. The author finds that much more work is needed in order to advantageously make use of FE programmes when studying the effects of time on pile capacity. For example, existing constitutive relationship can in principle not be used to describe time effects in sands due to non-isotach behaviour, cf. Part II. Other limitations and advantages of existing material models are discussed thouroughly in Liingaard et al. (2004) associated with Part II. Even though a consistent and robust model exists, development within numerical procedures and interface modelling associated with FE algorithms may be needed.

- *The effects of group action on set-up*.

- *The effects of maintained load on set-up*. As done for virtually all pile set-up research, the piles remained unloaded between tests. However, during construction the pile load is progressively increased. Therefore, it would be interesting to observe the set-up for piles subjected to maintained load between loading tests.

- *Development of time functions for piles in sand*. This is urgent as indicated by Jardine et al. (2005b, 2006) since pile capacity calculation procedures that take no account of time will be subject to considerable error unless they consider a tightly specified age range.

1.2.2 Time effects and the Danish practice for pile design

According to the Danish Code of Practice for foundation engineering, time is only assumed to influence the skin friction for piles in clay (DS415, 1998):

(4) $$q_{sik} = \frac{1}{1.5} m \cdot r \cdot S_u$$

where q_{sik} is the unit friction capacity, m is a material dependent factor (m = 1.0 for timber and concrete whereas m = 0.7 for steel), S_u is the undrained shear strength, and r is the regeneration factor. It should be noted that the determination of the unit skin friction is based on an α-approach, see Section 1.1.4, and in this case α equals $1/1.5 \cdot m \cdot r$. The r-factor is the ratio of the shear strength in a given depth at a given time after pile driving to the shear strength of the intact soil. Time influences the r-factor, and thereby the pile capacity, since time affects the shear strength. Further, the regeneration factor accounts both for the effects of dissipation of excess pore water pressures due to driving and ageing. DS415 (1998) recommend using r = 0.4 in the ultimate limit-state, if r has not been precisely specified by means of experiments.

DS415 (1998) postulates that the regeneration factor increases with decreasing shear strength; in this section the shear strength corresponds to the undisturbed soil state. This implies that at a given instant after installation the regeneration factor is greater for clays with low shear strengths compared to clays with high shear strengths. Therefore, Jensen et al. (2004) investigated a possible relation between time, t, undrained shear strength, S_u, based on vane shear tests, and the regeneration factor, r. They found that

(5) $$r = 2.31 \cdot \left(S_u\right)^{-0.26} \cdot \left(\frac{t}{t_{ref}}\right), \quad t \leq 70\text{days}$$

where t is in days, S_u in kPa, and t_{ref} is the reference time (= 70days). Equation (5) indicates that the regeneration factor increases with increasing time elapsed since installation and decreasing undrained shear strength. Equation (5) should be considered tentative since it is only based on seven cases including 13 static loading tests. Therefore, the results presented in Jensen et al. (2004) should be viewed upon as preliminary investigations on how to use existing data to develop a relation between time, strength and capacity of a pile. It should be mentioned that the cases involved are related to sites in Denmark. In the future, more tests should be analysed in order to calibrate and verify the model of the above-mentioned type.

1.3 Assessment of design methods for piles in clay

Even if a prediction method gives the correct answer for the total pile capacity, it may not give the correct end-bearing and distribution of skin friction with depth. In such cases, the method could be non-conservative for layered soil profiles. A predicted distribution of stresses can be verified by comparing it with a measured distribution obtained from instrumented loading tests. Such a comparison is, for example, given by Karlsrud et al. (2005) based on large diameter pile tests at Pentre and Tilbrook test sites in UK. In this thesis, focus is entirely paid to the capability of a given design method to predict the correct total pile capacity, which in this case equals the measured capacity. This implies that the distribution of stresses along the pile is not considered.

Database

As mentioned, the number of relevant pile tests are 268 and 111 sites constitute the available cases when considering piles in clay, see Augustesen et al. (2005a). Further, the established database represents a wide variety of soil and pile conditions. The average undrained shear strength for each pile ranges between eight and approximately 600kPa. The pile diameters range between 0.10m and 0.80m whereas the penetration depth of the longest pile exceeds 100m, cf. Augustesen et al. (2005a). The database, denoted AAU (after Aalborg University), consists of a great number of the pile tests included in the NGI database and cases found in connection with the present study. It should be mentioned that the database established by the Norwegian Geotechnical Institute is divided into primarily three groups. The conclusions drawn by Clausen and Aas (2000) are based on each one of the three groups or even subsets of those. In contrast, the conclusions drawn here are based on all available data. It should be mentioned that some of the cases employed in the NGI database, and thereby the AAU database, have been taken directly from the databases established by Flaate and Selnes (1977) and Semple and Rigden (1984).

Conclusions and recommendations

Uncertainty is introduced in several ways when assessing design methods and certain delimitations of this study have been presented (see Sections 1.1.1 and 1.1.4). Further, each design method requires soil parameters specific to that method. For example, NGI-99 is based on S_{uu}, which is the unconsolidated undrained shear strength determined by triaxial testing, and ICM-96 is based on the overconsolidation ratio, *OCR*, among other parameters. In most of the cases associated with the established database the clay property known is the undrained shear strength, S_u. A set of assumptions has therefore been employed to relate S_u with *OCR*, see Clausen and Aas (2000) and Augustesen et al. (2005a). In addition, since the kind of input shear strength used in the calculation procedures varies and since the shear strengths associated with the different cases have been established in different ways (triaxial test, vane shear test, CPT etc.), a routine that converts one type of shear strength to another have been employed. Thereby, the comparison of the methods is made consistent. However, the conversion procedures contribute to the mentioned uncertainty and it is a controversial matter within the profession of soil mechanics.

Time affects the capacity as described in Section 1.2. The loading tests represented in the database are performed at different times after initial driving and the calculation methods estimate capacities corresponding to the reference time (chosen to be 100 days). Thus, a time function that extrapolates the measured capacity at a given time to the capacity to the reference time have been employed. Consequently, it is possible to compare measured and predicted capacities, and thereby the different design methods, in a consistent manner. In the original work by Clausen and Aas (2000), the time function given by eq.(1) combined with eq.(2) have been employed. Further, time correction is associated with skin friction for the part of the pile located in clay. An alternative time function, given by eq.(1) combined with eq.(3), has been considered in order to study the effect of replacing time function when considering NGI-99 and API-RP2A. When investigating the reliability of ICM-96, eq. (3) can also be applied if S_{uu} is replaced by the consolidated undrained shear strength, S_{ciu}, and S^0_{uu} by S^0_{ciu} = 70 kPa (Augustesen et al., 2005a,c).

Bearing the above-mentioned assumptions, uncertainties and corrections in mind when comparing and assessing the design methods in consideration, the following can be concluded and recommended based on Augustesen et al. (2005a):

- Overall, NGI-99 provides the better description of the available data.

- ICM-96 can advantageously be applied to concrete piles. This statement is encumbered with great uncertainty due to the small number of tests available on concrete piles.

- It is recommended **not** to use ICM-96 for piles driven open-ended and loaded in compression. Further, API-RP2A can preferably be applied to piles driven open-ended and loaded in tension. In all other cases NGI-99 should be applied.

- Especially API-RP2A provides a skew distribution of *C*/*M*-ratios (see below) with penetration depth. Therefore, the effect of pile length has been investigated. It is recommended to use NGI-99 independent on pile length, driving conditions (open-ended or closed-ended), and loading conditions (compression or tension).

- The effect of pile diameter has also been elucidated. Generally, NGI-99 provides the better description independent on pile diameter. Alternatively, API-RP2A could be applied to piles with diameters in the range 0-0.3m, and ICM-96 for piles with diameters in the range 0.3-0.6m. The last statement may be affected by the fact that approximately 42% of the piles belonging to the category 0.3-0.6m are closed concrete piles loaded in compression. ICM-96 is especially reliable for these types of piles, whereas NGI-99 and API-RP2A are not.

- It is not evident whether it is an advantage to adapt corrections to undrained shear strength and time for all calculation methods. Generally, employing S_u conversions result in greater average *C/M*-ratios, which are the average of the ratios between the calculated capacities (*C*) and the corresponding measured capacities (*M*). Ideally, the average *C/M*-ratio equals 1 whereas the standard deviation should be equal to 0. The average *C/M*-ratios are reduced by employing time corrections. The effects on *C/M*-ratios are greater by making use of time correction than S_u conversions. More effort could advantageously be put into the revision of the conversion procedures for the undrained shear strength, S_u.

- The effects of replacing time function are not distinct. By employing the time functions proposed by Augustesen et al. (2005c), the calculation methods become slightly more accurate in the determination of the measured pile capacities when considering all the available tests. However, detailed analyses, not shown in this

thesis, show that the reliability of the design procedures is not improved by employing the time functions proposed by Augustesen et al. (2005c) compared to applying the time function based on $\Delta_{10} = 0.24$ (Augustesen et al., 2006). Hence, there is no benefit in making use of a complicated time function, which justifies the use of the time function based on $\Delta_{10} = 0.24$ as indicated by Augustesen et al. (2006). Independent on the time function employed, NGI-99 provides the most reliable prediction of the data.

- Generally, the calculation methods are very sensitive towards the way the soil profile and pile tests are interpreted.

The conclusions drawn should be looked upon as an impartial assessment of the different methods. However, the conclusions may be affected by the fact that 1) ICM-96 is based upon parameters that are not a part of routine site investigations, e.g. in all cases associated with this study the input parameters for ICM-96 are estimated and 2) it is assumed that the capacities determined by ICM-96 and API-RP2A correspond to the reference time (= 100days).

Finally, the choice of design method should rely on local test data if such data are available. Thus, if a number of piles have been tested in similar ground, the choice of calculation method should be based on *C/M*-ratios obtained for the given site.

Improvements and future work

The following improvements regarding the assessed design methods and suggestions for future work associated with calculation procedures in general could be considered:

- *Include more high quality data in the database and re-assess the design methods*. A modification of the conversion procedures related to the undrained shear strength needs to be considered.

- *Refine the calculation procedures* regarding the *effects of group action* and *loading conditions* different from static loading, e.g. cyclic and horizontal loads.

- Check the design methods ability to predict the *correct distribution of skin friction with depth*. This requires more heavily instrumented pile loading tests.

- *Additional studies of how the capacity of piles develops with time*. This is further discussed in Section 1.2.

- *More axial pile research is needed at actual design load levels* when considering design methods for offshore piles (Pelletier et al., 1993).

- Design methods are calibrated based on measured capacities. Whether piles are tested by means of CRP or ML, the rate of load application is much higher than the loading rate corresponding to that of a building under construction. Yet the ability of a pile to carry its load, and thereby the foundation for developing design methods, is judged on its behaviour under a comparatively rapid loading test (Tomlinson, 1995). Therefore, more effort could advantageously be put into investigations of *the influence of loading rate on pile capacity*. Well-knowing that the investigations in the laboratory (primarily 1D and conventional triaxial conditions) are very different from the conditions associated with large-scale loading tests (large strains, principal stress rotation, pile/soil interaction, 3D deformations), observations based on laboratory tests (see Part II) can eventually be applied in the design and analysis of tests relating loading rate to pile capacity. For example, the problem of load application is similar to the effects of strain rate discussed in Augustesen et al. (2004). Results show that the responses of clays subjected to slow Constant Rate of Strain tests (corresponds to CRP tests) are very different from responses of soils subjected to rapid CRS tests and conventional oedometer tests (corresponds to ML tests). This can be explained as follows: in connection with the slow CRS test ageing effects (structuration) leading to a gain in stiffness and strength can be deloped with time. This is not the case in connection with the other tests. Similarly, load-settlement curves depend on whether CRP or ML tests are performed, as well as the rate of load application. It should be mentioned that definitions of slow and rapid have not been clearly defined.

- Design method for piles in *permafrost, silt, and calcareous soils* (Lacasse, 1999).

- If design methods for piles driven in clay or sand are ever to progress beyond the current empirical approaches, then it is important to *include commercial FE programmes, and thereby constitutive modelling, to a greater extent in the development of design methods*. For example, by modelling a driving process knowledge can be gained regarding development of pore pressures, coring and plugging of piles, the degree of principal stress rotation, and the characteristics of the pile/soil interaction zone. Therefore, modelling of a driving process may reveal governing parameters related to pile capacity. In addition, if the driving situation is modelled correctly it could, together with a sophisticated constitutive model, lead to an explanation of why the skin friction is different when the pile subsequently to driving is loaded either in tension or compression. The results obtained may then be confirmed by loading tests. It should be mentioned that De Nicola and Randolph (1993) discuss from a theoretical point of view why tensile and compressive shaft capacities of piles in sand differ. However, they did not consider the effects of principal stress rotaion even though the mechanism has been noted from field measurements (Lehane et al., 1993). It should also be mentioned that modelling of a driving process requires stable and eventually advanced constitutive models and FE-algorithms.

The Norwegian Geotechnical Institute and Imperial College, London, have refined their calculation procedures after the completion of the research presented in this thesis. This implies that some of the above-mentioned suggestions of improvements have already been incorporated in the updated design methods. For example, according to Jardine et al. (2005c) the new sections of the Imperial College model include pile ageing; cyclic loading; group action; pile shape and seismic effects, as well as applications in calcareous and micaceous sands, diatomaceous clays and clay-silts. However, the governing static equations remain more or less unchanged. More detailed recommendations are made on parameter selection and practical implementation. According to Jardine et al. (2005c) the updated design method is described in details in Jardine et al. (2005a). In the modified NGI-model, the procedure for the skin friction is changed especially with focus on normally consolidated clay with low plasticity. For piles driven in overconsolidated clay the factor that takes driving conditions (open-ended or closed-ended) into account is also changed. For more details, see Karlsrud et al. (2005).

1.4 Assessment of design methods for piles in sand

As it was the case for piles in clay, focus is here entirely paid to the reliability of a given calculation procedure to predict the correct total pile capacity, which in this case equals the measured capacity. This implies that the distribution of stresses along the pile is not considered.

Database

As mentioned previously, the number of relevant pile tests are 152 and 59 sites constitute the available cases when considering piles in sand, see Augustesen et al. (2005b). Further, the established database represents a wide variety of soil and pile conditions. The average CPT tip resistance for each pile range between 2.5 and approximately 29MPa. The pile diameters range between 0.10m and 2.00m whereas the penetration depth of the longest pile is 94m, cf. Augustesen et al. (2005b). The database, denoted AAU (after Aalborg University), consists of a great number of the pile tests included in the NGI database and cases found in connection with the present study. It should be mentioned that the database established by the Norwegian Geotechnical Institute is divided into primarily four groups. The conclusions drawn by Clausen and Aas (2001b) are based on each one of the four groups or even subsets of those. In contrast, the conclusions drawn here are based on all available data. It should be mentioned that some of the cases employed in the NGI database, and thereby the AAU database, have been taken directly from the databases established by Olson (1988), Randolph et al. (1994), and Chow (1996).

Conclusions and recommendations

Uncertainty is introduced in several ways when assessing design methods and certain delimitations of this study have been presented (see Sections 1.1.1 and 1.1.4). Further, each design method requires soil parameters specific to that method. For example, ICM-96 is among other parameters based on the CPT tip resistance whereas the relative density is the governing parameter when calculating the shaft resistance associated with NGI-99. The relevant soil parameters are not all established in every case. In order to obtain a consistent treatment of the available data, conversion rules relating one parameter to another are employed. For each sand layer at least one of the following input parameters that relate to sand strength must be given: 1) CPT tip resistance, 2) SPT resistance, 3) relative density, or 4) angle of internal friction. If one of the mentioned parameters is known, the other three can be determined (Clausen and Aas, 2001b and reproduced in Augustesen et al., 2005b). This is done only if the parameter in consideration is not given as input. The

conversion is a controversial matter within the profession of soil mechanics and contributes to the mentioned uncertainty.

Time affects the capacity as described in Section 1.2. At the moment, no time correction formula is employed when re-assessing the design methods for the parts of the pile located in sand. However, in many of the cases associated with this study the time duration between installation and testing is unfortunately not known.

Bearing the above-mentioned assumptions, uncertainties and corrections in mind when comparing and assessing the design methods in consideration, the following can be concluded and recommended based on Augustesen et al. (2005b):

- Overall, API-RP2A provides the better description of the available data.
- Capacities of piles loaded in compression are best predicted by API-2 in terms of average *C/M*-ratio (defined in Section 1.3).
- ICM-96 can profitably be applied to concrete piles whereas API-RP2A and NGI-99 work best for piles made of steel.
- Especially API-RP2A provides a skew distribution of *C*/*M*-ratios with penetration depths. Therefore, the effect of pile length on the average *C/M*-ratios has been investigated. It is recommended to use NGI-99 for piles longer than 15m and ICM-96 for piles with penetration depths less than 15m independent on whether the piles are driven open-ended or closed-ended.
- The effect of pile diameter on the average *C/M*-ratios has also been elucidated. ICM-96 provides the most reliable description of piles with equivalent diameters less than 0.4m. API-RP2A is the most reliable method for piles with diameters exceeding 0.4m.
- Generally, the calculation methods are very sensitive towards the way the soil profile and pile tests are interpreted.

The conclusions drawn should be looked upon as an impartial assessment of the different methods. The choice of design method should rely on local test data if such data are available. Thus, if a number of piles have been tested in similar ground, the choice of calculation method should be based on *C/M*-ratios obtained for the given site.

Improvements and future work

The improvements and future work suggested for piles in clay (Section 1.3) do also apply for piles in sand.

It should be mentioned that the Norwegian Geotechnical Institute and Imperial College, London, have refined their calculation procedures after the completion of the research presented in this thesis. This implies that some of the suggestions of improvements have already been incorporated in the updated design methods. Comments, associated with the modification of the Imperial College model, are described in Section 1.3. In the modified NGI-model the fundamental equations are modified compared to NGI-99 and importantly, the modified version includes a term that is pile material dependent, i.e. the calculated shaft resistance depends on whether the pile material is concrete or steel. For more details, see Clausen et al. (2005).

According to Clausen et al. (2005) and Lehane et al. (2005c) two design methods for piles in sand have recently been proposed; one is developed by Fugro Engineers (Fugro, 2004) and the other is developed by Lehane and his co-workers at University of Western Australia (UWA), see Lehane et al. (2005a,b,c). At the moment, the author has no information on the Fugro-method whereas the UWA-model, at first sight, is based on the same fundamental considerations as ICM-96, see Augustesen et al. (2005b). Neither the Fugro nor the UWA-model is further considered in this thesis.

2 TIME EFFECTS IN SOILS - PART II

From real construction projects, it is well known that clay exhibit time-dependent behaviour. For example, Crawford and Morison (1996) report on settlements of a major wastewater treatment plant located on soft compressible soils, at least before pre-loading took place, nearby Vancouver in Canada. When the pre-loading and the construction period were finished after approximately three years settlements occurred for the next 19 years at a rate of 0.25m per log cycle of time (in years). Crawford and Morison (1996) concluded that the observed long-term settlements were due to creep since rapid drainage was observed in the upper layers. Another example, in Part I of this thesis the time-dependent behaviour of clays is quantified in terms of relating capacity of piles to time elapsed since the end of installation. Many other examples have been reported in the literature, especially when the subsoil conditions are clay. In contrast to clays, it is not widely accepted that sand shows considerable amounts of time-dependent behaviour. However, studies show that time effects in sands are not always negligible. For example, Hannink (1994) reports on settlements of ten buildings ranging from 12-storeys to 41-storeys in Rotterdam, Holland, for periods ranging from two to thirty years after construction. These buildings are supported by piles installed in 25m sandy soils. In one extreme case, the piles supporting a 100m high building settled about 130mm over a period of 19 years with 35% of the settlements occurring after the construction period. In addition to real construction projects, the effects of time on strength and deformation characteristics of soils have been observed extensively in the laboratory, see for example Augustesen et al. (2004) and Young and Townsend (1986).

2.1.1 Types of time effects

The words “time” and “time-dependency” can be understood in several ways. In this part of the thesis, time has nothing to do with dynamic effects where inertial forces are involved. Instead, time and time dependency is assumed to be related to viscous effects in the soil skeleton, such as creep, stress relaxation, rate effects, and accumulated effects. Therefore, the process of consolidation is not regarded as a true time effect either.

There is some confusion in the literature regarding the definition and the interpretation of the time-related phenomena. This especially concerns creep as discussed by Augustesen et al. (2004). In this thesis the following definitions have been applied:

- *Creep* is the development of strains under the assumption that the effective stresses are constant.
- *Relaxation* is the development of effective stresses under the assumption that the soil deformations (strains) are maintained constant.
- *Rate-effects* should be understood as how soil reacts to different rates of loading or straining. For instance, if the stress-strain relationship of a given soil depends on the rate at which the soil is loaded or deformed it is said to be rate-dependent.
- *Accumulated effects (or ageing effects)* deal with the soil behaviour, i.e. the stress-strain relation, when the soil is loaded after periods of ageing due to, for example, long periods of creep or stress relaxation. Ageing or accumulated effects are also related to the stress-strain behaviour at low strain or stress rates. The definition of low is not clearly defined (Augustesen et al., 2004). Structuration plays an important role in connection with ageing effects.

2.1.2 Aim and scope

Focus is aimed at time effects in soil in general. An understanding of the basic time mechanisms in soils, see Section 2.1.1, can be established by:

1. *Testing*. Laboratory or eventually in situ tests can be performed and analysed.
2. Analysing *constitutive relations* describing time-dependent behaviour of soils, i.e. localise advantages, limitations, and basic features of existing models. The relations can be based on laboratory experiments or in situ tests.

The two ways of investigating time effects in soils have been extensively studied and reported in the literature. "True" time effects have primarily been observed under well-defined conditions in the laboratory. Well-knowing that the test conditions in the laboratory do, in most cases, not match the in situ conditions, the starting point of this study is time effects observed in connection with laboratory tests and constitutive relations related hereto. This leads to the objectives of Part II and along with them the contribution of this part of the thesis to the area of geotechnical engineering:

- *Evaluation of time-dependent behaviour of soils*, see Augustesen et al. (2004). The purpose is to present the different time-related effects observed in soils and to remove the confusion regarding definitions which are found in the literature, i.e. a concise review is presented, which describes the observed trends within the field of time-dependent behaviour of soils.

- *Characterization of models for time-dependent behaviour of soils*, see Liingaard et al. (2004). The purpose is to give a survey of the models that exist for modelling the observed time effects and their limitations, i.e. a concise review which categorizes and describes the basic features of existing models as well as their advantages and limitations.

It was the author's hope to use the results of Part II to explain the ageing mechanisms associated with Part I but in the present form Part II should be looked upon as a step forward towards a better understanding of time effects in soil in general. Part II could be the start to improve methods and procedures used for solving time-dependent engineering problems. Eventually, the knowledge gained can help researchers to understand, for example, the ageing effects associated with pile set-up.

Delimination of the study
To keep the study within manageable limits, the following assumptions have been made:

- The influence of *temperature* on time effects in soils has not been considered.

- Results of *one-dimensional laboratory tests* and *conventional triaxial tests* are considered since time effects, to the author's knowledge, have not been observed under true triaxial conditions by means of, for example, a true triaxial apparatus or a hollow cylinder apparatus.

- The descriptions are restricted to factors that concern the *macro-mechanical* properties, such as stress, time, and strain. Hence, the macro-mechanical approach is based on general theories (elasticity, plasticity and viscosity) of ideal continua bodies and the physical nature of the materials (their structure and the changes thereof in a deformation process) is not subjected to close scrutiny. The material represents a "black box" and only the relations of input (e.g. load) and output (e.g. strain) are investigated (Feda, 1992). An alternative way to study time effects in soils is the micro-mechanical approach. In contrast to macro-mechanics, the micro-mechanical behaviour of soils is deduced from the physical ideas about their structure at atomic or molecular levels. In this kind of approach the soil behaviour is based on the interaction between structural units. The structural units are defined as aggregates (clusters) of elementary particles (grains) that acts as a whole and their structural response depends on their size, shape and composition (Feda, 1992). See Kamon et al. (1985), Feda (1992) and Mitchell (1993) for further details on micromechanical modelling of soils.

2.2 Evaluation of time-dependent behaviour of soils

Most of the past laboratory studies of the rheological behaviour of soils have focused on the characteristics of clayey soils. This is especially true when considering confined conditions. The time-dependent behaviour studied in connection with triaxial test conditions are usually carried out on clays as well, but in recent years increasing attention has been paid to experimental research into the behaviour of granular materials. Augustesen et al. (2004) present a concise review regarding observed time-dependent behaviour of soils.

The review by Augustesen et al. (2004) especially revealed an essential characteristic for soils. That is whether the time-dependent behaviour can be characterized as isotach or non-isotach. The behaviour symbolized by a unique relation between stresses and strains dependent on strain rate is denoted isotach behaviour (Figure 3 to the left), i.e. the phenomena of creep, relaxation, and strain-rate effects are governed by the same unique time-mechanism. This implies

Figure 3 Isotach behaviour is observed in clay for a) creep and relaxation and b) stepwise change in strain rate. Non-isotach behaviour is observed in sand for c) creep and relaxation and d) stepwise change in strain rate. q denotes deviator stress and ε is the strain. A superimposed dot indicates a rate.

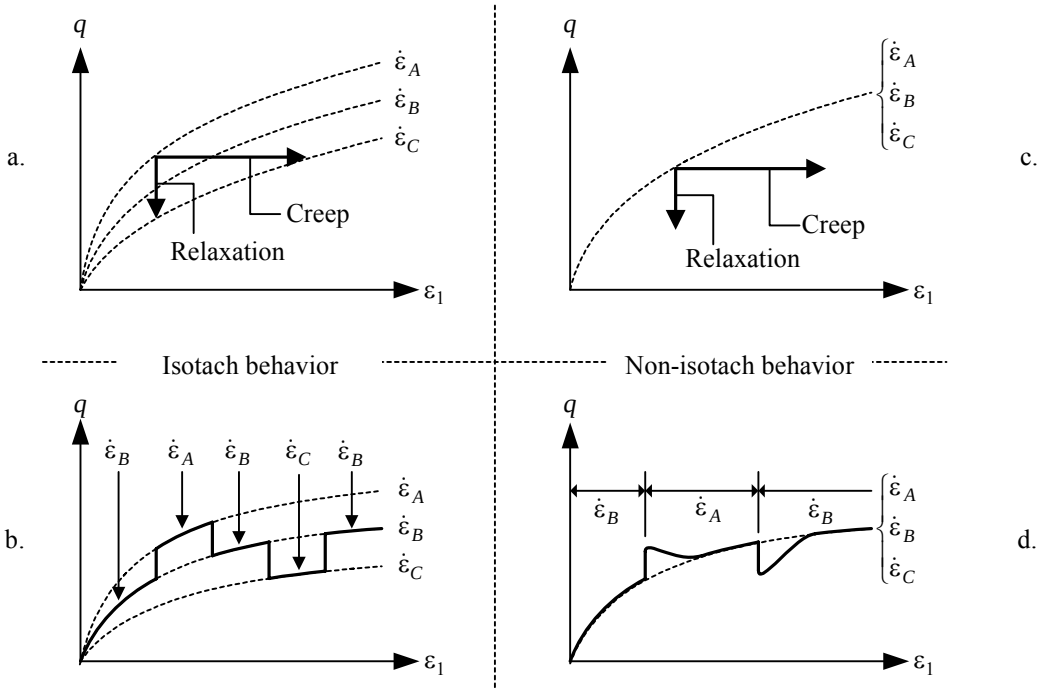

that creep properties can be obtained by Constant Rate of Strain (CRS) and relaxation tests and vice versa (Figure 4). Isotach behaviour corresponds to some extent to the observed behaviour of clay. The mechanism where creep, relaxation and rate dependency are considered to be due to the same basic time mechanism is also denoted the "correspondence principle" (Sheahan and Kaliakin, 1999). In contrast to clays, the sand tested by Matsushita et al. (1999) exhibited noticeable amounts of creep and relaxation but no strain rate effects (similar to Figure 3.c). This led to one of the main conclusions: The stress-strain relationship is independent on strain rate (Figure 3 to the right) and the phenomena of creep and relaxation cannot be predicted from results obtained in CRS loading tests on sand since changes of strain rate are temporary (similar to Figure 3.d). Therefore, sand exhibits non-isotach behaviour. It should be mentioned that the reported investigations of time-related phenomena in sand are few compared to the investigations of clay. Whether or not a given soil behaves in isotach or non-isotach matter is of paramount importance when considering the models used to predict the observed behaviour (Section 2.3).

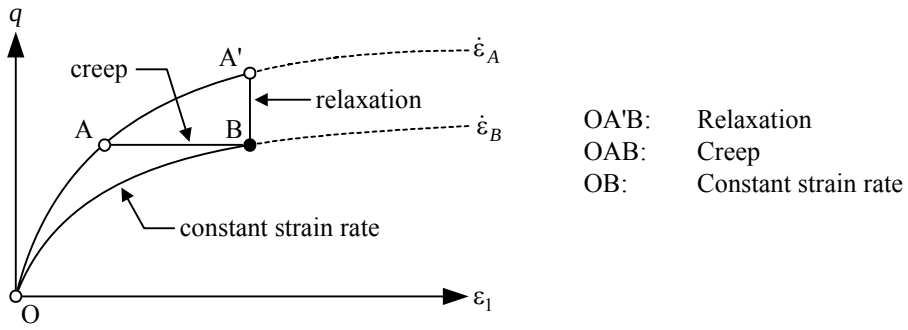

Figure 4 Isotach behaviour and the correspondence principle imply that the unique stress-strain-strain rate relation in B can be reached by creep (OAB), relaxation (OA'B) or by enforcing a constant rate of strain (OB), i.e. all three loading histories coincide in B.

Figure 5 a) Illustration of isotach and non-isotach behaviour for very slow ($\dot{\varepsilon} = \dot{\varepsilon}_C$) CRS tests. b) Illustration of isotach and non-isotach behaviour observed in connection with reloading ($\dot{\varepsilon} = \dot{\varepsilon}_A$) subsequent to ageing due to creep. Clays show the non-isotach behaviour in both cases.

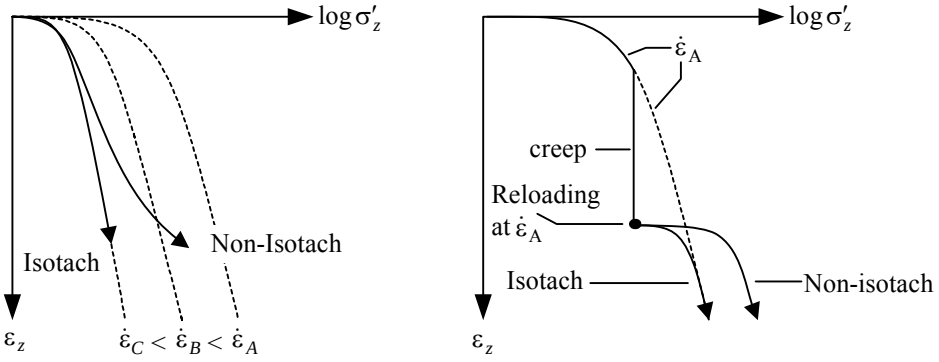

As mentioned, isotach behaviour is adequate to describe time effects in clays in many situations. However, there are some exceptions (Augustesen et al., 2004):

- *Time-dependent behaviour at very low strain rates* (Figure 5). Results obtained by very slow CRS tests showed disagreements with the unique stress-strain-strain rate relation. The definition of low is not clearly defined.

- *Loading after periods of ageing due to creep* (Figure 5).

As shown in Figure 5, compared to what is expected if the isotach behaviour is assumed valid for clay, additional strength and stiffness is gained. The change in strength and deformation characteristics is due to structuration, which is a result of ageing taking place. Leroueil et al. (1996) suggest that structuration in clays can be explained by strengthening of contacts between particles or aggregates due to thixotropy or cementation and may be influenced by the age of the clay. In summary, structuration cannot be explained by isotach behaviour. The subject is discussed in details in Augustesen et al. (2004). It should be mentioned that structuration effects also are observed in sand.

2.3 Characterization of models for time-dependent behaviour of soils

Liingaard et al. (2004) conclude that existing constitutive models for prediction of time-dependent behaviour of soils can roughly be categorized as follows:

1. *Empirical models* are mainly obtained by fitting experimental results from creep, stress relaxation, and constant rate of strain tests, and the constitutive relations are generally given by closed-form solutions or differential equations. This is similar to the approach applied when calibrating design methods for piles, see Part I. In addition, empirical models are strictly limited to specific boundary and loading conditions and they may be used as a basis for developing three-dimensional constitutive relations.

2. *Rheological models* describe uniaxial conditions and they are given as closed-form solutions or in a differential form. Often, they are used to obtain a conceptual understanding of time effects in soil.

3. *General stress-strain-time models* are in principle three-dimensional models. They are often given in incremental form. Therefore, they are readily adaptable to numerical implementation in, for example, commercial FE codes such as ABAQUS and PLAXIS. Further, the constitutive relations describe not only viscous effects but also the inviscid (time-independent) behaviour of soils, in principle, under any possible loading condition.

Advantages, limitations and basic features of the different types of constitutive relations are thoroughly presented in Liingaard et al. (2004).

To the author's knowledge none of the models developed so far can handle all the observed time effects in soils. Whether models are empirical, rheological, or general, they all make use of the correspondence principle. This implies that the same constitutive relationship can be used to predict creep, stress relaxation, and constant rate of strain behaviour by imposing appropriate boundary conditions on the soil element, i.e. a unique relation between stress, strain, and rate of strain is assumed. Consequently, relations making use of the correspondence principle can, in theory, model soils exhibiting isotach behaviour. It is therefore concluded that:

- Existing models and concepts *can* in principle be used when modelling time-dependent behaviour of clay.
- Existing models and concepts *cannot* be used when modelling time-dependent behaviour of sand.

However, ageing effects such as structuration cannot be modelled.

2.4 Improvements and future work

The following suggestions for future work regarding time effects in soils are related to both experimental investigations and the modelling aspect:

- *Systematic verification of the behaviour of clay*. It is important to determine whether the isotach behaviour is adequate for describing arbitrary loading situations. This verification is crucial in order to obtain general applicability of the existing constitutive models.
- *Comprehensive investigations of sand*. Due to the complex non-isotach behaviour of sand, investigations are required if constitutive relations for sand are to be formulated and in order to understand the phenomenon.
- Investigation of time-dependent behaviour of both sand and clay under *true triaxial conditions*.
- The influence of *principal stress direction*, *anisotropy* and *ageing effects* on the time-dependency of soils. For example, it would be interesting to quantify the effects of ageing (gain in strength and stiffness) depending on the duration of creep periods. Further, observing the effects of a change in principal stress direction when the soil is loaded subsequent to an ageing period is also relevant. According to Bowman and Soga (2003) any benefits of ageing is lost when the principal stresses are rotated or the load is removed. This may explain why the skin friction of tension piles is less than the skin friction observed in connection with piles loaded in compression (This is also discussed in Section 1.2). As a matter of fact, investigations of the effects of principal stress direction, anisotropy and structuration on the time-dependent behaviour of soils may be relevant when considering set-up for piles (see Part I) since 1) the soil surrounding the pile is an anisotropic material, 2) the principal stress directions are changed during installation and subsequent loading, and 3) the soil is loaded (sheared) due to construction or load testing after a period of ageing.
- In order to understand the basic mechanism that governs the overall time-dependent behaviour of soils, considerations at the *microscopic level* are required. Studies of the complex nature of the inter-particular bonding in sand and clays should be performed. Thereby, it might be possible to explain the different bonding in sand and clay. The bonding in sand seems to be temporary whereas the bonding in clays apparently is similar to cementation causing a persistent increase of inter-particular bonding.
- *Modelling of three-dimensional behaviour of clays and structuration*.
- *New concepts and models must be developed to describe time-dependent behaviour of sand*. Liingaard et al. (2004) discuss this subject in further details.
- It must be considered whether the constitutive relations should constitute a *unified model* or make use of the *coupling principle*. The decision influences the way in which the constitutive model is structured. A unified model is, as the name indicates, a model that combines all time effects (and other effects) in a set of constitutive equations, which are solved by numerical methods. For models making use of the coupling principle, a set of constitutive equations are coupled depending on the engineering problem that is solved. Therefore, the coupling principle implicitly assumes that different mechanisms control the different types of

time effects. For example, if a creep process is simulated the basic model, e.g. an existing elasto-plastic model, is coupled with the constitutive relation that models creep and all the other constitutive components are frozen. In reality, it may be physically impossible or hard to couple the different time effects. Further, for the unified approach, it may be impractical to develop a set of equations from which all time mechanisms can be modelled. That is, the same set of equations can probably not be used to describe e.g. crushing and stress relaxation in sand.

As indicated in the introduction to this chapter and numerous papers, time-dependent behaviour of soils is important to consider and in some cases it eventually leads to failure of a structure. Since time effects always occur, it is preferably to have a reliable and robust model to predict time-related phenomena. Since no general models exist for sand and there are some gaps associated with existing models for clayey soils, it may be of interest in the future to develop new constitutive relations based on, for example, laboratory tests and eventually implement them into commercial FE programs.

3 CONCLUSIONS

Elements related to pile design and time effects in soil in general have been studied and presented. Several conclusions can be drawn from the work presented in this thesis.

In respect of pile design, the present study was aimed at the determination of the axial capacity of piles by static design equations. Problems related to testing, pile driving formulae, installation and pile engineering practice in general were not the primary goals even though of major concern. Nevertheless, results of static tests were employed in order to fulfil the stated objectives. As presented in Part I, the study concerning pile design were divided into *time and its effects on capacity*, *assessment of design methods for piles in clay* and *assessment of design methods for piles in sand*.

The vertical bearing capacity of piles in clay has been assessed with focus on quantifying set-up. The idea was to suggest a practicable way in which consulting engineers and contractors can consider the additional capacity when designing pile foundations. In the literature it has been suggested that the pile capacity increases with the logarithm of time after installation. Augustesen et al. (2005c, 2006) confirm this semi-logarithmic relationship. In continuation of this it has been analysed whether the magnitude of set-up is related to the properties of the soil surrounding a pile. Augustesen et al. (2005c) propose a time function where the set-up factor, Δ_{10}, depends on the undrained shear strength In contrast, Augustesen et al. (2006) argue that $\Delta_{10} = 0.24$ when the reference time is chosen to be 100 days. It is recommended to use the time function based on $\Delta_{10} = 0.24$. Hence, the set-up factor for piles situated in clay is constant and independent of the soil properties. Finally, if another reference time than 100 days is preferred, the set-up factor should be adjusted according to Augustesen et al. (2006). According to the Danish Code of Practice for Foundation Engineering, time is only assumed to influence the skin friction through the regeneration factor. If this factor has not been precisely specified by means of experiments, it is assumed to be constant in the ultimate limit-state. Jensen et al. (2004) propose a relation between the regeneration factor, the time elapsed since installation and the undrained vane shear strength. The relation should be considered tentative since it is based on very few tests.

Design methods for piles in clay and sand have been a controversial matter within geotechnical engineering for many years due to their empirical nature. Therefore, the design of piles has remained a constant source of attention, especially with regard to the methodology for predicting the capacity. In this study, three very different design methods for piles in both clay and sand have been assessed based on established databases of static loading tests. The calculation procedures in consideration are NGI-99, ICM-96, and API-RP2A. API-RP2A is a part of the existing API (American Petroleum Institute) procedure. ICM-96 has been developed at Imperial College in London, whereas NGI-99 is proposed by the Norwegian Geotechnical Institute (NGI). Augustesen et al. (2005a) found that for piles in clay, NGI-99 provides the better prediction of pile capacities independent of pile length, driving conditions (open-ended or closed-ended) and loading conditions (compression or tension). Alternatively, API-RP2A can preferably be applied to piles driven open-ended and loaded in tension. However, Augustesen et al. (2005a) recommend that ICM-96 is not used for piles driven open-ended and loaded in compression. In order to evaluate the design methods in consideration for piles in clay it is necessary to correct for time between pile driving and pile testing. By employing the time functions proposed by Augustesen et al. (2005c, 2006), the calculation methods become slightly more accurate in the determination of the measured pile capacities compared to applying the time function proposed by NGI. However, the reliability of the design procedures is not improved by employing the time functions proposed by Augustesen et al. (2005c) compared to applying the time function based on $\Delta_{10} = 0.24$ (Augustesen et al., 2006). Hence, there is no benefit in making use of a more complicated time function, which justifies the use of the time function based on $\Delta_{10} = 0.24$.

For piles in sand, Augustesen et al. (2005b) recommend using NGI-99 for piles longer than 15m and ICM-96 for piles with penetration depths less than 15m independently of driving and loading conditions. However, API-2 generally provides the most reliable description of all the data available, piles with diameters exceeding 0.4m, and steel piles. Therefore, calculated capacities based on NGI-99 and ICM-96 should be compared to the outcome of a traditional API design. ICM-96 can profitably be applied to concrete piles.

In respect of time effects in soil in general, the present study was aimed at *evaluation of time-dependent behaviour of soils* and *characterization of models for time-dependent behaviour of soils* as described in Part II. Augustesen et al. (2004) present a concise review of time-related phenomena, such as creep, stress relaxation, rate effects and accumulated effects (ageing), observed in connection with laboratory tests. Focus is placed on one-dimensional tests and conventional triaxial tests on clay and sand. It has been shown that all the above-mentioned phenomena are present in both clay and sand. However, they are more pronounced in clay than sand. The review reveals essential characteristic situations for different types of soils, i.e. whether the time-dependent behaviour can be characterised as isotach or non-

isotach. It seems reasonable that the isotach behaviour is adequate for describing the time effects in clays in most situations. However, there are exceptions, such as the time-dependent behaviour at very low strain rates, where the effects of structuration play a role. The structuration effects cannot be explained by isotach behaviour. The isotach behaviour is not valid for sands.

Liingaard et al. (2004) give a survey of the models that exist for modelling the observed time effects and their limitations. They can roughly be categorized as one of the following types: 1) Empirical models, 2) Rheological models, and 3) General stress-strain-time models. Liingaard et al. (2004) conclude that existing models and concepts can in principle be used when modelling time-dependent behaviour of clay whereas this is not the case when considering sand.

4 REFERENCES

API (1993), Recommended practice for planning, designing and constructing fixed offshore platforms- working stress design, *API RP 2A-WSD, American Petroleum Institute, 20th edition*, July 1, 1993.

API (2000). Recommended practice for planning, designing and constructing fixed offshore platforms- working stress design. *API recommended practice 2A-WSD, American Petroleum Institute, 21st edition*.

Augustesen, A., Liingaard, M. and Lade, P.V. (2004), Evaluation of Time-Dependent Behavior of Soils, *International Journal of Geomechanics*, 4(3), pp.137-156.

Augustesen, A., Andersen, L., and Sørensen, C.S. (2005a), Capacity of Piles in Clay, *Available from the Department of Civil Engineering, Aalborg University, Denmark*, *Internal report*, ISSN: 1398-6465 R0502.

Augustesen, A., Andersen, L., and Sørensen, C.S. (2005b), Capacity of Piles in Sand, *Available from the Department of Civil Engineering, Aalborg University, Denmark*, *Internal report*, ISSN: 1398-6465 R0519.

Augustesen, A., Andersen, L., and Sørensen, C.S. (2005c), Time Function for Driven Piles in Clay, *Available from the Department of Civil Engineering, Aalborg University, Denmark*, *Internal report*, ISSN: 1398-6465 R0501.

Augustesen, A.H., Andersen, L., and Sørensen, C.S. (2006), Assessment of Time Functions for Piles Driven in Clay, *Available from the Department of Civil Engineering, Aalborg University, Denmark*, *DCE Technical Memorandum No.1*, ISSN: 1901-7278.

Axelsson, G. (1998), Long-term increase in shaft capacity of driven piles in sand, *Proceedings of 4th International Conference on Case Histories in Geotechnical Engineering*, St. Louis, Missouri, Paper no. 1.25, pp.301-308.

Axelsson, G. (2002), A Conceptual Model of Pile Set-up for Driven Piles in Non-cohesive Soil, *Proceedings of International deep foundations congress*, Orlando, Florida, Vol.1, (Geotechnical Special Technical Publication, ASCE, Vol.116), pp.64-79.

Bowles, J.E. (1996), Foundation analysis and design, *5th edition, The Mcgraw-Hill Companies, Inc*.

Bowman, E.T. and Soga, K. (2003), Creep, ageing and microstructural change in dense granular materials. *Soils and Foundations*, 43(4), pp.107-117.

Bowman. E.T. and Soga, K. (2005), Mechanisms of setup of displacement piles in sand: laboratory creep tests, *Canadian Geotechnical Journal*, 42(5), pp.1391-1407.

Bullock, P.J., Schmertmann, J.H., McVay, M.C., and Townsend, F.C. (2005a), Side shear setup. I: Test piles driven in Florida. *Journal of Geotechnical and Geoenvironmental Engineering*, 131(3), pp.292-300.

Bullock, P.J., Schmertmann, J.H., McVay, M.C., and Townsend, F.C. (2005b), Side shear setup. II: Results from Florida test piles. *Journal of Geotechnical and Geoenvironmental Engineering*, 131(3), pp.301-310.

Chow, F.C. (1996), Investigations into displacement pile behaviour for offshore foundations, *PhD dissertation, University of London (Imperial College), UK*.

Chow, F.C., Jardine, R.J., Brucy, F. and Nauroy, J.F. (1998), Effects of time on capacity of pipe piles in dense marine sand, *Journal of Geotechnical and Environmental Engineering*, 124(3), pp.254-264.

Clausen, C.J.F. and Aas, P.M. (2000), Bearing capacity of driven piles – Piles in clay, *NGI report 525211-1*, Norwegian Geotechnical Institute.

Clausen, C.J.F. and Aas, P.M. (2001a), Capacity of driven piles in clays and sands on the basis of pile load tests. *In the Proceedings of the 11th International Offshore and Polar Engineering Conference*, Stavanger, Norway, pp.581-586.

Clausen, C.J.F. and Aas, P.M. (2001b), Bearing capacity of driven piles – Piles in sand, *NGI report 525211-2*, Norwegian Geotechnical Institute.

Clausen, C.J.F., Aas, P.M. and Karlsrud, K. (2005), Bearing capacity of driven piles in sand, the NGI approach, *Proceedings of Frontiers in Offshore Geotechnics: ISFOG 2005*, (eds. Gourvenec and Cassidy), Perth, © 2005 Taylor & Francis Group, London.

Crawford, C.B. and Morrison, K.I. (1996), Case histories illustrate the importance of secondary-type consolidation settlements in the Frazer River Delta, *Canadian Geotechnical Journal*, 33, pp.866-878.

De Cock and Legrand (1997), Design of Axially Loaded Piles – European Practice. *Proceedings of the ERTC3 (The ISSMFE European Regional Technical Committee 3 "Piles"), Design of Axially Loaded Piles – European Practice*, (eds. De Cock and Legrand), Balkema, Rotterdam, ISBN: 90 5410 873 8.

De Nicola, A. and Randolph, M.F. (1993), Tensile and compressive shaft capacity of piles in sand, *Journal of Geotechnical Engineering*, 119(12), pp.1952-1973.

DS 415 (1998). *Norm for fundering, Code of Practice for foundation engineering*. Dansk Standard (in Danish).

Feda, J. (1992), Creep of soils and related phenomena, Development in geotechnical engineering 68, *Elsevier Science Publishers BV (North-Holland), Amsterdam, The Netherlands*.

Flaate, K. and Selnes, P. (1977), Side friction of piles in clay, *Prooceedings of the 9th International Conference on Soil Mechanics and Foundation Engineering*, Tokyo. Also NGI publication No.118, Norwegian Geotechnical Institute.

Fugro Engineers B.V. (Fugro) (2004), Axial pile capacity design method for offshore driven piles in sand, *Report P1003 presented to the American Petroleum Institute, issue 3*, August, 2004.

Hannink, G. (1994), Settlement of high-rise buildings in Rotterdam, *Proceedings of the 13th International Conference on Soil Mechanics and Foundation Engeenering*, New Delhi, Vol. 2, pp.441-444.

Horsnell, M.R. and Toolan, F.E. (1996), Risk of foundation failure of offshore jacket piles, *Offshore Technology Conference*, Houston, May 1996, Paper OTC 7997.

Jardine, R.J. and Chow, F.C. (1996), New design methods for offshore piles, *Marine technology directorate Ltd., publication MTD 96/103*, London, ISBN 1 870553 31 4.

Jardine, R.J. and Chow, F.C. (1997), Improved pile design methods from field testing research. *Proceedings of the ERTC3 (The ISSMFE European Regional Technical Committee 3 "Piles"), Design of Axially Loaded Piles – European Practice*, (eds. De Cock and Legrand), Balkema, Rotterdam. pp.27-38.

Jardine, R.J., Chow, F.C., Overy, R.F. and Standing, J.R. (2005a), ICP design methods for driven piles in sand and clay. *Thomas Telford, London*.

Jardine, R.J., Standing, J.R. and Chow, F.C. (2005b), Field research into the effects of time on the shaft capacity of piles driven in sand. *Proccedings of Frontiers in Offshore Geotechnics: ISFOG 2005* (eds. Gourvenec and Cassidy), Perth, © 2005 Taylor & Francis Group, London.

Jardine, R.J., Chow, F.C., Standing, J.R., Overy, R.F., Saldivar-Moguel, E. Strick van Linschoten, C. and Ridgway, A. (2005c), An updated assessment of the ICP pile capacity procedures. *Proccedings of Frontiers in Offshore Geotechnics: ISFOG 2005* (eds. Gourvenec and Cassidy), Perth, © 2005 Taylor & Francis Group, London, ISBN 0 415 39063 6.

Jardine, R.J., Standing, J.R., and Chow, F.C. (2006), Some observations of the effects of time on the capacity of piles driven in sand, *Geotechnique*, 56(4), pp.227-244.

Jensen, J.L, Augustesen, A. and Sørensen, C.S. (2004), The Influence of Time on the Bearing Capacity of Driven Piles, *In proceedings: NGM-2004 (Nordic Geotechnical Meeting), XIVth Nordiska Geoteknikermötet*, Ystad, 19.-21. May 2004, Sweden, pp.D103-D111.

Kamon, M., Matsui, T., Oda, M., Matsuoka, H., Tokue, T., Nakai, T. and Kitamura, R. (1985), Micrometric Approaches, Constitutive Laws of Soils, *Report of ISSMFE Subcommittee on Constitutive Laws of Soils and Proceedings of Discussion Session 1A,* ISSMFE Subcommittee on Constitutive Laws of Soils, 11th ICFMFE, San Francisco, pp.1-24.

Karlsrud, K. and Haugen, T. (1986), Axial static capacity of steel model piles in overconsolidated clay, *NGI Publication No.163*, Norwegian Geotechnical Institute. Also in the *Proceedings of 11th International Conference on Soil Mechanics and Foundation Engineering,* San Francisco, 1985, Vol.3, pp.1401-1406.

Karlsrud, K., Kalsnes, B. and Nowacki, F. (1992), Response of piles in soft clay and silt deposits to static and cyclic axial loading based on recent instrumented pile load tests, *Society of underwater testing*, London, Also NGI publication No.188, Norwegian Geotechnical Institute.

Karlsrud, K., Clausen, C.J.F. and Aas, P.M. (2005), Bearing capacity of driven piles in clay, the NGI approach, P*roceedings of Frontiers in Offshore Geotechnics: ISFOG 2005*, (eds. Gourvenec and Cassidy), Perth, © 2005 Taylor & Francis Group, London, ISBN 0 415 39063 6.

Lacasse, S. (1999), Ninth OTRC honors lecture: Geotechnical contributions to offshore development, *Offshore Technology Conference*, Houston, May 1999, Paper OTC 10822.

Lacasse, S. and Nadim, F. (1996), Model uncertainty in pile axial capacity predictions, *Offshore Technology Conference*, Houston, May 1996, Paper OTC 7996.

Lehane, B.M., Jardine, R.J., Bond, A.J. and Frank, R. (1993), Mechanisms of shaft friction in sand from instrumented pile tests, *Journal of Geotechnical Engineering*, 119(1), pp.19-35

Lehane, B.M., Schneider, J.A. and Xu, X. (2005a), Evaluation of design methods for displacement piles in sand, *University of Western Australia*, UWA Report, GEO: 05341.1.

Lehane, B.M., Schneider, J.A. and Xu, X. (2005b), CPT based design of driven piles in sand for offshore structures, *University of Western Australia*, UWA Report, GEO: 05345.

Lehane, B.M., Schneider, J.A. and Xu, X. (2005c), The UWA-05 method for prediction of axial capacity of driven piles in sand, *Proccedings of Frontiers in Offshore Geotechnics: ISFOG 2005* (eds. Gourvenec and Cassidy), Perth, © 2005 Taylor & Francis Group, London.

Leroueil, S., Perret, D. and Locat, J. (1996), Strain rate and structuring effects on compressibility of a young clay, *Measuring and Modeling Time Dependent Soil Behavior*, *Geotechnical Special Publication No. 61*, (Eds. Sheahan and Kaliakin), Am. Soc. of Civ. Engrg., Reston, VA, pp.1-60.

Liingaard, M., Augustesen, A. and Lade, P.V. (2004), Characterization of Models for Time-Dependent Behavior of Soils, *International Journal of Geomechanics*, 4(3), pp.157-177.

Long, J.M., Kerrigan, J.A. and Wysockey, M.H. (1999), Measured time effects for axial capacity of driven piling, *Transportation Research Record, Journal of the Transportation Research Board*, No.1663, pp.8-15.

Matsushita, M., Tatsouka, F., Koseki, J., Cazacliu, B., Benedetto, H. and Yasin, S.J.M. (1999), Time effects on the pre-peak deformation properties of sands, *Pre-failure Deformation Characteristics of geomaterials*, (Eds. Jamiolkowski, Lancellotta and Lo Presti), 1999, Balkema, Rotterdam, pp.681-689.

Miller, G.A. (1994), Behavior of displacement piles in overconsolidated clay, *PhD dissertation, Department of Civil and Environmental Engineering, University of Massachusetts Amherst, Amherst, Massachusetts, USA*.

Mitchell, J. K. (1993), Fundamentals of soil behavior, *2nd edition, John Wiley & Sons, Inc*.

Olson, R.E. (1988), Comparison of measured axial load capacities of steel pipe piles in sand with capacities calculated using the 1986 API Recommended Practice (RP2A), *Report to the American Petroleum Institute, Project PRAC 86-29A*, Austin, Texas.

Pelletier, J.H., Murff, J.D. and Young, A.C. (1993), Historical development and assessment of the current API design methods for axially loaded pipes, *Offshore Technology Conference*, Houston, May 1993, Paper OTC 7157, pp.253-282.

Pile Buck (2006), Material downloaded from http://www.vulcanhammer.net/download/driven-piles.php, Copyright Pile Buck, Inc., P.O. Bow 3609, Vero Beach, Florida 32964, USA

Randolph, M.F., Dolwin, J., and Beck, R. (1994), Design of driven piles in clay, *Geotechnique*, 44(3), p.427.

Schmertmann, J.H. (1991), The mechanical aging of soils, *Journal of Geotechnical Engineering*, 117(9), pp.1288-1330.

Semple, R.M. and Rigden, W.J. (1984), Shaft capacity of driven pipe piles in clay, *Proceedings of the Symposium on analysis and design of pile foundations*, ASCE (Ed. Meyer), p.59.

Skov, R. and Denver, H. (1988), Time-dependence of bearing capacity of piles, *Proceedings of the 3rd international conference on the application of stress-wave theory to piles*, Ottawa, Canada, (Ed. Fellenius, B.H.), pp.879-888.

Sheahan, T.C. and Kaliakin, V.N. (1999), Microstructural considerations and validity of the correspondence principle for cohesive soils, *Engineering Mechanics, Proceedings of the 13th Conference*, (Eds. Jones and Ghanem), ASCE pub., Baltimore, MD. 1999.

Tomlinson, M.J. (1995), Pile design and construction practice, *4th edition, E & FN Spon, an imprint of Chapman & Hall, London, UK*.

Vijayvergiya, V.N. (1977), Load-movement characteristics of piles, *Ports '77, Proc. 4th Annual Symposium of the Waterways, Ports, Coastal and Ocean Division of American Society of Civil Engineers*, 2, pp.269-284.

West, A.S. (1972), Piling practice, *Butterworth & Co, London, UK*.

Young, R.N. and Townsend, F.C. (1986) (editors), Consolidation of soils: Testing and evaluation, *ASTM Special Technical Publication, 892*, ASTM, Philadelphia.

5 ENCLOSED PAPERS AND REPORTS

Augustesen, A.H, Andersen, L., and Sørensen, C.S. (2006), Assessment of Time Functions for Piles Driven in Clay, *Available from the Department of Civil Engineering, Aalborg University, Denmark*, *DCE Technical Memorandum No.1*, ISSN: 1901-7278.

Augustesen, A., Andersen, L., and Sørensen, C.S. (2005), Time Function for Driven Piles in Clay, *Available from the Department of Civil Engineering, Aalborg University, Denmark*, *Internal report*, ISSN: 1398-6465 R0501.

Jensen, J.L, Augustesen, A. and Sørensen, C.S. (2004), The Influence of Time on the Bearing Capacity of Driven Piles, *In proceedings: NGM-2004 (Nordic Geotechnical Meeting), XIVth Nordiska Geoteknikermötet*, Ystad, 19.-21. May 2004, Sweden, pp.D103-D111.

Augustesen, A., Andersen, L., and Sørensen, C.S. (2005), Capacity of Piles in Clay, *Available from the Department of Civil Engineering, Aalborg University, Denmark*, *Internal report*, ISSN: 1398-6465 R0502.

Augustesen, A., Andersen, L., and Sørensen, C.S. (2005), Capacity of Piles in Sand, *Available from the Department of Civil Engineering, Aalborg University, Denmark*, *Internal report*, ISSN: 1398-6465 R0519.

Augustesen, A., Liingaard, M. and Lade, P.V. (2004), Evaluation of Time-Dependent Behavior of Soils, *International Journal of Geomechanics*, 4(3), pp.137-156.

Liingaard, M., Augustesen, A. and Lade, P.V. (2004), Characterization of Models for Time-Dependent Behavior of Soils, *International Journal of Geomechanics*, 4(3), pp.157-177.

Title:

Assessment of Time Functions for Piles Driven in Clay.

Authors:

Augustesen, A.H., Andersen, L., and Sørensen, C.S.

Year of publication:

2006

Published in:

Department of Civil Engineering, Aalborg University, Denmark, DCE Technical Memorandum No.1, ISSN: 1901-7278.

Remarks:

Parts of the memorandum are similar to parts of the report "Time Function for Driven Piles in Clay".
To be submitted for publication in an international journal.

Assessment of Time Functions for Piles Driven in Clay

A. H. Augustesen, L. Andersen, and C. S. Sørensen

The vertical bearing capacity of piles situated in clay is studied with regard to the long-term set-up. A statistical analysis is carried out on the basis of data from numerous static loading tests. The database covers a wide range of both soil and pile properties, which ensures a general applicability of the results. Firstly, it is validated that set-up leads to a linear increase of the capacity with the logarithm of time. This property is a basic assumption in most set-up models. Secondly, three different models suggested in the literature are assessed, and a comparison is made with two alternative models. In the first of these models, the rate of set-up is independent of the soil properties, whereas the second function depends on the undrained shear strength. Based on the available data, there is no statistical evidence that the magnitude of set-up depends on the properties of the soil. Hence, it is suggested that a constant set-up factor should be applied for the prediction of pile capacities at a given time after initial driving.

1 Introduction

For piles located in clay, sand or a combination of different soil types, experience shows that engineering time has an important effect on pile capacity. Thus, Wendel (1900) documented that the bearing capacity of timber piles located in clay continued to increase for two to three weeks after pile driving. This phenomenon is also known as set-up and has later been discussed extensively in the literature by, for example, Bullock et al. (2005a,b), Long et al. (1999) and Augustesen et al. (2005b). In particular, an attempt has been made to identify the causes of set-up, and empirical relations for quantifying the set-up have been offered. Such relations, in the following denoted *time functions*, may advantageously be employed in the design phase, since they will lead to economic savings through fewer, shorter or thinner piles.

This paper focus on assessment of time functions for axially loaded piles in clay. Time functions proposed in the literature are discussed and the possibility of introducing an alternative time function is investigated. The analysis is based on 18 cases with a total of 27 piles reported in the literature. In total, 88 pile tests are included in the database and only static tests are considered. The time between initial driving and the final static test on each pile varies from 22 to 9778 days. Further, the number of tests on each pile ranges from two to six.

2 Background

Skov and Denver (1988) described the relation between time, t, and vertical bearing capacity, Q, by a semi-logarithmic time function in the form

$$(1) \qquad Q = Q_0 \left\{ 1 + \Delta_{10} \log_{10} \left(\frac{t}{t_0} \right) \right\}$$

Here Q_0 is the reference capacity measured at the reference time t_0, and Δ_{10} is a factor providing the capacity increase corresponding to a ten-fold increase in time. In the following, Δ_{10} is referred to as the set-up factor.

Short-term effects regarding the bearing capacity of piles are related to both real time effects (ageing) and the equalisation of excess pore pressures built up during driving. In contrast, long-term effects are only due to ageing. Hence, different values of Δ_{10} are expected when either short- or long-term effects are investigated (Figure 1). The definition "short-term" can be misleading in connection with piles in clay because it may cover up a long period of time. If set-up is considered, the short-term component of Δ_{10} is greater than the long-term component, i.e. $\Delta_{10}^{\text{short-term}} > \Delta_{10}^{\text{long-term}}$. When relaxation, defined as a drop in capacity with time, takes place, $\Delta_{10}^{\text{short-term}}$ becomes negative. Relaxation have been reported and discussed by, for example, Davie and Bell (1991), Thompson and Thompson (1985), and York et at. (1994).

According to Skov and Denver (1988), the values of Δ_{10} in Eq. (1) for piles located in sand, clay and chalk are 0.2, 0.6 and 5.0, respectively. Correspondingly, the reference time, t_0, is assumed to be 0.5, 1.0 and 5.0 days. These values of t_0 ensure a stabilized increase of the capacity with time. Before this, the pore pressure has not reached the stationary state and soil remoulding continues to take place. Furthermore, Skov and Denver (1988) point out that there should be an upper limit to t for which Eq. (1) is used. However, no guidelines are given for this upper limit.

The assumption $t_0 = 0.5$, 1.0 or 5.0 for piles in sand, clay, and chalk, respectively, may be inconvenient if Q_0 is to be measured at the reference time. Therefore, Svinkin and Skov (2000) gave an alternative definition of Q_0 as the capacity at the end of initial driving and suggested the reference time $t_0 = 0.1$ days. Based on dynamic and static tests performed within a period of

Figure 1 Influence of short- and long-term effects on Δ_{10}. The time for equalisation of pore pressures due to pile installation is denoted t_{eoc}. Short-term effects are related to pore pressure dissipation and ageing whereas long-term effects are only due to ageing. It should be noted that both Δ_{10} and Q_0 depend on whether $t < t_{eoc}$ or $t > t_{eoc}$ are considered.

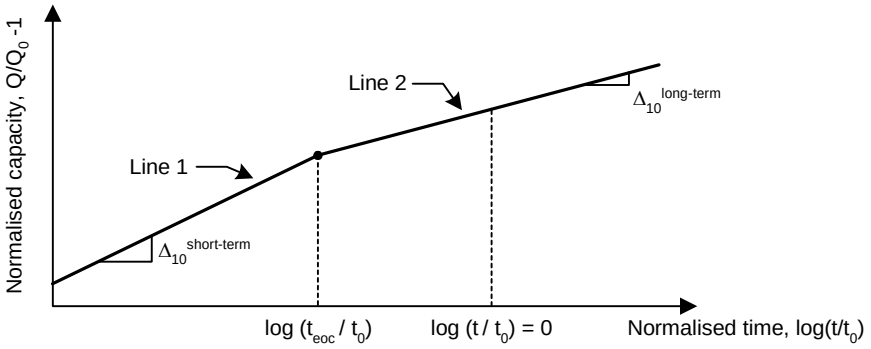

132 days after driving, Δ_{10} was found to vary between 1.14 and 3.50 for piles located in clayey soils.

Equation (1) concerns the total bearing capacity of a pile. However, Bullock et al. (2005a,b) report on similar development of the side-shear capacity with time for concrete piles driven into a variety of coastal plain soils in Florida. Δ_{10} is found to lie in the range 0.12 to 0.32. Piles located in clays generally experience higher values of Δ_{10} than piles in sand; but Δ_{10} does not depend significantly on the properties of the soil within each category. For design purposes Bullock et al. (2005b) recommend a value of $\Delta_{10} = 0.1$ (t_0 = 1day) for piles in clay when no test results are available for the specific site.

Whereas Skov and Denver (1988) and Bullock et al. (2005a,b) propose a constant value of Δ_{10}, Clausen and Aas (2000) postulate that the long-term set-up depends on the soil properties. Thus, Δ_{10} is a function of the plasticity index, I_p, and the over-consolidation ratio, *OCR*,

$$\Delta_{10} = 0.1 + 0.4\left(1 - \frac{I_p}{50}\right) OCR^{-0.8}, \qquad 0.1 \le \Delta_{10} \le 0.5 \qquad \text{NGI} \tag{2}$$

Equation (2) is based on very few tests. The reference time, t_0, is chosen to 100 days. The time function based on Eq. (2) is denoted NGI because it has been developed at the Norwegian Geotechnical Institute.

Other semi-empirical relations have been presented in the literature. Guang-Yu (1988) proposes a relation where the capacity of piles in soft ground corresponding to $t = 14$ days depend on the sensitivity, S_t, and Q_{eoid} (capacity at the "end of initial driving"). Huang (1988) postulates that the capacities for piles in soft Shanghai soils are a function of Q_{eoid}, the logarithm to time and a quantity denoted the maximum pile capacity. Svinkin et al. (1994) propose two exponential functions where the capacity is a function of Q_{eoid} and time. The study is based on testing five pre-stressed concrete piles driven in predominantly silty sands and dense soil at the lower third of the piles' embedded lengths.

In this study the assessment of time functions consists of validating the semi-logarithmic relation between capacity, Q, and time after driving, t, i.e. Eq. (1). Another objective is to compare existing expressions of Δ_{10}, and thereby the time functions, proposed by Skov and Denver (1988), Bullock et al. (2005a,b) and Clausen and Aas (2000). Thirdly, the possibility of introducing a new expression for Δ_{10} is investigated. However, firstly a common reference time should be chosen, and a careful interpretation of the test results forming the basis of the analyses has to be made.

2.1 Choice of reference time

As indicated in the former section, Skov and Denver (1988) and Bullock et al. (2005a,b) use an arbitrary, but practical, reference time of $t_0 = 1$ day. However, in the present study, t_0 is chosen to be 100 days. This value was applied by Clausen and Aas (2000). It is noted that the choice of reference time affects the value of both Q_0 and Δ_{10}, cf. Eq. (1). However, if the value of Δ_{10} for a different reference time is required, this may be found easily. Thus, defining two consistent sets of parameters ($t_{0,1}$, $Q_{0,1}$, $\Delta_{10,1}$) and ($t_{0,2}$, $Q_{0,2}$, $\Delta_{10,2}$), the following relationship is obtained from Eq. (1):

$$\begin{aligned} Q &= Q_{0,1}\left\{1 + \Delta_{10,1}\log_{10}\left(\frac{t}{t_{0,1}}\right)\right\} \\ &= Q_{0,2}\left\{1 + \Delta_{10,2}\log_{10}\left(\frac{t}{t_{0,2}}\right)\right\} \quad \forall\, t \qquad (3) \\ &\Rightarrow Q_{0,1}\cdot\Delta_{10,1}\cdot\log_{10}(t) = Q_{0,2}\cdot\Delta_{10,2}\cdot\log_{10}(t) \\ &\Rightarrow Q_{0,1}\cdot\Delta_{10,1} = Q_{0,2}\cdot\Delta_{10,2} \end{aligned}$$

Now, substitution of $Q_{0,2}$ with

$$(4) \qquad Q_{0,2} = Q_{0,1}\left\{1 + \Delta_{10,1}\log_{10}\left(\frac{t_{0,2}}{t_{0,1}}\right)\right\}$$

in Eq. (3) yields the relation

$$(5) \qquad \Delta_{10,1} - \Delta_{10,2} = \Delta_{10,1}\cdot\Delta_{10,2}\cdot\log_{10}\left(\frac{t_{0,2}}{t_{0,1}}\right)$$

Thus, t_0 may be chosen freely without loss of generality; but in order to compare the values of Δ_{10} suggested in the literature, they need to be converted to the same reference time in accordance with Eq. (5).

2.2 Choice of reference capacity

The reference capacity, Q_0, may be determined by some design method such as the API procedure proposed by the American Petroleum Institute (API, 1993) or the NGI-99 method which is developed at the Norwegian Geotechnical Institute (Clausen and Aas, 2000). However, as shown by Clausen and Aas (2000) and Augustesen et al. (2005a), even some of the widely accepted methods involve great amounts of uncertainty. Therefore, in the present work Q_0 is instead determined on the basis of the available test results by linear regression of $Q(t)$ versus $\log_{10}(t)$ for each pile, see Section 4. Q_0 is then the point on the regression line corresponding to $\log_{10}(t_0)$.

By choosing a small value of t_0, e.g. 1 day as proposed by Skov and Denver (1988) for clayey soils, small or even negative values of Q_0 may be obtained for piles which are only tested twice. In these circumstances, erroneous capacities are predicted. With t_0 = 100 days this problem is avoided. Hence, this reference time has been employed in the present analysis.

2.3 Interpretation of loading tests

A reliable measurement of set-up requires that the uncertainties related to the test procedure and the site conditions are minimized. First of all, the soil and pile conditions should be clearly defined. Further, the strata should be homogeneous and of such horizontal extent that several similar piles can be installed at approximately the same time in the same type of soil without group action taking place. Pile tests should be arranged as sketched in Figure 2. Thereby the effects of time can be separated from the effects of previous load testing of the same pile. If ageing is of interest, the first pile should be tested after equalisation of excess pore pressures. In contrast, if the goal is to establish the maximum set-up no considerations should be paid to excess pore pressures. Furthermore, the piles should be tested by the same procedure and the failure criterion should be defined uniquely. Though, the data in the present database are treated consistently and in most cases are of high quality, they do not punctually fulfil the above-mentioned recommendations.

2.3.1 Soil and pile conditions

In most of the cases constituting the present database, the strata are highly non-homogeneous and in some cases sand layers interbed the clay layers. This is not taken into consideration, i.e. the soil is assumed to consist solely of clay. The specific influence of the sand layers could be taken into consideration by measuring the side shear forces during testing but this is far from common in practice.

The properties of the soil are not determined in the same way in all cases in the database. For example, the undrained shear strength, S_u, may be measured by a vane shear test in some cases and by means of unconsolidated undrained triaxial tests in other cases. This complicates the application of time functions in which Δ_{10} depends on the soil properties, e.g. the NGI model, cf. Eq. (2). However, in order to obtain a consistent treatment of the available data, a unique set of rules based on Clausen and Aas (2000) that allow any strength to be calculated from another has been employed. This strength conversion is a controversial matter within the profession of soil mechanics. Further, if the plasticity index, I_p, and the overconsolidation ratio, *OCR*, are not provided, it is assumed that I_p = 25% and *OCR* is calculated by means of the SHANSEP relation (Ladd et al., 1977),

$$(6) \qquad \frac{S_u}{p_0} = \beta\cdot OCR^{\Lambda}$$

where S_u is the undrained shear strength, p_0 is the vertical effective stress, β is the normally consolidated undrained shear strength ratio $(S_u/p_0)_{nc}$, and Λ is a strength rebound parameter [-]. In this study, it is chosen to make use of the parameters β = 0.25 and Λ = 0.85, and S_u is assumed to be the unconsolidated undrained shear strength, S_{uu}. As is the case for S_u conversions, the dependence of S_u on *OCR* is also of controversial matter within geotechnical engineering. Limits on β and Λ as function of shear strength are discussed in Mayne (1988). It should be mentioned that in none of the cases associated with this study, *OCR* is measured.

Bullock et al. (2005b) postulate that Δ_{10} does not depend significantly on the pile length for penetration depths smaller than 25m. By contrast, the pile diameter

Figure 2 Ideal test series for studying the influence of time on the bearing capacity. The arrangement of pile tests implies that the effects of time are separated from the effects of previous load testing.

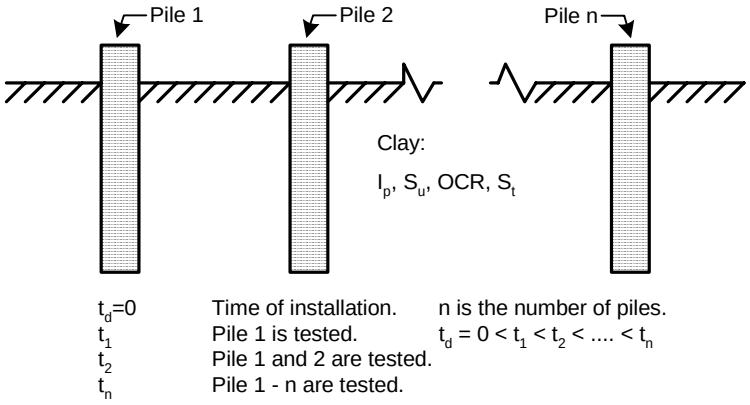

has an influence on the time development of set-up. In particular, excess pore pressures are induced by the penetration of a displacement pile with a maximum value of the pore pressure near the pile surface and diminishing to zero at some radial distance. As these pressures dissipate, the soil consolidates. The duration of this process is approximately proportional to the square of the pile diameter. Assuming that the pile displacement causes a destructuring gradient in the soil similar to the pore pressure gradient, the restructuring (ageing) may develop over time in a similar manner (Bullock et al., 2005b). Hence, the cross-sectional geometry of a pile affects the development of the capacity with time due to both consolidation and ageing. However, the geometry of the pile is not taken into consideration in the present analysis, i.e. piles are not divided into groups according to their cross-sectional geometry.

Since the pile and soil conditions are important parameters in set-up analyses, a quality ranking, Q_r, is specified for all available cases, cf. Table 1. Five categories are applied for the quality, namely $Q_r = 0$: not known; $Q_r = 1$: low; $Q_r = 2$: average; $Q_r = 3$: high; and $Q_r = 4$: very high.

2.3.2 Group action and staged loading

The interpretation of loading tests, and thereby the magnitudes of the measured capacities, may be influenced by group action and pre-shearing effects (staged loading). Thus, if a pile has been tested more than once, previous loading tests may have an effect on the capacity. However, in the light of their test results Bergdahl and Hult (1981) postulate that it is not possible to show any change in capacity as a result of previous loading tests for piles in clay.

In contrast to this, Karlsrud and Haugen (1986) as well as Bullock et al. (2005a,b) report that pre-shearing effects may be substantial. Thus, staged loading results in higher bearing capacities compared to the "intact equivalents", i.e. the capacities obtained by unstaged loading. Based on two examples in the literature and a research programme conducted at the University of Florida, Bullock et al. (2005b) recommend that the ratio $C_{st} = \Delta_{10,Unstaged}/\Delta_{10,Staged} = 0.4$ should be applied to convert the results of staged to unstaged tests when using $t_0 = 1$ day.

Unfortunately, only few results for unstaged loading are available in the literature. Hence, the starting point of this study is staged loading tests. However, employing the guidelines provided by Bullock et al. (2005b) the corresponding results for unstaged loading are readily obtained. Furthermore, when only staged loading tests are considered the data can be treated in a consistent manner. Finally, sufficiently many tests are available in the literature to ensure that statistically significant conclusions can be drawn.

Group action leads to an increase in set-up magnitudes as reported by Camp et al. (1993). Even if group effects are substantial they are not considered in the present work, simply because little information related to group action is provided in the cases forming the basis of this study.

2.3.3 Testing procedure

In this study attention is entirely paid to pile capacities based on static loading tests. Cases including dynamic tests could advantageously be incorporated in the database to improve the statistical foundation of the analyses. However, this implies that the capacities obtained from dynamic and static loading tests are strictly comparable. By focussing on static tests, uncertainty regarding this subject is neglected. The data are thereby treated in a consistent manner if the same failure criterion is applied in all cases. It should be mentioned that the influence of loading rate is not taken into consideration.

According to Bullock et al. (2005b) virtually all pile set-up research is based on piles being unloaded between consecutive tests. Those few tests carried out for piles that remain loaded between tests indicate that such piles exhibit conservatively more set-up than piles which are unloaded between tests. This has not been taken into consideration in the present study, i.e. no distinction is made with regard to the loading conditions between two subsequent tests.

In the database forming the basis of this study no distinction is made between piles loaded in compression and tension. As indicated in Table 2 only four of the 27 piles constituting the database are loaded in tension. Based on a study, the results of which are not included in this manuscript, it has been found that the results for three of these piles do not differ significantly from the results for the piles loaded in compression with respect to the formulation and calibration of a time function. However, results for the fourth pile, which belongs to the case with ID 9, differ significantly (Δ_{10} = -0.06), cf. Table 1 and Table 2. Therefore, this case has been omitted in all of the following analyses.

2.3.4 Failure criterion

The measured capacities associated with each case in the database are based on failure loads corresponding to settlements equal to 0.1d, where d is the equivalent pile diameter referring to an equivalent circle diameter for square and hexagonal piles. Experience shows that both the toe and shaft resistance are fully mobilised at this displacement (Vijayvergiya, 1977; API, 2000).

3 Presentation of cases

Key data for the cases that form the basis of this study are summarized in Table 1 and Table 2. The majority of the cases have been found in the literature and further data have been provided by the Danish company COWI A/S and the Norwegian Geotechnical Institute. The following comments are given regarding the database:

1. 18 cases including 27 piles constitute the database.
2. All piles have been subjected to staged static tests.
3. In total, 88 pile tests are included in the database.
4. The time elapsed between initial driving and the final static test of each pile varies from 22 to 9778 days. Further, the number of tests on each pile ranges from two to six.
5. Four piles are loaded in tension and 23 piles are loaded in compression.
6. Eleven piles are made of steel, three of timber, and four of concrete.
7. The diameters range from 0.1 m to 1.372 m and four piles are driven open-ended. The tip penetration range from five to 49 m.
8. The average unconsolidated undrained shear strength, S_{uu}, varies between approximately 12 and 136 kPa, the overconsolidation ratio, OCR, varies between 1.1 and 25.2, and the average plasticity index, I_p, varies between 15 and 47.

Both offshore and onshore piles are included and the different cases are grouped, specified by the quality ranking, Q_r, cf. Subsection 2.3.1.

4 Semi-logarithmic time function

The bearing capacity and the time scale for different piles and test sites may be very different, cf. Table 2. In order to test linearity between time, t, elapsed since initial driving and capacity, Q, as expressed in Eq. (1) and in order to compare results from different cases, the normalised versions of Q and t are investigated by plotting

$$(7) \qquad \left(\frac{Q_j}{Q_{0j}}-1\right)\Big/\Delta_{10j} \quad \text{versus} \quad \log_{10}\left(\frac{t}{t_0}\right)$$

Here Q_j is the measured capacity for pile j at time t after installation and Q_{0j} is the reference capacity for pile j corresponding to the reference time t_0 = 100 days, cf. Section 2.1.

Firstly, for each individual pile the Method of Least Squares is adopted for a linear regression analysis of $Q_j(t)$ versus $\log_{10}(t)$. Q_{0j} is then defined as the point on the regression line corresponding to $\log_{10}(t_0)$. Further, in accordance with Eq. (7), the set-up factor, Δ_{10j}, for pile j is determined as the inclination of the regression line obtained when plotting

$$(8) \qquad \frac{Q(t)}{Q_{0j}}-1 \text{ versus } \log_{10}\left(\frac{t}{t_0}\right)$$

Employing the values of Δ_{10j} obtained in this manner, Eq. (7) provides ideally a number of lines with the inclination β_1 = 1 and going through origo. The deviation of the normalised test data from this line forms the basis for testing the validity of the semi-logarithmic time function.

4.1.1 Linear regression

Based on Eq. (7) and the data presented in Table 1 and Table 2, the normalised capacities are plotted against normalised time in Figure 3. Every dot corresponds to one measured capacity, i.e. one pile test. By visual inspection it is concluded that the pile tests all fit into the assumed relation between Q and t, i.e. Eq. (1). However, cases including only two tests on the same pile

Table 1 Site specifications.

				Soil conditions				Pile conditions						
ID [g]	Name	Reference	Pile name	Q_r [h] [-]	I_p [i] [%]	OCR [j] [-]	S_{uu} [k] [kN/m^2]	Q_r [h] [-]	Open / Closed	Type [l]	Diam. [m] [m]	Wall [m] [mm]	Taper [m] [deg.]	Tippen. [n] [m]
1●	Houston	O'Neill et al. (1982a,b)	-	4	31	8.1	109.3	4	C	S	0.273	-	0	13.1
2●	Cowden	Powell et al. (2003) [a]	A	4	15	25.2	136.3	4	O	S	0.457	19	0	9.2
3●	Drammen	Eide et al. (1961)	-	3	21	1.1	20.6	3	C	T	0.150	-	0.44	15.5
4	St. Alban	Konrad and Roy (1987)	A	3	21	4.6	19.8	3	C	S	0.220	-	0	7.6
5	Sumatra	Trenter and Burt (1981)	-	3	40	2.3	35	3	O	S	0.400	12	0	43.3
6●	Canons Park	Powell et al. (2003) [b]	B, D	4	47	8.4	95.8-96.5	4	C	S	0.168	-	0	6.5 – 6.65
7●	Canons Park	Powell et al. (2003) [c]	A	4	45	8.5	104.7	4	C	S	0.168	-	0	6.63
8	Bothkennar	Clausen and Aas (2000) [d]	-	4	40	2.9	17.4	4	C	S	0.1016	-	0	6
9	West Delta	Chan and Birrell (1998) [e]	-	4	41	2.1	36.8	4	O	S	0.762	19.1	0	71.3
10	Algade	Geodan (1993) [f]	-	4	25*	9.7	134.7	2	C	C	0.255	-	0	13.35
11●	Motorvegbru Drammen	Tvedt and Fredriksen (2003)	P1-16 P2-16	4	25*	1.1	65.3	4	O, C	S	0.4 - 0.813	12.5	0	35
12	Drammen Stasjon	Falstad and Heyerdahl (1995)	P1	1	22	1.2	82.0	3	C	C	0.344	-	0	49
13●	Nitsund	Flaate (1972)	I, II	4	16	13.5-15.7	66.2-69.1	4	C	T	0.175 – 0.180	-	0.32 – 0.47	11.7 – 13.7
14●	Skå-Edeby	Bergdahl and Hult (1981)	A-E	4	40-41	3.9-4.1	11.8-12.3	4	C	T	0.127	-	0	14.5 – 15.3
15●	Haga	Karslrud and Haugen (1986)	-	4	18	7.3	41.5	4	C	S	0.153	-	0	5
16	Florida	Bullock et al. (2005a,b)	AUC, VLW	0	-	-	-	4	C	C	0.516	-	0	18.4 – 19.2
17	Northwestern	Finno et al. (1989)	Pipe	0	-	-	-	0	C	S	0.516	-	0	15.2
18	-	Svinkin et al. (1994)	TP2	0	-	-	-	0	O	C	1.372	0.127	0	24.4

a) Gallagher and St John (1980), Lehane and Jardine (1994).
b) Powell and Uglow (1988), Bond and Jardine (1991,1995) and Wardle et al. (1992).
c) Powell and Uglow (1988), Bond and Jardine (1991,1995) and Wardle et al. (1992).
d) Data taken directly from Clausen and Aas (2000).
e) Data taken directly from Clausen and Aas (2000).
f) Material provided by Kampsax Geodan, which is part of COWI A/S.
g) Cases marked with ● include piles belonging to the Group "Super Piles".
h) Quality ranking of soil and pile data: 0 = not known, 1= low, 2 = average, 3 = high, 4 = very high.
i) I_p is the average plasticity index. If not given I_p = 25% and marked with asterisk.
j) OCR is the average overconsolidation ratio based on S_{uu}-strengths.
k) S_{uu} is the average unconsolidated undrained shear strength.
l) Pile material indicator: S = steel, C = concrete, T = timber.
m) Diameter and wall thickness at pile tip, respectively. Wall thickness is only given in cases where the piles are driven open-ended. Taper denotes pile wall taper.
n) Tip penetration.

Table 2 Measured capacities.

ID - Pile #[a)]	Pile Name	CMP/ TNS[b)]	Q_0 [c)] [kN]	Δ_{10} [c)] [-]	Measured Capacity					
					Time / Cap [d)] [days / kN]	Time / Cap [d)] [days / kN]	Time / Cap [d)] [days / kN]	Time / Cap [d)] [days / kN]	Time / Cap [d)] [days / kN]	Time / Cap [d)] [days / kN]
1●	-	C	784	0.20	18 / 670	80 / 765	108 / 792	-	-	-
2●	A	C	1252	0.15	30 / 1140	396 / 1390	9125 / 1608	-	-	-
3●	-	C	259	0.19	31 / 220	71 / 270	799 / 300	-	-	-
4	A	C	103	0.36	4 / 47	8 / 67	20 / 77	33 / 83	-	-
5	-	C	1892	0.20	1.7 / 1225	10.5 / 1555	20.5 / 1670	32.5 / 1670	-	-
6.1●	D	C	174	0.34	108 / 189	496 / 200	1130 / 231	6200 / 291	-	-
6.2●	B	C	189	0.15	74 / 194	217 / 197	683 / 200	1312 / 221	6200 / 249	-
7●	A	C	160	0.20	31 / 159	134 / 161	248 / 163	525 / 170	1154 / 188	6200 / 231
8	-	C	36	0.18	4 / 27.34	32 / 32.91	-	-	-	-
9	-	T	5049	-0.06	116 / 5030	470 / 4850	-	-	-	-
10	-	C	741	0.13	14 / 660	9778 / 930	-	-	-	-
11.1●	P1-16	C	2699	0.26	16 / 2150	140 / 2800	-	-	-	-
11.2	P2-16	C	2082	0.41	14 / 1350	141 / 2210	-	-	-	-
12	P1	C	1572	0.44	21 / 1100	153 / 1700	-	-	-	-
13.1●	I	C	287	0.26	32 / 243	207 / 321	357 / 336	641 / 350	1043 / 350	-
13.2●	II	C	281	0.44	34 / 228	209 / 314	357 / 343	637 / 378	1023 / 414	-
14.1	B	C	69	0.61	39 / 52	75 / 64	-	-	-	-
14.2●	B	C	43	0.33	42 / 36	456 / 56	1116 / 54	-	-	-
14.3	C	C	75	0.54	30 / 54	75 / 70	-	-	-	-
14.4●	C	C	48	0.32	42 / 41	96 / 48	456 / 60	1116 / 62	-	-
14.5	D	C	69	0.47	30 / 52	75 / 65	-	-	-	-
14.6●	D	C	44	0.18	96 / 42	171 / 47	456 / 49	1116 / 51	-	-
15●	-	T	80	0.24	7 / 59	20 / 65	36 / 73	-	-	-
16.1	AUC	T	1616	0.17	3 / 1197	16.1 / 1427	65.1 / 1528	265 / 1712	1727 / 1982	-
16.2	VLW	T	751	0.20	3 / 519	19 / 635	157 / 783	-	-	-
17	Pipe	C	871	0.35	14 / 623	35 / 712	301 / 1024	-	-	-
18	TP2	C	4034	0.31	2 / 1913	9 / 2789	22 / 3189	-	-	-

a) ID refers to the case (see Table 1) and Pile # refers to the pile number, if there is more than one pile associated with the given case. Piles belonging to the Group "Super Piles" are marked with ●.
b) CMP and TNS denote piles loaded in compression and tension, respectively.
c) Estimated from the measured capacities by linear regression for every single case; the reference time t_0 = 100 days.
d) Measured capacity based on static test at the given time after installation.

will automatically create two points on the bisectional line with the inclination $\beta_1 = 1$. Thus, only cases involving at least three tests qualify for the verification of Eq. (1). In Table 3 the results of the regression analysis are presented. Since the regression coefficients are $\beta_1 = 1.0$ and $\beta_0 = 0$ there is a linear relation between normalised capacity and normalised time as expressed by Eq. (7). R^2 is loosely interpreted as the proportion of the total variation in the data that can be accounted for or explained by the regression line (Walpole and Myers, 1993). The range of R^2 is 0 to 1, with larger values indicating a better correlation. Thus, $R^2 = 0.96$, cf. Table 3, indicates an acceptable correlation.

4.1.2 Hypothesis testing

A reliability check of the estimated regression line can be performed by testing the two-sided hypothesis

Figure 3 Normalised capacity versus normalised time for piles tested more than two times. The dots are test results (one for each pile test), the solid line is the regression line, and the dotted lines mark the 95% confidence interval on the regression line. Dots deviating from the regression line imply that a semi-logarithmic relation does not describe the development of pile capacity with time.

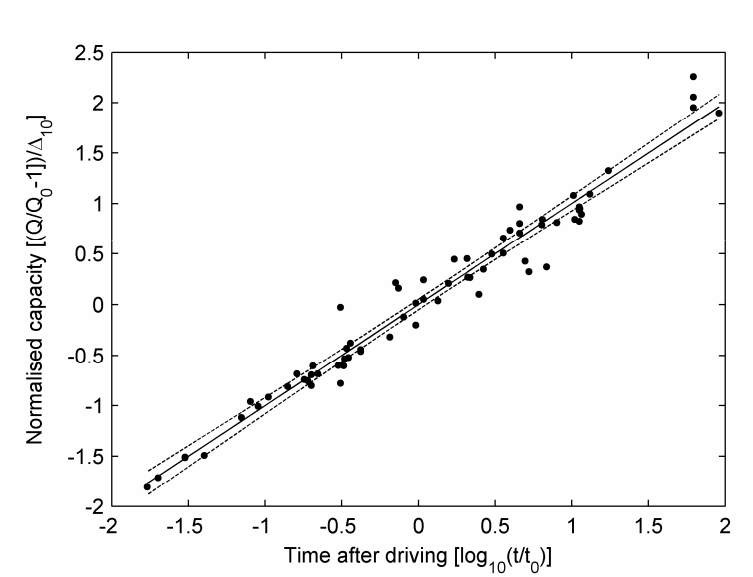

(9)
$$H_0: \ \beta_1 = 1.0$$
$$H_1: \ \beta_1 \neq 1.0$$

for e.g. a 1% level of significance ($\alpha = 0.01$). Analyses show that the null hypothesis cannot be rejected for a stated level of significance of 1%. Another common output of hypothesis testing is the *P*-value, which ranges from 0 to 1. It is defined as the smallest level of significance α that would lead to rejection of the null hypothesis H_0 (Walpole and Myers, 1993). Therefore, if the *P*-value is less than α, H_0 is rejected. In other words, the *P*-value is the probability of observing the given sample result under the assumption that the null hypothesis is true. A very small *P*-value casts doubt on the truth of the null hypothesis and the higher *P*-value the stronger evidence for accepting H_0. Therefore, the *P*-value contains more information than "reject" or "do not reject" (Walpole and Myers, 1993). When testing the hypothesis expressed by Eq. (9) on the available data, the *P*-value is approximately equal to 1. This strongly indicates that $\beta_1 = 1.0$, i.e. the validity of Eq. (1) has been verified.

4.1.3 Model adequacy checking

To identify possible statistical outliers with respect to the estimated regression line with the inclination $\beta_1 = 1$, the standardized residuals and the R-student are computed for each pile test (Montgomery, 2001). The standardized residuals are the raw residuals normalised by an estimate of their standard deviation. By contrast, the R-student is normalised by a so-called independent estimate of the standard deviation. Hence, the R-student is more sensitive to outliers.

Table 3 Linearity between capacity and the logarithm to time.

β_1 [a] / [CI] [b]	β_0 [c] / [CI] [b]	R^2 [d]
1.0 / [0.9538;1.0462]	0 / [-0.0409;0.0409]	0.96

a) Inclination of the regression line.
b) 95% confidence interval.
c) Intersection with the axis of the ordinate.
d) Sample coefficient of determination.

If the raw residuals are normally distributed with zero mean and variance σ^2, i.e. $N(0,\sigma^2)$, the standardized residuals should be normally distributed with zero mean and unit variance (Montgomery, 2001). Hence, R-students and standardized residuals greater than 3 or less than -3 are potential outliers. From Figure 5 it is concluded that there are no such data in the present database, though a few of the data are close to the limit.

4.1.4 Violation of assumptions

The analyses presented in the former sections assumes that the raw residuals 1) have zero mean, 2) have a constant variance across all values of normalised time, 3) are normally distributed, and 4) are independent (Ayyub and McCuen, 1997).

In Figure 5 the ordinary least square residuals are plotted as function of normalised time. In the actual case the mean is zero. Further, the ordinary least-square residuals show approximately constant variance when plotted

Figure 5 Residuals versus normalised time. Δ = ordinary raw least square residuals, • = standardized residuals, and x = externally studentized residuals (R-student). The solid line corresponds to residuals equal to zero.

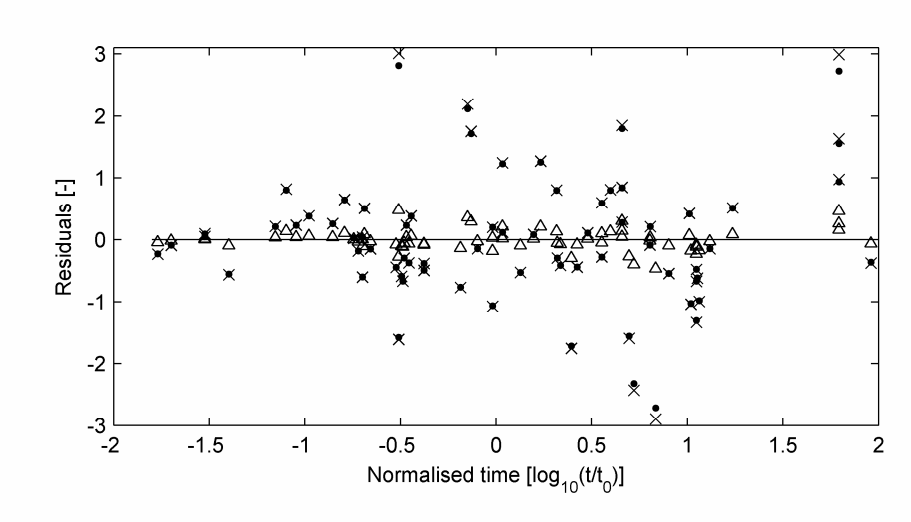

Figure 4 Check of normality of the raw residuals. A normal probability density function is superimposed on the discrete probability density function for the present data (*left*). The dotted line on the normality plot (*right*) is the line joining the first and third quartiles and hereafter extrapolated out to the ends of the sample to help evaluate the linearity of the data.

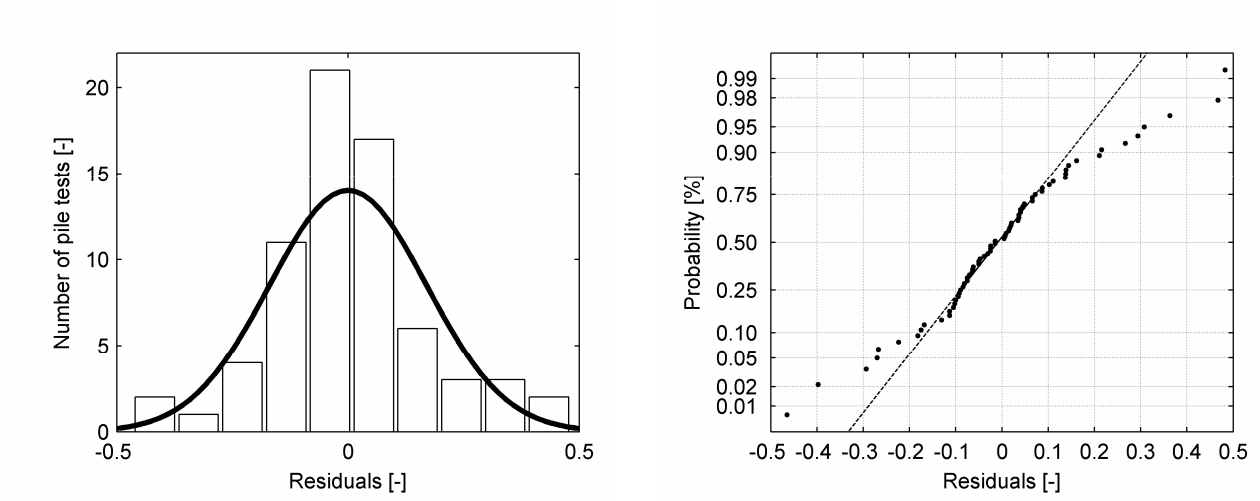

against the normalised time. A similar conclusion can be drawn if they are plotted against the normalised capacity. Other analyses, not presented here, indicate that for each pile there is no systematic "over"- and "undershooting", i.e. there is no tendency that the residuals systematically increase or decrease with normalised time.

Next, the normality assumption has been checked in Figure 4 by plotting a histogram of the ordinary raw least square residuals and the corresponding superimposed normal probability density function and by showing the normal probability plot. As seen, the tails of the residuals in the normal probability plot do not fit into a linear relation (dotted line) dictated by the first and third quartiles. The reason can be found by inspecting the histogram; the two columns located nearest to the mean contain too many pile tests, which implies that the values of the residuals corresponding to the first and third quartiles are close to the mean. Hence, according to Figure 4 the normality condition is not exactly fulfilled. However, a Lilliefors test (Conover, 1980) shows that the hypothesis, that the residuals have a normal distribution, cannot be rejected at a level of significance of 4%, which is acceptable. Therefore, it is concluded that the residuals are normally distributed.

The analyses forming the basis of testing the semi-logarithmic relation between capacity and time also assume that the residuals are independent. Since piles are tested more than ones, and since group action may influence pile capacities, the independence criterion is

not exactly fulfilled. In spite of this, there is no reason to suspect the model assumptions.

4.1.5 Tests to be included

When estimating Q_0 for a given pile, it has to be determined whether some test results should be omitted. According to Figure 1 and the discussion in Section 2, different rates of set-up are recorded before and after the end of primary consolidation. Since the present study concerns the long-term set-up, it is obvious to include tests performed after t_{eoc}. However, this instant is usually not known, and for each pile it has to be evaluated if tests performed earlier than, for example, 10 days should be excluded. Further, the lower limit on t should be as small as possible to include as many tests as possible in the calibration of the model, thereby minimising the statistical uncertainties. Analyses, not presented here, indicate that one day is the optimal choice in this study, i.e. test performed more than one day after installation have been employed. The outlier diagnostics also show that there are no significant outliers, which justify including tests, performed one day after installation.

5 Existing time functions

The time functions, proposed by Skov and Denver (1988), Bullock et al. (2005a,b) and Clausen and Aas (2000), are compared by examining the residuals obtained when applying the respective time functions to the available data, cf. Table 1 and Table 2. As mentioned previously, the measured capacities for the different piles and test sites are very different. Hence, in order to explicitly compare the residuals obtained for every single case and pile test, the residuals must be dimensionless, i.e. by normalizing the measured and the predicted capacities with respect to the reference capacity, the residual, r, defined as

$$(10) \qquad r = \frac{Q}{Q_0} - \frac{Q_{pred}}{Q_0}$$

becomes dimensionless and is a measure of how well a time function predicts an observed capacity. Q is the measured capacity at time t, Q_0 is the reference capacity at the reference time t_0 = 100 days, and Q_{pred} is the predicted capacity corresponding to the time function in consideration.

Now, substitution of Q_{pred} with Eq. (1) yields

$$(11) \qquad r = \frac{Q}{Q_0} - 1 - \Delta_{10} \log_{10}\left(\frac{t}{t_0}\right)$$

By defining Q_{meas} and Q_{est} as

$$(12) \qquad Q_{meas} = \frac{Q}{Q_0} - 1, \quad Q_{est} = \Delta_{10} \cdot \log_{10}\left(\frac{t}{t_0}\right)$$

The residual, r, can also be defined as

$$(13) \qquad r = Q_{meas} - Q_{est}$$

where Q_{meas} and Q_{est} are expressions of the measured and predicted capacities, respectively. In Eq. (12) Δ_{10} is the set-up factor corresponding to the time function in consideration. Further, Q, t, and Q_0 for every single pile in the database are shown in Table 2.

Since the Δ_{10}s proposed by Skov and Denver (1988) and Bullock et al. (2005a,b) are based on t_0 = 1 day rather than t_0 = 100 days, they must be converted in order to obtain a consistent comparison of the suggested time functions. This is done by applying Eq. (5). Hence, $\Delta_{10,Skov}$ = 0.27 when t_0 = 100 days whereas $\Delta_{10,Skov}$ = 0.6 for t_0 = 1 day, cf. Section 2. For piles subjected to unstaged loading, Bullock et al. (2005a,b) recommend $\Delta_{10,Unstaged}$ = 0.1 for t_0 = 1 day. This corresponds to $\Delta_{10,Staged}$ = 0.25 for t_0 = 1 day, cf. Section 2, which implies that $\Delta_{10,Bullock}$ = 0.17 when the reference time is t_0 = 100 days and staged loading is considered.

5.1.1 Comparison of existing time functions

In Figure 6, the residuals obtained by applying the time functions to the available data are plotted as functions of normalised time. Since $\Delta_{10,NGI}$ is based on the plasticity index, I_p, and overconsolidation ratio, OCR, cf. Eq. (2), and since the soil conditions are not provided in the cases with IDs 16-18, cf. Table 1, these have been omitted. Further, the case with ID 9 has also been omitted, because Δ_{10} in that case is less than zero, cf. Table 2. The models suggested by Clausen and Aas (2000) and by Bullock et al. (2005a,b) provide a skew distribution of the residuals, i.e. they are negative for $t < t_0$ and positive for $t > t_0$. On the other hand, the residuals in the model proposed by Skov and Denver (1988) are apparently independent of time, which characterises an adequate time function.

Next, the box plots in Figure 7 indicate that the three models produce almost symmetric distributions of the residuals; but the variation differs. This is also indicated in Table 4 and Figure 6. However, the standard deviations of the residuals are not significant different at a 1% level of significance, cf. Table 5.

Another measure of the time functions ability to predict the observed behaviour is the sum of squared residuals, SSR, defined as

Figure 6 Residuals plotted as function of normalised time and time function. The solid line corresponds to residuals equal to zero. The dotted lines mark the mean and the residuals corresponding to three times the standard deviation with respect to the mean.

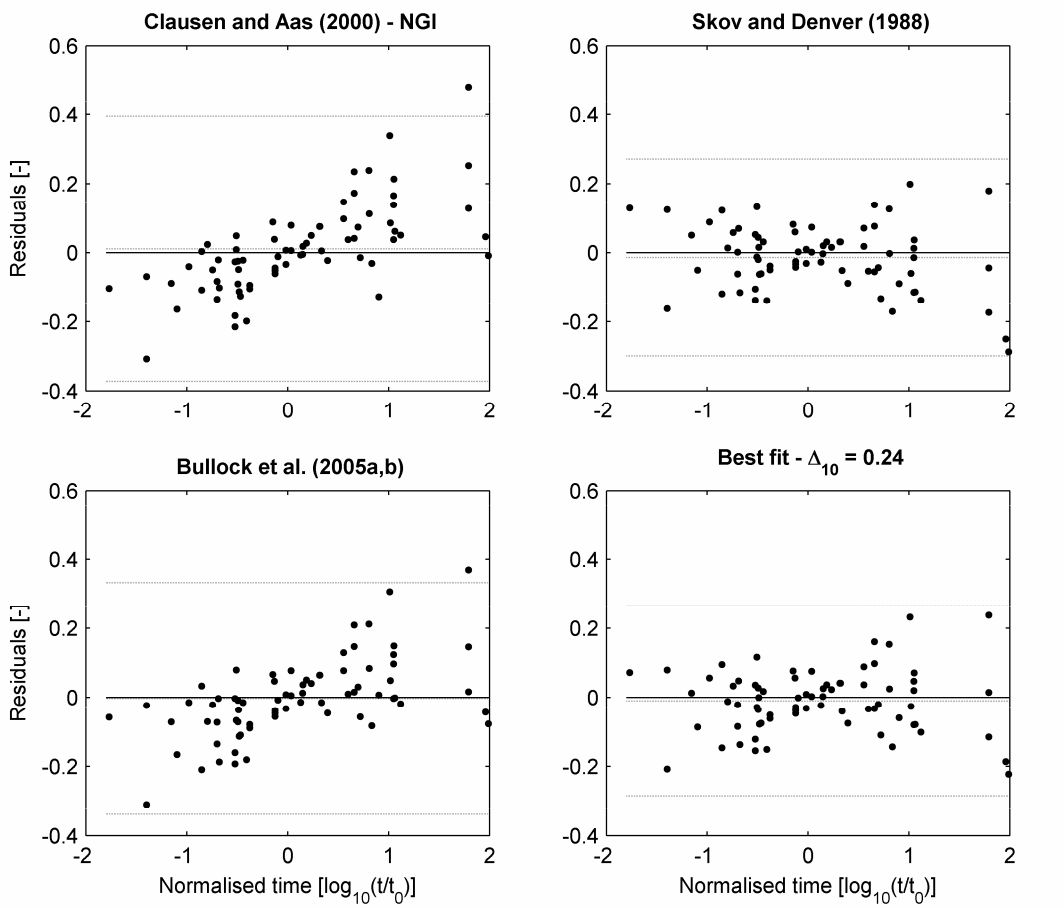

$$SSR = \sum r^2 \Rightarrow$$

$$SSR = \sum_{i=1}^{n} \sum_{j=1}^{k} \left(\frac{Q_j}{Q_{0i}} - 1 - \Delta_{10i} \cdot \log_{10}\left(\frac{t_j}{t_0} \right) \right)^2 \quad (14)$$

where Q_j is the measured capacity at time t_j, Q_{0i} is the reference capacity for pile i, t_j is the time elapsed since driving, t_0 is the reference time, k is number of static loading test on pile i, and n is the number of piles included in the analysis. An *SSR*-value equal to zero implies a perfect match between measured and predicted capacities, i.e. a small *SSR*-value indicates a good prediction of the pile capacity. The *SSR*s obtained by applying the time functions proposed by Skov and Denver (1988), Bullock et al. (2005a,b) and Clausen and Aas (2000) to the available data are shown in Table 4. The time function proposed by Skov and Denver (1988) provides the smaller *SSR*-value and therefore the better estimate of the measured capacities. Compared to this model, the *SSR*s obtained by the NGI model (Clausen and Aas, 2000) and the model proposed by Bullock et al. (2005a,b) are approximately 77% and 35% greater, respectively. This is primarily due to the relatively large residuals occurring at the tails of the normalised time range, see Figure 6. It should be mentioned that the largest residuals in the upper end of the time interval are associated with the piles with ID 6.2, 7, 14.6, and 13.2, see Table 2. These piles belong to cases of high quality, i.e. $Q_{r,soil} = Q_{r,pile} = 4$ (Table 1). This indicates that NGI (Clausen and Aas, 2000) and Bullock et al. (2005a,b) generally underestimate the long-term capacities, i.e. Δ_{10} is too small for these models. It is further noted that the diameters and penetration depths associated with the mentioned piles are relatively small, see Table 2.

Generally, the mean of the residuals, μ_r, should be zero. Therefore, the hypothesis

$$H_0: \ \mu_r = 0 \qquad H_1: \ \mu_r \neq 0 \quad (15)$$

with unknown variance has been tested for a 1% level of significance ($\alpha = 0.01$). The calculated μ_r does not differ significantly from zero for any of the time functions. However, there are great differences in the *P*-values (cf. Section 4) listed in Table 4. The large *P*-value obtained

by the Bullock time function is due to the small value of the mean, i.e. $\mu_r = -0.003$, see Table 4.

5.1.2 Model assumptions

The hypothesis tests require independent and normally distributed residuals. As mentioned in Section 4 the independence criterion is not exactly fulfilled. However, a Lilliefors test, not shown here, indicates that the hypothesis, that the residuals based on any of the three models have a normal distribution, cannot be rejected at a level of significance ranging from 1 to 20%, which is acceptable.

6 Calibration of time functions

The starting point, when investigating the possibilities of introducing an alternative time function to the models proposed by Skov and Denver (1988), Bullock et al. (2005a,b) and Clausen and Aas (2000), is to assume that Δ_{10} = constant. Subsequently it is investigated whether it is advantageous to make Δ_{10} a function of relevant soil parameters.

6.1 Constant set-up factor

In order to check the robustness of the calibrated time function, Δ_{10} = constant is calibrated based on all tests, for which $\Delta_{10,meas} > 0$, cf. Table 2, and a special subset of piles. The quality in terms of soil and pile conditions, including number and time range for the tests, are especially high for these piles. The subset is denoted "Super Piles", abbreviated *SP*, and they are marked with a ● in Table 1 and Table 2. It should be mentioned that *SP* consists of 9 cases including 13 piles and 48 pile tests, i.e. *SP* constitutes approximately 50% of the available data. For the case with ID 14, Skå-Edeby, piles tested more than two times are included in *SP*. The reason for not employing the other tests is that they reflect tests on the same piles initially located in other depths. Further, by not employing all tests, case 14 is not weighted as high in the calibration process. Thereby, the proposed time function reflects to a greater extent the trends observed in connection with relatively many cases instead of just a single case.

Figure 9 shows the sum of squared residuals, cf. Eq. (14), for different values of Δ_{10} = constant. Evidently the time function based on $\Delta_{10} = 0.24$ provides the better estimate of the measured capacities regardless of whether all tests or only the *SP* are employed in the calibration of Δ_{10}. This further implies that the time function based on the constant set-up factor $\Delta_{10} = 0.24$ is robust.

Figure 7 Box plot of the residuals. The box has lines at the lower quartile, median, and upper quartile values. Lines (whiskers) extend from the ends of the box to the minimum and maximum residuals.

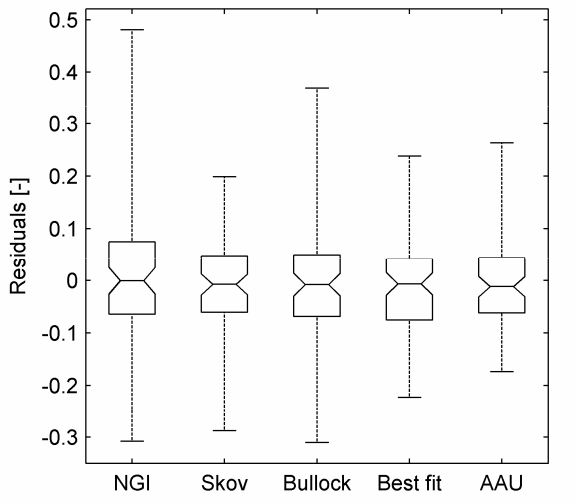

Table 4 Comparison of the time functions – residual statistics.

	NGI	Skov	Bullock	Best fit [e]	AAU [f]
μ_r [a]	0.011	-0.014	-0.003	-0.011	-0.005
σ_r [b]	0.128	0.095	0.112	0.092	0.087
SSR [c]	1.17	0.66	0.89	0.61	0.54
P-value [d]	0.46	0.22	0.80	0.33	0.60

a) Mean of the residuals.
b) Standard deviation of the residuals.
c) Squared Sum of the Residuals as defined in Eq. (14).
d) *P*-value associated with the test: H_0: $\mu_r = 0$, H_1: $\mu_r \neq 0$
e) Time function based on $\Delta_{10} = 0.24$, cf. Section 6.1.
f) Time function based on undrained shear strength, cf. Section 6.2.

Table 5 Testing the equality of residual variances as function of applied time functions, i.e. H_0: $\sigma^2_{r,1} = \sigma^2_{r,2}$, H_1: $\sigma^2_{r,1} \neq \sigma^2_{r,2}$, where 1 and 2 refer to one of the time functions: NGI, Skov, Bullock, Best fit, or AAU. 0 indicates that the null hypothesis cannot be rejected at a 1% significance level whereas 1 symbolizes that the null hypothesis can be rejected.

	NGI	Skov	Bullock	Best fit [a]	AAU [b]
NGI	-	0	0	1	1
Skov	0	-	0	0	0
Bullock	0	0	-	0	0
Best fit	1	0	0	-	0
AAU	1	0	0	0	-

a) Time function based on $\Delta_{10} = 0.24$, cf. Section 6.1.
b) Time function based on undrained shear strength, cf. Section 6.2.

6.1.1 Confidence interval for Δ_{10}

It is useful to obtain an estimate of the 95% confidence interval for Δ_{10}. Assume that $\Delta_{10} = 0.24$ is the estimate of the mean of Δ_{10} and the variance is unknown. A set of sample statistics, i.e. sample size, standard deviation etc., is needed to establish the confidence interval. Since such a set does not exist for Δ_{10}, the following assumptions are made:

1. The distribution of Δ_{10} is similar to the distribution of the measured Δ_{10}s.

2. The estimate of the standard deviation of Δ_{10} equals the standard deviation of the measured Δ_{10}s.

3. The sample size equals the number of measured Δ_{10}s. This is also equal to the number of piles associated with the database.

The measured Δ_{10}s, also denoted $\Delta_{10,meas}$, are the real set-up factors associated with every single pile. They are determined by means of regression analysis, cf. Section 4, and shown in Table 2. $\Delta_{10,meas}$ for case with ID 9 is negative. Therefore, it is omitted in the following and the sample size equals 26.

Figure 8 shows a histogram of the logarithm to the measured Δ_{10}s and the corresponding superimposed normal density function. It turns out that a lognormal distribution fits the measured Δ_{10}s better than a normal distribution; a Lilliefors test (Conover, 1980) shows that the hypothesis, that the $\Delta_{10,meas}$s have a lognormal distribution, cannot be rejected at a level of significance of 9%. The same conclusion can be drawn at a level of significance of 4% when testing the $\Delta_{10,meas}$s for normality. Therefore, it is assumed that Δ_{10} is lognormally distributed with a mean equal to $\log_{10}(0.24) = -0.62$. The estimated standard deviation of the logarithm to $\Delta_{10,meas}$, and thereby the logarithm to Δ_{10} equals 0.19 and the sample size is 26. By means of basic statistics, e.g. Montgomery (2001) or Walpole and Myers (1993), a 95% confidence interval for $\log_{10}(\Delta_{10})$ can be found to [-0.6975; -0.5439]. This implies that the 95% confidence interval for Δ_{10} is [0.20; 0.29] when the reference time is $t_0 = 100$ days and staged loading is considered.

If Eq. (5) and $C_{st} = 0.4$ ($t_0 = 1$ day) also hold true for confidence intervals, the upper and lower bounds of a 95% confidence interval for Δ_{10} can be determined for all other combinations of t_0 and loading conditions, i.e. staged or unstaged. Examples are shown in Table 6. The lower confidence limit when considering unstaged loading and $t_0 = 1$day is approximately 30% higher than the design set-up factor, $\Delta_{10,Bullock} = 0.1$, recommended by Bullock et al. (2005a,b). The mean is 80% higher. When considering staged loading and $t_0 = 1$ day, the mean and the upper confidence limit are approximately 23% lower

Figure 9 *SSR* versus Δ_{10}. $\Delta_{10} = 0.24$ whether Δ_{10} is calibrated based on all tests or piles belonging to *SP*.

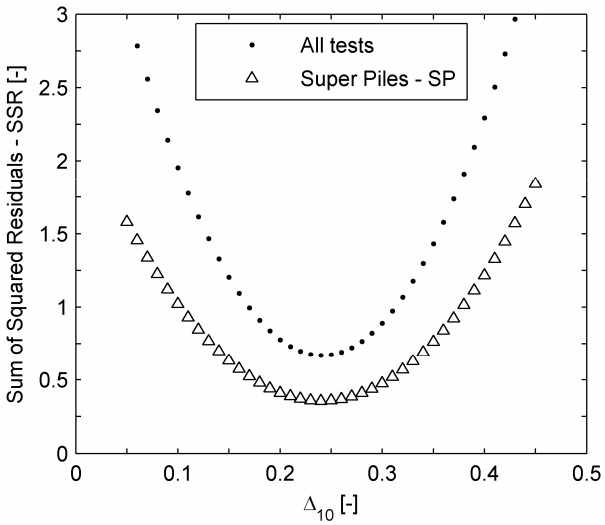

Figure 8 Histogram of the logarithm to the measured Δ_{10}s. $\Delta_{10,meas}$ is determined by regression analysis. Superimposed is the corresponding normal density function.

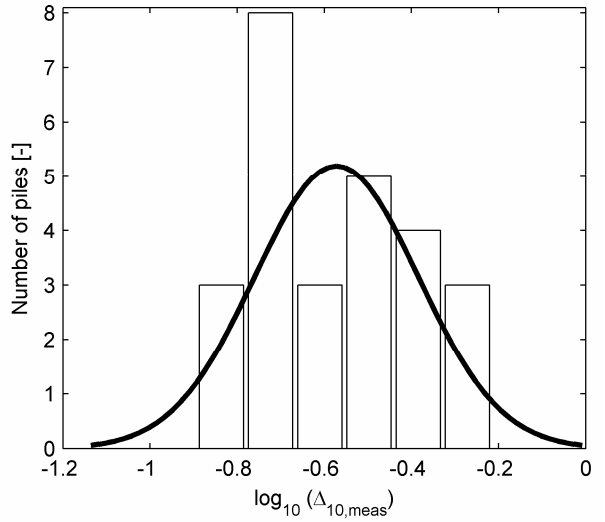

Table 6 Mean value and confidence intervals for Δ_{10} as function of t_0 and loading conditions.

Loading	t_0 [days] [a]	Δ_{10} [-] [b]	LL [-] [c]	UL [-] [d]
Staged	100	0.24	0.20	0.29
Staged	1	0.46	0.33	0.69
Unstaged	1	0.18	0.13	0.28
Unstaged	100	0.13	0.10	0.18

a) Reference time.
b) Mean value of the set-up factor.
c) Lower limit of a 95% confidence interval for Δ_{10}.
d) Upper limit of a 95% confidence interval for Δ_{10}.

Figure 10 Relation between $\Delta_{10,meas}$ and average soil parameters such as the plasticity index, I_p, unconsolidated undrained shear strength, S_{uu}, and overconsolidation ratio, *OCR*, depicted for every single pile in the database. Piles marked with a dot belong to *SP*. The first number in each plot label refers to the case and the second, if there is more than one pile associated with the given case, to pile number (see Table 1 and Table 2).

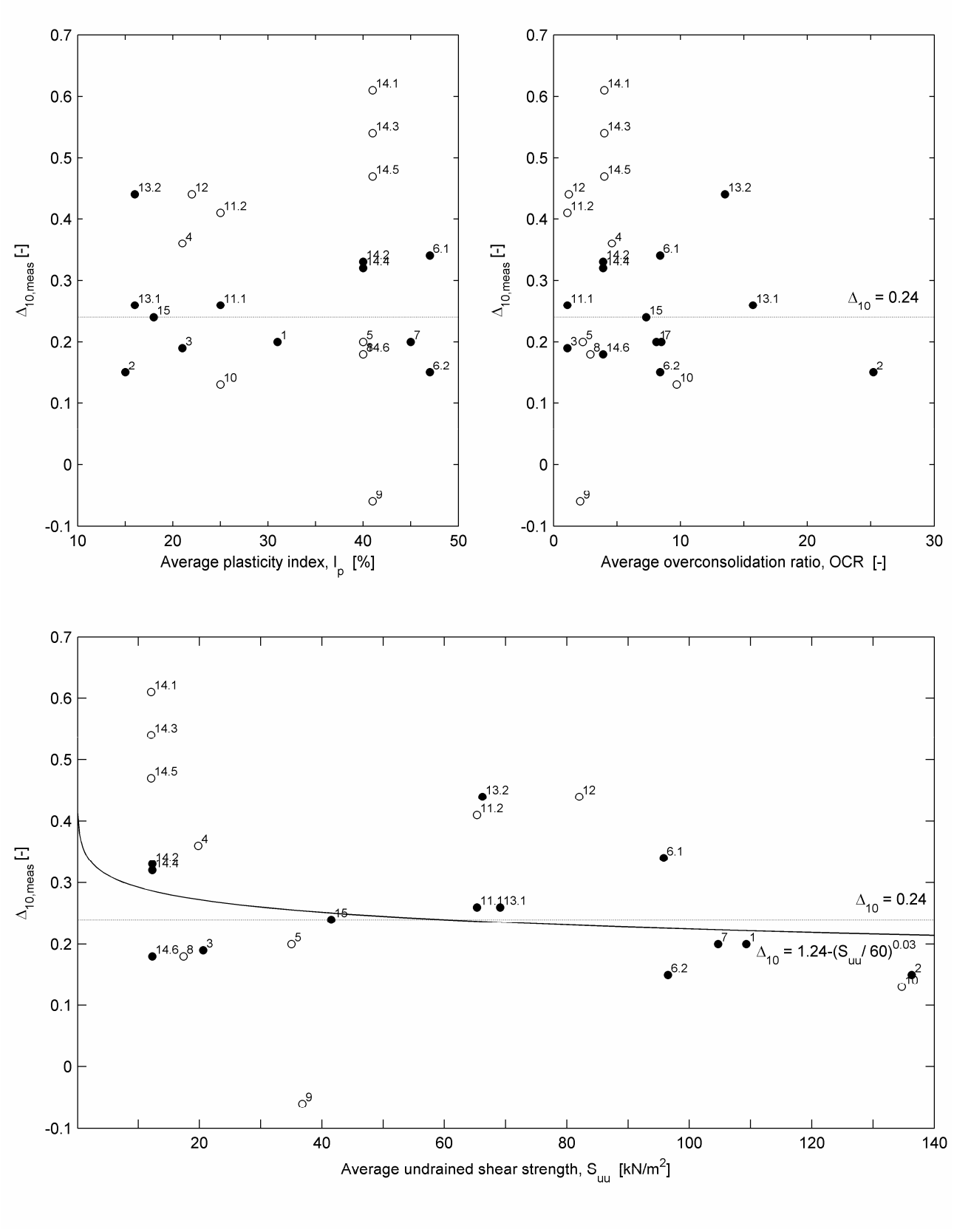

and 30% higher, respectively, than the set-up factor, $\Delta_{10,Skov} = 0.6$, proposed by Skov and Denver (1988).

The confidence limits presented in Table 6 are only intended as a guideline. They are encumbered with great uncertainty because the true distribution of Δ_{10} is unknown and so is a set of sample statistics. Further, the limits of the confidence intervals when inspecting unstaged loading or staged loading for $t_0 = 1$ day are determined based on Eq. (5) and $C_{st} = 0.4$, which in this situation may not be valid.

6.2 Set-up factor as function of undrained shear strength

The soil parameters influencing Δ_{10} are assumed to be the plasticity index, I_p, the overconsolidation ratio, *OCR*, and the unconsolidated undrained shear strength, S_{uu}. In Figure 10, the measured Δ_{10}s, denoted $\Delta_{10,meas}$, are depicted as function of these soil parameters. The values are listed in Table 1 and Table 2.

A natural starting point for the formulation of an enhanced time function appears to be a recalibration of the coefficients in the NGI model, cf. Eq. (2). However, Augustesen et al. (2005b) postulate that the form of Δ_{10} that best fits the observed behaviour is

$$\Delta_{10} = 1.24 - \left(\frac{S_{uu}}{60}\right)^{0.03} \qquad \text{AAU} \tag{16}$$

which is superimposed on Figure 10. Thus, Δ_{10} depends entirely on the average unconsolidated undrained shear strength, S_{uu}. The time function based on Eq. (16) is denoted AAU. As illustrated in Figure 10, Δ_{10} varies between 0.22 and 0.29 for the S_{uu} range examined. Considering the scatter of the data and the power of 0.03 in Eq. (16), there is no distinctive correlation between S_{uu} and the set-up factor. As such, the benefit is small compared to the model with a constant value of Δ_{10}.

6.3 Comparison of time functions

The AAU model and the time function based on the constant value $\Delta_{10} = 0.24$ have been applied to the same data as the existing models, cf. Section 5. The residuals obtained and relevant sample statistics are shown in Figure 6, Figure 7, Figure 11, and Table 4. Generally, the AAU model provides the better fit of the data in terms of *SSR*. In fact, the *SSR*-value obtained by AAU is 11% and 54% less than the *SSR*-values provided by the time function based on $\Delta_{10} = 0.24$ and the NGI model, respectively. For the AAU model and the time function based on $\Delta_{10} = 0.24$, the distributions of the residuals around $r = 0$ are symmetric and similar to the trends

Figure 11 Residuals plotted as function of normalised time. The solid line corresponds to residuals equal to zero. The dotted lines mark the mean and the residuals corresponding to three times the standard deviation with respect to the mean.

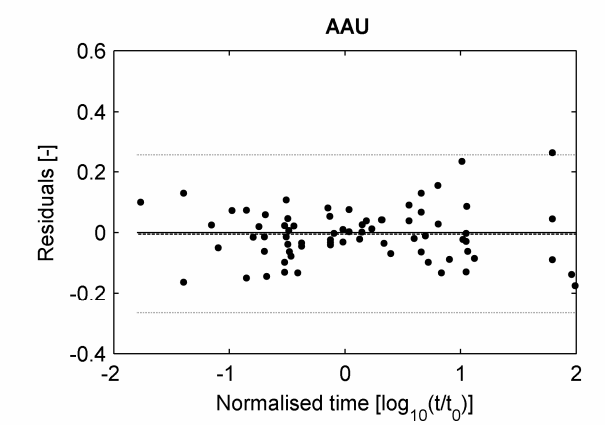

observed for Skov and Denver's model, cf. Figure 6, Figure 7, and Figure 11. The minimum standard deviation is obtained by the AAU model, see Table 4. However, the standard deviations and thereby the variances provided by the other models (except the NGI-model) are not significantly different at a 1% level of significance as indicated in Table 5.

Generally, the mean of the residuals, μ_r, should be zero. Compared to the other models, the time function proposed by Bullock et al. (2005a,b) results, on the average, in residuals closest to zero. However, based on hypothesis test like the one described by Eq. (15), it can be concluded that the estimated means of the residuals do not differ significantly from zero at a 1% level of significance regardless of the time function employed. This is also indicated by the *P*-values shown in Table 5.

6.4 Choice of time function

The time functions capability to predict the capacities associated with the piles in the database have been measured based on:

1. the magnitude of the sum of squared residuals, *SSR*,
2. the magnitude of the standard deviation of the residuals, σ_r,
3. the magnitude of the mean of the residuals, μ_r,
4. the visual distribution of the residuals, *r*, when plotted against normalised time,
5. the outcome of the test H_0: $\mu_r = 0$, H_1: $\mu_r \neq 0$,
6. the outcome of the hypothesis test H_0: $\sigma^2_{r,1} = \sigma^2_{r,2}$, H_1: $\sigma^2_{r,1} \neq \sigma^2_{r,2}$, where 1 and 2 refer to one of the time functions NGI, Skov, Bullock, Best fit (constant $\Delta_{10} = 0.24$), or AAU.

Based on these investigations, it can be concluded that AAU provides the better estimate of the available data,

Figure 12 Visualisation of how the time function based on $\Delta_{10} = 0.24$ (solid line) and NGI (dotted line) predict the observed behaviour for some selected cases in the database. Information regarding the cases is given in Table 1 and Table 2. EOD denotes End Of Driving.

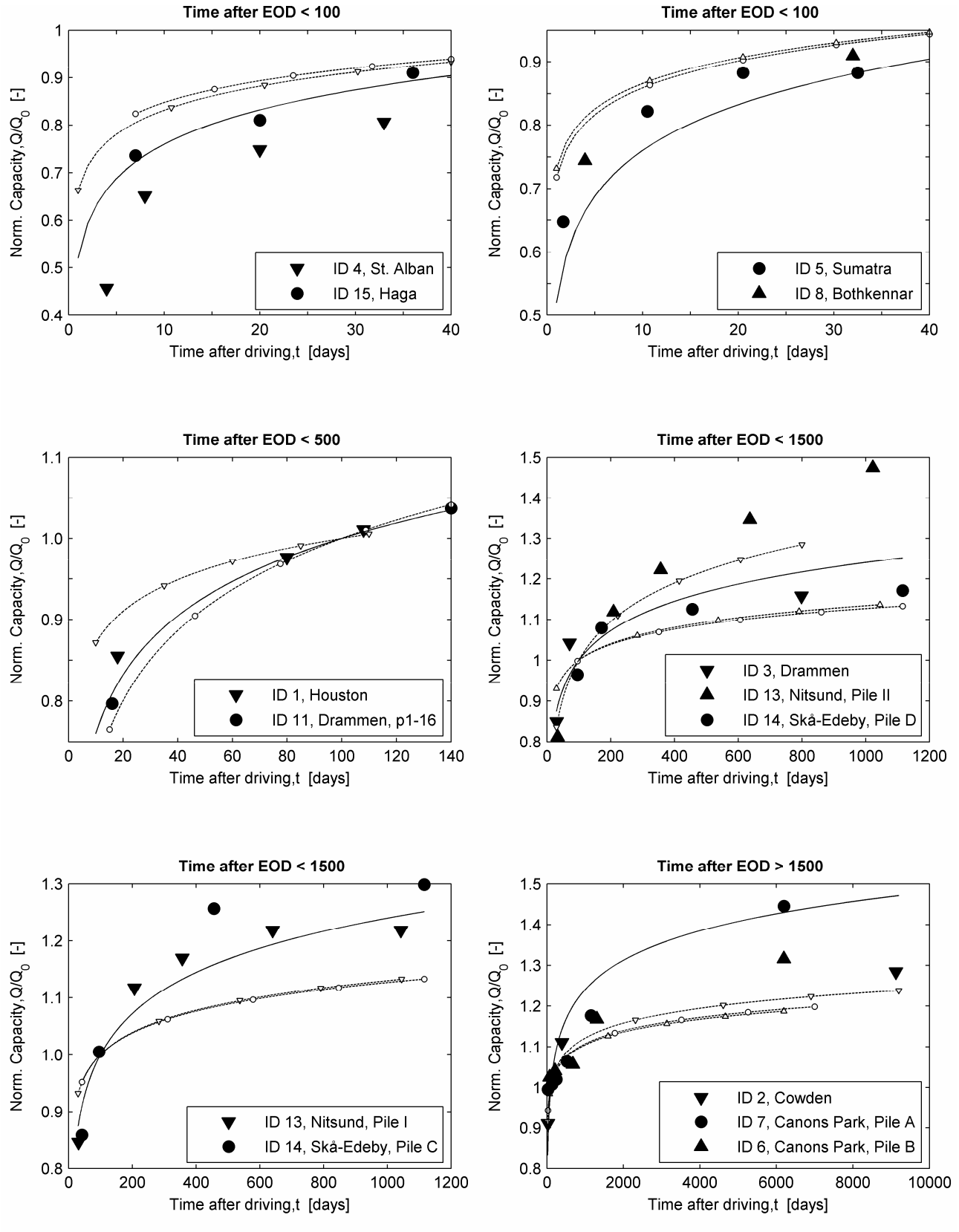

which is natural since the model is calibrated based on these data. The NGI-model provides the least suitable fit, whereas the time function based on $\Delta_{10} = 0.24$ is slightly better than the time function proposed by Skov and Denver (1988).

The time function based on $\Delta_{10} = 0.24$ almost fits the observed behaviour as well as AAU, which is also indicated by Figure 10. It is primarily in the tails of the S_{uu} range that the two models differ. Considering:

1. the non-distinctive correlation between S_{uu} and Δ_{10} for AAU,
2. that the variance of the residuals based on the two time functions do not differ significantly,
3. that the distribution of residuals around the mean is similar,
4. that *SSR* obtained for AAU is only 11% less than the *SSR*-value provided by the time function based on $\Delta_{10} = 0.24$,
5. that the time function based on $\Delta_{10} = 0.24$ provides a slightly better fit to the available data compared to the models proposed by Skov and Denver (1988), Bullock et al. (2005a,b), and by Clausen and Aas (2000).

it is recommend to make use of the time function based on $\Delta_{10} = 0.24$ when estimating the development of capacity with time based on staged loading and the reference time $t_0 = 100$ days. According to Table 6, Δ_{10} equals 0.13 for unstaged loading and $t_0 = 100$ days, whereas Δ_{10} equals 0.46 and 0.18 for staged and unstaged loading, respectively, when $t_0 = 1$ day.

Finally, in Figure 12 it is visualised how the time function based on $\Delta_{10} = 0.24$ predicts the actual behaviour compared to the NGI model.

7 Conclusions

The vertical bearing capacity of piles in clay has been assessed with the focus on its long-term development. The primary aim has been to quantify the rate of set-up. Further, it has been analysed whether the magnitude of set-up is related to the properties of the soil surrounding the pile. The analyses are based on 88 static pile tests, and the data represent a great variety of soil and pile properties. Therefore, the findings in this paper are of general applicability to piles in clay.

In the literature it has been suggested that the pile capacity increases with the logarithm of time after initial driving. Based on the available data, there is statistical evidence that this semi-logarithmic relationship is valid.

Concerning the set-up models proposed in the literature, the time function proposed by Skov and Denver (1988) provides the better fit of the available data. The model proposed by Bullock et al. (2005a,b) systematically under-predicts the capacity a long time after installation, which is also the case for the model proposed by Clausen and Aas (2000). Further, the maximum difference between the measured and predicted capacities is significantly smaller in the model suggested by Skov and Denver (1988) than in the two other models.

Skov and Denver (1988) as well as Bullock et al. (2005a,b) employ a constant value of the set-up factor, whereas Clausen and Aas (2000) propose that Δ_{10} depends on the properties of the soil. However, the present study indicates that neither of the undrained shear strength, the plasticity index or the overconsolidation ratio has a significant influence on the set-up.

Hence, in conclusion the set-up factor for piles situated in clay is constant and independent on the soil properties. The following relation may be applied to predict the bearing capacity at time *t* after initial driving:

$$Q = Q_0 \left\{ 1 + \Delta_{10} \log_{10} \left(\frac{t}{t_0} \right) \right\} \tag{17}$$

where t_0 and Q_0 are the reference time and capacity of the pile, respectively, while Δ_{10} is the set-up factor. For $t_0 = 1$ day and unstaged loading it has been found that $\Delta_{10} = 0.18$, whereas $\Delta_{10} = 0.13$ for staged loading. The listed values of the set-up factor are characteristic values determined as the lower limits of a 95% significance interval. It is worthwhile to note that the suggested value of $\Delta_{10} = 0.13$ is higher than the value proposed by Bullock et al. (2005a,b).

Finally, if another reference time than $t_0 = 1$ day is preferred, the set-up factor and reference capacity should be adjusted accordingly as described in Section 2.

8 Acknowledgement

The authors would like to thank the COWI A/S and the Norwegian Geotechnical Institute for kindly providing valuable pile test data.

9 References

API (1993), Recommended practice for planning, designing and constructing fixed offshore platforms- working stress design, API RP 2A-WSD, *American Petroleum Institute*, 20th edition, July 1, 1993.

API (2000), Recommended Practice for Planning, Designing and Constructing Fixed Offshore Platforms – Working Stress Design, *API recommended practice 2A-WSD (RP 2A-WSD), American Petroleum Institute*.

Augustesen, A., Andersen, L. and Sørensen, C.S. (2005a), Capacity of piles in clay, A*vailable from the Department of Civil Engineering, Aalborg University, Denmark*, *Internal report,* ISSN: 1398-6465 R0502.

Augustesen, A, Andersen, L. and Sørensen, C.S. (2005b), Time function for driven piles in clay, A*vailable from the Department of Civil Engineering, Aalborg University, Denmark*, *Internal report,* ISSN: 1398-6465 R0501.

Ayyub, B.M. and McCuen, R.H. (1997), Probability, statistics, & reliability for engineers, *CRC Press, Florida*.

Bergdahl, U. and Hult, G. (1981), Load tests on friction piles in clay, *Proc. 10th International conference on soil mechanics and foundation engineering*, Stockholm, Sweden, Vol.2, pp.625-630.

Bond, A.J. and Jardine, R.J. (1991), Effects of installing displacement piles in a high OCR clay, *Geotechnique*, 41(3), pp.341-363.

Bond, A.J. and Jardine, R.J. (1995), Shaft capacity of displacement piles in a high OCR clay, *Geotechnique*, 45(1), pp.3-23.

Bullock, P.J., Schmertmann, J.H., McVay, M.C., and Townsend, F.C. (2005a). Side shear setup. I: Test piles driven in Florida. *Journal of Geotechnical and Geoenvironmental Engineering*, 131(3), pp. 292-300.

Bullock, P.J., Schmertmann, J.H., McVay, M.C., and Townsend, F.C. (2005b). Side shear setup. II: Results from Florida test piles. *Journal of Geotechnical and Geoenvironmental Engineering*, 131(3), pp. 301-310.

Camp, W.M., Wright, W.B, and Hussein, M. (1993), The effect of overburden on pile capacity in a calcareous marl, *Proceedings of 18th Annual Members' Conference, Deep Foundations Institute*, Englewood Cliffs, N.J.

Chan, J.H.C. and Birrell, N.D. (1998), Project overview and organization – Tension pile study, *Offshore technology conference*, Houston, Texas, May 1998, OTC paper 8762.

Clausen, C.J.F. and Aas, P.M. (2000), Bearing capacity of driven piles in clays, *NGI-report, Norwegian Geotechnical Institute*.

Conover, W. J. (1980). Practical nonparametric statistics. *New York, Wiley.*

Davie, J.R. and Bell, K.R. (1991), A pile relaxation case history, *Ecole nationale des ponts et chaussees, Foundations profondes, presses de l'ecole nationale des ponts*, pp.421-429.

Eide, O., Hutchinson, J.N. and Landva, A. (1961), Short and long-term test loading of a friction pile in clay, *Proc. 5th International Conference on Soil Mechanics and Foundation Engineering*, Paris 1961, Also in NGI (Norwegian Geotechnical Institute) Publication no.45.

Falstad, B.A. and Heyerdahl, H. (1995), Construction of two railway bridges across Drammen river. Piling and related challenges, *Geoteknikkdagen*, 1995, Norway, pp.37.1-37.23.

Finno, R.J., Cosmao, T. and Gitskin, B. (1989), Results of foundation engineering congress pile load tests, *Results of pile prediction symposium (R.J. Finno, ed.), Geotechnical Special Publication, No.23, Geotechnical Engineering, ASCE*, pp.338-355.

Flaate, K. (1972), Effects of pile driving in clays, *Canadian Geotechnical Journal*, 9(1), pp.81-88.

Gallagher, K.A. and St. John, H.D. (1980), Field scale model studies of piles as anchorages for buoyant platforms, *Proc. European Offshore Petroleum Conference*, London, Paper EUR 135.

Guang-Yu, Z. (1988), Wave equation applications for piles in soft ground, *3rd International conference on the application of stress-wave theory to piles*, (Ed. Fellenius, B.H.), Ottawa, Canada, pp.830-836.

Huang, S.M. (1988), Application of dynamic measurement on long H-pile driven into soft ground in Shanghai, *3rd International conference on the application of stress-wave theory to piles*, (Ed. Fellenius, B.H.), Ottawa, Canada, pp.635-643.

Karlsrud, K. and Haugen, T. (1986), Axial static capacity of steel model piles in overconsolidated clay, *NGI Publication No.163*, Norwegian Geotechnical Institute. Also *Proc. 11th International Conference on Soil Mechanics and Foundation Engineering,* San Francisco, 1985, Vol.3, pp.1401-1406.

Konrad, J.M. and Roy, M. (1987), Bearing capacity of friction piles in marine clay, *Geotechnique*, 37(2), pp.163-175.

Ladd, C.C., Foott, R., Ishihara, K., Schlosser, F. and Poulos, H.G. (1977), Stress-deformation and strength characteristics, *State-of-the-art report, Proc. ICSMFE, Tokyo*, Vol.2.

Lehane, B.M. and Jardine, R.J. (1994), Displacement pile behaviour in glacial clay, *Canadian Geotechnical Journal*, .31(1), pp.79-90.

Long, J.M., Kerrigan, J.A. and Wysockey, M.H. (1999), Measured Time Effects for Axial Capacity of Driven Piling, *Transportation Research Record, Journal of the Transportation Research Board*, No.1663, pp.8-15.

Mayne, P.W. (1988), Determining OCR in clays from laboratory strength, *Journal of Geotechnical Engineering*, 114(1), pp.76-92.

Montgomery, D.C. (2001), Design and analysis of experiments, *5th edition, John Wileys & Sons, Inc., New York*.

O'Neill, M.W., Hawkins, R.A. and Audibert, J.M.E. (1982a), Installation of pile group in overconsolidated clay, *Journal of the Geotechnical Engineering Division*, 108(11).

O'Neill, M.W., Hawkins, R.A. and Audibert, J.M.E. (1982b), Load transfer mechanisms in piles and pile groups, *Journal of the Geotechnical Engineering Division*, 108(12).

Powell, J.J.M. and Uglow, I.M. (1988), Marchetti dilatometer testing in UK soils, *Penetration testing, ISOPT-1, De ruiter (ed.), Balkema Rotterdam*, ISBN 90 6191 801 4, pp.555-562.

Powell, J.J.M., Butcher, A.P. and Pellew, A. (2003), Capacity of driven piles with time – implifications of re-use, *Proc. XIII ECSMGE*, (eds. Vanicek et al.), Prague, Vol.2, pp.335-340.

Skov, R. and Denver, H. (1988), Time-dependence of bearing capacity of piles, *Proc. 3rd international conference on the application of stress-wave theory to piles, Ottawa, Canada, (Ed. Fellenius, B.H.)*, pp.879-888.

Svinkin, M.R., Morgano, C.M. and Morvant, M. (1994), Pile capacity as a function of time in clayey and sandy soils, *Proc. 5th International conference on piling and deep foundations*, Vol.5, Paper 1.11, pp.1-8.

Svinkin, M.R. and Skov, R. (2000), Set-up effect of cohesive soils in pile capacity, *Proc. 6th International Conference on the Application of stress wave theory to piles*, (Eds. Niyama, S. and Beim, J.), Sao Paolo, Brazil, pp.107-112.

Thompson, C.D. and Thompson, D.E. (1985), Real and Apparent Relaxation of Driven Piles, *Journal of Geotechnical Engineering*, 111(2), pp.225-237.

Trenter, N.A. and Burt, N.J. (1981), Steel pipe piles in silty clay soils at Belawan, Indonesia, *Proc. 10th International Conference on Soil Mechanics and Foundation Engineering*, Stockholm, Vol.2, p.873.

Tvedt, G. and Fredriksen, F. (2003), E18 Ny motorvegbru i Drammen. Prøvebelastning av Peler, *Proceedings from the conference on Rock Blasting and Geotechnics*, Oslo, 2003

Vijayvergiya, V.N. (1977), load-movement characteristics of piles, *Ports '77, Proc. 4th Annual Symposium of the Waterways, Ports, Coastal and Ocean Division of American Society of Civil Engineers*, 2, pp.269-284.

Walpole, R.E. and Myers, R.H. (1993), Probability and statistics for engineers and scientists, *5th edition, Prentice-Hall International, Inc., New Jersey*.

Wardle, I.F., Price, G. and Freeman, T.J. (1992), Effect of time and maintained load on the ultimate capacity of piles in stiff clay, *Piling: European practice and worldwide trends: Proceedings of a conference*, London, pp.92-99.

Wendel, E. (1900), On the test loading of piles and its application to foundation problems in Gothenburg, *Tekniska Samf. Goteberg handl.*, No.7, pp.3-62.

York, D.L., Brusey, W.G., Clemente, F.M. and Law, S.K. (1994), Setup and relaxation in glacial sand, *Journal of Geotechnical Engineering*, 120(9), pp.1498-1513.

Title:

Time Function for Driven Piles in Clay.

Authors:

Augustesen, A., Andersen, L., and Sørensen, C.S.

Year of publication:

2005

Published in:

Department of Civil Engineering, Aalborg University, Denmark, Internal report, ISSN: 1398-6465 R0501.

Remarks:

Parts of the report are similar to parts of the memorandum "Assessment of Time Functions for Piles Driven in Clay".

Time Function for Driven Piles in Clay

A. Augustesen, L. Andersen, and C.S. Sørensen

This report deals with the effects of time on the bearing capacity of single axially loaded piles located primarily in clays. The starting point of the study is a set of piles subjected to static loading tests and the purpose is twofold. Firstly, a general procedure/method is described by which existing data can be analysed in order to calibrate a time function, which describes the relation between time and axial bearing capacity (Section 2). Secondly, two time functions are proposed based on a set of piles that each have been tested statically a number of times after installation (Section 3). The functions are semi-logarithmic of nature and depend on the undrained shear strength. However, the correlation between the undrained shear strength and the set-up factor is not distinctive. For the range of undrained shear strength considered the set-up predicted by the time function lies between 0.22 and 0.29 per log cycle of time (in days). It is found that the smaller undrained shear strength the higher set-up. Assumptions and precautions concerning this study are discussed (Section 2). First, a concise review of the effects of time on the axial bearing capacity of driven piles in clay is presented (Section 1).

1 Introduction

For piles located entirely in either clay, sand or a combination of different soil types, the practical experience shows that engineering-time has an important effect on pile capacity. As early as 1900, Wendel (1900) documented time dependent increases for timber piles located in clay and reported that the axial capacity continued to increase for two to three weeks after driving. Up to present, several studies on the influence of time on the bearing capacity of piles have been reported in the literature - in chronological order: Bjerrum et al. (1958), Tavenas and Audy (1972), Flaate (1972), Bergdahl and Hult (1981), Karlsrud and Haugen (1986), Konrad and Roy (1987), Skov and Denver (1988), Fellenius et al. (1989), Preim et al. (1989), Davie and Bell (1991), Schmertmann (1991), Wardle et al. (1992), Svinkin et al. (1994), York et al. (1994), Joshi et al. (1995), Chow et al. (1998), Chen et al. (1999), Long et al. (1999), Seidel and Kalinowski (2000), Axelsson (2002), and Powell et al. (2003). In the following, focus is placed on axially loaded piles in clays.

1.1 Set-up and relaxation

Normally, the bearing capacity of a driven pile increases with time after installation, which is denoted set-up. In special cases, drops in capacity with time have been reported, which is denoted relaxation - see Parsons (1966), Yang (1970), Thompson and Thompson (1985), Davie and Bell (1991), and York et al. (1994). Whether set-up or relaxation occurs is related to:

- Characteristics of the subsoil in which a given pile is located.
- Flow of pore water.
- Time for equalisation of pore pressures.

In Table 1, clayey soils are categorised depending on sensitivity S_t: extra sensitive soils have sensitivity exceeding 8, sensitive clays has sensitivity between 2 and 4, and for normal clays the sensitivity does not exceed 2 (Yang, 1970). Some stiff clays with structural characteristics such as cracks and joints may have sensitivities below 1. The classification of sandy soils is related to their ability to dilate during shearing. Dense sand normally dilates whereas coarse and loose fine sands typically compress during shearing. In Table 1, the terms Q_d and Q_s denote the resistances at the end of initial driving and at the beginning of redriving, respectively. This implies that relaxation takes place if $Q_d > Q_s$ and set-up if $Q_s > Q_d$. According to Yang (1970), relaxation may only occur in connection with piles located in stiff clays, dense fine sands, and inorganic silts. In other cases set-up takes place. Furthermore, the more sensitive clay the greater amount of set-up and Mitchell (1993) postulates that the magnitudes of time effects in soils increase with increasing water content. In addition, Flaate (1968) has found for some Norwegian plastic clays and silty clays that set-up increases with decreasing plasticity index.

In general, the flow of pore water influence whether set-up or relaxation take place. During pile driving in dense sand or in clayey soils with high overconsolidation ratio, the soil surrounding the pile will eventually dilate. This results in negative pore pressures, which dissipate with time and thereby reduces the horizontal effective stresses acting against the pile wall. This implies a reduction in capacity with time. According to York et al. (1994), lateral stresses are further relieved even after the negative pore water pressures are dissipated. Soils that exhibit compression to failure experience the opposite tendencies.

Table 1 Soils exhibiting relaxation ($Q_d > Q_s$) or setup ($Q_d < Q_s$). Q_d is the capacity at the end of initial driving whereas Q_s is the capacity at the beginning of restriking. After Yang (1970).

Subsoil condition	Pile resistance
Stiff clay	$Q_d > Q_s$
Normal sensitive clay	$Q_d \approx Q_s$
Sensitive clay	$Q_d < Q_s$
Extra sensitive clay	$Q_d << Q_s$
Coarse sand	$Q_d \approx Q_s$
Loose fine sand	$Q_d < Q_s$
Dense fine sand	$Q_d > Q_s$
Organic silt	Similar to clay soils
Inorganic silt	Similar to fine sand

The time for equalisation of pore pressures and the time between driving and testing also affect set-up and relaxation tendencies. For example, if a pile is driven in dense sand, negative pore pressures occur due to driving. If the pile is tested within the equalisation period, it may seem like relaxation takes place. In contrast, if the pile is tested long after the end of consolidation, it may seem like set-up has occurred. In the latter case, the reason is that the effects of soil structure regeneration during and after consolidation are greater than the effects of dissipation of negative pore water pressures due to driving. Soils that undergo compression to failure will always exhibit set-up.

Long et al. (1999) and Powell et al. (2003) discuss to a limited extent the effects of driving, testing time, and ageing on set-up and relaxation tendencies. The question is whether real relaxation due to changes in the characteristics of the soil skeleton can occur. Seidel et al. (1992) postulate that relaxation can be observed in fractured, weak metamorphic rock, shale and silt stones. Further, relaxation occurs rapidly and there is no evidence of the long term effects of relaxation. It should be mentioned that the toe capacity decreased with time whereas the shaft friction increased. In addition, the lower parts of the piles were located in metamorphic rock whereas the rest were located in sand and clay. Thompson and Thompson (1985) conclude that relaxation of end-bearing driven piles in shale of the Georgian Bay Formation in the Bayfront area of downtown Toronto is a very real situation.

In the remaining part of this report, attention is primarily paid to set-up, which is more widely observed compared to relaxation.

1.2 Basic set-up mechanisms

It is commonly believed that set-up is due to:

1. *Dissipation of excess pore water pressures with time*. As the driving induced pore pressures dissipate, the soil consolidates. This leads to increased horizontal effective stresses acting against the pile wall implying increased mobilised skin friction with time. It should be mentioned that the duration of the process is approximately proportional to the pile diameter.
2. *Ageing*. Capacity increases with time due to changes in the characteristics of the soil skeleton, changes in the pile-soil interaction and/or changes in stress regime in the soil surrounding a given pile. For piles in clays thixotropy, cementation or bonding of clay particles with time also play a role.

The concept of, and experimental evidence for, pore pressure dissipation as a mechanism to explain increase in pile capacity with time is discussed by Soderberg (1962), Bjerrum et al. (1958), and Konrad and Roy (1987) among others. Furthermore, the effect of pore water flow is discussed in some details in Section 1.1 and will not be further examined. Instead, the main focus in this study is paid to "real" time effects associated with single piles located in clay.

Karlsrud and Haugen (1986) report that for piles at the Haga test site the measured set-up is likely associated with "bonding" of clay minerals rather than changes in stress conditions in the soil surrounding the piles. This is due to the fact that the increase in horizontal effective stresses did not match the corresponding increases in pile capacity. On the other hand, Karlsrud et al. (1992) conclude that also a gradual restoration of in situ stresses must be a major cause of set-up. Furthermore, in low plasticity deposits silo or arching effects occur. These effects may eventually decrease with time resulting in higher horizontal effective stresses and thereby higher capacity. That is, the arching phenomenon implies changes in the stress regime leading to set-up. See Chow et al. (1998) for further details on the arching mechanism.

Schmertmann (1991) discusses also plausible soil particle and soil-structure mechanisms perhaps responsible for the observed ageing effects. It is pointed out that ageing effects even in clays result from increased basic soil friction instead of increased cohesion, which is also indicated by Bullock et al. (2005a,b). Schmertmann (1991) postulates that the effective stresses drive the mechanisms involved. The mechanical effects include grain slippage, soil-structure dispersion, increased dilatancy, increased interlocking, and an internal arching of stresses. For information

Table 2 Increase in capacities for piles in clay – some case histories.

Reference	Soil description	Pile type [a)]	Pile dimension[b)]	Test [c)]	Max. time for tests	Results (Setup) [d)]
		Open/Closed, Material	Eq. diam. [mm], Emb. length [m]	Static, Dynamic	[Days]	Pile capacity increases:
Karlsrud and Haugen (1986)	Overconsolidated clay	C, S	153, ~5	S	35	5.9% per week. ~22% between 7 and 35 days
Powell et al. (2003)	Soft to very stiff clay	O and C, S	102 - 457, Up to 9.5	S	9125 (25 years)	10-20% in 1-3 months, 30-40% in 3-4 years
Konrad and Roy (1987)	Overconsolidated soft marine clay	C, S	220, Up to 7.6	S	33	12 times Q_{eoid} for friction along the shaft
Bergdahl and Hult (1981)	Normally consolidated clay	C, T	~110, 15	S	~1100	22% in 1-2 month, 45% between 1 and 40 month
Attwooll et al. (1999)	Lightly overconsolidated clay	C, S	324 - 610, 27 - 35	S and D	43	3.9 - 5.9 times Q_{eoid}
Long et al. (1999)	Clay	-	-	S and D	1000	1 - 6 times Q_{ref}, Largest setup within 20-30d
Bjerrum et al. (1958)	Normally consolidated clay	C, CO	395, 12 - 17	S	~200	1 month: Q is 50% of Q_{theo} 1 year: Q is 80-100% of Q_{theo}
Skov and Denver (1988)	Clay	C, CO	~280, Up to 21	S and D	~200	2.5 times Q_0, which is calculated capacity for t_0=1 day
Flaate (1972)	Clay	C, T	180, ~12 - ~14	S	1043	Average increase is ~ 60% between 32 and 1043 days
Bullock et al. (2005a,b)	Silty clay and fine sand	C, CO	516, ~19	S	1727	Q/Q_{ref} up to 2

a) O, C, S, T, and CO denote Open, Closed, Steel, Timber, and Concrete, respectively.
b) Eq. diam. is the equivalent diameter referring to an equivalent circle diameter for square and hexagonal piles. Emb. length is the embedded length.
c) S and D are Static and Dynamic, respectively.
d) Q, Q_{eoid}, Q_{ref} and Q_{theo} denote capacity at a given time after installation, capacity at the End Of Initial Driving, Reference capacity, and a theoretical determined capacity, respectively.

regarding the effects of increasing dilatancy, see Axelsson (1998,2002). On the other hand, Schmertmann (1991) also postulates that thixotropic ageing influences the time dependent response. However, the effect is weaker than the effects of mechanical ageing.

In summary, the mechanisms controlling the influence of time on pile capacity are complicated and not yet fully understood. In fact, limited information on basic mechanisms describing set-up for piles in clay have been reported. But it seems like changes in soil properties and stress regime in the soil are major contributors to the measured set-up. The phenomena are probably interrelated and it is therefore hard to decide which mechanism that is predominant. Axelsson (1998, 2002) and Chow et al. (1998) discuss these phenomena for piles in sand.

1.3 Observed magnitudes of set-up

Observed/measured set-up magnitudes reported in the literature vary a great deal even for piles located in the same type of soils. The term set-up is relative because it depends on the reference (for example the capacity at the end of driving or the capacity determined by means of static or dynamic load tests performed a given time after driving) from which it is calculated. Therefore, a direct comparison of the results from different studies reported in the literature should be taken with some precautions. Results of case histories are listed and summarized in Table 2. The list is not exhaustive but indicates the amount of set-up observed for a variety of pile types with different lengths subjected to different types of tests performed at a variety of times after installation. It should be mentioned that both piles loaded in tension and compression are included in Table 2; the latter accounts for the majority. References to other cases can be found in Appendix A and in the references listed in Table 2.

Karlsrud and Haugen (1986) report on the set-up due to ageing. Pore pressure instrumentation indicated that the excess pore pressures had dissipated 7 days after installation. However, the bearing capacity continued to increase for at least another 28 days. Similar conclusions have been drawn by Powell et al. (2003)

Figure 1 Setup of piles at a number of sites located in the UK. Typically, 10-20% increase in capacity within 1-3 months was observed and 30-40% after 3-4 years. Note that some of the piles have only been tested one time. After Powell et al. (2003).

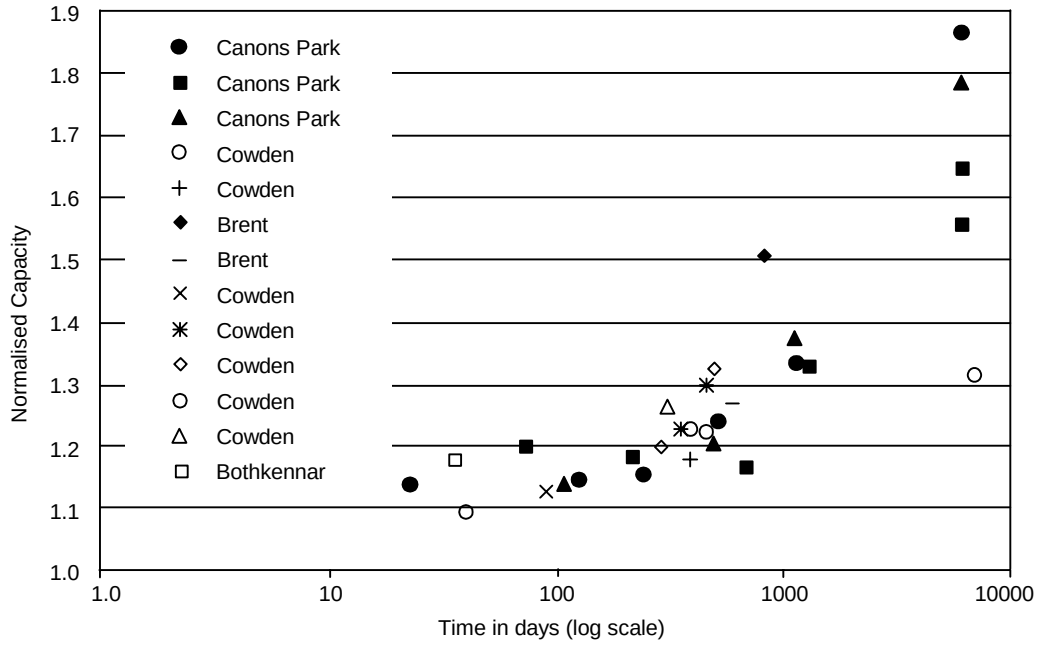

and Bullock et al. (2005a,b).

Attwooll et al. (1999) report on measured set-up for closed-ended steel piles. Set-up was defined as the difference between the capacity, Q_{eoid}, monitored dynamically at the end of driving and the axial compression load test capacity. Furthermore, a dynamic load test performed 93 days after installation on one of the piles showed a remarkable increase in shaft capacity that grows appreciably with depth, i.e. the amount of set-up increases with depth. Attwooll et al. (1999) mention that this observed increase could be influenced by the large number of production piles driven in the vicinity of the test pile after the load test but before companion pile restrike.

In Long et al. (1999), the reference capacity, Q_{ref}, is defined as the capacity from the first load test (either static or dynamic) or load estimate carried out on the pile. Long et al. (1999) present results from a database established from various pile tests reported in the literature. The database contains 80 pile load tests (both dynamic and static), which are sorted into three groups according to the primary subsurface profile: sands, clays and mixed soils. For piles in clay, the effect of time levels out around 100 days after driving. In contrast, for piles in sand set-up appears to continue for up to 500 days after driving but the increase is smaller than the increase exhibited by the piles in clay. For piles in mixed soils set-up magnitudes are similar to piles in clay. Therefore, set-up is most likely related to the proportion of clay in the soil profile, i.e. greater magnitudes are expected in mixed soil profiles with large percentages of clay. Most of the set-up for piles in clay develops within the 20 – 30 days after installation. Hence, Long et al. (1999) conclude that the increase in capacity is probably due to dissipation of excess pore pressures. Finally, no major difference in set-up between low and high displacement piles driven into mixed and clayey soils was found.

Powell et al. (2003) report on static loading tests performed within a period of 25 years in the UK. The results are presented in Figure 1. They define Q_{ref} as the capacity in initial testing. All the piles reported have been left after installation for pore pressures to equalise before initial testing. This implies that the observed set-up shown in Figure 1 is primarily due to ageing.

Bullock et al. (2005a,b) observed set-up ratios up to 2.0 for squared concrete piles installed in silty clay and fine sands within a period of 1727 days. The reference capacity, Q_{ref}, corresponds to t_0 = 1 day. Q_{ref} is determined by linear regression. The static tests were performed as O-cell tests and focus was placed on side shear friction because end bearing set-up is negligible compared to side shear set-up. Greater set-up was observed for piles located in clay than for piles in sand.

In summary, observed set-up for piles located in clays varies a lot and is both related to consolidation and ageing. The effects of excess pore pressure dissipation

Figure 2 Influence of short- and long-term effects on Δ_{10}. The time for equalisation of pore pressures due to pile installation is denoted t_{eoc}. Short-term effects are related to pore pressure dissipation and ageing whereas long-term effects are only due to ageing.

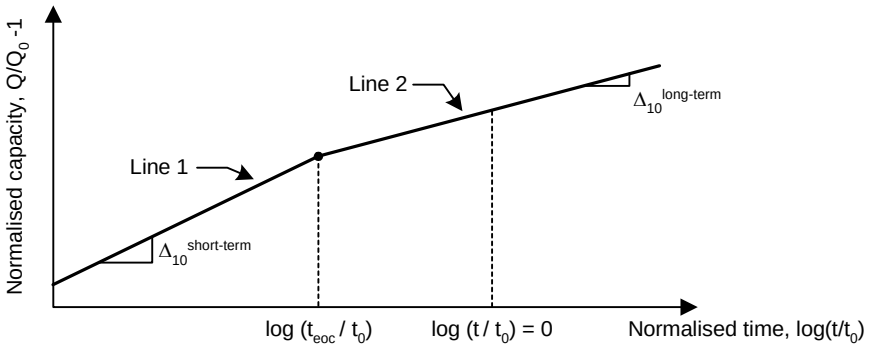

appear to be greater than the effects of ageing. In general, piles driven in soft clays tend to experience greater set-up than piles driven in stiff clays. Piles driven in loose sands and silts generally experience a smaller magnitude of set-up than those in soft clays. Set-up along the shaft is much bigger than the increase in end bearing. Further, the rate of increase in shaft capacity apparently grows with depth.

1.4 Time function

Skov and Denver (1988) described the relation between time after installation, t, and vertical bearing capacity, Q, by a semi-logarithmic function in the form:

$$(1) \qquad Q = Q_0 \left[1 + \Delta_{10} \log_{10} \left(\frac{t}{t_0} \right) \right]$$

Here Q_0 is the reference capacity measured at the reference time t_0, and Δ_{10} is a factor providing the capacity increase corresponding to a ten-fold increase in time. In the following, Δ_{10} is referred to as the set-up factor. A relation between time after installation and capacity as expressed, for example, by eq. (1) is denoted a time function.

Short-term effects regarding the bearing capacity of piles are related to both real time effects (ageing) and the equalisation of excess pore pressures built up during driving. In contrast, long-term effects are only due to ageing. Hence, different values of Δ_{10} are expected when either short- or long-term effects are investigated (Figure 2). The definition "short-term" can be misleading in connection with piles in clay because it may cover up a long period of time. If set-up is considered, the short-term component of Δ_{10} is greater than the long-term component, i.e. $\Delta_{10}^{\text{short-term}} > \Delta_{10}^{\text{long-term}}$. When relaxation, defined as a drop in capacity with time, takes place, $\Delta_{10}^{\text{short-term}}$ becomes negative.

According to Skov and Denver (1988), the values of Δ_{10} in eq. (1) for piles located in sand, clay and chalk are 0.2, 0.6 and 5.0, respectively. Correspondingly, the reference time, t_0, is assumed to be 0.5, 1.0 and 5.0 days. These values of t_0 ensure a stabilized increase of the capacity with time. Before this, the pore pressure has not reached the stationary state and soil remoulding continues to take place. Furthermore, Skov and Denver (1988) point out that there should be an upper limit to t for which eq. (1) is used. However, no guidelines are given for this upper limit.

The assumption $t_0 = 0.5$, 1.0 or 5.0 for piles in sand, clay, and chalk, respectively, may be inconvenient if Q_0 is to be measured at the reference time. Therefore, Svinkin and Skov (2000) gave an alternative definition of Q_0 as the capacity at the end of initial driving and suggested the reference time $t_0 = 0.1$ days. Based on dynamic and static tests performed within a period of 132 days after driving, Δ_{10} was found to vary between 1.14 and 3.50 for piles located in clayey soils.

Equation (1) concerns the total bearing capacity of a pile. However, Bullock et al. (2005a,b) report on similar development of the side-shear capacity with time for concrete piles driven into a variety of coastal plain soils in Florida. Δ_{10} is found to lie in the range 0.12 to 0.32. Piles located in clays generally experience higher values of Δ_{10} than piles in sand; but Δ_{10} does not depend significantly on the properties of the soil within each category. For design purposes Bullock et al. (2005b) recommend a value of $\Delta_{10} = 0.1$ ($t_0 = 1$ day) for piles in clay when no test results are available for the specific site.

Whereas Skov and Denver (1988) and Bullock et al. (2005a,b) propose a constant value of Δ_{10}, Clausen and

Aas (2000) postulate that the long-term set-up depends on the soil properties. Thus, Δ_{10} is a function of the plasticity index, I_p, and the overconsolidation ratio, OCR:

$$\Delta_{10} = 0.1 + 0.4\left(1 - \frac{I_p}{50}\right)OCR^{-0.8}, \quad 0.1 \le \Delta_{10} \le 0.5 \qquad \text{NGI1} \tag{2}$$

Equation (2) is based on very few tests. The reference time, t_0, is chosen to 100 days. The time function based on eq. (2) is denoted NGI because it has been developed at the Norwegian Geotechnical Institute.

Other semi-empirical relations have been presented in the literature. Guang-Yu (1988) proposes a relation where the capacity of piles in soft ground corresponding to $t = 14$ days depend on the sensitivity, S_t, and Q_{eoid} (capacity at the "end of initial driving"). Huang (1988) postulates that the capacities for piles in soft Shanghai soils are a function of Q_{eoid}, the logarithm to time and a quantity denoted the maximum pile capacity. Svinkin et al. (1994) propose two exponential functions where the capacity is a function of Q_{eoid} and time. The study is based on testing five pre-stressed concrete piles driven in predominantly silty sands and dense soil at the lower third of the piles' embedded lengths.

1.5 Discussion

All attempts to calculate/measure set-up have been investigated based on databases including pile load tests. The databases and the investigations suffer from one or more of the following shortcomings due to lack of relevant pile tests with respect to investigation of set-up. This implies a high degree of scatter in the results:

1. Capacities are determined by static and dynamic testing procedures. Although not strictly comparable, no distinction is made between dynamic and static loading tests.
2. Set-up is a relative quantity because it depends on the reference from which it is calculated. Differences exist in the definition of the reference capacity.
3. In connection with dynamic tests, the capacity may not be fully mobilized because the permanent set when restriking was too small (Axelsson, 2002). In that case the capacity, and thereby set-up, is underestimated. Similar conclusions may apply to static loading tests and in addition, measured capacities can be based on different failure criteria.
4. To study the effects of ageing on pile capacity, loading tests performed a long time after the end of consolidation are needed. Most tests have been performed within approximately 200 days after driving. Hence, information concerning long-term pile capacities is to some extent limited.
5. Some databases include piles that have only been tested one time. However, when piles are subjected to staged loading, the problem is to separate the effects of time and previous loading test. What seems like an increase in capacity with time is an effect of pre-shearing. Karlsrud and Haugen (1986) and Bullock et al. (2005a,b) report that for piles located in clays, pre-shearing effects can be substantial. However, Bergdahl and Hult (1981) postulate that it is not possible to show any change in bearing capacity as a result of previous pile load tests for piles in clay.
6. Both shaft resistances and total capacities (including shaft and toe resistance) are compared. Furthermore, both tension and compression tests are included in the analyses.
7. In general there can be huge differences in pile and soil conditions in the different case histories. However, in connection with some studies and databases this fact is not taken into account.
8. Load test results may be influenced by group action.

In order to consistently investigate the effects of time on pile capacity, a database that suffers least from the above-mentioned shortcomings has been established; see Table 3 and Table 4. However, it should be mentioned that no distinction between piles loaded in tension and compression have been made. Further, in respect of studying the effects of time on pile capacity, only few results for unstaged loading tests are available in the literature. Hence, the starting point of this study is piles subjected to staged static loading tests. Last, no information regarding group action is provided and has therefore not been considered. The results of the study are described in Section 2-5.

2 Preliminary considerations and general procedure

In this section, preliminary considerations regarding development of a time function are presented. Furthermore, assumptions, precautions and relations between the parameters entering this study are elucidated. Last, a general procedure is described by which existing data can be analysed in order to calibrate a time function.

Consider Table 4 which shows the results of static loading tests performed on the piles employed in this study. The corresponding pile and soil parameters are given in Table 3. The measured capacities associated with each case in the database are based on failure loads corresponding to settlements equal to $0.1d$, where d is the equivalent pile diameter referring to an equivalent

Figure 3 Development of pile capacity over time for Pile II (case 13 denoted Nitsund) to the left and Pile C (case 14 denoted Skå-Edeby) to the right. The dots denote the static capacity, Q, measured a given time, t, after installation whereas the solid line is the regression line. There is a linear relationship between Q and $\log(t)$. For more information about the piles, see Table 3 and Table 4.

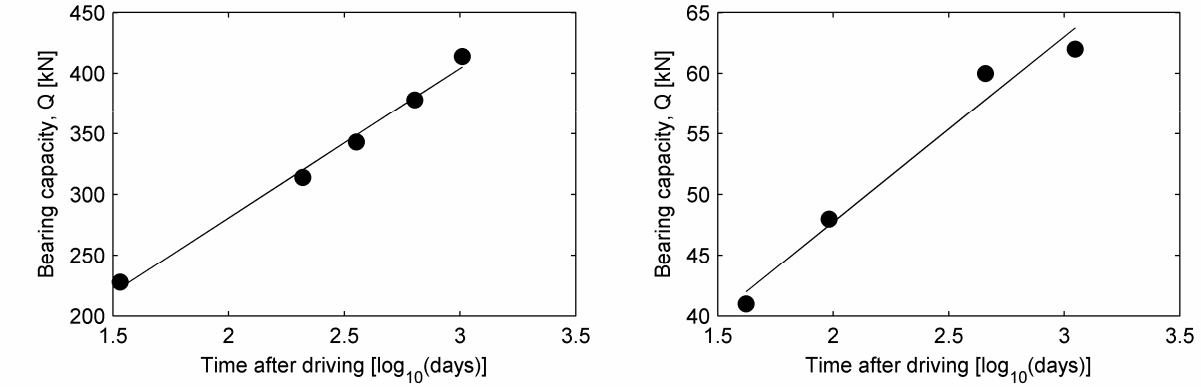

circle diameter for square and hexagonal piles. Experience shows that both the toe and shaft resistance are fully mobilised at this displacement (Vijayvergiya, 1977; API, 2000).

Now, consider pile II (13-16) and pile C (14-22) associated with case 13, Nitsund and case 14, Skå-Edeby, respectively (see Table 3 and Table 4). The development of capacity, Q, with time, t, for the two piles is depicted in Figure 3. Apparently, there is a linear relationship between the capacity and the logarithm to time. A relationship of this kind also appears to be representative for the remaining piles in the database.

As indicated in Section 1, Skov and Denver (1988) and Bullock et al. (2005a,b) have also found a semi-logarithmic relationship between capacity and time elapsed since installation for piles located in sand, clay and chalk. Similar observations have been reported by Chow et al. (1998) and Axelsson (2002) for piles in sand. Therefore, in order to generalize the observed trends, the starting point of this study is to assume that the relation between time and the vertical bearing capacity of piles located in clay can be described by the time function expressed by eq. (1). It is assumed that the material properties of the soil surrounding the pile are explicitly incorporated in Δ_{10}, i.e. Δ_{10} is a function of, for example, undrained shear strength, S_u, over-consolidation ratio, OCR, and plasticity index, I_p. In this study, special attention has been paid to the form of Δ_{10}.

The capacity and the time scale for different piles and test sites may be very different. In order to compare results from different cases, Q and t are normalised by plotting:

$$(3) \qquad \left(\frac{Q_j}{Q_{0j}}-1\right)\Big/\Delta_{10j} \quad \text{versus} \quad \log_{10}\left(\frac{t}{t_0}\right)$$

Here Q_j is the measured capacity for pile j at time t after installation, Q_{0j} is the reference capacity for pile j corresponding to t_0, and Δ_{10j} is the set-up factor for pile j. Δ_{10j} and Q_{0j} can be determined by linear regression as described in Section 2.3. Based on eq. (3), Table 3 and Table 4, the normalised capacities are plotted against the normalised time (t_0 = 100 days) in Figure 4. This plot may be utilized for visual inspection of whether a given pile test fits into the assumed relation between Q and t, i.e. eq. (1). In that case, the dot representing the measured capacity, i.e. the pile test in consideration, is located on the bisectional line. As indicated in Figure 4, the regression line equals the bisectional line and the 95% confidence interval on the line is relatively close to the regression line. It should be noted that cases including only two tests on the same pile will automatically create two points on the bisectional line. Thus, only cases involving at least three tests qualify for the verification of eq. (1). Based on the cases employed in this study and Figure 4, it is concluded that eq. (1) is representative for predicting set-up.

2.1 Choice of reference time

When calibrating a time function the reference time, t_0, can in principle be chosen freely. However, once chosen t_0 is assumed constant and should be used together with the corresponding calibrated time function. This is due to the fact that the development of Δ_{10} is highly dependent on Q_0 and thereby t_0, cf. eq. (1). The intention of this study is to explore especially the long-

Figure 4 Normalised capacity versus normalised time (t_0 = 100 days) for piles tested more than two times. The dots are test results (one for each pile test), the solid line a regression line, and the dotted lines mark the 95% confidence interval on the regression line. Dots deviating from the regression line imply that a semi-logarithmic relation does not describe the development of pile capacity with time.

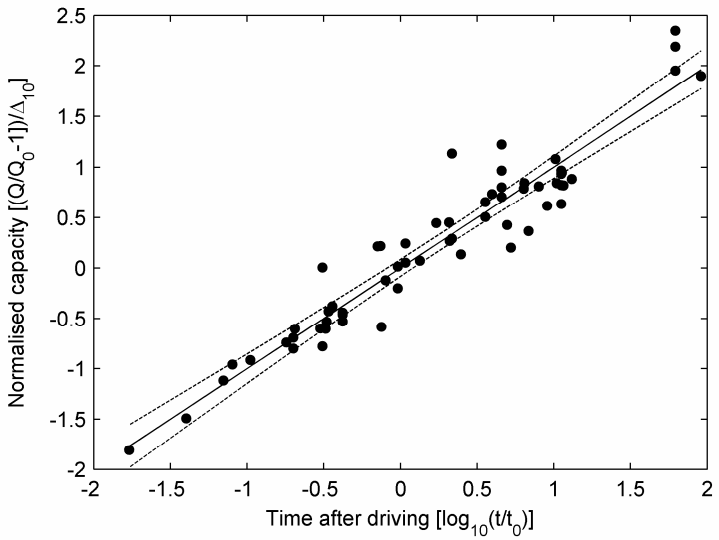

term effects, therefore it is chosen that $t_0 > t_{eoc}$, which is the time for equalisation of pore pressures due to driving. This implies that the capacity/time relationship in principle follows Line 2 instead of Line 1 in Figure 2. In this study t_0 = 100 days is chosen. Therefore, it is assumed that t_0 = 100 days ensures that $t_0 > t_{eoc}$ for all piles in the database. Accordingly, the reference capacity, Q_0, is the pile capacity 100 days after driving. It is denoted Q_{100}. t_0 = 100 days has also been used in the work by Clausen and Aas (2000).

Q_{100} may be determined by some design method such as the API procedure proposed by the American Petroleum Institute (API, 1993) or NGI-99, which is a model developed at Norwegian Geotechnical Institute (Clausen and Aas, 2000). As shown by Clausen and Aas (2000) and Augustesen et al. (2005) even some of the widely accepted methods involve great amounts of uncertainty. Therefore, in this study Q_{100} is instead determined on the basis of the available test results by linear regression of $Q(t)$ vs. $\log_{10}(t)$ for every single pile (Section 2.3). Hence, Q_{100} is the point on the regression line corresponding to $\log_{10}(t = 100)$.

When running the regression analysis, the problem is to determine if there are any test results in every single series of static loading tests on a given pile that should be omitted when estimating Q_{100} for the given pile, e.g. should tests performed earlier than 100 days be excluded or should tests performed after 10 days or more be included. This is due the fact that Q_{100} influences the magnitude of Δ_{10}. It is obvious to include tests performed after $t_0 = 100$ days > t_{eoc} because the capacity/time relationship then ideally follows the behaviour described by Line 2 (Figure 2) and that focus in this study is placed on long-term effects. Furthermore, it is also natural to employ tests conducted at times less than t_0, as long as the tests fit into the relationship described by Line 2 instead of Line 1. Inspection of the available tests indicate that 1 day is the optimal choice since it minimises statistical uncertainties without disturbing the model, i.e. test performed more than 1 day after installation have been used in the analyses. Attention should be paid to piles located in very soft clays due to a long reconsolidation phase.

2.2 Δ_{10} and soil parameters for clays

Section 2.2.1-2.2.3 deals with the problem of how to obtain a consistent set of soil parameters, and the relations between them, based on the available data. Section 2.2.4 deals with the relation between the soil parameters and Δ_{10}, which are based on available measurements from static loading tests and the procedure described in Section 2.3.

2.2.1 Relation between soil parameters

The starting point of this study is 15 cases (including 26 piles), which include piles subjected to staged static loading tests. Some of the cases have been found in the literature, and further data have been provided by Norwegian and Danish companies. A subset denoted ”Super time piles”, abbreviated STP, is used to calibrate

Table 3 Site specifications.

				Soil conditions							Pile conditions						
ID	Name	Reference	Pile name	Q_r [g] [-]	I_p [%]	OCR [h] [-]	S_{uu} [i] [kN/m^2]	S_{ciu} [i] [kN/m^2]	GWT [j] [m]	Z_{hole} [k] [m]	Q_r [g] [-]	Open / Closed	Type [l]	Diam. [m] [m]	Wall [m] [mm]	Taper [m] [deg.]	Tippen [n] [m]
1	Houston	O'Neill et al. (1982a,b)	-	4	31	8.1	109.3	116.6	2.4	3.0	4	C	S	0.273	-	0	13.1
2	Cowden	Powell et al. (2003) [a]	A	4	15	25.2	136.3	132.2	0.0	0.0	4	O	S	0.457	19	0	9.2
3	Drammen	Eide et al. (1961)	-	3	21	1.1	20.6	27.3	1.5	2.4	3	C	T	0.150	-	0.44	15.5
4	St. Alban	Konrad and Roy (1987)	A	3	21	4.6	19.8	23.2	0.6	0.0	3	C	S	0.220	-	0	7.6
5	Sumatra	Trenter and Burt (1981)	-	3	40	2.3	35	45.4	0.0	0.0	3	O	S	0.400	12	0	43.3
6	Canons Park	Powell et al. (2003) [b]	B, D	4	47	8.4	95.8-96.5	101.4-102.2	1.0	2.0	4	C	S	0.168	-	0	6.5 – 6.65
7	Canons Park	Powell et al. (2003) [c]	A	4	45	8.5	104.7	110.7	1.0	3.0	4	C	S	0.168	-	0	6.63
8	Bothkennar	Clausen and Aas (2000) [d]	-	4	40	2.9	17.4	21.0	1.0	1.1	4	C	S	0.1016	-	0	6
9	West Delta	Chan and Birrell (1998) [e]	-	4	41	2.1	36.8	47.9	-16.2	0.0	4	O	S	0.762	19.1	0	71.3
10	Algade	Geodan (1993) [f]	-	4	25	9.7	134.7	140.6	5.3	0.0	2	C	C	0.255	-	0	13.35
11	Motorvegbru Drammen	Tvedt and Fredriksen (2003)	P1-16 P2-16	4	25	1.1	65.3	86.1	2.8	0.0	4	O, C	S	0.4 - 0.813	12.5	0	35
12	Drammen Stasjon	Falstad and Heyerdahl (1995)	P1	1	22	1.2	82.0	107.8	1.0	0.0	3	C	C	0.344	-	0	49
13	Nitsund	Flaate (1972)	I, II	4	16	13.5-15.7	66.2-69.1	70.3-71.9	0.0	0.0	4	C	T	0.175 – 0.180	-	0.32 – 0.47	11.7 – 13.7
14	Skå-Edeby	Bergdahl and Hult (1981)	A-E	4	40-41	3.9-4.1	11.8-12.3	14.8-15.5	0.0	0.0	4	C	T	0.127	-	0	14.5 – 15.3
15	Haga	Karslrud and Haugen (1986)	-	4	18	7.3	41.5	46.8	0.0	0.2	4	C	S	0.153	-	0	5

a) Gallagher and St John (1980), Lehane and Jardine (1994a).
b) Powell and Uglow (1988), Bond and Jardine (1991,1995) and Wardle et al. (1992).
c) Powell and Uglow (1988), Bond and Jardine (1991,1995) and Wardle et al. (1992).
d) Data taken directly from Clausen and Aas (2000).
e) Data taken directly from Clausen and Aas (2000).
f) Material provided by Kampsax Geodan, which is part of COWI A/S.
g) Quality ranking of soil and pile data: 0 = not known, 1= low, 2 = average, 3 = high, 4 = very high (super piles).
h) *OCR* is based on S_{uu}-strengths.
i) S_{uu} / S_{ciu} is unconsolidated / consolidated undrained shear strength.
j) Depth from soil surface to ground water table, negative if site is submerged.
k) Depth below surface of an open or cased hole.
l) Pile material indicator: S = steel, C = concrete, T = timber.
m) Diameter and wall thickness at pile tip, respectively. Wall thickness is only given in cases where the piles are driven open-ended. Taper denotes pile wall taper.
n) Tip penetration.

Table 4 Measured capacities.

ID - Pile #[a]	Pile Name	CMP/ TNS[b]	Q_{100} [c] [kN]	Δ_{10} [c] [-]	Measured Capacity					
					Time / Cap [d] [days / kN]	Time / Cap [d] [days / kN]	Time / Cap [d] [days / kN]	Time / Cap [d] [days / kN]	Time / Cap [d] [days / kN]	Time / Cap [d] [days / kN]
1-1	-	C	784	0.20	18 / 670	80 / 765	108 / 792	-	-	-
2-2	A	C	1252	0.15	30 / 1140	396 / 1390	9125 / 1608	-	-	-
3-3	-	C	259	0.19	31 / 220	71 / 270	799 / 300	-	-	-
4-4	A	C	103	0.36	4 / 47	8 / 67	20 / 77	33 / 83	-	-
5-5	-	C	1892	0.20	1.7 / 1225	10.5 / 1555	20.5 / 1670	32.5 / 1670	-	-
6-6	D	C	174	0.34	108 / 189	496 / 200	1130 / 231	6200 / 291	-	-
6-7	B	C	185	0.22	74 / 194	217 / 197	683 / 200	1312 / 221	6200 / 274	-
7-8	A	C	159	0.19	31 / 159	134 / 161	248 / 163	525 / 165	1154 / 184	6200 / 231
8-9	-	C	36	0.18	4 / 27.34	32 / 32.91	-	-	-	-
9-10	-	T	5049	-0.06	116 / 5030	470 / 4850	-	-	-	-
10-11	-	C	741	0.13	14 / 660	9778 / 930	-	-	-	-
11-12	P1-16	C	2699	0.26	16 / 2150	140 / 2800	-	-	-	-
11-13	P2-16	C	2082	0.41	14 / 1350	141 / 2210	-	-	-	-
12-14	P1	C	1572	0.44	21 / 1100	153 / 1700	-	-	-	-
13-15	I	C	287	0.26	32 / 243	207 / 321	357 / 336	641 / 350	1043 / 350	-
13-16	II	C	281	0.44	34 / 228	209 / 314	357 / 343	637 / 378	1023 / 414	-
14-17	A	C	61	0.41	30 / 48	75 / 58	-	-	-	-
14-18	A	C	40	0.30	42 / 34	456 / 55	1116 / 48	-	-	-
14-19	B	C	69	0.61	39 / 52	75 / 64	-	-	-	-
14-20	B	C	43	0.33	42 / 36	456 / 56	1116 / 54	-	-	-
14-21	C	C	75	0.54	30 / 54	75 / 70	-	-	-	-
14-22	C	C	48	0.32	42 / 41	96 / 48	456 / 60	1116 / 62	-	-
14-23	D	C	69	0.47	30 / 52	75 / 65	-	-	-	-
14-24	D	C	44	0.18	96 / 42	171 / 47	456 / 49	1116 / 51	-	-
14-25	E	C	59	0.10	75 / 56	216 / 66	906 / 63	-	-	-
15-26	-	T	80	0.24	7 / 59	20 / 65	36 / 73	-	-	-

a) ID refers to the case (see Table 3) and Pile # refers to the given pile's number in the database. Piles that have been tested and then driven further down and hereafter tested again is counted as two, for example pile C associated with case 14, Skå-edeby.
b) CMP and TNS denote piles loaded in compression and tension, respectively.
c) Estimated from the measured capacities by linear regression for every single case.
d) Measured capacity based on static test at the given time after installation.

the different forms of Δ_{10}, see Section 3. The calibrated models are hereafter tested on all the cases in order to determine, which model that provides the better description of the data. STP consists of nine cases including 16 piles where pile, soil, and loading conditions are especially well described. It should be mentioned that since the pile and soil conditions are important parameters in set-up analyses, a quality ranking, Q_r, is specified for all available cases, cf. Table 3. Five categories are applied for the quality, namely $Q_r = 0$: not known; $Q_r = 1$: low; $Q_r = 2$: average; $Q_r = 3$: high; and $Q_r = 4$: very high. In Table 3, the cases belonging to STP have $Q_r = 4$ for both pile and soil and they are marked with asterisk in Appendix A. An exception is case 9, West Delta, because the capacity decreases with time, see Table 4. In connection with case 14, Skå-Edeby, piles tested more than two times are included in STP. The reason for not employing the other tests is that they reflect tests on the same piles initially located in other depths (see Appendix A). Furthermore, by not employing all tests, case 14 is not weighted as high in the calibration of the time functions. Thereby, the proposed time functions reflect to a greater extent the trends observed in connection with relatively

Figure 5 S_{uu} [kPa], I_p [%] and *OCR* [-] plotted against each other for the different cases forming the basis of this study.

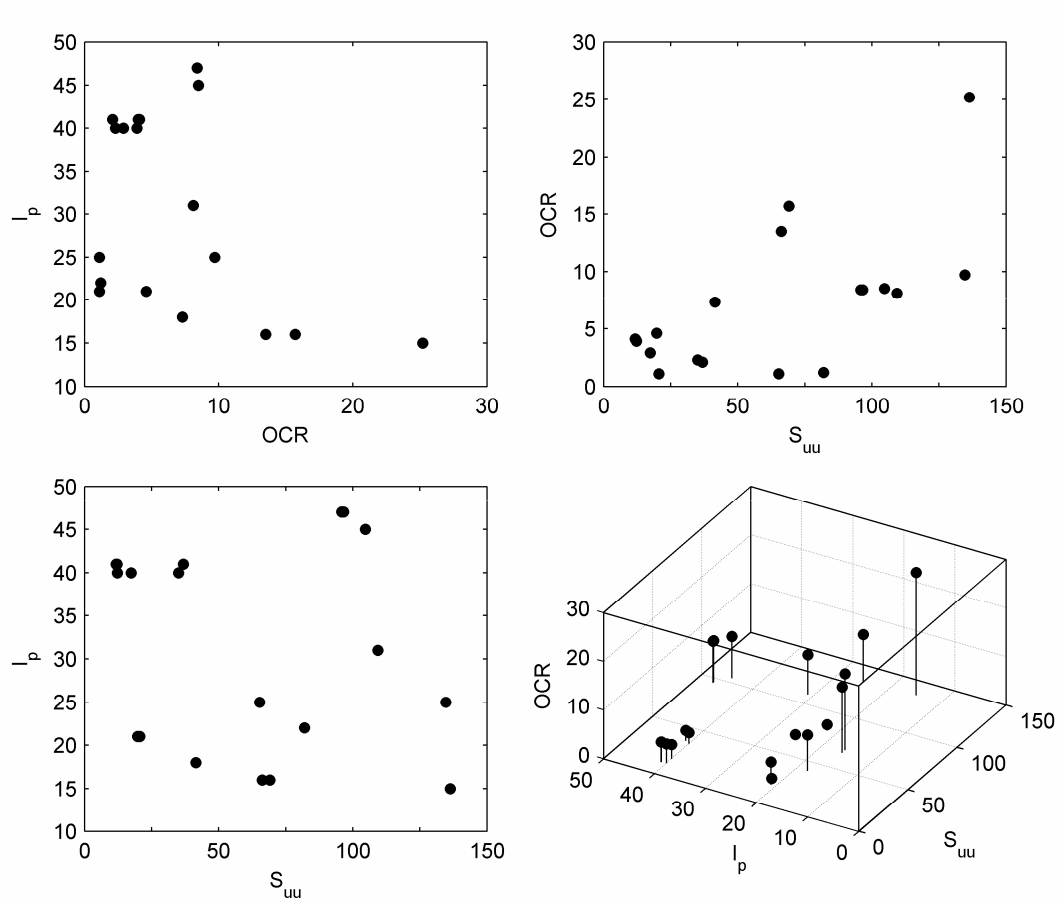

many cases instead of one. Detailed facts concerning the employed cases are presented in Table 3, Table 4, and Appendix A.

The relation between the soil parameters associated with the database is shown in Figure 5:

1. The plasticity index, I_p, decreases with increasing overconsolidation ratio, *OCR*.
2. The overconsolidation ratio, *OCR*, increases with increasing undrained shear strength, S_{uu}, determined by unconsolidated undrained triaxial compression tests.
3. There is no distinctive relation between I_p and S_{uu}.

The same tendencies are observed if the undrained shear strength, S_{ciu}, determined by means of consolidated undrained triaxial compression tests is plotted against I_p and *OCR*.

It should be noted that the range of I_p, *OCR*, and S_{uu} are approximately 15-47 %, and 1-25, and 12-137 kPa, respectively. For comparison, the range of S_{ciu} is 15-141 kPa.

The parameters plotted in Figure 5 are the weighted soil parameters for the entire pile. These form the basis of this study. Whether the soil parameters should be weighted is discussed in Section 2.2.3.

2.2.2 Determination and conversion of soil properties

In this section, it is discussed how to determine I_p and *OCR*, if they are not given. In relation hereto, it is examined how to convert one type of shear strength to another, and thereby create a consistent set of soil parameters.

Undrained shear strength

The undrained shear strength, S_u, can be determined in different ways. Some of the more well-known are consolidated/unconsolidated undrained triaxial compression/extension test, direct simple shear test, vane shear test, unconfined compression test, torvane and pocket penetrometer test, and field cone penetrometer test. In general, the magnitude of the undrained shear strength is influenced by testing method (Wroth, 1984).

For example, Sørensen et al. (1995) found that $S_{u,vane} = 0.86 \cdot S_{ciu}$ for clayey till investigated in connection with the construction of the Great Belt Link in Denmark. Since some of the proposed time functions, cf. Section 3, depend on the undrained shear strength, the calibration of those functions depends on the choice of reference strength. In this study, it is chosen to adopt two types of shear strength as reference; namely the unconsolidated (S_{uu}) and the consolidated (S_{ciu}) undrained triaxial shear strength.

The undrained shear strength is measured/determined in different ways in the different available cases (see Appendix A). In order to obtain a consistent calibration of the S_u-dependent time functions, it is necessary to establish a unique set of rules that allow any strength to be calculated from another. The procedure for calculating S_u-values based on other shear strengths is further discussed in Appendix B. According to Clausen and Aas (2000), the average strength correction is less than ± 20% for any given pile. It should be mentioned that this strength conversion is a controversial matter within the profession of soil mechanics.

Plasticity index and overconsolidation ratio

In far from all the cases, all necessary soil parameters (plasticity index, I_p, and overconsolidation ratio, *OCR*) are given. In such cases use has been made of default parameters. For example, it is assumed that the plasticity index I_p = 25% when the value of I_p is not provided. This appears reasonable according to Casagrande's work (reproduced for example by Mitchell (1993) and Larsen et al. (1988)) because most clays have plasticity indices below 50-60%.

If the overconsolidation ratio, *OCR*, is not given, it can be estimated based on Ladd et al. (1977):

$$(4) \qquad \frac{S_u}{p_0} = \beta \cdot OCR^{\Lambda} \Leftrightarrow OCR = \left(\beta^{-1} \cdot \frac{S_u}{p_0} \right)^{\frac{1.0}{\Lambda}}$$

where *OCR* is the overconsolidation ratio, [-], S_u/p_0 is the normalized strength to overburden ratio, [-], β is the normally consolidated undrained shear strength ratio (S_u/p_{0nc}), [-], and Λ is a strength rebound parameter, [-].

Based on eq. (4), the question arises: what are the magnitudes of β and Λ? According to Mayne (1988), β and Λ depend on the type of shear strength used as input because the undrained shear strength is not a unique soil property. The ranges of β and Λ depending on test method are shown in Table 5. It should be noted that the deviation on β is much bigger than the deviation on Λ when comparing the different test methods. In addition to Mayne (1988), Ladd et al. (1977) found that Λ = 0.8 in case of K_0-consolidated undrained direct simple shear tests, though a better fit is obtained if Λ is decreased from 0.85 to 0.75 with increasing *OCR*. Nothing is mentioned about the magnitude of β. According to Sørensen et al. (1995), for most Danish clays and till the range of β is 0.2-0.4 while Λ = 0.85 seems reasonably. β less than 0.3 can be applied for very soft clays whereas till lies in the upper end. This is based on CIUC (CIU) tests. In principle, values of β and Λ should be estimated from case to case and it should be noted that the determination is very sensitive towards the way the tests are performed.

Table 5 Limits for β and Λ, see eq. (4), as function of test method. Based on Mayne (1988).

	$\beta = S_u/p_0$ [e]	Λ [e]
CIUC (CIU) [a]	0.55 ≥ β ≥ 0.25	0.70
CAUC (CAU) [b]	0.45 ≥ β ≥ 0.2	0.78
DSS [c]	0.27 ≥ β ≥ 0.19	0.80
CAUE [d]	0.25 ≥ β ≥ 0.08	0.85

a) Isotropically consolidated undrained triaxial compression test.
b) Anisotropically consolidated undrained triaxial compression test.
c) Direct simple shear test.
d) Anisotropically consolidated undrained triaxial extension test.
e) Values of β and Λ are for *OCR*s less than 10.

In this study, it is chosen to make use of the parameters β = 0.25 and Λ = 0.85, when S_{uu} is employed as reference strength. This is also used in the work done at Norwegian Geotechnical Institute, see Clausen and Aas (2000). Presumably, eq. (4) with the given parameters provides useful results for $1 \leq OCR \leq 50$. At first sight, the chosen β-value appears too low whereas the Λ-value is maybe too high when comparing with Table 5. Nevertheless, it should be kept in mind that S_{uu} is chosen as reference strength. The reason for using a S_{uu}-based *OCR* in this study is that:

1. The original NGI-model (NGI1) based on I_p, and *OCR* is used as reference when analysing which model that provides the better description of the test results. Clausen and Aas (2000) assume that *OCR* should be calculated based on S_{uu}-strengths if *OCR* has not been provided.
2. *OCR* is also used in the calibration of the modified NGI-model (NGI2), which is based on I_p and *OCR*. (see Section 3). Again, *OCR* is assumed to be based on S_{uu}, if it is not provided.

Alternatively, the relationship between S_{ciu} and *OCR* proposed by Jardine and Chow (1996) may advantageously be adopted as described by Clausen and Aas (2000):

$$(5) \qquad \ln\left(\frac{S_{ciu}}{p_0}\right) = \ln\left(\frac{S_{cau}}{p_0}\right) = A + B \cdot \ln(OCR)$$

where $A = -0.82 - 0.019 I_p$ and $B = 0.75$. S_{ciu} is included in eq. (5) because there is not differentiated between S_{ciu} and S_{cau}. S_{ciu} and S_{cau} are the isotropically and anisotropically consolidated undrained shear strength determined by triaxial tests, respectively. Equation (5) is valid for $1 \leq OCR \leq 30$ and $20 \leq I_p \leq 30$.

It should be mentioned that the dependence of undrained shear strength on the overconsolidation ratio is of controversial matter within geotechnical engineering. Therefore, it is encumbered with some uncertainty.

2.2.3 Average values of S_u, I_p, and *OCR* for the entire pile

There are different ways to use eq. (1):

1. **Option 1**. Equation (1) is applied to every single soil layer. In this study, it is not a possibility because the contributions from the individual soil layers to the overall capacity are not measured. Thereby, a relation between the soil parameters and Δ_{10} cannot be established.
2. **Option 2**. Equation (1) is used for the entire pile. This implies that an average value of I_p, *OCR*, and S_u must be estimated for the soil surrounding the pile. This method is employed in this study.

In addition to Option 2, there are different possibilities to estimate I_p, *OCR* and S_u (after they have been corrected, see Section 2.2.2):

1. **Method 1**. Weighting the soil parameter by surface area.
2. **Method 2**. Weighting the soil parameter by the calculated capacity of the different layers by means of static design equations.

Consider for example I_p and Figure 6. By Method 1, the plasticity index, I_p, for the entire pile can be calculated as follows:

$$(6) \qquad I_p = \frac{\sum_{i=1}^{n} I_{pi} \cdot A_i}{\sum_{i=1}^{n} A_i}$$

where A_i is the area of the part of the pile that is located in layer *i*, [m^2], I_{pi} is the plasticity index for layer *i*, [%], and *n* is the number of soil layers surrounding the pile in consideration.

In contrast, according to Method 2 the plasticity index, I_p, for the entire pile can be expressed as:

$$(7) \qquad I_p = \sum_{i=1}^{n} I_{pi} \cdot \frac{Q_i}{Q_{total}}$$

where I_{pi} is the plasticity index for layer *i*, *n* is the number of soil layers surrounding the pile, Q_i is the contribution from the i^{th} layer to the total skin friction, and Q_{total} is the total skin friction mobilised along the pile.

Values of *OCR* and S_u can in a similar way be calculated for the entire pile, i.e. *OCR* and S_u can be determined by eq. (6) and eq. (7) by replacing I_p with *OCR* and S_u, respectively.

The advantages and disadvantages of Method 1 and 2 can be summarized as follows:

1. The advantage of Method 1 is that it does not depend on the static design equations whereas Method 2 does.
2. The advantage of Method 2 is that the parameters for a given layer are weighted corresponding to the layer's influence on the total capacity.
3. The static design equations associated with Method 2 do not always include all soil parameters. Thus, a certain "mean" parameter for the entire pile is evaluated by the influence of other parameters on the bearing capacity. Further, if a certain parameter is defective and used to estimate the capacity of a layer, great errors are introduced if this capacity is used to estimate parameters that are not included in the static design equations.
4. Method 1 does not take into account the effect of sand layers whereas Method 2 does.
5. In case of pipe piles, the capacity depends on whether the soil inside the pile behaves in a plugged or unplugged manner. However, the water and plug ratios are not always provided. This implies that *Q* cannot be determined, which of course is a disadvantage of Method 2.

In conclusion, Method 1 is preferred because its advantages exceed those of Method 2.

Figure 6 Example used to demonstrate the general principles behind Method 1 and Method 2. *d* and *l* denote equivalent pile diameter and magnitude of a soil layer, respectively. *Q* is mobilised skin friction in a given layer.

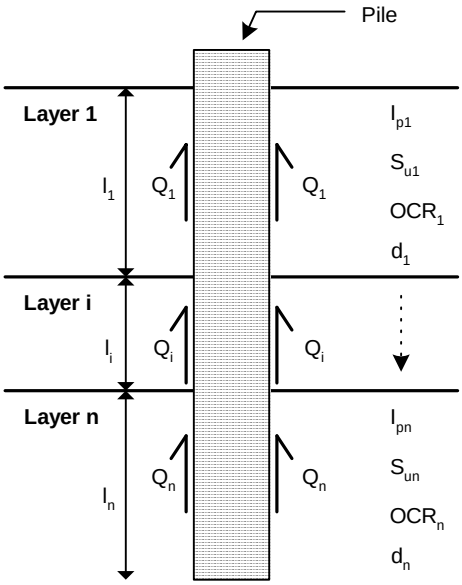

2.2.4 Relation between Δ_{10} and S_u, I_p and *OCR*

In order to calibrate a proposed time function and thereby Δ_{10}, a relation between "measured" Δ_{10}, based on static load tests, for a given pile and the corresponding soil parameters, based on site investigations at the location where the pile is driven, must be established. The soil parameters should be determined according to the criteria described in Sections 2.2.2 and 2.2.3 and Δ_{10} is determined as described in Section 2.3.

In Appendix C, the relation between Δ_{10} and the plasticity index I_p, unconsolidated undrained shear strength S_{uu}, and the overconsolidation ratio, *OCR*, are depicted for every single pile in the database (Figure C.1-C.3). In addition, the relation between Δ_{10} and the consolidated undrained shear strength, S_{ciu}, and *OCR* determined by eq. (5) are illustrated in Figure F.1 and Figure F.2 in Appendix F. It should be noted that even though the reference for undrained shear strength is changed, the relation between Δ_{10} and I_p still remains the same, whereas the relation between Δ_{10} and *OCR* changes because *OCR*, if not given, is determined based on S_u (see Section 2.2.2).

In Figure C.1-C.3 and Figure F.1-F.2 great uncertainties, due to inaccurate soil, pile and testing conditions, are related to piles marked by a circle. The first number in each plot label refers to the case (see Appendix A, Table 3, and Table 4) and the second to pile number, i.e. 6-7 indicates that the 7th pile in the database is a part of case number 6. The following observations are made based on visual inspection of Figure C.1-C.3 and Figure F.1-F.2:

1. Due to scatter there is no distinctive relation between Δ_{10} and either S_u, I_p, or *OCR*.
2. There is possibly a correlation between Δ_{10} and a combination of soil parameters.

2.3 General procedure for estimating and calibrating Δ_{10}

The general steps in calibrating a proposed form of Δ_{10} are as follows:

1. Obtain soil parameters for every single pile available by applying the criteria described in Section 2.2.2 and 2.2.3. In this study, a set of particularly well-described cases denoted super time piles (STP) is picked out. They form the basis for calibration of Δ_{10}. The rest of the cases are used together with STP when testing the validity and accuracy of the different formulae.
2. Determine the reference capacity Q_0 for each pile by investigating $Q(t)$ vs. $\log_{10}(t)$. The point on the regression line corresponding to $\log_{10}(t_0)$ is Q_0 where t_0 is the reference time. In this study the Method of Least Squares has been adopted to

estimate the regression line, and t_0 is selected as 100 days.

3. Δ_{10} is estimated in every single case belonging to the set of cases used to calibrate Δ_{10}. In this study it is STP. This can be done by plotting:

$$(8) \qquad \frac{Q(t)}{Q_0} - 1 \text{ vs. } \log_{10}\left(\frac{t}{t_0}\right)$$

for every single pile. Q is the capacity at time t, Q_0 is the reference capacity at the reference time, t_0, and t is time after driving. The reference capacity for every single pile is estimated in step 2. According to eq. (1), eq. (8) gives Δ_{10}, which is the inclination of a regression line in that type of diagram. Again, the Method of Least Squares has been adopted to estimate the regression line.

4. Different forms of Δ_{10} are calibrated to the soil parameters S_{uu} (or S_{ciu}), I_p, and *OCR* by the Method of Least Squares.
5. After calibrating Δ_{10}, the expression for Δ_{10} is used together with eq. (1) on all the tests to check how well the proposed model describes the observed behaviour. The models are evaluated by the overall residual, R_{ls}, which is defined as:

$$(9) \qquad R_{ls} = \sum_{i=1}^{n}\sum_{j=1}^{k}\left(\frac{Q_j}{Q_{0i}} - 1 - \Delta_{10i}\cdot\log_{10}\left(\frac{t_j}{t_0}\right)\right)^2$$

where Q_j is the measured capacity at time t_j, Q_{0i} is the reference capacity for pile i, t_j is time after driving, t_0 is the reference time, k is number of loading test on a single pile, and n is the number of cases and thereby piles included in the analysis. In this study, the number of cases is 15 but in total 26 piles are included. In the following, the method symbolized by eq. (9) for calculating the overall residual, R_{ls}, is denoted LS (Least Squares).

6. In order to check the method (LS) used to calibrate the models/formulae for Δ_{10} and to determine the overall residual for the model applied to all the tests, another approach has been used to estimate the overall residual. The approach is based on absolute deviations. In case of testing the entire model (the calibrated Δ_{10} combined with eq. (1)), the overall residual, R_{lad}, is defined as:

$$(10) \qquad R_{lad} = \sum_{i=1}^{n}\sum_{j=1}^{k}\text{abs}\left(\frac{Q_j}{Q_{0i}} - 1 - \Delta_{10i}\cdot\log_{10}\left(\frac{t_j}{t_0}\right)\right)$$

In the following, the method symbolized by eq. (10) for calculating the overall residual, R_{lad}, is denoted LAD (Least Absolute Deviations).

As an alternative to steps 4-6, a non-linear optimisation, or fitting, tool may be employed. However, studies indicate that most such algorithms are unable to locate the global minimum, and the solution is highly dependent on the initial "guess" of coefficients in the model for Δ_{10}. Therefore, the outlined approach is taken.

3 Results of data fitting

The outcome of calibrating different forms of Δ_{10} to the STPs and thereafter testing the models (Δ_{10} combined with eq. (1)) on all the cases in the database will be presented. See Appendix A, Table 3, and Table 4 for more details concerning the cases included in the database. Assumptions, precautions, relations between parameters, and the general procedure used to fit the data are described in Section 2.

3.1 Potential forms of Δ_{10}

The following general forms of Δ_{10} have been calibrated based on the available data well-knowing there is no distinctive relation between Δ_{10} and either S_u, I_p, or *OCR*, as mentioned in Section 2.2.4:

$$(11) \qquad \Delta_{10} = \Delta_{10}^0 + a\left(1 - \frac{I_p}{I_p^0}\right)OCR^{-b} \qquad \text{M1}$$

$$(12) \qquad \Delta_{10} = \Delta_{10}^0 - \left(\frac{S_u}{S_u^0}\right)^a \qquad \text{M2}$$

$$(13) \qquad \Delta_{10} = \Delta_{10}^0 + \left(\frac{S_u}{S_u^0}\right)^{-a} \qquad \text{M3}$$

$$(14) \qquad \Delta_{10} = \Delta_{10}^0 + \left(\frac{I_p}{I_p^0}\right)^{-a} \qquad \text{M4}$$

$$(15) \qquad \Delta_{10} = \Delta_{10}^0 - \left(\frac{I_p}{I_p^0}\right)^{a} \qquad \text{M5}$$

$$(16) \qquad \Delta_{10} = \Delta_{10}^0 + \left(\frac{S_u}{S_u^0}\right)^{-a}\cdot\left(1 - \frac{I_p}{I_p^0}\right) \qquad \text{M6}$$

Figure 7 Effects of the constants Δ_{10}^0 and a when eq. (12) is considered, i.e. Δ_{10}^0 fixes the regression curve along the Δ_{10}-axis whereas the parameter a governs the curvature.

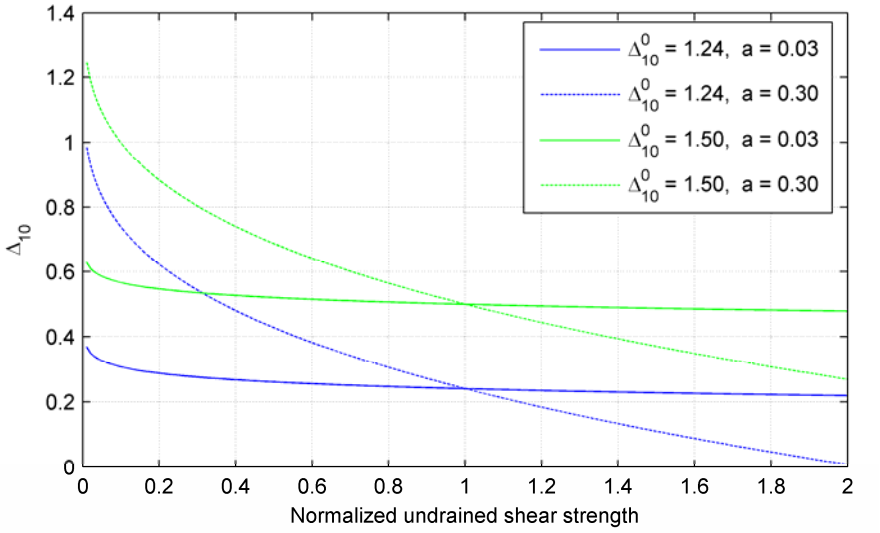

(17) $$\Delta_{10} = \Delta_{10}^0 - \left(\frac{S_u}{S_u^0}\right)^a \cdot \left(1 - \frac{I_p}{I_p^0}\right) \qquad \text{M7}$$

Here S_u is either S_{uu} or S_{ciu}. I_p and *OCR* are plasticity index and overconsolidation ratio, respectively. a, b, Δ_{10}^0, S_u^0, and I_p^0 are constants determined by regression.

The forms of Δ_{10} are chosen by presuming and considering that

- They approximately are capable of describing the observed tendencies between Δ_{10} and the soil parameters S_u, I_p, and *OCR*. Hence, power functions have been applied. Another criterion for Δ_{10} is that it can be applied to cases with soil parameters outside the range considered in this study. In addition, the chosen form of Δ_{10} should have a lower limit.
- In none of the cases employed in this study, *OCR* is actually measured. Instead, it is based on the undrained shear strength, S_u. Hence, either *OCR* or S_u should be omitted when calibrating Δ_{10}. Due to the fact that the determination of *OCR* is based on S_u and not the other way around, the uncertainty associated with Δ_{10} is reduced if it is a function of S_u instead of *OCR*.
- Δ_{10} is a function of either S_u or I_p, i.e. eqs. (12) to (15).
- Δ_{10} is a function of both S_u and I_p, i.e. eqs. (16) to (17).
- Δ_{10} is a function of both *OCR* and I_p as in case of NGI1, i.e. eq. (2).
- Only few regression constants are introduced to keep the functions simple. Furthermore, limited number of cases is available.
- The constant Δ_{10}^0 is used to fix the regression curve along the Δ_{10}-axis. The function of the constants S_u^0 and I_p^0 is to normalize a given soil parameter and thereby make Δ_{10} dimensionless. The constants a and b describe the curvature of the regression line. When considering eq. (12), the effects of Δ_{10}^0 and a are illustrated in Figure 7. The same reflections can be made in the other cases, eqs. (11) to (17). In general, if a minus is applied between Δ_{10}^0 and the next term, the power a should be positive and vice versa.

3.2 Calibrated Δ_{10} based on values of S_{uu}, I_p, and *OCR*

The results of testing the calibrated forms of Δ_{10}, combined with eq. (1), on all the tests by applying an LS-approach (see Section 2.3) are shown in Table 6. It should be mentioned that the overall residual, R_{ls}, is compared with the overall residual for the original NGI-model (NGI1), eq. (2) combined with eq. (1), which is a function of I_p and *OCR* based on S_{uu}-strengths. That is,

NGI1 is the reference when estimating a given model's capability to predict the observed behaviour.

As indicated in Table 6, the calibrated expression of M7 combined with eq. (1) is better to describe the overall behaviour compared to M2. Anyway, it is proposed to use the calibrated form of M2 instead because M7 has the problem that Δ_{10} turns negative for high values of S_{uu} and I_p, i.e. there is no lower limit on Δ_{10}. Further, M2 is much simpler than M7. The expression for M2 when calibrated is as follows:

$$\Delta_{10} = 1.24 - \left(\frac{S_{uu}}{60}\right)^{0.03} \qquad \text{AAU1} \tag{18}$$

Here S_{uu} is the unconsolidated undrained shear strength and Δ_{10} is the set-up factor. In Appendix D, eq. (18) is plotted together with the "measured" Δ_{10}s in the S_{uu}-range examined. Hence, eq. (18) implies that Δ_{10} varies between 0.22 and 0.29. Considering the scatter of the data and the power of 0.03 in eq. (18) there is no distinctive correlation between S_{uu} and the set-up factor. The time function given by a combination of eqs. (1) and (18) is denoted AAU1.

In addition to the LS-approach, the data and M2 have also been examined by means of a LAD-approach due to the relatively limited number of cases available. Thereby, the robustness of the LS-method is checked. It turns out that especially a in eq. (12) depends on whether LS or LAD is used to fit the data ($a = 0.03$ and $a = 0.06$ when LS and LAD are applied, respectively). Despite the differences in a, it does not matter whether LS or LAD fitted coefficients are introduced when evaluating the capability of M2 to fit the data based on a LS-approach. That is, approximately the same overall residual, when testing against all data by a LS-approach, is obtained whether the coefficients in M2 are determined by means of LS or LAD. A similar conclusion can be drawn if LAD is used to evaluate the accuracy of M2 calibrated by either LS or LAD. Therefore, the LS method adopted turns out robust.

It should be mentioned that NGI1 takes the following form when calibrated against the cases forming the basis of this study:

$$\Delta_{10} = 0.1 + 0.3\left(1 - \frac{I_p}{90}\right) OCR^{-0.2} \qquad \text{NGI2} \tag{19}$$

The time function described by a combination of eq. (1) and eq. (19) is denoted the modified NGI-model or NGI2. The power of OCR and the coefficient of I_p have changed significantly, when compared to NGI1. However, the coefficients in eqs. (2) and (19) are of the same order of magnitude.

Table 6 Comparison of the different calibrated expressions for Δ_{10} combined with eq. (1) and NGI1. M1-M7 refers to eqs. (11) to (17). + means that the given method is more accurate than NGI1.

M1	M2	M3	M4	M5	M6	M7
+47.3%	+51.3%	+48.0%	+47.7%	+47.7%	+50.9%	+57.7%

In Appendix E, it is visualized how AAU1 predicts the actual behaviour compared to the original NGI-model and NGI2. From this study, it can be concluded that AAU1 and the modified NGI-model give a better description of the observed behaviour compared to NGI1.

3.3 Calibrated Δ_{10} based on S_{ciu}

M2 is the only general form of Δ_{10} that has been calibrated based on consolidated undrained shear strengths, S_{ciu}, because it apparently describes the observed behaviour the best way, see Section 3.2.

When calibrated by the LS-approach, the general form of Δ_{10} as presented in eq. (12) is as follows:

$$\Delta_{10} = 1.24 - \left(\frac{S_{ciu}}{70}\right)^{0.03} \qquad \text{AAU2} \tag{20}$$

where S_{ciu} is the shear strength determined by means of consolidated undrained triaxial compression tests. The time function given by a combination of eq. (20) and eq. (1) is denoted AAU2.

Equation (20) is similar to eq. (18). Only the constant S_u^0, cf. eq. (12), differs. It takes the value 70 in eq. (20) and 60 in eq. (18). This seems reasonably because shear strengths based on consolidated undrained triaxial compression tests are normally higher than shear strengths based on unconsolidated undrained triaxial compression tests, i.e. $S_{ciu} > S_{uu}$. In Appendix G, eq. (20) is plotted together with the "measured" Δ_{10}s in the S_{ciu}-range in consideration. Again, considering the scatter of the data and the power of 0.03 in eq. (20) there is no distinctive correlation between S_{ciu} and the set-up factor.

Testing AAU2 on all cases in the database by applying a LS-approach shows that it is approximately 51.3% better to predict the observed behaviour than NGI1 when based on OCR related to S_{uu}-strengths. It should be noted that the same reference has been employed to evaluate AAU2 and the models presented in Section 3.2. By comparison, AAU1 and AAU2 predict the observed

Figure 8 Ideal test series for studying the influence of time on the bearing capacity. The arrangement of pile tests implies that the effects of time are separated from the effects of previous load testing.

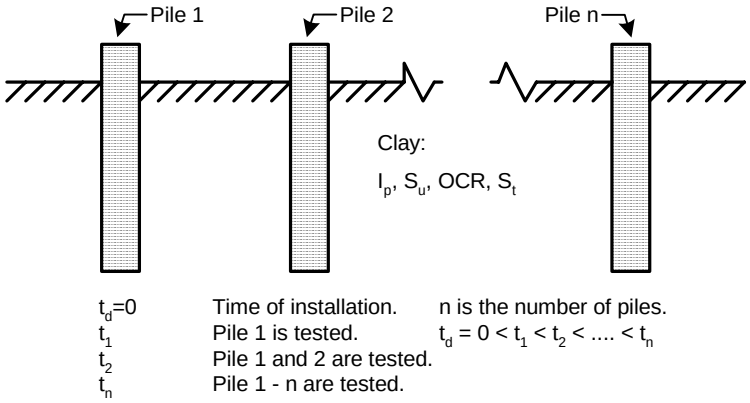

behaviour with the same accuracy. Furthermore, analyses show that NGI2 is also valid when *OCR* is based on S_{ciu}.

The data and M2, based on S_{ciu}, have also been examined by means of a LAD-approach in order to check the robustness of the LS-method. Again, the LS-approach turned out robust.

In Appendix H, it is visualized how AAU2 predicts the actual behaviour compared to NGI1 and NGI2. From this study, it can be concluded that AAU2 and NGI2 give a better description of the observed behaviour compared to NGI1.

4 Discussion

In light of the empirical nature of this study, the time functions presented in Section 3 are a result of a consistent treatment of more or less defective data. For example, in Appendix A and Table 3 the cases are ranked after the quality of the pile and soil descriptions. But what are the characteristics of an ideal case from which the influence of time on the bearing capacity can be studied? First of all, soil and pile conditions should be clearly defined. Furthermore, the strata should be homogeneous and of such horizontal extent that several similar piles can be installed at approximately the same time in the same type of soil without group effects taking place. Pile tests should be arranged as sketched in Figure 8. Thereby the effects of time can be separated from the effects of previous load testing of the same pile. If ageing is of interest the first pile should be tested after equalisation of excess pore pressures. In contrast, if the goal is to establish the maximum set-up no considerations should be paid to excess pore pressures. Furthermore, the piles should be tested by the same procedure and a failure criterion should be defined.

Though, the data are treated consistently and in most cases are of high quality, they do not punctually fulfil the above-mentioned recommendations. For example, time effects are examined by results of testing the same pile more than one time. Furthermore, the strata are non-homogeneous and in some cases even sand layers interbed the clay layers, which are not taken into consideration, i.e. all set-up is assumed to take place in the clay layers. In addition, the soil parameters are not determined in the same way. This is taken care of by the conversion procedures described in Section 2 and Appendix B. Relatively few cases have been reported where piles have been statically tested a long time after installation. If a correlation between results of static and dynamic tests were known, the number of cases will increase dramatically thereby reducing the degree of uncertainty associated with the developed time functions. Furthermore, if time functions are based on dynamic tests, it is not necessary to obtain weighted soil parameters for the entire pile, see Section 2, because the contribution from every single stratum to the total capacity is known. However, in this study focus is entirely placed on pile capacities based on static tests.

In this study, the soil parameters influencing Δ_{10} are assumed to be plasticity index, I_p, overconsolidation ratio, *OCR*, and undrained shear strength, S_u. Eventually, sensitivity, S_t, can advantageously and understandably be used instead of, or in company with, the others. This is due to the definition of S_t as the ratio of undisturbed shear strength to the remoulded strength. When the pile is installed, the surrounding soil is remoulded and the remoulded strength influences the pile capacity. The soil is regaining its strength with time and at the end of the day a new "undisturbed" strength is reached, thus adding to the pile capacity. So the gain

of capacity with time due to changes in undrained shear strength of the soil is reflected in S_t. Furthermore, according to Mitchell (1993), the time-related phenomena such as cementation and thixotropy contribute to the development of sensitivity. Since the undrained shear strength is a common parameter associated with geotechnical investigations and since S_t is a function of undrained shear strength, it is preferably to use the undrained shear strength in the time functions. But they should not both appear.

In none of the cases employed in this study, *OCR* is actually measured. Instead, it is based on the undrained shear strength, S_u, i.e. *OCR* and S_u are correlated. Therefore, either *OCR* or S_u should be omitted when calibrating Δ_{10}. Due to the fact that the determination of *OCR* is based on S_u and not the other way around, the uncertainty associated with Δ_{10} is reduced if it is a function of S_u instead of *OCR*.

In itself, I_p is not an obvious soil parameter for predicting set-up. What matters is probably the magnitude of the natural water content compared to the liquid and plastic limit. This is described by the liquidity index:

$$(21) \qquad LI = \frac{w_n - w_p}{w_l - w_p} = \frac{w_n - w_p}{I_p}$$

where w_n and I_p is the natural water content and plasticity index, respectively. w_p and w_l are water contents corresponding to the plastic and liquid limit, respectively. The magnitude of *LI* indicates how plastic the soil behaves. If it is chosen to use I_p, which is a common soil parameter, it can be used in company with S_t, *OCR* or S_u.

In summary, the undrained shear strengh is probably the most advantageously and understandably soil parameter to use when predicting set-up. It is common and it can easily be related to the gain in capacity with time. The results of this study also shows that the form of Δ_{10}, that best predicts the observed behaviour, depends on S_u and not on I_p and *OCR*.

5 Conclusions

From this study the following can be summarized:

1. The vertical bearing capacity of piles in clays increases with the logarithm of time, cf. eq. (1). In order to calibrate a time function (relation between capacity and time after installation as expressed by eq. (1)) knowledge about the reference time, t_0, the reference capacity, Q_0, and the set-up factor, Δ_{10}, which is the capacity increase corresponding to a ten-fold increase in time, must be obtained. In this study $t_0 = 100$ days is chosen and the corresponding capacity is $Q_0 = Q_{100}$. Furthermore, it is assumed that Δ_{10} depends explicitly on the material properties of the soil surrounding a given pile. The primary focus of this study has been paid to the form and calibration of Δ_{10}.
2. In order to calibrate Δ_{10} a consistent set of data is needed. The relation between the available data have been presented and it is discussed how to make them consistent.
3. A general procedure for calibration of a proposed time function has been presented. The method can be used to develop new functions or update existing formulae when new tests are available.
4. Based on the available data, it has been found that Δ_{10} should depend on the undrained shear strength rather than overconsolidation ratio and plasticity index or other characteristic soil quantities. Thus, the set-up factors suggested in the present work based on S_{uu} and S_{ciu} provide the better predictions of the observed behaviour; approximately 50% better than an existing model developed at Norwegian Geotechnical Institute, which is used as reference when testing the different models capability to describe the observed behaviour. However, it should be mentioned that the proposed set-up factors do not depend significantly on the undrained shear strengths.

6 Acknowledgement

The authors would like to thank the Norwegian Geotechnical Institute for kindly providing the FORTRAN code PILCAP and valuable pile test data.

7 References

API (1993), Recommended practice for planning, designing and constructing fixed offshore platforms- working stress design, API RP 2A-WSD, *American Petroleum Institute*, 20th edition, July 1, 1993.

API (2000), Recommended Practice for Planning, Designing and Constructing Fixed Offshore Platforms – Working Stress Design, *API recommended practice 2A-WSD (RP 2A-WSD), American Petroleum Institute*.

Attwooll, W.J., Holloway, D.M., Rollins, K.M., Esrig, M.I., Sakhai, S. and Hemenway, D. (1999), Measured Pile Setup During Load testing and Production Piling- I-15 Corridor reconstruction Project in Salt Lake City, Utah, *Transportation Research Record, Journal of the Transportation Research Board*, No.1663, pp.1-7.

Augustesen, A., Andersen, L. and Sørensen, C.S. (2005), Capacity of piles in clay, *Available from the Department of Civil Engineering, Aalborg University, Denmark*, *Internal report*, ISSN: 1398-6465 R0502.

Axelsson, G. (1998), Long-term Increase in Shaft Capacity of driven Piles in Sand, *Proc. 4th International Conference on Case Histories in Geotechnical Engineering*, St. Louis, Missouri, Paper no. 1.25, pp.301-308.

Axelsson, G. (2002), A Conceptual Model of Pile Set-up for Driven Piles in Non-cohesive Soil, *Proc. International deep foundations congress*, Orlando, Florida, Vol.1, (Geotechnical Special Technical Publication, ASCE, Vol.116), pp.64-79.

Bergdahl, U. and Hult, G. (1979), Load tests on friction piles in sand – Field tests with different test procedures, *Swedish Commission on Pile Research*, Stockholm, In Swedish with English summary.

Bergdahl, U. and Hult, G. (1981), Load tests on friction piles in clay, *Proc. 10th International conference on soil mechanics and foundation engineering*, Stockholm, Sweden, Vol.2, pp.625-630.

Bjerrum, L., Brinch Hansen, J. and Sevaldson. R. (1958), Geotechnical investigations for a quay structure in Horten, *NGI publication No.28*, Norwegian Geotechnical Institute, pp.1-18.

Bjerrum, L. (1973), Problems of soil mechanics and construction on soft clays, *State-of-the-art report, Session IV, Proc. 8th International Conference on Soil Mechanics and Foundation Engineering,* Moscow, 1973, Also in *NGI Publication No.100*, Norwegian Geotechnical Institute.

Bond, A.J. and Jardine, R.J. (1991), Effects of installing displacement piles in a high OCR clay, *Geotechnique*, 41(3), pp.341-363.

Bond, A.J. and Jardine, R.J. (1995), Shaft capacity of displacement piles in a high OCR clay, *Geotechnique*, 45(1), pp.3-23.

Bullock, P.J., Schmertmann, J.H., McVay, M.C., and Townsend, F.C. (2005a). Side shear setup. I: Test piles driven in Florida. *Journal of Geotechnical and Geoenvironmental Engineering*, 131(3), pp. 292-300.

Bullock, P.J., Schmertmann, J.H., McVay, M.C., and Townsend, F.C. (2005b). Side shear setup. II: Results from Florida test piles. *Journal of Geotechnical and Geoenvironmental Engineering*, 131(3), pp.301-310.

Chan, J.H.C. and Birrell, N.D. (1998), Project overview and organization – Tension pile study, *Offshore technology conference*, Houston, Texas, May 1998, OTC paper 8762.

Chen, Y.-J and Kulhawy, F.H, (1993), Undrained strength interrelationships among CIUC, UU, and UC tests, *Journal of Geotechnical Engineering*, 119(11), pp.1732-1750.

Chen, C.S., Liew, S.S. and Tan, Y.C. (1999), Time effects on the bearing capacity of driven piles, *11th Asian Regional Conference on Soil Mechanics and Geotechnical Engineering*, (Eds. Hong et al.), Balkema, Rotterdam, pp.175-178.

Chow, F.C., Jardine, R.J., Brucy, F. and Nauroy, J.F. (1998), Effects of Time on Capacity of Pipe Piles in Dense Marine Sand, *Journal of Geotechnical and Environmental Engineering*, 124(3), pp.254-264.

Clausen, C.J.F. and Aas, P.M. (2000), Bearing capacity of driven piles in clays, *NGI-report, Norwegian Geotechnical Institute*.

Davie, J.R. and Bell, K.R. (1991), A pile relaxation case history, *Ecole nationale des ponts et chaussees, Foundations profondes, presses de l'ecole nationale des ponts*, pp.421-429.

Eide, O., Hutchinson, J.N. and Landva, A. (1961), Short and long-term test loading of a friction pile in clay, *Proc. 5th International Conference on Soil Mechanics and Foundation Engineering*, Paris 1961, Also in NGI (Norwegian Geotechnical Institute) Publication no.45.

Falstad, B.A. and Heyerdahl, H. (1995), Construction of two railway bridges across Drammen river. Piling and related challenges, *Geoteknikkdagen*, 1995, Norway, pp.37.1-37.23.

Fellenius, B.H., Riker, R.E., O'Brien, A.J. and Tracy, G.R. (1989), Dynamic and Static Soil Exhibiting Set-Up, *Journal of Geotechnical Engineering*, 115(7), pp.984-1002.

Flaate, K. (1968), Bearing capacity of friction piles in clay, *NGF stipend 1967-1968, Veglaboratoriet*, Oslo (in Norwegian).

Flaate, K. (1972), Effects of pile driving in clays, *Canadian Geotechnical Journal*, 9(1), pp.81-88.

Gallagher, K.A. and St. John, H.D. (1980), Field scale model studies of piles as anchorages for buoyant platforms, *Proc. European Offshore Petroleum Conference*, London, Paper EUR 135.

Guang-Yu, Z. (1988), Wave equation applications for piles in soft ground, *3rd International conference on the application of stress-wave theory to piles*, (Ed. Fellenius, B.H.), Ottawa, Canada, pp.830-836.

Huang, S.M. (1988), Application of dynamic measurement on long H-pile driven into soft ground in Shanghai, *3rd International conference on the application of stress-wave theory to piles*, (Ed. Fellenius, B.H.), Ottawa, Canada, pp.635-643.

Jardine, R.J. and Chow, F.C. (1996), New design methods for offshore piles, *Marine Technology Directorate Ltd., Publication MTD 96/103, London 1996, ISBN 1 870553 31 4*.

Joshi, R.C., Achari, G., Kaniraj, S.R. and Wijeweera, H. (1995), Effect of aging on the penetration resistance of sands, *Canadian Geotechnical Journal*, 32, pp.767-782.

Karlsrud, K. and Haugen, T. (1986), Axial static capacity of steel model piles in overconsolidated clay, *NGI Publication No.163*, Norwegian Geotechnical Institute. Also *Proc. 11th International Conference on Soil Mechanics and Foundation Engineering,* San Francisco, 1985, Vol.3, pp.1401-1406.

Karlsrud, K., Kalsnes, B. and Nowacki, F. (1992), Response of piles in soft clay and silt deposits to static and cyclic axial loading based on recent instrumented pile load tests, *Society of underwater testing*, London, Also NGI publication No.188, Norwegian Geotechnical Institute.

Konrad, J.M. and Roy, M. (1987), Bearing capacity of friction piles in marine clay, *Geotechnique*, 37(2), pp.163-175.

Ladd, C.C. (1991), Stability evaluation during stage construction, *Journal of Geotechnical Engineering*, 117(4), pp.540-615.

Ladd, C.C., Foott, R., Ishihara, K., Schlosser, F. and Poulos, H.G. (1977), Stress-deformation and strength characteristics, *State-of-the-art report, Proc. ICSMFE, Tokyo*, Vol.2.

Larsen, G., Frederiksen, J., Villumsen, A, Fredericia, J., Gravesen, P., Foged, N., Knudsen, B. and Baumann, J. (1988), Vejledning I ingeniørgeologisk prøvebeskrivelse, *DGF Bulletin 1, Juli 1988*, (in Danish).

Lehane, B.M. and Jardine, R.J. (1994a), Displacement pile behaviour in glacial clay, *Canadian Geotechnical Journal*, .31(1), pp.79-90.

Lehane, B.M. and Jardine, R. (1994b), Displacement-pile behaviour in soft marine clay, *Canadian geotechnical Journal*, 31(2), pp.181-191.

Long, J.M., Kerrigan, J.A. and Wysockey, M.H. (1999), Measured Time Effects for Axial Capacity of Driven Piling, *Transportation Research Record, Journal of the Transportation Research Board*, No.1663, pp.8-15.

Mayne, P.W. (1988), Determining OCR in clays from laboratory strength, *Journal of Geotechnical Engineering*, 114(1), pp.76-92.

Mitchell, J.K. (1993), Fundamentals of soil behavior, *2nd edition, John Wileys and Sons, Inc., New York*.

O'Neill, M.W., Hawkins, R.A. and Audibert, J.M.E. (1982a), Installation of pile group in overconsolidated clay, *Journal of the Geotechnical Engineering Division*, 108(11).

O'Neill, M.W., Hawkins, R.A. and Audibert, J.M.E. (1982b), Load transfer mechanisms in piles and pile groups, *Journal of the Geotechnical Engineering Division*, 108(12).

Parsons, J.D. (1966), Piling difficulties in the New York area, *Journal of the Soil Mechanics and Foundations Division*, 92(SM1), pp.43-64.

Powell, J.J.M. and Uglow, I.M. (1988), Marchetti dilatometer testing in UK soils, *Penetration testing, ISOPT-1, De ruiter (ed.), Balkema Rotterdam*, ISBN 90 6191 801 4, pp.555-562.

Powell, J.J.M., Butcher, A.P. and Pellew, A. (2003), Capacity of driven piles with time – implifications of re-use, *Proc. XIII ECSMGE*, (eds. Vanicek et al.), Prague, Vol.2, pp.335-340.

Preim, M.J., March, R. and Hussein, M. (1989), Bearing Capacity of Piles in Soils with Time Dependent Characteristics, *Proc., International Conference on Piling and Deep Foundations,* (eds. Burland, J.B. and Mitchell, J.M.), London, pp.363-370.

Schmertmann, J.H. (1991), The Mechanical Aging of Soils, *Journal of Geotechnical Engineering*, 117(9), pp.1288-1330.

Seidel, J.P., Anderson, G.D. and Morrison, N.J. (1992), The effects of pile relaxation on toe capacity and stiffness, *Proc. 4th Application of Stress-Wave Theory to Piles*, (Ed. Barends, F.B.J.), The Hague, The Netherlands, pp.619-626.

Seidel, J.P. and Kalinowski, M. (2000), Pile set-up in sands, *Proc. 6th International Conference on the Application of Stress-Wave Theory to Piles*, (eds. Niyama and Beim), Sao Paulo City, Brazil.

Skov, R. and Denver, H. (1988), Time-dependence of bearing capacity of piles, *Proc. 3rd internatonal conference on the application of stress-wave theory to piles, Ottawa, Canada, (Ed. Fellenius, B.H.)*, pp.879-888.

Svinkin, M.R., Morgano, C.M. and Morvant, M. (1994), Pile capacity as a function of time in clayey and sandy soils, *Proc. 5th International conference on piling and deep foundations*, Vol.5, Paper 1.11, pp.1-8.

Svinkin, M.R. and Skov, R. (2000), Set-up effect of cohesive soils in pile capacity, *Proc. 6th International Conference on the Application of stress wave theory to piles*, (Eds. Niyama, S. and Beim, J.), Sao Paolo, Brazil, pp.107-112.

Soderberg, L.O. (1962), Consolidation Theory Applied to Foundation Pile Time Effects, *Géotechnique*, 12(3), pp.217-225.

Sørensen, C.S., Steenfelt, J.S. and Mortensen, J.K. (1995), Foundation of the East Bridge for the Storebælt link, *Proc. of the 11th European Geotechnical conference, Copenhagen, Denmark*. Also in DGF- bulletin 11 (Danish Geotechnical Society), Vol.5, pp.5.31-5.42.

Tavenas, F. and Audy, R. (1972), Limitations of the Driving Formulas for Predicting the Bearing Capacities of Piles in Sand, *Canadian Geotechnical Journal*, 9(1), pp.47-62.

Thompson, C.D. and Thompson, D.E. (1985), Real and Apparent Relaxation of Driven Piles, *Journal of Geotechnical Engineering*, 111(2), pp.225-237.

Trenter, N.A. and Burt, N.J. (1981), Steel pipe piles in silty clay soils at Belawan, Indonesia, *Proc. 10th International Conference on Soil Mechanics and Foundation Engineering*, Stockholm, Vol.2, p.873.

Tvedt, G. and Fredriksen, F. (2003), E18 Ny motorvegbru i Drammen. Prøvebelastning av Peler, *Proceedings from the conference on Rock Blasting and Geotechnics*, Oslo, 2003

Vijayvergiya, V.N. (1977), load-movement characteristics of piles, *Ports '77, Proc. 4th Annual Symposium of the Waterways, Ports, Coastal and Ocean Division of American Society of Civil Engineers*, 2, pp.269-284.

Wardle, I.F., Price, G. and Freeman, T.J. (1992), Effect of time and maintained load on the ultimate capacity of piles in stiff clay, *Piling: European practice and worldwide trends: Proceedings of a conference*, London, pp.92-99.

Wendel, E. (1900), On the test loading of piles and its application to foundation problems in Gothenburg, *Tekniska Samf. Goteberg handl.*, No.7, pp.3-62.

Wroth, C.P. (1984), Interpretation of in situ soil tests, *Geotechnique*, 34(4), pp.449-489.

Yang, N.C. (1970), Relaxation of piles in sand and inorganic silt, *Journal of Soil Mechanics and Foundation Divison*, 96(2), pp.395-409.

York, D.L., Brusey, W.G., Clemente, F.M. and Law, S.K. (1994), Setup and Relaxation in Gacial Sand, *Journal of Geotechnical Engineering*, 120(9), pp.1498-1513.

Appendix

1. Appendix A: Cases.
2. Appendix B: Conversion procedure.
3. Appendix C: Relation between Δ_{10} and I_p, S_{uu} and *OCR*.
4. Appendix D: M2 based on S_{uu} applied to all tests.
5. Appendix E: Capacity vs. time.
6. Appendix F: Relation between Δ_{10}, S_{ciu}, and *OCR*.
7. Appendix G: M2 based on S_{ciu} applied to all tests.
8. Appendix H: Capacity vs. time.

Appendix A:
Cases

```
PILES IN CLAY     CLAY DATABASE                                        09 AUG 2005

    15   NUMSIT   Number of different sites
     0   INTER    Run program in interactive mode (0=no 1=yes)

     6   ICSAND   Code for method to calculate sand skin friction, see below
     6   ICCLAY   Code for method to calculate clay skin friction, see below

   100   ATMPRS   Atmospheric pressure    (100 kPa  in S.I. units)
    10   GAMWAT   Unit weight of water    (10 kN/m3 in S.I. units)
    78   GAMSTL   Unit weight of steel    (78 kN/m3 in S.I. units)
    25   GAMCON   Unit weight of concrete (25 kN/m3 in S.I. units)
     9   GAMWOD   Unit weight of wood     ( 9 kN/m3 in S.I. units)

     1   MODFSU   Code for change of Su values to Su.UU or Su.DSS (0=No 1=Yes)
   100   TIMEFC   Time needed for development of full pile clay capacity, days
   .00   DELT10   Pile capacity increase for 10-fold time increase
  1.00   PLGFCT   Plug factor, ratio inside/outside friction force

  0  0   INCQRC   Include sites with same or higher soil and pile quality rating code
 1 1 1   INCMAT   Include piles with material code STEEL/CONCRETE/WOOD (0=No 1=Yes)
  1  1   INCMTN   Include piles loaded in compression/tension (0=No 1=Yes)
 0 100   DIAINC   Include piles with diameter within given range
 0 200   PENINC   Include piles with penetration within given range
 0 99999 CAPINC   Include piles with measured capacity within given range
 0 10000 TIMINC   Include piles with time from driving to testing within given range
 0 10.0  SUPINC   Include piles with average Su/po' ratio within given range

  4.5   65  3.0  0.05 0.2   SAND 1-5    Parameters used to calculate pile skin
  .40  .75  .30  2.0  .125  SAND 6-10   friction in sand by NGI-1999 method

 1 1 0            Codes for plotting, 0=NO 1=YES (SAND/CMP  SAND/TNS  CLAY/CMP&TNS)

  ================================    ======================================
  SAND SKIN FRICTION CODES            CLAY SKIN FRICTION CODES
  ================================    ======================================
  1 = API 1972 to 1984 (K=0.5/0.7)    1 = API 1979 to 1987 (24-72 kPa)
  2 = API 1984 to now  (K=0.8/0.8)    2 = API 1987 to now  (ALPHA=f(Su/SIGZ))
  3 = API 1984 to now  (K=0.5/0.7)    3 = API/NGI 1992
  4 = Not used                        4 = NGI 1990
  5 = Imperial College 1996           5 = Imperial College 1996
  6 = NGI 1999                        6 = NGI 1999
  7 = Not used                        7 = Not used
  ================================    ======================================

Data given below for each location and pile include :

  NUMLAY        Number of soil layers
  NUMPIL        Number of different piles or penetration depths
  GWT           Depth from soil surface to ground water table, neg. if submerged site
  GAMPWP        Water unit weight to calculate pore water pressure at pile tip
  SIGSRF        Vertical stress at soil surface
  ZHOLE         Depth below surface of open or cased hole
  QR.SOIL       Quality rating for soil and pile data :
  QR.PILE       0 = Not known  1 = Low  2 = Average  3 = High

  DEPTH BOTTM   Depth to bottom of layer
  GAMMA EFF     Effective unit weight
  TYPE          Soil type indicator (1=Clay 2=Silt 3=Sand)
  Q.CPT         Cone Penetrometer Test tip resistance qc
  SPT           Standard Penetration Test, blows/foot
  OCR           Over-consolidation ratio for CPT to Dr conversion
  SuTop         Undrained shear strength at top of layer
  SuBot         Undrained shear strength at bottom of layer
  TYP           Type of undrained shear strength measurement, see below
  St            Clay sensitivity
  Ip            Clay plasticity index = Wl - Wp
  D50           Sand grain average diameter, mm
  Dr            Sand relative density
  PHI           Sand angle of internal friction
  CLC.FLG       Flag for calcareous soils
  MISC 1-3      MISC(1) is Delta.Sig.PC, used to find OCR.  2-3 not used.

  OPN.CLS       Pile driven open ended (=1) or closed ended (=2)
  MAT.TYP       Pile material type id (1=steel 2=concrete 3=wood)
  DIAM.TIP      Pile tip diameter
  TAPER         Pile wall taper, degrees
  WALL.TIP      Wall thickness at pile tip
  TOTAL.LNGTH   Total pile length from pile but to pile tip
  TIP.PENTR     Depth of pile tip penetration
  PLUG.RATIO    Ratio soil plug length to tip penetration
  WATER.RATIO   Ratio water plug length to tip penetration
  COMPRSSN      Measured pile capacity in compression
  TENSION       Measured pile capacity in tension
  DAYS          Number of days between pile driving and pile testing
  TBF           Value 1 flags that the pile has been tested before
  MISC(1)=  1   Value 1 flags that failure was not reached
  MISC(2)= -1   No correction for time between driving and testing
  MISC(3)= -1   Skip plug capacity control
  MISC(3)=  0   Clay tip tensile force : Undrained conditions
```

MISC(3)= 1 Clay tip tensile force : Drained conditions
MISC(3)= 2 Clay tip tensile force : Zero force at pile tip

Undrained shear strength codes (TYP) :

-1 = Estimated value 0 = Not known

1 = Torvane, pocket pentr. 8 = Field vane test
2 = Unconfined compr. test 9 = Field cone penetrometer test
3 = UU triaxial test 10 = Other field test
4 = CIU/CAU triaxial test
5 = Direct simple shear
6 = Lab vane
7 = Other lab test

*** # 001**

O'Neill et al (1982a,b) Reference piles for 9-pile group
Houston ? Last modified :

NUMLAY	NUMPIL	GWT	GAMPWP	SIGSRF	ZHOLE	QR.SOIL	QR.PILE
4	3	2.4	10	0.0	3.0	4	4

LAYER	DEPTH BOTTM	GAMMA EFF	TYPE ClSiSa	Q.CPT TIP	SPT N	OCR	CLAY SuTop	CLAY SuBot	CLAY TYP	CLAY St	CLAY Ip	SAND D50	SAND Dr	SAND PHI	CLC FLG	MISCELLANEOUS 1	MISCELLANEOUS 2	MISCELLANEOUS 3
1	3.6	10.6	1	1700	0	0	115	115	3	0	30	0	0	0	0	0	0	0
2	7.9	9.3	1	2700	0	0	86	86	3	1	50	0	0	0	0	0	0	0
3	9.2	10.8	1	2100	0	0	38	38	3	0	15	0	0	0	0	0	0	0
4	14.4	10.6	1	3500	0	0	158	158	3	1	15	0	0	0	0	0	0	0

PILE NO	OPN CLS	MAT TYP	DIAM TIP	TAPER degr	WALL TIP	TOTAL LNGTH	TIP PENTR	PLUG RATIO	WATER RATIO	-- MEASURED CAPACITIES -- COMPRSSN	TENSION	DAYS	TBF	MISCELLANEOUS 1	MISCELLANEOUS 2	MISCELLANEOUS 3
1	2	1	.273	.0	.0093	14.1	13.1	0.0	0.0	670	0	18	0	0	0	0
2	2	1	.273	.0	.0093	14.1	13.1	0.0	0.0	765	0	80	1	0	0	0
3	2	1	.273	.0	.0093	14.1	13.1	0.0	0.0	792	0	108	1	0	0	0

*** # 002**

Gallagher & St John (1980), Powell et al. (2003), Lehane and Jardine (1994a)
Cowden, Piles A (open)

NUMLAY	NUMPIL	GWT	GAMPWP	SIGSRF	ZHOLE	QR.SOIL	QR.PILE
4	3	0.0	10	0.0	0.0	4	4

LAYER	DEPTH BOTTM	GAMMA EFF	TYPE ClSiSa	Q.CPT TIP	SPT N	OCR	CLAY SuTop	CLAY SuBot	CLAY TYP	CLAY St	CLAY Ip	SAND D50	SAND Dr	SAND PHI	CLC FLG	MISCELLANEOUS 1	MISCELLANEOUS 2	MISCELLANEOUS 3
1	1.3	10.5	1	1225	0	0	60	85	9	0	15	0	0	0	0	0	0	0
2	2.7	10.5	1	4050	0	0	215	255	9	0	15	0	0	0	0	0	0	0
3	4.7	10.5	1	2700	0	0	190	120	9	0	15	0	0	0	0	0	0	0
4	10.0	10.5	1	2100	0	0	120	110	9	0	15	0	0	0	0	0	0	0

PILE NO	OPN CLS	MAT TYP	DIAM TIP	TAPER degr	WALL TIP	TOTAL LNGTH	TIP PENTR	PLUG RATIO	WATER RATIO	-- MEASURED CAPACITIES -- COMPRSSN	TENSION	DAYS	TBF	MISCELLANEOUS 1	MISCELLANEOUS 2	MISCELLANEOUS 3
1	1	1	.457	.00	.019	12.0	9.2	0.5?	0.5?	1140	0	30	0	0	0	0
2	1	1	.457	.00	.019	12.0	9.2	0.5?	0.5?	1390	0	396	1	0	0	0
3	1	1	.457	.00	.019	12.0	9.2	0.5?	0.5?	1608	0	9125	1	0	0	0

In the old database, Pile A was only tested one time- after 390 days and the capacity was 1440kN. In order to obtain a consistent set of data, the new data substitutes the old data. That is, 390 days and 1440kN is substituted with 396 days and 1390 kN.

 # 003

Eide et al (1961) Timber pile with short- and long-term tests
Drammen Last modified :

NUMLAY	NUMPIL	GWT	GAMPWP	SIGSRF	ZHOLE	QR.SOIL	QR.PILE
5	3	1.5	10	0.0	2.4	3	3

LAYER	DEPTH BOTTM	GAMMA EFF	TYPE ClSiSa	Q.CPT TIP	SPT N	OCR	CLAY SuTop	CLAY SuBot	CLAY TYP	CLAY St	CLAY Ip	SAND D50	SAND Dr	SAND PHI	CLC FLG	MISCELLANEOUS 1	MISCELLANEOUS 2	MISCELLANEOUS 3
1	1.5	19	3	0	0	0	0	0	0	0	0	0	0	35	0	0	0	0
2	3.5	7.8	1	0	0	0	20	20	8	7	25	0	0	0	0	0	0	0
3	7.0	7.8	1	0	0	0	12	12	8	7	25	0	0	0	0	0	0	0
4	13.0	8.1	1	0	0	0	12	20	8	5	20	0	0	0	0	0	0	0
5	20.0	8.8	1	0	0	0	15	30	8	4	13	0	0	0	0	0	0	0

PILE NO	OPN CLS	MAT TYP	DIAM TIP	TAPER degr	WALL TIP	TOTAL LNGTH	TIP PENTR	PLUG RATIO	WATER RATIO	-- MEASURED CAPACITIES -- COMPRSSN	TENSION	DAYS	TBF	MISCELLANEOUS 1	MISCELLANEOUS 2	MISCELLANEOUS 3
1	2	3	.150	.44	.075	15.5	15.5	0.0	0.0	220	0	31	0	0	0	0
2	2	3	.150	.44	.075	15.5	15.5	0.0	0.0	270	0	71	1	0	0	0
3	2	3	.150	.44	.075	15.5	15.5	0.0	0.0	300	0	799	1	0	0	0

 # 004
Konrad & Roy (1987) Field tests in stiff clay, time effects
St Alban Canada Last modified :

NUMLAY	NUMPIL	GWT	GAMPWP	SIGSRF	ZHOLE	QR.SOIL	QR.PILE
3	4	0.6	10	0.0	0.0	3	3

LAYER	DEPTH	GAMMA	TYPE	Q.CPT	SPT	OCR	CLAY					SAND			CLC	MISCELLANEOUS		
	BOTTM	EFF	ClSiSa	TIP	N		SuTop	SuBot	TYP	St	Ip	D50	Dr	PHI	FLG	1	2	3
1	0.6	13.0	2.5	0	0	0	0	0	0	0	0	0	0	25	0	0	0	0
2	1.6	7.3	1	0	0	0	35	10	8	5	30	0	0	0	0	0	0	0
3	9.8	6.2	1	0	0	0	9	32	8	18	20	0	0	0	0	0	0	0

PILE NO	OPN CLS	MAT TYP	DIAM TIP	TAPER degr	WALL TIP	TOTAL LNGTH	TIP PENTR	PLUG RATIO	WATER RATIO	-- MEASURED CAPACITIES -- COMPRSSN	TENSION	DAYS	TBF	MISCELLANEOUS 1	2	3	
1	2	1	.220	.0	.008	7.6	7.6	0.0	0.0	47	0	4	0	0	0	0	Pile A
2	2	1	.220	.0	.008	7.6	7.6	0.0	0.0	67	0	8	1	0	0	0	Pile A
3	2	1	.220	.0	.008	7.6	7.6	0.0	0.0	77	0	20	1	0	0	0	Pile A
4	2	1	.220	.0	.008	7.6	7.6	0.0	0.0	83	0	33	1	0	0	0	Pile A

 # 005
Trenter & Burt (1981) Open steel piles in soft silty clay, Offshore test P4
Sumatra Last modified :

NUMLAY	NUMPIL	GWT	GAMPWP	SIGSRF	ZHOLE	QR.SOIL	QR.PILE
3	4	0.0	10	0.0	0.0	3	3

LAYER	DEPTH	GAMMA	TYPE	Q.CPT	SPT	OCR	CLAY					SAND			CLC	MISCELLANEOUS		
	BOTTM	EFF	ClSiSa	TIP	N		SuTop	SuBot	TYP	St	Ip	D50	Dr	PHI	FLG	1	2	3
1	18.0	5.8	1	0	0	0	10	35	8	2	40	0	0	0	0	0	0	0
2	19.0	9.0	3	0	0	0	0	0	0	0	0	0	0.6	0	0	0	0	0
3	48.0	6.2	1	0	0	0	35	70	8	2	40	0	0	0	0	0	0	0

PILE NO	OPN CLS	MAT TYP	DIAM TIP	TAPER degr	WALL TIP	TOTAL LNGTH	TIP PENTR	PLUG RATIO	WATER RATIO	-- MEASURED CAPACITIES -- COMPRSSN	TENSION	DAYS	TBF	MISCELLANEOUS 1	2	3
1	1	1	.400	.0	.012	44.3	43.3	0.5?	0.98?	1225	0	1.7	0	0	0	0
2	1	1	.400	.0	.012	44.3	43.3	0.5?	0.98?	1555	0	10.5	1	0	0	0
3	1	1	.400	.0	.012	44.3	43.3	0.5?	0.98?	1670	0	20.5	1	0	0	0
4	1	1	.400	.0	.012	44.3	43.3	0.5?	0.98?	1670	0	32.5	1	0	0	0

*** # 006**
Powell et al. (2003), Powell and Uglow (1988), Bond and Jardine (1991,1995), Wardle et al. (1992)
Canons Park, Pile B and D

NUMLAY	NUMPIL	GWT	GAMPWP	SIGSRF	ZHOLE	QR.SOIL	QR.PILE
3	9	1.0	10	0.0	2.0	4	4

LAYER	DEPTH	GAMMA	TYPE	Q.CPT	SPT	OCR	CLAY					SAND			CLC	MISCELLANEOUS		
	BOTTM	EFF	ClSiSa	TIP	N		SuTop	SuBot	TYP	St	Ip	D50	Dr	PHI	FLG	1	2	3
1	2.0	20.0	1	0	0	0	10	63	3	0	55	0	0	0	0	0	0	0
2	4.1	10.0	1	0	0	0	63	78	3	0	55	0	0	0	0	0	0	0
3	7.0	10.0	1	0	0	0	118	118	3	0	40	0	0	0	0	0	0	0

PILE NO	OPN CLS	MAT TYP	DIAM TIP	TAPER degr	WALL TIP	TOTAL LNGTH	TIP PENTR	PLUG RATIO	WATER RATIO	-- MEASURED CAPACITIES -- COMPRSSN	TENSION	DAYS	TBF	MISCELLANEOUS 1	2	3	
1	2	1	.168	.00	.0064	7.0	6.5	0.0	0.0	189	0	108	1	0	0	0	D
2	2	1	.168	.00	.0064	7.0	6.5	0.0	0.0	200	0	496	1	0	0	0	D
3	2	1	.168	.00	.0064	7.0	6.5	0.0	0.0	231	0	1130	1	0	0	0	D
4	2	1	.168	.00	.0064	7.0	6.5	0.0	0.0	291	0	6200	1	0	0	0	D
5	2	1	.168	.00	.0064	7.0	6.65	0.0	0.0	194	0	74	1	0	0	0	B
6	2	1	.168	.00	.0064	7.0	6.65	0.0	0.0	197	0	217	1	0	0	0	B
7	2	1	.168	.00	.0064	7.0	6.65	0.0	0.0	200	0	683	1	0	0	0	B
8	2	1	.168	.00	.0064	7.0	6.65	0.0	0.0	221	0	1312	1	0	0	0	B
9	2	1	.168	.00	.0064	7.0	6.65	0.0	0.0	274	0	6200	1	0	0	0	B

Failure loads for pile B are estimated from Table 1 in Wardle et al. (1992) and Powell et al (2003). Because the ratios Cal/meas are approximately the same for pile B and D (load-settlement curves are given), it is assumed that the head loads given in Wardle et al. (1992) are failure loads.
"Good agreement" between Fig. 4 in Powell et al. (2003) and Tab. 1 in Wardle et al. (1992).
Static tests after 0 and 1day have not been included in the database.

*** # 007**
Powell et al. (2003), Powell and Uglow (1988), Bond and Jardine (1991,1995), Wardle et al. (1992)
Canons Park, Pile A

NUMLAY	NUMPIL	GWT	GAMPWP	SIGSRF	ZHOLE	QR.SOIL	QR.PILE
3	6	1.0	10	0.0	3.0	4	4

LAYER	DEPTH	GAMMA	TYPE	Q.CPT	SPT	OCR	CLAY					SAND			CLC	MISCELLANEOUS		
	BOTTM	EFF	ClSiSa	TIP	N		SuTop	SuBot	TYP	St	Ip	D50	Dr	PHI	FLG	1	2	3
1	2.0	20.0	1	0	0	0	10	63	3	0	55	0	0	0	0	0	0	0
2	4.1	10.0	1	0	0	0	63	78	3	0	55	0	0	0	0	0	0	0
3	7.0	10.0	1	0	0	0	118	118	3	0	40	0	0	0	0	0	0	0

PILE NO	OPN CLS	MAT TYP	DIAM TIP	TAPER degr	WALL TIP	TOTAL LNGTH	TIP PENTR	PLUG RATIO	WATER RATIO	-- MEASURED CAPACITIES -- COMPRSSN	TENSION	DAYS	TBF	MISCELLANEOUS 1	2	3	
1	2	1	.168	.00	.0064	7.0	6.63	0.0	0.0	159	0	31	1	0	0	0	A
2	2	1	.168	.00	.0064	7.0	6.63	0.0	0.0	161	0	134	1	0	0	0	A
3	2	1	.168	.00	.0064	7.0	6.63	0.0	0.0	163	0	248	1	0	0	0	A
4	2	1	.168	.00	.0064	7.0	6.63	0.0	0.0	165	0	525	1	0	0	0	A
5	2	1	.168	.00	.0064	7.0	6.63	0.0	0.0	184	0	1154	1	0	0	0	A
6	2	1	.168	.00	.0064	7.0	6.63	0.0	0.0	231	0	6200	1	0	0	0	A

Failure loads for pile A are estimated from Table 1 in Wardle et al. (1992) and Powell et al (2003). Because the ratios Cal/meas are approximately the same for pile A, B and D (load-settlement curves are given), it is assumed that the head loads given in Wardle et al. (1992) are failure loads. "Not that good agreement" between Fig. 4 in Powell et al. (2003) and Tab. 1 in Wardle et al. (1992). The static test after 0days have not been included in the database.

*** # 008**
Bothkennar
Bothkennar Last modified : Dec 1999

NUMLAY	NUMPIL	GWT	GAMPWP	SIGSRF	ZHOLE	QR.SOIL	QR.PILE
3	2	1.0	10.0	0.0	1.1	4	4

LAYER	DEPTH	GAMMA	TYPE	Q.CPT	SPT	OCR	CLAY					SAND			CLC	MISCELLANEOUS		
	BOTTM	EFF	ClSiSa	TIP	N		SuTop	SuBot	TYP	St	Ip	D50	Dr	PHI	FLG	1	2	3
1	1.0	13.5	1	600	0	0	12	13	3	0	25	0	0	0	0	0	0	0
2	4.5	6.5	1	215	0	0	13	19	3	0	35	0	0	0	0	0	0	0
3	7.0	5.5	1	355	0	0	19	23	3	0	51	0	0	0	0	0	0	0

PILE NO	OPN CLS	MAT TYP	DIAM TIP	TAPER degr	WALL TIP	TOTAL LNGTH	TIP PENTR	PLUG RATIO	WATER RATIO	-- MEASURED CAPACITIES -- COMPRSSN	TENSION	DAYS	TBF	MISCELLANEOUS 1	2	3
1	2	1	.1016	.0	.0103	7.0	6.00	0.0	0.0	27.34	0	4	0	0	0	0
2	2	1	.1016	.0	.0103	7.0	6.01	0.0	0.0	32.91	0	32	1	0	0	0

Failure load computed from given average skin friction
Data taken directly from Clausen and Aas (2000).
For information concerning soil profile at Bothkennar see for example Lehane and Jardine (1994b)

 # 009
Chan & Birrell (1998) OTC-8762/8767 Also NGI 514166-4 & 882016-4 and OTC-6513
West Delta Last modified : 17 Feb 2000

NUMLAY	NUMPIL	GWT	GAMPWP	SIGSRF	ZHOLE	QR.SOIL	QR.PILE
3	2	-16.2	12.72	0.0	0.0	4	4

LAYER	DEPTH	GAMMA	TYPE	Q.CPT	SPT	OCR	CLAY					SAND			CLC	MISCELLANEOUS		
	BOTTM	EFF	ClSiSa	TIP	N		SuTop	SuBot	TYP	St	Ip	D50	Dr	PHI	FLG	1	2	3
1	21	2.8	1	0	0	0	5	25	3	1.5	40	0	0	0	0	0	0	0
2	47	5.12	1	0	0	0	25	42	3	1.5	30	0	0	0	0	0	0	0
3	76	2.01?	1	0	0	0	42	72	3	2.3	55	0	0	0	0	0	0	0

PILE NO	OPN CLS	MAT TYP	DIAM TIP	TAPER degr	WALL TIP	TOTAL LNGTH	TIP PENTR	PLUG RATIO	WATER RATIO	-- MEASURED CAPACITIES -- COMPRSSN	TENSION	DAYS	TBF	MISCELLANEOUS 1	2	3
1	1	1	.762	.0	.0191	71.2	71.2	1.0?	0.0	0	5030	116	0	0	0	0
2	1	1	.762	.0	.0191	71.3	71.3	1.0?	0.0	0	4850	470	1	0	0	0

17 Feb 2000 : The above mudline forces are based upon OTC-8767, and verified against NGI 882016-4.
Data taken directly from Clausen and Aas (2000).

 # 010
Algade, Aalborg Site 1 Pile(s) 1 - 1 Precast concrete
Algade, Aalborg, P4

NUMLAY	NUMPIL	GWT	GAMPWP	SIGSRF	ZHOLE	QR.SOIL	QR.PILE
6	2	5.3	10	0.0	0.0	4	2

LAYER	DEPTH	GAMMA	TYPE	Q.CPT	SPT	OCR	CLAY					SAND			CLC	MISCELLANEOUS		
	BOTTM	EFF	ClSiSa	TIP	N		SuTop	SuBot	TYP	St	Ip	D50	Dr	PHI	FLG	1	2	3
1	4.5	15.0	1	0	0	0	25	25	8	0	0	0	0	0	0	0	0	0
2	5.3	15.6	1	0	0	0	120	120	8	1.7	0	0	0	0	0	0	0	0
3	6.0	9.0	3	0	5	0	0	0	0	0	0	0	0	0	0	0	0	0
4	8.5	9.0	1	0	0	0	110	110	8	2.0	0	0	0	0	0	0	0	0
5	11.0	9.2	1	0	0	0	170	170	8	3.0	0	0	0	0	0	0	0	0
6	13.5	9.2	1	0	0	0	225	225	8	3.8	0	0	0	0	0	0	0	0

PILE NO	OPN CLS	MAT TYP	DIAM TIP	TAPER degr	WALL TIP	TOTAL LNGTH	TIP PENTR	PLUG RATIO	WATER RATIO	-- MEASURED CAPACITIES -- COMPRSSN	TENSION	DAYS	TBF	MISCELLANEOUS 1	2	3
1	2	2	.255	.00	.1275	13.35	13.35	0.0	0.0	660	0	14	0	0	0	0
2	2	2	.255	.00	.1275	13.35	13.35	0.0	0.0	930	0	9778	1	1	0	0

Uncertainty on the pile length.
The first two layers are categorized as clay. They are actually a fill and a organic layer, respectively.
The strength and the weight of the fill layer are estimated.
It looks like the concrete crushed in connection with the tests after 9778 days.
Pile is a squared prec. concrete pile (sidelength 20cm). Diameter calculation based on surface area.
Soil profile based mainly on boring 2.
Load tests for other piles are presented. They are not included in the database because failure was not reached due to the definition: Load corresponding to total deformations equal 10% of pile diameter.

*** # 011**

Motorvegbru Drammen Site 1 Pile(s) 1 - 2 Steel tube and HP-profile
Tvedt and Fredriksen (2003), Pile P1 og P2 (Akse 16)

NUMLAY	NUMPIL	GWT	GAMPWP	SIGSRF	ZHOLE	QR.SOIL	QR.PILE
6	4	2.8	10	0.0	0.0	4	4

LAYER	DEPTH	GAMMA	TYPE	Q.CPT	SPT	OCR	CLAY					SAND			CLC	MISCELLANEOUS		
	BOTTM	EFF	ClSiSa	TIP	N		SuTop	SuBot	TYP	St	Ip	D50	Dr	PHI	FLG	1	2	3
1	2.8	18.0	3	5500	0	0	0	0	0	0	0	0	.52	36	0	0	0	0
2	15.5	8.0	3	5500	0	0	0	0	0	0	0	0	.52	36	0	0	0	0
3	30.0	9.0	1	0	0	0	40	110	4	0	0	0	0	0	0	0	0	0
4	32.5	9.0	1	0	0	0	110	110	4	0	0	0	0	0	0	0	0	0
5	36.0	9.0	1	0	0	0	85	85	4	0	0	0	0	0	0	0	0	0
6	40.0	9.0	1	0	0	0	110	110	4	0	0	0	0	0	0	0	0	0

PILE NO	OPN CLS	MAT TYP	DIAM TIP	TAPER degr	WALL TIP	TOTAL LNGTH	TIP PENTR	PLUG RATIO	WATER RATIO	-- MEASURED CAPACITIES -- COMPRSSN	TENSION	DAYS	TBF	MISCELLANEOUS 1 2 3	
1	1	1	.813	.00	.0125	36.0	35.0	0.21	1.0	2150	0	16	1	0 0 0	P1-16
2	1	1	.813	.00	.0125	36.0	35.0	0.21	1.0	2800	0	140	1	0 0 0	P1-16
3	2	1	.400	.00	.200	39.0	35.0	0.0	0.0	1350	0	14	1	0 0 0	P2-16
4	2	1	.400	.00	.200	39.0	35.0	0.0	0.0	2210	0	141	1	0 0 0	P2-16

The piles have also been dynamic tested.
Static tests after 1day have not been included in the database.
Pile no.2 is a steel pile with H-profile. This profile is equated with a "solid/closed" circular profile.
When calculating the water ratio, the water level inside the pile is assumed to correspond to the level of the ground surface.
Some uncertainty associated with the determination of the plug ratio.

 # 012

Drammen Stasjon Site 1 Pile(s) 1 - 2 Precast concrete
Falstad and Heyerdahl (1995), Pæle P1, P2

NUMLAY	NUMPIL	GWT	GAMPWP	SIGSRF	ZHOLE	QR.SOIL	QR.PILE
5	2	1.0	10	0.0	0.0	1	3

LAYER	DEPTH	GAMMA	TYPE	Q.CPT	SPT	OCR	CLAY					SAND			CLC	MISCELLANEOUS		
	BOTTM	EFF	ClSiSa	TIP	N		SuTop	SuBot	TYP	St	Ip	D50	Dr	PHI	FLG	1	2	3
1	1.0	19.0	3	2000	0	0	0	0	0	0	0	.80	0	0	0	0	0	0
2	11.0	9.0	3	2000	0	0	0	0	0	0	0	.80	0	0	0	0	0	0
3	14.1	10.3	3	2000	0	0	0	0	0	0	0	.13	0	0	0	0	0	0
4	25.0	8.7	1	0	0	0	50	75	8	8.3	22	0	0	0	0	0	0	0
5	50.0	9.0	1	0	0	0	75	75	8	0	22	0	0	0	0	0	0	0

PILE NO	OPN CLS	MAT TYP	DIAM TIP	TAPER degr	WALL TIP	TOTAL LNGTH	TIP PENTR	PLUG RATIO	WATER RATIO	-- MEASURED CAPACITIES -- COMPRSSN	TENSION	DAYS	TBF	MISCELLANEOUS 1 2 3
1	2	2	.344	.00	.172	50.6	49.0	0.0	0.0	1100	0	21	0	0 0 0
2	2	2	.344	.00	.172	50.6	49.0	0.0	0.0	1700	0	153	1	1 0 0

Boring 6 and "tryksondering" are ended 22m and app. 40m under surface level. Clay anticipated all way down to pile tip. Characteristica based on reports, borings and "tryksonderinger".
The sand is loose and characteristica for the layers are based on reports and other borings.
The top 9m is sandfill. GammaEff is estimated.
Piles are sq. prec. concrete pile (sidelength 27cm). Diameter calculation based on surface area.

*** # 013**

Flaate (1972)
Nitsund test site, Pile I and II

NUMLAY	NUMPIL	GWT	GAMPWP	SIGSRF	ZHOLE	QR.SOIL	QR.PILE
2	10	0.0	10	0.0	0.0	4	4

LAYER	DEPTH	GAMMA	TYPE	Q.CPT	SPT	OCR	CLAY					SAND			CLC	MISCELLANEOUS		
	BOTTM	EFF	ClSiSa	TIP	N		SuTop	SuBot	TYP	St	Ip	D50	Dr	PHI	FLG	1	2	3
1	3.8	10.1	1	0	0	0	80	46	8	4	16	0	0	0	0	0	0	0
2	14.0	9.7	1	0	0	0	46	46	8	5	16	0	0	0	0	0	0	0

PILE NO	OPN CLS	MAT TYP	DIAM TIP	TAPER degr	WALL TIP	TOTAL LNGTH	TIP PENTR	PLUG RATIO	WATER RATIO	-- MEASURED CAPACITIES -- COMPRSSN	TENSION	DAYS	TBF	MISCELLANEOUS 1 2 3	
1	2	3	.180	.47	.09	11.9	11.7	0.0	0.0	243	0	32	0	0 0 0	I
2	2	3	.180	.47	.09	11.9	11.7	0.0	0.0	321	0	207	1	0 0 0	I
3	2	3	.180	.47	.09	11.9	11.7	0.0	0.0	336	0	357	1	0 0 0	I
4	2	3	.180	.47	.09	11.9	11.7	0.0	0.0	350	0	641	1	0 0 0	I
5	2	3	.180	.47	.09	11.9	11.7	0.0	0.0	350	0	1043	1	1 0 0	I
6	2	3	.175	.32	.0875	13.9	13.7	0.0	0.0	228	0	34	0	0 0 0	II
7	2	3	.175	.32	.0875	13.9	13.7	0.0	0.0	314	0	209	1	0 0 0	II
8	2	3	.175	.32	.0875	13.9	13.7	0.0	0.0	343	0	357	1	0 0 0	II
9	2	3	.175	.32	.0875	13.9	13.7	0.0	0.0	378	0	637	1	0 0 0	II
10	2	3	.175	.32	.0875	13.9	13.7	0.0	0.0	414	0	1023	1	0 0 0	II

Ground water table assumed to be located at surface level.
The boring is stopped in depth of 10m. The second clay layer is extended to the depth of 14m.

*** # 014**

Bergdahl and Hult (1981)
Skå-Edeby, Pile A-D

NUMLAY	NUMPIL	GWT	GAMPWP	SIGSRF	ZHOLE	QR.SOIL	QR.PILE
2	25	0.0	10	0.0	0.0	4	4

LAYER	DEPTH	GAMMA	TYPE	Q.CPT	SPT	OCR	CLAY					SAND			CLC	MISCELLANEOUS		
	BOTTM	EFF	ClSiSa	TIP	N		SuTop	SuBot	TYP	St	Ip	D50	Dr	PHI	FLG	1	2	3
1	5.0	4.0	1	0	0	0	9	9	8	9	60	0	0	0	0	0	0	0
2	15.6	6.0	1	0	0	0	9	24	8	9	31	0	0	0	0	0	0	0

PILE NO	OPN CLS	MAT TYP	DIAM TIP	TAPER degr	WALL TIP	TOTAL LNGTH	TIP PENTR	PLUG RATIO	WATER RATIO	-- MEASURED CAPACITIES -- COMPRSSN	TENSION	DAYS	TBF	MISCELLANEOUS 1	2	3	
1	2	3	.127	.0	.0635	15.5	15.0	0.0	0.0	48	0	30	0	0	0	0	A
2	2	3	.127	.0	.0635	15.5	15.0	0.0	0.0	58	0	75	1	0	0	0	A
3	2	3	.127	.0	.0635	15.5	15.3	0.0	0.0	34	0	42	0	0	0	0	A
4	2	3	.127	.0	.0635	15.5	15.3	0.0	0.0	55	0	456	1	0	0	0	A
5	2	3	.127	.0	.0635	15.5	15.3	0.0	0.0	48	0	1116	1	0	0	0	A
6	2	3	.127	.0	.0635	15.5	15.0	0.0	0.0	52	0	39	0	0	0	0	B
7	2	3	.127	.0	.0635	15.5	15.0	0.0	0.0	64	0	75	1	0	0	0	B
8	2	3	.127	.0	.0635	15.5	15.3	0.0	0.0	36	0	42	0	0	0	0	B
9	2	3	.127	.0	.0635	15.5	15.3	0.0	0.0	56	0	456	1	0	0	0	B
10	2	3	.127	.0	.0635	15.5	15.3	0.0	0.0	54	0	1116	1	0	0	0	B
11	2	3	.127	.0	.0635	15.5	15.0	0.0	0.0	54	0	30	0	0	0	0	C
12	2	3	.127	.0	.0635	15.5	15.0	0.0	0.0	70	0	75	1	0	0	0	C
13	2	3	.127	.0	.0635	15.5	15.3	0.0	0.0	41	0	42	0	0	0	0	C
14	2	3	.127	.0	.0635	15.5	15.3	0.0	0.0	48	0	96	1	0	0	0	C
15	2	3	.127	.0	.0635	15.5	15.3	0.0	0.0	60	0	456	1	0	0	0	C
16	2	3	.127	.0	.0635	15.5	15.3	0.0	0.0	62	0	1116	1	0	0	0	C
17	2	3	.127	.0	.0635	15.5	15.0	0.0	0.0	52	0	30	0	0	0	0	D
18	2	3	.127	.0	.0635	15.5	15.0	0.0	0.0	65	0	75	1	0	0	0	D
19	2	3	.127	.0	.0635	15.5	15.3	0.0	0.0	42	0	96	0	0	0	0	D
20	2	3	.127	.0	.0635	15.5	15.3	0.0	0.0	47	0	171	1	0	0	0	D
21	2	3	.127	.0	.0635	15.5	15.3	0.0	0.0	49	0	456	1	0	0	0	D
22	2	3	.127	.0	.0635	15.5	15.3	0.0	0.0	51	0	1116	1	0	0	0	D
23	2	3	.127	.0	.0635	15.5	14.5	0.0	0.0	56	0	75	0	0	0	0	E
24	2	3	.127	.0	.0635	15.5	14.5	0.0	0.0	66	0	216	1	0	0	0	E
25	2	3	.127	.0	.0635	15.5	14.5	0.0	0.0	63	0	906	1	0	0	0	E

Ground water table assumed to be located at surface level.
Some of the test piles are loaded in different ways. Furthermore, different test procedures are used during load tests of a single pile.
Failure loads are ultimate loads.
Four of the piles (A-D) were driven further 0,2m after the second load test. Hereafter, the pile is treated as a new pile. That is, the effects of former tests are negligible.
Uncertainty in the determination of the time for testing.
Piles are squared wood piles (sidelength 10cm). Diameter calculations based on surface area.
It is assumed that the piles are loaded in compression.

*** # 015**

Karlsrud & Haugen (1986) Haga model piles, typical results
Haga Last modified : 3 Feb 2000

NUMLAY	NUMPIL	GWT	GAMPWP	SIGSRF	ZHOLE	QR.SOIL	QR.PILE
3	3	0.0	0.0	0.0	0.2	4	4

LAYER	DEPTH	GAMMA	TYPE	Q.CPT	SPT	OCR	CLAY					SAND			CLC	MISCELLANEOUS		
	BOTTM	EFF	ClSiSa	TIP	N		SuTop	SuBot	TYP	St	Ip	D50	Dr	PHI	FLG	1	2	3
1	1.5	21	1	0	0	0	20	34	5	4	13	0	0	0	0	0	0	0
2	4.5	16.7	1	0	0	0	34	34	5	4	16	0	0	0	0	0	0	0
3	5.6	16.7	1	0	0	0	48	48	5	4	40	0	0	0	0	0	0	0

PILE NO	OPN CLS	MAT TYP	DIAM TIP	TAPER degr	WALL TIP	TOTAL LNGTH	TIP PENTR	PLUG RATIO	WATER RATIO	-- MEASURED CAPACITIES -- COMPRSSN	TENSION	DAYS	TBF	MISCELLANEOUS 1	2	3
1	2	1	.153	.0	.0045	5.15	5.0?	0.0	0.0	0	59	7	0	0	0	0
2	2	1	.153	.0	.0045	5.15	5.0?	0.0	0.0	0	65	20	0	0	0	0
3	2	1	.153	.0	.0045	5.15	5.0?	0.0	0.0	0	73	36	0	0	0	0

Typical time development results, not individual tests, see Karlsrud and Haugen (1986).

****
DATA BASE LOG
****

Date	By	Description
09.08.2004	AA	All piles from the different old databases collected. Taken from Clausen and Aas (2000).
09.08.2004	AA	Old and new database collected.
09.08.2004	AA	Case 364 Cowden from the old database substituted with data from additional database.
10.01.2005	AA	Including case 015 Haga.
03.03.2005	AA	Change reference for case 008 Bothkennar.
09.05.2005	AA	Taper changed in connection with case 013 Nitsund.
09.08.2005	AA	Qr.soil changed to 4 for case 013 Nitsund.

Appendix B: Conversion procedure

The procedure employed to convert one type of shear strength to another is presented. The following is based on Clausen and Aas (2000).

For each soil layer in each case, the undrained shear strength is given at the top and the bottom of the layer, see Appendix A. Every shear strength is associated with a type, which is indicated in the TYP-column. For example, undrained shear strengths determined by means of unconsolidated undrained triaxial compression tests is of type 3, i.e. TYP = 3 (see Appendix A). Table B.1 indicates the TYP associated with the different types of shear strengths.

Each test type is assumed to belong to one of the five groups indicated in the last column in Table B.1. For example, undrained shear strengths determined by means of consolidated undrained triaxial compression tests belongs to group 3. Another example, if the undrained shear strength comes from CPT, it is implicitly assumed that the N_k factor used to convert cone tip resistance to undrained shear strength was selected such that the calculated strength corresponds to a UU triaxial value (Clausen and Aas, 2000). So the conversion procedure consists in using relations that combine the strengths belonging to the different groups. It is assumed that the following quantities are given:

1. Vertical effective stress at a given depth, p_0.
2. Plasticity index, I_p.
3. Undrained shear strength, S_u, for one of the five groups in Table B.1.

In the following the relevant equations are given and afterwards it is presented how the conversion procedure works in practice. It should be mentioned that the subscripts associated with each undrained shear strength refer to Table B.1.

Conversion equations

For normally consolidated clays it is assumed that (Clausen and Aas, 2000; Ladd, 1991):

$$\text{(B.1)} \quad \frac{S_{ciu}}{p_0} = \beta^{ciu} = 0.32$$

$$\text{(B.2)} \quad \frac{S_{DSS}}{p_0} = \beta^{DSS} = 0.22 + 0.06\frac{I_p}{100}$$

β^{ciu} lies in the lower end of the range proposed by Mayne (1988). S_{ciu} and S_{DSS} are shear strengths based on consolidated undrained triaxial compression test and directional shear test, respectively. β^{ciu} and β^{DSS} are the normally consolidated undrained shear strength ratios depending on whether S_{ciu} or S_{DSS} are employed as reference shear strength.

Table B.1 Undrained shear strength types and groups. After Clausen and Aas (2000).

TYP	Undrained shear strength test type	Group
-1	Estimated value	1 : UCT
0	Not known	1 : UCT
1	TV/PP: Torvane, Pocket penetrometer test	1 : UCT
2	UCT: Unconfined compression test	1 : UCT
3	UU: Unconsolidated undrained triaxial test	2: UU
4	CIU/CAU: Consolidated undrained triaxial test	3: CIU
5	DSS: Direct simple shear	4: DSS
6	LV: Laboratory vane test	5: Vane
7	Other laboratory test	1 : UCT
8	FV: Field vane test	5: Vane
9	CPT: Field cone penetrometer test	2: UU
10	Other field test	2: UU

For overconsolidated clays, it is assumed that S_{ciu} and S_{DSS} strengths follow the SHANSEP model, based upon Clausen and Aas (2000), Ladd et al. (1977), and Mayne (1988):

$$\text{(B.3)} \quad \frac{S_{ciu}}{p_0} = \beta^{ciu} \cdot OCR^{\Lambda} \quad \text{and} \quad \frac{S_{DSS}}{p_0} = \beta^{DSS} \cdot OCR^{\Lambda}$$

where OCR is the overconsolidation ratio, [-]. β is the normally consolidated undrained shear strength ratio, S_u/p_{0nc}, given by eq. (B.1) and eq. (B.2) depending on whether CIU tests or DSS tests are investigated. Λ is a strength rebound parameter, [-]. It is assumed that Λ = 0.85. OCR is defined as:

$$\text{(B.4)} \quad OCR = \frac{\sigma_{pc}}{p_0} = \frac{p_0 + \Delta\sigma_{pc}}{p_0}$$

where σ_{pc} is the effective preconsolidation pressure.

The relationship between S_{uu} and S_{ciu} based upon Clausen and Aas (2000) and Chen and Kulhawy (1993) is as follows:

$$\text{(B.5)} \quad \frac{S_{uu}}{S_{ciu}} = 0.63 + 0.12 \cdot OCR^{0.5}, \quad 0.75 \le \frac{S_{uu}}{S_{ciu}} \le 1.10$$

where S_{uu} is the unconsolidated undrained triaxial shear strength.

The relationship between S_{uct} and S_{ciu} based upon Clausen and Aas (2000) and Chen and Kulhawy (1993) is as follows:

$$\text{(B.6)} \quad \frac{S_{uct}}{S_{ciu}} = 0.55 + 0.17 \cdot OCR^{0.5}, \;\; 0.72 \le \frac{S_{uct}}{S_{ciu}} \le 1.10$$

where S_{uct} is the shear strength based on unconfined compression test.

The relationship between S_{vane} and S_{DSS} based upon Clausen and Aas (2000) and Bjerrum (1973) is as follows:

$$\text{(B.7)} \quad \frac{S_{vane}}{S_{DSS}} = \begin{cases} 0.9 + 0.8\dfrac{I_p}{100} & \text{for } I_p < 75\% \\ 1.50 & \text{for } I_p \ge 75\% \end{cases}$$

where S_{vane} is the vane shear strength.

Conversion procedure

The conversion procedure is as follows:

1. If *OCR* is not given; calculate *OCR* corresponding to a given type and magnitude of an undrained shear strength by combining some of the equations in the former section, i.e. eqs. (B.1) to (B.7). If the calculated overconsolidation ratio $OCR_{calc} \le 1$ then $OCR = 1$ in the conversion procedure. Furthermore, if S_{uu}/S_{ciu}, S_{uct}/S_{ciu}, and S_{vane}/S_{DSS} are less or greater than the given lower and upper bounds, use must be made of the values of the lower and upper bounds, respectively. Finally, if $p_0 < 0.01p_{atm}$ (for example at the surface) then $p_0 = 0.01p_{atm}$ must be introduced in eqs. (B.1) to (B.7) where $p_{atm} = 100$ kPa is the atmospheric pressure.
2. The magnitude of an undrained shear strength of another type is then calculated by inserting the *OCR* found in step 1, if it is not given, in relevant equations from the former section, i.e. combining eqs. (B.1) to (B.7).

Example: Calculate a S_{uu} strength based on a given S_{uct} strength.

1. By combining eq. (B.1), eq. (B.3), and eq. (B.6), *OCR* can be calculated based on the given S_{uct} strength. It should be mentioned that an iteration procedure might profitably be applied.
2. By inserting the calculated *OCR* found in step 1 in eq. (B.5) and combining this equation with eq. (B.1) and eq. (B.3), the corresponding S_{uu} strength can be calculated.

By similar considerations and calculations, four unknown strengths, see Table B.1, can be calculated based on the known fifth strength.

Appendix C:
Relation between Δ_{10} and I_p, S_{uu} and *OCR*

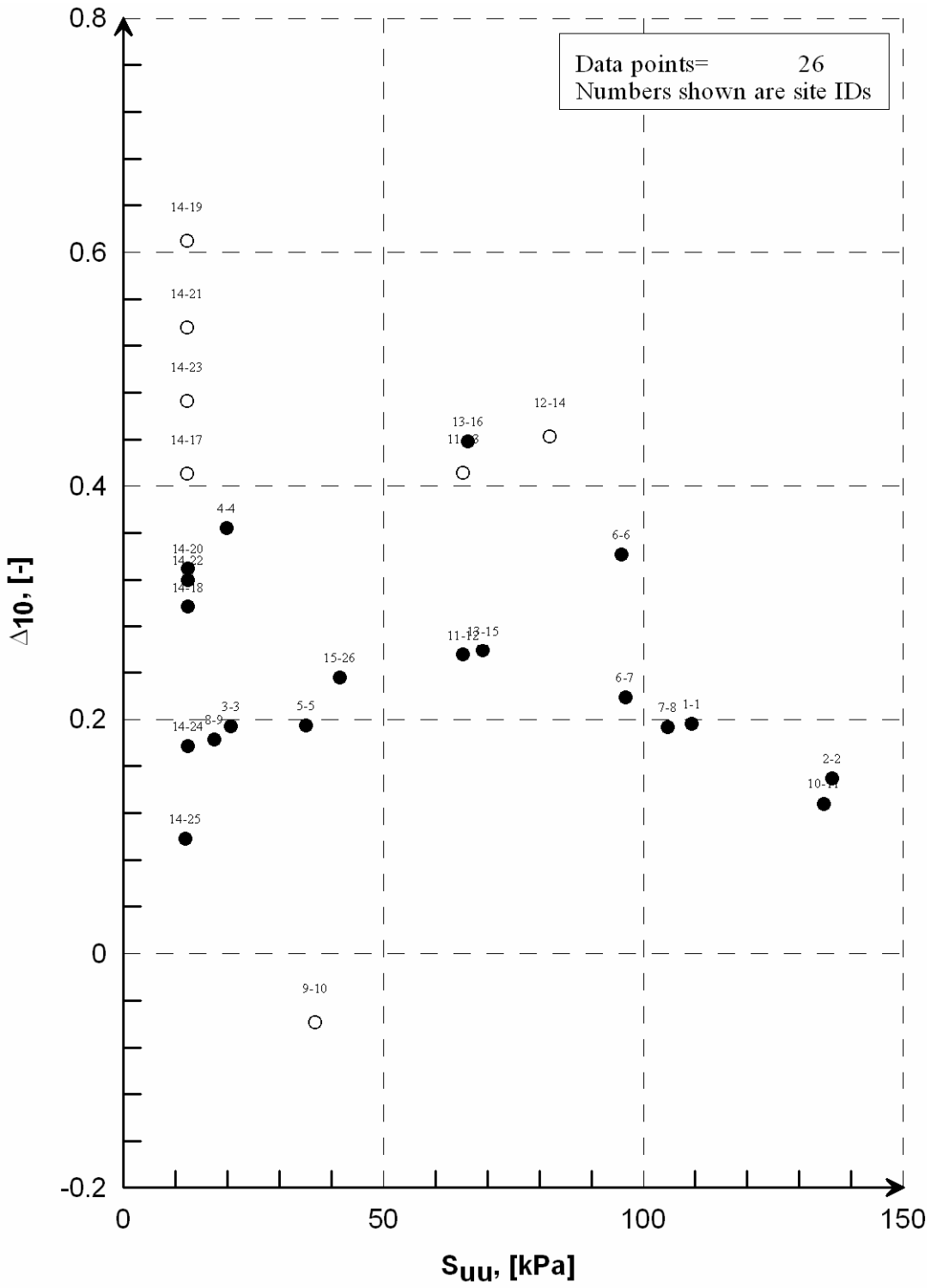

Figure C.1 Relation between "measured" Δ_{10} and the unconsolidated undrained shear strength, S_{uu}, for all the cases in the database. The first number in each plot label refers to the case and the second to pile number, see Appendix A, Table 3 and Table 4, i.e. 6-7 indicates that the 7th pile in the database is a part of case number 6. Piles symbolized by circles are associated with great uncertainty.

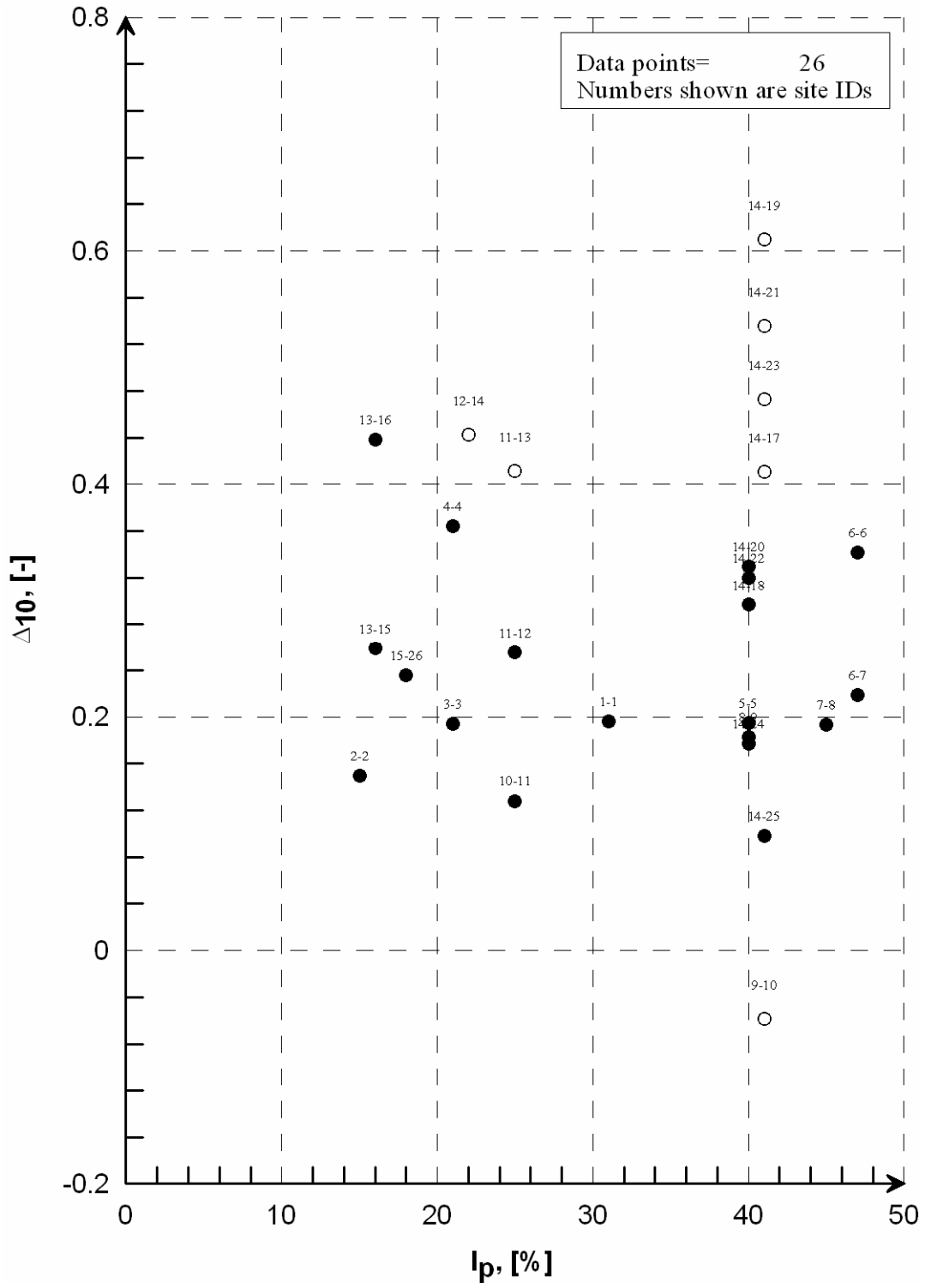

Figure C.2 Relation between "measured" Δ_{10} and the plasticity index, I_p, for all the cases in the database. The first number in each plot label refers to the case and the second to pile number, see Appendix A, Table 3 and Table 4, i.e. 6-7 indicates that the 7th pile in the database is a part of case number 6. Piles symbolized by circles are associated with great uncertainty.

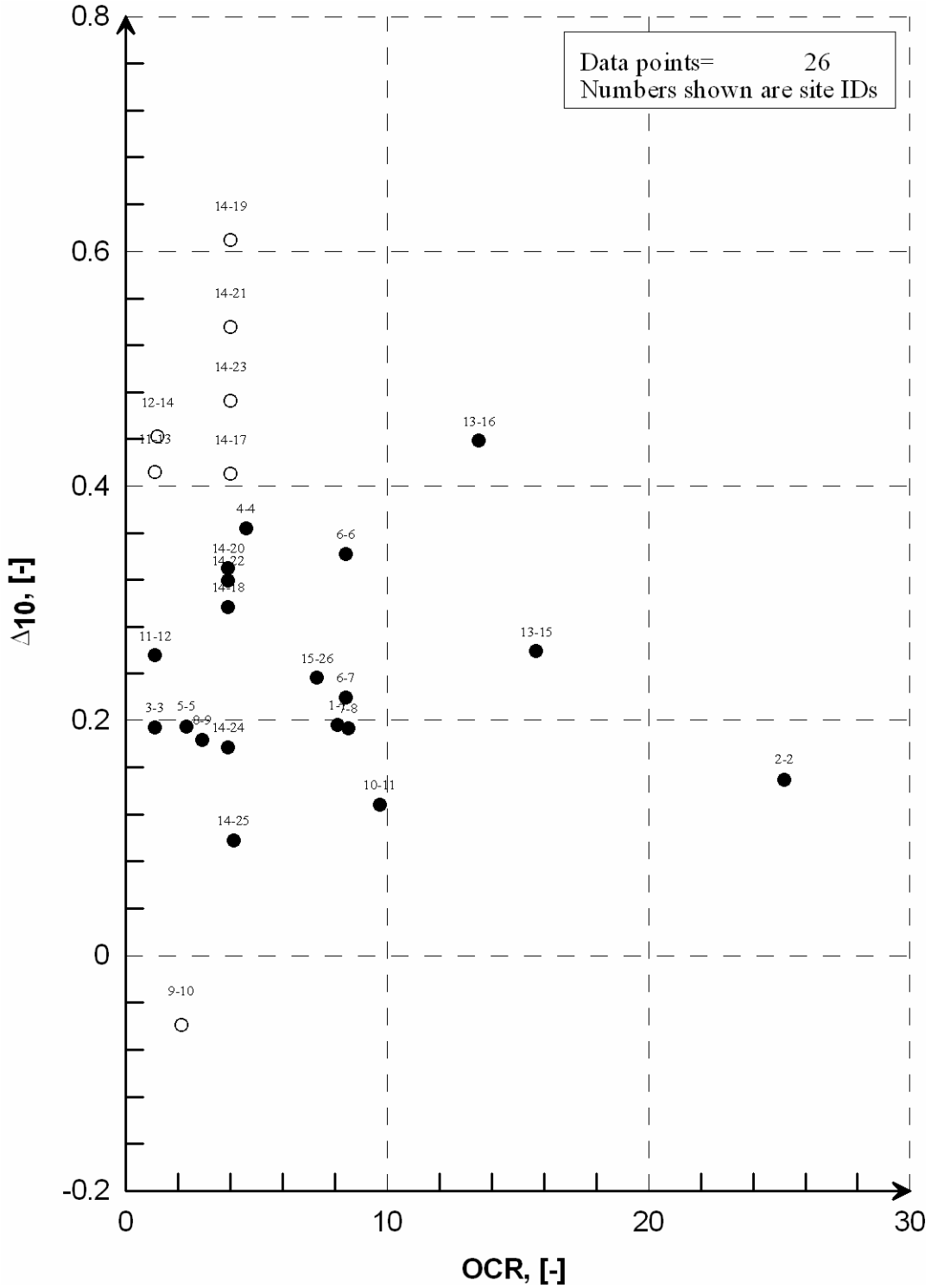

Figure C.3 Relation between "measured" Δ_{10} and the overconsolidation ratio, *OCR*, for all the cases in the database. The first number in each plot label refers to the case and the second to pile number, see Appendix A, Table 3 and Table 4, i.e. 6-7 indicates that the 7th pile in the database is a part of case number 6. Piles symbolized by circles are associated with great uncertainty.

Appendix D:
M2 based on S_{uu} applied to all tests.

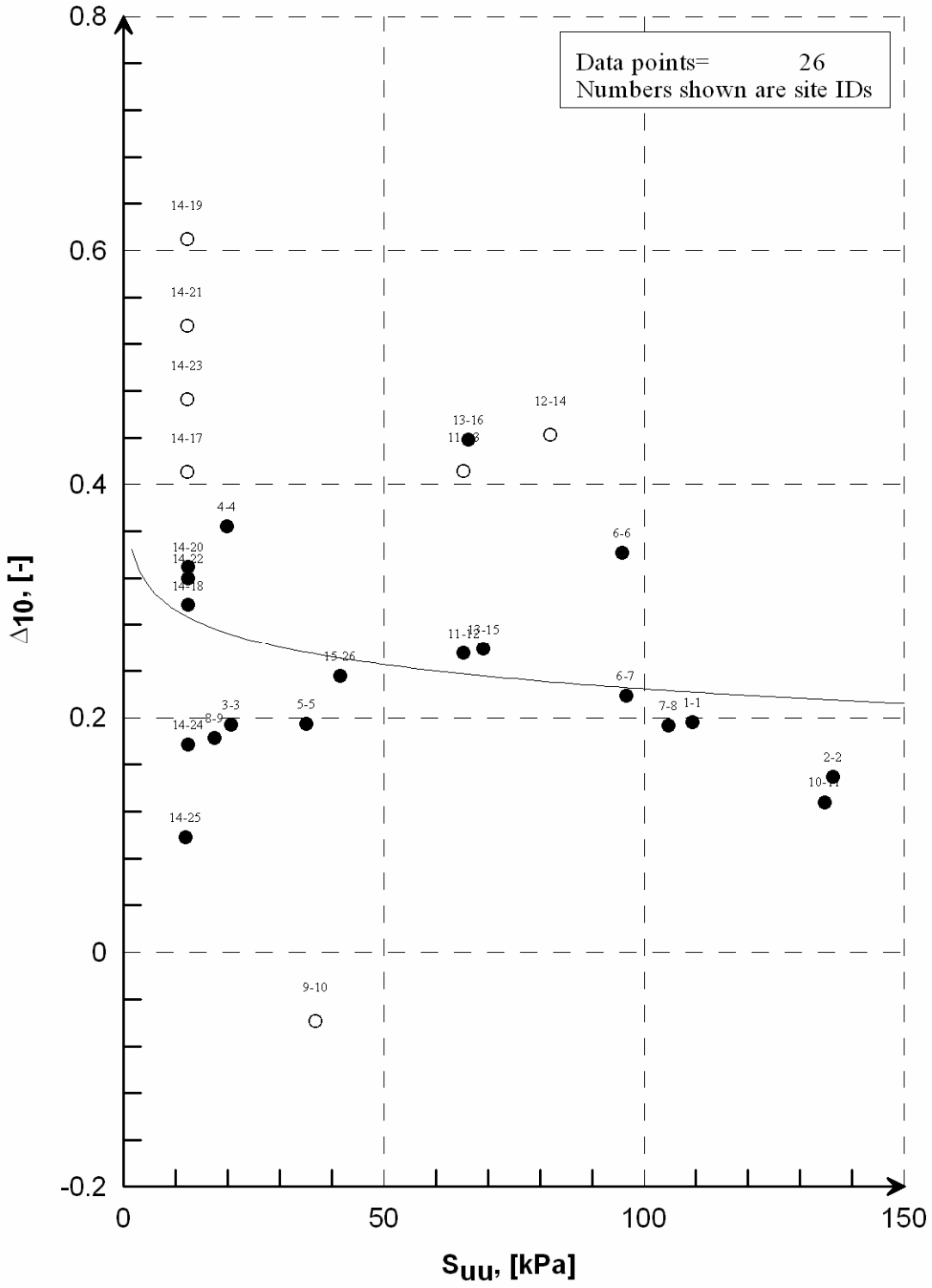

Figure D.1 M2 (solid line) plotted together with the "measured" Δ_{10}s in the S_u-range in consideration. The first number in each plot label refers to the case and the second to pile number, see Appendix A, Table 3 and Table 4, i.e. 6-7 indicates that the 7th pile in the database is a part of case number 6.

Appendix E:
Capacity vs. Time

In the following, it is shown how the different models predict the observed behaviour for the 26 piles in the database, see Appendix A. In connection with all the figures:

Green line	Original NGI-model
Blue line	Modified NGI-model
Black line	AAU1
*	Test results

In each figure, a label like *-* is mentioned. The first * refers to the case and the second to pile number, see Appendix A, Table 3 and Table 4, i.e. 6-7 indicates that the 7th pile in the database is a part of case number 6.

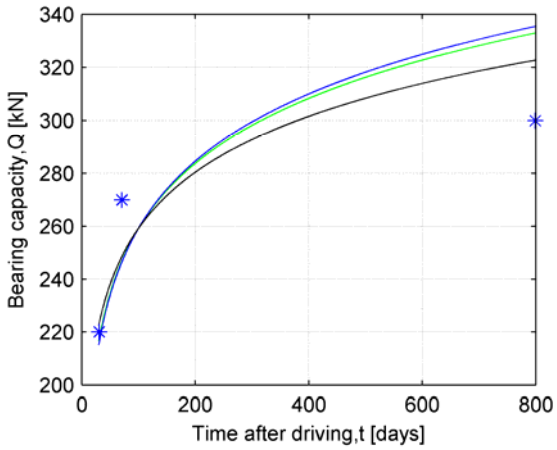

Case: Drammen, 3-3.

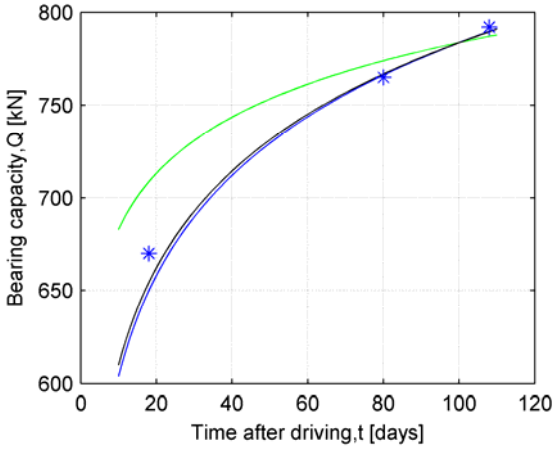

Case: Houston, 1-1.

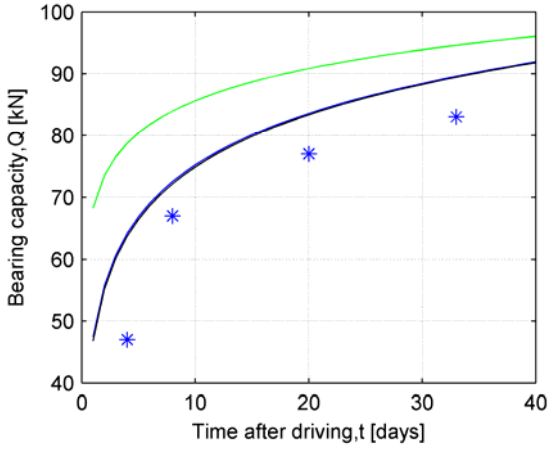

Case: St. Alban, 4-4, Pile A.

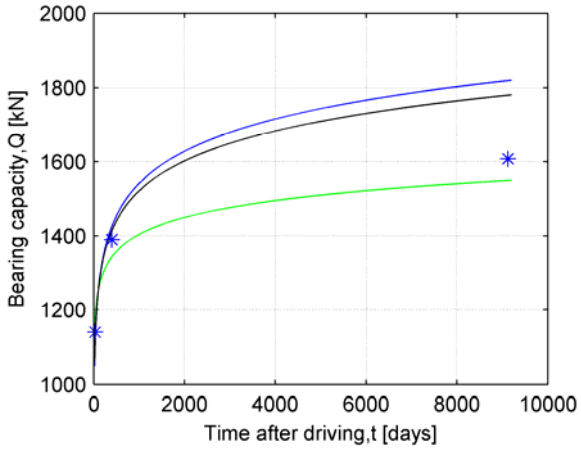

Case: Cowden, 2-2, Pile A.

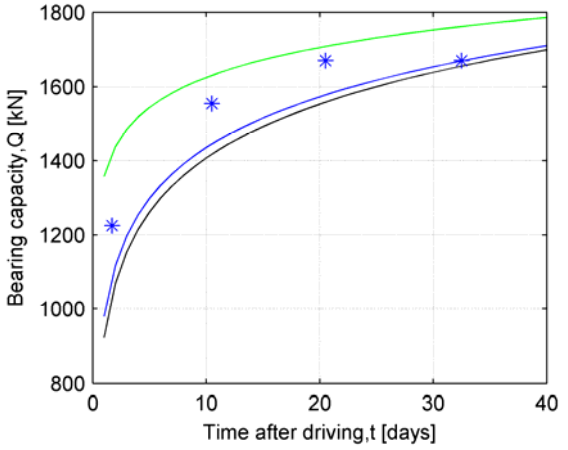

Case: Sumatra, 5-5.

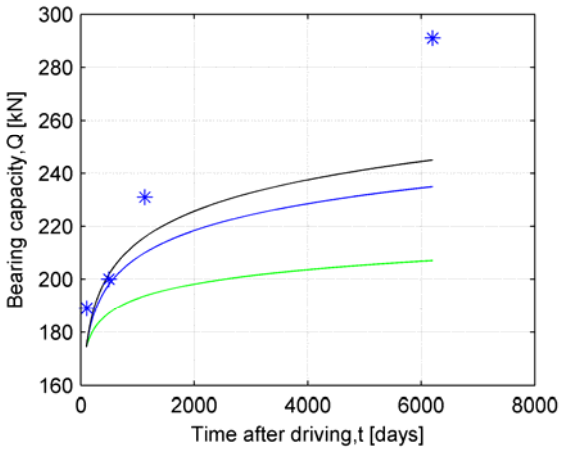

Case: Canons Park, 6-6, Pile D.

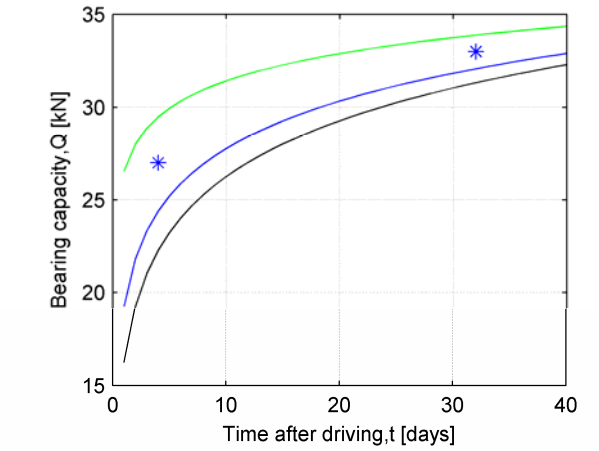

Case: Bothkennar, 8-9.

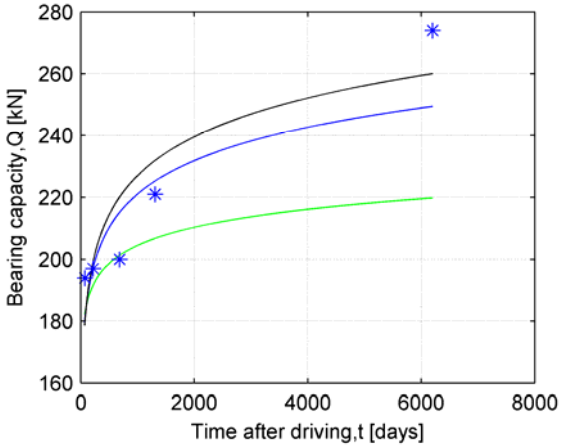

Case: Canons Park, 6-7, Pile B.

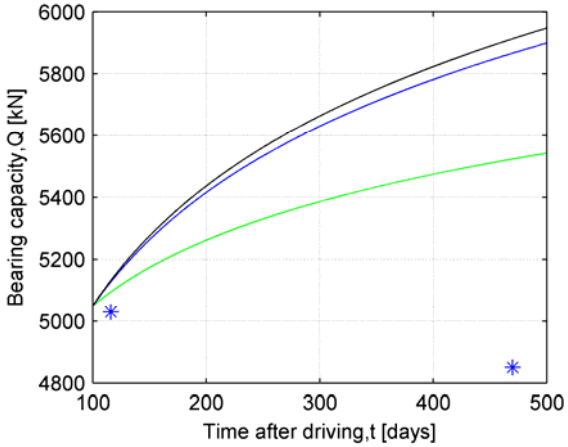

Case: West Delta, 9-10.

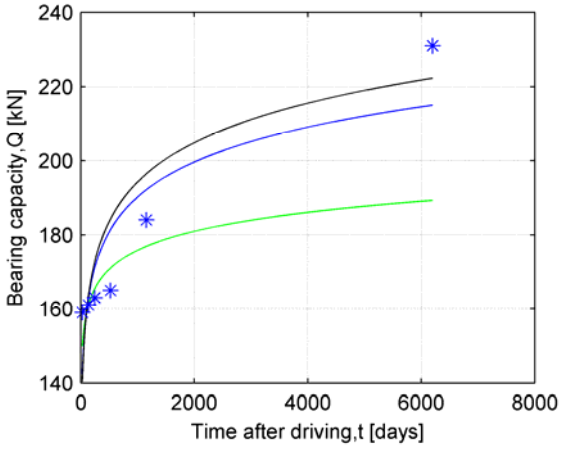

Case: Canons Park, 7-8, Pile A.

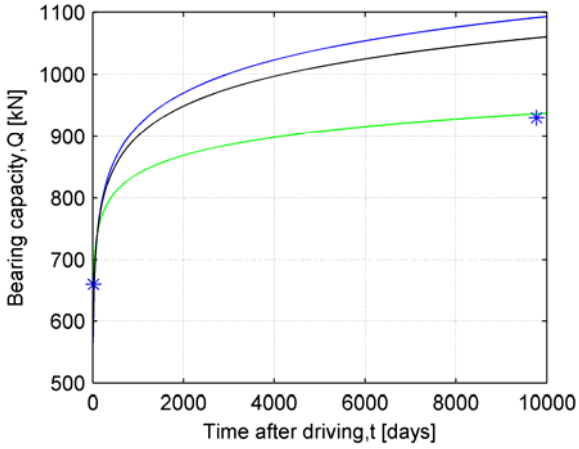

Case: Algade, 10-11.

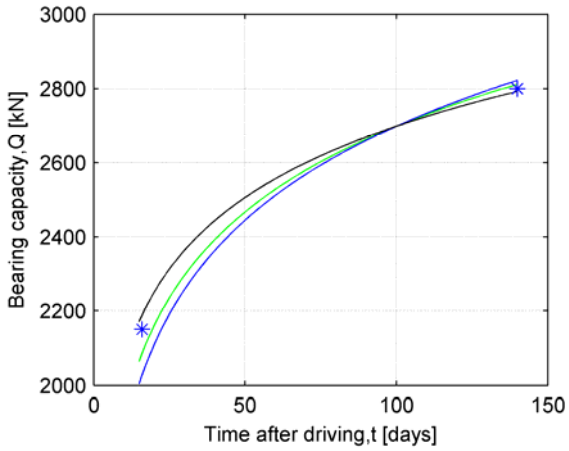

Case: Motorvegbru Drammen, 11-12, Pile P1-16.

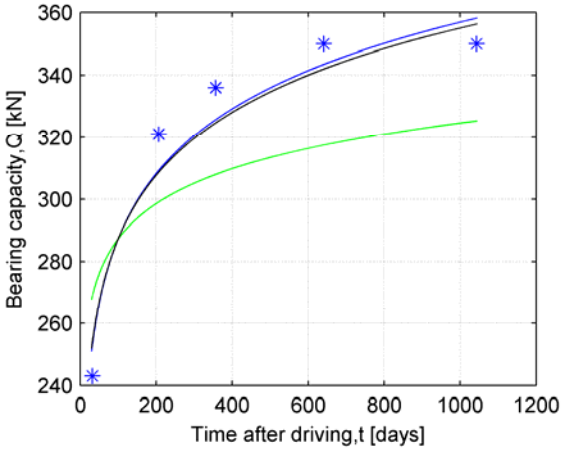

Case: Nitsund, 13-15, Pile I.

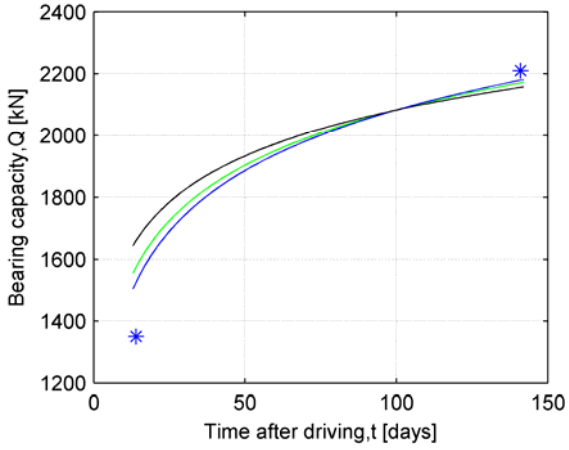

Case: Motorvegbru Drammen, 11-13, Pile P2-16.

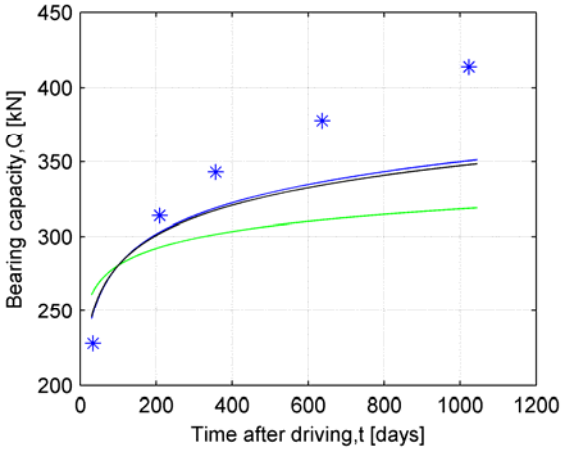

Case: Nitsund, 13-16, Pile II.

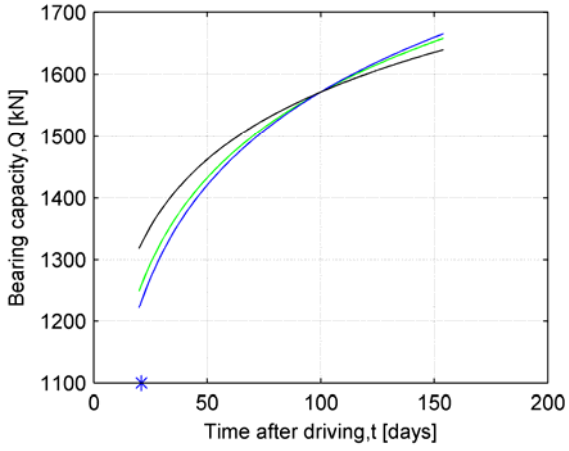

Case: Drammen Stasjon, 12-14.

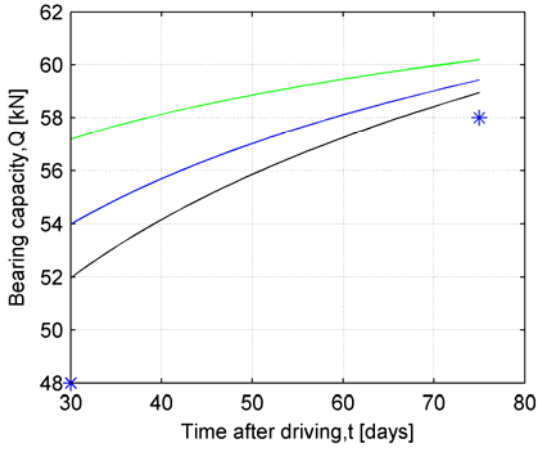

Case: Skå-Edeby, 14-17, Pile A.

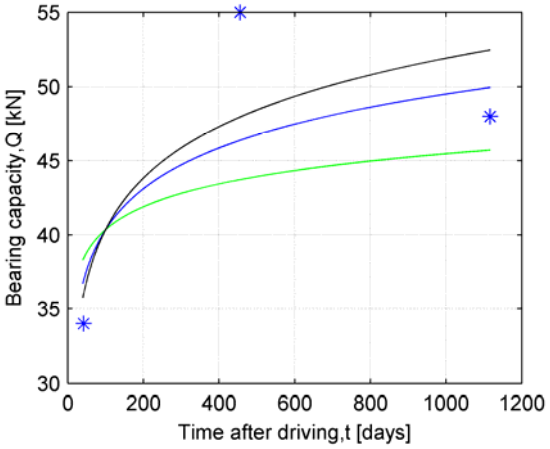

Case: Skå-Edeby, 14-18, Pile A.

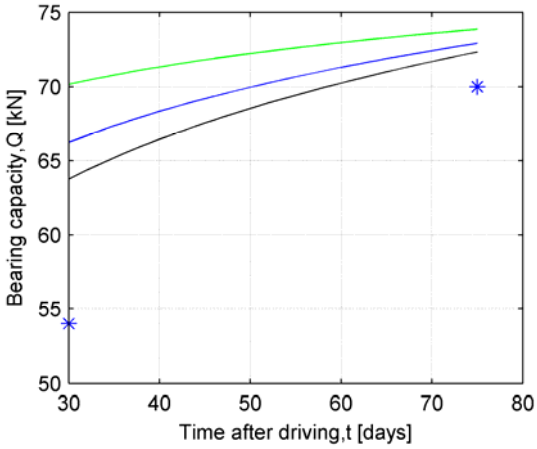

Case: Skå-Edeby, 14-21, Pile C.

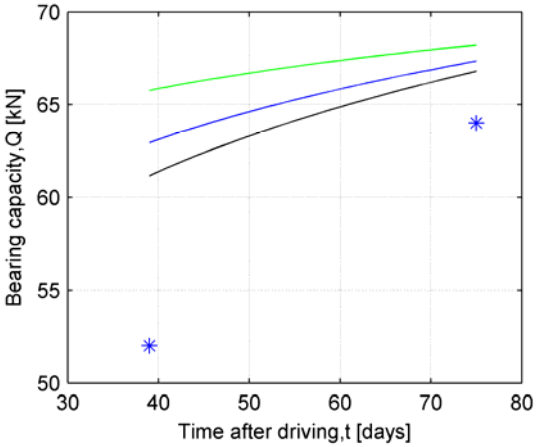

Case: Skå-Edeby, 14-19, Pile B.

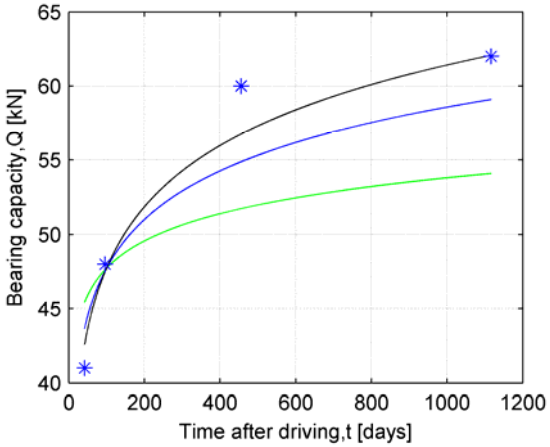

Case: Skå-Edeby, 14-22, Pile C.

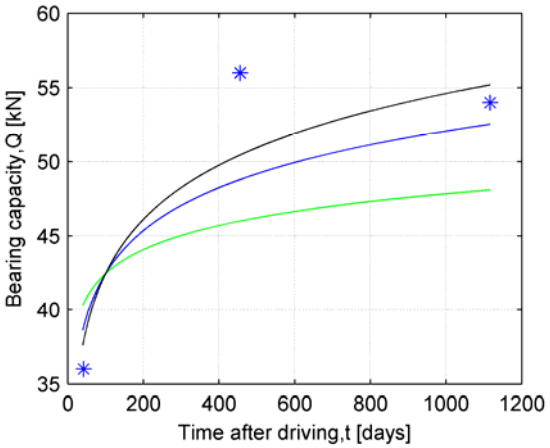

Case: Skå-Edeby, 14-20, Pile B.

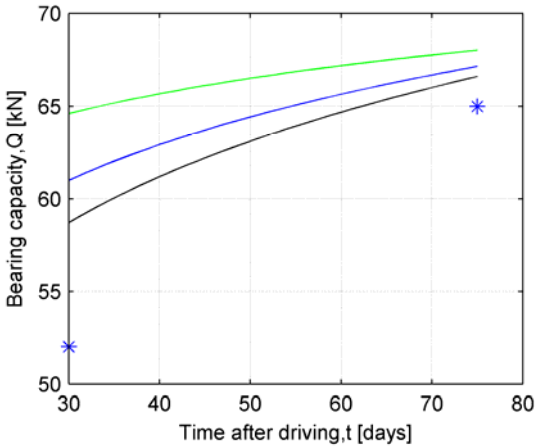

Case: Skå-Edeby, 14-23, Pile D.

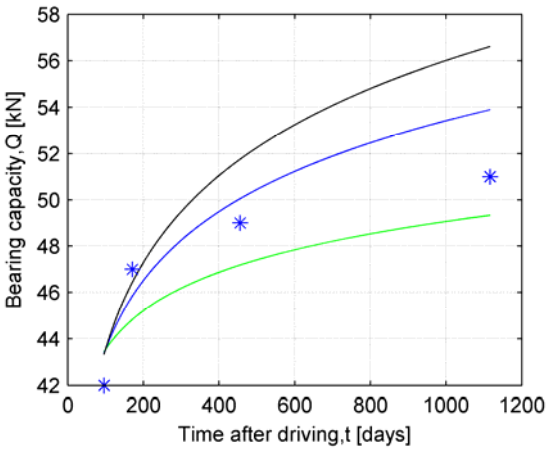

Case: Skå-Edeby, 14-24, Pile D.

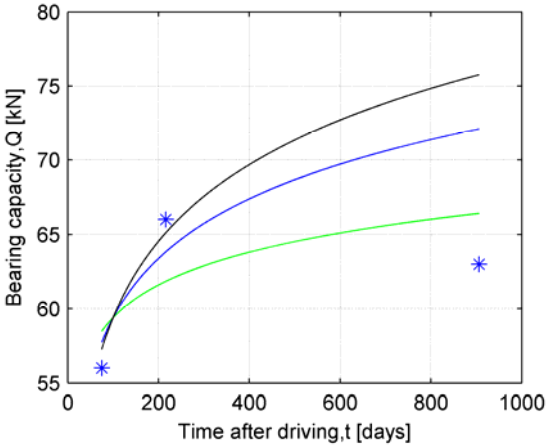

Case: Skå-Edeby, 14-25, Pile E.

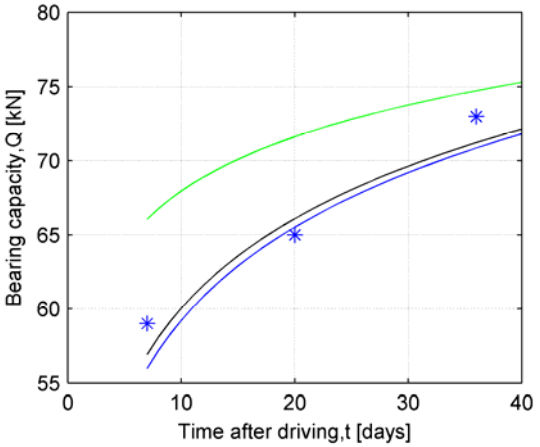

Case: Haga, 15-26.

Appendix F:
Relation between Δ_{10}, S_{ciu}, and *OCR*

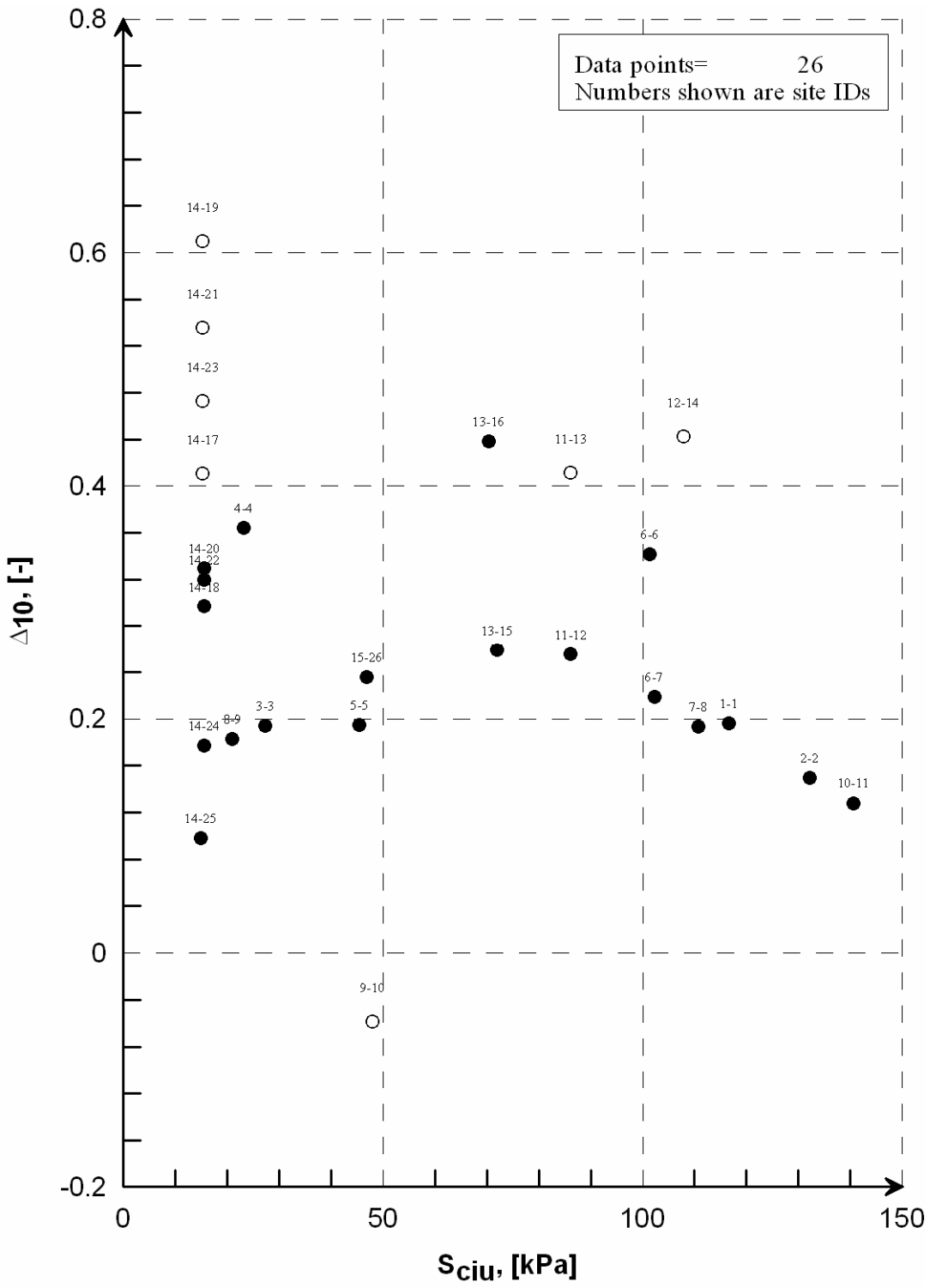

Figure F.1 Relation between "measured" Δ_{10} and the consolidated undrained shear strength, S_{ciu}, for all the cases in the database. The first number in each plot label refers to the case and the second to pile number, see Appendix A, Table 3 and Table 4, i.e. 6-7 indicates that the 7th pile in the database is a part of case number 6. Piles symbolized by circles are associated with great uncertainty.

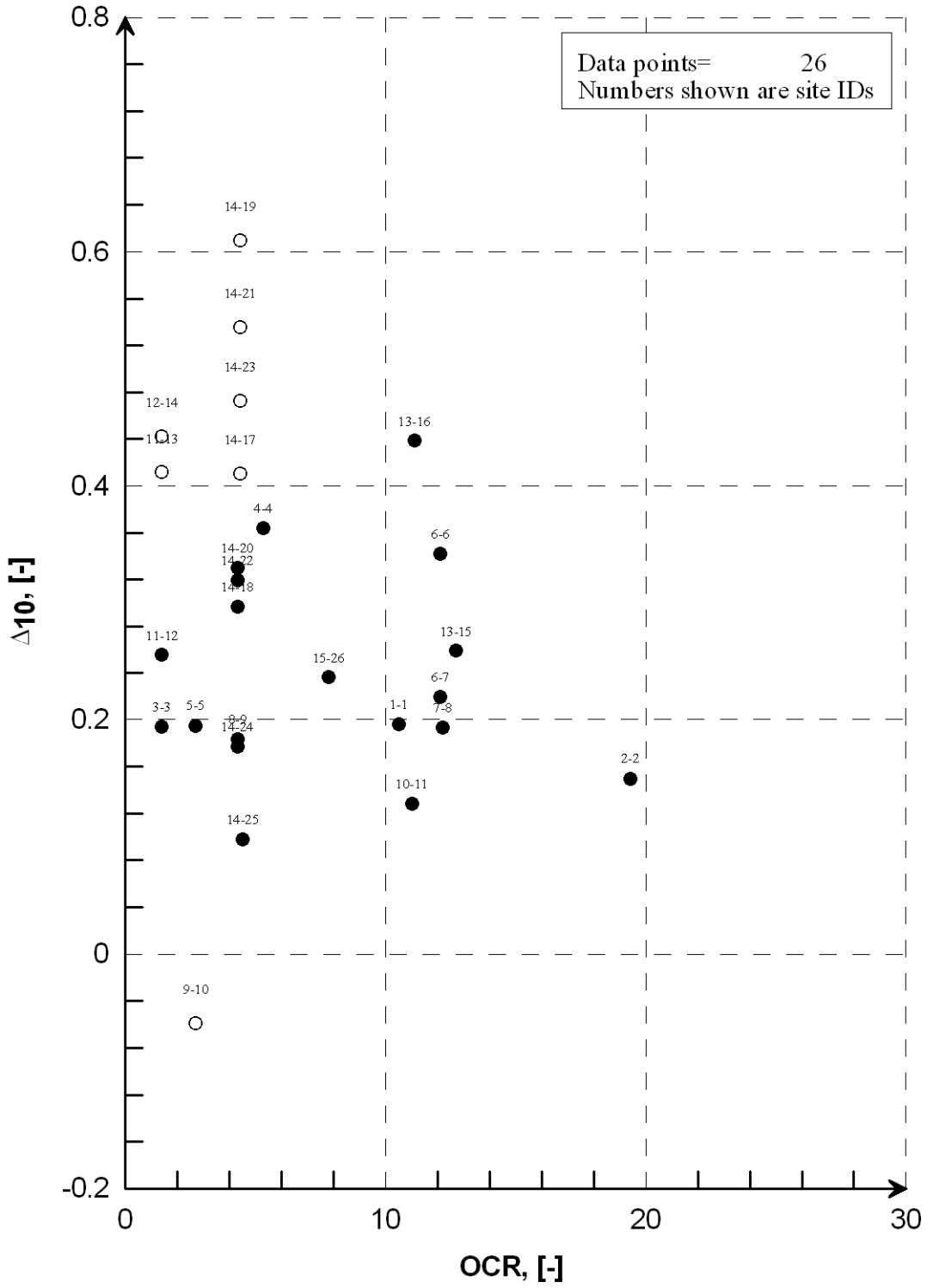

Figure F.2 Relation between "measured" Δ_{10} and the overconsolidation ratio, *OCR*, for all the cases in the database. The first number in each plot label refers to the case and the second to pile number, see Appendix A, Table 3 and Table 4, i.e. 6-7 indicates that the 7th pile in the database is a part of case number 6. Piles symbolized by circles are associated with great uncertainty.

Appendix G:
M2 based on S_{ciu} applied to all tests.

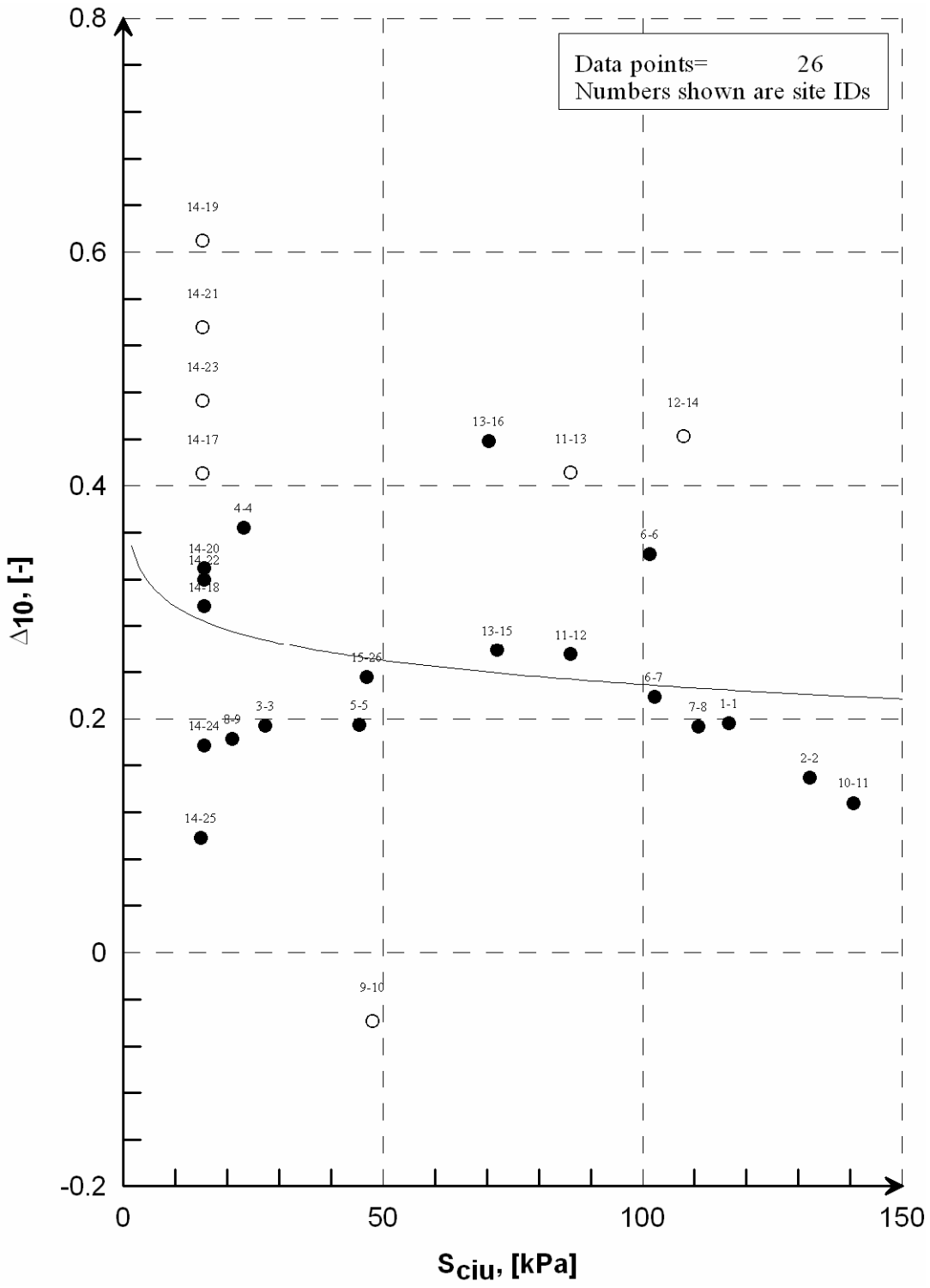

Figure G.1 M2 (solid line) plotted together with the "measured" Δ_{10}s in the S_u-range in consideration. The first number in each plot label refers to the case and the second to pile number, see Appendix A, Table 3 and Table 4, i.e. 6-7 indicates that the 7th pile in the database is a part of case number 6.

Appendix H:
Capacity vs. time

In the following, it is shown how the different models predict the observed behaviour for the 26 piles in the database, see Appendix A. In connection with all the figures:

Green line	Original NGI-model
Blue line	Modified NGI-model
Black line	AAU2
*	Test results

In each figure, a label like *-* is mentioned. The first * refers to the case and the second to pile number, see Appendix A, Table 3 and Table 4, i.e. 6-7 indicates that the 7th pile in the database is a part of case number 6.

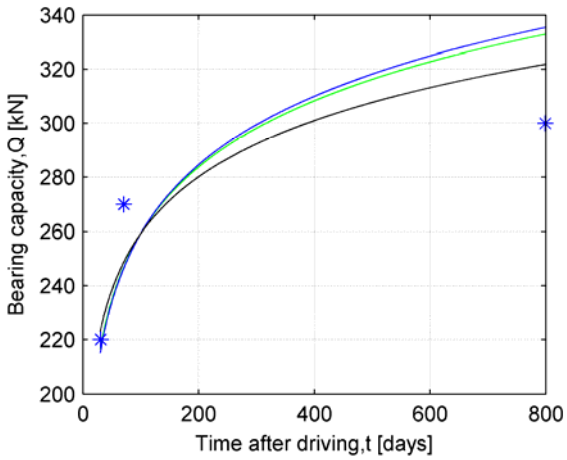

Case: Drammen, 3-3.

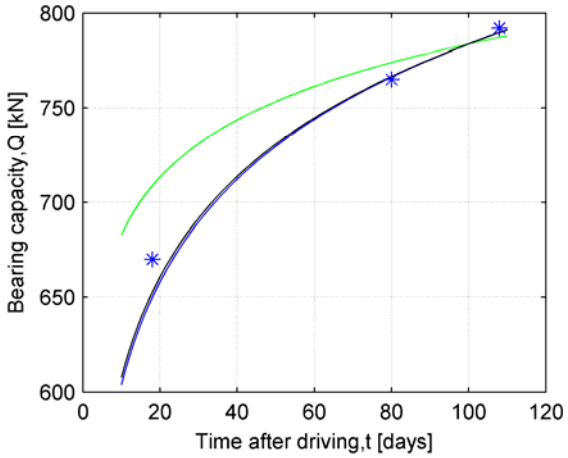

Case: Houston, 1-1

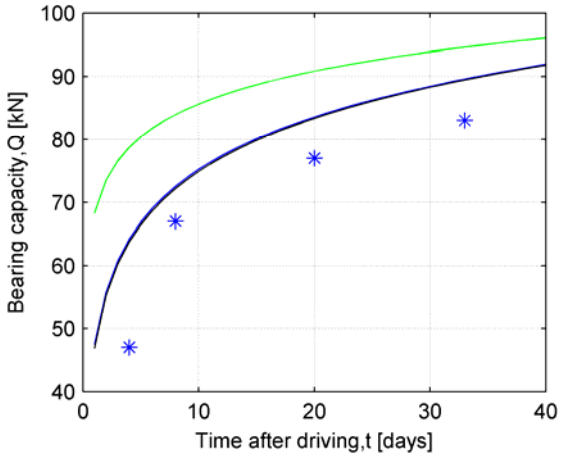

Case: St. Alban, 4-4, Pile A.

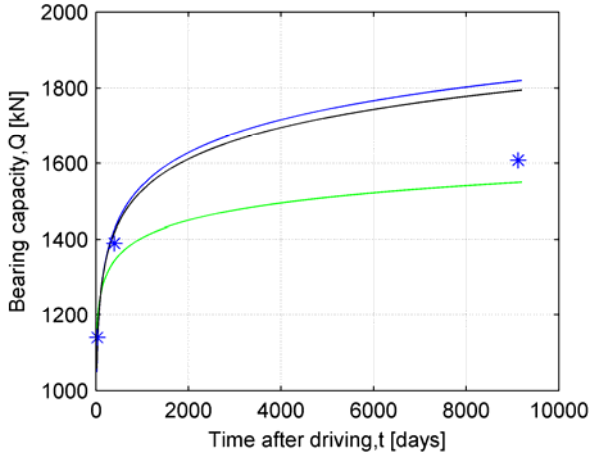

Case: Cowden, 2-2, Pile A

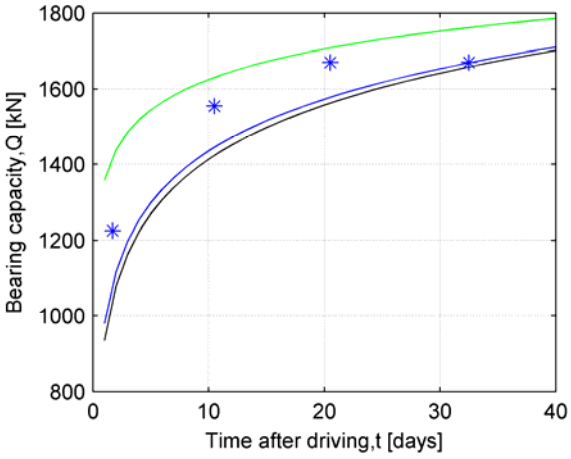

Case: Sumatra, 5-5.

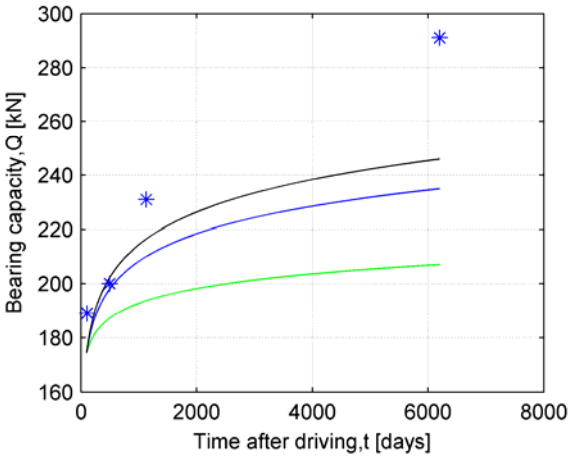

Case: Canons Park, 6-6, Pile D.

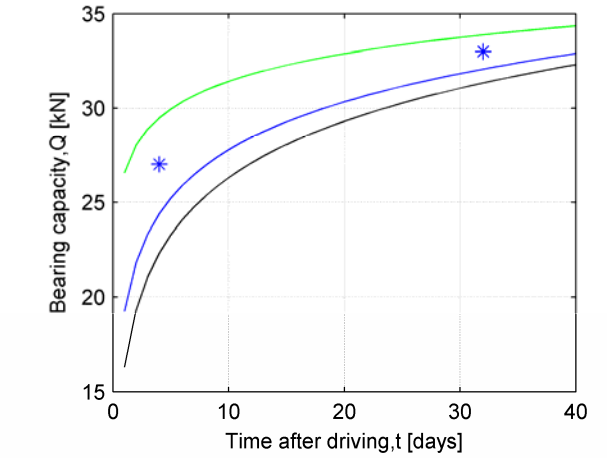

Case: Bothkennar, 8-9.

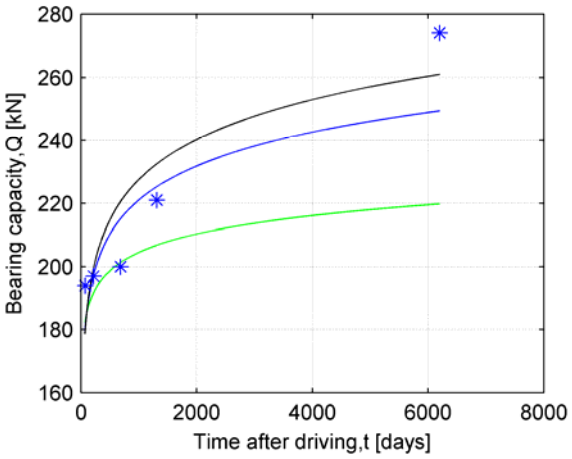

Case: Canons Park, 6-7, Pile B.

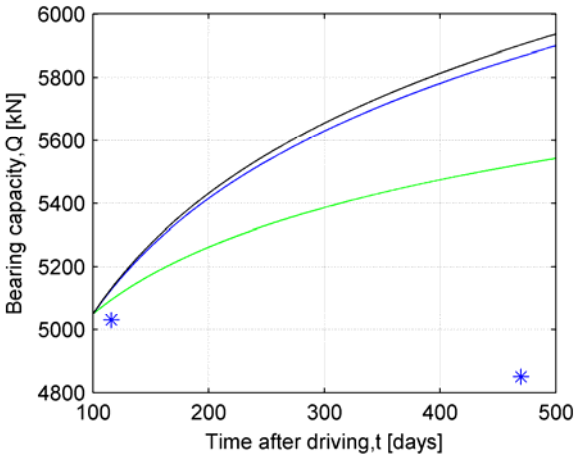

Case: West Delta, 9-10.

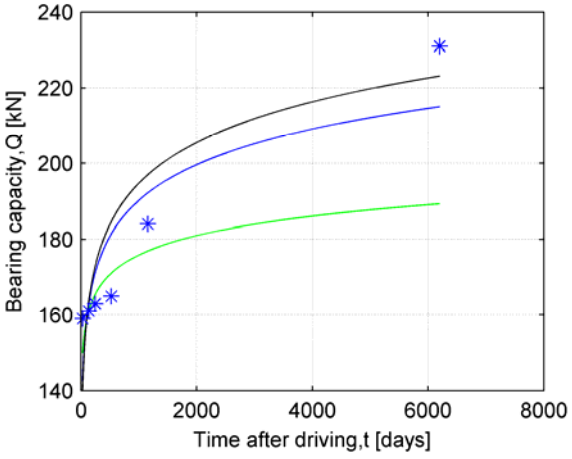

Case: Canons Park, 7-8, Pile A.

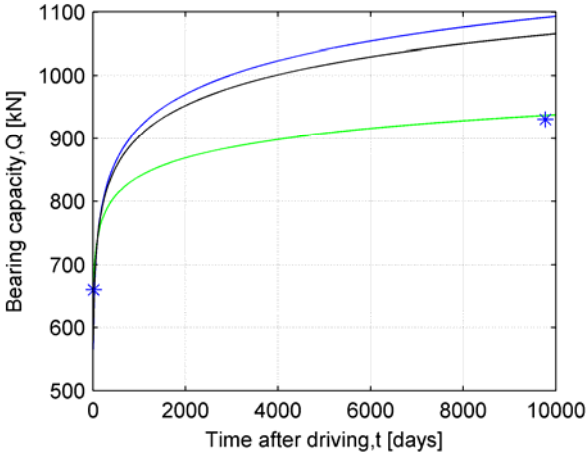

Case: Algade, 10-11.

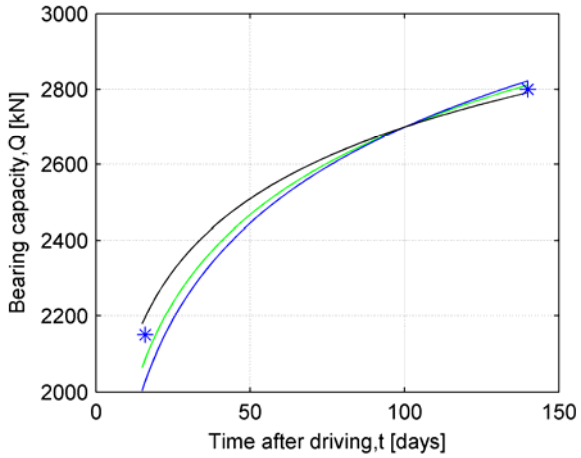

Case: Motorvegbru Drammen, 11-12, Pile P1-16.

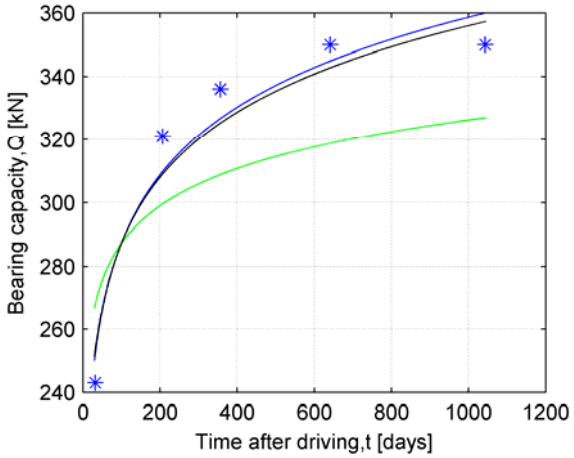

Case: Nitsund, 13-15, Pile I.

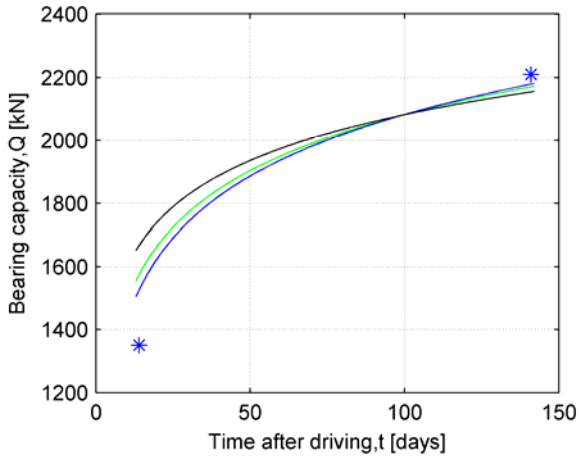

Case: Motorvegbru Drammen, 11-13, Pile P2-16.

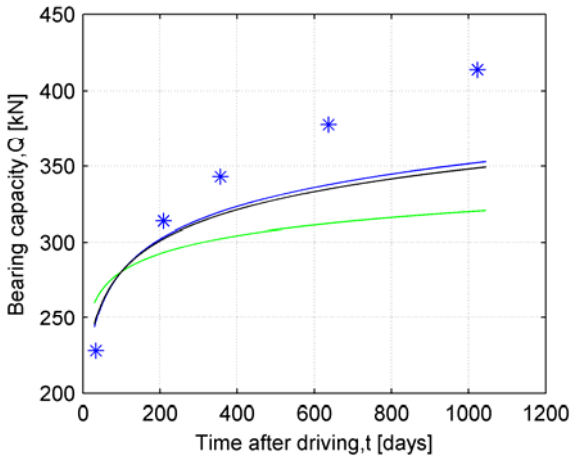

Case: Nitsund, 13-16, Pile II.

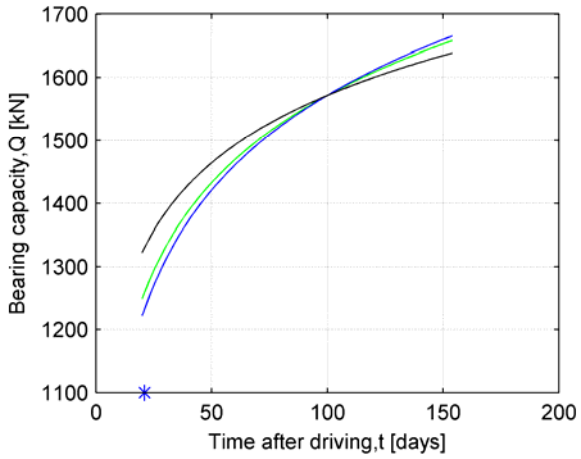

Case: Drammen Stasjon, 12-14.

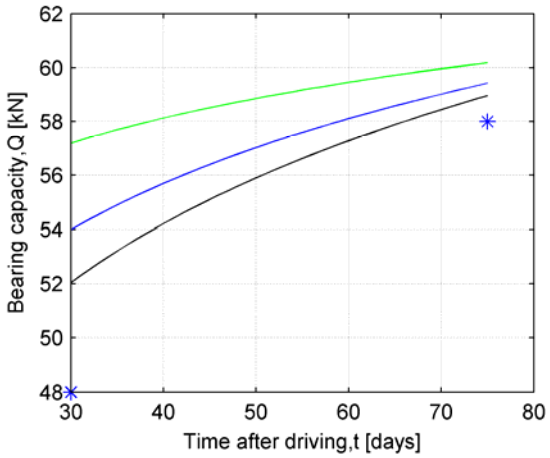

Case: Skå-Edeby, 14-17, Pile A.

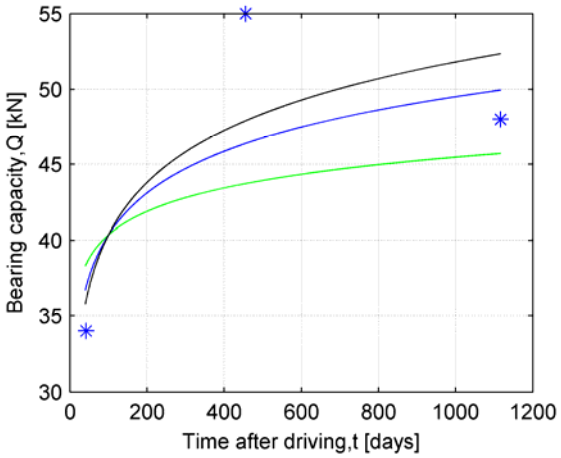

Case: Skå-Edeby, 14-18, Pile A.

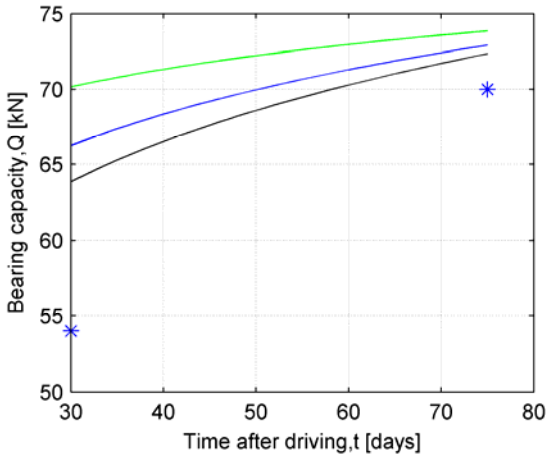

Case: Skå-Edeby, 14-21, Pile C.

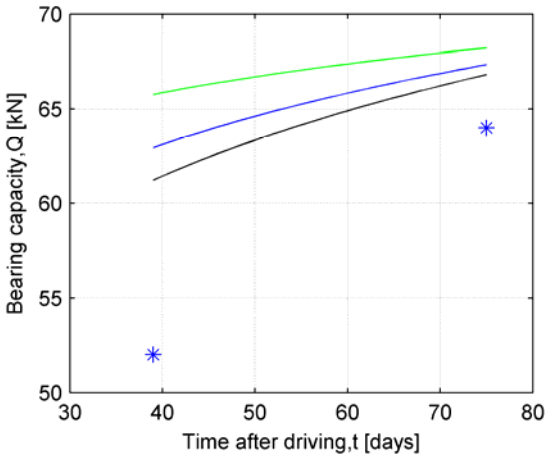

Case: Skå-Edeby, 14-19, Pile B.

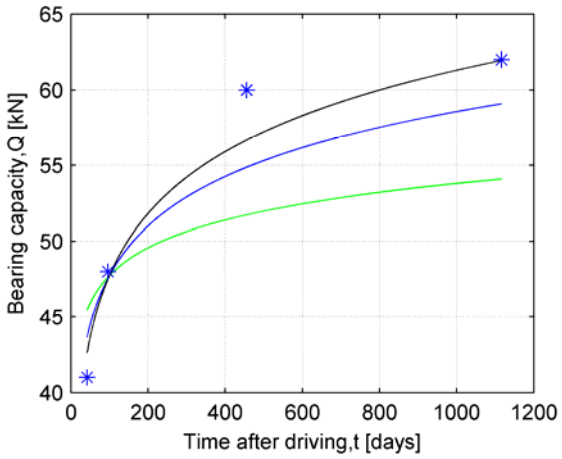

Case: Skå-Edeby, 14-22, Pile C.

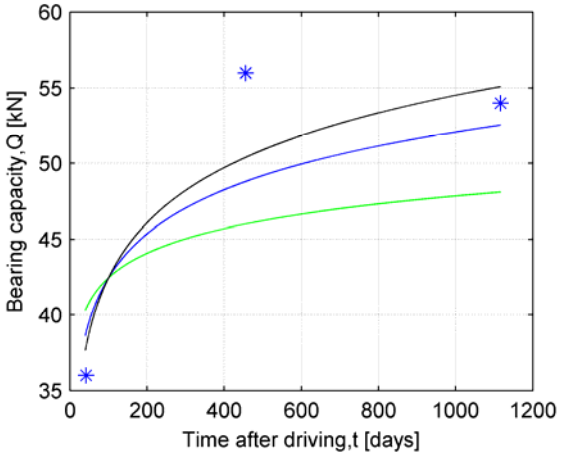

Case: Skå-Edeby, 14-20, Pile B.

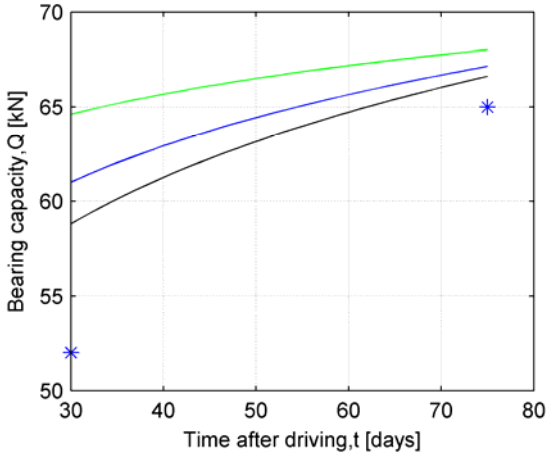

Case: Skå-Edeby, 14-23, Pile D.

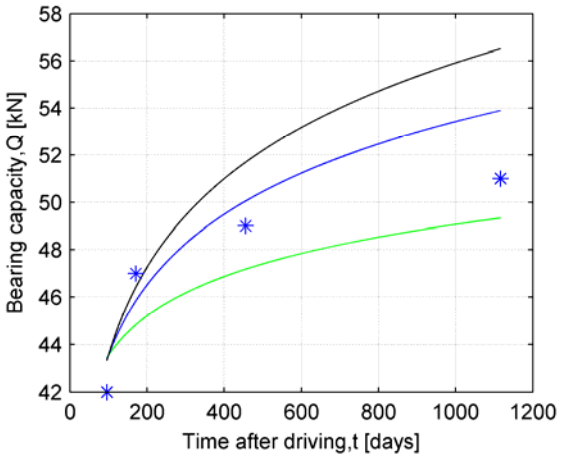

Case: Skå-Edeby, 14-24, Pile D.

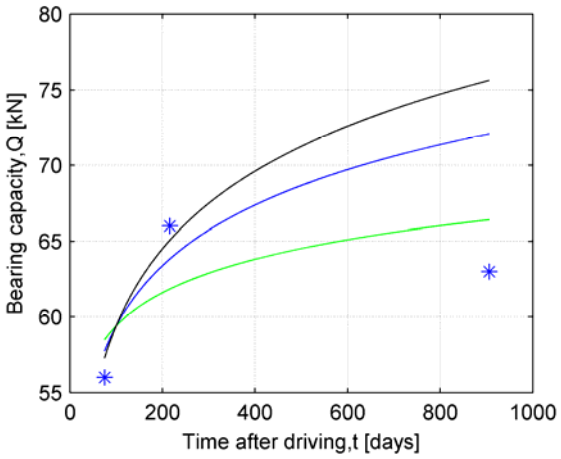

Case: Skå-Edeby, 14-25, Pile D.

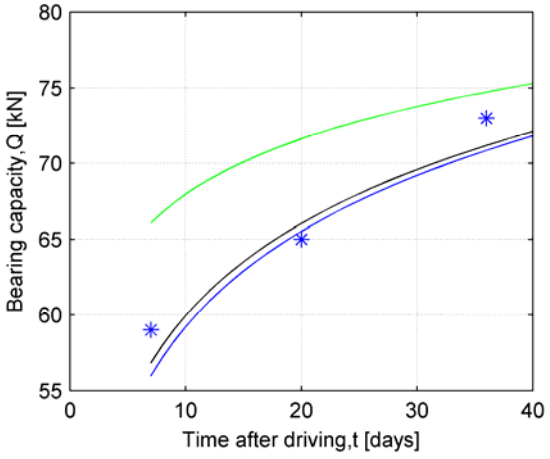

Case: Haga, 15-26.

Title:

The Influence of Time on the Bearing Capacity of Driven Piles.

Authors:

Jensen, J.L., Augustesen, A. and Sørensen, C.S.

Year of publication:

2004

Published in:

In proceedings: NGM-2004 (Nordic Geotechnical Meeting), XIVth Nordiska Geoteknikermötet, Ystad, 19.-21. May 2004, Sweden, pp.D103-D112.

Remarks:

The Influence of Time on the Bearing Capacity of Driven Piles

J. Lysebjerg Jensen
Aalborg University, Denmark, lyseb99@civil.auc.dk
A. Augustesen
Aalborg University, Department of Civil Engineering, Denmark, i5aa@civil.auc.dk
C. S. Sørensen
Aalborg University, Department of Civil Engineering, Denmark,i5css@civil.auc.dk

Abstract: In Danish engineering practice, one of the ways to determine the ultimate bearing capacity of an axially loaded pile is by means of geostatic formulas. In the equation describing the contribution from the shaft friction to the total bearing capacity for piles located entirely or partly in clay, a regeneration factor appears. The regeneration factor accounts for effects of dissipation of pore pressure due to pile driving and true time effects such as ageing on the ultimate bearing capacity. Normally the factor is 0.4 but in this paper, the influence of the undrained shear strength and time on the regeneration factor is investigated. A relation between the quantities is proposed, which in the end may imply an economical benefit in the design of pile foundations.

1 INTRODUCTION

In Denmark, driven squared concrete piles are very commonly used. During pile installation, the soil close to the pile surface is remoulded, and depending on the soil, negative or excess pore-water pressures develop (see for example Tomlinson 1994; Bond & Jardine, 1991). That is, the soil that surrounds the pile will not have the same strength immediately after the installation as it had before pile driving took place.

The excess pore-water pressures dissipate over time, which implies that some of the strength lost during the installation of the pile will be recreated over time. Furthermore, even though the excess pore-water pressures are dissipated the strength of the soil and thereby the ultimate bearing capacity of a pile can increase over time. This is due to true time effects denoted ageing. For further details on the influence of time on soil strength and ultimate bearing capacity of piles, see for example Augustesen *et al.* (2002); Schmertmann (1991); Bergdahl & Hult (1981); Karlsrud & Haugen (1986); Wardle *et al.* (1992); Powell *et al.* (2003); Soderberg (1962); Flaate (1972); Chow *et al.* (1998); Long *et al.* (1999); Chen *et al.* (1999); Axelsson (2000); Fellenius *et al.* (1989) and Skov & Denver (1988).

In connection with geostatic formulas used in Danish engineering practice to calculate the ultimate bearing capacity of an axially loaded pile, time (consoli-dation and ageing effects) is only assumed to influence the calculated skin friction in clay (DS 415, 1998). In reality, time may also play a role in connection with skin friction in sand and toe resistance in both sand and clay. See for example Axelsson (1998); Chow *et al.* (1997) and Konrad & Roy (1987) for comments regarding skin friction in sand and clay and toe resistance in clay.

In Denmark, the regeneration factor r accounts for the effects of time on the strength of the soil surrounding the pile and thereby the ultimate bearing capacity. Furthermore, it is only incorporated in the equation for the skin friction in clay (see Appendix). The r-factor is the ratio between the shear strength in a given depth at a given time after pile driving and the shear strength in the same depth before pile driving took place. That is, since time influences the shear strength, time also influences the r-factor and thereby the bearing capacity. According to the Danish Code of Practice for foundation engineering (DS 415, 1998) the regeneration factor r equals 0.4 if the value of r is not more precisely specified by means of experiments.

The purpose of this paper is to propose a relation between time, shear strength and the regeneration factor r. This can in the end imply a better estimate on r (instead of using r = 0.4) and eventually lead to an economical benefit. The relation is based upon a database (section 2), which is a collection of Danish cases involving static loading tests. In sections 3 and 4, the proposed relation is described and discussed in some details. The geostatic formulas used in Danish engineering practice are mentioned in the appendix.

2 DATABASE

The cases, and thereby the static loading tests from which the relation between time, the regeneration factor, and undrained shear strength is investigated, are listed in Table 1.

As indicated in Table 1, 7 cases are at present time included in the database. In total 12 piles have been subjected to static compression tests and 1 of the them has been tested more than ones. All the piles are squared concrete piles. The side length varies between 0.2m and 0.4m whereas the embedded length varies between approximately 8m and 31m. Furthermore, the piles are located onshore and the thickness of the clay layers varies at the different locations. In connection with the static loading tests all piles did not fail and the time duration between testing and pile driving lies in the interval 13 – 11600 days. In addition, one of the tests was performed as a Constant Rate of Penetration test (Aalborg H. for the 0.3×0.3m pile) and the others as tests with stepwise increase in load. The influence of testing procedure in connection with static loading tests on the stress-strain curve for the

pile and the soil that surrounds is not taken into account. For details on this subject for piles located in clay, see Bergdahl & Hult (1981).

Table 1 Overview of the cases used. # piles and # tests denote the total number of piles and the number of tests performed on each pile, respectively. The column "soil" shows the total length of the part of the pile that is located in clay in percentage of the total embedded length. Furthermore, the type of soil that surrounds the tip is indicated. Failure, Comp./Tension and time state if failure occurred during testing, if the pile was loaded in compression or tension and the time between pile driving and testing, respectively. Clay covers soil types with marked cohesive tendencies.

Case	# piles/ # tests	Cross Section [m]	Embedded length [m]	Soil [% Clay/ Tip]	Failure	Comp./ Tension [C or T]	Time [days]
Budolfi	3/1 or 2	0.2 × 0.2	12.0 – 13.6	50/sand	Yes		22
				91/clay	Yes	C	14/9399
				46/sand	No		18
Fynsværket	2/1	0.3 × 0.3	25.9 – 26.4	84/clay	No	C	26
					No		27
Fynsværket	2/1	0.35 × 0.35	25.8 – 29.0	84/clay	No	C	11600
					No		11600
Hanstholm	1/1	0.3 × 0.3	11.4 – 16.8	39/sand	No	C	13
Aalborg H.	1/1	0.3 × 0.3	30.8	37/gravel	Yes	C	15
Aalborg H.	1/1	0.35 × 0.35	28.0	41/gravel	Yes	C	20
Århus Ø.	2/1	0.4 × 0.4	8.3 – 15.5	63-80/clay	No	C	29
					No		79

3 REGENERATION FACTOR AS FUNCTION OF TIME AND UNDRAINED SHEAR STRENGTH

In this section a relation between the regeneration factor r, time t, and undrained shear strength c_u (determined by means of field vane test), is discussed. The relation is based on experimental load-settlement curves associated with the cases in the database and an approach to reproduce load-settlement curves proposed by Vijayvergiya (1977). First, the assumptions applied in this study related to the Vijayvergiya method are discussed.

3.1 Vijayvergiya method for reproducing measured load-settlement curves

Vijayvergiya (1977) proposes a method to reproduce load-settlement curves for piles by means of equations describing the mobilization of the skin friction and the

base resistance. The method is combined with the geostatic formulas given in DS 415 (1998). Furthermore, the formulas are used to calculate the maximum skin friction and the base resistance. The method is also capable of extending the load-settlement curves for piles, which have not been loaded to failure in connection with a static load test and thereby determine the ultimate resistance.

Vijayvergiya (1977) states that the maximum skin friction and the base resistance are mobilized at a critical movement z_c of the pile skin and the pile base, respectively. The skin friction is fully mobilized at a critical movement $z_{c,skin}$ of 0.2 – 0.3 inches (Vijayvergiya, 1977), whereas Tomlinson (1994) states that $z_{c,skin}$ is 0.3 – 1.0% of the pile diameter. In this analysis $z_{c,skin}$ = 4mm is used, which is approximately the average of the values stated above for piles normally used in Denmark. In this study it is assumed that the base resistance is fully mobilized at a critical movement $z_{c,base}$ equal to 5% of the pile diameter. For comparison, Vijayvergiya (1977) and Tomlinson (1994) for example postulate that $z_{c,base}$ = 4 – 6% and $z_{c,base}$ = 10 – 20% of the pile diameter, respectively.

In DS 415 (1998) the regeneration factor r, the bearing capacity factor N_m, and the material factor m associated with the geostatic formulas have predefined values (see Appendix). In this study, the values of r and N_m for each layer along the pile shaft are fitted in such a way that the calculated load-settlement curve for a given pile by using Vijayvergiya's method is identical to the load-settlement curve obtained by a static load test performed on the same pile. In this way, different values for r and N_m are obtained for each layer along the pile and the relation between undrained shear strength of the different layers surrounding the pile, the regeneration factor, and time, can be studied.

Vijayvergiya's method has been demonstrated by Jensen (2004); Sørensen & Jensen (1996) and Mosher & Dawkins (2000).

3.2 Regeneration factor vs. Undrained shear strength and time.

By using Vijayvergiya's method on every case mentioned in Table 1, it has been possible to investigate the influence of time and undrained shear strength on the regeneration factor. The results are illustrated in Figure 1.

In Figure 1, every single curve represents the fitted regeneration factor for every single cohesive soil layer surrounding the pile as a function of the undrained shear strength for that given layer. That is, the accentuated points (points marked with ▲, ■, x or ○) on each curve symbolize the regeneration factor for a given layer with a certain undrained shear strength at a given time after installation of a given pile. Furthermore, the results are divided into time categories depending on the time duration between pile driving and testing. For example, in the case "Budolfi" the undrained shear strengths for the cohesive soil layers surrounding one of the piles

are 25, 110, 120, 140 and 225kPa, respectively. The corresponding regeneration factors (estimated by reproducing the load-settlement curve for the pile by means of Vijayvergiya's method) are 1.10, 0.92, 0.90, 0.88 and 0.85. The pile was tested statically 9399 days after the installation.

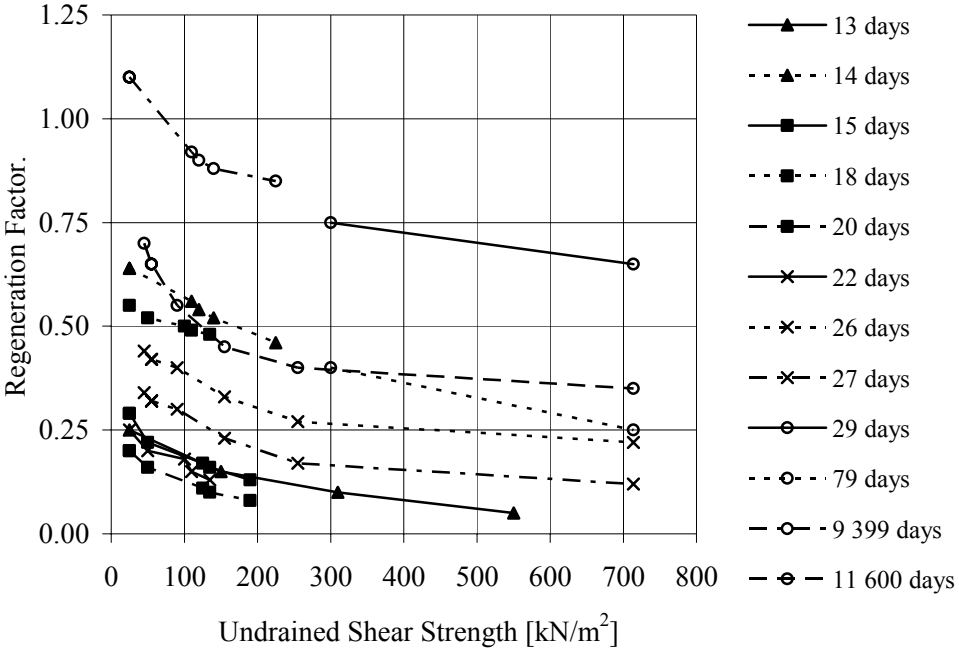

Figure 1 The regeneration factor vs. the undrained shear strength. Time is divided into t ≤ 2 weeks (▲), 2 weeks < t ≤ 3 weeks (■), 3 weeks < t ≤ 4 weeks (x), t > 4 weeks (○). (After Jensen, 2004)

For each time interval the results presented in Figure 1 have been fitted with a curve and depicted in Figure 2. It appears that the curves for the different time intervals are similar in shape. Furthermore, Figure 1 and Figure 2 indicate that the regeneration factor increases when the undrained shear strength decreases. In addition, it seems like the regeneration factor increases with time. If the pile is left untouched for 4 weeks or more, the regeneration factor will exceed 0.4 for undrained shear strengths below 714 kPa. In that case r = 0.4 as proposed by DS 415 (1998) may be too conservative.

The tendencies illustrated in Figure 2 can approximately be described by the following equation:

$$r = 2.31 c_u^{-0.26} \left(\frac{t}{t_{ref}} \right) \quad , \quad t \le 70 \text{ days} \qquad (1)$$

where t is time in days, c_u is the undrained shear strength determined by means of field vane test, and t_{ref} is the reference time. The reference time t_{ref} is found to be

70 days in order to get the best fit. The curves in Figure 2 do almost coincide with curves based on Eq.(1) for t = 14, 21, 28 and 70 days, respectively.

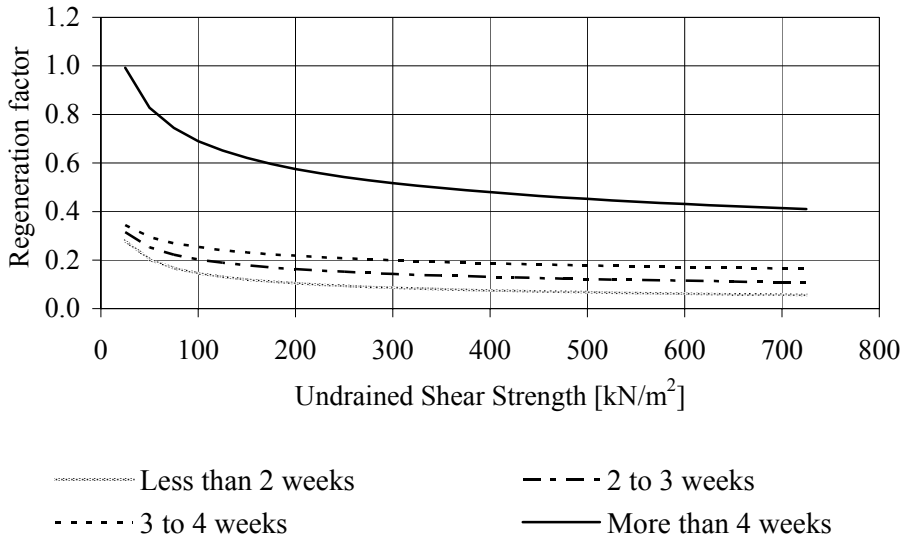

Figure 2 The regeneration factor as a function of undrained shear strength and time. (After Jensen, 2004)

4 DISCUSSION

The above mentioned results should be viewed upon as preliminary investigations on how to use existing data to develop a relation between time, strength and capacity of a pile. In the future, more tests should be subjected to such an analysis in order to calibrate and verify the model. If it turns out that the relation described by Eq.(1) is able to describe the regeneration factor as a function of time, it may imply an economical benefit if the piles can be left untouched for more than 4 weeks.

Some uncertainties and limitations are associated with the analysis of the cases in Table 1. First, the regeneration factor includes effects of pore pressure dissipation and "true" time effects. Since the drainage conditions for the soils associated with the different cases are not the same, the magnitude of the regeneration factor will vary from case to case even though the dimensions of the piles, the time for testing, and the undrained shear strengths of the layers considered, are the same. Secondly, failure did not occur in all the tests associated with the cases in Table 1. Therefore, some uncertainty is connected to the reproduction of these load-settlement curves and thereby the estimation of the regeneration factor. In addition, in the analyses it is chosen that the skin friction and the base resistance for every pile segment are fully mobilized corresponding to deformations equal to 4mm and 5% of the pile diameter, respectively (section 3.1). It can be discussed whether these values are "correct". It seems like the values of the critical deformations do not affect the magnitude of the regeneration factor for the different cohesive soil layers. Thirdly, piles driven within close distance of the tested pile may influence the regeneration factor. This has not been taken into account, but it could be the case in connection

with “Fynsværket”, where the distance between the test piles and the surrounding piles are approximately 1.6m. As mentioned earlier, the type of test (Constant Rate of Penetration or tests with stepwise increment in load) influences the load-settlement curve and thereby the regeneration factor. It should also be mentioned that Eq.(1) is based on undrained shear strengths measured by field vane test. At last, pore pressures were not measured during driving, i.e. whether negative or excess pore pressures were present during driving is not known. This might also affect the magnitude of the regeneration factor at a given time after pile driving and thereby Eq.(1).

5 CONCLUSION

This paper deals with the influence of time and undrained shear strength on the regeneration factor, which is the quantity in connection with Danish engineering practice that accounts for the effects of time on the bearing capacity of an axially loaded pile. 7 cases (13 static pile load tests) have been investigated by means of the approach by Vijayvergiya (1977) and the geostatic formulas used in Danish engineering practice. A relation (Eq. (1)) between time, undrained shear strength and the regeneration factor has been found. If a pile is left untouched for approximately 4 weeks after pile driving, it seems like the Danish Code of Practice for foundation engineering (DS 415, 1998) are to conservative compared to the relation (Eq.(1) and Fig. 2) proposed in this paper regarding the magnitude of the regeneration factor. That is, the proposed relation may imply an economical benefit in the design of pile foundations.

ACKNOWLEDGEMENT

The Authors would like to thank all those who provided data from their archives: Per Aarsleff A/S, Rambøll, COWI A/S and Carl Bro.

APPENDIX

In Denmark the bearing capacity of a single axially loaded pile can be determined by means of geostatic formulas as given in DS 415 (1998). The characteristic value of the total bearing capacity R_{ck} is calculated as the sum of the skin friction R_{sk} and the toe resistance R_{bk}:

$$R_{ck} = R_{bk} + R_{sk} \qquad (2)$$

The characteristic value of the skin friction R_{sk} is calculated by means of empirical equations:

$$R_{sk}=\sum_{i=1}^{n} q_{sik}A_{si} \quad \Rightarrow \quad q_{sik}=\frac{1}{1.5}mrc_u \qquad \text{for cohesion soil}$$
$$q_{sik}=\frac{1}{1.5}N_m q'_m \qquad \text{for cohesionless soil} \tag{3}$$

where q_{sik} is the characteristic value of the skin friction per unit area in the i^{th} layer, A_{si} is the pile skin area in the i^{th} layer, m is a material factor, r is the regeneration factor, c_u is the undrained shear strength, N_m is a bearing capacity factor, and q'_m is the effective vertical stress at the middle of the i^{th} layer.

The characteristic value of the toe resistance R_{bk} is:

$$R_{bk}=q_{bk}A_b \quad \Rightarrow \quad q_{bk}=\frac{1}{1.5}9c_u \quad \text{for cohesion soil} \tag{4}$$

where q_{bk} is the characteristic toe resistance per unit area and A_b is the cross area of the pile toe. In till with cohesive tendencies, the factor 9 can be increased to 18.

In cohesionless soils, it is recommended not to use the geostatic formulas to calculate the toe resistance, but to use the Danish Driving Formula.

REFERENCES

Augustesen, A., Liingaard, M. & Lade, P.V. 2002. Evaluation of Time Dependent Behavior of Soils *International Journal of Geomechanics*. In press.

Axelsson, G. 1998. Long-term Increase in Shaft Capacity of driven Piles in Sand. *Proc. 4th International Conference on Case Histories in Geotechnical Engineering, St. Louis, Missouri* Paper no. 1.25: 301-308.

Axelsson, G. 2000. *Long-term set-up of driven piles in sand*. Ph.D. Thesis, Kungl Tekniska Högskolan (Royal Insitute of Technology), Stockholm, Sweden.

Bergdahl, U. & Hult, G. 1981. Load tests on friction piles in clay. Proc. 10th international conference on soil mechanics and foundation engineering, Stockholm, Sweden 2: 625-630.

Bond, A.J. & Jardine, R.J. 1991. Effects of installing displacement piles in a high OCR clay. *Géotechnique* 41(3): 341-363.

Chen, C.S., Liew, S.S. & Tan, Y.C. 1999. Time effects on the bearing capacity of driven piles. 11th Asian Regional Conference on Soil Mechanics and Geotechnical Engineering, Balkema, Rotterdam, Hong et al. (eds.): 175-178.

Chow, F.C., Jardine, R.J., Brucy, F. & Nauroy, J.F. 1998. Effects of Time on Capacity of Pipe Piles in Dense Marine Sand. *Journal of Geotechnical and Environmental Engineering* 124(3): 254-264.

Chow, F.C., Jardine, R.J., Nauroy, J.F. & Brucy, F. 1997. Time-related increases in the shaft capacities of driven piles in sand. *Géotechnique* .47(2): 353-361.

DS 415 1998. Norm for fundering, Code of Practice for foundation engineering. Dansk Standard (in Danish)

Fellenius, B.H., Riker, R.E., O'Brien, A.J. & Tracy, G.R. 1989. Dynamic and Static Soil Exhibiting Set-Up. *Journal of Geotechnical Engineering* 115(7): 984-1002.

Flaate, K. 1972. Effects of pile driving in clays. *Canadian Geotechnical Journal* 9(1): 81-88.

Jensen, J.L. 2004. *Aksialbelastede betonpæle – statisk analyse af bæreevneforøgelse*. M.Sc. Thesis. Aalborg Universitet. (in Danish)

Karlsrud, K. & Haugen, T. 1986. Axial static capacity of steel model piles in over-consolidated clay, *Publication No.163*, *Norwegian Geotechnical Institute*, have also been published in the *Proc. of 11th International Conference on Soil Mechanics and Foundation Engineering, San fransisco, 1985* 3: 1401-1406.

Konrad, J.M. & Roy, M. 1987. Bearing capacity of friction piles in marine clay. *Géotechnique* 37(2): 163-175.

Long, J.M., Kerrigan, J.A. & Wysockey, M.H. 1999. Measured Time Effects for Axial Capacity of Driven Piling. *Transportation Research Record, Journal of the Transportation Research Board* 1663: 8-15.

Mosher, R.L. & Dawkins, W.P. 2000. *Theoretical Manual for Pile Foundation.,* Engineer Research and Development Center, US Army Corps of Engineers, Washington, DC.

Powell, J.J.M., Butcher, A.P. & Pellew, A. 2003. Capacity of driven piles with time – implifications of re-use. *Proc. XIII ECSMGE, Prague (eds. Vanicek et al.)* 2: 335-340.

Schmertmann, J.H. 1991. The Mechanical Aging of Soils. *Journal of Geotechnical Engineering* 117(9): 1288-1330.

Skov, R. & Denver, H. 1988. Time-dependence of bearing capacity of piles. *Proc. 3rd internatonal conference on the application of stress-wave theory to piles, Ottawa, Canada, (Ed. Fellenius, B.H.)*: 879-888.

Soderberg, L.O. 1962. Consolidation Theory Applied to Foundation Pile Time Effects. *Géotechnique* 12(3): 217-225.

Sørensen, C.S. & Jensen B.S. 1996. Fodpæles bæreevnetilvækst. *XII Nordiska Geoteknikermötet, Reykjavik 26.-28. juni 1996* 1. (in Danish)

Tomlinson, M.J. 1994. *Pile Design and Construction Practice*. London: E & FN SPON. Fourth Edition. ISBN: 0-419-18450-3.

Vijayvergiya, V.N. 1977. Load-movement characteristics of pile. *Ports '77, Proc. 4th Annual Symposium of the Waterways, Ports, Costal and Ocean Division of American Society of Civil Engineers* 2: 269-284.

Wardle, I.F., Price, G. & Freeman, T.J. 1992. Effect of time and maintained load on the ultimate capacity of piles in stiff clay. *Piling: European practice and worldwide trends: Proceedings of a conference.* London: 92-99.

Title:

Capacity of Piles in Clay.

Authors:

Augustesen, A., Andersen, L., and Sørensen, C.S.

Year of publication:

2005

Published in:

Department of Civil Engineering, Aalborg University, Denmark, Internal report, ISSN: 1398-6465 R0502.

Remarks:

The first part of the report is similar to parts of the report "Capacity of Piles in Sand".
To be submitted for publication in an international journal in a shorter version.

Capacity of Piles in Clay

A. Augustesen, L. Andersen, and C.S. Sørensen

Abstract: In the literature, numerous methods are available for the prediction of the axial bearing capacity of piles in clay. However, the reliability of the various methods depends on the soil and pile properties. In this report three models are considered, namely API-RP2A (1987 to present), NGI-99, and ICM-96. The first is developed by the American Petroleum Institute, the last by Jardine and his co-workers at Imperial College in London whereas NGI-99 is a calculation method proposed by Clausen and Aas at the Norwegian Geotechnical Institute. The reliability of the methods is studied by comparison with cases from the literature and static field test performed by Danish and Norwegian companies. Further comparisons between predicted and measured capacities are made based on a number of cases from a database established by the Norwegian Geotechnical Institute. In order to make a consistent evaluation of the calculation procedures, corrections related to undrained shear strength and time between pile driving and testing have been employed. The study indicates that the interpretation of the field tests is of paramount importance, both with regard to the soil profile and the loading conditions. Based on analyses of 268 pile tests distributed on 111 sites it is generally recommended to use NGI-99 independent on pile length, driving conditions (open-ended and closed-ended), loading conditions (compression and tension) and pile diameter. Especially ICM-96 should not be used for piles driven open-ended and loaded in compression, whereas API-RP2A could alternatively be applied to piles driven open-ended and loaded in tension. ICM-96 can advantageously be applied to concrete piles. It is not evident whether it is an advantage to adapt corrections to undrained shear strength and time for all calculation procedures.

1 Introduction

Design methods for piles in clay have been a controversial matter within geotechnical engineering in many years. Calculation methods have been developed, and the issue has been elucidated through dynamic and static testing procedures. In this report, results of a case-study of the axial bearing capacity based upon measured capacities from static loading tests are presented. According to Clausen and Aas (2001a), several similar studies have been carried out during the last 30 years, see for example: Vijayvergiya and Focht (1972), Burland (1973), Meyerhof (1976), Flaate and Selnes (1977), Kraft et al. (1981), Dennis and Olson (1983), Semple and Rigden (1984), Randolph and Murphy (1985), Toolan and Ims (1988), Karlsrud et al. (1992), Nowacki et al. (1992), Mirza (1995), Kolk and Velde (1996), Chow (1996) and Jardine and Chow (1996).

The capacity of driven piles cannot entirely be predicted by theoretical methods. This is due to the fact that stresses acting against the pile and the mechanical properties of the disturbed pile/soil contact zone are not known (Clausen and Aas, 2001a). Therefore, in the authors opinion a design method must be based on a semi-empirical approach and calibrated against a database containing a representative set of, for example, static loading tests. The purpose of this report is to elucidate the advantages and limitations of such well-known calculation procedures. The methods employed are NGI-99, ICM-96, and API-RP2A (API, 1993), which in the following is denoted API-2. The last is a part of the existing API (American Petroleum Institute) procedure, and it is included in this study because many off-shore piles have been designed based on the API recommendations. ICM-96 has been developed at Imperial College in London by Jardine and his co-workers (Jardine and Chow, 1996, 1997), whereas NGI-99 is proposed by Clausen and Aas (2000) at the Norwegian Geotechnical Institute (NGI). The comparison is made by testing the methods against a database (denoted AAU after Aalborg University) based on loading tests, see Section 3. In addition to this, the calculation procedures have also been tested against an existing NGI database (see Section 4 and Clausen and Aas, 2000) and against a combination of the two (Section 5). Based on an evaluation of the methods' ability to predict the measured capacities, guidelines are given for the choice of calculation method to use in different circumstances (e.g. load specifications, length of pile, pile material etc.).

Even if a prediction method gives the correct answer for the total pile capacity, it may not give the correct distribution of skin friction with depth. In such cases, the method could be non-conservative for layered soil profiles. In this report, focus is entirely paid to the reliability of a given calculation procedure to predict the correct total pile capacity. Furthermore, the comparison of the models is based upon characteristic values of the soil parameters, so no safeties in terms of partial coefficients or total factor of safety are introduced. The guidelines given are not based on conservative reasons for design but instead sober facts concerning which model that provides the better description of the data available. If the calculation procedures are applied in limit state design, safety should be employed through partial coefficients or a reasonable total factor of safety.

Figure 1 Flow diagram of PILCAP. The parameter *n* indicates the number of cases. *C*, *TC*, and *SF* denote total capacity, tip capacity, and skin friction, respectively. They are all calculated by means of NGI-99, API-2 or ICM-96 and they correspond to the capacities after 100 days.

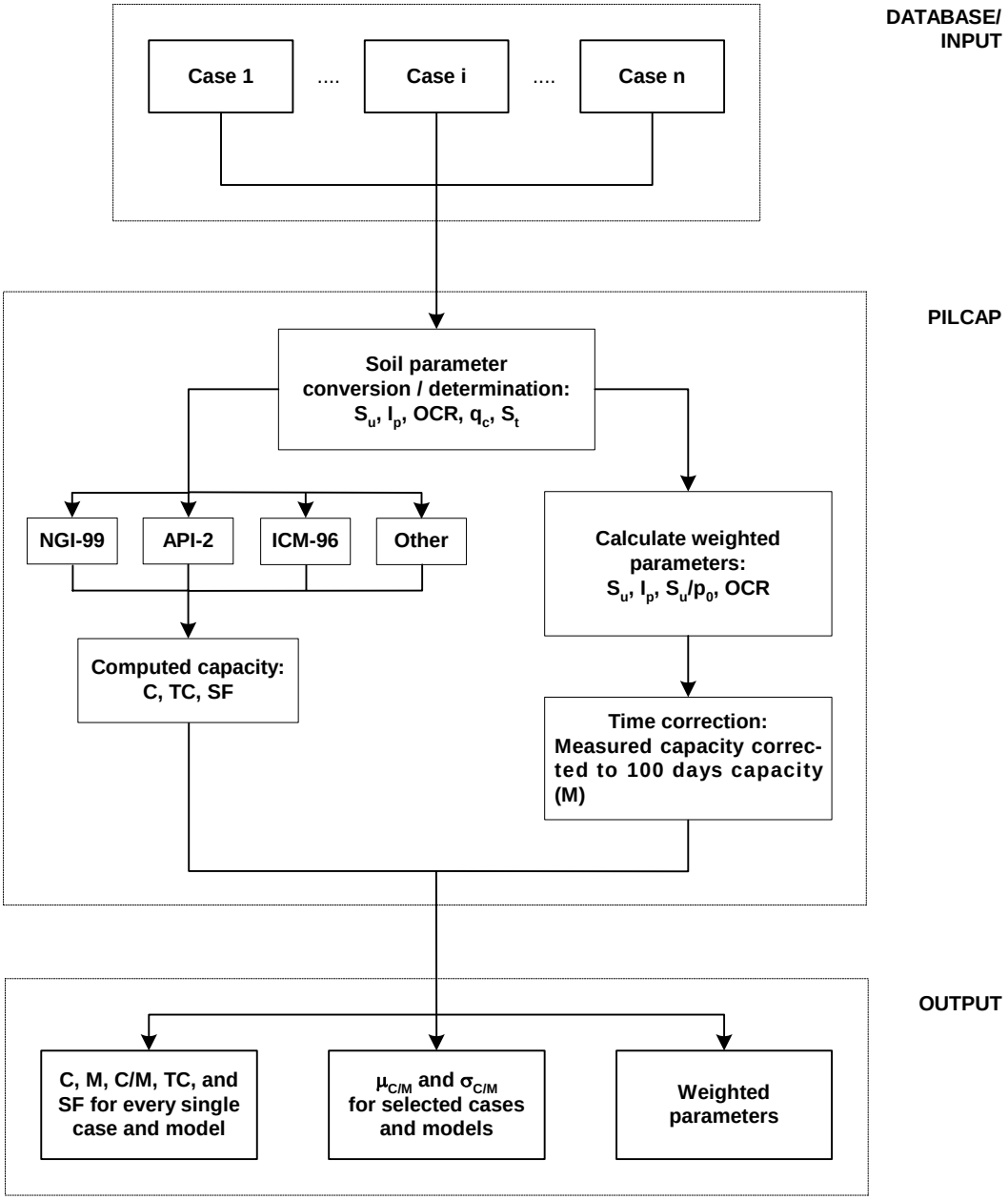

The starting point of this study is the studies done at Norwegian Geotechnical Institute during the last decade. Further, this report is supplementary to the work performed by NGI (Clausen and Aas, 2000, 2001a). A significant number of cases (the AAU database) are added to the NGI database and the conclusions drawn are the results of impartially investigations of the three methods capability to predict measured pile capacities.

Existing calculation methods, API-2, ICM-96 and NGI-99, take only to a limited extent the influence of time into account when predicting the axial capacity of piles. As a matter of fact the database processing program PILCAP used for analyses in this study, see Section 2, includes a time function, which is a function relating capacity to time. The present time function is based on little information. Therefore, an alternative time function based on Augustesen et al. (2005) is implemented in PILCAP. Results of testing the

calculation procedures against the available data by employing a time modified version of PILCAP are presented.

2 Background

As indicated, the analyses are performed by means of the database processing program PILCAP (Figure 1) developed by the Norwegian Geotechnical Institute, see Clausen and Aas (2000). In principle, from every single analysed case, PILCAP reads soil and pile data as well as measured capacities based on loading tests and returns quantities of interests, e.g. the *C/M*-ratio, which is the calculated capacity, *C*, divided by the measured capacity, *M*, at a given reference time (in this case 100 days). That is, the *C/M*-value is a good parameter to use when investigating a certain method's ability to estimate the measured capacities correctly and when comparing the different calculation procedures. Though numerous other parameters are returned by PILCAP, see Clausen and Aas (2000, 2001b) and Appendix G, focus in this report is paid to the average *C/M*-ratio, $\mu_{C/M}$, and the corresponding standard deviation, $\sigma_{C/M}$, when testing the calculation methods against the data being considered. A mean value, $\mu_{C/M}$, equal to unity represents that, on the average, the predicted capacity equals the measured capacity. For $\mu_{C/M} < 0$, the method under consideration tends to underestimate the capacity, and for $\mu_{C/M} > 0$, the method has a tendency to overpredict the capacity. A measure for scatter exhibited by a predictive method is quantified by the standard deviation, $\sigma_{C/M}$. If $\sigma_{C/M} = 0$ there is no scatter in the results, i.e. the capacity is systematically over- or underpredicted.

Uncertainty is introduced in several ways when comparing measured and calculated capacities:

1. Interpretation of soil conditions,
2. Conversion/determination of soil parameters,
3. Interpretation of loading tests,
4. Time correction,
5. Calculation procedures,
6. Pre-shearing and group effects.

As mentioned, the purpose of this report is to estimate the reliability of the calculation procedures NGI-99, API-2, and ICM-96. Except for pre-shearing and group effects, items 1-4 have been carefully considered in order to obtain a consistent treatment of the data and thereby to reach a reliable validation of the methods (item 5). In the remaining part of this section, the most important corrections and assumptions related to PILCAP and this study will be discussed. The subsections refer to Figure 1:

1. **Definition of failure.** All loading tests represented in the database are analysed based on the same failure criterion, see Section 2.1.
2. **Soil parameter determination** (Section 2.2). The different calculation procedures and time correction formulae depend on different soil parameters. Further, the undrained shear strengths associated with the different cases are not established in the same way. Therefore, a unique set of rules have been used to convert one type of shear strength to another, see Clausen and Aas (2000) and Appendix A. In addition to this, default values for plasticity index, I_p, sensitivity, S_t, CPT tip resistance, q_c, pile/soil friction angle, δ_f, and overconsolidation ratio, *OCR*, are determined if they are not given. In Appendix F the input file of all available data and thereby the original values of the soil parameters can be seen, whereas Appendix G shows an output file where the modified soil parameters can be studied.
3. **Time correction**. The measured capacities are compared to the calculated capacities, which correspond to the capacities of the piles 100 days after installation – in the following referred to as the 100-days capacities. In order to make a consistent comparison, the measured capacities are time corrected to corresponding 100-days capacities, see Section 2.3. The function applied for time correction is based on average soil parameters, i.e. an average undrained shear strength, *OCR* and I_p is associated with every single pile, see Clausen and Aas (2000) and Augustesen et al. (2005) for further details.
4. **Prediction methods**. A brief introduction to the calculation procedures API-2, NGI-99, and ICM-96 is given in Section 2.4.

2.1 Failure criterion

The measured capacities associated with each case in the database are based on failure loads corresponding to settlements equal to $0.1d$, where d is the equivalent pile diameter referring to an equivalent circle diameter for square and hexagonal piles. It is chosen to make use of this definition because it is most likely that both the toe and shaft resistance are fully mobilised (Vijayvergiya, 1977; API, 2000).

In addition to the failure criterion, the loading test results, and thereby the magnitudes of the measured capacities, may also be influenced by group effects and pre-shearing effects. That is, if a pile has been tested more than one time the effects of previous loading tests may influence the capacity. Karlsrud and Haugen (1986) and Bullock et al. (2005a,b) report that pre-shearing effects can be substantial and that pre-shearing

results in higher capacities compared to the "intact equivalents". However, Bergdahl and Hult (1981) postulate in the light of their tests that it is not possible to show any change in capacity as a result of previous loading tests for piles in clay. In contrast, Jardine et al. (2005c) found for piles in sand that any aged pile loses a substantial part of its capacity as it undergoes first time failure and relaxation to zero load. If the pile is allowed to rest, it develops a degree of capacity recovery. But pre-tested piles appear to always fall short of their "intact equivalents". Pre-shearing effects have not been taken into consideration in this study even though some of the piles represented in the databases have been subjected to several loading tests. Group effects are also not considered here.

2.2 Soil parameter determination

Of the strength and deformation parameters associated with clayey soils, the unconsolidated undrained shear strength, S_{uu}, and plasticity index, I_p, are the key parameters in NGI-99, see Section 2.4 and Appendix B. If I_p is not given it is assumed that $I_p = 25\%$.

ICM-96 is primarily based on *OCR*, sensitivity, S_t, CPT tip resistance, q_c, and the pile/soil friction angle, δ, which is correlated to the plasticity index, I_p (Section 2.4). If S_t is not given it is determined according to:

$$(1) \qquad S_t = 2\frac{p_0}{S_u}, \quad 1.0 \le S_t \le 8.0$$

where p_0 is the vertical effective normal stress at a given depth. If not given *OCR* and q_c are determined based on the consolidated undrained shear strength, S_{ciu}, see Appendix D and Augustesen et al. (2005). It should be mentioned that in many of the cases associated with this study the input parameters for ICM-96 are estimated, which naturally introduces some uncertainty in the predictions. This may influence the conclusions drawn in the following sections.

The key soil parameters associated with API-2 are the unconsolidated undrained shear strength, S_{uu}, and the strength to effective overburden pressure ratio, S_{uu}/p_0 (Section 2.4 and Appendix C), which is highly correlated with *OCR*.

In summary, all three calculation procedures depend explicitly or implicitly on the undrained shear strength, S_u. Since the kind of input shear strength used in the calculation procedures varies and since the shear strengths associated with the different cases have been established in different ways (triaxial test, vane shear test, CPT etc.), PILCAP includes a routine that converts one type of shear strength to another. Thereby, the comparison of the methods is made consistent even though the conversion is a controversial matter within the profession of soil mechanics. For more details see Augustesen et al. (2005) and Appendix A.

2.3 Time correction

Time correction is at the moment only associated with skin friction for the part of the pile located in clay. Since the loading tests represented in the database are performed at different times after initial driving, PILCAP includes a time function that extrapolates the measured capacity at a given time to the capacity to a given reference time. Furthermore, if it is assumed that the calculation methods estimate capacities corresponding to the same reference time, the calculated *C/M*-ratios are directly comparable.

The time function employed in this study for correction of measured capacities can be expressed as:

$$(2) \qquad Q(t) = Q_0 \cdot \left\{1 + \Delta_{10} \cdot \log_{10}\left(\frac{t}{t_0}\right)\right\}$$

where Q is the capacity at time t [days] after the end of installation and Q_0 is the capacity corresponding to the reference time, t_0. Finally, Δ_{10} is the capacity increase corresponding to a ten-fold increase in time. Equation (2) is supported by Augustesen et al. (2005). Further, it relates time and capacity for fully consolidated piles due to ageing, cf. Clausen and Aas (2000) and Karlsrud et al. (2005). t_0 can in principle be chosen freely. However, once chosen t_0 is assumed constant and should be used together with the corresponding calibrated time function. This is due to the fact that Δ_{10} depends on t_0, cf. eq. (2). In this study it is chosen that t_0 = 100 days. Hence, Q_0 equals the 100-days capacity.

Based on Flaate (1968) and seven cases from the existing NGI database Clausen and Aas (2000) assume that Δ_{10} can be estimated from:

$$(3) \qquad \Delta_{10} = 0.1 + 0.4\left(1 - \frac{I_p}{50}\right) \cdot OCR^{-0.8}$$

with the limitation that Δ_{10} shall be within the range 0.1 to 0.5. Due to the fact that the limits of Δ_{10} are based on few tests, they are encumbered with great uncertainty. Further, it is noted that eq. (3) implies a particularly high increase in capacity per log cycle of time for soft clays of low plasticity. The time function given by a combination of eq. (2) and eq. (3) is denoted NGI. The

Figure 2 Factors influencing skin friction and toe resistance for piles clay.

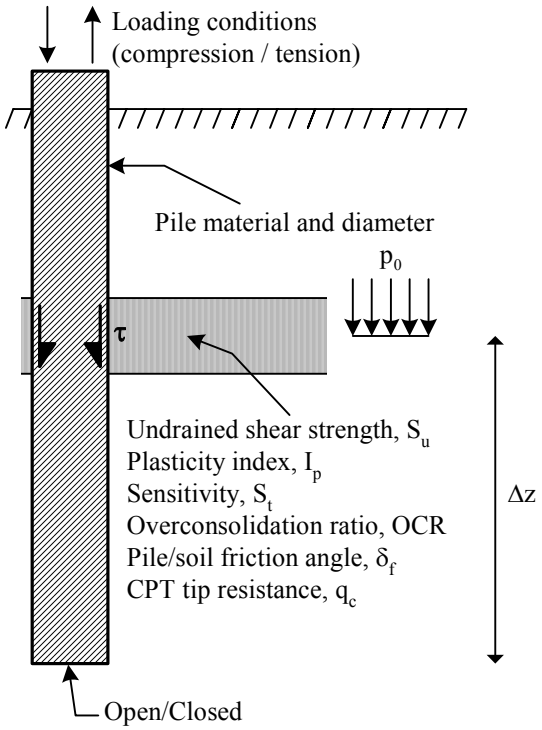

influence of employing a time function different from NGI in PILCAP is presented in Section 5.

The pile capacity, *C*, estimated by NGI-99 corresponds to a 100-days capacity. Whether this is also the case for API-2 and ICM-96 is unclear, since the reference time has not been specified in these methods. It is likely that the capacity is predicted at the time t_{eoc} for the end of primary consolidation, which is a function of pile diameter (since t_{eoc} is proportional to d^2/c_v where d is the pile diameter and c_v is the consolidation coefficient), drainage conditions etc. If this is the case the measured capacity should be corrected to $Q(t_{eoc})$ rather than $Q_0 = Q(100)$. However, for simplicity it shall be assumed that all prediction methods provide 100-days capacities.

2.4 Prediction methods

Characteristics, of the calculation procedures employed, are brief listed below and some of the dominant parameters related hereto are indicated in Figure 2.

1. **API-2** is an S_u based method. The shaft resistance is a function of the undrained shear strength, S_u, and the strength to the effective overburden pressure ratio, S_u/p_0, which is highly correlated with *OCR*. The toe resistance is function of the undrained shear strength. API (1993) states that unconsolidated undrained triaxial compression tests are recommended for establishing the strength profile variation, i.e. S_{uu} is the preferable strength measure to employ when applying API-2 (Clausen and Aas, 2000). More information on API-2 can be found in API (1993) and Appendix C.
2. **NGI-99** is a mixed effective stress and S_u based method, a so-called α-β approach (also denoted λ approach) when considering the skin friction. α and β are closely interrelated and they result from data fitting. β is a function of I_p and *OCR*. If not given, *OCR* is determined based on the normalised strength ratio, S_u/p_0. In fact, *OCR* has not been provided in any of the cases associated with this study. α depends on the tip condition (open-ended or closed-ended), S_u/p_0, and the distance from the level considered to the pile toe, Δz. That is, NGI-99 includes a length factor so "friction fatigue effects" are taken into account. Further, compared to API-2, NGI-99 also accounts for the effects of whether a pile is driven open-ended or closed-ended when calculating the shaft resistance. Even if an open-ended pile behaves in a plugged manner or if the pile is closed-ended, the toe resistance is calculated the same way for NGI-99 as for API-2. That is, the toe resistance depends only on S_u. The shear strength, S_{uu}, determined by means of un-consolidated undrained triaxial tests is the reference

Table 1 Specification of AAU data. For more information on the AAU database, see Appendix E.

ID	Site, Reference	No. of piles	With time [a]	No time [b]	$Q_{r,soil}$ / $Q_{r,pile}$ [c]	Soil conditions			Depth [m] [g]
						S_{uu} [kPa] [d]	I_p [%] [e]	OCR [-] [f]	
901	Singapore Port Leung et al. (1991)	1		1	1 / 3	44.1	25 [n]	8.2	28
902	Aalborg Havnefront [h]	2		2	0 / 4	149.5	25 [n]	4.9	28-31
903, 904	Egå Renseanlæg [i]	2		2	2 / 3	194.4 - 210.4	25 [n]	14.1 - 14.2	24, 25.2
905	Algade [j]	1	1		4 / 2	134.7	25 [n]	9.7	13
906	Motorvegbru Drammen Tvedt and Fredriksen (2003)	2	2		4 / 4	65.3	25 [n]	1.1	35
907	Drammen Stasjon Falstad and Heyerdahl (1995)	2	1	1	1 / 3	82.0	22	1.2	30-49
908, 909	Canons Park Powell et al.(2003) [k]	3	3		4 / 4	95.8 – 104.7	45 – 47	8.4 – 8.5	6.5
910	Cowden Powell et al. (2003) [l]	1	1		4 / 4	136.3	15	25.2	9
911	Nitsund Flaate (1972)	2	2		4 / 4	66.2 - 69.1	16	13.5 – 15.7	12-14
912	Skå-Edeby Bergdahl and Hult (1981)	9	9		4 / 4	11.8 – 12.3	40 – 41	3.9 - 4.1	15
913	Fynsværket [m]	1	1		0 / 2	336.9	25 [n]	12.6	28.7
	Total	26	20	6	-			-	-

a) Piles have been tested more than one time.
b) Piles have only been subjected to one static test.
c) Quality ranking of soil and pile data: 0 = not known, 1 = low, 2 = average, 3 = high, 4 = very high (super piles).
d) Average unconsolidated undrained shear strength along the pile shaft.
e) Average plasticity index along the pile shaft.
f) Average overconsolidation ratio along the pile shaft.
g) Embedded depth.
h) Material provided by Per Aarsleff A/S, Denmark.
i) Material provided by CP test A/S, which is a part of Per Aarsleff A/S, Denmark.
j) Material provided by Kampsax Geodan, which now is part of COWI A/S, Denmark.
k) In addition: Powell and Uglow (1988), Bond and Jardine (1991,1995), Wardle et al. (1992).
l) In addition: Gallagher and St. John (1980), Lehane and Jardine (1994)
m) Material provided by Carl Bro A/S, Odense, Denmark
n) Default parameters, see Section 2.2.

strength. More information on NGI-99 can be found in Appendix B, which is taken from Clausen and Aas (2000).

3. **ICM-96** is an effective stress based method when considering the skin friction. The shaft resistance depends on the sensitivity, S_t, the distance from the layer considered to the pile toe, Δz, the pile diameter, the pile/soil friction angle, δ_f (depends on I_p), and OCR, i.e. some of the input parameters are not normally measured in routine site investigations (Jardine and Chow, 1997). If S_t and OCR have not been provided, they are estimated based on the consolidated undrained shear strength from trixial tests, see Appendix D, i.e. S_{ciu} is the reference strength. However, Jardine and Chow (1996) include alternative expressions, based upon parameters to be determined from oedometer tests, rather than direct use of S_t. Like NGI-99, ICM-96 includes a length, or friction fatigue, factor. In addition to this, ICM-96 also accounts for the effects of whether a pile is driven open-ended or closed-ended when calculating the shaft resistance. The toe resistance when the pile is located in clay is a function of the CPT tip resistance, q_c. ICM-96 also accounts for the effects of whether a pile is driven open-ended or closed-ended or behaves in a plugged or unplugged manner when estimating the toe resistance. More information on ICM-96 can be found in Jardine and Chow (1996, 1997) and Appendix D.

Whichever model employed, PILCAP also accounts for whether the toe conditions are drained or undrained for piles loaded in tension.

In some of the cases associated with this study, the shaft of the pile is partly embedded in sand and the toe may also be located in sand. How the three models incorporate this can be studied in API (1993), Clausen and Aas (2001b), and Jardine and Chow (1996).

Norwegian Geotechnical Institute and Imperial College, London, have modified their calculation procedures upon the final completion of the research reported in this document. For more details on the modified versions of the Imperial College model and the NGI approach, see Jardine et al. (2005a) and Karlsrud et al. (2005). According to Jardine et al. (2005b), the new sections of the model include pile ageing; cyclic loading; group action; pile shape and seismic effects, as well as applications in calcareous and micaceous sands, diatomaceous clays and clay-silts. Further, more detailed recommendations are made on parameter selection and practical implementation. Fundamentally, the governing static equations remain more or less unchanged. In the modified NGI-model the unconsolidated undrained shear strength, S_{uu}, and the plasticity index, I_p, are still the key parameters. The procedure for the skin friction is changed especially with focus on normally consolidated clay with low plasticity. For piles driven in overconsolidated clay the factor that takes driving conditions (open-ended or closed-ended) into account is also changed. For more details, see Karlsrud et al. (2005).

3 AAU data

An overview of the data initially collated in connection with this study (AAU database) is presented herein. The cases have been found in the literature and provided by Norwegian and Danish companies. The data were collected based on the following criteria:

1. Only loading tests in which failure occurs are included. In this case failure is defined when the movements equal 10% of the pile diameter.
2. Piles tested within approximately a week after driving have not been included. During that time period the measured capacity is highly questionable because it is influenced by driving. Furthermore, converting a measured capacity determined within few days after installation to a 100-days capacity by means of a time correction function based on long term tests may introduce large errors.
3. Only cases with reasonably good information regarding soil, pile, and testing conditions have been included. Both offshore and onshore piles are included and the different cases are divided into five groups, i.e. Group 0 to 4, depending on the quality of the soil and pile data available. Cases belonging to Group 4 ($Q_{r,soil}$ = 4 and $Q_{r,pile}$ = 4 as indicated in Table 1) are especially well-described in terms of pile, soil, and test information, whereas Group 0 contains the cases of poorest quality.

Details regarding the available data are presented in Table 1. In summary:

1. If a pile is driven to a given depth and tested and then driven further down and tested again, the pile will be counted as "two" piles and included in the "no time" category in Table 1.
2. The average soil parameters along the pile shaft are weighted in terms of surface area. An average undrained shear strength, S_u, an average overconsolidation ratio, *OCR*, and an average plasticity index, I_p is associated with every single pile. S_{uu} is the unconsolidated undrained shear strength determined by triaxial test. For more information on average soil parameters, see Augustesen et al. (2005).
3. 26 piles distributed on 13 sites have been included in the analyses.
4. Six piles have been subjected to loading tests one time whereas 20 piles are tested more than once. In total, 70 tests on piles in clay have been included.
5. All the piles are loaded in compression.
6. The embedded lengths of the piles vary between 6.5 and 49 m.
7. Two piles are driven open-ended whereas 24 are driven closed-ended.
8. Seven piles have circular cross sections and 18 rectangular. The remaining one pile is an H-profile, which is equated with a "solid/closed" circular profile.
9. Of the 26 piles, six are made of steel, nine of concrete and 11 of timber.

The data in terms of pile tip level and average strength ratio, S_{uu}/p_0 is shown in Figure 3. S_{uu} is the average unconsolidated undrained shear strength for the soil along the pile shaft. Soil and pile data for the different sites are shown in Appendix E.

3.1 Results of analyses

In Figure 4, *C/M*-ratios (calculated capacity, *C*, divided by the measured capacity, *M*) are plotted as function of pile penetration depth and average strength ratio, S_u/p_0, for every single pile depending on calculation method. p_0 is the average normal effective vertical stress. Results can be summarised as follows:

1. When including corrections to time and undrained shear strength, the average *C*/*M*-ratio for both NGI-99 and API-2 is 1.14 whereas the standard

Figure 3 Range covered by the AAU database in terms of depth (pile tip level) and average strength ratio, S_{uu}/p_0. Numbers associated with each point refer to site identification numbers (see Table 1).

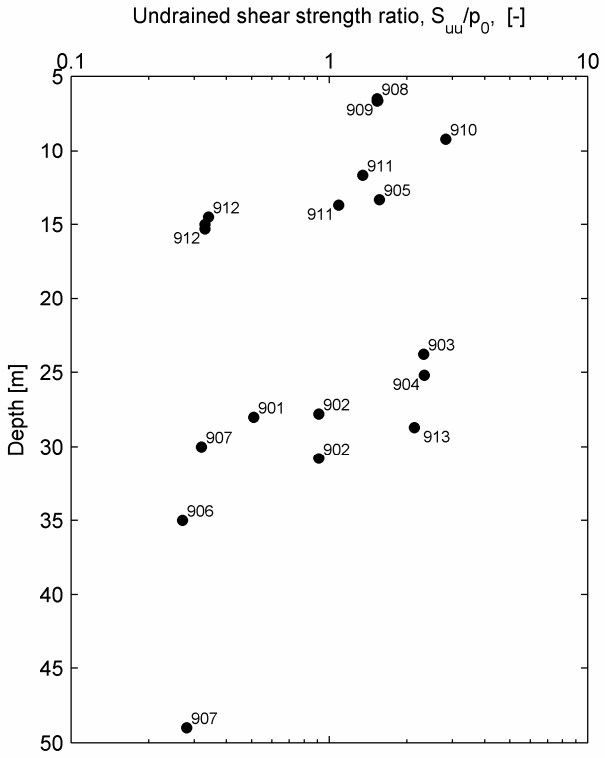

Table 2 NGI-99, API-2, and ICM-96 tested against piles with penetration depths greater or less than 20m.[a)]

Depth [b)]	No. of piles	NGI-99 $\mu_{C/M}$ / $\sigma_{C/M}$ [c)]	API-2 $\mu_{C/M}$ / $\sigma_{C/M}$ [c)]	ICM-96 $\mu_{C/M}$ / $\sigma_{C/M}$ [c)]
< 20	55	1.08 / 0.26	1.05 / 0.35	0.85 / 0.19
> 20	12	1.38 / 0.50	1.55 / 0.52	1.26 / 0.35

a) Corrections to S_u and time have been applied.
b) Penetration depth, [m].
c) μ and σ are the mean value and the standard deviation of the *C/M*-ratios.

deviations are 0.34 and 0.42, respectively. In contrast, the average *C/M*-ratio and standard deviation for ICM-96 are 0.93 and 0.27, respectively. That is, ICM-96 provides a better description of the data compared to NGI-99 and API-2. It should be noted that cases with IDs 908-910 are a part of the cases forming the basis of ICM-96. This may contribute to the fact that ICM-96 provides a better result than the two other methods.

2. Figure 4 indicates that there is a skew distribution of *C*/*M*-ratios with penetration depth when applying especially API-2 to the available data. This is confirmed by inspecting Table 2. For all the methods the average *C/M*-ratios, $\mu_{C/M}$, are significant higher for piles longer than 20m compared to piles with penetration depths less than 20m. API-2 generally overestimates the capacity of piles longer than 20m more than NGI-99 and ICM-96 do. A reason might be that NGI-99 and ICM-96 include a length factor, which takes "friction fatigue effects" into consideration, whereas API-2 does not. Similar trends are observed if the three calculation methods are tested against piles with penetration depths greater and less than 10m, respectively. The conclusions drawn may be influenced by the fact that the number of pile tests associated with piles longer than 20m is 12. Further, the number of tests associated with piles shorter than 20m is dominated by the case with ID 912, Skå-Edeby, i.e. the number of tests constitutes approximately 45% of the total number of tests for that group. A skew distribution of data points obtained for API-2 has also been observed by Jardine and Chow (1997) and Jardine et al. (2005b).
3. Some results deviate more than others, e.g. the case with ID 907, Drammen Stasjon (see Table 1). This may be due to an inadequate soil description. For the case with ID 906, Motorvegbru Drammen, information concerning plug ratios was insufficient and the H-shaped pile cross section was looked upon as rectangular. For the cases with

Figure 4 NGI-99, API-2, and ICM-96 tested on AAU data. Ratios, *C/M*, of calculated capacities corresponding to 100 days, *C*, divided by associated time corrected measured capacities, *M*, are plotted as function of pile penetration depth and average strength ratio, S_u/p_0. ● and ○ refer to closed compression piles and open compression piles, respectively. A line through data points indicate that the data points belong to the same case. The corresponding plot label refers to site ID (see Table 1).

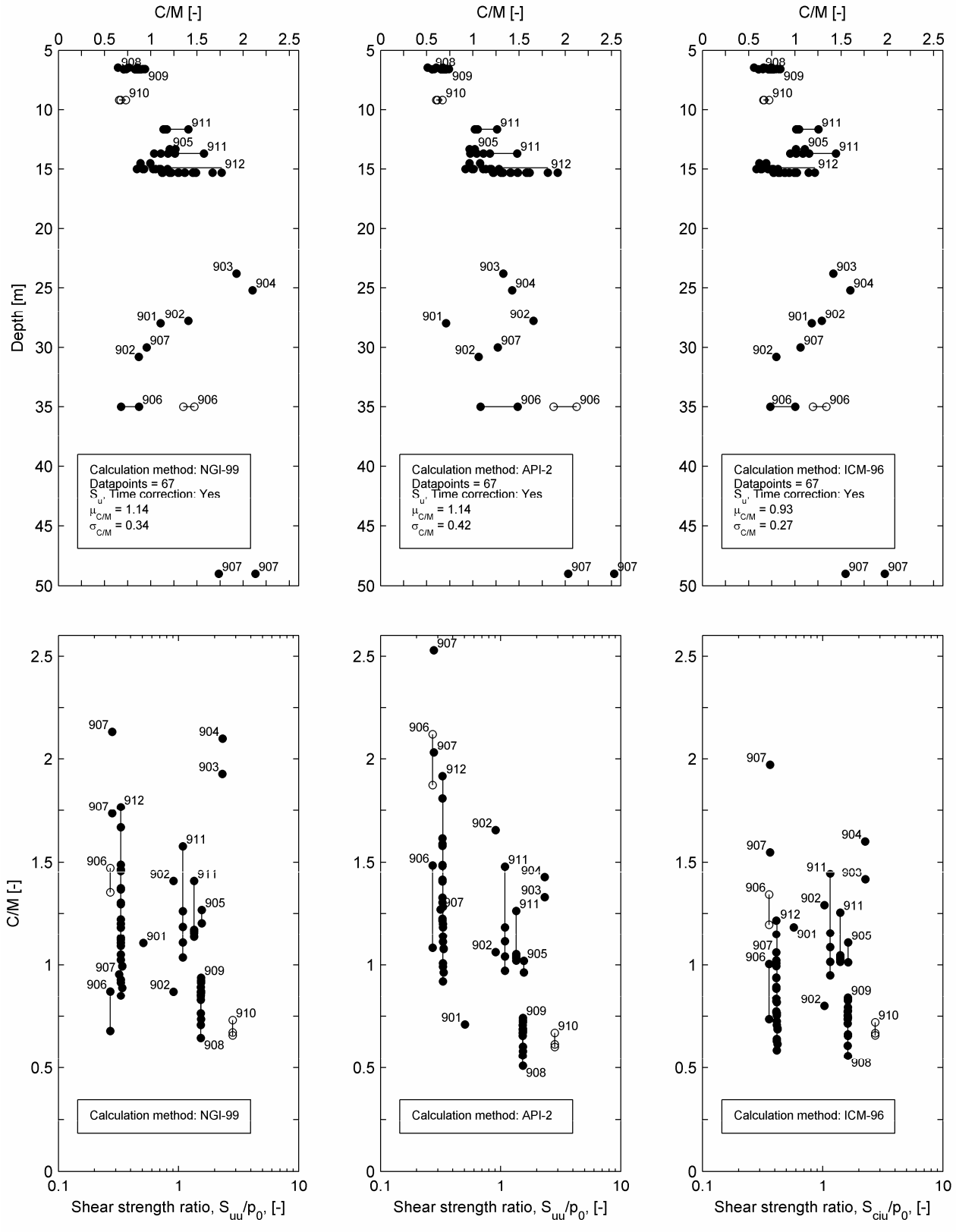

Figure 5 Influence of short- and long-term effects on Δ_{10}. The time for equalisation of pore pressures due to pile installation is denoted t_{eoc}. Short-term effects are related to pore pressure dissipation and ageing whereas long-term effects are only due to ageing.

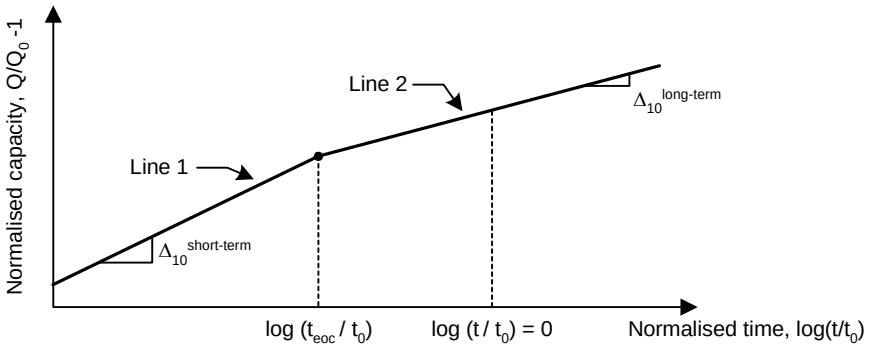

Figure 6 Differences in employing $\Delta_{10}^{short\text{-}term}$ and $\Delta_{10}^{long\text{-}term}$ when time correcting capacities from loading tests performed shortly after installation. ○ indicates that the pile in consideration is tested for the first time. In contrast, Δ indicates that a given pile has been tested several times. That is, the effects of pre-shearing result in higher time corrected capacities, *M*.

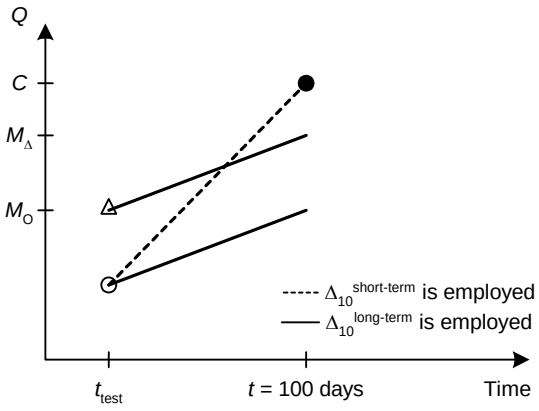

IDs 903 and 904, Egå Renseanlæg, the measured capacities based on static tests may be influenced by the fact that the piles also have been subjected to dynamic tests. In addition to this, uncertainty is associated with the evaluation of strengths and effective unit weights of the granular materials. In the case with ID 911, Nitsund, the *C/M*-ratios may be affected by the fact that the deepest located clay layer associated with the soil profile is virtually extended approximately 4m because no information regarding the soil associated with the lower 4m of the pile is available. In the case with ID 912, Skå-Edeby, different test methods have been applied. In the case with ID 908, Canons Park, uncertainty is associated with the determination of failure loads. The above mentioned listed reasons are not comprehensive. For further details, Appendix E can be studied for every single case.

4. The case with ID 913, Fynsværket, is omitted because it is a statistical deviant (*C/M* ≈ 6). For example, if NGI-99 is tested on the additional cases, the average *C/M*-ratio is 1.36 if "Fynsværket" is included and 1.14 if it is omitted. The *C/M*-ratio may be affected by the fact that the fourth clay layer (see Appendix E) is virtually extended approximately 4m because no information regarding the soil associated with the lower 4m of the pile is available. Furthermore, uncertainty is associated with the determination of the vane shear strength due to equipment limitations. Even though the case is excluded in the following it is still a part of the database.

In general, the *C/M*-ratios decrease with increasing time between driving and testing. For example, for Pile II (the embedded depth is 13.7m) associated with the case with ID 911, Nitsund, *C/M*-ratios equal 1.58, 1.26, 1.19, 1.11 and 1.04, see Figure 4, when the given pile has been situated 34, 209, 357, 637, and 1023 days in the ground, respectively. The calculation method employed is NGI-99. Similarly, consider the closed compression pile associated with the case with ID 906, Motorvegbru Drammen. *C/M*-ratios equal 0.87 and 0.68 if the pile is tested 14 and 141 days after installation, respectively. Again, NGI-99 is applied. As a matter of fact, all the piles that have been tested more than one time show the described tendencies. Plausible reasons can be summarised as follows:

1. The calculated capacity, *C*, always corresponds to the 100-days capacity and it is constant for a given pile located at a given depth in given soil conditions. Therefore, if *C/M* decreases with increasing time between installation and testing, *M* must be subjected to changes.
2. The increase in capacity per log cycle of time, Δ_{10} cf. eq. (2), is dependent on whether short- or long-term effects are investigated (Figure 5). Short-term

Table 3 NGI-99, API-2, and ICM-96 tested against the AAU data [a)].

	No. of piles / No. of sites	NGI-99 $\mu_{C/M}$ / $\sigma_{C/M}$ [b)]	API-2 $\mu_{C/M}$ / $\sigma_{C/M}$ [b)]	ICM-96 $\mu_{C/M}$ / $\sigma_{C/M}$ [b)]
All piles [c)]:				
Time and S_u correction[d)]	70 / 13	1.36 / 1.14	1.30 / 0.86	1.08 / 0.78
All piles:				
Time and S_u correction [d)]	67 / 12	1.14 / 0.34	1.14 / 0.42	0.93 / 0.27
No time or S_u correction[e)]	67 / 12	1.11 / 0.37	1.13 / 0.49	0.83 / 0.26
S_u correction, no time correction[f)]	67 / 12	1.13 / 0.39	1.13 / 0.48	0.92 / 0.32
Time correction, no S_u correction[g)]	67 / 12	1.12 / 0.32	1.14 / 0.44	0.84 / 0.21
Steel piles:				
Time and S_u correction [d)]	22 / 4	0.86 / 0.20	0.83 / 0.43	0.79 / 0.18
No time or S_u correction [e)]	22 / 4	0.86 / 0.29	0.85 / 0.55	0.74 / 0.22
S_u correction, no time correction [f)]	22 / 4	0.84 / 0.26	0.82 / 0.50	0.77 / 0.24
Time correction, no S_u correction [g)]	22 / 4	0.88 / 0.23	0.86 / 0.49	0.75 / 0.17
Timber piles:				
Time and S_u correction [d)]	35 / 2	1.21 / 0.22	1.26 / 0.25	0.91 / 0.20
No time or S_u correction [e)]	35 / 2	1.18 / 0.28	1.25 / 0.33	0.79 / 0.17
S_u correction, no time correction [f)]	35 / 2	1.18 / 0.25	1.23 / 0.28	0.89 / 0.21
Time correction, no S_u correction [g)]	35 / 2	1.21 / 0.26	1.28 / 0.31	0.81 / 0.16
Concrete piles:				
Time and S_u correction [d)]	10 / 6	1.47 / 0.47	1.40 / 0.55	1.30 / 0.34
No time or S_u correction [e)]	10 / 6	1.41 / 0.50	1.33 / 0.58	1.18 / 0.34
S_u correction, no time correction [f)]	10 / 6	1.55 / 0.55	1.48 / 0.65	1.36 / 0.42
Time correction, no S_u correction [g)]	10 / 6	1.33 / 0.40	1.26 / 0.48	1.11 / 0.27
Group 4 [h)]:				
Time and S_u correction [d)]	57 / 5	1.08 / 0.27	1.09 / 0.39	0.86 / 0.20
No time or S_u correction [e)]	57 / 5	1.06 / 0.32	1.10 / 0.47	0.77 / 0.19
S_u correction, no time correction [f)]	57 / 5	1.05 / 0.30	1.07 / 0.42	0.84 / 0.23
Time correction, no S_u correction [g)]	57 / 5	1.08 / 0.29	1.12 / 0.44	0.79 / 0.16

a) The time function proposed by NGI, eqs. (2)-(3), has been applied to time correct the measured data.
b) μ and σ are the mean value and the standard deviation of the *C/M*-ratios.
c) The case with ID 913, Fynsværket, is only included in these investigations.
d) Corrections to time and undrained shear strength have been employed (Section 2).
e) Time and undrained shear strength corrections have not been employed (Section 2).
f) Corrections to undrained shear strength have been employed whereas corrections concerning time have not been taken into account (Section 2).
g) Corrections to time have been employed whereas corrections concerning the undrained shear strength have not been taken into account (Section 2).
h) This category includes all cases, where soil and pile data belong to Group 4, i.e. cases, where soil and pile data are especially well-described.

effects are related to both equalisation of pore pressures due to driving and ageing. In contrast, long-term effects are only due to ageing. If set-up is considered, the short-term component of Δ_{10} is greater than the long-term component, i.e. $\Delta_{10}^{\text{short-term}} > \Delta_{10}^{\text{long-term}}$. The definition "short-term" can be misleading in connection with piles in clay because it may cover a long period of time. That is, t_{eoc} (Figure 5) can easily vary from few days to over 100 days depending on the characteristics of the subsoil. Capacities measured shortly after installation should in principle be time corrected by employing $\Delta_{10}^{\text{short-term}}$ whereas capacities based on loading tests performed long after equalisation of excess pore pressures should in principle be time corrected by applying $\Delta_{10}^{\text{long-term}}$. In this study, a Δ_{10} corresponding to Line 2, cf. eqs. (3)-(5), in Figure 5 is employed. This implies that *M*s based on loading tests performed soon after driving are too low (see Figure 6). Therefore, as described in the beginning of this section, piles tested within approximately one week after driving have not been included in this study.

3. Pre-shearing effects can have a significant effect on the measured capacities as reported, for example, by Karlsrud and Haugen (1986). This implies that piles subjected to staged loading develop greater capacities compared to results from corresponding unstaged loading tests (see Figure 6). This result in greater *C/M*-ratios for piles subjected to unstaged loading compared to piles that have been tested before. In addition to this, group effects also influence the magnitude of measured capacities.

Results from more detailed analyses using PILCAP are shown in Table 3 from which it can be concluded:

1. In general, NGI-99 provides a more reliable estimate of the bearing capacity than API-2. The average *C/M*-ratio computed with the two methods

are the same for the cases analysed, but the standard deviation is smaller for NGI-99. It should be mentioned that all the piles are closed-ended compression piles.
2. ICM-96 provides a better description of the data than API-2 and NGI-99. An exception is steel piles and piles belonging to Group 4, which are characterized by well-described soil and pile data. It should be noted that only five sites but 57 piles are included in Group 4.
3. For NGI-99 and API-2 it is not evident whether it is an advantage to adapt corrections to undrained shear strengths and time, cf. Sections 2.2 and 2.3. In contrast, for ICM-96 it is in general better to employ both S_u and time conversions.
4. Both NGI-99 and API-2 overestimate the capacities for concrete and timber piles whereas they underestimate the capacities for steel piles.
5. Of the cases available only five of the piles are driven open-ended; two piles associated with the case with ID 906, Motorvegbru Drammen, and three piles related to the case with ID 910, Cowden, see Appendix E. Therefore, further investigations into the effects of piles driven open-ended are not carried out.

As mentioned, detailed studies indicate that it is not always an advantage in terms of reliability to employ time correction. The time function, i.e. eq. (2) combined with eq. (3), is based on the plasticity index, I_p, and the overconsolidation ratio, *OCR*. In some cases these quantities are estimated, thereby introducing some uncertainty in the correction of the measured capacities. This may affect the overall reliability of a given method. The results of employing a time function alternative to NGI in PILCAP are presented in Section 5.

4 NGI data

Most offshore piles have been designed based on API recommendations. Therefore, the motivation of the work done by Clausen and Aas (2000) is:

1. To check how well the API-RP2A method (API, 1993) predicts well-documented pile tests compared to other calculation methods.
2. To develop a revised calculation procedure, denoted NGI-99, which better predicts the actual load test data compared to other existing methods.

In case of piles located in clay, API-2 was compared to:

1. NGI-99 (Clausen and Aas, 2000 and Appendix B).
2. API-1 (API-RP2A, 1975 to 1986), which is replaced by API-2 (API, 1993 and Appendix C).
3. NGI-90 (Karlsrud and Nadim, 1990).
4. NGI-92 (Nowacki et al., 1992), which to some extent is an adjustment and refinement of API-2.
5. ICM-96 (Jardine and Chow, 1996 and Appendix D).

In Clausen and Aas (2000) and also in this report, most effort is put into the comparison of API-2, ICM-96 and NGI-99 because:

1. API-2 has replaced API-1. Therefore, API-1 has mainly a historical interest.
2. NGI-92 is to some extent an adjustment and refinement of API-2.
3. For piles in clay, the established databases have focussed on available information on shear strength rather than results from compressibility tests, i.e. in none of the cases investigated, *OCR* have been measured but instead estimated based on shear strength. Furthermore, NGI-90 and ICM-96 are based on key soil parameters (*OCR* and pile/soil friction angle, δ_f) that normally are not a part of a soil investigation for offshore platforms and they give the designer a considerable freedom of choice for the key parameters involved (Clausen and Aas, 2000). So in principle, ICM-96 and NGI-90 should be omitted in the analyses but ICM-96 is included because it is developed at Imperial College, London, and is thereby an alternative to NGI-90, NGI-92, and NGI-99.

Due to the fact that this section is included to sum up the conclusions drawn by Clausen and Aas (2000), API-1, NGI-90 and NGI-92 are only discussed in the present section.

The calculation procedures are compared based on a database established by the Norwegian Geotechnical Institute (NGI) over the last decade. Static load tests and matching soil and pile data, which quality are of a more or less high standard, are included in the database. Both off- and onshore piles are included and the database is mainly based on published data.

Facts concerning the database are as follows:

1. The database consists, in total, of 202 different pile tests.
2. 100 sites have been investigated and the piles range from few meters to above 100 m.
3. Tension, compression, open-ended and closed-ended piles are included.
4. A subset consisting of 43 piles denoted “super piles” are used to calibrate and develop NGI-99 (Clausen and Aas, 2000). These cases belong to Group 4 ($Q_{r,soil}$ = 4 and $Q_{r,pile}$ = 4 as explained in Section 3). They are especially well-described in terms of pile, soil, and test information. Therefore, they have been carefully checked against the data

Table 4 Calculation methods tested against the NGI database.

	Clay-I [a] $\mu_{C/M}$ / $\sigma_{C/M}$ [e]	Clay-II [b] $\mu_{C/M}$ / $\sigma_{C/M}$ [e]	Clay-III [c] $\mu_{C/M}$ / $\sigma_{C/M}$ [e]	Group 4 ("super piles") [d] $\mu_{C/M}$ / $\sigma_{C/M}$ [e]
Number of pile tests	44	33	127	43
API-1	1.26 / 0.31	1.01 / 0.25	1.08 / 0.35	1.12 / 0.36
API-2	1.06 / 0.21	1.12 / 0.30	0.98 / 0.40	1.10 / 0.54
NGI-90	0.93 / 0.25	1.06 / 0.26	0.86 / 0.40	0.97 / 0.56
NGI-92	1.02 / 0.20	1.10 / 0.30	0.97 / 0.36	1.05 / 0.47
ICM-96	0.96 / 0.38	0.66 / 0.12	0.90 / 0.49	1.04 / 0.71
NGI-99	0.96 / 0.24	1.03 / 0.27	0.97 / 0.26	0.98 / 0.19

a) Data taken directly from Flaate and Selnes (1977).
b) Data taken directly from Semple and Rigden (1984).
c) Pile test source data collected and interpreted as part of the study presented in Clausen and Aas (2000).
d) A subset of Clay-III. NGI-99 is calibrated based on these cases.
e) μ and σ are the mean value and standard deviation of *C/M*-ratios.

presented in the original publications.

5. As indicated in Table 4, the NGI database is divided into primarily three groups denoted Clay-I, Clay-II, and Clay-III. Some cases are included in more than one group, which is the reason why the total number of pile tests (202) does not match the sum of all pile tests related to Clay-I, Clay-II, and Clay-III, respectively (see Table 4).

4.1 Results and recommendations

In Table 4, average *C/M*-ratios obtained by applying the calculation methods to the NGI data are shown. Overall, the methods predict the measured capacities quiet well because the average *C/M*-ratios, $\mu_{C/M}$, and standard deviations, $\sigma_{C/M}$, are relatively close to unity and zero, respectively. Furthermore, NGI-99 generally provides the best fit. With reference to Table 4 there is no particular reason why ICM-96 on the average underestimates the capacities of Clay-II piles significantly with low scatter. Though, it should be noted that Clay-II is entirely based on compression piles. On the other hand, the high scatter associated with ICM-96 and API-2 when testing against the piles belonging to Group 4 is due to uncertainty in the prediction of capacities of the piles loaded in tension - $\sigma_{C/M}$ = 0.82 and 0.61 when employing ICM-96 and API-2, respectively. In addition, API-2 and ICM-96 specially fail to match the measured capacities associated with the case denoted "Lierstranda", see Jardine et al. (2005b). In contrast, NGI-99 is calibrated against pile tests belonging to Group 4, which of course implies a low standard deviation, $\sigma_{C/M}$, and a mean value, $\mu_{C/M}$, close to unity. All pile tests categorised as Group 4 are made of steel.

As mentioned, the NGI database consists, in total, of 202 different pile tests distributed on 100 sites. Results of testing NGI-99, API-2, and ICM-96 against these data are shown in Table 5. When employing the NGI time function, eq. (2) combined with eq. (3), it can be concluded that NGI-99 provides the better description of the data in terms of average *C/M*-ratio. In contrast, API-2 presents the best estimate when employing the AAU time function (see Section 5), eq. (2) combined with eqs. (4)-(5).

Clausen and Aas (2000, 2001a) conclude and recommend the following for piles in clay:

1. API-2 produces a skew distribution of *C/M*-ratios when plotted against the strength ratio S_u/p_0 or penetration depth. That is, for short piles (<20-30m) API-2 underpredicts the capacity, whereas it overestimates the capacity for longer piles (>20-30m). Similar trends are reported by Jardine et al. (2005b) and observed in connection with testing the calculation procedures against the AAU data, see Section 3.
2. API-2 fails to predict the low observed skin friction for piles in normally consolidated clay. Therefore, the method should not be used for piles located in such soils. As the preconsolidation increases, the difference between API-2 and the other methods is reduced.
3. For soil profiles that do not include normally consolidated clays of low plasticity, it is proposed to take the pile capacity as the highest of the values calculated by API-2 and NGI-99.
4. For piles in overconsolidated clay there is an effect on the skin friction of whether the pile is driven open- or closed-ended. The capacity for closed-ended piles is 10-30% higher. API-2 does not differentiate between open- and closed-ended piles

Table 5 NGI-99, API-2, and ICM-96 tested against the NGI database, the AAU data and a combination of the two.

		NGI time function [a]			AAU time function [b]		
	No. of piles / No. of sites	NGI-99 $\mu_{C/M}$ / $\sigma_{C/M}$ [c]	API-2 $\mu_{C/M}$ / $\sigma_{C/M}$ [c]	ICM-96 $\mu_{C/M}$ / $\sigma_{C/M}$ [c]	NGI-99 $\mu_{C/M}$ / $\sigma_{C/M}$ [c]	API-2 $\mu_{C/M}$ / $\sigma_{C/M}$ [c]	ICM-96 $\mu_{C/M}$ / $\sigma_{C/M}$ [c]
NGI database	202 / 100	0.98 / 0.26	1.03 / 0.35	0.88 / 0.44	0.96 / 0.27	1.00 / 0.38	0.86 / 0.47
AAU data	67 / 12	1.14 / 0.34	1.14 / 0.42	0.93 / 0.27	1.16 / 0.33	1.16 / 0.43	0.95 / 0.27
All data	268 / 111	1.02 / 0.28	1.06 / 0.37	0.89 / 0.40	1.01 / 0.30	1.04 / 0.40	0.88 / 0.43

a) The time function proposed by NGI, eqs. (2)-(3), has been employed to time correct the measured data.
b) The time function proposed by AAU, eqs. (2), (4)-(5), has been employed to time correct the measured data.
c) μ and σ are mean value and standard deviation of the *C/M*-ratios.

in connection with predicting the skin friction in clay, see Section 2.4.

5. For piles belonging to the Group 4, the pile diameter does not have a significant influence on *C/M*-ratios.
6. API-2 is more sensitive towards the way the undrained shear strengths are determined than NGI-99.
7. It is recommended that more high quality tests should be implemented in the database and a study of the development of pile capacity with time should be performed. The latter has been investigated by Augustesen et al. (2005) and the former is a part of the study presented in this report. Furthermore, NGI-99 should be checked that the models for piles in clay and sand produce a smooth transition as the soil changes from sand to silt to clay.

5 Combination of AAU and NGI

In this section, the three calculation procedures are tested against a combination of the AAU and NGI data by employing the NGI time function, eqs. (2)-(3), or the alternative AAU time function described in Section 5.2. For further details on time correction, see Section 2.3. Initially, it should be mentioned that the total number of pile tests analysed are 268. 111 sites constitute the cases. The input file for the combined AAU and NGI database is shown in Appendix F. The corresponding output file can be seen in Appendix G.

5.1 NGI time function

Average *C/M*-ratios, $\mu_{C/M}$, and standard deviations, $\sigma_{C/M}$, obtained when applying NGI-99, ICM-96, and API-2 to the AAU data, the NGI data and to a combination of the two are shown in Table 5 and Table 6. If the NGI time function, cf. eqs. (2) and (3), is used to time correct the measured capacities, the following comments and conclusions can be made:

1. NGI-99 provides in general a better description of the measured capacities compared to API-2 and ICM-96.
2. Average *C/M*-ratios, $\mu_{C/M}$, and standard deviations, $\sigma_{C/M}$, increase slightly when the AAU data are added to the NGI database.
3. The accuracy of NGI-99 is better than that of API-2 and ICM-96 when investigating timber piles and piles belonging to Group 4 if S_u and time corrections are taken into account. Again, cases belonging to Group 4 are characterised by especially well-described soil and pile data. In general, NGI-99 and API-2 are more precise compared to ICM-96 when considering steel piles, whereas ICM-96 is better when considering concrete piles.
4. Generally, ICM-96 is less reliable in terms of average *C/M*-ratio than the two other methods. The reason may be that this model is based upon parameters that are not a part of routine site investigations, see Section 2.4. Therefore, in all cases associated with this study the input parameters for ICM-96 are estimated, which naturally introduces some uncertainty in the predictions.
5. Based on Table 6 no distinct conclusions can be drawn regarding piles loaded in compression/ tension and the effects of driving conditions (open-ended or closed-ended) except that ICM-96 is unreliable in terms of average *C/M*-ratio, $\mu_{C/M}$, when considering piles loaded in compression or piles driven open-ended. Detailed studies are shown in Table 7. It is recommended not to use ICM-96 for piles driven open-ended and loaded in compression. Further, API-2 can preferably be applied to piles driven open-ended and loaded in tension. In all other cases NGI-99 should be applied. It should be noted that the number of piles loaded in compression is much larger than the number of piles loaded in tension.
6. It is not evident whether it is an advantage to adapt corrections to undrained shear strength and time for all calculation methods. Generally, employing S_u

Table 6 NGI-99, API-2, and ICM-96 tested against all available data for piles in clay. [a)]

	No. of piles / No. of sites	NGI-99 $\mu_{C/M}$ / $\sigma_{C/M}$ [b)]	API-2 $\mu_{C/M}$ / $\sigma_{C/M}$ [b)]	ICM-96 $\mu_{C/M}$ / $\sigma_{C/M}$ [b)]
All cases [c)]:				
Time and S_u correction [d)]	268 / 111	**1.02 / 0.28**	**1.06 / 0.37**	**0.89 / 0.40**
No time and S_u correction [e)]	-	1.04 / 0.30	1.06 / 0.39	0.84 / 0.45
S_u correction, no time correction [f)]	-	1.05 / 0.30	1.09 / 0.43	0.92 / 0.48
Time correction, no S_u correction [g)]	-	1.02 / 0.28	1.03 / 0.35	0.81 / 0.37
Piles loaded in compression [d)]	215	**1.02 / 0.30**	**1.05 / 0.34**	**0.86 / 0.31**
Piles loaded in tension [d)]	53	**1.02 / 0.21**	**1.06 / 0.50**	**1.01 / 0.65**
Piles driven open-ended [d)]	83	**1.01 / 0.23**	**1.05 / 0.30**	**0.76 / 0.26**
Piles driven closed-ended [d)]	185	**1.03 / 0.31**	**1.06 / 0.40**	**0.95 / 0.45**
Steel:				
Time and S_u correction [d)]	154 / 76	**0.97 / 0.24**	**0.99 / 0.41**	**0.84 / 0.45**
No time and S_u correction [e)]	-	1.01 / 0.27	1.02 / 0.41	0.81 / 0.53
S_u correction, no time correction [f)]	-	1.01 / 0.26	1.05 / 0.50	0.88 / 0.55
Time correction, no S_u correction [g)]	-	0.97 / 0.26	0.97 / 0.36	0.77 / 0.42
Piles loaded in compression [d)]	107	**0.95 / 0.25**	**0.97 / 0.34**	**0.75 / 0.26**
Piles loaded in tension [d)]	47	**1.00 / 0.21**	**1.05 / 0.53**	**1.03 / 0.68**
Piles driven open-ended [d)]	83	**1.01 / 0.23**	**1.05 / 0.30**	**0.76 / 0.26**
Piles driven closed-ended [d)]	71	**0.91 / 0.25**	**0.93 / 0.50**	**0.92 / 0.59**
Timber:				
Time and S_u correction [d)]	79 / 22	**1.03 / 0.28**	**1.12 / 0.27**	**0.90 / 0.30**
No time and S_u correction [e)]	-	1.02 / 0.30	1.08 / 0.32	0.81 / 0.29
S_u correction, no time correction [f)]	-	1.03 / 0.28	1.11 / 0.27	0.90 / 0.31
Time correction, no S_u correction [g)]	-	1.03 / 0.30	1.08 / 0.32	0.81 / 0.28
Piles loaded in compression [d)]	79	**1.03 / 0.28**	**1.12 / 0.27**	**0.90 / 0.30**
Piles loaded in tension [d)]	0	- / -	- / -	- / -
Piles driven open-ended [d)]	0	- / -	- / -	- / -
Piles driven closed-ended [d)]	79	**1.03 / 0.28**	**1.12 / 0.27**	**0.90 / 0.30**
Concrete:				
Time and S_u correction [d)]	35 / 17	**1.23 / 0.37**	**1.19 / 0.37**	**1.09 / 0.34**
No time and S_u correction [e)]	-	1.27 / 0.33	1.23 / 0.38	1.03 / 0.29
S_u correction, no time correction [f)]	-	1.29 / 0.40	1.25 / 0.42	1.14 / 0.37
Time correction, no S_u correction [g)]	-	1.21 / 0.29	1.17 / 0.33	0.98 / 0.26
Piles loaded in compression [d)]	29	**1.25 / 0.40**	**1.19 / 0.41**	**1.14 / 0.35**
Piles loaded in tension [d)]	6	**1.12 / 0.07**	**1.16 / 0.10**	**0.82 / 0.14**
Piles driven open-ended [d)]	0	- / -	- / -	- / -
Piles driven closed-ended [d)]	35	**1.23 / 0.37**	**1.19 / 0.37**	**1.09 / 0.34**
Group 4 [h)]:				
Time and S_u correction [d)]	131 / 35	**1.01 / 0.25**	**1.02 / 0.44**	**0.89 / 0.46**
No time and S_u correction [e)]	-	1.03 / 0.28	1.04 / 0.45	0.85 / 0.54
S_u correction, no time correction [f)]	-	1.03 / 0.27	1.06 / 0.53	0.92 / 0.57
Time correction, no S_u correction [g)]	-	1.00 / 0.27	1.00 / 0.40	0.82 / 0.42
Piles loaded in compression [d)]	88	**1.01 / 0.27**	**1.01 / 0.38**	**0.82 / 0.25**
Piles loaded in tension [d)]	43	**1.00 / 0.22**	**1.04 / 0.55**	**1.02 / 0.70**
Piles driven open-ended [d)]	38	**1.02 / 0.21**	**1.00 / 0.33**	**0.82 / 0.28**
Piles driven closed-ended [d)]	93	**1.00 / 0.27**	**1.03 / 0.48**	**0.91 / 0.51**

a) The time function proposed by NGI, eqs. (2)-(3), has been employed to time correct the measured data.
b) μ and σ are the mean value and the standard deviation of the *C/M*-ratios.
c) The case with ID 913, Fynsværket, is not included in any of the analyses, see Section 3.
d) Corrections to time and undrained shear strength have been employed see Section 2.
e) Time and undrained shear strength corrections have not been employed see Section 2.
f) Corrections to undrained shear strength have been employed whereas corrections concerning time have not been taken into account (Section 2).
g) Corrections to time have been employed whereas corrections concerning the undrained shear strength have not been taken into account (Section 2).
h) This category includes all cases, where soil and pile data belong to Group 4 ($Q_{r,soil} = Q_{r,pile} = 4$), i.e. cases, where soil and pile data are especially well-described.

conversions result in greater average *C/M*-ratios. In contrast, the average *C/M*-ratios are reduced by employing time corrections. The effects on *C/M*-ratios are greater by making use of time correction than S_u conversions. This is not the case when applying ICM-96 to the available data.

7. On the average, API-2 overestimates the capacity of piles installed in depths greater than 20m more than the capacity of piles installed in depths less than 20m, see Table 8. That is, API-2 produces a skew distribution of *C/M*-ratios with penetration depth. ICM-96 and NGI-99 also produce a skew

Table 7 Effects of driving and loading conditions. [a)]

Driving / Loading [b)]	No. of piles	NGI-99 $\mu_{C/M}$ / $\sigma_{C/M}$ [c)]	API-2 $\mu_{C/M}$ / $\sigma_{C/M}$ [c)]	ICM-96 $\mu_{C/M}$ / $\sigma_{C/M}$ [c)]
Open / TNS	23	1.07 / 0.32	0.99 / 0.26	0.95 / 0.30
Open / CMP	60	0.99 / 0.23	1.07 / 0.32	0.69 / 0.20
Closed / TNS	30	0.98 / 0.21	1.11 / 0.63	1.06 / 0.82
Closed / CMP	155	1.03 / 0.32	1.05 / 0.35	0.93 / 0.32

a) Corrections to S_u and time have been applied.
b) Diving and loading conditions; Open = piles driven open-ended, Closed = piles driven closed-ended, TNS = piles loaded in tension, CMP = piles loaded in compression.
c) μ and σ are the mean value and the standard deviation of the *C/M*-ratios.

Table 8 NGI-99, API-2, and ICM-96 tested against piles with penetration depths greater or less than 20m.[a)]

Depth [b)]	No. of piles	NGI-99 $\mu_{C/M}$ / $\sigma_{C/M}$ [c)]	API-2 $\mu_{C/M}$ / $\sigma_{C/M}$ [c)]	ICM-96 $\mu_{C/M}$ / $\sigma_{C/M}$ [c)]
< 20	183	0.99 / 0.28	0.96 / 0.30	0.86 / 0.31
> 20	85	1.09 / 0.29	1.26 / 0.43	0.96 / 0.56

a) Piles driven open-ended and closed-ended as well as loaded in compression and tension are included. Further, corrections to S_u and time have been applied.
b) Penetration depth, [m].
c) μ and σ are the mean value and the standard deviation of the *C/M*-ratios.

Table 9 Effect of pile diameter.

Diameter [m] [a)]	No. of piles	NGI-99 $\mu_{C/M}$ / $\sigma_{C/M}$ [b)]	API-2 $\mu_{C/M}$ / $\sigma_{C/M}$ [b)]	ICM-96 $\mu_{C/M}$ / $\sigma_{C/M}$ [b)]
0 – 0.3	154	0.98 / 0.27	1.02 / 0.39	0.89 / 0.44
0.3 – 0.6	69	1.08 / 0.34	1.13 / 0.36	0.94 / 0.39
> 0.6	45	1.06 / 0.22	1.07 / 0.33	0.83 / 0.26

a) Equivalent pile diameter.
b) μ and σ are the mean value and the standard deviation of the *C/M*-ratios.

distribution of *C*/*M*-ratios with penetration depth but it is not as distinct. A possible reason for the observed tendencies is that API-2 does not include a length factor accounting for "friction fatigue effects", whereas NGI-99 and ICM-96 do. Similar conclusions have been made by testing the calculation procedures against the AAU database, cf. Section 3.

8. Based on Table 8 it is recommended to use NGI-99 independent on pile length. Detailed studies indicate that similar conclusions can be drawn if either piles driven open-ended or closed-ended are investigated as well as piles loaded in either compression or tension.
9. In Table 9 the effect of pile diameter on the average *C/M*-ratio is shown. Generally, NGI-99 provides the better description of piles belonging to the three categories. Alternatively, API-2 could be applied to piles with diameters in the range 0-0.3m, and ICM-96 for piles with diameters in the range 0.3-0.6m. This result may be affected by the fact that approximately 42% of the piles belonging to the category 0.3-0.6m are closed concrete piles loaded in compression. According to Table 6, ICM-96 is especially reliable in terms of average *C/M*-ratio for these types of piles, whereas NGI-99 and API-2 are not.
10. The especially low *C/M*-ratio obtained when applying ICM-96 to piles with diameters greater than 0.6m is due to the fact these piles are primarily steel piles driven open-ended. Further, approximately 50% of the piles are loaded in compression.

5.2 AAU time function

Based on a comprehensive study of the relation between time after installation and the axial bearing capacity of piles, Augustesen et al. (2005) propose the following relations for Δ_{10} in eq. (2) depending on the type of shear strength used as reference:

$$\Delta_{10} = 1.24 - \left(\frac{S_{uu}}{60}\right)^{0.03} \quad (4)$$

$$\Delta_{10} = 1.24 - \left(\frac{S_{ciu}}{70}\right)^{0.03} \quad (5)$$

S_{uu} [kPa] and S_{ciu} [kPa] are shear strengths determined by means of unconsolidated and consolidated undrained triaxial tests, respectively. The time functions given by a combination of eq. (2) and either eq. (4) or eq. (5) are denoted AAU. It is assumed that t_0 = 100 days. It should be mentioned that S_{uu} is one of the key parameters associated with NGI-99 and API-2, whereas ICM-96 is based on *OCR*, and if not given *OCR* is determined by means of S_{ciu}. That is, eq. (4) is employed when using NGI-99 and API-2 whereas eq. (5) is used in connection with ICM-96.

The AAU time functions have been implemented in PILCAP as an alternative to the NGI time function. The effects of replacing time function on the overall performance of NGI-99, API-2, and ICM-96 can be studied from Table 5 and Table 10:

1. The average *C/M*-ratio increases slightly by employing the AAU time function on piles belonging to the AAU data.

Table 10 NGI-99, API-2, and ICM-96 tested against all available data for piles in clay.

		NGI time function [a]			AAU time function [b]		
	No. of piles / No. of sites	NGI-99 $\mu_{C/M}$ / $\sigma_{C/M}$ [c]	API-2 $\mu_{C/M}$ / $\sigma_{C/M}$ [c]	ICM-96 $\mu_{C/M}$ / $\sigma_{C/M}$ [c]	NGI-99 $\mu_{C/M}$ / $\sigma_{C/M}$ [c]	API-2 $\mu_{C/M}$ / $\sigma_{C/M}$ [c]	ICM-96 $\mu_{C/M}$ / $\sigma_{C/M}$ [c]
All cases	268 / 111	1.02 / 0.28	1.06 / 0.37	0.89 / 0.40	1.01 / 0.30	1.04 / 0.40	0.88 / 0.43
Steel piles	154 / 76	0.97 / 0.24	0.99 / 0.41	0.84 / 0.45	0.95 / 0.25	0.98 / 0.44	0.83 / 0.49
Timber piles	79 / 22	1.03 / 0.28	1.12 / 0.27	0.90 / 0.30	1.04 / 0.29	1.13 / 0.28	0.91 / 0.30
Concrete piles	35 / 17	1.23 / 0.37	1.19 / 0.37	1.09 / 0.34	1.19 / 0.39	1.14 / 0.40	1.05 / 0.36
Group 4 [d]	131 / 35	1.01 / 0.25	1.02 / 0.44	0.89 / 0.46	1.00 / 0.28	1.02 / 0.48	0.89 / 0.50

a) The time function proposed by NGI, eqs. (2)-(3), has been employed to time correct the measured data.
b) The time function proposed by AAU, eqs. (2), (4)-(5) has been employed to time correct the measured data.
c) μ and σ are the mean value and the standard deviation of the *C/M*-ratios.
d) This category includes all cases, where soil and pile data belong to Group 4, i.e. cases, where soil and pile data are especially well-described.

2. The average *C/M*-ratio decreases slightly by employing the AAU time function on piles belonging to the existing NGI database.
3. API-2 and ICM-96 are more accurate than NGI-99 in terms of average *C/M*-ratio when investigating the NGI and AAU data, respectively.
4. In general, by employing the time function proposed by Augustesen et al. (2005) the calculation methods, NGI-99 and API-2, become slightly more accurate in the determination of the measured pile capacities when considering all the available tests. Of the three calculation procedures, NGI-99 provides the best prediction of the data.
5. In terms of average *C/M*-ratios, the effects of replacing the time function are not distinct.
6. Detailed analyses show that the general conclusions drawn by applying the NGI time function to the available data, cf. Section 5.1, are also applicable when employing the AAU time function on the same data.

6 Summary and recommendations

The purpose of this report is to elucidate which calculation procedure (NGI-99, API-2, or ICM-96) that provides the better description of the axial capacity of piles in clay. This is done by comparing measured and calculated capacities based on relatively well-documented cases. Facts regarding the established data (denoted AAU) have been introduced. The database is based on static loading tests reported in the literature and provided by Danish and Norwegian companies. 70 tests on piles in clay constitute the AAU data. The piles are distributed on 13 sites. One case - including three pile tests – is omitted in the analyses because it is a statistical deviant.

The methods have been tested against the AAU data and also an existing NGI database by means of the database processing program PILCAP, which has been developed at the Norwegian Geotechnical Institute. Results of applying the calculation procedures to the AAU data and the NGI data are presented in Section 3 and 4, respectively, and will not be repeated here. Instead, recommendations based on testing the models on a combination of the AAU and NGI data and thereby on all available tests will be emphasized.

For piles in clay, the following is concluded and recommended based on analyses of 268 static loading tests distributed on 111 sites:

1. Overall, NGI-99 provides the better description of the data.
2. ICM-96 can advantageously be applied to concrete piles. This statement is encumbered with great uncertainty due to the small number of tests available on concrete piles.
3. It is recommended **not** to use ICM-96 for piles driven open-ended and loaded in compression. Further, API-2 can preferably be applied to piles driven open-ended and loaded in tension. In all other cases NGI-99 should be applied.
4. Especially API-2 provides a skew distribution of *C/M*-ratios with penetration depth. Therefore, the effect of pile length on the average *C/M*-ratios has been investigated. Based on this study it is recommended to use NGI-99 independent on pile length, driving conditions (open-ended or closed-ended), and loading conditions (compression or tension).
5. The effect of pile diameter on the average *C/M*-ratios has also been elucidated. Generally, NGI-99 provides the better description independent on pile diameter. Alternatively, API-2 could be applied to piles with diameters in the range 0-0.3m, and ICM-96 for piles with diameters in the range 0.3-0.6m.

The last statement may be affected by the fact that approximately 42% of the piles belonging to the category 0.3-0.6m are closed concrete piles loaded in compression. ICM-96 is especially reliable in terms of average *C/M*-ratio for these types of piles, whereas NGI-99 and API-2 are not.

6. It is not evident whether it is an advantage to adapt corrections to undrained shear strength and time for all calculation methods. Generally, employing S_u conversions result in greater average *C/M*-ratios. In contrast, the average *C/M*-ratios are reduced by employing time corrections. The effects on *C/M*-ratios are greater by making use of time correction than S_u conversions. More effort could advantageously be put into the revision of the conversion procedures for the undrained shear strength, S_u.
7. The effects of replacing the time function (used for time correction) originally implemented in PILCAP have been investigated and they are not distinct. By employing the time function proposed by Augustesen et al. (2005), the calculation methods become slightly more accurate in the determination of the measured pile capacities when considering all the available tests. NGI-99 provides the most reliable prediction of the data.
8. Generally, the calculation methods are very sensitive towards the way the soil profile and pile tests are interpreted.

Uncertainty is introduced in several ways when comparing measured and calculated capacities. Uncertainty is associated with:

1. Interpretation of soil conditions,
2. Conversion of soil parameters,
3. Interpretation of loading tests,
4. Time correction,
5. Calculation procedures,
6. Pre-shearing and group effects.

As mentioned, the purpose of this paper is to elucidate the reliability of the calculation procedures NGI-99, API-2, and ICM-96. Except for pre-shearing and group effects, items 1-4 have been carefully taken care of in order to obtain a consistent treatment of the data and thereby reaching a reliable validation of the methods.

It should be mentioned that ICM-96 is based upon parameters that are not a part of routine site investigations, see Section 2.4. Therefore, in all cases associated with this study the input parameters for ICM-96 are estimated, which naturally introduces some uncertainty in the predictions. This may influence the above mentioned conclusions.

Finally, it is noted that the choice of calculation method should rely on local test data if such data are available. Thus, if a number of piles have been tested in similar ground, the choice of calculation method should be based on *C/M*-ratios obtained for the given site.

7 Acknowledgement

The authors would like to thank the Norwegian Geotechnical Institute for kindly providing the FORTRAN code PILCAP and numerous pile test data.

8 References

API (1993), Recommended practice for planning, designing and constructing fixed offshore platforms- working stress design, API RP 2A-WSD, *American Petroleum Institute*, 20th edition, July 1, 1993.

API (2000). Recommended practice for planning, designing and constructing fixed offshore platforms- working stress design. API recommended practice 2A-WSD, American Petroleum Institute, 21th edition, December, 2000.

Augustesen, A, Andersen, L. and Sørensen, C.S. (2005), Time function for driven piles in clay, *Available from the Department of Civil Engineering, Aalborg University, Denmark*, *Internal report*, ISSN: 1398-6465 R0501.

Bergdahl, U. and Hult, G. (1981), Load tests on friction piles in clay, *Proc. 10th International conference on soil mechanics and foundation engineering*, Stockholm, Sweden, Vol.2, pp.625-630.

Bjerrum, L. (1973). Problems of soil mechanics and construction on soft clays. State-of-the-art report, Session IV. *Proc. of the 8th International Conference on Soil Mechanics and Foundation Engineering*, Moscow, 1973. Also in NGI Publication No.100, Norwegian Geotechnical Institute.

Bond, A.J. and Jardine, R.J. (1991), Effects of installing displacement piles in a high OCR clay, *Geotechnique*, 41(3), pp.341-363.

Bond, A.J. and Jardine, R.J. (1995), Shaft capacity of displacement piles in a high OCR clay, *Geotechnique*, 45(1), pp.3-23.

Bullock, P.J., Schmertmann, J.H., McVay, M.C., and Townsend, F.C. (2005a), Side shear setup. I: Test piles driven in Florida. *Journal of Geotechnical and Geoenvironmental Engineering*, 131(3), pp.292-300.

Bullock, P.J., Schmertmann, J.H., McVay, M.C., and Townsend, F.C. (2005b), Side shear setup. II: Results from Florida test piles. *Journal of Geotechnical and Geoenvironmental Engineering*, 131(3), pp.301-310.

Burland, J.B. (1973), Shaft capacity of piles in clay – a simple fundamental approach, *Ground Engineering*, 6(2).

Chen, Y.-J, and Kulhawy, F.H. (1993). Undrained strength interrelationships among CIUC, UU, and UC tests, *Journal of Geotechnical Engineering*, 119(11), pp.1732-1750.

Chow, F.C. (1996), Investigations into displacement pile behaviour for offshore foundations, *Ph.D. Thesis, University of London (Imperial College)*.

Clausen, C.J.F. and Aas, P.M. (2000), Bearing capacity of driven piles – Piles in clay, *NGI report 525211-1*, Norwegian Geotechnical Institute.

Clausen, C.J.F. and Aas, P.M. (2001a), Capacity of driven piles in clays and sands on the basis of pile load tests. *ISOPE conference*.

Clausen, C.J.F. and Aas, P.M. (2001b), Bearing capacity of driven piles – Piles in sand, *NGI report 525211-2*, Norwegian Geotechnical Institute.

Dennis, N.D. and Olson, R.E. (1983), Axial capacity of steel pipe piles in clay, *Proc. Geotechnical practice in offshore engineering*, Austin, Texas (1983).

Falstad, B.A. and Heyerdahl, H. (1995), Construction of two railway bridges across Drammen river. Piling and related challenges, *Geoteknikkdagen*, 1995, Norway, pp.37.1-37.23.

Flaate, K. (1968), Bearing capacity of friction piles in clay, *NGF stipend 1967-1968, Veglaboratoriet*, Oslo (in Norwegian).

Flaate, K. (1972), Effects of pile driving in clays, *Canadian Geotechnical Journal*, 9(1), pp.81-88.

Flaate, K. and Selnes, P. (1977), Side friction of piles in clay, *Proc. 9th International Conference on Soil Mechanics and Foundation Engineering*, Tokyo, Also in NGI publication No.118, Norwegian Geotechnical Institute.

Gallagher, K.A. and St. John, H.D. (1980), Field scale model studies of piles as anchorages for buoyant platforms, *Proc. European Offshore Petroleum Conference*, London, Paper EUR 135.

Jardine, R.J. and Chow, F.C. (1996), New design methods for offshore piles, *Marine technology directorate Ltd., publication MTD 96/103*, London, ISBN 1 870553 31 4.

Jardine, R.J. and Chow (1997). Improved pile design methods from field testing research. *In* proceedings of the ERTC3 (The ISSMFE European Regional Technical Committee 3 "Piles"), Design of Axially Loaded Piles – European Practice (eds. De Cock and Legrand), Belgium, Balkema, Rotterdam. pp.27-38.

Jardine, R.J., Chow, F.C., Overy, R.F. and Standing, J.R. (2005a), ICP design methods for driven piles in sand and clay. *Thomas Telford, London*.

Jardine, R.J., Chow, F.C., Standing, J.R., Overy, R.F., Saldivar-Moguel, E. Strick van Linschoten, C. and Ridgway, A. (2005b), An updated assessment of the ICP pile capacity procedures. *Proccedings of Frontiers in Offshore Geotechnics: ISFOG 2005* (eds. Gourvenec and Cassidy), Perth, © 2005 Taylor & Francis Group, London, ISBN 0 415 39063 6.

Jardine, R.J., Standing, J.R. and Chow, F.C. (2005c), Field research into the effects of time on the shaft capacity of piles driven in sand. *Proccedings of Frontiers in Offshore Geotechnics: ISFOG 2005* (eds. Gourvenec and Cassidy), Perth, © 2005 Taylor & Francis Group, London.

Karlsrud, K. and Haugen, T. (1986), Axial static capacity of steel model piles in overconsolidated clay, *NGI Publication No.163*, Norwegian Geotechnical Institute. Also *Proc. 11th International Conference on Soil Mechanics and Foundation Engineering,* San Francisco, 1985, Vol.3, pp.1401-1406.

Karlsrud, K. and Nadim, F. (1990), Axial static capacity of offshore piles in clay, *Offshore Technology Conference*, Houston, May 1990, Paper OTC 6245. Also NGI publication No.188, Norwegian Geotechnical Institute.

Karlsrud, K., Kalsnes, B. and Nowacki, F. (1992), Response of piles in soft clay and silt deposits to static and cyclic axial loading based on recent instrumented pile load tests, *Society of underwater testing*, London, Also NGI publication No.188, Norwegian Geotechnical Institute.

Karlsrud, K., Clausen, C.J.F. and Aas, P.M. (2005), Bearing capacity of driven piles in clay, the NGI approach, P*roceedings of Frontiers in Offshore Geotechnics: ISFOG 2005*, (eds. Gourvenec and Cassidy), Perth, © 2005 Taylor & Francis Group, London, ISBN 0 415 39063 6.

Kolk, H.J. and Velde, E.v.d. (1996), A reliable method to determine friction capacity of piles driven into clays, *Offshore Technology Conference*, Houston, May 1996, Paper OTC 7993.

Kraft, L.M., Focht, J.A. and Amerasinghe, S.F. (1981), Friction capacity of piles driven into clay, *ASCE, JGED*, 107(GT11).

Ladd, C.C. (1991). Stability evaluation during stage construction. *Journal of Geotechnical Engineering*, 117(4), pp.540-615.

Ladd, C.C., Foott, R., Ishihara, K., Schlosser, F., and Poulos, H.G. (1977). Stress-deformation and strength characteristics, State-of-the-art report. *Proc. of the International Conference on Soil Mechanics and Foundation Engineering*, Tokyo, Vol.2.

Lehane, B.M. and Jardine, R.J. (1994), Displacement pile behaviour in glacial clay, *Canadian Geotechnical Journal*, .31(1), pp.79-90.

Leung, C.F., Radhakrishnan, R. and Tan, S.A. (1991), Performance of precast driven piles in marine clay, *Journal of Geotechnical Engineering*, 117(4), pp.637-657.

Mayne, P.W. (1988). Determining OCR in clays from laboratory strength. *Journal of Geotechnical Engineering*, 114(1), pp.76-92.

Meyerhof, G.G. (1976), Bearing capacity and settlement of pile foundations, *ASCE, JGED*, 102(GT3).

Mirza, U.A.A. (1995), A simple approach for calculating pile skin friction in clays, *Preprint, ISOPE Conf.*, Holland.

Nowacki, F., Karlsrud, K. and Sparrevik, P. (1992), Comparison of recent tests on OC clay and implications for design, *Proc. Large-scale pile tests in clay, ICE*, London (Ed. Clarke), Published by Thomas Telford Ltd.

Powell, J.J.M. and Uglow, I.M. (1988), Marchetti dilatometer testing in UK soils, *Penetration testing, ISOPT-1, De ruiter (ed.), Balkema Rotterdam*, ISBN 90 6191 801 4, pp.555-562.

Powell, J.J.M., Butcher, A.P. and Pellew, A. (2003), Capacity of driven piles with time – implifications of re-use, *Proc. XIII ECSMGE*, (eds. Vanicek et al.), Prague, Vol.2, pp.335-340.

Randolph, M.F. and Murphy, B.S. (1985), Shaft capacity of driven piles in clay, *Offshore Technology Conference*, Houston, May 1985, Paper OTC 4883.

Semple, R.M. and Rigden, W.J. (1984), Shaft capacity of driven pipe piles in clay, *Proc., Symposium on analysis and design of pile foundations*, ASCE (Ed. Meyer), p.59.

Toolan, F.E. and Ims, B.W. (1988), Impact of recent changes in the API recommended practice for offshore piles in sand and clays, *Preprint, Oceanology international 1988*.

Tvedt, G. and Fredriksen, F. (2003), E18 Ny motorvegbru i Drammen. Prøvebelastning av Peler, *Proceedings from the conference on Rock Blasting and Geotechnics*, Oslo, 2003

Vijayvergiya, V.N. (1977), Load-movement characteristics of piles, *Ports '77, Proc. 4th Annual Symposium of the Waterways, Ports, Coastal and Ocean Division of American Society of Civil Engineers*, 2, pp.269-284.

Vijayvergiya, V.N. and Focht, J.A. (1972), A new way to predict capacity of piles in clay, *Offshore Technology Conference*, Houston, May 1972, Paper OTC 1718.

Wardle, I.F., Price, G. and Freeman, T.J. (1992), Effect of time and maintained load on the ultimate capacity of piles in stiff clay, *Piling: European practice and worldwide trends: Proceedings of a conference*, London, pp.92-99.

Appendix

The following appendices are included in the report:

1. Appendix A: Conversion procedures
2. Appendix B: NGI-99
3. Appendix C: API-2
4. Appendix D: ICM-96
5. Appendix E: AAU clay database
6. Appendix F: AAU and NGI data
7. Appendix G: Calculated results

Appendix A:
Conversion procedures

The procedure employed to convert one type of shear strength to another is presented. The following is based on Clausen and Aas (2000). For further information see Augustesen et al. (2005).

Undrained shear strengths are assumed to belong to one of the five groups indicated in the last column in Table A.1 depending on the way they are measured. For example, undrained shear strengths determined by means of consolidated undrained triaxial compression tests belongs to group 3. Another example, if the undrained shear strength comes from CPT, it is implicitly assumed that the N_k factor used to convert cone tip resistance to undrained shear strength is selected such that the calculated strength corresponds to a UU triaxial value (Clausen and Aas, 2000). Thus, the conversion procedures consist in using relations that combine the strengths belonging to the different groups. It is assumed that the following quantities are given:

1. Vertical effective stress at a given depth, p_0.
2. Plasticity index, I_p.
3. Undrained shear strength, S_u, for one of the five groups in Table A.1.

In the following, the subscripts associated with the undrained shear strength refer to Table A.1.

Table A.1 Undrained shear strength types and groups. After Clausen and Aas (2000).

Undrained shear strength test type	Group
Estimated value	1 : UCT
Not known	1 : UCT
TV/PP: Torvane, Pocket penetrometer test	1 : UCT
UCT: Unconfined compression test	1 : UCT
UU: Unconsolidated undrained triaxial test	2: UU
CIU/CAU: Consolidated undrained triaxial test	3: CIU
DSS: Direct simple shear	4: DSS
LV: Laboratory vane test	5: Vane
Other laboratory test	1 : UCT
FV: Field vane test	5: Vane
CPT: Field cone penetrometer test	2: UU
Other field test	2: UU

Conversion equations

For normally consolidated clays it is assumed that (Clausen and Aas, 2000; Ladd, 1991):

$$\text{(A.1)} \quad \frac{S_{ciu}}{p_0} = \beta^{ciu} = 0.32$$

$$\text{(A.2)} \quad \frac{S_{DSS}}{p_0} = \beta^{DSS} = 0.22 + 0.06\frac{I_p}{100}$$

β^{ciu} lies in the lower end of the range proposed by Mayne (1988). S_{ciu} and S_{DSS} are shear strengths based on consolidated undrained triaxial compression test and directional shear test, respectively. β^{ciu} and β^{DSS} are the normally consolidated undrained shear strength ratios depending on whether S_{ciu} or S_{DSS} are employed as reference shear strength.

For overconsolidated clays, it is assumed that S_{ciu} and S_{DSS} strengths follow the SHANSEP model, based upon Clausen and Aas (2000), Ladd et al. (1977) and Mayne (1988):

$$\text{(A.3)} \quad \frac{S_{ciu}}{p_0} = \beta^{ciu} \cdot OCR^{\Lambda} \quad \text{and} \quad \frac{S_{DSS}}{p_0} = \beta^{DSS} \cdot OCR^{\Lambda}$$

where OCR is the overconsolidation ratio, [-]. β is the normally consolidated undrained shear strength ratio, S_u/p_{0nc}, given by eq. (A.1) and eq. (A.2) depending on whether CIU tests or DSS tests are investigated. Λ is a strength rebound parameter, [-]. It is assumed that Λ = 0.85. OCR is defined as:

$$\text{(A.4)} \quad OCR = \frac{\sigma_{pc}}{p_0} = \frac{p_0 + \Delta\sigma_{pc}}{p_0}$$

where σ_{pc} is the effective preconsolidation pressure.

The relationship between S_{uu} and S_{ciu} based upon Clausen and Aas (2000) and Chen and Kulhawy (1993) is as follows:

$$\text{(A.5)} \quad \frac{S_{uu}}{S_{ciu}} = 0.63 + 0.12 \cdot OCR^{0.5}, \quad 0.75 \le \frac{S_{uu}}{S_{ciu}} \le 1.10$$

where S_{uu} is the unconsolidated undrained triaxial shear strength.

The relationship between S_{uct} and S_{ciu} based upon Clausen and Aas (2000) and Chen and Kulhawy (1993) is as follows:

(A.6) $$\frac{S_{\text{uct}}}{S_{\text{ciu}}} = 0.55 + 0.17 \cdot OCR^{0.5}, \;\; 0.72 \le \frac{S_{\text{uct}}}{S_{\text{ciu}}} \le 1.10$$

where S_{uct} is the shear strength based on unconfined compression test.

The relationship between S_{vane} and S_{DSS} based upon Clausen and Aas (2000) and Bjerrum (1973) is as follows:

(A.7) $$\frac{S_{\text{vane}}}{S_{\text{DSS}}} = \begin{cases} 0.9 + 0.8\dfrac{I_p}{100} & \text{for } I_{\text{p}} < 75\% \\ 1.50 & \text{for } I_{\text{p}} \ge 75\% \end{cases}$$

where S_{vane} is the vane shear strength.

Conversion procedure

The conversion procedure is as follows:

1. If *OCR* is not given; calculate *OCR* corresponding to a given type and magnitude of an undrained shear strength by combining some of the equations in the former section, i.e. eqs. (A.1) to (A.7). If the calculated overconsolidation ratio $OCR_{\text{calc}} \le 1$ then $OCR = 1$ in the conversion procedure. Furthermore, if $S_{\text{uu}}/S_{\text{ciu}}$, $S_{\text{uct}}/S_{\text{ciu}}$, and $S_{\text{vane}}/S_{\text{DSS}}$ are less or greater than the given lower and upper bounds, use must be made of the values of the lower and upper bounds, respectively. Finally, if $p_0 < 0.01p_{\text{atm}}$ (for example at the surface) then $p_0 = 0.01p_{\text{atm}}$ must be introduced in eqs. (A.1) to (A.7) where $p_{\text{atm}} = 100$ kPa is the atmospheric pressure.
2. The magnitude of an undrained shear strength of another type is then calculated by inserting the *OCR* found in step 1, if it is not given, in relevant equations from the former section, i.e. combining eqs. (A.1) to (A.7).

Example: Calculate a S_{uu} strength based on a given S_{uct} strength.

1. By combining eq. (A.1), eq. (A.3), and eq. (A.6), *OCR* can be calculated based on the given S_{uct} strength. It should be mentioned that an iteration procedure might profitably be applied.
2. By inserting the calculated *OCR* found in step 1 in eq. (A.5) and combining this equation with eq. (A.1) and eq. (A.3), the corresponding S_{uu} strength can be calculated.

By similar considerations and calculations, four unknown strengths, see Table A.1, can be calculated based on the known fifth strength.

Appendix B: NGI-99

The method assumes that the values of the following parameters are known:

- The vertical effective free field stress, p_0, at a given depth.
- The undrained unconsolidated shear strength, S_{uu}, determined by triaxial tests - in the following denoted S_u.
- Plasticity index, I_p.
- Distance Δz from the level considered to the pile tip.
- Pile tip condition during driving, open- or closed ended.

This appendix is entirely based on Clausen and Aas (2000).

Skin friction

The following algorithm is used to calculate the skin friction:

(B.1) $$\tau_{skin} = \beta \cdot p_0 + \alpha \cdot \Delta S_u$$

where:

(B.2) $$\Delta S_u = S_u - 0.25 \cdot p_0$$

(B.3) $$S_u = \max\left(0.25 \cdot p_0, S_{uu}\right)$$

(B.4) $$\alpha = 0.37 \cdot F_{Length} \cdot F_{Tip} \cdot F_{Strength}$$

(B.5) $$F_{Strength} = \min\left(1.0 + 0.25 \cdot \ln\left(\psi\right), 1.5\right)$$

(B.6) $$\psi = \frac{S_u}{p_0}$$

(B.7) $F_{Tip} = 1.0$ for piles driven open ended

(B.8) $F_{Tip} = 1.4$ for piles closed ended

(B.9) $$F_{Length} = \frac{\Delta z + 10}{1.5\Delta z + 10}$$

(B.10) $$\beta = 0.107 \cdot \sqrt[3]{I_{pc}}$$

(B.11) $$I_{pc} = I_p - \frac{12}{OCR}, \quad I_{pc} > 0.0$$

(B.12) $$OCR = \sqrt[0.85]{4 \cdot \psi}$$ if not given as input

(B.13) $$0.05 < \beta < 0.23$$

The following restrictions are valid for τ_{skin}:

(B.14) $$0.05 p_0 < \tau_{skin} < S_u \quad \wedge \quad \tau_{skin} < \tau_{max}$$

where

(B.15) $$\tau_{max} = 0.7 \cdot \sigma_h$$

(B.16) $$\sigma_h = \min\left(\sigma_{h1}, \sigma_{h2}\right)$$

(B.17) $$\sigma_{h2} = p_0 + 2S_u$$

(B.18) $$\sigma_{h1} = 4.6 \cdot p_0$$

Eq. (B.3) involves that S_u cannot be less than the normally consolidated undrained shear strength estimated as $0.25 \cdot p_0$.

Pile tip capacity

When calculating the pile tip capacity the following notation and quantities are used (Figure B.1):

- t is wall thickness.
- D_i is the inside diameter.
- L is the length of the soil plug.
- GW is the weight of the water plug.
- GP is the total weight of the soil plug.
- τ_i is the inside average skin friction.
- u is the pore pressure at the pile tip.
- σ_v is the vertical effective free field stress at the pile tip.
- σ_w is the vertical total stress acting against the pile wall at the pile tip.
- σ_p is the vertical total stress acting against the soil plug at the pile tip.
- A_i is the soil plug cross section area.
- A_w is the pile wall cross section area.
- A_s is the soil plug side area.

The pile tip stress is normally calculated as 9 times S_{uu}. However, NGI-99 also takes the following into account:

1. The pile is open-ended and coring (Figure B.1).
2. The pile is partly filled with water and soil (Figure B.1).
3. Drained or undrained conditions at pile tip.
4. Cavitation at pile tip when loaded in tension.

The following equations are used when the pile tip is located in clay and the pile is subjected to compression:

(B.19) $\sigma_{p1} = u + \sigma_v + 9 \cdot S_u$

(B.20) $\sigma_{p2} = \dfrac{GW + GP + A_s \cdot \tau_i}{A_i}$

(B.21) Plugged pile if $\sigma_{p1} < \sigma_{p2}$:

(B.22) $\sigma_w = \sigma_p = \sigma_{p1}$

(B.23) Coring pile if $\sigma_{p1} > \sigma_{p2}$

(B.24) $q_1 = u + \sigma_v$

(B.25) $q_2 = \sigma_{p2}$

(B.26) $q = \min(q_1, q_2)$

(B.27) $\sigma_w = 9 \cdot S_u + q$

(B.28) $\sigma_p = \sigma_{p2}$

Equations used when the pile tip is located in clay and the pile is subjected to tension, short-term:

(B.29) $\sigma_{p1} = u + \sigma_v - 9 \cdot S_u$

(B.30) $\sigma_{p1} = \max(\sigma_{p1}, -100\text{kPa})$

(B.31) $\sigma_{p2} = \dfrac{GW + GP - A_s \cdot \tau_i}{A_i}$

(B.32) Plugged pile if $\sigma_{p1} > \sigma_{p2}$:

(B.33) $\sigma_w = \sigma_p = \sigma_{p1}$

(B.34) Coring pile if $\sigma_{p1} < \sigma_{p2}$:

(B.35) $\sigma_w = \sigma_{p1}$

(B.36) $\sigma_p = \sigma_{p2}$

Equations used when the pile tip is located in clay and the pile is subjected to tension, long-term:

(B.37) $\sigma_w = \sigma_p = u$

This implies that the soil plug follows the pile and that a crack forms underneath the pile tip and that this crack has hydrostatic pressure. If the internal plug has been removed, the pore pressure in the above expression should be replaced by $u = GW / A_i$.

Figure B.1 Parameters associated with calculation of tip resistance. After Clausen and Aas (2000)

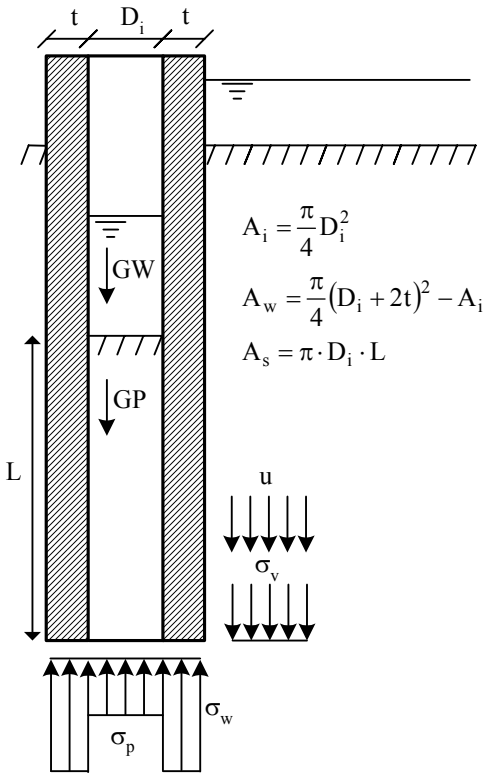

Appendix C:
API-2

The method assumes that the values of the following parameters are known:

- The vertical effective free field stress, p_0, at a given depth.
- The undrained shear strength, S_u [kPa], of the soil at the point in question.

This appendix is based on API (1993) and Clausen and Aas (2000).

Skin friction

The following algorithm is used to calculate the skin friction:

$$\tau_{skin} = \alpha \cdot S_u \quad \text{(C.1)}$$

where:

$$\begin{aligned} \alpha &= 0.5 \cdot \psi^{-0.50}, \quad \psi \le 1.0 \\ \alpha &= 0.5 \cdot \psi^{-0.25}, \quad \psi > 1.0 \end{aligned} \quad \text{(C.2)}$$

$$\psi = \frac{S_u}{p_0} \quad \text{(C.3)}$$

In the commentary to the code, Section C.2.6.4, it is stated that "Unconsolidated-undrained triaxial compression tests on high quality samples, preferably taken by pushing a thin-walled sampler with diameter of 3.0 inches or more, are recommended for establishing strength profile variation because og their consistency and repeatability". Therefore, in this report S_{uu} is taken as the reference strength when applying API-2

Pile tip capacity

For piles end bearing in cohesive soils, the unit end bearing, q [kPa], can be calculated as

$$q = 9 \cdot S_u \quad \text{(C.4)}$$

Again, S_u is the unconsolidated undrained shear strength determined by means of triaxial compression tests.

Appendix D: ICM-96

This appendix is based on Jardine and Chow (1997) and Clausen and Aas (2000).

Skin friction

The following algorithm is used to calculate the skin friction:

$$\tau_{skin} = 0.8 \cdot \sigma_{rc} \cdot \tan\delta \quad \text{(D.1)}$$

where:

- δ is the ultimative interface shear friction angle. δ is measured in appropriate laboratory tests or evaluated from the charts given by Jardine and Chow (1996).
- σ_{rc} is the radial effective stress after installation, see Figure D.1.

The radial effective stress after installation, σ_{rc}, can be calculated by employing either eq. (D.2) or eq. (D.3):

$$\sigma_{rc} = p_0 \left(2.2 + 0.016 \cdot YSR - 0.87\Delta I_{vy}\right) \cdot YSR^{0.42} \left(\frac{\Delta z}{R}\right)^{-0.20} \quad \text{(D.2)}$$

$$\sigma_{rc} = p_0 \left(2 - 0.625 I_{vr}\right) \cdot YSR^{0.42} \left(\frac{\Delta z}{R}\right)^{-0.20} \quad \text{(D.3)}$$

where:

- p_0 is the free field vertical effective stress.
- YSR is the yield stress ratio or the apparent overconsolidation ratio. In this study OCR is introduced instead of YSR.
- The initial sensitivity of the clay can be expressed by either ΔI_{vy} or I_{vr}, which are obtained by comparing the oedometer curves of intact and reconstituted samples. Alternatively, $\Delta I_{vy} = \log(S_t)$ where S_t is the sensitivity. In this study, eq. (D.2) is applied and $\Delta I_{vy} = \log(S_t)$.
- Δz is the distance from the layer considered to the pile toe and R is the radius of the pile, i.e. $\Delta z / R$ is an expression for friction fatigue effects. If $\Delta z / R > 8$ the equations should be evaluated with $\Delta z / R = 8$

Figure D.1 Parameters associated with calculation of skin friction.

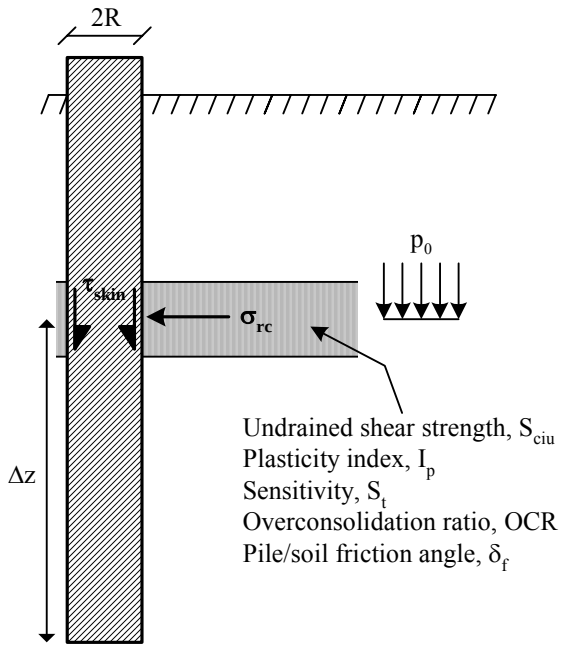

The above expressions apply for closed-ended or plugged piles. For open-ended piles, R should be replaced by:

$$R = \sqrt{\left(R_{outer}^2 - R_{inner}^2\right)} \quad \text{(D.4)}$$

where R_{outer} and R_{inner} are the outer and inner radius, respectively.

In none of the cases associated with this study, the overconsolidation ratio, OCR, and the sensitivity, S_t, are given. OCR can be determined from the known shear strength, S_u, and the vertical effective stress, p_0, based on a study of K_0-consolidated undrained triaxial compression tests, see Jardine and Chow (1996). That is, the anisotropically consolidated undrained shear strength, S_{cau}, associated with triaxial compression tests is the reference strength associated with ICM-96. In this study there is not differentiated between S_{cau} and the isotropically consolidated undrained shear strength, S_{ciu}, determined by triaxial test, i.e. $S_{ciu} = S_{cau}$, see Appendix A. So in practice S_{ciu} is the reference strength when applying ICM-96 to the available data. The relation between OCR, p_0, and S_{ciu} proposed by Jardine and Chow (1996) may advantageously be described by eq. (D.5), see Clausen and Aas (2000):

(D.5) $$\ln\left(\frac{S_{ciu}}{p_0}\right) = \ln\left(\frac{S_{cau}}{p_0}\right) = A + B \cdot \ln(OCR)$$

where $A = -0.82 - 0.019 I_p$ and $B = 0.75$. I_p is the plasticity index.

In this study the sensitivity, S_t, is calculated by means of eq. (D.6):

(D.6) $$S_t = 2\frac{p_0}{S_{ciu}}, \quad 1.0 \le S_t \le 8.0$$

Pile tip capacity

ICM-96 incorporates different rules for evaluating base resistance, and the potential for plugging for open-ended piles located in cohesive soils. These rely principally on the local CPT resistance.

For closed-ended piles the base resistance, Q_b, can be calculated as:

(D.7) $$Q_b = 0.8 \cdot q_c \cdot A_{tip}$$

where q_c is the local CPT tip resistance and A_{tip} is the cross-section area.

For plugging piles driven open-ended the end bearing capacity, Q_b, can be determined as follows:

(D.8) $$Q_b = 0.4 \cdot q_c \cdot A_{tip}$$

For open-ended coring piles the end bearing capacity is determined according to (D.9):

(D.9) $$Q_b = q_c \cdot \pi \cdot \left(R_{outer}^2 - R_{inner}^2\right)$$

where R_{outer} and R_{inner} are the outer and inner radius of the pile, respectively.

According to Jardine and Chow (1997) there is more information regarding the calculation procedure in Jardine and Chow (1996)

Appendix E:
AAU clay database

```
PILES IN CLAY     TILLÆGSCASES TIL NGI DATABASE - OPDATERET          09 MAY 2005

    13   NUMSIT   Number of different sites
     0   INTER    Run program in interactive mode (0=no 1=yes)

     6   ICSAND   Code for method to calculate sand skin friction, see below
     6   ICCLAY   Code for method to calculate clay skin friction, see below

   100   ATMPRS   Atmospheric pressure    (100 kPa  in S.I. units)
    10   GAMWAT   Unit weight of water    (10 kN/m3 in S.I. units)
    78   GAMSTL   Unit weight of steel    (78 kN/m3 in S.I. units)
    25   GAMCON   Unit weight of concrete (25 kN/m3 in S.I. units)
     9   GAMWOD   Unit weight of wood     ( 9 kN/m3 in S.I. units)

     1   MODFSU   Code for change of Su values to Su.UU or Su.DSS (0=No 1=Yes)
   100   TIMEFC   Time needed for development of full pile clay capacity, days
   .00   DELT10   Pile capacity increase for 10-fold time increase
  1.00   PLGFCT   Plug factor, ratio inside/outside friction force

  0  0   INCQRC   Include sites with same or higher soil and pile quality rating code
 1 1 1   INCMAT   Include piles with material code STEEL/CONCRETE/WOOD (0=No 1=Yes)
  1  1   INCMTN   Include piles loaded in compression/tension (0=No 1=Yes)
 0 100   DIAINC   Include piles with diameter within given range
 0 200   PENINC   Include piles with penetration within given range
 0 99999 CAPINC   Include piles with measured capacity within given range
 0 10000 TIMINC   Include piles with time from driving to testing within given range
 0 10.0  SUPINC   Include piles with average Su/po' ratio within given range

  4.5   65  3.0  0.05 0.2   SAND 1-5    Parameters used to calculate pile skin
  .40  .75  .30  2.0  .125  SAND 6-10   friction in sand by NGI-1999 method

 1 1 0            Codes for plotting, 0=NO 1=YES (SAND/CMP  SAND/TNS  CLAY/CMP&TNS)

  ================================    ======================================
  SAND SKIN FRICTION CODES            CLAY SKIN FRICTION CODES
  ================================    ======================================
  1 = API 1972 to 1984 (K=0.5/0.7)    1 = API 1979 to 1987 (24-72 kPa)
  2 = API 1984 to now  (K=0.8/0.8)    2 = API 1987 to now  (ALPHA=f(Su/SIGZ))
  3 = API 1984 to now  (K=0.5/0.7)    3 = API/NGI 1992
  4 = Not used                        4 = NGI 1990
  5 = Imperial College 1996           5 = Imperial College 1996
  6 = NGI 1999                        6 = NGI 1999
  7 = Not used                        7 = Not used
  ================================    ======================================

Data given below for each location and pile include :

  NUMLAY        Number of soil layers
  NUMPIL        Number of different piles or penetration depths
  GWT           Depth from soil surface to ground water table, neg. if submerged site
  GAMPWP        Water unit weight to calculate pore water pressure at pile tip
  SIGSRF        Vertical stress at soil surface
  ZHOLE         Depth below surface of open or cased hole
  QR.SOIL       Quality rating for soil and pile data :
  QR.PILE       0 = Not known  1 = Low  2 = Average  3 = High

  DEPTH BOTTM   Depth to bottom of layer
  GAMMA EFF     Effective unit weight
  TYPE          Soil type indicator (1=Clay 2=Silt 3=Sand)
  Q.CPT         Cone Penetrometer Test tip resistance qc
  SPT           Standard Penetration Test, blows/foot
  OCR           Over-consolidation ratio for CPT to Dr conversion
  SuTop         Undrained shear strength at top of layer
  SuBot         Undrained shear strength at bottom of layer
  TYP           Type of undrained shear strength measurement, see below
  St            Clay sensitivity
  Ip            Clay plasticity index = Wl - Wp
  D50           Sand grain average diameter, mm
  Dr            Sand relative density
  PHI           Sand angle of internal friction
  CLC.FLG       Flag for calcareous soils
  MISC 1-3      MISC(1) is Delta.Sig.PC, used to find OCR.  2-3 not used.

  OPN.CLS       Pile driven open ended (=1) or closed ended (=2)
  MAT.TYP       Pile material type id (1=steel 2=concrete 3=wood)
  DIAM.TIP      Pile tip diameter
  TAPER         Pile wall taper, degrees
  WALL.TIP      Wall thickness at pile tip
  TOTAL.LNGTH   Total pile length from pile but to pile tip
  TIP.PENTR     Depth of pile tip penetration
  PLUG.RATIO    Ratio soil plug length to tip penetration
  WATER.RATIO   Ratio water plug length to tip penetration
  COMPRSSN      Measured pile capacity in compression
  TENSION       Measured pile capacity in tension
  DAYS          Number of days between pile driving and pile testing
  TBF           Value 1 flags that the pile has been tested before
  MISC(1)=  1   Value 1 flags that failure was not reached
  MISC(2)= -1   No correction for time between driving and testing
```

```
  MISC(3)= -1   Skip plug capacity control
  MISC(3)=  0   Clay tip tensile force : Undrained conditions
  MISC(3)=  1   Clay tip tensile force : Drained conditions
  MISC(3)=  2   Clay tip tensile force : Zero force at pile tip

Undrained shear strength codes :

  -1 = Estimated value              0 = Not known

   1 = Torvane, pocket pentr.       8 = Field vane test
   2 = Unconfined compr. test       9 = Field cone penetrometer test
   3 = UU triaxial test            10 = Other field test
   4 = CIU/CAU triaxial test
   5 = Direct simple shear
   6 = Lab vane
   7 = Other lab test


#  901
Leung et al. (1991), ASCE JOGE, Vol.117, No.4
Singapore Port

 NUMLAY   NUMPIL   GWT   GAMPWP    SIGSRF   ZHOLE   QR.SOIL   QR.PILE
    4       1      0.0     10        0.0     0.0      1         3

 LAYER  DEPTH  GAMMA TYPE  Q.CPT  SPT  OCR  -------- CLAY -------   ----SAND----  CLC  MISCELLANEOUS
        BOTTM   EFF ClSiSa  TIP    N        SuTop SuBot TYP St Ip   D50  Dr  PHI  FLG    1   2   3
   1     6.6    7.0   1      0    14    0    90    90    3   0  0    0    0   0    0     0   0   0
   2    22.8    6.0   1      0     0    0    20    20    3   0  0    0    0   0    0     0   0   0
   3    27.2    6.0   1      0     8    0    10    10    3   0  0    0    0   0    0     0   0   0
   4    29.2   11.0   3      0   144    0     0     0    0   0  0    0    0   0    0     0   0   0

 PILE OPN MAT  DIAM TAPER  WALL  TOTAL  TIP   PLUG  WATER   -- MEASURED CAPACITIES --  MISCELLANEOUS
  NO  CLS TYP   TIP degr   TIP   LNGTH PENTR  RATIO RATIO   COMPRSSN TENSION DAYS TBF  1 2 3
   1   2   2   .331  0    .1655  30.0  28.0   0.0   0.0      2100        0     7   0   0 0 0

4th. layer is soft shale. Characterized as sand (information on SPT) in order to run the program.
GammaEff is estimated.
Ground water table assumed to be located at surface level.
Pile is a squared prec. concrete pile (sidelength 26cm). Diameter calculation based on surface area.
Load test for another pile is presented. It is not included in the database because failure was not
reached due to the definition: Load corresponding to total deformations equal 10% of pile diameter.



#  902
Aalborg havnefront byggefelt 1 & 2

 NUMLAY   NUMPIL   GWT   GAMPWP    SIGSRF   ZHOLE   QR.SOIL   QR.PILE
    4       2      1.3     10        0.0    10.0      0         4

 LAYER  DEPTH  GAMMA TYPE  Q.CPT  SPT  OCR  -------- CLAY -------   ----SAND----  CLC  MISCELLANEOUS
        BOTTM   EFF ClSiSa  TIP    N        SuTop SuBot TYP St Ip   D50  Dr  PHI  FLG    1   2   3
   1    12.3   10.0   3      0     0    0     0     0    0   0  0    0    0  33    0     0   0   0
   2    17.3    4.5   1      0     0    0   170   150    8   0  0    0    0   0    0     0   0   0
   3    26.3    8.0   1      0     0    0   100   150    8   0  0    0    0   0    0     0   0   0
   4    31.0   10.0   3      0     0    0     0     0    0   0  0    0    0  33    0     0   0   0

 PILE OPN MAT  DIAM TAPER  WALL  TOTAL  TIP   PLUG  WATER   -- MEASURED CAPACITIES --  MISCELLANEOUS
  NO  CLS TYP   TIP degr   TIP   LNGTH PENTR  RATIO RATIO   COMPRSSN TENSION DAYS TBF  1 2 3
   1   2   2   .382  0    .191   32.0  30.8   0.0   0.0      2540        0    18   1   0 0 0
   2   2   2   .446  0    .223   29.0  27.8   0.0   0.0      1800        0    18   1   0 0 0

Piles are squared prec. concrete piles (sidelengths 30cm and 35cm). Diameter calculation based on
surface area.
The clay layer is really an organic layer. Here it is categorized as clay.
The triaxial friction angles are estimated.
The unit weight for the sand is estimated.
Both ML (maintained load) tests and CRP (Constant rate of penetration) are performed.



#  903
Egå Rensenanlæg  Site 1   Pile(s) 1 - 1   Precast concrete
Egå Rensenanlæg, P4

 NUMLAY   NUMPIL   GWT   GAMPWP    SIGSRF   ZHOLE   QR.SOIL   QR.PILE
    4       1      0.3     10        0.0     0.0      2         3

 LAYER  DEPTH  GAMMA TYPE  Q.CPT  SPT  OCR  -------- CLAY -------   ----SAND----  CLC  MISCELLANEOUS
        BOTTM   EFF ClSiSa  TIP    N        SuTop SuBot TYP St Ip   D50  Dr  PHI  FLG    1   2   3
   1     4.0    8.0   3    5800    0    0     0     0    0   0  0    0    0   0    1     0   0   0
   2    15.5    5.0   1       0    0    0   100   100    8 2.5  0    0    0   0    1     0   0   0
   3    16.5   11.5   3   30000    0    0     0     0    0   0  0    0    0   0    1     0   0   0
   4    30.0   10.0   1       0    0    0   230   380    8   2  0    0    0   0    1     0   0   0

 PILE OPN MAT  DIAM TAPER  WALL  TOTAL  TIP   PLUG  WATER   -- MEASURED CAPACITIES --  MISCELLANEOUS
  NO  CLS TYP   TIP degr   TIP   LNGTH PENTR  RATIO RATIO   COMPRSSN TENSION DAYS TBF  1 2 3
   1   2   2   .318 .00    .159   25.0  23.8   0.0   0.0      1400        0    27   1   0 0 0

Pile is a squared prec. concrete pile (sidelength 25cm). Diameter calculation based on surface area.
Dynamic tests have also been performed on the test site. Each pile has been tested several times.
Some uncertainty associated with the determination of especially sand parameters.
```

904
Egå Rensenanlæg Site 2 Pile(s) 1 - 1 Precast concrete
Egå Rensenanlæg, P10

NUMLAY	NUMPIL	GWT	GAMPWP	SIGSRF	ZHOLE	QR.SOIL	QR.PILE
4	1	0.4	10	0.0	0.0	2	3

LAYER	DEPTH	GAMMA	TYPE	Q.CPT	SPT	OCR	CLAY					SAND			CLC	MISCELLANEOUS		
	BOTTM	EFF	ClSiSa	TIP	N		SuTop	SuBot	TYP	St	Ip	D50	Dr	PHI	FLG	1	2	3
1	2.0	8.0	3	7000	0	0	0	0	0	0	0	0	0	0	0	0	0	0
2	14.0	4.4	1	0	0	0	60	60	8	0	0	0	0	0	1	0	0	0
3	15.5	11.5	3	35000	0	0	0	0	0	0	0	0	0	0	1	0	0	0
4	30.0	10.0	1	0	0	0	230	340	8	2.2	0	0	0	0	1	0	0	0

PILE NO	OPN CLS	MAT TYP	DIAM TIP	TAPER degr	WALL TIP	TOTAL LNGTH	TIP PENTR	PLUG RATIO	WATER RATIO	-- MEASURED CAPACITIES -- COMPRSSN	TENSION	DAYS	TBF	MISCELLANEOUS 1 2 3
1	2	2	.382	.00	.191	26.5	25.2	0.0	0.0	1671	0	28	1	0 0 0

Pile is a squared prec. concrete pile (sidelength 30cm). Diameter calculation based on surface area.
Dynamic tests have also been performed on the test site. Each pile has been tested several times.
Some uncertainty associated with the determination of especiall sand parameters.

905
Algade, Aalborg Site 1 Pile(s) 1 - 1 Precast concrete
Algade, Aalborg, P4

NUMLAY	NUMPIL	GWT	GAMPWP	SIGSRF	ZHOLE	QR.SOIL	QR.PILE
6	2	5.3	10	0.0	0.0	4	2

LAYER	DEPTH	GAMMA	TYPE	Q.CPT	SPT	OCR	CLAY					SAND			CLC	MISCELLANEOUS		
	BOTTM	EFF	ClSiSa	TIP	N		SuTop	SuBot	TYP	St	Ip	D50	Dr	PHI	FLG	1	2	3
1	4.5	15.0	1	0	0	0	25	25	8	0	0	0	0	0	0	0	0	0
2	5.3	15.6	1	0	0	0	120	120	8	1.7	0	0	0	0	0	0	0	0
3	6.0	9.0	3	0	5	0	0	0	0	0	0	0	0	0	0	0	0	0
4	8.5	9.0	1	0	0	0	110	110	8	2.0	0	0	0	0	0	0	0	0
5	11.0	9.2	1	0	0	0	170	170	8	3.0	0	0	0	0	0	0	0	0
6	13.5	9.2	1	0	0	0	225	225	8	3.8	0	0	0	0	0	0	0	0

PILE NO	OPN CLS	MAT TYP	DIAM TIP	TAPER degr	WALL TIP	TOTAL LNGTH	TIP PENTR	PLUG RATIO	WATER RATIO	-- MEASURED CAPACITIES -- COMPRSSN	TENSION	DAYS	TBF	MISCELLANEOUS 1 2 3
1	2	2	.255	.00	.1275	13.35	13.35	0.0	0.0	660	0	14	0	0 0 0
2	2	2	.255	.00	.1275	13.35	13.35	0.0	0.0	930	0	9778	1	1 0 0

Uncertainty on the pile length.
The first two layers are categorized as clay. They are actually a fill and a organic layer, respectively.
The strength and the weight of the fill layer are estimated.
It looks like the concrete crushed in connection with the tests after 9778 days.
Pile is a squared prec. concrete pile (sidelength 20cm). Diameter calculation based on surface area.
Soil profile based mainly on boring 2.
Load tests for other piles are presented. They are not included in the database because failure was not reached due to the definition: Load corresponding to total deformations equal 10% of pile diameter.

906
Motorvegbru Drammen Site 1 Pile(s) 1 - 2 Steel tube and HP-profile
Tvedt and Fredriksen (2003), Pile P1 og P2 (Akse 16)

NUMLAY	NUMPIL	GWT	GAMPWP	SIGSRF	ZHOLE	QR.SOIL	QR.PILE
6	4	2.8	10	0.0	0.0	4	4

LAYER	DEPTH	GAMMA	TYPE	Q.CPT	SPT	OCR	CLAY					SAND			CLC	MISCELLANEOUS		
	BOTTM	EFF	ClSiSa	TIP	N		SuTop	SuBot	TYP	St	Ip	D50	Dr	PHI	FLG	1	2	3
1	2.8	18.0	3	5500	0	0	0	0	0	0	0	0	.52	36	0	0	0	0
2	15.5	8.0	3	5500	0	0	0	0	0	0	0	0	.52	36	0	0	0	0
3	30.0	9.0	1	0	0	0	40	110	4	0	0	0	0	0	0	0	0	0
4	32.5	9.0	1	0	0	0	110	110	4	0	0	0	0	0	0	0	0	0
5	36.0	9.0	1	0	0	0	85	85	4	0	0	0	0	0	0	0	0	0
6	40.0	9.0	1	0	0	0	110	110	4	0	0	0	0	0	0	0	0	0

PILE NO	OPN CLS	MAT TYP	DIAM TIP	TAPER degr	WALL TIP	TOTAL LNGTH	TIP PENTR	PLUG RATIO	WATER RATIO	-- MEASURED CAPACITIES -- COMPRSSN	TENSION	DAYS	TBF	MISCELLANEOUS 1 2 3	
1	1	1	.813	.00	.0125	36.0	35.0	0.21	1.0	2150	0	16	1	0 0 0	P1-16
2	1	1	.813	.00	.0125	36.0	35.0	0.21	1.0	2800	0	140	1	0 0 0	P1-16
3	2	1	.400	.00	.200	39.0	35.0	0.0	0.0	1350	0	14	1	0 0 0	P2-16
4	2	1	.400	.00	.200	39.0	35.0	0.0	0.0	2210	0	141	1	0 0 0	P2-16

The piles have also been dynamic tested.
Static tests after 1day have not been included in the database.
Pile no.2 is a steel pile with H-profile. This profile is equated with a "solid/closed" circular profile.
When calculating the water ratio, the water level inside the pile is assumed to correspond to the level of the ground surface.
Some uncertainty associated with the determination of the plug ratio.

907
Drammen Stasjon Site 1 Pile(s) 1 - 2 Precast concrete
Falstad and Heyerdahl (1995), Pæle P1, P2

NUMLAY	NUMPIL	GWT	GAMPWP	SIGSRF	ZHOLE	QR.SOIL	QR.PILE
5	3	1.0	10	0.0	0.0	1	3

LAYER	DEPTH	GAMMA	TYPE		Q.CPT	SPT	OCR	CLAY					SAND			CLC	MISCELLANEOUS		
	BOTTM	EFF	Cl	Si	Sa	TIP	N		SuTop	SuBot	TYP	St	Ip	D50	Dr	PHI	FLG	1	2	3
1	1.0	19.0	3			2000	0	0	0	0	0	0	0	.80	0	0	0	0	0	0
2	11.0	9.0	3			2000	0	0	0	0	0	0	0	.80	0	0	0	0	0	0
3	14.1	10.3	3			2000	0	0	0	0	0	0	0	.13	0	0	0	0	0	0
4	25.0	8.7	1			0	0	0	50	75	8	8.3	22	0	0	0	0	0	0	0
5	50.0	9.0	1			0	0	0	75	75	8	0	22	0	0	0	0	0	0	0

PILE NO	OPN CLS	MAT TYP	DIAM TIP	TAPER degr	WALL TIP	TOTAL LNGTH	TIP PENTR	PLUG RATIO	WATER RATIO	-- MEASURED CAPACITIES -- COMPRSSN	TENSION	DAYS	TBF	MISCELLANEOUS 1 2 3
1	2	2	.344	.00	.172	50.6	49.0	0.0	0.0	1100	0	21	0	0 0 0
2	2	2	.344	.00	.172	50.6	49.0	0.0	0.0	1700	0	153	1	1 0 0
3	2	2	.344	.00	.172	31.5	30.0	0.0	0.0	960	0	24	0	0 0 0

Boring 6 and "tryksondering" are ended 22m and app. 40m under surface level. Clay anticipated all way down to pile tip. Characteristica based on reports, borings and "tryksonderinger".
The sand is loose and characteristica for the layers are based on reports and other borings.
The top 9m is sandfill. GammaEff is estimated.
Piles are sq. prec. concrete pile (sidelength 27cm). Diameter calculation based on surface area.

908
Powell et al. (2003), Powell and Uglow (1988), Bond and Jardine (1991,1995), Wardle et al. (1992)
Canons Park, Pile B and D

NUMLAY	NUMPIL	GWT	GAMPWP	SIGSRF	ZHOLE	QR.SOIL	QR.PILE
3	9	1.0	10	0.0	2.0	4	4

LAYER	DEPTH	GAMMA	TYPE		Q.CPT	SPT	OCR	CLAY					SAND			CLC	MISCELLANEOUS		
	BOTTM	EFF	Cl	Si	Sa	TIP	N		SuTop	SuBot	TYP	St	Ip	D50	Dr	PHI	FLG	1	2	3
1	2.0	20.0	1			0	0	0	10	63	3	0	55	0	0	0	0	0	0	0
2	4.1	10.0	1			0	0	0	63	78	3	0	55	0	0	0	0	0	0	0
3	7.0	10.0	1			0	0	0	118	118	3	0	40	0	0	0	0	0	0	0

PILE NO	OPN CLS	MAT TYP	DIAM TIP	TAPER degr	WALL TIP	TOTAL LNGTH	TIP PENTR	PLUG RATIO	WATER RATIO	-- MEASURED CAPACITIES -- COMPRSSN	TENSION	DAYS	TBF	MISCELLANEOUS 1 2 3
1	2	1	.168	.00	.0064	7.0	6.5	0.0	0.0	189	0	108	1	0 0 0 D
2	2	1	.168	.00	.0064	7.0	6.5	0.0	0.0	200	0	496	1	0 0 0 D
3	2	1	.168	.00	.0064	7.0	6.5	0.0	0.0	231	0	1130	1	0 0 0 D
4	2	1	.168	.00	.0064	7.0	6.5	0.0	0.0	291	0	6200	1	0 0 0 D
5	2	1	.168	.00	.0064	7.0	6.65	0.0	0.0	194	0	74	1	0 0 0 B
6	2	1	.168	.00	.0064	7.0	6.65	0.0	0.0	197	0	217	1	0 0 0 B
7	2	1	.168	.00	.0064	7.0	6.65	0.0	0.0	200	0	683	1	0 0 0 B
8	2	1	.168	.00	.0064	7.0	6.65	0.0	0.0	221	0	1312	1	0 0 0 B
9	2	1	.168	.00	.0064	7.0	6.65	0.0	0.0	274	0	6200	1	0 0 0 B

Failure loads for pile B are estimated from Table 1 in Wardle et al. (1992) and Powell et al. (2003).
Because the ratios Cal/meas are approximately the same for pile B and D (load-settlement curves are given), it is assumed that the head loads given in Wardle et al. (1992) are failure loads.
"Good agreement" between Fig. 4 in Powell et al. (2003) and Tab. 1 in Wardle et al. (1992).
Addition to existing database #541. GammaEff is here corrected compared to the original database.
Static tests after 0 and 1day have not been included in the database.

909
Powell et al. (2003), Powell and Uglow (1988), Bond and Jardine (1991,1995), Wardle et al. (1992)
Canons Park, Pile A

NUMLAY	NUMPIL	GWT	GAMPWP	SIGSRF	ZHOLE	QR.SOIL	QR.PILE
3	6	1.0	10	0.0	3.0	4	4

LAYER	DEPTH	GAMMA	TYPE		Q.CPT	SPT	OCR	CLAY					SAND			CLC	MISCELLANEOUS		
	BOTTM	EFF	Cl	Si	Sa	TIP	N		SuTop	SuBot	TYP	St	Ip	D50	Dr	PHI	FLG	1	2	3
1	2.0	20.0	1			0	0	0	10	63	3	0	55	0	0	0	0	0	0	0
2	4.1	10.0	1			0	0	0	63	78	3	0	55	0	0	0	0	0	0	0
3	7.0	10.0	1			0	0	0	118	118	3	0	40	0	0	0	0	0	0	0

PILE NO	OPN CLS	MAT TYP	DIAM TIP	TAPER degr	WALL TIP	TOTAL LNGTH	TIP PENTR	PLUG RATIO	WATER RATIO	-- MEASURED CAPACITIES -- COMPRSSN	TENSION	DAYS	TBF	MISCELLANEOUS 1 2 3
1	2	1	.168	.00	.0064	7.0	6.63	0.0	0.0	159	0	31	1	0 0 0 A
2	2	1	.168	.00	.0064	7.0	6.63	0.0	0.0	161	0	134	1	0 0 0 A
3	2	1	.168	.00	.0064	7.0	6.63	0.0	0.0	163	0	248	1	0 0 0 A
4	2	1	.168	.00	.0064	7.0	6.63	0.0	0.0	165	0	525	1	0 0 0 A
5	2	1	.168	.00	.0064	7.0	6.63	0.0	0.0	184	0	1154	1	0 0 0 A
6	2	1	.168	.00	.0064	7.0	6.63	0.0	0.0	231	0	6200	1	0 0 0 A

Failure loads for pile A are estimated from Table 1 in Wardle et al. (1992) and Powell et al (2003).
Because the ratios Cal/meas are approximately the same for pile A, B and D (load-settlement curves are given), it is assumed that the head loads given in Wardle et al. (1992) are failure loads.
"Not that good agreement" between Fig. 4 in Powell et al. (2003) and Tab. 1 in Wardle et al. (1992).
Addition to existing database #541. GammaEff is here corrected compared to the original database.
The static test after 0days have not been included in the database.

910
Powell et al. (2003), Gallagher and St John (1980), Lehane and Jardine (1994)
Cowden, Pile A

NUMLAY	NUMPIL	GWT	GAMPWP	SIGSRF	ZHOLE	QR.SOIL	QR.PILE
4	3	0.0	10	0.0	0.0	4	4

LAYER	DEPTH	GAMMA	TYPE	Q.CPT	SPT	OCR	CLAY					SAND			CLC	MISCELLANEOUS		
	BOTTM	EFF	ClSiSa	TIP	N		SuTop	SuBot	TYP	St	Ip	D50	Dr	PHI	FLG	1	2	3
1	1.3	10.5	1	1225	0	0	60	85	9	0	15	0	0	0	0	0	0	0
2	2.7	10.5	1	4050	0	0	215	255	9	0	15	0	0	0	0	0	0	0
3	4.7	10.5	1	2700	0	0	190	120	9	0	15	0	0	0	0	0	0	0
4	10.0	10.5	1	2100	0	0	120	110	9	0	15	0	0	0	0	0	0	0

PILE NO	OPN CLS	MAT TYP	DIAM TIP	TAPER degr	WALL TIP	TOTAL LNGTH	TIP PENTR	PLUG RATIO	WATER RATIO	-- MEASURED CAPACITIES -- COMPRSSN	TENSION	DAYS	TBF	MISCELLANEOUS 1 2 3
1	1	1	.457	.00	.019	12.0	9.2	0.5?	0.5?	1140	0	30	0	0 0 0
2	1	1	.457	.00	.019	12.0	9.2	0.5?	0.5?	1390	0	396	1	0 0 0
3	1	1	.457	.00	.019	12.0	9.2	0.5?	0.5?	1608	0	9125	1	0 0 0

Addition to existing database #509.

911
Flaate (1972)
Nitsund test site, Pile I and II

NUMLAY	NUMPIL	GWT	GAMPWP	SIGSRF	ZHOLE	QR.SOIL	QR.PILE
2	10	0.0	10	0.0	0.0	4	4

LAYER	DEPTH	GAMMA	TYPE	Q.CPT	SPT	OCR	CLAY					SAND			CLC	MISCELLANEOUS		
	BOTTM	EFF	ClSiSa	TIP	N		SuTop	SuBot	TYP	St	Ip	D50	Dr	PHI	FLG	1	2	3
1	3.8	10.1	1	0	0	0	80	46	8	4	16	0	0	0	0	0	0	0
2	14.0	9.7	1	0	0	0	46	46	8	5	16	0	0	0	0	0	0	0

PILE NO	OPN CLS	MAT TYP	DIAM TIP	TAPER degr	WALL TIP	TOTAL LNGTH	TIP PENTR	PLUG RATIO	WATER RATIO	-- MEASURED CAPACITIES -- COMPRSSN	TENSION	DAYS	TBF	MISCELLANEOUS 1 2 3
1	2	3	.180	.47	.09	11.9	11.7	0.0	0.0	243	0	32	0	0 0 0 I
2	2	3	.180	.47	.09	11.9	11.7	0.0	0.0	321	0	207	1	0 0 0 I
3	2	3	.180	.47	.09	11.9	11.7	0.0	0.0	336	0	357	1	0 0 0 I
4	2	3	.180	.47	.09	11.9	11.7	0.0	0.0	350	0	641	1	0 0 0 I
5	2	3	.180	.47	.09	11.9	11.7	0.0	0.0	350	0	1043	1	1 0 0 I
6	2	3	.175	.32	.0875	13.9	13.7	0.0	0.0	228	0	34	0	0 0 0 II
7	2	3	.175	.32	.0875	13.9	13.7	0.0	0.0	314	0	209	1	0 0 0 II
8	2	3	.175	.32	.0875	13.9	13.7	0.0	0.0	343	0	357	1	0 0 0 II
9	2	3	.175	.32	.0875	13.9	13.7	0.0	0.0	378	0	637	1	0 0 0 II
10	2	3	.175	.32	.0875	13.9	13.7	0.0	0.0	414	0	1023	1	0 0 0 II

Ground water table assumed to be located at surface level.
The boring is stopped in depth of 10m. The second clay layer is extended to the depth of 14m.
It is possible that some piles also are included in the Flaate and Selnes (1977) database (#301-#322). Though it does not seem like that. The pile, soil and test results do not coincide. It is still postulated because there is some uncertainty associated with pile, soil and test conditions, i.e. notice the differences in ranking (This case compared to #301-#322).

912
Bergdahl and Hult (1981)
Skå-Edeby, Pile A-D

NUMLAY	NUMPIL	GWT	GAMPWP	SIGSRF	ZHOLE	QR.SOIL	QR.PILE
2	25	0.0	10	0.0	0.0	4	4

LAYER	DEPTH	GAMMA	TYPE	Q.CPT	SPT	OCR	CLAY					SAND			CLC	MISCELLANEOUS		
	BOTTM	EFF	ClSiSa	TIP	N		SuTop	SuBot	TYP	St	Ip	D50	Dr	PHI	FLG	1	2	3
1	5.0	4.0	1	0	0	0	9	9	8	9	60	0	0	0	0	0	0	0
2	15.6	6.0	1	0	0	0	9	24	8	9	31	0	0	0	0	0	0	0

PILE NO	OPN CLS	MAT TYP	DIAM TIP	TAPER degr	WALL TIP	TOTAL LNGTH	TIP PENTR	PLUG RATIO	WATER RATIO	-- MEASURED CAPACITIES -- COMPRSSN	TENSION	DAYS	TBF	MISCELLANEOUS 1 2 3
1	2	3	.127	.0	.0635	15.5	15.0	0.0	0.0	48	0	30	0	0 0 0 A
2	2	3	.127	.0	.0635	15.5	15.0	0.0	0.0	58	0	75	1	0 0 0 A
3	2	3	.127	.0	.0635	15.5	15.3	0.0	0.0	34	0	42	0	0 0 0 A
4	2	3	.127	.0	.0635	15.5	15.3	0.0	0.0	55	0	456	1	0 0 0 A
5	2	3	.127	.0	.0635	15.5	15.3	0.0	0.0	48	0	1116	1	0 0 0 A
6	2	3	.127	.0	.0635	15.5	15.0	0.0	0.0	52	0	39	0	0 0 0 B
7	2	3	.127	.0	.0635	15.5	15.0	0.0	0.0	64	0	75	1	0 0 0 B
8	2	3	.127	.0	.0635	15.5	15.3	0.0	0.0	36	0	42	0	0 0 0 B
9	2	3	.127	.0	.0635	15.5	15.3	0.0	0.0	56	0	456	1	0 0 0 B
10	2	3	.127	.0	.0635	15.5	15.3	0.0	0.0	54	0	1116	1	0 0 0 B
11	2	3	.127	.0	.0635	15.5	15.0	0.0	0.0	54	0	30	0	0 0 0 C
12	2	3	.127	.0	.0635	15.5	15.0	0.0	0.0	70	0	75	1	0 0 0 C
13	2	3	.127	.0	.0635	15.5	15.3	0.0	0.0	41	0	42	0	0 0 0 C
14	2	3	.127	.0	.0635	15.5	15.3	0.0	0.0	48	0	96	1	0 0 0 C
15	2	3	.127	.0	.0635	15.5	15.3	0.0	0.0	60	0	456	1	0 0 0 C
16	2	3	.127	.0	.0635	15.5	15.3	0.0	0.0	62	0	1116	1	0 0 0 C
17	2	3	.127	.0	.0635	15.5	15.0	0.0	0.0	52	0	30	0	0 0 0 D
18	2	3	.127	.0	.0635	15.5	15.0	0.0	0.0	65	0	75	1	0 0 0 D
19	2	3	.127	.0	.0635	15.5	15.3	0.0	0.0	42	0	96	0	0 0 0 D
20	2	3	.127	.0	.0635	15.5	15.3	0.0	0.0	47	0	171	1	0 0 0 D
21	2	3	.127	.0	.0635	15.5	15.3	0.0	0.0	49	0	456	1	0 0 0 D
22	2	3	.127	.0	.0635	15.5	15.3	0.0	0.0	51	0	1116	1	0 0 0 D
23	2	3	.127	.0	.0635	15.5	14.5	0.0	0.0	56	0	75	0	0 0 0 E
24	2	3	.127	.0	.0635	15.5	14.5	0.0	0.0	66	0	216	1	0 0 0 E
25	2	3	.127	.0	.0635	15.5	14.5	0.0	0.0	63	0	906	1	0 0 0 E

Ground water table assumed to be located at surface level.
Some of the test piles are loaded in different ways. Furthermore, different test procedures are used during load tests of a single pile.
Failure loads are ultimate loads.
Four of the piles (A-D) were driven further 0,2m after the second load test. Hereafter, the pile is treated as a new pile. That is, the effect of former tests are negligible.
Uncertainty in the determination of the time for testing.
Piles are squared wood piles (sidelength 10cm). Diameter calculations based on surface area.
It is assumed that the piles are loaded in compression.

913
Fynsværket Site 1 Pile(s) 1 - 1 Precast concrete
Fynsværket, P1

NUMLAY	NUMPIL	GWT	GAMPWP	SIGSRF	ZHOLE	QR.SOIL	QR.PILE
4	3	0.0	10	0.0	0.0	0	2

LAYER	DEPTH BOTTM	GAMMA EFF	TYPE ClSiSa	Q.CPT TIP	SPT N	OCR	CLAY SuTop	CLAY SuBot	CLAY TYP	CLAY St	CLAY Ip	SAND D50	SAND Dr	SAND PHI	CLC FLG	MISCELLANEOUS 1	MISCELLANEOUS 2	MISCELLANEOUS 3
1	1.9	11.0	1	0	0	0	50	50	8	3.3	0	0	0	0	0	0	0	0
2	9.6	10.3	1	0	0	0	50	70	8	6.0	0	0	0	0	0	0	0	0
3	15.2	10.5	1	0	0	0	110	190	8	12.2	0	0	0	0	0	0	0	0
4	29.1	13.0	1	0	0	0	240	715	8	2.0	0	0	0	0	0	0	0	0

PILE NO	OPN CLS	MAT TYP	DIAM TIP	TAPER degr	WALL TIP	TOTAL LNGTH	TIP PENTR	PLUG RATIO	WATER RATIO	MEASURED CAPACITIES -- COMPRSSN	TENSION	DAYS	TBF	MISCELLANEOUS 1	2	3
1	2	2	.382	.00	.191	29.0	28.7	0.0	0.0	1140	0	50	0	0	0	0
2	2	2	.382	.00	.191	29.0	28.7	0.0	0.0	1149	0	52	1	0	0	0
3	2	2	.382	.00	.191	29.0	28.7	0.0	0.0	1219	0	73	1	0	0	0

Capacities determined by static tests after 52 and 73 days, respectively, are reduced 14% because the loading rate in both cases was "fast". For more details see geotechnical report.
Pile is a squared prec. concrete pile (sidelength 30cm). Diameter calculation based on surface area.
Excavation is taken into account (discussed in geotechnical report). "surface" in kote -0,4.
The boring is stopped app. 26m under the surface level. It is anticipated that the soil in depth between 26m and 29.1m is the same as the soil in the depth of 26m.
Dynamic tests have also been performed in the area. Failure were not reached.

****
DATA BASE: TILLÆGSCASES TIL NGI-DATABASE - PILES IN CLAY LOG
****

Date	By	Description
10 Dec 2003	AA	Cases approved by CJFC/NGI and PMA/NGI.
15 Dec 2003	AA	Piles with non-circular cross-sections are equated with circular cross-sections. Equivalent diameter based on surface area instead of cross-section area. Soil and pile quality rating. Tests performed within some days of driving are omitted. Case Aalborg værft is removed. Included in the sand database.
16 Dec 2003	AA	Changed the sequence of the cases.
07 Mar 2005	AA	PSG Domicil KBH. moved to Sand database.
09 May 2005	AA	Taper changed in connection with case #911 Nitsund
09 Aug 2005	AA	Qr.soil changed to 4 for Nitsund

Appendix F:
AAU and NGI data

The following pages present the PILCAP input file for the combination of the AAU and NGI data. It should be mentioned that the references in the database cannot all be found in the list of references.

```
PILES IN CLAY     CLAY DATABASE - ALL PILES IN OLD AND NEW DATABASE                    09 MAY 2005

   114   NUMSIT   Number of different sites
     0   INTER    Run program in interactive mode (0=no 1=yes)

     6   ICSAND   Code for method to calculate sand skin friction, see below
     6   ICCLAY   Code for method to calculate clay skin friction, see below

   100   ATMPRS   Atmospheric pressure    (100 kPa  in S.I. units)
    10   GAMWAT   Unit weight of water    (10 kN/m3 in S.I. units)
    78   GAMSTL   Unit weight of steel    (78 kN/m3 in S.I. units)
    25   GAMCON   Unit weight of concrete (25 kN/m3 in S.I. units)
     9   GAMWOD   Unit weight of wood     ( 9 kN/m3 in S.I. units)

     1   MODFSU   Code for change of Su values to Su.UU or Su.DSS (0=No 1=Yes)
   100   TIMEFC   Time needed for development of full pile clay capacity, days
   .00   DELT10   Pile capacity increase for 10-fold time increase
  1.00   PLGFCT   Plug factor, ratio inside/outside friction force

  0  0   INCQRC   Include sites with same or higher soil and pile quality rating code
 1 1 1   INCMAT   Include piles with material code STEEL/CONCRETE/WOOD (0=No 1=Yes)
  1  1   INCMTN   Include piles loaded in compression/tension (0=No 1=Yes)
 0 100   DIAINC   Include piles with diameter within given range
 0 200   PENINC   Include piles with penetration within given range
 0 99999 CAPINC   Include piles with measured capacity within given range
 0 10000 TIMINC   Include piles with time from driving to testing within given range
 0 10.0  SUPINC   Include piles with average Su/po' ratio within given range

  4.5   65  3.0  0.05 0.2   SAND 1-5    Parameters used to calculate pile skin
  .40  .75  .30  2.0  .125  SAND 6-10   friction in sand by NGI-1999 method

 1 1 0            Codes for plotting, 0=NO 1=YES (SAND/CMP  SAND/TNS  CLAY/CMP&TNS)

  ================================    ======================================
  SAND SKIN FRICTION CODES            CLAY SKIN FRICTION CODES
  ================================    ======================================
  1 = API 1972 to 1984 (K=0.5/0.7)    1 = API 1979 to 1987 (24-72 kPa)
  2 = API 1984 to now  (K=0.8/0.8)    2 = API 1987 to now  (ALPHA=f(Su/SIGZ))
  3 = API 1984 to now  (K=0.5/0.7)    3 = API/NGI 1992
  4 = Not used                        4 = NGI 1990
  5 = Imperial College 1996           5 = Imperial College 1996
  6 = NGI 1999                        6 = NGI 1999
  7 = Not used                        7 = Not used
  ================================    ======================================

Data given below for each location and pile include :

  NUMLAY        Number of soil layers
  NUMPIL        Number of different piles or penetration depths
  GWT           Depth from soil surface to ground water table, neg. if submerged site
  GAMPWP        Water unit weight to calculate pore water pressure at pile tip
  SIGSRF        Vertical stress at soil surface
  ZHOLE         Depth below surface of open or cased hole
  QR.SOIL       Quality rating for soil and pile data :
  QR.PILE       0 = Not known  1 = Low  2 = Average  3 = High

  DEPTH BOTTM   Depth to bottom of layer
  GAMMA EFF     Effective unit weight
  TYPE          Soil type indicator (1=Clay 2=Silt 3=Sand)
  Q.CPT         Cone Penetrometer Test tip resistance qc
  SPT           Standard Penetration Test, blows/foot
  OCR           Over-consolidation ratio for CPT to Dr conversion
  SuTop         Undrained shear strength at top of layer
  SuBot         Undrained shear strength at bottom of layer
  TYP           Type of undrained shear strength measurement, see below
  St            Clay sensitivity
  Ip            Clay plasticity index = Wl - Wp
  D50           Sand grain average diameter, mm
  Dr            Sand relative density
  PHI           Sand angle of internal friction
  CLC.FLG       Flag for calcareous soils
  MISC 1-3      MISC(1) is Delta.Sig.PC, used to find OCR.  2-3 not used.

  OPN.CLS       Pile driven open ended (=1) or closed ended (=2)
  MAT.TYP       Pile material type id (1=steel 2=concrete 3=wood)
  DIAM.TIP      Pile tip diameter
  TAPER         Pile wall taper, degrees
  WALL.TIP      Wall thickness at pile tip
  TOTAL.LNGTH   Total pile length from pile but to pile tip
  TIP.PENTR     Depth of pile tip penetration
  PLUG.RATIO    Ratio soil plug length to tip penetration
  WATER.RATIO   Ratio water plug length to tip penetration
  COMPRSSN      Measured pile capacity in compression
  TENSION       Measured pile capacity in tension
  DAYS          Number of days between pile driving and pile testing
  TBF           Value 1 flags that the pile has been tested before
  MISC(1)=  1   Value 1 flags that failure was not reached
  MISC(2)= -1   No correction for time between driving and testing
  MISC(3)= -1   Skip plug capacity control
  MISC(3)=  0   Clay tip tensile force : Undrained conditions
  MISC(3)=  1   Clay tip tensile force : Drained conditions
  MISC(3)=  2   Clay tip tensile force : Zero force at pile tip

Undrained shear strength codes :

  -1 = Estimated value              0 = Not known

   1 = Torvane, pocket pentr.       8 = Field vane test
```

```
   2 = Unconfined compr. test        9 = Field cone penetrometer test
   3 = UU triaxial test             10 = Other field test
   4 = CIU/CAU triaxial test
   5 = Direct simple shear
   6 = Lab vane
   7 = Other lab test


#  301
Flaate & Selnes (1977)   Site 1   Pile(s) 1 - 1   Timber
F&S 1-1

 NUMLAY   NUMPIL   GWT   GAMPWP    SIGSRF   ZHOLE   QR.SOIL   QR.PILE
    1       1      0.0     10        0.0     0.0       2         1

 LAYER  DEPTH  GAMMA TYPE  Q.CPT  SPT  OCR  -------- CLAY -------   ----SAND----  CLC  MISCELLANEOUS
        BOTTM   EFF ClSiSa  TIP    N        SuTop SuBot TYP St Ip   D50  Dr  PHI  FLG    1   2   3
   1    14.11  13.3   1      0     0    0    12    40    2?  7 12    0    0   0    0     0   0   0

 PILE OPN MAT  DIAM TAPER  WALL  TOTAL  TIP   PLUG  WATER   -- MEASURED CAPACITIES --  MISCELLANEOUS
  NO  CLS TYP   TIP degr   TIP   LNGTH PENTR  RATIO RATIO   COMPRSSN TENSION DAYS TBF  1 2 3
   1   2   3   .150 .75   .075   14.1  14.1   0.0   0.0       392        0    90   0   0 0 0


#  302
Flaate & Selnes (1977)   Site 2   Pile(s) 2 - 2   Timber
F&S 2-2

 NUMLAY   NUMPIL   GWT   GAMPWP    SIGSRF   ZHOLE   QR.SOIL   QR.PILE
    1       1      0.0     10        0.0     0.0       2         1

 LAYER  DEPTH  GAMMA TYPE  Q.CPT  SPT  OCR  -------- CLAY -------   ----SAND----  CLC  MISCELLANEOUS
        BOTTM   EFF ClSiSa  TIP    N        SuTop SuBot TYP St Ip   D50  Dr  PHI  FLG    1   2   3
   1    13.01  15.4   1      0     0    0     2    28    2?  7 19    0    0   0    0     0   0   0

 PILE OPN MAT  DIAM TAPER  WALL  TOTAL  TIP   PLUG  WATER   -- MEASURED CAPACITIES --  MISCELLANEOUS
  NO  CLS TYP   TIP degr   TIP   LNGTH PENTR  RATIO RATIO   COMPRSSN TENSION DAYS TBF  1 2 3
   1   2   3   .150 .45   .075   13.0  13.0   0.0   0.0       265        0    90   0   0 0 0


#  303
Flaate & Selnes (1977)   Site 3   Pile(s) 3 - 3   Timber
F&S 3-3

 NUMLAY   NUMPIL   GWT   GAMPWP    SIGSRF   ZHOLE   QR.SOIL   QR.PILE
    1       1      0.0     10        0.0     0.0       2         1

 LAYER  DEPTH  GAMMA TYPE  Q.CPT  SPT  OCR  -------- CLAY -------   ----SAND----  CLC  MISCELLANEOUS
        BOTTM   EFF ClSiSa  TIP    N        SuTop SuBot TYP St Ip   D50  Dr  PHI  FLG    1   2   3
   1    11.71   9.1   1      0     0    0    11    35    2?  5 14    0    0   0    0     0   0   0

 PILE OPN MAT  DIAM TAPER  WALL  TOTAL  TIP   PLUG  WATER   -- MEASURED CAPACITIES --  MISCELLANEOUS
  NO  CLS TYP   TIP degr   TIP   LNGTH PENTR  RATIO RATIO   COMPRSSN TENSION DAYS TBF  1 2 3
   1   2   3   .200 .50   .100   11.7  11.7   0.0   0.0       157        0    90   0   0 0 0


#  304
Flaate & Selnes (1977)   Site 4   Pile(s) 4 - 5   Timber
F&S 4-5

 NUMLAY   NUMPIL   GWT   GAMPWP    SIGSRF   ZHOLE   QR.SOIL   QR.PILE
    1       2      0.0     10        0.0     0.0       2         1

 LAYER  DEPTH  GAMMA TYPE  Q.CPT  SPT  OCR  -------- CLAY -------   ----SAND----  CLC  MISCELLANEOUS
        BOTTM   EFF ClSiSa  TIP    N        SuTop SuBot TYP St Ip   D50  Dr  PHI  FLG    1   2   3
   1    14.61   9.4   1      0     0    0    13    43    2?  3  9    0    0   0    0     0   0   0

 PILE OPN MAT  DIAM TAPER  WALL  TOTAL  TIP   PLUG  WATER   -- MEASURED CAPACITIES --  MISCELLANEOUS
  NO  CLS TYP   TIP degr   TIP   LNGTH PENTR  RATIO RATIO   COMPRSSN TENSION DAYS TBF  1 2 3
   1   2   3   .160 .37   .080   14.6  14.6   0.0   0.0       196        0    90   0   0 0 0
   2   2   3   .175 .38   .0875  11.6  11.6   0.0   0.0       167        0    90   0   0 0 0


#  305
Flaate & Selnes (1977)   Site 5   Pile(s) 6 - 8   Timber
F&S 6-8

 NUMLAY   NUMPIL   GWT   GAMPWP    SIGSRF   ZHOLE   QR.SOIL   QR.PILE
    1       3      0.0     10        0.0     0.0       2         1

 LAYER  DEPTH  GAMMA TYPE  Q.CPT  SPT  OCR  -------- CLAY -------   ----SAND----  CLC  MISCELLANEOUS
        BOTTM   EFF ClSiSa  TIP    N        SuTop SuBot TYP St Ip   D50  Dr  PHI  FLG    1   2   3
   1    17.51  10.8   1      0     0    0     8    41    2?  6 43    0    0   0    0     0   0   0

 PILE OPN MAT  DIAM TAPER  WALL  TOTAL  TIP   PLUG  WATER   -- MEASURED CAPACITIES --  MISCELLANEOUS
  NO  CLS TYP   TIP degr   TIP   LNGTH PENTR  RATIO RATIO   COMPRSSN TENSION DAYS TBF  1 2 3
   1   2   3   .143 .06   .0715  17.5  17.5   0.0   0.0       226        0    90   0   0 0 0
   2   2   3   .156 .13   .078   14.4  14.4   0.0   0.0       255        0    90   0   0 0 0
   3   2   3   .153 .15   .0765  15.0  15.0   0.0   0.0       265        0    90   0   0 0 0


#  306
Flaate & Selnes (1977)   Site 6   Pile(s) 9 - 12  Timber
F&S 9-12

 NUMLAY   NUMPIL   GWT   GAMPWP    SIGSRF   ZHOLE   QR.SOIL   QR.PILE
    1       4      0.0     10        0.0     0.0       2         1

 LAYER  DEPTH  GAMMA TYPE  Q.CPT  SPT  OCR  -------- CLAY -------   ----SAND----  CLC  MISCELLANEOUS
        BOTTM   EFF ClSiSa  TIP    N        SuTop SuBot TYP St Ip   D50  Dr  PHI  FLG    1   2   3
   1    17.31   6.4   1      0     0    0     2    34    2?  6 98    0    0   0    0     0   0   0

 PILE OPN MAT  DIAM TAPER  WALL  TOTAL  TIP   PLUG  WATER   -- MEASURED CAPACITIES --  MISCELLANEOUS
  NO  CLS TYP   TIP degr   TIP   LNGTH PENTR  RATIO RATIO   COMPRSSN TENSION DAYS TBF  1 2 3
   1   2   3   .159 .01   .0795  11.9  11.9   0.0   0.0        78        0    90   0   0 0 0
   2   2   3   .150 .11   .075   13.8  13.8   0.0   0.0       113        0    90   0   0 0 0
   3   2   3   .150 .17   .075   15.9  15.9   0.0   0.0       123        0    90   0   0 0 0
   4   2   3   .140 .19   .070   17.3  17.3   0.0   0.0       123        0    90   0   0 0 0
```

307
Flaate & Selnes (1977) Site 7 Pile(s) 13 - 19 Timber
F&S 13-19

NUMLAY	NUMPIL	GWT	GAMPWP	SIGSRF	ZHOLE	QR.SOIL	QR.PILE
1	7	0.0	10	0.0	0.0	2	1

LAYER	DEPTH	GAMMA	TYPE	Q.CPT	SPT	OCR	CLAY				SAND			CLC	MISCELLANEOUS		
	BOTTM	EFF	ClSiSa	TIP	N		SuTop	SuBot	TYP	St Ip	D50	Dr	PHI	FLG	1	2	3
1	12.71	8.3	1	0	0	0	5	28	2?	6 44	0	0	0	0	0	0	0

PILE NO	OPN CLS	MAT TYP	DIAM TIP	TAPER degr	WALL TIP	TOTAL LNGTH	TIP PENTR	PLUG RATIO	WATER RATIO	-- MEASURED CAPACITIES -- COMPRSSN	TENSION	DAYS	TBF	MISCELLANEOUS 1 2 3
1	2	3	.135	.29	.0675	8.1	8.1	0.0	0.0	49	0	90	0	0 0 0
2	2	3	.192	.29	.0960	9.6	9.6	0.0	0.0	96	0	90	0	0 0 0
3	2	3	.156	.29	.078	11.5	11.5	0.0	0.0	98	0	90	0	0 0 0
4	2	3	.147	.29	.0735	11.6	11.6	0.0	0.0	108	0	90	0	0 0 0
5	2	3	.167	.29	.0835	12.7	12.7	0.0	0.0	142	0	90	0	0 0 0
6	2	3	.165	.29	.0825	7.7	7.7	0.0	0.0	49	0	90	0	0 0 0
7	2	3	.138	.29	.069	9.4	9.4	0.0	0.0	54	0	90	0	0 0 0

308
Flaate & Selnes (1977) Site 8 Pile(s) 20 - 22 Timber
F&S 20-22

NUMLAY	NUMPIL	GWT	GAMPWP	SIGSRF	ZHOLE	QR.SOIL	QR.PILE
1	3	0.0	10	0.0	0.0	2	1

LAYER	DEPTH	GAMMA	TYPE	Q.CPT	SPT	OCR	CLAY				SAND			CLC	MISCELLANEOUS		
	BOTTM	EFF	ClSiSa	TIP	N		SuTop	SuBot	TYP	St Ip	D50	Dr	PHI	FLG	1	2	3
1	12.01	6.4	1	0	0	0	1	24	2?	0 54	0	0	0	0	0	0	0

PILE NO	OPN CLS	MAT TYP	DIAM TIP	TAPER degr	WALL TIP	TOTAL LNGTH	TIP PENTR	PLUG RATIO	WATER RATIO	-- MEASURED CAPACITIES -- COMPRSSN	TENSION	DAYS	TBF	MISCELLANEOUS 1 2 3
1	2	3	.135	.20	.0675	8.0	8.0	0.0	0.0	39	0	90	0	0 0 0
2	2	3	.135	.30	.0675	10.0	10.0	0.0	0.0	69	0	90	0	0 0 0
3	2	3	.155	.36	.0775	12.0	12.0	0.0	0.0	88	0	90	0	0 0 0

309
Flaate & Selnes (1977) Site 9 Pile(s) 23 - 26 Timber
F&S 23-26

NUMLAY	NUMPIL	GWT	GAMPWP	SIGSRF	ZHOLE	QR.SOIL	QR.PILE
1	4	0.0	10	0.0	0.0	2	1

LAYER	DEPTH	GAMMA	TYPE	Q.CPT	SPT	OCR	CLAY				SAND			CLC	MISCELLANEOUS		
	BOTTM	EFF	ClSiSa	TIP	N		SuTop	SuBot	TYP	St Ip	D50	Dr	PHI	FLG	1	2	3
1	14.11	3.7	1	0	0	0	6	35	2?	8 73	0	0	0	0	0	0	0

PILE NO	OPN CLS	MAT TYP	DIAM TIP	TAPER degr	WALL TIP	TOTAL LNGTH	TIP PENTR	PLUG RATIO	WATER RATIO	-- MEASURED CAPACITIES -- COMPRSSN	TENSION	DAYS	TBF	MISCELLANEOUS 1 2 3
1	2	3	.190	.29	.095	13.8	13.8	0.0	0.0	137	0	90	0	0 0 0
2	2	3	.220	.26	.110	10.2	10.2	0.0	0.0	69	0	90	0	0 0 0
3	2	3	.235	.31	.1175	14.1	14.1	0.0	0.0	177	0	90	0	0 0 0
4	2	3	.190	.31	.095	10.1	10.1	0.0	0.0	62	0	90	0	0 0 0

310
Flaate & Selnes (1977) Site 10 Pile(s) 27 - 30 Spliced timber piles
F&S 27-30

NUMLAY	NUMPIL	GWT	GAMPWP	SIGSRF	ZHOLE	QR.SOIL	QR.PILE
1	4	0.0	10	0.0	0.0	2	1

LAYER	DEPTH	GAMMA	TYPE	Q.CPT	SPT	OCR	CLAY				SAND			CLC	MISCELLANEOUS		
	BOTTM	EFF	ClSiSa	TIP	N		SuTop	SuBot	TYP	St Ip	D50	Dr	PHI	FLG	1	2	3
1	24.21	11.8	1	0	0	0	1	39	2?	6 16	0	0	0	0	0	0	0

PILE NO	OPN CLS	MAT TYP	DIAM TIP	TAPER degr	WALL TIP	TOTAL LNGTH	TIP PENTR	PLUG RATIO	WATER RATIO	-- MEASURED CAPACITIES -- COMPRSSN	TENSION	DAYS	TBF	MISCELLANEOUS 1 2 3
1	2	3	.150	.27	.075	24.2	24.2	0.0	0.0	441	0	90	0	0 0 0
2	2	3	.150	.29	.075	24.2	24.2	0.0	0.0	491	0	90	0	0 0 0
3	2	3	.150	.32	.075	24.2	24.2	0.0	0.0	540	0	90	0	0 0 0
4	2	3	.150	.32	.075	24.2	24.2	0.0	0.0	589	0	90	0	0 0 0

311
Flaate & Selnes (1977) Site 11 Pile 31 Timber
F&S 31

NUMLAY	NUMPIL	GWT	GAMPWP	SIGSRF	ZHOLE	QR.SOIL	QR.PILE
1	1	0.0	10	0.0	0.0	2	1

LAYER	DEPTH	GAMMA	TYPE	Q.CPT	SPT	OCR	CLAY				SAND			CLC	MISCELLANEOUS		
	BOTTM	EFF	ClSiSa	TIP	N		SuTop	SuBot	TYP	St Ip	D50	Dr	PHI	FLG	1	2	3
1	17.11	12.5	1	0	0	0	39	73	2?	5 12	0	0	0	0	0	0	0

PILE NO	OPN CLS	MAT TYP	DIAM TIP	TAPER degr	WALL TIP	TOTAL LNGTH	TIP PENTR	PLUG RATIO	WATER RATIO	-- MEASURED CAPACITIES -- COMPRSSN	TENSION	DAYS	TBF	MISCELLANEOUS 1 2 3
1	2	3	.150	.38	.075	17.1	17.1	0.0	0.0	343	0	90	0	0 0 0

312
Flaate & Selnes (1977) Site 12 Pile 32 Timber
F&S 32

NUMLAY	NUMPIL	GWT	GAMPWP	SIGSRF	ZHOLE	QR.SOIL	QR.PILE
1	1	0.0	10	0.0	0.0	2	1

LAYER	DEPTH	GAMMA	TYPE	Q.CPT	SPT	OCR	CLAY				SAND			CLC	MISCELLANEOUS		
	BOTTM	EFF	ClSiSa	TIP	N		SuTop	SuBot	TYP	St Ip	D50	Dr	PHI	FLG	1	2	3
1	12.71	5.8	1	0	0	0	6	32	2?	16 20	0	0	0	0	0	0	0

PILE NO	OPN CLS	MAT TYP	DIAM TIP	TAPER degr	WALL TIP	TOTAL LNGTH	TIP PENTR	PLUG RATIO	WATER RATIO	-- MEASURED CAPACITIES -- COMPRSSN	TENSION	DAYS	TBF	MISCELLANEOUS 1 2 3
1	2	3	.232	.29	.116	12.7	12.7	0.0	0.0	206	0	90	0	0 0 0

313
Flaate & Selnes (1977) Site 13 Pile 33 Timber
F&S 33

NUMLAY	NUMPIL	GWT	GAMPWP	SIGSRF	ZHOLE	QR.SOIL	QR.PILE
1	1	0.0	10	0.0	0.0	2	1

LAYER	DEPTH	GAMMA	TYPE	Q.CPT	SPT	OCR	CLAY					SAND			CLC	MISCELLANEOUS		
	BOTTM	EFF	ClSiSa	TIP	N		SuTop	SuBot	TYP	St	Ip	D50	Dr	PHI	FLG	1	2	3
1	15.51	10.1	1	0	0	0	56	87	2?	3	12	0	0	0	0	0	0	0

PILE NO	OPN CLS	MAT TYP	DIAM TIP	TAPER degr	WALL TIP	TOTAL LNGTH	TIP PENTR	PLUG RATIO	WATER RATIO	-- MEASURED CAPACITIES -- COMPRSSN	TENSION	DAYS	TBF	MISCELLANEOUS 1 2 3
1	2	3	.175	.29	.0875	15.5	15.5	0.0	0.0	441	0	90	0	0 0 0

314
Flaate & Selnes (1977) Site 14 Pile 34 Timber
F&S 34

NUMLAY	NUMPIL	GWT	GAMPWP	SIGSRF	ZHOLE	QR.SOIL	QR.PILE
1	1	0.0	10	0.0	0.0	2	1

LAYER	DEPTH	GAMMA	TYPE	Q.CPT	SPT	OCR	CLAY					SAND			CLC	MISCELLANEOUS		
	BOTTM	EFF	ClSiSa	TIP	N		SuTop	SuBot	TYP	St	Ip	D50	Dr	PHI	FLG	1	2	3
1	11.51	10.8	1	0	0	0	60	83	2?	3	13	0	0	0	0	0	0	0

PILE NO	OPN CLS	MAT TYP	DIAM TIP	TAPER degr	WALL TIP	TOTAL LNGTH	TIP PENTR	PLUG RATIO	WATER RATIO	-- MEASURED CAPACITIES -- COMPRSSN	TENSION	DAYS	TBF	MISCELLANEOUS 1 2 3
1	2	3	.175	.29	.0875	11.5	11.5	0.0	0.0	226	0	90	0	0 0 0

315
Flaate & Selnes (1977) Site 15 Pile 35 Timber
F&S 35

NUMLAY	NUMPIL	GWT	GAMPWP	SIGSRF	ZHOLE	QR.SOIL	QR.PILE
1	1	0.0	10	0.0	0.0	2	1

LAYER	DEPTH	GAMMA	TYPE	Q.CPT	SPT	OCR	CLAY					SAND			CLC	MISCELLANEOUS		
	BOTTM	EFF	ClSiSa	TIP	N		SuTop	SuBot	TYP	St	Ip	D50	Dr	PHI	FLG	1	2	3
1	10.01	9.2	1	0	0	0	41	61	2?	4	8	0	0	0	0	0	0	0

PILE NO	OPN CLS	MAT TYP	DIAM TIP	TAPER degr	WALL TIP	TOTAL LNGTH	TIP PENTR	PLUG RATIO	WATER RATIO	-- MEASURED CAPACITIES -- COMPRSSN	TENSION	DAYS	TBF	MISCELLANEOUS 1 2 3
1	2	3	.230	.31	.115	10.0	10.0	0.0	0.0	196	0	90	0	0 0 0

316
Flaate & Selnes (1977) Site 16 Pile 36 Timber
F&S 36

NUMLAY	NUMPIL	GWT	GAMPWP	SIGSRF	ZHOLE	QR.SOIL	QR.PILE
1	1	0.0	10	0.0	0.0	2	1

LAYER	DEPTH	GAMMA	TYPE	Q.CPT	SPT	OCR	CLAY					SAND			CLC	MISCELLANEOUS		
	BOTTM	EFF	ClSiSa	TIP	N		SuTop	SuBot	TYP	St	Ip	D50	Dr	PHI	FLG	1	2	3
1	10.01	16.0	1	0	0	0	25	45	2?	4	14	0	0	0	0	0	0	0

PILE NO	OPN CLS	MAT TYP	DIAM TIP	TAPER degr	WALL TIP	TOTAL LNGTH	TIP PENTR	PLUG RATIO	WATER RATIO	-- MEASURED CAPACITIES -- COMPRSSN	TENSION	DAYS	TBF	MISCELLANEOUS 1 2 3
1	2	3	.170	.28	.085	10.0	10.0	0.0	0.0	196	0	90	0	0 0 0

317
Flaate & Selnes (1977) Site 17 Pile 37 Timber
F&S 37

NUMLAY	NUMPIL	GWT	GAMPWP	SIGSRF	ZHOLE	QR.SOIL	QR.PILE
1	1	0.0	10	0.0	0.0	2	1

LAYER	DEPTH	GAMMA	TYPE	Q.CPT	SPT	OCR	CLAY					SAND			CLC	MISCELLANEOUS		
	BOTTM	EFF	ClSiSa	TIP	N		SuTop	SuBot	TYP	St	Ip	D50	Dr	PHI	FLG	1	2	3
1	9.41	10.9	1	0	0	0	19	37	2?	11	31	0	0	0	0	0	0	0

PILE NO	OPN CLS	MAT TYP	DIAM TIP	TAPER degr	WALL TIP	TOTAL LNGTH	TIP PENTR	PLUG RATIO	WATER RATIO	-- MEASURED CAPACITIES -- COMPRSSN	TENSION	DAYS	TBF	MISCELLANEOUS 1 2 3
1	2	3	.293	.24	.1465	9.4	9.4	0.0	0.0	191	0	90	0	0 0 0

318
Flaate & Selnes (1977) Site 18 Piles 38 - 39 Concrete
F&S 38-39

NUMLAY	NUMPIL	GWT	GAMPWP	SIGSRF	ZHOLE	QR.SOIL	QR.PILE
1	2	0.0	10	0.0	0.0	2	1

LAYER	DEPTH	GAMMA	TYPE	Q.CPT	SPT	OCR	CLAY					SAND			CLC	MISCELLANEOUS		
	BOTTM	EFF	ClSiSa	TIP	N		SuTop	SuBot	TYP	St	Ip	D50	Dr	PHI	FLG	1	2	3
1	14.31	12.2	1	0	0	0	8	36	2?	0	34	0	0	0	0	0	0	0

PILE NO	OPN CLS	MAT TYP	DIAM TIP	TAPER degr	WALL TIP	TOTAL LNGTH	TIP PENTR	PLUG RATIO	WATER RATIO	-- MEASURED CAPACITIES -- COMPRSSN	TENSION	DAYS	TBF	MISCELLANEOUS 1 2 3
1	2	2	.260	.00	.130	14.3	14.3	0.0	0.0	255	0	90	0	0 0 0
2	2	2	.260	.00	.130	14.3	14.3	0.0	0.0	235	0	90	0	0 0 0

319
Flaate & Selnes (1977) Site 19 Piles 40 - 41 Concrete
F&S 40-41

NUMLAY	NUMPIL	GWT	GAMPWP	SIGSRF	ZHOLE	QR.SOIL	QR.PILE
1	2	0.0	10	0.0	0.0	2	1

LAYER	DEPTH	GAMMA	TYPE	Q.CPT	SPT	OCR	CLAY					SAND			CLC	MISCELLANEOUS		
	BOTTM	EFF	ClSiSa	TIP	N		SuTop	SuBot	TYP	St	Ip	D50	Dr	PHI	FLG	1	2	3
1	22.51	5.2	1	0	0	0	22	67	2?	0	27	0	0	0	0	0	0	0

PILE NO	OPN CLS	MAT TYP	DIAM TIP	TAPER degr	WALL TIP	TOTAL LNGTH	TIP PENTR	PLUG RATIO	WATER RATIO	-- MEASURED CAPACITIES -- COMPRSSN	TENSION	DAYS	TBF	MISCELLANEOUS 1 2 3
1	2	2	.470	.00	.235	22.5	22.5	0.0	0.0	863	0	90	0	0 0 0
2	2	2	.470	.00	.235	22.5	22.5	0.0	0.0	1069	0	90	0	0 0 0

```
#  320
Flaate & Selnes (1977)   Site 20  Pile 42   Steel
F&S 42

 NUMLAY   NUMPIL   GWT   GAMPWP    SIGSRF   ZHOLE   QR.SOIL   QR.PILE
    1       1      0.0     10        0.0     0.0       2         1

 LAYER  DEPTH  GAMMA TYPE  Q.CPT  SPT  OCR  -------- CLAY -------   ----SAND----  CLC  MISCELLANEOUS
        BOTTM   EFF ClSiSa  TIP    N        SuTop SuBot TYP St Ip   D50  Dr  PHI  FLG    1   2   3
   1   13.41  11.8   1      0     0    0      9    35    2?  0 32    0    0   0    0     0   0   0

 PILE OPN MAT  DIAM TAPER  WALL  TOTAL  TIP   PLUG  WATER   -- MEASURED CAPACITIES --  MISCELLANEOUS
  NO  CLS TYP   TIP degr   TIP   LNGTH PENTR  RATIO RATIO   COMPRSSN TENSION DAYS TBF  1 2 3
   1   2?  1   .270 .00   .010?  13.4  13.4   0.0   0.0       206        0    90   0   0 0 0

#  321
Flaate & Selnes (1977)   Site 21  Pile 43   Steel
F&S 43

 NUMLAY   NUMPIL   GWT   GAMPWP    SIGSRF   ZHOLE   QR.SOIL   QR.PILE
    1       1      0.0     10        0.0     0.0       2         1

 LAYER  DEPTH  GAMMA TYPE  Q.CPT  SPT  OCR  -------- CLAY -------   ----SAND----  CLC  MISCELLANEOUS
        BOTTM   EFF ClSiSa  TIP    N        SuTop SuBot TYP St Ip   D50  Dr  PHI  FLG    1   2   3
   1   13.51  20.4   1      0     0    0     127  154    2?  0 14    0    0   0    0     0   0   0

 PILE OPN MAT  DIAM TAPER  WALL  TOTAL  TIP   PLUG  WATER   -- MEASURED CAPACITIES --  MISCELLANEOUS
  NO  CLS TYP   TIP degr   TIP   LNGTH PENTR  RATIO RATIO   COMPRSSN TENSION DAYS TBF  1 2 3
   1   2?  1   .305 .00   .010?  13.5  13.5   0.0   0.0       697        0    90   0   0 0 0

#  322
Flaate & Selnes (1977)   Site 22  Pile 44   Steel
F&S 44

 NUMLAY   NUMPIL   GWT   GAMPWP    SIGSRF   ZHOLE   QR.SOIL   QR.PILE
    1       1      0.0     10        0.0     0.0       2         1

 LAYER  DEPTH  GAMMA TYPE  Q.CPT  SPT  OCR  -------- CLAY -------   ----SAND----  CLC  MISCELLANEOUS
        BOTTM   EFF ClSiSa  TIP    N        SuTop SuBot TYP St Ip   D50  Dr  PHI  FLG    1   2   3
   1    5.51  15.6   1      0     0    0      24   35    2?  0 45    0    0   0    0     0   0   0

 PILE OPN MAT  DIAM TAPER  WALL  TOTAL  TIP   PLUG  WATER   -- MEASURED CAPACITIES --  MISCELLANEOUS
  NO  CLS TYP   TIP degr   TIP   LNGTH PENTR  RATIO RATIO   COMPRSSN TENSION DAYS TBF  1 2 3
   1   2?  1   .305 .00   .010?   5.5   5.5   0.0   0.0       216        0    90   0   0 0 0

#  323
Semple & Rigden (1984)   API Data Base Identifier =  8
S&R (1984)

 NUMLAY   NUMPIL   GWT   GAMPWP    SIGSRF   ZHOLE   QR.SOIL   QR.PILE
    2       1      0.0     10        0       5.8       2         1

 LAYER  DEPTH  GAMMA TYPE  Q.CPT  SPT  OCR  -------- CLAY -------   ----SAND----  CLC  MISCELLANEOUS
        BOTTM   EFF ClSiSa  TIP    N        SuTop SuBot TYP St Ip   D50  Dr  PHI  FLG    1   2   3
   1    5.80   9.0   1      0     0    0      7     7    2   0  0    0    0   0    0     0   0   0
   2   26.21   9.0   1      0     0    0      7    53    2   0  0    0    0   0    0     0   0   0

 PILE OPN MAT  DIAM TAPER  WALL  TOTAL  TIP   PLUG  WATER   -- MEASURED CAPACITIES --  MISCELLANEOUS
  NO  CLS TYP   TIP degr   TIP   LNGTH PENTR  RATIO RATIO   COMPRSSN TENSION DAYS TBF  1 2 3
   1   1   1   .762  .0   .001   26.2  26.2    1.0   1.0      1567        0     0   0   0 0 0


#  324
Semple & Rigden (1984)   API Data Base Identifier =  6,20
S&R (1984)

 NUMLAY   NUMPIL   GWT   GAMPWP    SIGSRF   ZHOLE   QR.SOIL   QR.PILE
    2       1      0.0     10        0       5.6       2         1

 LAYER  DEPTH  GAMMA TYPE  Q.CPT  SPT  OCR  -------- CLAY -------   ----SAND----  CLC  MISCELLANEOUS
        BOTTM   EFF ClSiSa  TIP    N        SuTop SuBot TYP St Ip   D50  Dr  PHI  FLG    1   2   3
   1    5.60   9.0   1      0     0    0      6     6    2   0  0    0    0   0    0     0   0   0
   2   27.21   9.0   1      0     0    0      6    56    2   0  0    0    0   0    0     0   0   0

 PILE OPN MAT  DIAM TAPER  WALL  TOTAL  TIP   PLUG  WATER   -- MEASURED CAPACITIES --  MISCELLANEOUS
  NO  CLS TYP   TIP degr   TIP   LNGTH PENTR  RATIO RATIO   COMPRSSN TENSION DAYS TBF  1 2 3
   1   1   1   .457  .0   .001   27.2  27.2    1.0   1.0       976        0     0   0   0 0 0


#  325
Semple & Rigden (1984)   API Data Base Identifier =  3,7,17
S&R (1984)

 NUMLAY   NUMPIL   GWT   GAMPWP    SIGSRF   ZHOLE   QR.SOIL   QR.PILE
    2       1      0.0     10        0       6.2       2         1

 LAYER  DEPTH  GAMMA TYPE  Q.CPT  SPT  OCR  -------- CLAY -------   ----SAND----  CLC  MISCELLANEOUS
        BOTTM   EFF ClSiSa  TIP    N        SuTop SuBot TYP St Ip   D50  Dr  PHI  FLG    1   2   3
   1    6.20   9.0   1      0     0    0      9     9    2   0  0    0    0   0    0     0   0   0
   2   25.41   9.0   1      0     0    0      9    53    2   0  0    0    0   0    0     0   0   0

 PILE OPN MAT  DIAM TAPER  WALL  TOTAL  TIP   PLUG  WATER   -- MEASURED CAPACITIES --  MISCELLANEOUS
  NO  CLS TYP   TIP degr   TIP   LNGTH PENTR  RATIO RATIO   COMPRSSN TENSION DAYS TBF  1 2 3
   1   1   1   .610  .0   .001   25.4  25.4    1.0   1.0      1269        0     0   0   0 0 0


#  326
Semple & Rigden (1984)   API Data Base Identifier =  478,489
S&R (1984)

 NUMLAY   NUMPIL   GWT   GAMPWP    SIGSRF   ZHOLE   QR.SOIL   QR.PILE
    2       1      0.0     10        0      42.2       2         1

 LAYER  DEPTH  GAMMA TYPE  Q.CPT  SPT  OCR  -------- CLAY -------   ----SAND----  CLC  MISCELLANEOUS
        BOTTM   EFF ClSiSa  TIP    N        SuTop SuBot TYP St Ip   D50  Dr  PHI  FLG    1   2   3
   1   42.20   9.0   1      0     0    0     10    87    2   0  0    0    0   0    0     0   0   0
   2   57.41   9.0   1      0     0    0     87   121    2   0  0    0    0   0    0     0   0   0

 PILE OPN MAT  DIAM TAPER  WALL  TOTAL  TIP   PLUG  WATER   -- MEASURED CAPACITIES --  MISCELLANEOUS
  NO  CLS TYP   TIP degr   TIP   LNGTH PENTR  RATIO RATIO   COMPRSSN TENSION DAYS TBF  1 2 3
   1   1   1   .356  .0   .001   57.4  57.4    1.0   1.0      1965        0     0   0   0 0 0
```

327
Semple & Rigden (1984)   API Data Base Identifier = 491,493
S&R (1984)

NUMLAY	NUMPIL	GWT	GAMPWP	SIGSRF	ZHOLE	QR.SOIL	QR.PILE
2	1	0.0	10	0	73.7	2	1

LAYER	DEPTH	GAMMA	TYPE	Q.CPT	SPT	OCR	-------- CLAY -------					----SAND----			CLC	MISCELLANEOUS		
	BOTTM	EFF	ClSiSa	TIP	N		SuTop	SuBot	TYP	St	Ip	D50	Dr	PHI	FLG	1	2	3
1	73.70	9.0	1	0	0	0	10	148	2	0	0	0	0	0	0	0	0	0
2	85.91	9.0	1	0	0	0	148	176	2	0	0	0	0	0	0	0	0	0

PILE NO	OPN CLS	MAT TYP	DIAM TIP	TAPER degr	WALL TIP	TOTAL LNGTH	TIP PENTR	PLUG RATIO	WATER RATIO	-- MEASURED CAPACITIES -- COMPRSSN	TENSION	DAYS	TBF	MISCELLANEOUS 1 2 3
1	1	1	.356	.0	.001	85.9	85.9	1.0	1.0	2368	0	0	0	0 0 0

328
Semple & Rigden (1984)   API Data Base Identifier = 854,855
S&R (1984)

NUMLAY	NUMPIL	GWT	GAMPWP	SIGSRF	ZHOLE	QR.SOIL	QR.PILE
1	1	0.0	10	0.0	0.0	2	1

LAYER	DEPTH	GAMMA	TYPE	Q.CPT	SPT	OCR	-------- CLAY -------					----SAND----			CLC	MISCELLANEOUS		
	BOTTM	EFF	ClSiSa	TIP	N		SuTop	SuBot	TYP	St	Ip	D50	Dr	PHI	FLG	1	2	3
1	43.91	7.4	1	0	0	0	1	76	6	0	0	0	0	0	0	0	0	0

PILE NO	OPN CLS	MAT TYP	DIAM TIP	TAPER degr	WALL TIP	TOTAL LNGTH	TIP PENTR	PLUG RATIO	WATER RATIO	-- MEASURED CAPACITIES -- COMPRSSN	TENSION	DAYS	TBF	MISCELLANEOUS 1 2 3
1	1	1	.305	.0	.001	43.9	43.9	1.0	1.0	1313	0	0	0	0 0 0

329
Semple & Rigden (1984)   API Data Base Identifier = 868
S&R (1984)

NUMLAY	NUMPIL	GWT	GAMPWP	SIGSRF	ZHOLE	QR.SOIL	QR.PILE
1	1	0.0	10	0.0	0.0	2	1

LAYER	DEPTH	GAMMA	TYPE	Q.CPT	SPT	OCR	-------- CLAY -------					----SAND----			CLC	MISCELLANEOUS		
	BOTTM	EFF	ClSiSa	TIP	N		SuTop	SuBot	TYP	St	Ip	D50	Dr	PHI	FLG	1	2	3
1	96.01	7.4	1	0	0	0	1	160	2	0	0	0	0	0	0	0	0	0

PILE NO	OPN CLS	MAT TYP	DIAM TIP	TAPER degr	WALL TIP	TOTAL LNGTH	TIP PENTR	PLUG RATIO	WATER RATIO	-- MEASURED CAPACITIES -- COMPRSSN	TENSION	DAYS	TBF	MISCELLANEOUS 1 2 3
1	1	1	.610	.0	.001	96.0	96.0	1.0	1.0	8516	0	0	0	0 0 0

330
Semple & Rigden (1984)   API Data Base Identifier = 869
S&R (1984)

NUMLAY	NUMPIL	GWT	GAMPWP	SIGSRF	ZHOLE	QR.SOIL	QR.PILE
1	1	0.0	10	0.0	0.0	2	1

LAYER	DEPTH	GAMMA	TYPE	Q.CPT	SPT	OCR	-------- CLAY -------					----SAND----			CLC	MISCELLANEOUS		
	BOTTM	EFF	ClSiSa	TIP	N		SuTop	SuBot	TYP	St	Ip	D50	Dr	PHI	FLG	1	2	3
1	73.81	7.4	1	0	0	0	1	134	2	0	0	0	0	0	0	0	0	0

PILE NO	OPN CLS	MAT TYP	DIAM TIP	TAPER degr	WALL TIP	TOTAL LNGTH	TIP PENTR	PLUG RATIO	WATER RATIO	-- MEASURED CAPACITIES -- COMPRSSN	TENSION	DAYS	TBF	MISCELLANEOUS 1 2 3
1	1	1	.610	.0	.001	73.8	73.8	1.0	1.0	7080	0	0	0	0 0 0

331
Semple & Rigden (1984)   API Data Base Identifier = 873
S&R (1984)

NUMLAY	NUMPIL	GWT	GAMPWP	SIGSRF	ZHOLE	QR.SOIL	QR.PILE
2	1	0.0	10	0	61.0	2	1

LAYER	DEPTH	GAMMA	TYPE	Q.CPT	SPT	OCR	-------- CLAY -------					----SAND----			CLC	MISCELLANEOUS		
	BOTTM	EFF	ClSiSa	TIP	N		SuTop	SuBot	TYP	St	Ip	D50	Dr	PHI	FLG	1	2	3
1	61.00	9.0	1	0	0	0	10	144	2	0	0	0	0	0	0	0	0	0
2	83.61	9.0	1	0	0	0	144	196	2	0	0	0	0	0	0	0	0	0

PILE NO	OPN CLS	MAT TYP	DIAM TIP	TAPER degr	WALL TIP	TOTAL LNGTH	TIP PENTR	PLUG RATIO	WATER RATIO	-- MEASURED CAPACITIES -- COMPRSSN	TENSION	DAYS	TBF	MISCELLANEOUS 1 2 3
1	1	1	.767	.0	.001	83.6	83.6	1.0	1.0	11276	0	0	0	0 0 0

332
Semple & Rigden (1984)   API Data Base Identifier = 451
S&R (1984)

NUMLAY	NUMPIL	GWT	GAMPWP	SIGSRF	ZHOLE	QR.SOIL	QR.PILE
1	1	0.0	10	0.0	0.0	2	1

LAYER	DEPTH	GAMMA	TYPE	Q.CPT	SPT	OCR	-------- CLAY -------					----SAND----			CLC	MISCELLANEOUS		
	BOTTM	EFF	ClSiSa	TIP	N		SuTop	SuBot	TYP	St	Ip	D50	Dr	PHI	FLG	1	2	3
1	66.41	6.7	1	0	0	0	1	120	2	0	0	0	0	0	0	0	0	0

PILE NO	OPN CLS	MAT TYP	DIAM TIP	TAPER degr	WALL TIP	TOTAL LNGTH	TIP PENTR	PLUG RATIO	WATER RATIO	-- MEASURED CAPACITIES -- COMPRSSN	TENSION	DAYS	TBF	MISCELLANEOUS 1 2 3
1	1	1	.325	.0	.001	66.4	66.4	1.0	1.0	2205	0	0	0	0 0 0

333
Semple & Rigden (1984)   API Data Base Identifier = 42
S&R (1984)

NUMLAY	NUMPIL	GWT	GAMPWP	SIGSRF	ZHOLE	QR.SOIL	QR.PILE
2	1	0.0	10	0	1.8	2	1

LAYER	DEPTH	GAMMA	TYPE	Q.CPT	SPT	OCR	-------- CLAY -------					----SAND----			CLC	MISCELLANEOUS		
	BOTTM	EFF	ClSiSa	TIP	N		SuTop	SuBot	TYP	St	Ip	D50	Dr	PHI	FLG	1	2	3
1	1.80	9.0	1	0	0	0	10	10	2	0	0	0	0	0	0	0	0	0
2	32.31	9.0	1	0	0	0	10	80	2	0	0	0	0	0	0	0	0	0

PILE NO	OPN CLS	MAT TYP	DIAM TIP	TAPER degr	WALL TIP	TOTAL LNGTH	TIP PENTR	PLUG RATIO	WATER RATIO	-- MEASURED CAPACITIES -- COMPRSSN	TENSION	DAYS	TBF	MISCELLANEOUS 1 2 3
1	1	1	.325	.0	.001	32.3	32.3	1.0	1.0	971	0	0	0	0 0 0

334
Semple & Rigden (1984) API Data Base Identifier = 444,450
S&R (1984)

NUMLAY	NUMPIL	GWT	GAMPWP	SIGSRF	ZHOLE	QR.SOIL	QR.PILE
1	1	0.0	10	0.0	0.0	2	1

LAYER	DEPTH BOTTM	GAMMA EFF	TYPE ClSiSa	Q.CPT TIP	SPT N	OCR	CLAY SuTop	CLAY SuBot	TYP	St	Ip	SAND D50	SAND Dr	SAND PHI	CLC FLG	MISCELLANEOUS 1	2	3
1	45.71	6.5	1	0	0	0	1	104	2	0	0	0	0	0	0	0	0	0

PILE NO	OPN CLS	MAT TYP	DIAM TIP	TAPER degr	WALL TIP	TOTAL LNGTH	TIP PENTR	PLUG RATIO	WATER RATIO	-- MEASURED CAPACITIES -- COMPRSSN	TENSION	DAYS	TBF	MISCELLANEOUS 1 2 3
1	1	1	.325	.0	.001	45.7	45.7	1.0	1.0	1097	0	0	0	0 0 0

335
Semple & Rigden (1984) API Data Base Identifier = 507,508
S&R (1984)

NUMLAY	NUMPIL	GWT	GAMPWP	SIGSRF	ZHOLE	QR.SOIL	QR.PILE
1	1	0.0	10	0.0	0.0	2	1

LAYER	DEPTH BOTTM	GAMMA EFF	TYPE ClSiSa	Q.CPT TIP	SPT N	OCR	CLAY SuTop	CLAY SuBot	TYP	St	Ip	SAND D50	SAND Dr	SAND PHI	CLC FLG	MISCELLANEOUS 1	2	3
1	29.01	7.2	1	0	0	0	6	72	2	0	0	0	0	0	0	0	0	0

PILE NO	OPN CLS	MAT TYP	DIAM TIP	TAPER degr	WALL TIP	TOTAL LNGTH	TIP PENTR	PLUG RATIO	WATER RATIO	-- MEASURED CAPACITIES -- COMPRSSN	TENSION	DAYS	TBF	MISCELLANEOUS 1 2 3
1	1	1	.330	.0	.001	29.0	29.0	1.0	1.0	1252	0	0	0	0 0 0

336
Semple & Rigden (1984) API Data Base Identifier = 30
S&R (1984)

NUMLAY	NUMPIL	GWT	GAMPWP	SIGSRF	ZHOLE	QR.SOIL	QR.PILE
2	1	0.0	10	0	5.6	2	1

LAYER	DEPTH BOTTM	GAMMA EFF	TYPE ClSiSa	Q.CPT TIP	SPT N	OCR	CLAY SuTop	CLAY SuBot	TYP	St	Ip	SAND D50	SAND Dr	SAND PHI	CLC FLG	MISCELLANEOUS 1	2	3
1	5.60	9.0	1	0	0	0	10	29	2	0	0	0	0	0	0	0	0	0
2	19.31	9.0	1	0	0	0	29	61	2	0	0	0	0	0	0	0	0	0

PILE NO	OPN CLS	MAT TYP	DIAM TIP	TAPER degr	WALL TIP	TOTAL LNGTH	TIP PENTR	PLUG RATIO	WATER RATIO	-- MEASURED CAPACITIES -- COMPRSSN	TENSION	DAYS	TBF	MISCELLANEOUS 1 2 3
1	1	1	.325	.0	.001	19.3	19.3	1.0	1.0	637	0	0	0	0 0 0

337
Semple & Rigden (1984) API Data Base Identifier = 150
S&R (1984)

NUMLAY	NUMPIL	GWT	GAMPWP	SIGSRF	ZHOLE	QR.SOIL	QR.PILE
1	1	0.0	10	0.0	0.0	2	1

LAYER	DEPTH BOTTM	GAMMA EFF	TYPE ClSiSa	Q.CPT TIP	SPT N	OCR	CLAY SuTop	CLAY SuBot	TYP	St	Ip	SAND D50	SAND Dr	SAND PHI	CLC FLG	MISCELLANEOUS 1	2	3
1	18.31	5.6	1	0	0	0	12	54	2	0	0	0	0	0	0	0	0	0

PILE NO	OPN CLS	MAT TYP	DIAM TIP	TAPER degr	WALL TIP	TOTAL LNGTH	TIP PENTR	PLUG RATIO	WATER RATIO	-- MEASURED CAPACITIES -- COMPRSSN	TENSION	DAYS	TBF	MISCELLANEOUS 1 2 3
1	1	1	.325	.0	.001	18.3	18.3	1.0	1.0	638	0	0	0	0 0 0

338
Semple & Rigden (1984) API Data Base Identifier = 45
S&R (1984)

NUMLAY	NUMPIL	GWT	GAMPWP	SIGSRF	ZHOLE	QR.SOIL	QR.PILE
1	1	0.0	10	0.0	0.0	2	1

LAYER	DEPTH BOTTM	GAMMA EFF	TYPE ClSiSa	Q.CPT TIP	SPT N	OCR	CLAY SuTop	CLAY SuBot	TYP	St	Ip	SAND D50	SAND Dr	SAND PHI	CLC FLG	MISCELLANEOUS 1	2	3
1	48.21	6.3	1	0	0	0	9	119	2	0	0	0	0	0	0	0	0	0

PILE NO	OPN CLS	MAT TYP	DIAM TIP	TAPER degr	WALL TIP	TOTAL LNGTH	TIP PENTR	PLUG RATIO	WATER RATIO	-- MEASURED CAPACITIES -- COMPRSSN	TENSION	DAYS	TBF	MISCELLANEOUS 1 2 3
1	1	1	.610	.0	.001	48.2	48.2	1.0	1.0	3802	0	0	0	0 0 0

339
Semple & Rigden (1984) API Data Base Identifier = 844,846,848,851
S&R (1984)

NUMLAY	NUMPIL	GWT	GAMPWP	SIGSRF	ZHOLE	QR.SOIL	QR.PILE
1	1	0.0	10	0.0	0.0	2	1

LAYER	DEPTH BOTTM	GAMMA EFF	TYPE ClSiSa	Q.CPT TIP	SPT N	OCR	CLAY SuTop	CLAY SuBot	TYP	St	Ip	SAND D50	SAND Dr	SAND PHI	CLC FLG	MISCELLANEOUS 1	2	3
1	11.61	7.6	1	0	0	0	8	34	6	0	0	0	0	0	0	0	0	0

PILE NO	OPN CLS	MAT TYP	DIAM TIP	TAPER degr	WALL TIP	TOTAL LNGTH	TIP PENTR	PLUG RATIO	WATER RATIO	-- MEASURED CAPACITIES -- COMPRSSN	TENSION	DAYS	TBF	MISCELLANEOUS 1 2 3
1	1	1	.114	.0	.001	11.6	11.6	1.0	1.0	59	0	0	0	0 0 0

340
Semple & Rigden (1984) API Data Base Identifier = 856
S&R (1984)

NUMLAY	NUMPIL	GWT	GAMPWP	SIGSRF	ZHOLE	QR.SOIL	QR.PILE
1	1	0.0	10	0.0	0.0	2	1

LAYER	DEPTH BOTTM	GAMMA EFF	TYPE ClSiSa	Q.CPT TIP	SPT N	OCR	CLAY SuTop	CLAY SuBot	TYP	St	Ip	SAND D50	SAND Dr	SAND PHI	CLC FLG	MISCELLANEOUS 1	2	3
1	12.21	5.4	1	0	0	0	2	30	7	0	0	0	0	0	0	0	0	0

PILE NO	OPN CLS	MAT TYP	DIAM TIP	TAPER degr	WALL TIP	TOTAL LNGTH	TIP PENTR	PLUG RATIO	WATER RATIO	-- MEASURED CAPACITIES -- COMPRSSN	TENSION	DAYS	TBF	MISCELLANEOUS 1 2 3
1	1	1	.168	.0	.001	12.2	12.2	1.0	1.0	70	0	0	0	0 0 0

341
Semple & Rigden (1984) API Data Base Identifier = 325
S&R (1984)

NUMLAY	NUMPIL	GWT	GAMPWP	SIGSRF	ZHOLE	QR.SOIL	QR.PILE
1	1	0.0	10	0.0	0.0	2	1

LAYER	DEPTH	GAMMA	TYPE	Q.CPT	SPT	OCR	CLAY					SAND				CLC	MISCELLANEOUS		
	BOTTM	EFF	ClSiSa	TIP	N		SuTop	SuBot	TYP	St	Ip	D50	Dr	PHI	FLG		1	2	3
1	14.01	8.4	1	0	0	0	14	46	8	0	0	0	0	0	0		0	0	0

PILE NO	OPN CLS	MAT TYP	DIAM TIP	TAPER degr	WALL TIP	TOTAL LNGTH	TIP PENTR	PLUG RATIO	WATER RATIO	-- MEASURED CAPACITIES -- COMPRSSN	TENSION	DAYS	TBF	MISCELLANEOUS 1 2 3
1	1	1	.351	.0	.001	14.0	14.0	1.0	1.0	401	0	0	0	0 0 0

342
Semple & Rigden (1984) API Data Base Identifier = 67
S&R (1984)

NUMLAY	NUMPIL	GWT	GAMPWP	SIGSRF	ZHOLE	QR.SOIL	QR.PILE
2	1	0.0	10	0	13.2	2	1

LAYER	DEPTH	GAMMA	TYPE	Q.CPT	SPT	OCR	CLAY					SAND				CLC	MISCELLANEOUS		
	BOTTM	EFF	ClSiSa	TIP	N		SuTop	SuBot	TYP	St	Ip	D50	Dr	PHI	FLG		1	2	3
1	13.20	9.0	1	0	0	0	10	119	2	0	0	0	0	0	0		0	0	0
2	52.81	9.0	1	0	0	0	119	211	2	0	0	0	0	0	0		0	0	0

PILE NO	OPN CLS	MAT TYP	DIAM TIP	TAPER degr	WALL TIP	TOTAL LNGTH	TIP PENTR	PLUG RATIO	WATER RATIO	-- MEASURED CAPACITIES -- COMPRSSN	TENSION	DAYS	TBF	MISCELLANEOUS 1 2 3
1	1	1	.274	.0	.001	52.8	52.8	1.0	1.0	2868	0	0	0	0 0 0

343
Semple & Rigden (1984) API Data Base Identifier = 43
S&R (1984)

NUMLAY	NUMPIL	GWT	GAMPWP	SIGSRF	ZHOLE	QR.SOIL	QR.PILE
1	1	0.0	10	0.0	0.0	2	1

LAYER	DEPTH	GAMMA	TYPE	Q.CPT	SPT	OCR	CLAY					SAND				CLC	MISCELLANEOUS		
	BOTTM	EFF	ClSiSa	TIP	N		SuTop	SuBot	TYP	St	Ip	D50	Dr	PHI	FLG		1	2	3
1	30.51	6.0	1	0	0	0	17	87	2	0	0	0	0	0	0		0	0	0

PILE NO	OPN CLS	MAT TYP	DIAM TIP	TAPER degr	WALL TIP	TOTAL LNGTH	TIP PENTR	PLUG RATIO	WATER RATIO	-- MEASURED CAPACITIES -- COMPRSSN	TENSION	DAYS	TBF	MISCELLANEOUS 1 2 3
1	1	1	.610	.0	.001	30.5	30.5	1.0	1.0	2022	0	0	0	0 0 0

344
Semple & Rigden (1984) API Data Base Identifier = 443,449
S&R (1984)

NUMLAY	NUMPIL	GWT	GAMPWP	SIGSRF	ZHOLE	QR.SOIL	QR.PILE
1	1	0.0	10	0.0	0.0	2	1

LAYER	DEPTH	GAMMA	TYPE	Q.CPT	SPT	OCR	CLAY					SAND				CLC	MISCELLANEOUS		
	BOTTM	EFF	ClSiSa	TIP	N		SuTop	SuBot	TYP	St	Ip	D50	Dr	PHI	FLG		1	2	3
1	22.91	7.9	1	0	0	0	26	78	2	0	0	0	0	0	0		0	0	0

PILE NO	OPN CLS	MAT TYP	DIAM TIP	TAPER degr	WALL TIP	TOTAL LNGTH	TIP PENTR	PLUG RATIO	WATER RATIO	-- MEASURED CAPACITIES -- COMPRSSN	TENSION	DAYS	TBF	MISCELLANEOUS 1 2 3
1	1	1	.325	.0	.001	22.9	22.9	1.0	1.0	691	0	0	0	0 0 0

345
Semple & Rigden (1984) API Data Base Identifier = 368,369
S&R (1984)

NUMLAY	NUMPIL	GWT	GAMPWP	SIGSRF	ZHOLE	QR.SOIL	QR.PILE
1	1	0.0	10	0.0	0.0	2	1

LAYER	DEPTH	GAMMA	TYPE	Q.CPT	SPT	OCR	CLAY					SAND				CLC	MISCELLANEOUS		
	BOTTM	EFF	ClSiSa	TIP	N		SuTop	SuBot	TYP	St	Ip	D50	Dr	PHI	FLG		1	2	3
1	25.91	7.6	1	0	0	0	31	91	2	0	0	0	0	0	0		0	0	0

PILE NO	OPN CLS	MAT TYP	DIAM TIP	TAPER degr	WALL TIP	TOTAL LNGTH	TIP PENTR	PLUG RATIO	WATER RATIO	-- MEASURED CAPACITIES -- COMPRSSN	TENSION	DAYS	TBF	MISCELLANEOUS 1 2 3
1	1	1	.325	.0	.001	25.9	25.9	1.0	1.0	971	0	0	0	0 0 0

346
Semple & Rigden (1984) API Data Base Identifier = 435,436,437,438
S&R (1984)

NUMLAY	NUMPIL	GWT	GAMPWP	SIGSRF	ZHOLE	QR.SOIL	QR.PILE
2	1	0.0	10	0	14.4	2	1

LAYER	DEPTH	GAMMA	TYPE	Q.CPT	SPT	OCR	CLAY					SAND				CLC	MISCELLANEOUS		
	BOTTM	EFF	ClSiSa	TIP	N		SuTop	SuBot	TYP	St	Ip	D50	Dr	PHI	FLG		1	2	3
1	14.40	9.0	1	0	0	0	10	156	2	0	0	0	0	0	0		0	0	0
2	39.71	9.0	1	0	0	0	156	214	2	0	0	0	0	0	0		0	0	0

PILE NO	OPN CLS	MAT TYP	DIAM TIP	TAPER degr	WALL TIP	TOTAL LNGTH	TIP PENTR	PLUG RATIO	WATER RATIO	-- MEASURED CAPACITIES -- COMPRSSN	TENSION	DAYS	TBF	MISCELLANEOUS 1 2 3
1	1	1	.274	.0	.001	39.7	39.7	1.0	1.0	2048	0	0	0	0 0 0

347
Semple & Rigden (1984) API Data Base Identifier = 70
S&R (1984)

NUMLAY	NUMPIL	GWT	GAMPWP	SIGSRF	ZHOLE	QR.SOIL	QR.PILE
1	1	0.0	10	0.0	0.0	2	1

LAYER	DEPTH	GAMMA	TYPE	Q.CPT	SPT	OCR	CLAY					SAND				CLC	MISCELLANEOUS		
	BOTTM	EFF	ClSiSa	TIP	N		SuTop	SuBot	TYP	St	Ip	D50	Dr	PHI	FLG		1	2	3
1	14.91	8.9	1	0	0	0	36	70	2	0	0	0	0	0	0		0	0	0

PILE NO	OPN CLS	MAT TYP	DIAM TIP	TAPER degr	WALL TIP	TOTAL LNGTH	TIP PENTR	PLUG RATIO	WATER RATIO	-- MEASURED CAPACITIES -- COMPRSSN	TENSION	DAYS	TBF	MISCELLANEOUS 1 2 3
1	1	1	.528	.0	.001	14.9	14.9	1.0	1.0	819	0	0	0	0 0 0

348
Semple & Rigden (1984) API Data Base Identifier = 998
S&R (1984)

NUMLAY	NUMPIL	GWT	GAMPWP	SIGSRF	ZHOLE	QR.SOIL	QR.PILE
1	1	0.0	10	0.0	0.0	2	1

LAYER	DEPTH	GAMMA	TYPE	Q.CPT	SPT	OCR	CLAY					SAND				MISCELLANEOUS		
	BOTTM	EFF	ClSiSa	TIP	N		SuTop	SuBot	TYP	St	Ip	D50	Dr	PHI	FLG	1	2	3
1	32.01	8.8	1	0	0	0	78	152	2	0	0	0	0	0	0	0	0	0

PILE NO	OPN CLS	MAT TYP	DIAM TIP	TAPER degr	WALL TIP	TOTAL LNGTH	TIP PENTR	PLUG RATIO	WATER RATIO	-- MEASURED CAPACITIES -- COMPRSSN	TENSION	DAYS	TBF	MISCELLANEOUS 1 2 3
1	1	1	.274	.0	.001	32.0	32.0	1.0	1.0	1728	0	0	0	0 0 0

349
Semple & Rigden (1984) API Data Base Identifier = 106
S&R (1984)

NUMLAY	NUMPIL	GWT	GAMPWP	SIGSRF	ZHOLE	QR.SOIL	QR.PILE
2	1	0.0	10	0	5.8	2	1

LAYER	DEPTH	GAMMA	TYPE	Q.CPT	SPT	OCR	CLAY					SAND				MISCELLANEOUS		
	BOTTM	EFF	ClSiSa	TIP	N		SuTop	SuBot	TYP	St	Ip	D50	Dr	PHI	FLG	1	2	3
1	5.80	9.0	1	0	0	0	10	81	6	0	0	0	0	0	0	0	0	0
2	18.61	9.0	1	0	0	0	81	111	6	0	0	0	0	0	0	0	0	0

PILE NO	OPN CLS	MAT TYP	DIAM TIP	TAPER degr	WALL TIP	TOTAL LNGTH	TIP PENTR	PLUG RATIO	WATER RATIO	-- MEASURED CAPACITIES -- COMPRSSN	TENSION	DAYS	TBF	MISCELLANEOUS 1 2 3
1	1	1	.325	.0	.001	18.6	18.6	1.0	1.0	798	0	0	0	0 0 0

350
Semple & Rigden (1984) API Data Base Identifier = 547,549
S&R (1984)

NUMLAY	NUMPIL	GWT	GAMPWP	SIGSRF	ZHOLE	QR.SOIL	QR.PILE
2	1	0.0	10	0	1.2	2	1

LAYER	DEPTH	GAMMA	TYPE	Q.CPT	SPT	OCR	CLAY					SAND				MISCELLANEOUS		
	BOTTM	EFF	ClSiSa	TIP	N		SuTop	SuBot	TYP	St	Ip	D50	Dr	PHI	FLG	1	2	3
1	1.20	9.0	1	0	0	0	10	81	2	0	0	0	0	0	0	0	0	0
2	18.01	9.0	1	0	0	0	81	119	2	0	0	0	0	0	0	0	0	0

PILE NO	OPN CLS	MAT TYP	DIAM TIP	TAPER degr	WALL TIP	TOTAL LNGTH	TIP PENTR	PLUG RATIO	WATER RATIO	-- MEASURED CAPACITIES -- COMPRSSN	TENSION	DAYS	TBF	MISCELLANEOUS 1 2 3
1	1	1	.610	.0	.001	18.0	18.0	1.0	1.0	2085	0	0	0	0 0 0

351
Semple & Rigden (1984) API Data Base Identifier = 31,32
S&R (1984)

NUMLAY	NUMPIL	GWT	GAMPWP	SIGSRF	ZHOLE	QR.SOIL	QR.PILE
2	1	0.0	10	0	5.6	2	1

LAYER	DEPTH	GAMMA	TYPE	Q.CPT	SPT	OCR	CLAY					SAND				MISCELLANEOUS		
	BOTTM	EFF	ClSiSa	TIP	N		SuTop	SuBot	TYP	St	Ip	D50	Dr	PHI	FLG	1	2	3
1	5.60	9.0	1	0	0	0	10	121	2	0	0	0	0	0	0	0	0	0
2	19.31	9.0	1	0	0	0	121	153	2	0	0	0	0	0	0	0	0	0

PILE NO	OPN CLS	MAT TYP	DIAM TIP	TAPER degr	WALL TIP	TOTAL LNGTH	TIP PENTR	PLUG RATIO	WATER RATIO	-- MEASURED CAPACITIES -- COMPRSSN	TENSION	DAYS	TBF	MISCELLANEOUS 1 2 3
1	1	1	.325	.0	.001	19.3	19.3	1.0	1.0	1015	0	0	0	0 0 0

352
Semple & Rigden (1984) API Data Base Identifier = 829,830
S&R (1984)

NUMLAY	NUMPIL	GWT	GAMPWP	SIGSRF	ZHOLE	QR.SOIL	QR.PILE
2	1	0.0	10	0	2.3	2	1

LAYER	DEPTH	GAMMA	TYPE	Q.CPT	SPT	OCR	CLAY					SAND				MISCELLANEOUS		
	BOTTM	EFF	ClSiSa	TIP	N		SuTop	SuBot	TYP	St	Ip	D50	Dr	PHI	FLG	1	2	3
1	2.30	9.0	1	0	0	0	10	95	3	0	0	0	0	0	0	0	0	0
2	15.41	9.0	1	0	0	0	95	125	3	0	0	0	0	0	0	0	0	0

PILE NO	OPN CLS	MAT TYP	DIAM TIP	TAPER degr	WALL TIP	TOTAL LNGTH	TIP PENTR	PLUG RATIO	WATER RATIO	-- MEASURED CAPACITIES -- COMPRSSN	TENSION	DAYS	TBF	MISCELLANEOUS 1 2 3
1	1	1	.274	.0	.001	15.4	15.4	1.0	1.0	674	0	0	0	0 0 0

353
Semple & Rigden (1984) API Data Base Identifier = 495,497
S&R (1984)

NUMLAY	NUMPIL	GWT	GAMPWP	SIGSRF	ZHOLE	QR.SOIL	QR.PILE
2	1	0.0	10	0	1.4	2	1

LAYER	DEPTH	GAMMA	TYPE	Q.CPT	SPT	OCR	CLAY					SAND				MISCELLANEOUS		
	BOTTM	EFF	ClSiSa	TIP	N		SuTop	SuBot	TYP	St	Ip	D50	Dr	PHI	FLG	1	2	3
1	1.40	9.0	1	0	0	0	10	185	6	0	0	0	0	0	0	0	0	0
2	21.81	9.0	1	0	0	0	185	231	6	0	0	0	0	0	0	0	0	0

PILE NO	OPN CLS	MAT TYP	DIAM TIP	TAPER degr	WALL TIP	TOTAL LNGTH	TIP PENTR	PLUG RATIO	WATER RATIO	-- MEASURED CAPACITIES -- COMPRSSN	TENSION	DAYS	TBF	MISCELLANEOUS 1 2 3
1	1	1	.610	.0	.001	21.8	21.8	1.0	1.0	4187	0	0	0	0 0 0

354
Semple & Rigden (1984) API Data Base Identifier = See Table 1 (*)
S&R (1984)

NUMLAY	NUMPIL	GWT	GAMPWP	SIGSRF	ZHOLE	QR.SOIL	QR.PILE
2	1	0.0	10	0	1.4	2	1

LAYER	DEPTH	GAMMA	TYPE	Q.CPT	SPT	OCR	CLAY					SAND				MISCELLANEOUS		
	BOTTM	EFF	ClSiSa	TIP	N		SuTop	SuBot	TYP	St	Ip	D50	Dr	PHI	FLG	1	2	3
1	1.40	9.0	1	0	0	0	10	134	6	0	0	0	0	0	0	0	0	0
2	10.51	9.0	1	0	0	0	134	154	6	0	0	0	0	0	0	0	0	0

PILE NO	OPN CLS	MAT TYP	DIAM TIP	TAPER degr	WALL TIP	TOTAL LNGTH	TIP PENTR	PLUG RATIO	WATER RATIO	-- MEASURED CAPACITIES -- COMPRSSN	TENSION	DAYS	TBF	MISCELLANEOUS 1 2 3
1	1	1	.450	.0	.001	10.5	10.5	1.0	1.0	1166	0	0	0	0 0 0

355
Semple & Rigden (1984) API Data Base Identifier = 23,24
S&R (1984)

NUMLAY	NUMPIL	GWT	GAMPWP	SIGSRF	ZHOLE	QR.SOIL	QR.PILE
2	1	0.0	10	0	3.7	2	1

LAYER	DEPTH BOTTM	GAMMA EFF	TYPE ClSiSa	Q.CPT TIP	SPT N	OCR	CLAY SuTop	CLAY SuBot	TYP	St	Ip	SAND D50	SAND Dr	SAND PHI	CLC FLG	MISCELLANEOUS 1	2	3
1	3.70	9.0	1	0	0	0	10	314	2	0	0	0	0	0	0	0	0	0
2	22.01	9.0	1	0	0	0	314	356	2	0	0	0	0	0	0	0	0	0

PILE NO	OPN CLS	MAT TYP	DIAM TIP	TAPER degr	WALL TIP	TOTAL LNGTH	TIP PENTR	PLUG RATIO	WATER RATIO	-- MEASURED CAPACITIES -- COMPRSSN	TENSION	DAYS	TBF	MISCELLANEOUS 1 2 3
1	1	1	.762	.0	.001	22.0	22.0	1.0	1.0	8212	0	0	0	0 0 0

356
Holmberg (1970) Hollow octogonal concrete pile
Thailand Last modified :

NUMLAY	NUMPIL	GWT	GAMPWP	SIGSRF	ZHOLE	QR.SOIL	QR.PILE
5	1	0.0	10	0.0	0.0	3	3

LAYER	DEPTH BOTTM	GAMMA EFF	TYPE ClSiSa	Q.CPT TIP	SPT N	OCR	CLAY SuTop	CLAY SuBot	TYP	St	Ip	SAND D50	SAND Dr	SAND PHI	CLC FLG	MISCELLANEOUS 1	2	3
1	1.5	9.0	3	0	0	0	0	0	0	0	0	0	0	33	0	0	0	0
2	2.7	6.5	1	0	0	0	70	70	8	10	40	0	0	0	0	0	0	0
3	6.0	4.5	1	0	0	0	20	35	8	5	50	0	0	0	0	0	0	0
4	9.0	8.5	1	0	0	0	50	220	8	2	30	0	0	0	0	0	0	0
5	15.5	9.5	1	0	0	0	220	250	8	2	35	0	0	0	0	0	0	0

PILE NO	OPN CLS	MAT TYP	DIAM TIP	TAPER degr	WALL TIP	TOTAL LNGTH	TIP PENTR	PLUG RATIO	WATER RATIO	-- MEASURED CAPACITIES -- COMPRSSN	TENSION	DAYS	TBF	MISCELLANEOUS 1	2	3
1	2	2	.580	.0	.100	13.5	13.5	0.0	0.0	1570	0	28	0	0	0	0

357
Holmberg (1970) 0.22m x 0.22m concrete piles
Thailand Last modified :

NUMLAY	NUMPIL	GWT	GAMPWP	SIGSRF	ZHOLE	QR.SOIL	QR.PILE
4	3	0.0	10	0.0	0.0	3	3

LAYER	DEPTH BOTTM	GAMMA EFF	TYPE ClSiSa	Q.CPT TIP	SPT N	OCR	CLAY SuTop	CLAY SuBot	TYP	St	Ip	SAND D50	SAND Dr	SAND PHI	CLC FLG	MISCELLANEOUS 1	2	3
1	1.4	9.0	3	0	0	0	0	0	0	0	0	0	0	33	0	0	0	0
2	4.3	5.5	1	0	0	0	15	22	8	5	35	0	0	0	0	0	0	0
3	10.3	4.5	1	0	0	0	22	30	8	8	50	0	0	0	0	0	0	0
4	16.3	9.0	1	0	0	0	150	300	8	2	35	0	0	0	0	0	0	0

PILE NO	OPN CLS	MAT TYP	DIAM TIP	TAPER degr	WALL TIP	TOTAL LNGTH	TIP PENTR	PLUG RATIO	WATER RATIO	-- MEASURED CAPACITIES -- COMPRSSN	TENSION	DAYS	TBF	MISCELLANEOUS 1	2	3
1	2	2	.248	.0	.124	10.0	10.0	0.0	0.0	-167	0	60	1	0	0	0
2	2	2	.248	.0	.124	13.0	13.0	0.0	0.0	313	0	60	1	0	0	0
3	2	2	.248	.0	.124	16.0	16.0	0.0	0.0	580	0	60	1	0	0	0

Remark : Pile has been removed, its tip may be located in stiff clay

358
Ostenfeld et al (1970) Lilleb'lt concrete and steel test piles B2-B3-S2-S3
Lilleb'lt Last modified :

NUMLAY	NUMPIL	GWT	GAMPWP	SIGSRF	ZHOLE	QR.SOIL	QR.PILE
2	4	-15.3	10	0.0	0.0	3	3

LAYER	DEPTH BOTTM	GAMMA EFF	TYPE ClSiSa	Q.CPT TIP	SPT N	OCR	CLAY SuTop	CLAY SuBot	TYP	St	Ip	SAND D50	SAND Dr	SAND PHI	CLC FLG	MISCELLANEOUS 1	2	3
1	7.7	9.5	3	0	0	0	0	0	0	0	0	0	0	35	0	0	0	0
2	30.0	8.3	1	0	0	0	270	450	8	5	100?	0	0	0	0	0	0	0

PILE NO	OPN CLS	MAT TYP	DIAM TIP	TAPER degr	WALL TIP	TOTAL LNGTH	TIP PENTR	PLUG RATIO	WATER RATIO	-- MEASURED CAPACITIES -- COMPRSSN	TENSION	DAYS	TBF	MISCELLANEOUS 1	2	3
1	2	2	.410	.0	.205	40.0	23.8	0.0	0.0	3237	0	0	0	0	0	0 B2
2	2	2	.410	.0	.205	34.0	16.8	0.0	0.0	1864	0	0	0	0	0	0 B3
3	2	1	.267	.0	.035	45.0	27.1	0.0	0.0	1776	0	0	0	0	0	0 S2
4	2	1	.267	.0	.035	45.0	27.1	0.0	0.0	1884	0	0	0	0	0	0 S3

359
Kraft et al (1981a) Empire 14 inch conductor segment, Pile 1
Empire LA Last modified : 2 Dec 1999

NUMLAY	NUMPIL	GWT	GAMPWP	SIGSRF	ZHOLE	QR.SOIL	QR.PILE
2	1	0.0	10	0.0	35.1	4	4

LAYER	DEPTH BOTTM	GAMMA EFF	TYPE ClSiSa	Q.CPT TIP	SPT N	OCR	CLAY SuTop	CLAY SuBot	TYP	St	Ip	SAND D50	SAND Dr	SAND PHI	CLC FLG	MISCELLANEOUS 1	2	3
1	35.1	6.00	1	0	0	0	10	47	8	0	60	0	0	0	0	0	0	0
2	50.31	6.00	1	0	0	0	48	71	3	0	60	0	0	0	0	0	0	0

PILE NO	OPN CLS	MAT TYP	DIAM TIP	TAPER degr	WALL TIP	TOTAL LNGTH	TIP PENTR	PLUG RATIO	WATER RATIO	-- MEASURED CAPACITIES -- COMPRSSN	TENSION	DAYS	TBF	MISCELLANEOUS 1	2	3
1	1	1	.356	.0	.0001	50.3	50.3	0.30	0.30	1113	0	7	0	0	0	0

Su.vane values in 2nd layer replaced by Su.UU values, 2 Dec 1999

360
Kraft et al (1981a) Empire 14 inch conductor segment, Pile 2
Empire LA Last modified : 2 Dec 1999

NUMLAY	NUMPIL	GWT	GAMPWP	SIGSRF	ZHOLE	QR.SOIL	QR.PILE
2	1	0.0	10	0.0	62.8	4	4

LAYER	DEPTH BOTTM	GAMMA EFF	TYPE ClSiSa	Q.CPT TIP	SPT N	OCR	CLAY SuTop	CLAY SuBot	TYP	St	Ip	SAND D50	SAND Dr	SAND PHI	CLC FLG	MISCELLANEOUS 1	2	3
1	62.8	6.36	1	0	0	0	10	77	8	0	50	0	0	0	0	0	0	0
2	78.01	6.36	1	0	0	0	90	113	3	0	50	0	0	0	0	0	0	0

PILE NO	OPN CLS	MAT TYP	DIAM TIP	TAPER degr	WALL TIP	TOTAL LNGTH	TIP PENTR	PLUG RATIO	WATER RATIO	-- MEASURED CAPACITIES -- COMPRSSN	TENSION	DAYS	TBF	MISCELLANEOUS 1	2	3
1	1	1	.356	.0	.0001	78.0	78.0	0.19	0.19	1936	0	9	0	0	0	0

Su.vane values in 2nd layer replaced by Su.UU values, 2 Dec 1999

\# 361
Kraft et al (1981a) Empire 14 inch conductor segment, Pile 3
Empire LA Last modified : 2 Dec 1999

NUMLAY	NUMPIL	GWT	GAMPWP	SIGSRF	ZHOLE	QR.SOIL	QR.PILE
2	1	0.0	10	0.0	82.3	4	4

LAYER	DEPTH BOTTM	GAMMA EFF	TYPE ClSiSa	Q.CPT TIP	SPT N	OCR	-------- CLAY ------- SuTop	SuBot	TYP	St	Ip	----SAND---- D50	Dr	PHI	CLC FLG	MISCELLANEOUS 1	2	3
1	82.3	6.97	1	0	0	0	10	107	8	0	55	0	0	0	0	0	0	0
2	94.51	6.97	1	0	0	0	124	124	3	0	55	0	0	0	0	0	0	0

PILE NO	OPN CLS	MAT TYP	DIAM TIP	TAPER degr	WALL TIP	TOTAL LNGTH	TIP PENTR	PLUG RATIO	WATER RATIO	-- MEASURED CAPACITIES -- COMPRSSN	TENSION	DAYS	TBF	MISCELLANEOUS 1	2	3
1	1	1	.356	.0	.0001	94.5	94.5	0.13	0.13	2127	0	10	0	0	0	0

Su.vane values in 2nd layer replaced by Su.UU values, 2 Dec 1999

\# 362
Kraft et al (1981a) Empire 14 inch conductor segment, Pile 4
Empire LA Last modified : 2 Dec 1999

NUMLAY	NUMPIL	GWT	GAMPWP	SIGSRF	ZHOLE	QR.SOIL	QR.PILE
2	1	0.0	10	0.0	97.5	4	4

LAYER	DEPTH BOTTM	GAMMA EFF	TYPE ClSiSa	Q.CPT TIP	SPT N	OCR	-------- CLAY ------- SuTop	SuBot	TYP	St	Ip	----SAND---- D50	Dr	PHI	CLC FLG	MISCELLANEOUS 1	2	3
1	97.5	6.94	1	0	0	0	10	150	8	0	50	0	0	0	0	0	0	0
2	109.71	6.94	1	0	0	0	174	174	3	0	50	0	0	0	0	0	0	0

PILE NO	OPN CLS	MAT TYP	DIAM TIP	TAPER degr	WALL TIP	TOTAL LNGTH	TIP PENTR	PLUG RATIO	WATER RATIO	-- MEASURED CAPACITIES -- COMPRSSN	TENSION	DAYS	TBF	MISCELLANEOUS 1	2	3
1	1	1	.356	.0	.0001	109.7	109.7	0.11	0.11	2354	0	4	0	0	0	0

Su.vane values in 2nd layer replaced by Su.UU values, 2 Dec 1999

\# 363
O'Neill et al (1982a,b) Reference piles for 9-pile group
Houston ? Last modified :

NUMLAY	NUMPIL	GWT	GAMPWP	SIGSRF	ZHOLE	QR.SOIL	QR.PILE
4	3	2.4	10	0.0	3.0	4	4

LAYER	DEPTH BOTTM	GAMMA EFF	TYPE ClSiSa	Q.CPT TIP	SPT N	OCR	-------- CLAY ------- SuTop	SuBot	TYP	St	Ip	----SAND---- D50	Dr	PHI	CLC FLG	MISCELLANEOUS 1	2	3
1	3.6	10.6	1	1700	0	0	115	115	3	0	30	0	0	0	0	0	0	0
2	7.9	9.3	1	2700	0	0	86	86	3	1	50	0	0	0	0	0	0	0
3	9.2	10.8	1	2100	0	0	38	38	3	0	15	0	0	0	0	0	0	0
4	14.4	10.6	1	3500	0	0	158	158	3	1	15	0	0	0	0	0	0	0

PILE NO	OPN CLS	MAT TYP	DIAM TIP	TAPER degr	WALL TIP	TOTAL LNGTH	TIP PENTR	PLUG RATIO	WATER RATIO	-- MEASURED CAPACITIES -- COMPRSSN	TENSION	DAYS	TBF	MISCELLANEOUS 1	2	3
1	2	1	.273	.0	.0093	14.1	13.1	0.0	0.0	670	0	18	0	0	0	0
2	2	1	.273	.0	.0093	14.1	13.1	0.0	0.0	765	0	80	1	0	0	0
3	2	1	.273	.0	.0093	14.1	13.1	0.0	0.0	792	0	108	1	0	0	0

\# 364
Gallagher & St John (1980),Powell et al. (2003), Lehane and Jardine (1994)
Cowden, Piles A (open) and B (closed) in clay till

NUMLAY	NUMPIL	GWT	GAMPWP	SIGSRF	ZHOLE	QR.SOIL	QR.PILE
4	4	0.0	10	0.0	0.0	4	4

LAYER	DEPTH BOTTM	GAMMA EFF	TYPE ClSiSa	Q.CPT TIP	SPT N	OCR	-------- CLAY ------- SuTop	SuBot	TYP	St	Ip	----SAND---- D50	Dr	PHI	CLC FLG	MISCELLANEOUS 1	2	3
1	1.3	10.5	1	1225	0	0	60	85	9	0	15	0	0	0	0	0	0	0
2	2.7	10.5	1	4050	0	0	215	255	9	0	15	0	0	0	0	0	0	0
3	4.7	10.5	1	2700	0	0	190	120	9	0	15	0	0	0	0	0	0	0
4	10.0	10.5	1	2100	0	0	120	110	9	0	15	0	0	0	0	0	0	0

PILE NO	OPN CLS	MAT TYP	DIAM TIP	TAPER degr	WALL TIP	TOTAL LNGTH	TIP PENTR	PLUG RATIO	WATER RATIO	-- MEASURED CAPACITIES -- COMPRSSN	TENSION	DAYS	TBF	MISCELLANEOUS 1	2	3
1	1	1	.457	.00	.019	12.0	9.2	0.5?	0.5?	1140	0	30	0	0	0	0
2	1	1	.457	.00	.019	12.0	9.2	0.5?	0.5?	1390	0	396	1	0	0	0
3	1	1	.457	.00	.019	12.0	9.2	0.5?	0.5?	1608	0	9125	1	0	0	0
4	2	1	.457	.0	.019	12.0	9.2	0.0	0.0	1670	0	390	1	0	0	0

Addition to existing database #509 (In this database #364).
In the old database, Pile A was only tested one time- after 390 days and the capacity was 1440kN. In order to obtain a consistent set of data, the new data substitutes the old data. That is, 390 days and 1440kN is substituted with 396 days and 1390 kN.

\# 365
Karlsrud et al (1992a) Pentre pile segment test A5
Pentre A5 Last modified : 17 feb 2000

NUMLAY	NUMPIL	GWT	GAMPWP	SIGSRF	ZHOLE	QR.SOIL	QR.PILE
6	1	1.0	10.37	0.0	17.5	4	4

LAYER	DEPTH BOTTM	GAMMA EFF	TYPE ClSiSa	Q.CPT TIP	SPT N	OCR	-------- CLAY ------- SuTop	SuBot	TYP	St	Ip	----SAND---- D50	Dr	PHI	CLC FLG	MISCELLANEOUS 1	2	3
1	1.0	19.2	1	0	0	0	100	100	3	0	25	0	0	0	0	0	0	0
2	15.0	9.0	1	0	0	0	35	35	3	0	12	0	0	0	0	0	0	0
3	25.0	8.5	1	0	0	0	36	62	3	0	14	0	0	0	0	0	0	0
4	35.0	8.5	1	0	0	0	62	88	3	0	18	0	0	0	0	0	0	0
5	48.0	9.15	1	0	0	0	88	120	3	0	23	0	0	0	0	0	0	0
6	60.0	12.33	1	0	0	0	120	150	3	0	16	0	0	0	0	0	0	0

PILE NO	OPN CLS	MAT TYP	DIAM TIP	TAPER degr	WALL TIP	TOTAL LNGTH	TIP PENTR	PLUG RATIO	WATER RATIO	-- MEASURED CAPACITIES -- COMPRSSN	TENSION	DAYS	TBF	MISCELLANEOUS 1	2	3
1	2	1	.219	.0	.016	25.0	25.0	0.0	0.0	0	154	31	0	0	0	2

The loads given for A5 and A6 below correspond to the top transducer level, located 2.5 m below the bottom of the cased hole, increased by the weight of the pile above, and assuming zero pile tip force.

366
Karlsrud et al (1992a) Pentre pile segment test A6
Pentre A6 Last modified : 17 Feb 2000

NUMLAY	NUMPIL	GWT	GAMPWP	SIGSRF	ZHOLE	QR.SOIL	QR.PILE
6	1	1.0	10.2	0.0	22.5	4	4

LAYER	DEPTH	GAMMA	TYPE	Q.CPT	SPT	OCR	CLAY					SAND				CLC	MISCELLANEOUS		
	BOTTM	EFF	ClSiSa	TIP	N		SuTop	SuBot	TYP	St	Ip	D50	Dr	PHI	FLG		1	2	3
1	1.0	19.2	1	0	0	0	100	100	3	0	25	0	0	0	0		0	0	0
2	15.0	9.0	1	0	0	0	35	35	3	0	12	0	0	0	0		0	0	0
3	25.0	8.5	1	0	0	0	36	62	3	0	14	0	0	0	0		0	0	0
4	35.0	8.5	1	0	0	0	62	88	3	0	18	0	0	0	0		0	0	0
5	48.0	9.15	1	0	0	0	88	120	3	0	23	0	0	0	0		0	0	0
6	60.0	12.33	1	0	0	0	120	150	3	0	16	0	0	0	0		0	0	0

PILE NO	OPN CLS	MAT TYP	DIAM TIP	TAPER degr	WALL TIP	TOTAL LNGTH	TIP PENTR	PLUG RATIO	WATER RATIO	-- MEASURED CAPACITIES -- COMPRSSN	TENSION	DAYS	TBF	MISCELLANEOUS 1	2	3
1	2	1	.219	.0	.016	32.5	32.5	0.0	0.0	0	361	31	0	0	0	2

367
Karlsrud et al (1992a) Tilbrook pile segment tests A-C-D
Tilbrook Last modified :

NUMLAY	NUMPIL	GWT	GAMPWP	SIGSRF	ZHOLE	QR.SOIL	QR.PILE
4	3	2.0	8.6	0.0	3.0	4	4

LAYER	DEPTH	GAMMA	TYPE	Q.CPT	SPT	OCR	CLAY					SAND				CLC	MISCELLANEOUS		
	BOTTM	EFF	ClSiSa	TIP	N		SuTop	SuBot	TYP	St	Ip	D50	Dr	PHI	FLG		1	2	3
1	2.0	20.7	1	0	0	0	260	260	3	0	25	0	0	0	0		0	0	0
2	17.5	13.3	1	0	0	0	350	490	3	0	23	0	0	0	0		0	0	0
3	25.0	12.7	1	0	0	0	420	750	3	0	32	0	0	0	0		0	0	0
4	31.0	12.6	1	0	0	0	650	490	3	0	32	0	0	0	0		0	0	0

PILE NO	OPN CLS	MAT TYP	DIAM TIP	TAPER degr	WALL TIP	TOTAL LNGTH	TIP PENTR	PLUG RATIO	WATER RATIO	-- MEASURED CAPACITIES -- COMPRSSN	TENSION	DAYS	TBF	MISCELLANEOUS 1	2	3	
1	2	1	.219	.0	.016	12.5	12.5	0.0	0.0	0	1238	60	0	0	0	0	A
2	2	1	.219	.0	.016	17.5	17.5	0.0	0.0	0	1995	60	0	0	0	2	C
3	1	1	.273	.0	.016	17.5	17.5	0.0	0.0	0	1891	60	0	0	0	0	D

Remark : Pile C has tip extension piece

368
Karlsrud et al (1992a) Tilbrook pile segment test B
Tilbrook B Last modified :

NUMLAY	NUMPIL	GWT	GAMPWP	SIGSRF	ZHOLE	QR.SOIL	QR.PILE
4	1	2.0	8.6	0.0	17.5	4	4

LAYER	DEPTH	GAMMA	TYPE	Q.CPT	SPT	OCR	CLAY					SAND				CLC	MISCELLANEOUS		
	BOTTM	EFF	ClSiSa	TIP	N		SuTop	SuBot	TYP	St	Ip	D50	Dr	PHI	FLG		1	2	3
1	2.0	20.7	1	0	0	0	260	260	3	0	25	0	0	0	0		0	0	0
2	17.5	13.3	1	0	0	0	350	490	3	0	23	0	0	0	0		0	0	0
3	25.0	12.7	1	0	0	0	420	750	3	0	32	0	0	0	0		0	0	0
4	31.0	12.6	1	0	0	0	650	490	3	0	32	0	0	0	0		0	0	0

PILE NO	OPN CLS	MAT TYP	DIAM TIP	TAPER degr	WALL TIP	TOTAL LNGTH	TIP PENTR	PLUG RATIO	WATER RATIO	-- MEASURED CAPACITIES -- COMPRSSN	TENSION	DAYS	TBF	MISCELLANEOUS 1	2	3	
1	2	1	.219	.0	.016	25.5	25.5	0.0	0.0	0	1684	60	0	0	0	2	B

Remark : Pile B has tip extension piece

369
Karlsrud et al (1992b) Pile segment tests at Ons”y, Piles A1-C1-C2-B1
Ons”y Last modified : 2 Feb 2000

NUMLAY	NUMPIL	GWT	GAMPWP	SIGSRF	ZHOLE	QR.SOIL	QR.PILE
2	4	1.0	11.1	11.0	5.0	4	4

LAYER	DEPTH	GAMMA	TYPE	Q.CPT	SPT	OCR	CLAY					SAND				CLC	MISCELLANEOUS		
	BOTTM	EFF	ClSiSa	TIP	N		SuTop	SuBot	TYP	St	Ip	D50	Dr	PHI	FLG		1	2	3
1	15.0	5.1	1	0	0	0	10	20.5	5	5?	40	0	0	0	0		0	0	0
2	40.0	5.1	1	0	0	0	20.5	55.5	5	5?	40	0	0	0	0		0	0	0

PILE NO	OPN CLS	MAT TYP	DIAM TIP	TAPER degr	WALL TIP	TOTAL LNGTH	TIP PENTR	PLUG RATIO	WATER RATIO	-- MEASURED CAPACITIES -- COMPRSSN	TENSION	DAYS	TBF	MISCELLANEOUS 1	2	3	
1	2	1	.219	.0	.010	15.0	15.0	0.0	0.0	0	130	50?	0	0	0	2	A1
2	2	1	.219	.0	.010	35.0	35.0	0.0	0.0	0	465	50?	0	0	0	2	C1
3	2	1	.219	.0	.010	35.0	35.0	0.0	0.0	0	510?	50?	0	0	0	2	C2
4	1	1	.812	.0	.010	15.0	15.0	0.0	0.0	0	469	50?	0	0	0	2	B1

Remarks : Wall thickness, tip condition and failure load adjusted to give failure tau.skin reported

370
Karlsrud et al (1992b) Pile segment tests at Ons”y, Pile A2
Ons”y Last modified : 2 Feb 2000

NUMLAY	NUMPIL	GWT	GAMPWP	SIGSRF	ZHOLE	QR.SOIL	QR.PILE
2	1	1.0	11.1	11.0	12.5	4	4

LAYER	DEPTH	GAMMA	TYPE	Q.CPT	SPT	OCR	CLAY					SAND				CLC	MISCELLANEOUS		
	BOTTM	EFF	ClSiSa	TIP	N		SuTop	SuBot	TYP	St	Ip	D50	Dr	PHI	FLG		1	2	3
1	15.0	5.1	1	0	0	0	10	20.5	5	5?	40	0	0	0	0		0	0	0
2	40.0	5.1	1	0	0	0	20.5	55.5	5	5?	40	0	0	0	0		0	0	0

PILE NO	OPN CLS	MAT TYP	DIAM TIP	TAPER degr	WALL TIP	TOTAL LNGTH	TIP PENTR	PLUG RATIO	WATER RATIO	-- MEASURED CAPACITIES -- COMPRSSN	TENSION	DAYS	TBF	MISCELLANEOUS 1	2	3	
1	2	1	.219	.0	.010	22.5	22.5	0.0	0.0	0	161	50?	0	0	0	2	A2

371
Karlsrud et al (1992b) Pile segment tests at Ons”y, Pile A3
Ons”y Last modified : 2 Feb 2000

NUMLAY	NUMPIL	GWT	GAMPWP	SIGSRF	ZHOLE	QR.SOIL	QR.PILE
2	1	1.0	11.1	11.0	20.0	4	4

LAYER	DEPTH	GAMMA	TYPE	Q.CPT	SPT	OCR	CLAY					SAND				CLC	MISCELLANEOUS		
	BOTTM	EFF	ClSiSa	TIP	N		SuTop	SuBot	TYP	St	Ip	D50	Dr	PHI	FLG		1	2	3
1	15.0	5.1	1	0	0	0	10	20.5	5	5?	40	0	0	0	0		0	0	0
2	40.0	5.1	1	0	0	0	20.5	55.5	5	5?	40	0	0	0	0		0	0	0

```
 PILE OPN MAT  DIAM TAPER  WALL  TOTAL  TIP   PLUG  WATER   -- MEASURED CAPACITIES --  MISCELLANEOUS
  NO  CLS TYP   TIP degr   TIP   LNGTH PENTR  RATIO RATIO   COMPRSSN TENSION DAYS TBF    1   2   3
   1   2   1   .219  .0   .010   30.0  30.0   0.0   0.0         0      216    50?  0     0   0   2 A3

#  372
Karlsrud et al (1992b)  Pile segment tests at Ons”y, Pile A4
Ons”y                   Last modified : 2 Feb 2000

 NUMLAY   NUMPIL   GWT   GAMPWP    SIGSRF   ZHOLE   QR.SOIL   QR.PILE
    2       1      1.0    11.1      11.0    27.5      4         4

 LAYER  DEPTH  GAMMA TYPE  Q.CPT  SPT  OCR  -------- CLAY -------   ----SAND----  CLC  MISCELLANEOUS
        BOTTM   EFF ClSiSa  TIP    N        SuTop SuBot TYP St Ip   D50  Dr  PHI  FLG    1   2   3
   1    15.0    5.1   1      0     0    0     10    20.5  5  5? 40    0    0   0    0     0   0   0
   2    40.0    5.1   1      0     0    0     20.5  55.5  5  5? 40    0    0   0    0     0   0   0

 PILE OPN MAT  DIAM TAPER  WALL  TOTAL  TIP   PLUG  WATER   -- MEASURED CAPACITIES --  MISCELLANEOUS
  NO  CLS TYP   TIP degr   TIP   LNGTH PENTR  RATIO RATIO   COMPRSSN TENSION DAYS TBF    1   2   3
   1   2   1   .219  .0   .010   37.5  37.5   0.0   0.0         0      258    50?  0     0   0   2 A4

#  373
Karlsrud et al (1992b)  Pile segment tests at Lierstranda, Piles A7 & B2
Lierstranda             Last modified : 19 Feb 2000

 NUMLAY   NUMPIL   GWT   GAMPWP    SIGSRF   ZHOLE   QR.SOIL   QR.PILE
    4       2      0.0     10        0.0     5.0      4         4

 LAYER  DEPTH  GAMMA TYPE  Q.CPT  SPT  OCR  -------- CLAY -------   ----SAND----  CLC  MISCELLANEOUS
        BOTTM   EFF ClSiSa  TIP    N        SuTop SuBot TYP St Ip   D50  Dr  PHI  FLG    1   2   3
   1     2.0     10   3      0     0    0      0     0    0   0 0    0   .5   0    0     0   0   0
   2    13.0    6.9   1      0     0    0     21    21    5  5? 23   0    0   0    0     0   0   0
   3    26.0    7.1  1.9     0     0    0     24    27    5  5? 14   0    0   0    0     0   0   0
   4    40.0    7.5  1.9     0     0    0     31    40    5  5? 12   0    0   0    0     0   0   0

 PILE OPN MAT  DIAM TAPER  WALL  TOTAL  TIP   PLUG  WATER   -- MEASURED CAPACITIES --  MISCELLANEOUS
  NO  CLS TYP   TIP degr   TIP   LNGTH PENTR  RATIO RATIO   COMPRSSN TENSION DAYS TBF    1   2   3
   1   2   1   .219  .0   .010   15.0  15.0   0.0   0.0         0      86.1   29   0     0   0   2 A7
   2   1   1   .812  .0   .010   15.0  15.0   0.0   0.0         0      374    55   0     0   0   2 B2

 19 Feb 2000 : The Su values for sites 518-519-520-521 changed from "Su.lab"
               values based upon above paper, to Su.DSS values from NGI report 52523-21, Fig. 04.
               Time from driving to testing changed from 50 to 30.

#  374
Karlsrud et al (1992b)  Pile segment tests at Lierstranda, Pile A8
Lierstranda             Last modified : 19 Feb 2000

 NUMLAY   NUMPIL   GWT   GAMPWP    SIGSRF   ZHOLE   QR.SOIL   QR.PILE
    4       1      0.0     10        0.0    12.5      4         4

 LAYER  DEPTH  GAMMA TYPE  Q.CPT  SPT  OCR  -------- CLAY -------   ----SAND----  CLC  MISCELLANEOUS
        BOTTM   EFF ClSiSa  TIP    N        SuTop SuBot TYP St Ip   D50  Dr  PHI  FLG    1   2   3
   1     2.0     10   3      0     0    0      0     0    0   0 0    0   .5   0    0     0   0   0
   2    13.0    6.9   1      0     0    0     21    21    5  5? 23   0    0   0    0     0   0   0
   3    26.0    7.1  1.9     0     0    0     24    27    5  5? 14   0    0   0    0     0   0   0
   4    40.0    7.5  1.9     0     0    0     31    40    5  5? 12   0    0   0    0     0   0   0

 PILE OPN MAT  DIAM TAPER  WALL  TOTAL  TIP   PLUG  WATER   -- MEASURED CAPACITIES --  MISCELLANEOUS
  NO  CLS TYP   TIP degr   TIP   LNGTH PENTR  RATIO RATIO   COMPRSSN TENSION DAYS TBF    1   2   3
   1   2   1   .219  .0   .010   22.5  22.5   0.0   0.0         0      89.2   32   0     0   0   2 A8


#  375
Karlsrud et al (1992b)  Pile segment tests at Lierstranda, Pile A9
Lierstranda             Last modified : 19 Feb 2000

 NUMLAY   NUMPIL   GWT   GAMPWP    SIGSRF   ZHOLE   QR.SOIL   QR.PILE
    4       1      0.0     10        0.0    20.0      4         4

 LAYER  DEPTH  GAMMA TYPE  Q.CPT  SPT  OCR  -------- CLAY -------   ----SAND----  CLC  MISCELLANEOUS
        BOTTM   EFF ClSiSa  TIP    N        SuTop SuBot TYP St Ip   D50  Dr  PHI  FLG    1   2   3
   1     2.0     10   3      0     0    0      0     0    0   0 0    0   .5   0    0     0   0   0
   2    13.0    6.9   1      0     0    0     21    21    5  5? 23   0    0   0    0     0   0   0
   3    26.0    7.1  1.9     0     0    0     24    27    5  5? 14   0    0   0    0     0   0   0
   4    40.0    7.5  1.9     0     0    0     31    40    5  5? 12   0    0   0    0     0   0   0

 PILE OPN MAT  DIAM TAPER  WALL  TOTAL  TIP   PLUG  WATER   -- MEASURED CAPACITIES --  MISCELLANEOUS
  NO  CLS TYP   TIP degr   TIP   LNGTH PENTR  RATIO RATIO   COMPRSSN TENSION DAYS TBF    1   2   3
   1   2   1   .219  .0   .010   30.0  30.0   0.0   0.0         0      104.1  31   0     0   0   2 A9


#  376
Karlsrud et al (1992b)  Pile segment tests at Lierstranda, Pile A10
Lierstranda             Last modified : 19 Feb 2000

 NUMLAY   NUMPIL   GWT   GAMPWP    SIGSRF   ZHOLE   QR.SOIL   QR.PILE
    4       1      0.0     10        0.0    27.5      4         4

 LAYER  DEPTH  GAMMA TYPE  Q.CPT  SPT  OCR  -------- CLAY -------   ----SAND----  CLC  MISCELLANEOUS
        BOTTM   EFF ClSiSa  TIP    N        SuTop SuBot TYP St Ip   D50  Dr  PHI  FLG    1   2   3
   1     2.0     10   3      0     0    0      0     0    0   0 0    0   .5   0    0     0   0   0
   2    13.0    6.9   1      0     0    0     21    21    5  5? 23   0    0   0    0     0   0   0
   3    26.0    7.1  1.9     0     0    0     24    27    5  5? 14   0    0   0    0     0   0   0
   4    40.0    7.5  1.9     0     0    0     31    40    5  5? 12   0    0   0    0     0   0   0

 PILE OPN MAT  DIAM TAPER  WALL  TOTAL  TIP   PLUG  WATER   -- MEASURED CAPACITIES --  MISCELLANEOUS
  NO  CLS TYP   TIP degr   TIP   LNGTH PENTR  RATIO RATIO   COMPRSSN TENSION DAYS TBF    1   2   3
   1   2   1   .219  .0   .010   37.5  37.5   0.0   0.0         0      94.8   30   0     0   0   2 A10


# -377
Bjerrum et al (1969) and Johannessen (1965)  S”renga, Pile C, Negative skin friction test
S”renga                                      Last modified : Removed 29 Feb 2000

 NUMLAY   NUMPIL   GWT   GAMPWP    SIGSRF   ZHOLE   QR.SOIL   QR.PILE
    2       1      2.0     10       10.0     0.0      2         2

 LAYER  DEPTH  GAMMA TYPE  Q.CPT  SPT  OCR  -------- CLAY -------   ----SAND----  CLC  MISCELLANEOUS
        BOTTM   EFF ClSiSa  TIP    N        SuTop SuBot TYP St Ip   D50  Dr  PHI  FLG    1   2   3
   1    15.0    9.0  3.5     0     0    0      0     0    0   0 0    0    0   33   0     0   0   0
   2    60.0    9.0  1.3     0     0    0     25   100?   8   3 17   0    0   0    0     0   0   0
```

PILE NO	OPN CLS	MAT TYP	DIAM TIP	TAPER degr	WALL TIP	TOTAL LNGTH	TIP PENTR	PLUG RATIO	WATER RATIO	-- MEASURED CAPACITIES -- COMPRSSN	TENSION	DAYS	TBF	MISCELLANEOUS 1	2	3
1	2	1	.500	.0	.008	57.0	57.0	0.0	0.0	0	2950	720	0	0	0	0

29 Feb 2000 : These results and soil strengths need to be checked further, calculated capacity is much higher than measured, possibly caused by the slow "loading"

378
Hutchinson & Jensen (1968) Port Khorramshahr pile tests, non-coated piles
Iran Last modified :

NUMLAY	NUMPIL	GWT	GAMPWP	SIGSRF	ZHOLE	QR.SOIL	QR.PILE
3	9	2.0	10	0.0	0.0	3	3

LAYER	DEPTH BOTTM	GAMMA EFF	TYPE ClSiSa	Q.CPT TIP	SPT N	OCR	-------- CLAY ------- SuTop	SuBot	TYP	St	Ip	----SAND---- D50	Dr	PHI	CLC FLG	MISCELLANEOUS 1	2	3
1	2.0	18.3	1.3	0	0	0	21	25	8	3	30	0	0	0	0	0	0	0
2	8.0	8.3	1.3	0	0	0	25	36	8	3	22	0	0	0	0	0	0	0
3	20.0	8.3	1.3	0	0	0	36	58	8	3	28	0	0	0	0	0	0	0

PILE NO	OPN CLS	MAT TYP	DIAM TIP	TAPER degr	WALL TIP	TOTAL LNGTH	TIP PENTR	PLUG RATIO	WATER RATIO	-- MEASURED CAPACITIES -- COMPRSSN	TENSION	DAYS	TBF	MISCELLANEOUS 1	2	3	
1	2	2	.382	.0	.191	14.0	13.3	0.0	0.0	335	0	44	0	0	0	0	P1
2	2	2	.382	.0	.191	16.0	15.0	0.0	0.0	335	0	90	0	0	0	0	P2
3	2	2	.382	.0	.191	20.0	19.1	0.0	0.0	515	0	44	0	0	0	0	P6
4	2	2	.382	.0	.191	16.0	15.05	0.0	0.0	400	0	42	0	0	0	0	P10
5	2	2	.382	.0	.191	18.0	16.6	0.0	0.0	380	0	48	0	0	0	0	P14
6	2	2	.382	.0	.191	16.0	15.0	0.0	0.0	410	0	71	0	0	0	0	P18
7	2	3	.350	.0	.175	17.0	17.0	0.0	0.0	610	0	33	0	0	0	0	P19
8	2	3	.350	.0	.175	17.2	17.1	0.0	0.0	590	0	36	0	0	0	0	P20
9	2	1	.35	.0	.010?	14.2	13.9	0.0	0.0	400	0	584	0	0	0	0	P21

379
Karlsrud & Haugen (1985) Haga model piles, typical results
Haga Last modified : 3 Feb 2000

NUMLAY	NUMPIL	GWT	GAMPWP	SIGSRF	ZHOLE	QR.SOIL	QR.PILE
3	3	0.0	0.0	0.0	0.2	4	4

LAYER	DEPTH BOTTM	GAMMA EFF	TYPE ClSiSa	Q.CPT TIP	SPT N	OCR	-------- CLAY ------- SuTop	SuBot	TYP	St	Ip	----SAND---- D50	Dr	PHI	CLC FLG	MISCELLANEOUS 1	2	3
1	1.5	21	1	0	0	0	20	34	5	4	13	0	0	0	0	0	0	0
2	4.5	16.7	1	0	0	0	34	34	5	4	16	0	0	0	0	0	0	0
3	5.6	16.7	1	0	0	0	48	48	5	4	40	0	0	0	0	0	0	0

PILE NO	OPN CLS	MAT TYP	DIAM TIP	TAPER degr	WALL TIP	TOTAL LNGTH	TIP PENTR	PLUG RATIO	WATER RATIO	-- MEASURED CAPACITIES -- COMPRSSN	TENSION	DAYS	TBF	MISCELLANEOUS 1	2	3
1	2	1	.153	.0	.0045	5.15	5.0?	0.0	0.0	0	59	7	0	0	0	0
2	2	1	.153	.0	.0045	5.15	5.0?	0.0	0.0	0	65	20	0	0	0	0
3	2	1	.153	.0	.0045	5.15	5.0?	0.0	0.0	0	73	36	0	0	0	0

Remark : Typical time development results, not individual tests

380
Eide et al (1961) Timber pile with short- and long-term tests
Drammen Last modified :

NUMLAY	NUMPIL	GWT	GAMPWP	SIGSRF	ZHOLE	QR.SOIL	QR.PILE
5	3	1.5	10	0.0	2.4	3	3

LAYER	DEPTH BOTTM	GAMMA EFF	TYPE ClSiSa	Q.CPT TIP	SPT N	OCR	-------- CLAY ------- SuTop	SuBot	TYP	St	Ip	----SAND---- D50	Dr	PHI	CLC FLG	MISCELLANEOUS 1	2	3
1	1.5	19	3	0	0	0	0	0	0	0	0	0	0	35	0	0	0	0
2	3.5	7.8	1	0	0	0	20	20	8	7	25	0	0	0	0	0	0	0
3	7.0	7.8	1	0	0	0	12	12	8	7	25	0	0	0	0	0	0	0
4	13.0	8.1	1	0	0	0	12	20	8	5	20	0	0	0	0	0	0	0
5	20.0	8.8	1	0	0	0	15	30	8	4	13	0	0	0	0	0	0	0

PILE NO	OPN CLS	MAT TYP	DIAM TIP	TAPER degr	WALL TIP	TOTAL LNGTH	TIP PENTR	PLUG RATIO	WATER RATIO	-- MEASURED CAPACITIES -- COMPRSSN	TENSION	DAYS	TBF	MISCELLANEOUS 1	2	3
1	2	3	.150	.44	.075	15.5	15.5	0.0	0.0	220	0	31	0	0	0	0
2	2	3	.150	.44	.075	15.5	15.5	0.0	0.0	270	0	71	1	0	0	0
3	2	3	.150	.44	.075	15.5	15.5	0.0	0.0	300	0	799	1	0	0	0

381
Fellenius & Samson (1976) Concrete pile no. 9, tension test
Montreal Last modified :

NUMLAY	NUMPIL	GWT	GAMPWP	SIGSRF	ZHOLE	QR.SOIL	QR.PILE
2	1	0.9	10	0.0	1.0	3	3

LAYER	DEPTH BOTTM	GAMMA EFF	TYPE ClSiSa	Q.CPT TIP	SPT N	OCR	-------- CLAY ------- SuTop	SuBot	TYP	St	Ip	----SAND---- D50	Dr	PHI	CLC FLG	MISCELLANEOUS 1	2	3
1	0.9	16.5	1	0	0	0	50	50	8	20	35	0	0	0	0	0	0	0
2	18.0	6.5	1	0	0	0	40	67	8	20	35	0	0	0	0	0	0	0

PILE NO	OPN CLS	MAT TYP	DIAM TIP	TAPER degr	WALL TIP	TOTAL LNGTH	TIP PENTR	PLUG RATIO	WATER RATIO	-- MEASURED CAPACITIES -- COMPRSSN	TENSION	DAYS	TBF	MISCELLANEOUS 1	2	3
1	2	2	.300	.0	.150	18.6	16.8	0.0	0.0	0	458	71	0	0	0	0

382
Blanchet et al (1980) Bridge pier, comparison between different pile types
Maskinonge Canada Last modified :

NUMLAY	NUMPIL	GWT	GAMPWP	SIGSRF	ZHOLE	QR.SOIL	QR.PILE
4	5	1.3	10	0.0	0.0	3	3

LAYER	DEPTH BOTTM	GAMMA EFF	TYPE ClSiSa	Q.CPT TIP	SPT N	OCR	-------- CLAY ------- SuTop	SuBot	TYP	St	Ip	----SAND---- D50	Dr	PHI	CLC FLG	MISCELLANEOUS 1	2	3
1	1.3	18.0	2.5	0	0	0	0	0	0	0	0	0	0	30	0	0	0	0
2	5.3	8.0	2.5	0	0	0	0	0	0	0	0	0	0	30	0	0	0	0
3	15.4	6.5	1	0	0	0	14	40	8	6	30	0	0	0	0	0	0	0
4	40.0	6.5	1	0	0	0	40	105	8	6	55	0	0	0	0	0	0	0

PILE NO	OPN CLS	MAT TYP	DIAM TIP	TAPER degr	WALL TIP	TOTAL LNGTH	TIP PENTR	PLUG RATIO	WATER RATIO	-- MEASURED CAPACITIES -- COMPRSSN	TENSION	DAYS	TBF	MISCELLANEOUS 1	2	3
1	2	3	.222	.28	.111	15.25	15.25	0.0	0.0	698	0	58	0	0	0	0
2	2	3	.222	.28	.111	15.25	15.25	0.0	0.0	640	0	58	0	0	0	0
3	2	2	.242	.0	.121	23.8	23.8	0.0	0.0	585	0	58	0	0	0	0
4	2	1	.219	.0	.00635	23.8	23.8	0.0	0.0	390	0	58	0	0	0	0
5	2	2	.242	.0	.121	37.5	37.5	0.0	0.0	845	0	58	0	0	0	0

383
Bengtsson & S„llfors (1983) Tension test on concrete pile, Fig. 13
G”teborg   Last modified :

NUMLAY	NUMPIL	GWT	GAMPWP	SIGSRF	ZHOLE	QR.SOIL	QR.PILE
2	1	1.0?	10	10.0?	8.0	3	3

LAYER	DEPTH BOTTM	GAMMA EFF	TYPE ClSiSa	Q.CPT TIP	SPT N	OCR	CLAY SuTop	CLAY SuBot	CLAY TYP	CLAY St	CLAY Ip	SAND D50	SAND Dr	SAND PHI	CLC FLG	MISCELLANEOUS 1	2	3
1	4.0	9.0	3	0	0	0	0	0	0	0	0	0	0	30	0	0	0	0
2	35.0	5.9	1	0	0	0	23	80	8	15	40?	0	0	0	0	0	0	0

PILE NO	OPN CLS	MAT TYP	DIAM TIP	TAPER degr	WALL TIP	TOTAL LNGTH	TIP PENTR	PLUG RATIO	WATER RATIO	-- MEASURED CAPACITIES -- COMPRSSN	TENSION	DAYS	TBF	MISCELLANEOUS 1	2	3
1	2	2	.340	.0	.170	35.0	34.0	0.0	0.0	0	900	46	0	0	0	0

-384
Not used

385
Indraratna et al (1992) Tension tetsts on concrete pile in Bangkok clay
Bangkok   Last modified :

NUMLAY	NUMPIL	GWT	GAMPWP	SIGSRF	ZHOLE	QR.SOIL	QR.PILE
4	4	2.0	10	0.0	0.0	3	3

LAYER	DEPTH BOTTM	GAMMA EFF	TYPE ClSiSa	Q.CPT TIP	SPT N	OCR	CLAY SuTop	CLAY SuBot	CLAY TYP	CLAY St	CLAY Ip	SAND D50	SAND Dr	SAND PHI	CLC FLG	MISCELLANEOUS 1	2	3
1	2.0	15.7	1	0	0	0	30	30	-1	5?	40	0	0	0	0	0	0	0
2	4.0	5.7	1	0	0	0	10	10	4	5?	40	0	0	0	0	0	0	0
3	12.0	3.9	1	0	0	0	10	25	4	5?	70	0	0	0	0	0	0	0
4	20.1	5.7	1	0	0	0	25	52	4	5?	60	0	0	0	0	0	0	0

PILE NO	OPN CLS	MAT TYP	DIAM TIP	TAPER degr	WALL TIP	TOTAL LNGTH	TIP PENTR	PLUG RATIO	WATER RATIO	-- MEASURED CAPACITIES -- COMPRSSN	TENSION	DAYS	TBF	MISCELLANEOUS 1	2	3
1	2	2	.400	.0	.075	8.0	8.0	0.0	0.0	0	110	8.5	0	0	0	0
2	2	2	.400	.0	.075	12.0	12.0	0.0	0.0	0	165	8.5	0	0	0	0
3	2	2	.400	.0	.075	16.0	16.0	0.0	0.0	0	245	8.5	0	0	0	0
4	2	2	.400	.0	.075	20.0	20.0	0.0	0.0	0	425	8.5	0	0	0	0

386
Konrad & Roy (1987) Field tests in stiff clay, time effects
St Alban   Canada   Last modified :

NUMLAY	NUMPIL	GWT	GAMPWP	SIGSRF	ZHOLE	QR.SOIL	QR.PILE
3	5	0.6	10	0.0	0.0	3	3

LAYER	DEPTH BOTTM	GAMMA EFF	TYPE ClSiSa	Q.CPT TIP	SPT N	OCR	CLAY SuTop	CLAY SuBot	CLAY TYP	CLAY St	CLAY Ip	SAND D50	SAND Dr	SAND PHI	CLC FLG	MISCELLANEOUS 1	2	3
1	0.6	13.0	2.5	0	0	0	0	0	0	0	0	0	0	25	0	0	0	0
2	1.6	7.3	1	0	0	0	35	10	8	5	30	0	0	0	0	0	0	0
3	9.8	6.2	1	0	0	0	9	32	8	18	20	0	0	0	0	0	0	0

PILE NO	OPN CLS	MAT TYP	DIAM TIP	TAPER degr	WALL TIP	TOTAL LNGTH	TIP PENTR	PLUG RATIO	WATER RATIO	-- MEASURED CAPACITIES -- COMPRSSN	TENSION	DAYS	TBF	MISCELLANEOUS 1	2	3	
1	2	1	.220	.0	.008	7.6	7.6	0.0	0.0	47	0	4	0	0	0	0	Pile A
2	2	1	.220	.0	.008	7.6	7.6	0.0	0.0	67	0	8	1	0	0	0	Pile A
3	2	1	.220	.0	.008	7.6	7.6	0.0	0.0	77	0	20	1	0	0	0	Pile A
4	2	1	.220	.0	.008	7.6	7.6	0.0	0.0	83	0	33	1	0	0	0	Pile A
5	2	1	.220	.0	.008	7.6	7.6	0.0	0.0	86	0	720	0	0	0	0	Pile B

387
Togrol (1973) Two steel piles in clay/silt, one with tip in sand
Izmir   Last modified :

NUMLAY	NUMPIL	GWT	GAMPWP	SIGSRF	ZHOLE	QR.SOIL	QR.PILE
3	4	-13.0	10	0.0	0.0	2	3

LAYER	DEPTH BOTTM	GAMMA EFF	TYPE ClSiSa	Q.CPT TIP	SPT N	OCR	CLAY SuTop	CLAY SuBot	CLAY TYP	CLAY St	CLAY Ip	SAND D50	SAND Dr	SAND PHI	CLC FLG	MISCELLANEOUS 1	2	3
1	6.0	6.2	1.9	0	0	0	20	20	3?	0	30	0	0	0	0	0	0	0
2	16.0	10.0	1.5	0	0	0	75	75	2	0	13	0	0	0	0	0	0	0
3	19.0	10.0	3	0	40	0	0	0	0	0	0	0	0	0	0	0	0	0

PILE NO	OPN CLS	MAT TYP	DIAM TIP	TAPER degr	WALL TIP	TOTAL LNGTH	TIP PENTR	PLUG RATIO	WATER RATIO	-- MEASURED CAPACITIES -- COMPRSSN	TENSION	DAYS	TBF	MISCELLANEOUS 1	2	3
1	1	1	.528	.0	.010	32.0?	17.0	0.5?	0.9?	1410	0	60	0	0	0	0
2	1	1	.528	.0	.010	32.0?	17.0	0.5?	0.9?	0	710	60	1	0	0	0
3	1	1	.528	.0	.010	30.0?	15.0	0.5?	0.9?	780	0	30	0	0	0	0
4	1	1	.528	.0	.010	30.0?	15.0	0.5?	0.9?	0	590	30	1	0	0	0

388
Lehane & Jardine (1992)   Tests with instrumented model pile, glacial till
Cowden   Last modified :

NUMLAY	NUMPIL	GWT	GAMPWP	SIGSRF	ZHOLE	QR.SOIL	QR.PILE
3	3	0.0	10	0.0	2.5	4	4

LAYER	DEPTH BOTTM	GAMMA EFF	TYPE ClSiSa	Q.CPT TIP	SPT N	OCR	CLAY SuTop	CLAY SuBot	CLAY TYP	CLAY St	CLAY Ip	SAND D50	SAND Dr	SAND PHI	CLC FLG	MISCELLANEOUS 1	2	3
1	2.5	11.5	1	0	0	0	170	170	3	0	20	0	0	0	0	0	0	0
2	4.0	11.5	1	0	0	0	180	180	3	0	20	0	0	0	0	0	0	0
3	7.0	11.5	1	0	0	0	100	100	3	0	18	0	0	0	0	0	0	0

PILE NO	OPN CLS	MAT TYP	DIAM TIP	TAPER degr	WALL TIP	TOTAL LNGTH	TIP PENTR	PLUG RATIO	WATER RATIO	-- MEASURED CAPACITIES -- COMPRSSN	TENSION	DAYS	TBF	MISCELLANEOUS 1	2	3
1	2	1	.102	.0	.008?	6.65	6.15	0.0	0.0	136	0	4	0	0	0	0
2	2	1	.102	.0	.008?	6.90	6.40	0.0	0.0	0	90	5	0	0	0	0
3	2	1	.102	.0	.008?	6.93	6.43	0.0	0.0	108	0	4	0	0	0	0

389
Meyerhof et al (1981) Concrete piles in clay till
NovaScotia   Last modified : 7 Feb 2000 Time set to 7? days

NUMLAY	NUMPIL	GWT	GAMPWP	SIGSRF	ZHOLE	QR.SOIL	QR.PILE
2	2	1.0?	10	10.0	0.0	3	3

LAYER	DEPTH BOTTM	GAMMA EFF	TYPE ClSiSa	Q.CPT TIP	SPT N	OCR	CLAY SuTop	CLAY SuBot	CLAY TYP	CLAY St	CLAY Ip	SAND D50	SAND Dr	SAND PHI	CLC FLG	MISCELLANEOUS 1	2	3
1	7.0	12.5	1.5	0	0	0	190	150	4	0	9	0	0	0	0	0	0	0
2	15.0	12.8	1.5	0	0	0	190	220	4	0	15	0	0	0	0	0	0	0

PILE NO	OPN CLS	MAT TYP	DIAM TIP	TAPER degr	WALL TIP	TOTAL LNGTH	TIP PENTR	PLUG RATIO	WATER RATIO	-- MEASURED CAPACITIES -- COMPRSSN	TENSION	DAYS	TBF	MISCELLANEOUS 1	2	3
1	2	2	.243	.0	.1215	12.5	12.0	0.0	0.0	1240	0	7?	0	0	0	0
2	2	2	.340	.0	.170	13.5	13.0	0.0	0.0	1950	0	7?	0	0	0	0

Piles tested "a few days" after driving.

390
Trenter & Burt (1981) Open steel piles in soft silty clay, Offshore test P4
Sumatra Last modified :

NUMLAY	NUMPIL	GWT	GAMPWP	SIGSRF	ZHOLE	QR.SOIL	QR.PILE
3	4	0.0	10	0.0	0.0	3	3

LAYER	DEPTH BOTTM	GAMMA EFF	TYPE ClSiSa	Q.CPT TIP	SPT N	OCR	CLAY SuTop	CLAY SuBot	CLAY TYP	CLAY St	CLAY Ip	SAND D50	SAND Dr	SAND PHI	CLC FLG	MISCELLANEOUS 1	2	3
1	18.0	5.8	1	0	0	0	10	35	8	2	40	0	0	0	0	0	0	0
2	19.0	9.0	3	0	0	0	0	0	0	0	0	0	0.6	0	0	0	0	0
3	48.0	6.2	1	0	0	0	35	70	8	2	40	0	0	0	0	0	0	0

PILE NO	OPN CLS	MAT TYP	DIAM TIP	TAPER degr	WALL TIP	TOTAL LNGTH	TIP PENTR	PLUG RATIO	WATER RATIO	-- MEASURED CAPACITIES -- COMPRSSN	TENSION	DAYS	TBF	MISCELLANEOUS 1	2	3
1	1	1	.400	.0	.012	44.3	43.3	0.5?	0.98?	1225	0	1.7	0	0	0	0
2	1	1	.400	.0	.012	44.3	43.3	0.5?	0.98?	1555	0	10.5	1	0	0	0
3	1	1	.400	.0	.012	44.3	43.3	0.5?	0.98?	1670	0	20.5	1	0	0	0
4	1	1	.400	.0	.012	44.3	43.3	0.5?	0.98?	1670	0	32.5	1	0	0	0

391
McCammon & Golder (1970) Geotetechnique June 1970 p. 171 Pile 2
L Arrow Lake Last modified : 3 Feb 2000

NUMLAY	NUMPIL	GWT	GAMPWP	SIGSRF	ZHOLE	QR.SOIL	QR.PILE
3	5	0.0	10.9	0.0	0.0	4	4

LAYER	DEPTH BOTTM	GAMMA EFF	TYPE ClSiSa	Q.CPT TIP	SPT N	OCR	CLAY SuTop	CLAY SuBot	CLAY TYP	CLAY St	CLAY Ip	SAND D50	SAND Dr	SAND PHI	CLC FLG	MISCELLANEOUS 1	2	3
1	6.1	5.2	1	0	0	0	14	14	8	5	45?	0	0	0	0	0	0	0
2	22.9	6.6	1	0	0	0	57	72	8	4	40	0	0	0	0	0	0	0
3	48.8	7.3	1	0	0	0	91	105	2	0	30	0	0	0	0	0	0	0

PILE NO	OPN CLS	MAT TYP	DIAM TIP	TAPER degr	WALL TIP	TOTAL LNGTH	TIP PENTR	PLUG RATIO	WATER RATIO	-- MEASURED CAPACITIES -- COMPRSSN	TENSION	DAYS	TBF	MISCELLANEOUS 1 2 3	Name
1	1	1	.610	0	.0127	32.5	30.5	0.00	1.0?	1558	0	1.1	0	0 0 0	2A
2	1	1	.610	0	.0127	32.5	30.5	0.00	1.0?	1958	0	10	1	0 0 0	2B
3	1	1	.610	0	.0127	48.6	46.6	0.00	1.0?	2626	0	1.3	1	0 0 0	2C
4	2	1	.610	0	.0127	50.2	48.2	0.19	1.0?	3160	0	3	1	0 0 0	2D
5	2	1	.610	0	.0127	50.3	48.3	0.19	1.0?	3649	0	170	1	0 0 0	2E

392
Clarke et al (1985) Geotechnique December 1985 p. 393
West Sole Last modified :

NUMLAY	NUMPIL	GWT	GAMPWP	SIGSRF	ZHOLE	QR.SOIL	QR.PILE
4	12	0.0	10	0.0	0.0	4	4

LAYER	DEPTH BOTTM	GAMMA EFF	TYPE ClSiSa	Q.CPT TIP	SPT N	OCR	CLAY SuTop	CLAY SuBot	CLAY TYP	CLAY St	CLAY Ip	SAND D50	SAND Dr	SAND PHI	CLC FLG	MISCELLANEOUS 1	2	3
1	8.0	12.5	1	6000	0	0	200	360	3	0	20	0	0	0	0	0	0	0
2	11.0	12.5	1	8000	0	0	500	500	3	0	19	0	0	0	0	0	0	0
3	15.0	11.0	1	7000	0	0	450	450	3	0	22	0	0	0	0	0	0	0
4	19.0	11.5	1	9000	0	0	600	600	3	0	21	0	0	0	0	0	0	0

PILE NO	OPN CLS	MAT TYP	DIAM TIP	TAPER degr	WALL TIP	TOTAL LNGTH	TIP PENTR	PLUG RATIO	WATER RATIO	-- MEASURED CAPACITIES -- COMPRSSN	TENSION	DAYS	TBF	MISCELLANEOUS 1 2 3	Name
1	1	1	.762	0	.0318	6.0	6.0	1.0	1.0	0	2438	4.9	0	0 -1 0	A
2	1	1	.762	0	.0318	9.0	9.0	1.0	1.0	0	2873	0.3	0	0 -1 0	A
3	1	1	.762	0	.0318	12.0	12.0	1.0	1.0	0	4466	0.2	0	0 -1 0	A
4	1	1	.762	0	.0318	15.0	15.0	1.0	1.0	0	5240	0.4	0	0 -1 0	A
5	1	1	.762	0	.0318	18.0	18.0	1.0	1.0	0	6734	0.4	0	0 -1 0	A
6	1	1	.762	0	.0318	3.0	3.0	1.0	1.0	1406	961	2.6	0	0 -1 0	B
7	1	1	.762	0	.0318	6.0	6.0	1.0	1.0	3051	1726	0.4	0	0 -1 0	B
8	1	1	.762	0	.0318	9.0	9.0	1.0	1.0	5471	2642	0.2	0	0 -1 0	B
9	1	1	.762	0	.0318	9.0	9.0	0.9	1.0	0	3079	5.9	1	0 -1 0	B
10	1	1	.762	0	.0318	12.0	12.0	0.8	1.0	6681	4457	0.3	0	0 -1 0	B
11	1	1	.762	0	.0318	15.0	15.0	0.7	1.0	6788	4510	0.2	0	0 -1 0	B
12	1	1	.762	0	.0318	18.0	18.0	0.5	1.0	8344	6023	0.2	0	0 -1 0	B

Remarks : Short time between driving and testing. Pile A has driving shoe.

393
Cox et al (1992) Thomas Telford : "Large-Scale Pile Tests in Clay"
Pentre Last modified :

NUMLAY	NUMPIL	GWT	GAMPWP	SIGSRF	ZHOLE	QR.SOIL	QR.PILE
6	1	1.0	10.2	0.0	15.0	4	4

LAYER	DEPTH BOTTM	GAMMA EFF	TYPE ClSiSa	Q.CPT TIP	SPT N	OCR	CLAY SuTop	CLAY SuBot	CLAY TYP	CLAY St	CLAY Ip	SAND D50	SAND Dr	SAND PHI	CLC FLG	MISCELLANEOUS 1	2	3
1	1.0	19.2	1	0	0	0	100	100	3	0	25	0	0	0	0	0	0	0
2	15.0	9.0	1	0	0	0	35	35	3	0	12	0	0	0	0	0	0	0
3	25.0	8.5	1	0	0	0	36	62	3	0	14	0	0	0	0	0	0	0
4	35.0	8.5	1	0	0	0	62	88	3	0	18	0	0	0	0	0	0	0
5	48.0	9.15	1	0	0	0	88	120	3	0	23	0	0	0	0	0	0	0
6	60.0	12.33	1	0	0	0	120	150	3	0	16	0	0	0	0	0	0	0

PILE NO	OPN CLS	MAT TYP	DIAM TIP	TAPER degr	WALL TIP	TOTAL LNGTH	TIP PENTR	PLUG RATIO	WATER RATIO	-- MEASURED CAPACITIES -- COMPRSSN	TENSION	DAYS	TBF	MISCELLANEOUS 1	2	3
1	1	1	.762	0	.015	56.0	55.0	0.76	0.76	6030	0	44	0	0	0	0

394
Cox et al (1992) Thomas Telford : "Large-Scale Pile Tests in Clay"
Tilbrook Last modified : 7 Feb 2000 Plug & Water ratio set to 0.55

NUMLAY	NUMPIL	GWT	GAMPWP	SIGSRF	ZHOLE	QR.SOIL	QR.PILE
4	1	2.0	8.6	0.0	0.0	4	4

LAYER	DEPTH	GAMMA	TYPE	Q.CPT	SPT	OCR	-------- CLAY -------					----SAND----				CLC	MISCELLANEOUS		
	BOTTM	EFF	ClSiSa	TIP	N		SuTop	SuBot	TYP	St	Ip	D50	Dr	PHI	FLG		1	2	3
1	2.0	20.7	1	0	0	0	260	260	3	0	25	0	0	0	0		0	0	0
2	17.5	13.3	1	0	0	0	350	490	3	0	23	0	0	0	0		0	0	0
3	25.0	12.7	1	0	0	0	420	750	3	0	32	0	0	0	0		0	0	0
4	31.0	12.6	1	0	0	0	650	490	3	0	32	0	0	0	0		0	0	0

PILE	OPN	MAT	DIAM	TAPER	WALL	TOTAL	TIP	PLUG	WATER	-- MEASURED CAPACITIES --				MISCELLANEOUS		
NO	CLS	TYP	TIP	degr	TIP	LNGTH	PENTR	RATIO	RATIO	COMPRSSN	TENSION	DAYS	TBF	1	2	3
1	1	1	.762	0	.030	31.0	30.0	0.55	0.55	16131	0	130	0	0	0	0

\# 395
Clarke et al (1993) Tilbrook Grange additional tension test
Tilbrook Last modified : 7 Feb 2000 ZHOLE reduced from 2.5 to 1.6 m

NUMLAY	NUMPIL	GWT	GAMPWP	SIGSRF	ZHOLE	QR.SOIL	QR.PILE
4	1	2.0	8.6	0.0	1.6	4	4

LAYER	DEPTH	GAMMA	TYPE	Q.CPT	SPT	OCR	-------- CLAY -------					----SAND----				CLC	MISCELLANEOUS		
	BOTTM	EFF	ClSiSa	TIP	N		SuTop	SuBot	TYP	St	Ip	D50	Dr	PHI	FLG		1	2	3
1	2.0	20.7	1	0	0	0	260	260	3	0	25	0	0	0	0		0	0	0
2	17.5	13.3	1	0	0	0	350	490	3	0	23	0	0	0	0		0	0	0
3	25.0	12.7	1	0	0	0	420	750	3	0	32	0	0	0	0		0	0	0
4	31.0	12.6	1	0	0	0	650	490	3	0	32	0	0	0	0		0	0	0

PILE	OPN	MAT	DIAM	TAPER	WALL	TOTAL	TIP	PLUG	WATER	-- MEASURED CAPACITIES --				MISCELLANEOUS		
NO	CLS	TYP	TIP	degr	TIP	LNGTH	PENTR	RATIO	RATIO	COMPRSSN	TENSION	DAYS	TBF	1	2	3
1	1	1	.762	.0	.035	32.0	29.4	0.063	0.063?	0	16200	700?	0	0	0	0

\# 396
Bond & Jardine (1995) Geotechnique March OD = 0.102 m test piles
Canons Prk Last modified :

NUMLAY	NUMPIL	GWT	GAMPWP	SIGSRF	ZHOLE	QR.SOIL	QR.PILE
3	8	1.0	10.0	0.0	2.0	4	4

LAYER	DEPTH	GAMMA	TYPE	Q.CPT	SPT	OCR	-------- CLAY -------					----SAND----				CLC	MISCELLANEOUS		
	BOTTM	EFF	ClSiSa	TIP	N		SuTop	SuBot	TYP	St	Ip	D50	Dr	PHI	FLG		1	2	3
1	2.0	15.5	1	0	0	0	10	63	3	0	55	0	0	0	0		0	0	0
2	4.1	8.8	1	0	0	0	63	78	3	0	55	0	0	0	0		0	0	0
3	6.2	8.8	1	0	0	0	118	118	3	0	40	0	0	0	0		0	0	0

PILE	OPN	MAT	DIAM	TAPER	WALL	TOTAL	TIP	PLUG	WATER	-- MEASURED CAPACITIES --				MISCELLANEOUS			
NO	CLS	TYP	TIP	degr	TIP	LNGTH	PENTR	RATIO	RATIO	COMPRSSN	TENSION	DAYS	TBF	1	2	3	
1	2	1	.102	.0	.010	7.0	5.20	0.0	0.0	0	90	109	0	0	-1	0	CP0F
2	2	1	.102	.0	.010	7.0	5.28	0.0	0.0	68	0	79	0	0	-1	0	CP1S
3	2	1	.102	.0	.010	7.0	5.95	0.0	0.0	110	0	63	0	0	-1	0	CP2F
4	2	1	.102	.0	.010	7.0	5.87	0.0	0.0	78	0	2	0	0	-1	0	CP3FS
5	2	1	.102	.0	.010	7.0	6.16	0.0	0.0	0	119	20	0	0	-1	0	CP4F
6	2	1	.102	.0	.010	7.0	5.92	0.0	0.0	0	105	2	0	0	-1	0	CP5F
7	2	1	.102	.0	.010	7.0	5.80	0.0	0.0	0	105	2	0	0	-1	0	CP6D
8	1	1	.102	.0	.010	7.0	5.70	0.3	0.3	0	94	2	0	0	-1	0	CP7DO

\# 397
Powell et al. (2003), Powell and Uglow (1988), Bond and Jardine (1991,1995), Wardle et al. (1992)
Canons Park, Pile B and D

NUMLAY	NUMPIL	GWT	GAMPWP	SIGSRF	ZHOLE	QR.SOIL	QR.PILE
3	9	1.0	10	0.0	2.0	4	4

LAYER	DEPTH	GAMMA	TYPE	Q.CPT	SPT	OCR	-------- CLAY -------					----SAND----				CLC	MISCELLANEOUS		
	BOTTM	EFF	ClSiSa	TIP	N		SuTop	SuBot	TYP	St	Ip	D50	Dr	PHI	FLG		1	2	3
1	2.0	20.0	1	0	0	0	10	63	3	0	55	0	0	0	0		0	0	0
2	4.1	10.0	1	0	0	0	63	78	3	0	55	0	0	0	0		0	0	0
3	7.0	10.0	1	0	0	0	118	118	3	0	40	0	0	0	0		0	0	0

PILE	OPN	MAT	DIAM	TAPER	WALL	TOTAL	TIP	PLUG	WATER	-- MEASURED CAPACITIES --				MISCELLANEOUS		
NO	CLS	TYP	TIP	degr	TIP	LNGTH	PENTR	RATIO	RATIO	COMPRSSN	TENSION	DAYS	TBF	1	2	3
1	2	1	.168	.00	.0064	7.0	6.5	0.0	0.0	189	0	108	1	0	0	0 D
2	2	1	.168	.00	.0064	7.0	6.5	0.0	0.0	200	0	496	1	0	0	0 D
3	2	1	.168	.00	.0064	7.0	6.5	0.0	0.0	231	0	1130	1	0	0	0 D
4	2	1	.168	.00	.0064	7.0	6.5	0.0	0.0	291	0	6200	1	0	0	0 D
5	2	1	.168	.00	.0064	7.0	6.65	0.0	0.0	194	0	74	1	0	0	0 B
6	2	1	.168	.00	.0064	7.0	6.65	0.0	0.0	197	0	217	1	0	0	0 B
7	2	1	.168	.00	.0064	7.0	6.65	0.0	0.0	200	0	683	1	0	0	0 B
8	2	1	.168	.00	.0064	7.0	6.65	0.0	0.0	221	0	1312	1	0	0	0 B
9	2	1	.168	.00	.0064	7.0	6.65	0.0	0.0	274	0	6200	1	0	0	0 B

Failure loads for pile B are estimated from Table 1 in Wardle et al. (1992) and Powell et al (2003).
Because the ratios Cal/meas are approximately the same for pile B and D (load-settlement curves are given), it is assumed that the head loads given in Wardle et al. (1992) are failure loads.
"Good agreement" between Fig. 4 in Powell et al. (2003) and Tab. 1 in Wardle et al. (1992).
Addition to existing database #541 (#396 in this database).
GammaEff is here corrected compared to the original database.
Static tests after 0 and 1day have not been included in the database.

\# 398
Powell et al. (2003), Powell and Uglow (1988), Bond and Jardine (1991,1995), Wardle et al. (1992)
Canons Park, Pile A

NUMLAY	NUMPIL	GWT	GAMPWP	SIGSRF	ZHOLE	QR.SOIL	QR.PILE
3	6	1.0	10	0.0	3.0	4	4

LAYER	DEPTH	GAMMA	TYPE	Q.CPT	SPT	OCR	-------- CLAY -------					----SAND----				CLC	MISCELLANEOUS		
	BOTTM	EFF	ClSiSa	TIP	N		SuTop	SuBot	TYP	St	Ip	D50	Dr	PHI	FLG		1	2	3
1	2.0	20.0	1	0	0	0	10	63	3	0	55	0	0	0	0		0	0	0
2	4.1	10.0	1	0	0	0	63	78	3	0	55	0	0	0	0		0	0	0
3	7.0	10.0	1	0	0	0	118	118	3	0	40	0	0	0	0		0	0	0

PILE	OPN	MAT	DIAM	TAPER	WALL	TOTAL	TIP	PLUG	WATER	-- MEASURED CAPACITIES --				MISCELLANEOUS		
NO	CLS	TYP	TIP	degr	TIP	LNGTH	PENTR	RATIO	RATIO	COMPRSSN	TENSION	DAYS	TBF	1	2	3
1	2	1	.168	.00	.0064	7.0	6.63	0.0	0.0	159	0	31	1	0	0	0 A
2	2	1	.168	.00	.0064	7.0	6.63	0.0	0.0	161	0	134	1	0	0	0 A
3	2	1	.168	.00	.0064	7.0	6.63	0.0	0.0	163	0	248	1	0	0	0 A
4	2	1	.168	.00	.0064	7.0	6.63	0.0	0.0	165	0	525	1	0	0	0 A
5	2	1	.168	.00	.0064	7.0	6.63	0.0	0.0	184	0	1154	1	0	0	0 A
6	2	1	.168	.00	.0064	7.0	6.63	0.0	0.0	231	0	6200	1	0	0	0 A

Failure loads for pile A are estimated from Table 1 in Wardle et al. (1992) and Powell et al (2003).
Because the ratios Cal/meas are approximately the same for pile A, B and D (load-settlement curves are given), it is assumed that the head loads given in Wardle et al. (1992) are failure loads.

"Not that good agreement" between Fig. 4 in Powell et al. (2003) and Tab. 1 in Wardle et al. (1992).
Addition to existing database #541 (#396 in this database).
GammaEff is here corrected compared to the original database.
The static test after 0days have not been included in the database.

399
E.P. Heerema (1979) 24" steel piles in Boom clay OTC paper 3490
Kontich Last modified : 7 Feb 2000 Comp/Tens tests separated

NUMLAY	NUMPIL	GWT	GAMPWP	SIGSRF	ZHOLE	QR.SOIL	QR.PILE
4	4	1.0	10.0	10.0	1.5	2	3

LAYER	DEPTH	GAMMA	TYPE	Q.CPT	SPT	OCR	CLAY					SAND			CLC	MISCELLANEOUS		
	BOTTM	EFF	ClSiSa	TIP	N		SuTop	SuBot	TYP	St	Ip	D50	Dr	PHI	FLG	1	2	3
1	1.5	10.0	3	0	0	0	0	0	0	0	0	0	.5	0	0	0	0	0
2	4.0	9.0	1	1300	0	0	60	85	-1	0	52?	0	0	0	0	0	0	0
3	14.0	9.0	1	2800	0	0	120	200	-1	0	52?	0	0	0	0	0	0	0
4	25.0	9.0	1	0	0	0	200	225	-1	0	52?	0	0	0	0	0	0	0

PILE	OPN	MAT	DIAM	TAPER	WALL	TOTAL	TIP	PLUG	WATER	-- MEASURED CAPACITIES --				MISCELLANEOUS		
NO	CLS	TYP	TIP	degr	TIP	LNGTH	PENTR	RATIO	RATIO	COMPRSSN	TENSION	DAYS	TBF	1	2	3
1	1	1	.610	.0	.017?	23.5	23.5	0.9	0.9	4840	0	21	0	0	0	0
2	1	1	.610	.0	.017?	23.5	23.5	0.9	0.9	0	4100	26	0	0	0	0
3	1	1	.610	.0	.017?	20.1	20.1	1.0	1.0	3380	0	12	0	0	0	0
4	1	1	.610	.0	.017?	20.1	20.1	1.0	1.0	0	2420	16	0	0	0	0

Remark : Tension tests 4-5 days after compression, pile 2 has internal driving shoe
No soil data below 17 m in EPH paper,

400
Doyle & Pelletier (1985) Long Beach Beta Pile Tests
Long Beach Last modified : 8 Feb 2000 Use Pelletier & Doyle (1992) soil data

NUMLAY	NUMPIL	GWT	GAMPWP	SIGSRF	ZHOLE	QR.SOIL	QR.PILE
2	1	0.0	10.0	0.0	57.9	4	4

LAYER	DEPTH	GAMMA	TYPE	Q.CPT	SPT	OCR	CLAY					SAND			CLC	MISCELLANEOUS		
	BOTTM	EFF	ClSiSa	TIP	N		SuTop	SuBot	TYP	St	Ip	D50	Dr	PHI	FLG	1	2	3
1	57.9	9.86	1	0	0	0	230	365	3	0	16	0	0	0	0	0	0	0
2	80.51	9.07	1	0	0	0	365	365	3	0	16	0	0	0	0	0	0	0

PILE	OPN	MAT	DIAM	TAPER	WALL	TOTAL	TIP	PLUG	WATER	-- MEASURED CAPACITIES --				MISCELLANEOUS		
NO	CLS	TYP	TIP	degr	TIP	LNGTH	PENTR	RATIO	RATIO	COMPRSSN	TENSION	DAYS	TBF	1	2	3
1	1	1	.762	.0	.045	80.5	80.5	0.28?	0.28?	0	10710	60	0	0	0	0

401
Bustamante et al (1994) New Dehli, Vol. 2, p.685 Piles 5 & 6 average
Napoli Last modified :

NUMLAY	NUMPIL	GWT	GAMPWP	SIGSRF	ZHOLE	QR.SOIL	QR.PILE
3	1	0.0	10.0	0.0	3.0	3	3

LAYER	DEPTH	GAMMA	TYPE	Q.CPT	SPT	OCR	CLAY					SAND			CLC	MISCELLANEOUS		
	BOTTM	EFF	ClSiSa	TIP	N		SuTop	SuBot	TYP	St	Ip	D50	Dr	PHI	FLG	1	2	3
1	9.0	7.1	1	0	0	0	120	40	9	0	40	0	0	0	0	0	0	0
2	19.0	7.1	1	0	0	0	40	45	9	0	35	0	0	0	0	0	0	0
3	50.0	7.1	1	0	0	0	45	170	9	0	30	0	0	0	0	0	0	0

PILE	OPN	MAT	DIAM	TAPER	WALL	TOTAL	TIP	PLUG	WATER	-- MEASURED CAPACITIES --				MISCELLANEOUS		
NO	CLS	TYP	TIP	degr	TIP	LNGTH	PENTR	RATIO	RATIO	COMPRSSN	TENSION	DAYS	TBF	1	2	3
1	2	1	.356	.03	.007?	48.5	48.5	1.0	1.0	2348	0	0	0	0	0	0

Remark : OD = 0.406 m and 0.356 m, concrete filled, given capacity correspond to
measured skin friction + tip force in Su = 164 kPa clay.

402
Totani et al (1994) New Dehli ISSMFE Conf., Vol. 2, p.695
Livorno Last modified :

NUMLAY	NUMPIL	GWT	GAMPWP	SIGSRF	ZHOLE	QR.SOIL	QR.PILE
4	2	4.0	10.0	0.0	0.0	4	4

LAYER	DEPTH	GAMMA	TYPE	Q.CPT	SPT	OCR	CLAY					SAND			CLC	MISCELLANEOUS		
	BOTTM	EFF	ClSiSa	TIP	N		SuTop	SuBot	TYP	St	Ip	D50	Dr	PHI	FLG	1	2	3
1	4.0	15.5	1	0	0	0	30	30	0	0	70	0	0	0	0	0	0	0
2	20.0	5.5	1	0	0	0	20	30	0	0	60	0	0	0	0	0	0	0
3	51.0	9.5	1.9	0	0	0	30	120	0	0	14	0	0	0	0	0	0	0
4	60.0	10.0	3	7000	0	0	0	0	0	0	0	0	0	0	0	0	0	0

PILE	OPN	MAT	DIAM	TAPER	WALL	TOTAL	TIP	PLUG	WATER	-- MEASURED CAPACITIES --				MISCELLANEOUS		
NO	CLS	TYP	TIP	degr	TIP	LNGTH	PENTR	RATIO	RATIO	COMPRSSN	TENSION	DAYS	TBF	1	2	3
1	2	1	.457	.03	.007	50.0	50.0	0.0	0.0	2400	0	19	0	0	0	0
2	2	1	.457	.03	.007	57.0	57.0	1.0	1.0	4200	0	28	0	0	0	0

Remark : OD = 0.508 m and 0.457 m, concrete filled

403
Jardine & Lehane (1993) DoE Report OTH 93 401
Bothkennar Last modified : Dec 1999

NUMLAY	NUMPIL	GWT	GAMPWP	SIGSRF	ZHOLE	QR.SOIL	QR.PILE
3	5	1.0	10.0	0.0	1.1	4	4

LAYER	DEPTH	GAMMA	TYPE	Q.CPT	SPT	OCR	CLAY					SAND			CLC	MISCELLANEOUS		
	BOTTM	EFF	ClSiSa	TIP	N		SuTop	SuBot	TYP	St	Ip	D50	Dr	PHI	FLG	1	2	3
1	1.0	13.5	1	600	0	0	12	13	3	0	25	0	0	0	0	0	0	0
2	4.5	6.5	1	215	0	0	13	19	3	0	35	0	0	0	0	0	0	0
3	7.0	5.5	1	355	0	0	19	23	3	0	51	0	0	0	0	0	0	0

PILE	OPN	MAT	DIAM	TAPER	WALL	TOTAL	TIP	PLUG	WATER	-- MEASURED CAPACITIES --				MISCELLANEOUS			
NO	CLS	TYP	TIP	degr	TIP	LNGTH	PENTR	RATIO	RATIO	COMPRSSN	TENSION	DAYS	TBF	1	2	3	
1	2	1	.1016	.0	.0103	7.0	6.00	0.0	0.0	27.34	0	4	0	0	0	0	
2	2	1	.1016	.0	.0103	7.0	6.01	0.0	0.0	32.91	0	32	1	0	0	0	
3	2	1	.1016	.0	.0103	7.0	6.00	0.0	0.0	0.0	25.54	1	0	0	0	2	>>>> ???
4	2	1	.1016	.0	.0103	7.0	3.15	0.0	0.0	15.28	0	4	0	0	0	0	
5	2	1	.1016	.0	.0103	7.0	5.95	0.0	0.0	25.69	0	2	0	0	0	0	

Failure load computed from given average skin friction

404
Chan & Birrell (1998) OTC-8762/8767 Also NGI 514166-4 & 882016-4 and OTC-6513
West Delta Last modified : 17 Feb 2000

NUMLAY	NUMPIL	GWT	GAMPWP	SIGSRF	ZHOLE	QR.SOIL	QR.PILE
3	2	-16.2	12.72	0.0	0.0	4	4

LAYER	DEPTH	GAMMA	TYPE	Q.CPT	SPT	OCR	CLAY					SAND				CLC	MISCELLANEOUS		
	BOTTM	EFF	ClSiSa	TIP	N		SuTop	SuBot	TYP	St	Ip	D50	Dr	PHI	FLG		1	2	3
1	21	2.8	1	0	0	0	5	25	3	1.5	40	0	0	0	0		0	0	0
2	47	5.12	1	0	0	0	25	42	3	1.5	30	0	0	0	0		0	0	0
3	76	2.01?	1	0	0	0	42	72	3	2.3	55	0	0	0	0		0	0	0

PILE NO	OPN CLS	MAT TYP	DIAM TIP	TAPER degr	WALL TIP	TOTAL LNGTH	TIP PENTR	PLUG RATIO	WATER RATIO	-- MEASURED CAPACITIES -- COMPRSSN	TENSION	DAYS	TBF	MISCELLANEOUS 1	2	3
1	1	1	.762	.0	.0191	71.2	71.2	1.0?	0.0	0	5030	116	0	0	0	0
2	1	1	.762	.0	.0191	71.3	71.3	1.0?	0.0	0	4850	470	1	0	0	0

17 Feb 2000 : The above mudline forces are based upon OTC-8767, and verified against NGI 882016-4.

405
Leung et al. (1991), ASCE JOGE, Vol.117, No.4
Singapore Port

NUMLAY	NUMPIL	GWT	GAMPWP	SIGSRF	ZHOLE	QR.SOIL	QR.PILE
4	1	0.0	10	0.0	0.0	1	3

LAYER	DEPTH	GAMMA	TYPE	Q.CPT	SPT	OCR	CLAY					SAND				CLC	MISCELLANEOUS		
	BOTTM	EFF	ClSiSa	TIP	N		SuTop	SuBot	TYP	St	Ip	D50	Dr	PHI	FLG		1	2	3
1	6.6	7.0	1	0	14	0	90	90	3	0	0	0	0	0	0		0	0	0
2	22.8	6.0	1	0	0	0	20	20	3	0	0	0	0	0	0		0	0	0
3	27.2	6.0	1	0	8	0	10	10	3	0	0	0	0	0	0		0	0	0
4	29.2	11.0	3	0	144	0	0	0	0	0	0	0	0	0	0		0	0	0

PILE NO	OPN CLS	MAT TYP	DIAM TIP	TAPER degr	WALL TIP	TOTAL LNGTH	TIP PENTR	PLUG RATIO	WATER RATIO	-- MEASURED CAPACITIES -- COMPRSSN	TENSION	DAYS	TBF	MISCELLANEOUS 1	2	3
1	2	2	.331	0	.1655	30.0	28.0	0.0	0.0	2100	0	7	0	0	0	0

4th. layer is soft shale. Characterized as sand (information on SPT) in order to run the program.
GammaEff is estimated.
Ground water table assumed to be located at surface level.
Pile is a squared prec. concrete pile (sidelength 26cm). Diameter calculation based on surface area.
Load test for another pile is presented. It is not included in the database because failure was not reached due to the definition: Load corresponding to total deformations equal 10% of pile diameter.

406
Aarsleff (1997)
Aalborg havnefront byggefelt 1 & 2

NUMLAY	NUMPIL	GWT	GAMPWP	SIGSRF	ZHOLE	QR.SOIL	QR.PILE
4	2	1.3	10	0.0	10.0	0	4

LAYER	DEPTH	GAMMA	TYPE	Q.CPT	SPT	OCR	CLAY					SAND				CLC	MISCELLANEOUS		
	BOTTM	EFF	ClSiSa	TIP	N		SuTop	SuBot	TYP	St	Ip	D50	Dr	PHI	FLG		1	2	3
1	12.3	10.0	3	0	0	0	0	0	0	0	0	0	0	33	0		0	0	0
2	17.3	4.5	1	0	0	0	170	150	8	0	0	0	0	0	0		0	0	0
3	26.3	8.0	1	0	0	0	100	150	8	0	0	0	0	0	0		0	0	0
4	31.0	10.0	3	0	0	0	0	0	0	0	0	0	0	33	0		0	0	0

PILE NO	OPN CLS	MAT TYP	DIAM TIP	TAPER degr	WALL TIP	TOTAL LNGTH	TIP PENTR	PLUG RATIO	WATER RATIO	-- MEASURED CAPACITIES -- COMPRSSN	TENSION	DAYS	TBF	MISCELLANEOUS 1	2	3
1	2	2	.382	0	.191	32.0	30.8	0.0	0.0	2540	0	18	1	0	0	0
2	2	2	.446	0	.223	29.0	27.8	0.0	0.0	1800	0	18	1	0	0	0

Piles are squared prec. concrete piles (sidelengths 30cm and 35cm). Diameter calculation based on surface area.
The clay layer is really an organic layer. Here it is categorized as clay.
The triaxial friction angles are estimated.
The unit weight for the sand is estimated.
Both ML (maintained load) tests and CRP (Constant rate of penetration) are performed.

407
Egå Rensenanlæg Site 1 Pile(s) 1 - 1 Precast concrete
Egå Rensenanlæg, P4

NUMLAY	NUMPIL	GWT	GAMPWP	SIGSRF	ZHOLE	QR.SOIL	QR.PILE
4	1	0.3	10	0.0	0.0	2	3

LAYER	DEPTH	GAMMA	TYPE	Q.CPT	SPT	OCR	CLAY					SAND				CLC	MISCELLANEOUS		
	BOTTM	EFF	ClSiSa	TIP	N		SuTop	SuBot	TYP	St	Ip	D50	Dr	PHI	FLG		1	2	3
1	4.0	8.0	3	5800	0	0	0	0	0	0	0	0	0	0	1		0	0	0
2	15.5	5.0	1	0	0	0	100	100	8	2.5	0	0	0	0	1		0	0	0
3	16.5	11.5	3	30000	0	0	0	0	0	0	0	0	0	0	1		0	0	0
4	30.0	10.0	1	0	0	0	230	380	8	2	0	0	0	0	1		0	0	0

PILE NO	OPN CLS	MAT TYP	DIAM TIP	TAPER degr	WALL TIP	TOTAL LNGTH	TIP PENTR	PLUG RATIO	WATER RATIO	-- MEASURED CAPACITIES -- COMPRSSN	TENSION	DAYS	TBF	MISCELLANEOUS 1	2	3
1	2	2	.318	.00	.159	25.0	23.8	0.0	0.0	1400	0	27	1	0	0	0

Pile is a squared prec. concrete pile (sidelength 25cm). Diameter calculation based on surface area.
Dynamic tests have also been performed on the test site. Each pile has been tested several times.
Some uncertainty associated with the determination of especially sand parameters.

408
Egå Rensenanlæg Site 2 Pile(s) 1 - 1 Precast concrete
Egå Rensenanlæg, P10

NUMLAY	NUMPIL	GWT	GAMPWP	SIGSRF	ZHOLE	QR.SOIL	QR.PILE
4	1	0.4	10	0.0	0.0	2	3

LAYER	DEPTH	GAMMA	TYPE	Q.CPT	SPT	OCR	CLAY					SAND				CLC	MISCELLANEOUS		
	BOTTM	EFF	ClSiSa	TIP	N		SuTop	SuBot	TYP	St	Ip	D50	Dr	PHI	FLG		1	2	3
1	2.0	8.0	3	7000	0	0	0	0	0	0	0	0	0	0	0		0	0	0
2	14.0	4.4	1	0	0	0	60	60	8	0	0	0	0	0	1		0	0	0
3	15.5	11.5	3	35000	0	0	0	0	0	0	0	0	0	0	1		0	0	0
4	30.0	10.0	1	0	0	0	230	340	8	2.2	0	0	0	0	1		0	0	0

PILE NO	OPN CLS	MAT TYP	DIAM TIP	TAPER degr	WALL TIP	TOTAL LNGTH	TIP PENTR	PLUG RATIO	WATER RATIO	-- MEASURED CAPACITIES -- COMPRSSN	TENSION	DAYS	TBF	MISCELLANEOUS 1	2	3
1	2	2	.382	.00	.191	26.5	25.2	0.0	0.0	1671	0	28	1	0	0	0

Pile is a squared prec. concrete pile (sidelength 30cm). Diameter calculation based on surface area.
Dynamic tests have also been performed on the test site. Each pile has been tested several times.
Some uncertainty associated with the determination of especiall sand parameters.

409
Algade, Aalborg Site 1 Pile(s) 1 - 1 Precast concrete
Algade, Aalborg, P4

NUMLAY	NUMPIL	GWT	GAMPWP	SIGSRF	ZHOLE	QR.SOIL	QR.PILE
6	2	5.3	10	0.0	0.0	4	2

LAYER	DEPTH BOTTM	GAMMA EFF	TYPE ClSiSa	Q.CPT TIP	SPT N	OCR	CLAY SuTop	CLAY SuBot	CLAY TYP	CLAY St	CLAY Ip	SAND D50	SAND Dr	SAND PHI	CLC FLG	MISCELLANEOUS 1	MISCELLANEOUS 2	MISCELLANEOUS 3
1	4.5	15.0	1	0	0	0	25	25	8	0	0	0	0	0	0	0	0	0
2	5.3	15.6	1	0	0	0	120	120	8	1.7	0	0	0	0	0	0	0	0
3	6.0	9.0	3	0	5	0	0	0	0	0	0	0	0	0	0	0	0	0
4	8.5	9.0	1	0	0	0	110	110	8	2.0	0	0	0	0	0	0	0	0
5	11.0	9.2	1	0	0	0	170	170	8	3.0	0	0	0	0	0	0	0	0
6	13.5	9.2	1	0	0	0	225	225	8	3.8	0	0	0	0	0	0	0	0

PILE NO	OPN CLS	MAT TYP	DIAM TIP	TAPER degr	WALL TIP	TOTAL LNGTH	TIP PENTR	PLUG RATIO	WATER RATIO	-- MEASURED CAPACITIES -- COMPRSSN	TENSION	DAYS	TBF	MISCELLANEOUS 1 2 3
1	2	2	.255	.00	.1275	13.35	13.35	0.0	0.0	660	0	14	0	0 0 0
2	2	2	.255	.00	.1275	13.35	13.35	0.0	0.0	930	0	9778	1	1 0 0

Uncertainty on the pile length.
The first two layers are categorized as clay. They are actually a fill and a organic layer, respectively.
The strength and the weight of the fill layer are estimated.
It looks like the concrete crushed in connection with the tests after 9778 days.
Pile is a squared prec. concrete pile (sidelength 20cm). Diameter calculation based on surface area.
Soil profile based mainly on boring 2.
Load tests for other piles are presented. They are not included in the database because failure was not reached due to the definition: Load corresponding to total deformations equal 10% of pile diameter.

410
Motorvegbru Drammen Site 1 Pile(s) 1 - 2 Steel tube and HP-profile
Motorvegbru Drammen, Pile P1 og P2 (Åkse 16)

NUMLAY	NUMPIL	GWT	GAMPWP	SIGSRF	ZHOLE	QR.SOIL	QR.PILE
6	4	2.8	10	0.0	0.0	4	4

LAYER	DEPTH BOTTM	GAMMA EFF	TYPE ClSiSa	Q.CPT TIP	SPT N	OCR	CLAY SuTop	CLAY SuBot	CLAY TYP	CLAY St	CLAY Ip	SAND D50	SAND Dr	SAND PHI	CLC FLG	MISCELLANEOUS 1	MISCELLANEOUS 2	MISCELLANEOUS 3
1	2.8	18.0	3	5500	0	0	0	0	0	0	0	0	.52	36	0	0	0	0
2	15.5	8.0	3	5500	0	0	0	0	0	0	0	0	.52	36	0	0	0	0
3	30.0	9.0	1	0	0	0	40	110	4	0	0	0	0	0	0	0	0	0
4	32.5	9.0	1	0	0	0	110	110	4	0	0	0	0	0	0	0	0	0
5	36.0	9.0	1	0	0	0	85	85	4	0	0	0	0	0	0	0	0	0
6	40.0	9.0	1	0	0	0	110	110	4	0	0	0	0	0	0	0	0	0

PILE NO	OPN CLS	MAT TYP	DIAM TIP	TAPER degr	WALL TIP	TOTAL LNGTH	TIP PENTR	PLUG RATIO	WATER RATIO	-- MEASURED CAPACITIES -- COMPRSSN	TENSION	DAYS	TBF	MISCELLANEOUS 1 2 3
1	1	1	.813	.00	.0125	36.0	35.0	0.21	1.0	2150	0	16	1	0 0 0 P1-16
2	1	1	.813	.00	.0125	36.0	35.0	0.21	1.0	2800	0	140	1	0 0 0 P1-16
3	2	1	.400	.00	.200	39.0	35.0	0.0	0.0	1350	0	14	1	0 0 0 P2-16
4	2	1	.400	.00	.200	39.0	35.0	0.0	0.0	2210	0	141	1	0 0 0 P2-16

The piles have also been dynamic tested.
Static tests after 1day have not been included in the database.
Pile no.2 is a steel pile with H-profile. This profile is equated with a "solid/closed" circular profile.
When calculating the water ratio, the water level inside the pile is assumed to correspond to the level of the ground surface.
Some uncertainty associated with the determination of the plug ratio.

411
Drammen Stasjon Site 1 Pile(s) 1 - 2 Precast concrete
Drammen Stasjon, Pæle P1, P2

NUMLAY	NUMPIL	GWT	GAMPWP	SIGSRF	ZHOLE	QR.SOIL	QR.PILE
5	3	1.0	10	0.0	0.0	1	3

LAYER	DEPTH BOTTM	GAMMA EFF	TYPE ClSiSa	Q.CPT TIP	SPT N	OCR	CLAY SuTop	CLAY SuBot	CLAY TYP	CLAY St	CLAY Ip	SAND D50	SAND Dr	SAND PHI	CLC FLG	MISCELLANEOUS 1	MISCELLANEOUS 2	MISCELLANEOUS 3
1	1.0	19.0	3	2000	0	0	0	0	0	0	0	.80	0	0	0	0	0	0
2	11.0	9.0	3	2000	0	0	0	0	0	0	0	.80	0	0	0	0	0	0
3	14.1	10.3	3	2000	0	0	0	0	0	0	0	.13	0	0	0	0	0	0
4	25.0	8.7	1	0	0	0	50	75	8	8.3	22	0	0	0	0	0	0	0
5	50.0	9.0	1	0	0	0	75	75	8	0	22	0	0	0	0	0	0	0

PILE NO	OPN CLS	MAT TYP	DIAM TIP	TAPER degr	WALL TIP	TOTAL LNGTH	TIP PENTR	PLUG RATIO	WATER RATIO	-- MEASURED CAPACITIES -- COMPRSSN	TENSION	DAYS	TBF	MISCELLANEOUS 1 2 3
1	2	2	.344	.00	.172	50.6	49.0	0.0	0.0	1100	0	21	0	0 0 0
2	2	2	.344	.00	.172	50.6	49.0	0.0	0.0	1700	0	153	1	1 0 0
3	2	2	.344	.00	.172	31.5	30.0	0.0	0.0	960	0	24	0	0 0 0

Boring 6 and "tryksondering" are ended 22m and app. 40m under surface level. Clay anticipated all way down to pile tip. Characteristica based on reports, borings and "tryksonderinger".
The sand is loose and characteristica for the layers are based on reports and other borings.
The top 9m is sandfill. GammaEff is estimated.
Piles are sq. prec. concrete pile (sidelength 27cm). Diameter calculation based on surface area.

412
Flaate (1972)
Nitsund test site, Pile I and II

NUMLAY	NUMPIL	GWT	GAMPWP	SIGSRF	ZHOLE	QR.SOIL	QR.PILE
2	10	0.0	10	0.0	0.0	4	4

LAYER	DEPTH BOTTM	GAMMA EFF	TYPE ClSiSa	Q.CPT TIP	SPT N	OCR	CLAY SuTop	CLAY SuBot	CLAY TYP	CLAY St	CLAY Ip	SAND D50	SAND Dr	SAND PHI	CLC FLG	MISCELLANEOUS 1	MISCELLANEOUS 2	MISCELLANEOUS 3
1	3.8	10.1	1	0	0	0	80	46	8	4	16	0	0	0	0	0	0	0
2	14.0	9.7	1	0	0	0	46	46	8	5	16	0	0	0	0	0	0	0

PILE NO	OPN CLS	MAT TYP	DIAM TIP	TAPER degr	WALL TIP	TOTAL LNGTH	TIP PENTR	PLUG RATIO	WATER RATIO	-- MEASURED CAPACITIES -- COMPRSSN	TENSION	DAYS	TBF	MISCELLANEOUS 1 2 3
1	2	3	.180	.47	.09	11.9	11.7	0.0	0.0	243	0	32	0	0 0 0 I
2	2	3	.180	.47	.09	11.9	11.7	0.0	0.0	321	0	207	1	0 0 0 I
3	2	3	.180	.47	.09	11.9	11.7	0.0	0.0	336	0	357	1	0 0 0 I
4	2	3	.180	.47	.09	11.9	11.7	0.0	0.0	350	0	641	1	0 0 0 I
5	2	3	.180	.47	.09	11.9	11.7	0.0	0.0	350	0	1043	1	1 0 0 I
6	2	3	.175	.32	.0875	13.9	13.7	0.0	0.0	228	0	34	0	0 0 0 II
7	2	3	.175	.32	.0875	13.9	13.7	0.0	0.0	314	0	209	1	0 0 0 II
8	2	3	.175	.32	.0875	13.9	13.7	0.0	0.0	343	0	357	1	0 0 0 II
9	2	3	.175	.32	.0875	13.9	13.7	0.0	0.0	378	0	637	1	0 0 0 II
10	2	3	.175	.32	.0875	13.9	13.7	0.0	0.0	414	0	1023	1	0 0 0 II

Ground water table assumed to be located at surface level.
The boring is stopped in depth of 10m. The second clay layer is extended to the depth of 14m.
It is possible that some piles also are included in the Flaate and Selnes (1977) database (#301-#322).
Though it does not seem like that. The pile, soil and test results do not coincide. It is still postula-
ted because there is some uncertainty associated with pile, soil and test conditions, i.e. notice the
differences in ranking (This case compared to #301-#322).

\# 413
Bergdahl and Hult (1981)
Skå-Edeby, Pile A-D

NUMLAY	NUMPIL	GWT	GAMPWP	SIGSRF	ZHOLE	QR.SOIL	QR.PILE
2	25	0.0	10	0.0	0.0	4	4

LAYER	DEPTH BOTTM	GAMMA EFF	TYPE ClSiSa	Q.CPT TIP	SPT N	OCR	CLAY SuTop	CLAY SuBot	CLAY TYP	CLAY St	CLAY Ip	SAND D50	SAND Dr	SAND PHI	CLC FLG	MISCELLANEOUS 1	2	3
1	5.0	4.0	1	0	0	0	9	9	8	9	60	0	0	0	0	0	0	0
2	15.6	6.0	1	0	0	0	9	24	8	9	31	0	0	0	0	0	0	0

PILE NO	OPN CLS	MAT TYP	DIAM TIP	TAPER degr	WALL TIP	TOTAL LNGTH	TIP PENTR	PLUG RATIO	WATER RATIO	-- MEASURED CAPACITIES -- COMPRSSN	TENSION	DAYS	TBF	MISCELLANEOUS 1 2 3
1	2	3	.127	.0	.0635	15.5	15.0	0.0	0.0	48	0	30	0	0 0 0 A
2	2	3	.127	.0	.0635	15.5	15.0	0.0	0.0	58	0	75	1	0 0 0 A
3	2	3	.127	.0	.0635	15.5	15.3	0.0	0.0	34	0	42	0	0 0 0 A
4	2	3	.127	.0	.0635	15.5	15.3	0.0	0.0	55	0	456	1	0 0 0 A
5	2	3	.127	.0	.0635	15.5	15.3	0.0	0.0	48	0	1116	1	0 0 0 A
6	2	3	.127	.0	.0635	15.5	15.0	0.0	0.0	52	0	39	0	0 0 0 B
7	2	3	.127	.0	.0635	15.5	15.0	0.0	0.0	64	0	75	1	0 0 0 B
8	2	3	.127	.0	.0635	15.5	15.3	0.0	0.0	36	0	42	0	0 0 0 B
9	2	3	.127	.0	.0635	15.5	15.3	0.0	0.0	56	0	456	1	0 0 0 B
10	2	3	.127	.0	.0635	15.5	15.3	0.0	0.0	54	0	1116	1	0 0 0 B
11	2	3	.127	.0	.0635	15.5	15.0	0.0	0.0	54	0	30	0	0 0 0 C
12	2	3	.127	.0	.0635	15.5	15.0	0.0	0.0	70	0	75	1	0 0 0 C
13	2	3	.127	.0	.0635	15.5	15.3	0.0	0.0	41	0	42	0	0 0 0 C
14	2	3	.127	.0	.0635	15.5	15.3	0.0	0.0	48	0	96	1	0 0 0 C
15	2	3	.127	.0	.0635	15.5	15.3	0.0	0.0	60	0	456	1	0 0 0 C
16	2	3	.127	.0	.0635	15.5	15.3	0.0	0.0	62	0	1116	1	0 0 0 C
17	2	3	.127	.0	.0635	15.5	15.0	0.0	0.0	52	0	30	0	0 0 0 D
18	2	3	.127	.0	.0635	15.5	15.0	0.0	0.0	65	0	75	1	0 0 0 D
19	2	3	.127	.0	.0635	15.5	15.3	0.0	0.0	42	0	96	0	0 0 0 D
20	2	3	.127	.0	.0635	15.5	15.3	0.0	0.0	47	0	171	1	0 0 0 D
21	2	3	.127	.0	.0635	15.5	15.3	0.0	0.0	49	0	456	1	0 0 0 D
22	2	3	.127	.0	.0635	15.5	15.3	0.0	0.0	51	0	1116	1	0 0 0 D
23	2	3	.127	.0	.0635	15.5	14.5	0.0	0.0	56	0	75	0	0 0 0 E
24	2	3	.127	.0	.0635	15.5	14.5	0.0	0.0	66	0	216	1	0 0 0 E
25	2	3	.127	.0	.0635	15.5	14.5	0.0	0.0	63	0	906	1	0 0 0 E

Ground water table assumed to be located at surface level.
Some of the test piles are loaded in different ways. Furthermore, different test procedures are used
during load tests of a single pile.
Failure loads are ultimate loads.
Four of the piles (A-D) were driven further 0,2m after the second load test. Hereafter, the pile is
treated as a new pile. That is, the effect of former tests are negligible.
Uncertainty in the determination of the time for testing.
Piles are squared wood piles (sidelength 10cm). Diameter calculations based on surface area.
It is assumed that the piles are loaded in compression.

\# 414
Fynsværket Site 1   Pile(s) 1 - 1   Precast concrete
Fynsværket, P1

NUMLAY	NUMPIL	GWT	GAMPWP	SIGSRF	ZHOLE	QR.SOIL	QR.PILE
4	3	0.0	10	0.0	0.0	0	2

LAYER	DEPTH BOTTM	GAMMA EFF	TYPE ClSiSa	Q.CPT TIP	SPT N	OCR	CLAY SuTop	CLAY SuBot	CLAY TYP	CLAY St	CLAY Ip	SAND D50	SAND Dr	SAND PHI	CLC FLG	MISCELLANEOUS 1	2	3
1	1.9	11.0	1	0	0	0	50	50	8	3.3	0	0	0	0	0	0	0	0
2	9.6	10.3	1	0	0	0	50	70	8	6.0	0	0	0	0	0	0	0	0
3	15.2	10.5	1	0	0	0	110	190	8	12.2	0	0	0	0	0	0	0	0
4	29.1	13.0	1	0	0	0	240	715	8	2.0	0	0	0	0	0	0	0	0

PILE NO	OPN CLS	MAT TYP	DIAM TIP	TAPER degr	WALL TIP	TOTAL LNGTH	TIP PENTR	PLUG RATIO	WATER RATIO	-- MEASURED CAPACITIES -- COMPRSSN	TENSION	DAYS	TBF	MISCELLANEOUS 1 2 3
1	2	2	.382	.00	.191	29.0	28.7	0.0	0.0	1140	0	50	0	0 0 0
2	2	2	.382	.00	.191	29.0	28.7	0.0	0.0	1149	0	52	1	0 0 0
3	2	2	.382	.00	.191	29.0	28.7	0.0	0.0	1219	0	73	1	0 0 0

Capacities determined by static tests after 52 and 73 days, respectively, are reduced 14% because
the loading rate in both cases was "fast". For more details see geotechnical report.
Pile is a squared prec. concrete pile (sidelength 30cm). Diameter calculation based on surface area.
Excavation is taken into account (discussed in geotechnical report). "surface" in kote -0,4.
The boring is stopped app. 26m under the surface level. It is anticipated that the soil in depth
between 26m and 29.1m is the same as the soil in the depth of 26m.
Dynamic tests have also been performed in the area. Failure were not reached.

****
DATA BASE LOG
****

Date	By	Description
09.08.2004	AA	All piles from the different old databases collected. Taken from Clausen and Aas (2000).
09.08.2004	AA	Old and new database collected.
09.08.2004	AA	#364 Cowden. Data from old database substituted with data from additinal database.
07.03.2005	AA	PSG Domicil kbh. moved to to sand database.
09.05.2005	AA	Taper changed in connection with case #412 Nitsund.
09.08.2005	AA	Qr.soil changed to 4 for Nitsund

Appendix G:
Calculated results

The following pages present an output file generated by the program PILCAP based on the input file shown in Appendix F: AAU and NGI data.

In the output file the text shown on the top of each column should be interpreted in the following way (taken directly from Clausen and Aas, 2000):

SITE NO PILE NO	Site number and pile number in the database.
LOCATION NAME	Short mnemonic name taken from the input file for each different site.
DIAM M	Pile outer diameter, m.
MAT O/C	Pile material type (steel, concrete or timber) and code for pile driven open-ended (o) or closed-ended (c).
TIP SOIL	Type of soil at the pile tip, sand or clay.
TIME DAYS	Number of days between end of pile driving and testing.
CMP TNS	Indicator for pile tested in compression or tension. When both a compression and a tension test was carried out on the same pile, and at the same depth, this is included as two pile tests in the database.
MEASURED (kN) TCOR:N TCOR:Y	Measured pile capacity in kN. TCOR:N value has not been time corrected, the TCOR:Y value has been time corrected. A "+" symbol after the value flags that this pile test did not reach failure, i.e. the actual capacity is higher than the value given.
SHAFT SAND%	Length of pile located in sand layers / total length times 100.
SAND CLAY	Codes "s" and "c" flag that the skin friction mainly comes from sand and clay layers, respectively.
SIGV SIGV	Average vertical stress, same value for sand and clay.
NqCPT Su	Ratio q_{CPT} / σ'_z at pile tip for sand, average undrained shear strength along the shaft for piles in clay.
SPT Ip	Average SPT (blows/ft) along the shaft for sand, average plasticity index for clay.
Dr Su/SIGV	Average relative density for sand, average S_u / σ'_z ratio for clay.
PHI OCR	Average angle of internal friction for sand, average overconsolidation ratio for clay.

CALCD TAUSK	Calculated average skin friction (kPa) along pile shaft.
CALCULATED (kN) TOTAL SKN% WGH% TIP%	Calculated total pile capacity (kN) followed by skin friction, pile/plug weight and tip resistance in % of the total capacity. A positive value acts in the same direction as the skin friction force. Total stresses are used. A "*" symbol after the tip value flags the pile tip is coring according to the calculated results.
CALC MEAS	Ratio between calculated and measured pile capacity.

Program PILCAP Version 05 Jan 2001 Time = 00 MAY 2000 16:57:46

PILES IN CLAY CLAY DATABASE - ALL PILES IN OLD AND NEW DATABASE 09 MAY 20

SAND SKIN FRICTION BY METHOD : NGI 1999 SOIL DATA QUALITY RATING = 0 CORRECTIONS INCLUDED
CLAY SKIN FRICTION BY METHOD : NGI 1999 PILE DATA QUALITY RATING = 0 Su : Yes Time : Yes

SITE No / PILE No	LOCATION NAME	DIAM M	MAT O/C	PENTR M	TIP SOIL	TIME DAYS	CMP TNS	MEASURED (kN) TCOR:N	MEASURED (kN) TCOR:Y	SHAFT SAND%	SHAFT CLAY	SIGV SIGV	NqCPT Su	SPT Ip	Dr Su/SIGV	PHI OCR	CALCD TAUSKN	CALCULATED (kN) TOTAL	SKN%	WGH%	TIP%	CALC MEAS
301.01	F&S 1-1	0.335	T C	14.10	CLAY	90.0	CMP	392	395	0	C	76.5	25.5	12	0.33	3.6	11.6	199	87	-6	19	0.50
302.01	F&S 2-2	0.252	T C	13.00	CLAY	90.0	CMP	265	268	0	C	86.6	21.8	19	0.25	1.3	18.1	205	91	-3	12	0.76
303.01	F&S 3-3	0.302	T C	11.70	CLAY	90.0	CMP	157	158	0	C	47.2	22.1	14	0.47	4.8	13.6	170	89	-5	16	1.08
304.01	F&S 4-5	0.254	T C	14.60	CLAY	90.0	CMP	196	198	0	C	60.1	26.7	9	0.44	4.6	11.7	153	89	-5	16	0.77
304.02	F&S 4-5	0.252	T C	11.60	CLAY	90.0	CMP	167	168	0	C	49.0	24.1	9	0.49	5.3	11.6	121	88	-4	16	0.72
305.01	F&S 6-8	0.161	T C	17.50	CLAY	90.0	CMP	226	227	0	C	90.9	26.0	43	0.29	2.4	22.0	206	95	-2	7	0.91
305.02	F&S 6-8	0.189	T C	14.40	CLAY	90.0	CMP	255	256	0	C	73.3	22.5	43	0.31	2.7	18.3	167	93	-2	9	0.65
305.03	F&S 6-8	0.192	T C	15.00	CLAY	90.0	CMP	265	266	0	C	75.5	22.9	43	0.30	2.7	18.7	181	93	-2	9	0.68
306.01	F&S 9-12	0.161	T C	11.90	CLAY	90.0	CMP	78	78	0	C	37.9	13.2	75	0.35	2.2	10.0	66	91	-3	12	0.85
306.02	F&S 9-12	0.176	T C	13.80	CLAY	90.0	CMP	113	113	0	C	42.0	14.4	75	0.34	2.1	11.0	91	92	-3	11	0.80
306.03	F&S 9-12	0.197	T C	15.90	CLAY	90.0	CMP	123	124	0	C	46.8	15.9	75	0.34	2.0	12.1	128	93	-3	10	1.04
306.04	F&S 9-12	0.197	T C	17.30	CLAY	90.0	CMP	123	124	0	C	50.0	16.8	75	0.34	2.0	12.9	147	94	-3	9	1.19
307.01	F&S 13-19	0.176	T C	8.10	CLAY	90.0	CMP	49	49	0	C	31.0	12.1	44	0.39	3.7	8.7	44	90	-4	14	0.89
307.02	F&S 13-19	0.241	T C	9.60	CLAY	90.0	CMP	96	96	0	C	37.2	13.5	44	0.36	3.3	10.0	83	88	-5	17	0.86
307.03	F&S 13-19	0.214	T C	11.50	CLAY	90.0	CMP	98	98	0	C	43.4	14.9	44	0.34	3.0	11.4	97	91	-4	13	0.98
307.04	F&S 13-19	0.206	T C	11.60	CLAY	90.0	CMP	108	109	0	C	43.6	14.9	44	0.34	3.0	11.4	93	92	-4	12	0.86
307.05	F&S 13-19	0.231	T C	12.70	CLAY	90.0	CMP	142	143	0	C	47.8	15.9	44	0.33	2.9	12.3	125	91	-4	13	0.87
307.06	F&S 13-19	0.204	T C	7.70	CLAY	90.0	CMP	49	49	0	C	29.9	11.8	44	0.39	3.7	8.5	48	87	-5	18	0.98
307.07	F&S 13-19	0.186	T C	9.40	CLAY	90.0	CMP	54	54	0	C	35.7	13.1	44	0.37	3.4	9.7	59	91	-4	13	1.08

Program PILCAP Version 05 Jan 2001 Time = 00 MAY 2000 16:57:46

PILES IN CLAY CLAY DATABASE - ALL PILES IN OLD AND NEW DATABASE 09 MAY 20

SAND SKIN FRICTION BY METHOD : NGI 1999 SOIL DATA QUALITY RATING = 0 CORRECTIONS INCLUDED
CLAY SKIN FRICTION BY METHOD : NGI 1999 PILE DATA QUALITY RATING = 0 Su : Yes Time : Yes

SITE No / PILE No	LOCATION NAME	DIAM M	MAT O/C	PENTR M	TIP SOIL	TIME DAYS	CMP TNS	MEASURED (kN) TCOR:N	MEASURED (kN) TCOR:Y	SHAFT SAND%	SHAFT SAND	SHAFT CLAY	SIGV SIGV	NqCPT Su	SPT Ip	Dr Su/SIGV	PHI OCR	CALCD TAUSKN	CALCULATED (kN) TOTAL	CALCULATED (kN) SKN%	CALCULATED (kN) WGH%	CALCULATED (kN) TIP%	CALC MEAS
308.01	F&S 20-22	0.163	T C	8.00	CLAY	90.0	CMP	39	39	0	C		24.1	8.4	54	0.35	2.1	6.4	30	88	-5	17	0.75
308.02	F&S 20-22	0.187	T C	10.00	CLAY	90.0	CMP	69	69	0	C		29.0	9.9	54	0.34	2.0	7.6	49	90	-5	15	0.71
308.03	F&S 20-22	0.230	T C	12.00	CLAY	90.0	CMP	88	88	0	C		34.2	11.5	54	0.34	1.9	8.9	85	91	-5	14	0.96
309.01	F&S 23-26	0.260	T C	13.80	CLAY	90.0	CMP	137	138	0	C		23.2	18.8	73	0.81	6.9	10.8	134	91	-5	14	0.98
309.02	F&S 23-26	0.266	T C	10.20	CLAY	90.0	CMP	69	69	0	C		17.8	15.8	73	0.89	7.9	9.1	90	87	-6	19	1.30
309.03	F&S 23-26	0.311	T C	14.10	CLAY	90.0	CMP	177	178	0	C		24.0	19.2	73	0.80	6.8	11.1	172	89	-6	17	0.97
309.04	F&S 23-26	0.245	T C	10.10	CLAY	90.0	CMP	62	62	0	C		17.3	15.5	73	0.90	8.0	9.0	79	88	-6	18	1.26
310.01	F&S 27-30	0.264	T C	24.20	CLAY	90.0	CMP	441	448	0	C		122.2	29.9	16	0.24	1.1	20.9	448	94	-3	9	1.00
310.02	F&S 27-30	0.272	T C	24.20	CLAY	90.0	CMP	491	498	0	C		121.4	29.7	16	0.24	1.1	20.8	460	93	-3	10	0.92
310.03	F&S 27-30	0.285	T C	24.20	CLAY	90.0	CMP	540	548	0	C		120.2	29.4	16	0.24	1.1	20.6	478	93	-3	10	0.87
310.04	F&S 27-30	0.285	T C	24.20	CLAY	90.0	CMP	589	598	0	C		120.2	29.4	16	0.24	1.1	20.6	478	93	-3	10	0.80
311.01	F&S 31	0.263	T C	17.10	CLAY	90.0	CMP	343	345	0	C		91.5	54.3	12	0.59	7.1	30.2	453	94	-2	8	1.31
312.01	F&S 32	0.296	T C	12.70	CLAY	90.0	CMP	206	207	0	C		34.2	18.3	20	0.53	4.6	11.6	155	88	-5	17	0.75
313.01	F&S 33	0.253	T C	15.50	CLAY	90.0	CMP	441	444	0	C		70.2	70.0	12	1.00	11.2	37.9	495	94	-1	7	1.12
314.01	F&S 34	0.233	T C	11.50	CLAY	90.0	CMP	226	227	0	C		56.9	70.3	13	1.23	13.4	38.4	347	93	-1	8	1.53
315.01	F&S 35	0.284	T C	10.00	CLAY	90.0	CMP	196	197	0	C		43.1	50.2	8	1.16	12.5	26.1	262	89	-2	13	1.33
316.01	F&S 36	0.219	T C	10.00	CLAY	90.0	CMP	196	197	0	C		74.0	34.9	14	0.47	5.6	21.2	162	90	-2	12	0.82
317.01	F&S 37	0.332	T C	9.40	CLAY	90.0	CMP	191	192	0	C		49.2	28.0	31	0.57	6.3	17.7	206	84	-4	20	1.08
318.01	F&S 38-39	0.260	C C	14.30	CLAY	90.0	CMP	255	257	0	C		87.2	24.9	34	0.29	2.4	21.2	265	93	-7	14	1.03

Program PILCAP Version 05 Jan 2001 Time = 00 MAY 2000 16:57:46

PILES IN CLAY CLAY DATABASE - ALL PILES IN OLD AND NEW DATABASE 09 MAY 20

SAND SKIN FRICTION BY METHOD : NGI 1999 SOIL DATA QUALITY RATING = 0 CORRECTIONS INCLUDED
CLAY SKIN FRICTION BY METHOD : NGI 1999 PILE DATA QUALITY RATING = 0 Su : Yes Time : Yes

SITE No / PILE No	LOCATION NAME	DIAM M	MAT O/C	PENTR M	TIP SOIL	TIME DAYS	CMP TNS	MEASURED (kN) TCOR:N	MEASURED (kN) TCOR:Y	SHAFT SAND%	SHAFT CLAY	SIGV SIGV	NqCPT Su	SPT Ip	Dr Su/SIGV	PHI OCR	CALCD TAUSKN	CALCULATED (kN) TOTAL	SKN%	WGH%	TIP%	CALC MEAS
318.02	F&S 38-39	0.260	C C	14.30	CLAY	90.0	CMP	235	237	0	C	87.2	24.9	34	0.29	2.4	21.2	265	93	-7	14	1.12
319.01	F&S 40-41	0.470	C C	22.50	CLAY	90.0	CMP	863	867	0	C	58.5	44.5	27	0.76	7.1	25.5	913	93	-11	18	1.05
319.02	F&S 40-41	0.470	C C	22.50	CLAY	90.0	CMP	1069	1075	0	C	58.5	44.5	27	0.76	7.1	25.5	913	93	-11	18	0.85
320.01	F&S 42	0.270	S C	13.40	CLAY	90.0	CMP	206	207	0	C	79.1	23.5	32	0.30	2.6	19.5	249	89	-3	14	1.20
321.01	F&S 43	0.305	S C	13.50	CLAY	90.0	CMP	697	701	0	C	137.7	140.7	14	1.02	11.0	78.0	1131	89	-1	12	1.61
322.01	F&S 44	0.305	S C	5.50	CLAY	90.0	CMP	216	217	0	C	42.9	29.8	45	0.69	7.8	18.3	126	76	-3	27	0.58
323.01	S&R (1984)	0.762	S O	26.20	CLAY	0.0	CMP	1567	0	0	C	144.0	34.6	25	0.24	1.0	33.1	1727	94	-20	26	1.10
324.01	S&R (1984)	0.457	S O	27.20	CLAY	0.0	CMP	976	0	0	C	147.6	35.4	25	0.24	1.0	33.9	1093	96	-12	16	1.12
325.01	S&R (1984)	0.610	S O	25.40	CLAY	0.0	CMP	1269	0	0	C	142.2	34.3	25	0.24	1.0	32.7	1272	95	-17	22	1.00
326.01	S&R (1984)	0.356	S O	57.40	CLAY	0.0	CMP	1965	0	0	C	448.2	108.5	25	0.24	1.0	103.1	1805	97	-9	12	0.92
327.01	S&R (1984)	0.356	S O	85.90	CLAY	0.0	CMP	2368	0	0	C	718.2	172.4	25	0.24	1.0	165.2	2330	97	-11	14	0.98
328.01	S&R (1984)	0.305	S O	43.90	CLAY	0.0	CMP	1313	0	0	C	162.4	39.5	25	0.24	1.1	37.4	1590	99	-6	7	1.21
329.01	S&R (1984)	0.610	S O	96.00	CLAY	0.0	CMP	8516	0	0	C	355.2	85.7	25	0.24	1.0	81.7	15190	99	-5	6	1.78
330.01	S&R (1984)	0.610	S O	73.80	CLAY	0.0	CMP	7080	0	0	C	273.1	70.1	25	0.26	1.1	63.1	9074	98	-7	9	1.28
331.01	S&R (1984)	0.767	S O	83.60	CLAY	0.0	CMP	11276	0	0	C	650.7	176.2	25	0.27	1.1	152.4	8748	95	-13	18	0.78
332.01	S&R (1984)	0.325	S O	66.40	CLAY	0.0	CMP	2205	0	0	C	222.4	62.6	25	0.28	1.2	52.5	3595	99	-4	5	1.63
333.01	S&R (1984)	0.325	S O	32.30	CLAY	0.0	CMP	971	0	0	C	153.5	46.3	25	0.30	1.4	37.0	1185	97	-7	10	1.22
334.01	S&R (1984)	0.325	S O	45.70	CLAY	0.0	CMP	1097	0	0	C	148.5	53.7	25	0.36	1.6	37.8	1803	98	-6	8	1.64
335.01	S&R (1984)	0.330	S O	29.00	CLAY	0.0	CMP	1252	0	0	C	104.4	39.9	25	0.38	2.5	27.2	849	96	-8	12	0.68

Program PILCAP Version 05 Jan 2001 Time = 00 MAY 2000 16:57:46

PILES IN CLAY CLAY DATABASE - ALL PILES IN OLD AND NEW DATABASE 09 MAY 20

SAND SKIN FRICTION BY METHOD : NGI 1999 SOIL DATA QUALITY RATING = 0 CORRECTIONS INCLUDED
CLAY SKIN FRICTION BY METHOD : NGI 1999 PILE DATA QUALITY RATING = 0 Su : Yes Time : Yes

SITE No / PILE No	LOCATION NAME	DIAM M	MAT O/C	PENTR M	TIP SOIL	TIME DAYS	CMP TNS	MEASURED (kN) TCOR:N	TCOR:Y	SHAFT SAND%	SAND CLAY	SIGV SIGV	NqCPT Su	SPT Ip	Dr Su/SIGV	PHI OCR	CALCD TAUSKN	CALCULATED (kN) TOTAL	SKN%	WGH%	TIP%	CALC MEAS
336.01	S&R (1984)	0.325	S O	19.30	CLAY	0.0	CMP	637	0	0	C	112.1	45.7	25	0.41	1.9	30.1	451	93	-11	18	0.71
337.01	S&R (1984)	0.325	S O	18.30	CLAY	0.0	CMP	638	0	0	C	51.2	33.1	25	0.65	5.5	17.5	352	93	-11	18	0.55
338.01	S&R (1984)	0.610	S O	48.20	CLAY	0.0	CMP	3802	0	0	C	151.8	65.1	25	0.43	2.8	41.2	3978	96	-9	13	1.05
339.01	S&R (1984)	0.114	S O	11.60	CLAY	0.0	CMP	59	0	0	C	44.1	21.9	25	0.50	4.7	13.1	56	97	-6	9	0.95
340.01	S&R (1984)	0.168	S O	12.20	CLAY	0.0	CMP	70	0	0	C	32.9	16.1	25	0.49	3.0	9.7	65	95	-11	16	0.93
341.01	S&R (1984)	0.351	S O	14.00	CLAY	0.0	CMP	401	0	0	C	58.8	31.8	25	0.54	5.5	18.3	307	92	-13	21	0.77
342.01	S&R (1984)	0.274	S O	52.80	CLAY	0.0	CMP	2868	0	0	C	297.0	164.8	25	0.55	2.8	90.7	3173	97	-3	6	1.11
343.01	S&R (1984)	0.610	S O	30.50	CLAY	0.0	CMP	2022	0	0	C	91.5	52.4	25	0.57	4.7	28.8	1821	92	-13	21	0.90
344.01	S&R (1984)	0.325	S O	22.90	CLAY	0.0	CMP	691	0	0	C	90.5	52.5	25	0.58	5.5	28.9	714	95	-8	13	1.03
345.01	S&R (1984)	0.325	S O	25.90	CLAY	0.0	CMP	971	0	0	C	98.4	61.5	25	0.62	5.9	32.7	910	95	-7	12	0.94
346.01	S&R (1984)	0.274	S O	39.70	CLAY	0.0	CMP	2048	0	0	C	243.5	182.1	25	0.75	3.9	89.7	2041	96	-3	7	1.00
347.01	S&R (1984)	0.528	S O	14.90	CLAY	0.0	CMP	819	0	0	C	66.3	53.2	25	0.80	8.2	26.3	755	86	-13	27	0.92
348.01	S&R (1984)	0.274	S O	32.00	CLAY	0.0	CMP	1728	0	0	C	140.8	115.3	25	0.82	8.4	55.2	1582	96	-4	8	0.92
349.01	S&R (1984)	0.325	S O	18.60	CLAY	0.0	CMP	798	0	0	C	109.8	106.5	25	0.97	5.5	50.2	726	90	-6	16	0.91
350.01	S&R (1984)	0.610	S O	18.00	CLAY	0.0	CMP	2085	0	0	C	86.4	99.3	25	1.15	9.6	45.5	1720	85	-9	24	0.83
351.01	S&R (1984)	0.325	S O	19.30	CLAY	0.0	CMP	1015	0	0	C	112.1	131.2	25	1.17	6.9	59.7	930	90	-5	15	0.92
352.01	S&R (1984)	0.274	S O	15.40	CLAY	0.0	CMP	674	0	0	C	79.7	110.0	25	1.38	9.8	49.6	615	91	-4	13	0.91
353.01	S&R (1984)	0.610	S O	21.80	CLAY	0.0	CMP	4187	0	0	C	104.4	257.9	25	2.47	21.2	108.1	4852	87	-4	17	1.16
354.01	S&R (1984)	0.450	S O	10.50	CLAY	0.0	CMP	1166	0	0	C	53.5	185.0	25	3.46	27.0	82.3	1310	81	-4	23	1.12

Program PILCAP Version 05 Jan 2001 Time = 00 MAY 2000 16:57:46

PILES IN CLAY CLAY DATABASE - ALL PILES IN OLD AND NEW DATABASE 09 MAY 20

SAND SKIN FRICTION BY METHOD : NGI 1999 SOIL DATA QUALITY RATING = 0 CORRECTIONS INCLUDED
CLAY SKIN FRICTION BY METHOD : NGI 1999 PILE DATA QUALITY RATING = 0 Su : Yes Time : Yes

SITE No PILE No	LOCATION NAME	DIAM M	MAT O/C	PENTR M	TIP SOIL	TIME DAYS	CMP TNS	MEASURED (kN) TCOR:N	TCOR:Y	SHAFT SAND%	SAND CLAY	SIGV SIGV	NqCPT Su	SPT Ip	Dr Su/SIGV	PHI OCR	CALCD TAUSKN	CALCULATED (kN) TOTAL	SKN%	WGH%	TIP%	CALC MEAS
355.01	S&R (1984)	0.762	S O	22.00	CLAY	0.0	CMP	8212	0	0	C	115.7	325.0	25	2.81	22.1	141.3	7467	83	-4	21	0.91
356.01	Thailand	0.580	C C	13.50	CLAY	28.0	CMP	1570	1624	0	C	53.0	161.0	38	3.04	17.8	100.9	2888	76	-2	26	1.78
357.02	Thailand	0.248	C C	13.00	CLAY	60.0	CMP	313	318	0	C	42.7	67.3	43	1.58	7.2	43.8	506	78	-3	25	1.59
357.03	Thailand	0.248	C C	16.00	CLAY	60.0	CMP	580	590	0	C	53.1	117.4	41	2.21	10.0	74.7	999	85	-2	17	1.69
358.01	Lilleb‘lt	0.410	C C	23.80	CLAY	0.0	CMP	3237	0	2	C	140.0	269.1	75	1.92	11.9	150.9	3518	91	-4	13	1.09
358.02	Lilleb‘lt	0.410	C C	16.80	CLAY	0.0	CMP	1864	0	7	C	110.9	253.7	75	2.29	14.1	149.7	2168	87	-5	18	1.16
358.03	Lilleb‘lt	0.267	S C	27.10	CLAY	0.0	CMP	1776	0	2	C	153.7	276.4	75	1.80	11.2	152.6	2633	96	-3	7	1.48
358.04	Lilleb‘lt	0.267	S C	27.10	CLAY	0.0	CMP	1884	0	2	C	153.7	276.4	75	1.80	11.2	152.6	2633	96	-3	7	1.40
359.01	Empire LA	0.356	S O	50.30	CLAY	7.0	CMP	1113	1239	0	C	256.2	61.5	60	0.24	1.0	58.9	1107	90	-4	14	0.89
360.01	Empire LA	0.356	S O	78.00	CLAY	9.0	CMP	1936	2135	0	C	447.7	107.5	50	0.24	1.0	103.0	1945	90	-2	12	0.91
361.01	Empire LA	0.356	S O	94.50	CLAY	10.0	CMP	2127	2330	0	C	616.1	147.9	55	0.24	1.0	141.7	2201	88	-2	14	0.94
362.01	Empire LA	0.356	S O	109.70	CLAY	4.0	CMP	2354	2680	0	C	719.0	178.4	50	0.25	1.0	165.5	2574	88	-1	13	0.96
363.01	Houston	0.273	S C	13.10	CLAY	18.0	CMP	670	731	0	C	81.4	109.3	31	1.34	8.1	63.3	637	86	-1	15	0.87
363.02	Houston	0.273	S C	13.10	CLAY	80.0	CMP	765	773	0	C	81.4	109.3	31	1.34	8.1	63.3	637	86	-1	15	0.82
363.03	Houston	0.273	S C	13.10	CLAY	108.0	CMP	792	789	0	C	81.4	109.3	31	1.34	8.1	63.3	637	86	-1	15	0.81
364.01	Cowden, Pi	0.457	S O	9.20	CLAY	30.0	CMP	1140	1204	0	C	48.3	136.3	15	2.82	25.2	55.1	880	83	-5	22	0.73
364.02	Cowden, Pi	0.457	S O	9.20	CLAY	396.0	CMP	1390	1309	0	C	48.3	136.3	15	2.82	25.2	55.1	880	83	-5	22	0.67
364.03	Cowden, Pi	0.457	S O	9.20	CLAY	9125.0	CMP	1608	1337	0	C	48.3	136.3	15	2.82	25.2	55.1	880	83	-5	22	0.66
364.04	Cowden, Pi	0.457	S C	9.20	CLAY	390.0	CMP	1670	1571	0	C	48.3	136.3	15	2.82	25.2	67.0	1056	84	-2	18	0.67

Program PILCAP Version 05 Jan 2001 Time = 00 MAY 2000 16:57:46

PILES IN CLAY CLAY DATABASE - ALL PILES IN OLD AND NEW DATABASE 09 MAY 20

SAND SKIN FRICTION BY METHOD : NGI 1999 SOIL DATA QUALITY RATING = 0 CORRECTIONS INCLUDED
CLAY SKIN FRICTION BY METHOD : NGI 1999 PILE DATA QUALITY RATING = 0 Su : Yes Time : Yes

SITE No / PILE No	LOCATION NAME	DIAM M	MAT O/C	PENTR M	TIP SOIL	TIME DAYS	CMP TNS	MEASURED (kN) TCOR:N	TCOR:Y	SHAFT SAND%	SAND SIGV	CLAY SIGV	NqCPT Su	SPT Ip	Dr Su/SIGV	PHI OCR	CALCD TAUSKN	CALCULATED (kN) TOTAL	SKN%	WGH%	TIP%	CALC MEAS
365.01	Pentre A5	0.219	S C	25.00	CLAY	31.0	TNS	154	190	0	C	198.3	52.3	14	0.26	1.1	30.4	177	89	11	0	0.93
366.01	Pentre A6	0.219	S C	32.50	CLAY	31.0	TNS	361	437	0	C	251.4	68.5	17	0.27	1.1	50.8	375	93	7	0	0.86
367.01	Tilbrook	0.219	S C	12.50	CLAY	60.0	TNS	1238	1271	0	C	117.9	401.9	23	3.41	24.2	246.1	1626	99	1	0	1.28
367.02	Tilbrook	0.219	S C	17.50	CLAY	60.0	TNS	1995	2049	0	C	151.1	424.5	23	2.81	20.3	248.5	2493	99	1	0	1.22
367.03	Tilbrook	0.273	S O	17.50	CLAY	60.0	TNS	1891	1942	0	C	151.1	424.5	23	2.81	20.3	188.4	2363	99	1	0*	1.22
368.01	Tilbrook B	0.219	S C	25.50	CLAY	60.0	TNS	1684	1730	0	C	298.3	588.6	32	1.97	11.3	347.2	1931	99	1	0	1.12
369.01	Ons″y	0.219	S C	15.00	CLAY	50.0	TNS	130	137	0	C	62.0	17.9	40	0.29	1.2	15.0	111	93	7	0	0.81
369.02	Ons″y	0.219	S C	35.00	CLAY	50.0	TNS	465	491	0	C	113.0	29.0	40	0.26	1.1	26.2	560	97	3	0	1.14
369.03	Ons″y	0.219	S C	35.00	CLAY	50.0	TNS	510	538	0	C	113.0	29.0	40	0.26	1.1	26.2	560	97	3	0	1.04
369.04	Ons″y	0.812	S O	15.00	CLAY	50.0	TNS	469	494	0	C	62.0	17.9	40	0.29	1.2	14.8	407	93	7	0	0.82
370.01	Ons″y	0.219	S C	22.50	CLAY	50.0	TNS	161	170	0	C	100.3	24.6	40	0.25	1.0	23.1	170	93	7	0	1.00
371.01	Ons″y	0.219	S C	30.00	CLAY	50.0	TNS	216	228	0	C	138.5	34.6	40	0.25	1.0	31.9	235	93	7	0	1.03
372.01	Ons″y	0.219	S C	37.50	CLAY	50.0	TNS	258	273	0	C	176.8	44.7	40	0.25	1.0	40.8	300	94	6	0	1.10
373.01	Lierstrand	0.219	S C	15.00	CLAY	29.0	TNS	86	100	0	C	75.2	24.8	21	0.33	1.5	17.6	129	94	6	0	1.29
373.02	Lierstrand	0.812	S O	15.00	CLAY	55.0	TNS	374	402	0	C	75.2	24.8	21	0.33	1.5	17.1	465	94	6	0	1.16
374.01	Lierstrand	0.219	S C	22.50	CLAY	32.0	TNS	89	110	0	C	127.9	32.2	14	0.25	1.0	18.3	137	92	8	0	1.25
375.01	Lierstrand	0.219	S C	30.00	CLAY	31.0	TNS	104	130	0	C	181.4	43.9	13	0.24	1.0	17.6	136	89	11	0	1.05
376.01	Lierstrand	0.219	S C	37.50	CLAY	30.0	TNS	95	120	0	C	237.0	56.9	12	0.24	1.0	11.8	101	81	19	0	0.84
378.01	Iran	0.382	C C	13.30	CLAY	44.0	CMP	335	352	0	C	73.7	33.4	26	0.45	3.9	22.5	390	92	-10	18	1.11

Program PILCAP Version 05 Jan 2001 Time = 00 MAY 2000 16:57:46

PILES IN CLAY CLAY DATABASE - ALL PILES IN OLD AND NEW DATABASE 09 MAY 20

SAND SKIN FRICTION BY METHOD : NGI 1999 SOIL DATA QUALITY RATING = 0 CORRECTIONS INCLUDED
CLAY SKIN FRICTION BY METHOD : NGI 1999 PILE DATA QUALITY RATING = 0 Su : Yes Time : Yes

SITE No / PILE No	LOCATION NAME	DIAM M	MAT O/C	PENTR M	TIP SOIL	TIME DAYS	CMP TNS	MEASURED (kN) TCOR:N	TCOR:Y	SHAFT SAND%	SAND CLAY	SIGV SIGV	NqCPT Su	SPT Ip	Dr Su/SIGV	PHI OCR	CALCD TAUSKN	CALCULATED (kN) TOTAL	SKN%	WGH%	TIP%	CALC MEAS
378.02	Iran	0.382	C C	15.00	CLAY	90.0	CMP	335	337	0	C	80.9	34.6	26	0.43	3.6	23.8	460	93	-10	17	1.37
378.03	Iran	0.382	C C	19.10	CLAY	44.0	CMP	515	543	0	C	98.2	37.6	26	0.38	3.1	27.0	656	95	-9	14	1.21
378.04	Iran	0.382	C C	15.05	CLAY	42.0	CMP	400	422	0	C	81.1	34.6	26	0.43	3.6	23.8	463	93	-10	17	1.10
378.05	Iran	0.382	C C	16.60	CLAY	48.0	CMP	380	397	0	C	87.7	35.7	26	0.41	3.4	25.0	531	94	-10	16	1.34
378.06	Iran	0.382	C C	15.00	CLAY	71.0	CMP	410	419	0	C	80.9	34.6	26	0.43	3.6	23.8	460	93	-10	17	1.10
378.07	Iran	0.350	T C	17.00	CLAY	33.0	CMP	610	659	0	C	89.4	36.0	26	0.40	3.3	25.4	531	89	-3	14	0.81
378.08	Iran	0.350	T C	17.10	CLAY	36.0	CMP	590	633	0	C	89.8	36.1	26	0.40	3.3	25.4	535	89	-3	14	0.85
378.09	Iran	0.350	S C	13.90	CLAY	584.0	CMP	400	362	0	C	76.2	33.8	26	0.44	3.8	22.9	401	87	-3	16	1.11
379.01	Haga	0.153	S C	5.00	CLAY	7.0	TNS	59	72	0	C	49.1	41.5	18	0.84	7.3	25.2	62	94	1	5	0.86
379.02	Haga	0.153	S C	5.00	CLAY	20.0	TNS	65	73	0	C	49.1	41.5	18	0.84	7.3	25.2	62	94	1	5	0.85
379.03	Haga	0.153	S C	5.00	CLAY	36.0	TNS	73	78	0	C	49.1	41.5	18	0.84	7.3	25.2	62	94	1	5	0.79
380.01	Drammen	0.269	T C	15.50	CLAY	31.0	CMP	220	256	0	C	80.5	20.6	21	0.26	1.1	16.2	181	92	-5	13	0.71
380.02	Drammen	0.269	T C	15.50	CLAY	71.0	CMP	270	282	0	C	80.5	20.6	21	0.26	1.1	16.2	181	92	-5	13	0.64
380.03	Drammen	0.269	T C	15.50	CLAY	799.0	CMP	300	240	0	C	80.5	20.6	21	0.26	1.1	16.2	181	92	-5	13	0.75
381.01	Montreal	0.300	C C	16.80	CLAY	71.0	TNS	458	467	0	C	66.9	54.2	35	0.81	5.5	31.3	517	90	6	4	1.11
382.01	Maskinonge	0.297	T C	15.25	CLAY	58.0	CMP	698	735	10	C	85.8	23.8	30	0.28	1.1	20.5	213	90	-5	15	0.29
382.02	Maskinonge	0.297	T C	15.25	CLAY	58.0	CMP	640	674	10	C	85.8	23.8	30	0.28	1.1	20.5	213	90	-5	15	0.32
382.03	Maskinonge	0.242	C C	23.80	CLAY	58.0	CMP	585	607	3	C	115.5	30.2	41	0.26	1.1	27.0	403	98	-7	9	0.66
382.04	Maskinonge	0.219	S C	23.80	CLAY	58.0	CMP	390	404	3	C	115.5	30.2	41	0.26	1.1	27.0	378	94	-2	8	0.94

Program PILCAP Version 05 Jan 2001 Time = 00 MAY 2000 16:57:46

PILES IN CLAY CLAY DATABASE - ALL PILES IN OLD AND NEW DATABASE 09 MAY 20

SAND SKIN FRICTION BY METHOD : NGI 1999 SOIL DATA QUALITY RATING = 0 CORRECTIONS INCLUDED
CLAY SKIN FRICTION BY METHOD : NGI 1999 PILE DATA QUALITY RATING = 0 Su : Yes Time : Yes

SITE No PILE No	LOCATION NAME	DIAM M	MAT O/C	PENTR M	TIP SOIL	TIME DAYS	CMP TNS	MEASURED (kN) TCOR:N	TCOR:Y	SHAFT SAND%	SAND CLAY	SIGV SIGV	NqCPT Su	SPT Ip	Dr Su/SIGV	PHI OCR	CALCD TAUSKN	CALCULATED (kN) TOTAL	SKN%	WGH%	TIP%	CALC MEAS
382.05	Maskinonge	0.242	C C	37.50	CLAY	58.0	CMP	845	868	1	C	160.0	41.9	47	0.26	1.1	37.4	943	98	-5	7	1.09
383.01	G"teborg	0.340	C C	34.00	CLAY	46.0	TNS	900	953	0	C	146.3	44.8	40	0.31	1.3	36.1	1083	92	7	1	1.14
385.01	Bangkok	0.400	C C	8.00	CLAY	8.5	TNS	110	123	0	C	38.5	15.8	55	0.41	5.3	11.8	135	88	11	1	1.10
385.02	Bangkok	0.400	C C	12.00	CLAY	8.5	TNS	165	185	0	C	47.7	16.1	60	0.34	3.9	12.9	216	90	11	-1	1.17
385.03	Bangkok	0.400	C C	16.00	CLAY	8.5	TNS	245	274	0	C	57.1	18.1	60	0.32	3.2	14.8	331	90	9	1	1.20
385.04	Bangkok	0.400	C C	20.00	CLAY	8.5	TNS	425	476	0	C	67.4	21.4	60	0.32	2.8	17.3	480	91	8	1	1.01
386.01	St Alban	0.220	S C	7.60	CLAY	4.0	CMP	47	57	0	C	30.5	19.8	21	0.65	4.6	12.4	71	85	-4	19	1.25
386.02	St Alban	0.220	S C	7.60	CLAY	8.0	CMP	67	79	0	C	30.5	19.8	21	0.65	4.6	12.4	71	85	-4	19	0.90
386.03	St Alban	0.220	S C	7.60	CLAY	20.0	CMP	77	85	0	C	30.5	19.8	21	0.65	4.6	12.4	71	85	-4	19	0.83
386.04	St Alban	0.220	S C	7.60	CLAY	33.0	CMP	83	89	0	C	30.5	19.8	21	0.65	4.6	12.4	71	85	-4	19	0.80
386.05	St Alban	0.220	S C	7.60	CLAY	720.0	CMP	86	77	0	C	30.5	19.8	21	0.65	4.6	12.4	71	85	-4	19	0.92
387.01	Izmir	0.528	S O	17.00	SAND	60.0	CMP	1410	1430	26	C	61.5	53.0	19	0.86	7.5	25.4	1494	61	-3	42*	1.04
387.02	Izmir	0.528	S O	17.00	SAND	60.0	TNS	710	728	26	C	61.5	53.0	19	0.86	7.5	25.4	884	94	13	-7	1.21
387.03	Izmir	0.528	S O	15.00	CLAY	30.0	CMP	780	825	0	C	56.8	51.5	20	0.91	7.8	24.7	744	83	-14	31	0.90
387.04	Izmir	0.528	S O	15.00	CLAY	30.0	TNS	590	639	0	C	56.8	51.5	20	0.91	7.8	24.7	779	79	14	7	1.22
388.01	Cowden	0.102	S C	6.15	CLAY	4.0	CMP	136	163	0	C	49.7	132.9	19	2.67	19.4	82.4	104	93	-1	8	0.64
388.02	Cowden	0.102	S C	6.40	CLAY	5.0	TNS	90	107	0	C	51.2	130.8	19	2.56	18.7	80.7	104	97	1	2	0.96
388.03	Cowden	0.102	S C	6.43	CLAY	4.0	CMP	108	129	0	C	51.3	130.5	19	2.54	18.6	80.5	109	93	-1	8	0.84
389.01	NovaScotia	0.243	C C	12.00	CLAY	7.0	CMP	1240	1442	0	C	85.3	180.1	11	2.11	18.5	96.8	965	92	-2	10	0.67

Program PILCAP Version 05 Jan 2001 Time = 00 MAY 2000 16:57:46

PILES IN CLAY CLAY DATABASE - ALL PILES IN OLD AND NEW DATABASE 09 MAY 20

SAND SKIN FRICTION BY METHOD : NGI 1999 SOIL DATA QUALITY RATING = 0 CORRECTIONS INCLUDED
CLAY SKIN FRICTION BY METHOD : NGI 1999 PILE DATA QUALITY RATING = 0 Su : Yes Time : Yes

SITE No / PILE No	LOCATION NAME	DIAM M	MAT O/C	PENTR M	TIP SOIL	TIME DAYS	CMP TNS	MEASURED (kN) TCOR:N	MEASURED (kN) TCOR:Y	SHAFT SAND%	SAND CLAY	SIGV SIGV	NqCPT Su	SPT Ip	Dr Su/SIGV	PHI OCR	CALCD TAUSKN	CALCULATED (kN) TOTAL	SKN%	WGH%	TIP%	CALC MEAS
389.02	NovaScotia	0.340	C C	13.00	CLAY	7.0	CMP	1950	2265	0	C	91.7	180.9	12	1.97	17.6	97.1	1501	90	-2	12	0.66
390.01	Sumatra	0.400	S O	43.30	CLAY	1.7	CMP	1225	1571	3	C	130.6	35.0	40	0.27	2.3	30.7	1702	99	-8	9	1.08
390.02	Sumatra	0.400	S O	43.30	CLAY	10.5	CMP	1555	1773	3	C	130.6	35.0	40	0.27	2.3	30.7	1702	99	-8	9	0.96
390.03	Sumatra	0.400	S O	43.30	CLAY	20.5	CMP	1670	1828	3	C	130.6	35.0	40	0.27	2.3	30.7	1702	99	-8	9	0.93
390.04	Sumatra	0.400	S O	43.30	CLAY	32.5	CMP	1670	1779	3	C	130.6	35.0	40	0.27	2.3	30.7	1702	99	-8	9	0.96
391.01	L Arrow La	0.610	S O	30.50	CLAY	1.1	CMP	1558	2066	0	C	93.6	59.3	39	0.63	5.0	31.3	1769	103	-3	0*	0.86
391.02	L Arrow La	0.610	S O	30.50	CLAY	10.0	CMP	1958	2239	0	C	93.6	59.3	39	0.63	5.0	31.3	1769	103	-3	0*	0.79
391.03	L Arrow La	0.610	S O	46.60	CLAY	1.3	CMP	2626	3561	0	C	150.0	73.7	36	0.49	3.9	43.3	3781	102	-2	0*	1.06
391.04	L Arrow La	0.610	S C	48.20	CLAY	3.0	CMP	3160	3875	0	C	155.7	74.8	35	0.48	3.8	48.0	4697	94	-6	12	1.21
391.05	L Arrow La	0.610	S C	48.30	CLAY	170.0	CMP	3649	3551	0	C	156.1	74.9	35	0.48	3.8	48.0	4712	94	-6	12	1.33
392.01	West Sole	0.762	S O	6.00	CLAY	4.9	TNS	2438	0	0	C	37.5	260.0	20	6.93	43.2	104.3	1680	89	6	5	0.69
392.02	West Sole	0.762	S O	9.00	CLAY	0.3	TNS	2873	0	0	C	56.2	304.4	20	5.41	37.9	132.1	3096	92	5	3	1.08
392.03	West Sole	0.762	S O	12.00	CLAY	0.2	TNS	4466	0	0	C	74.9	349.2	20	4.66	34.5	153.5	4727	93	5	2	1.06
392.04	West Sole	0.762	S O	15.00	CLAY	0.4	TNS	5240	0	0	C	93.0	369.3	20	3.97	30.9	160.3	6140	94	4	2	1.17
392.05	West Sole	0.762	S O	18.00	CLAY	0.4	TNS	6734	0	0	C	110.6	407.8	20	3.69	28.9	176.7	8065	94	4	2	1.20
392.07	West Sole	0.762	S O	6.00	CLAY	0.4	CMP	3051	0	0	C	37.5	260.0	20	6.93	43.2	104.3	2764	54	-4	50	0.91
392.07	West Sole	0.762	S O	6.00	CLAY	0.4	TNS	1726	0	0	C	37.5	260.0	20	6.93	43.2	104.3	1680	89	6	5	0.97
392.08	West Sole	0.762	S O	9.00	CLAY	0.2	CMP	5471	0	0	C	56.2	304.4	20	5.41	37.9	132.1	4827	59	-3	44	0.88
392.08	West Sole	0.762	S O	9.00	CLAY	0.2	TNS	2642	0	0	C	56.2	304.4	20	5.41	37.9	132.1	3096	92	5	3	1.17
392.09	West Sole	0.762	S O	9.00	CLAY	5.9	TNS	3079	0	0	C	56.2	304.4	20	5.41	37.9	132.1	3088	92	5	3	1.00

Program PILCAP Version 05 Jan 2001 Time = 00 MAY 2000 16:57:46

PILES IN CLAY CLAY DATABASE - ALL PILES IN OLD AND NEW DATABASE 09 MAY 20

SAND SKIN FRICTION BY METHOD : NGI 1999 SOIL DATA QUALITY RATING = 0 CORRECTIONS INCLUDED
CLAY SKIN FRICTION BY METHOD : NGI 1999 PILE DATA QUALITY RATING = 0 Su : Yes Time : Yes

SITE No / PILE No	LOCATION NAME	DIAM M	MAT O/C	PENTR M	TIP SOIL	TIME DAYS	CMP TNS	MEASURED (kN) TCOR:N	MEASURED (kN) TCOR:Y	SHAFT SAND%	SAND SIGV	CLAY SIGV	NqCPT Su	SPT Ip	Dr Su/SIGV	PHI OCR	CALCD TAUSKN	CALCULATED (kN) TOTAL	SKN%	WGH%	TIP%	CALC MEAS
392.10	West Sole	0.762	S O	12.00	CLAY	0.3	CMP	6681	0	0	C	74.9	349.2	20	4.66	34.5	153.5	6182	71	-3	32	0.93
392.10	West Sole	0.762	S O	12.00	CLAY	0.3	TNS	4457	0	0	C	74.9	349.2	20	4.66	34.5	153.5	4706	94	4	2	1.06
392.11	West Sole	0.762	S O	15.00	CLAY	0.2	CMP	6788	0	0	C	93.0	369.3	20	3.97	30.9	160.3	7523	77	-3	26	1.11
392.11	West Sole	0.762	S O	15.00	CLAY	0.2	TNS	4510	0	0	C	93.0	369.3	20	3.97	30.9	160.3	6102	94	4	2	1.35
392.12	West Sole	0.762	S O	18.00	CLAY	0.2	CMP	8344	0	0	C	110.6	407.8	20	3.69	28.9	176.7	10010	76	-2	26	1.20
392.12	West Sole	0.762	S O	18.00	CLAY	0.2	TNS	6023	0	0	C	110.6	407.8	20	3.69	28.9	176.7	7989	95	3	2	1.33
393.01	Pentre	0.762	S O	55.00	CLAY	44.0	CMP	6030	6705	0	C	320.4	87.3	18	0.27	1.1	65.8	6678	94	-10	16	1.00
394.01	Tilbrook	0.762	S O	30.00	CLAY	130.0	CMP	16131	15950	0	C	212.2	477.8	27	2.25	19.1	199.5	16374	87	-2	15	1.03
395.01	Tilbrook	0.762	S O	29.40	CLAY	700.0	TNS	16200	14723	0	C	219.4	489.3	27	2.23	17.6	207.8	14220	97	2	1	0.97
396.01	Canons Prk	0.102	S C	5.20	CLAY	109.0	TNS	90	0	0	C	45.1	86.8	50	1.93	11.0	53.6	58	95	3	2	0.64
396.02	Canons Prk	0.102	S C	5.28	CLAY	79.0	CMP	68	0	0	C	45.4	87.6	50	1.93	11.0	54.0	65	88	-2	14	0.95
396.03	Canons Prk	0.102	S C	5.95	CLAY	63.0	CMP	110	0	0	C	48.4	92.7	48	1.92	10.9	56.7	80	90	-2	12	0.73
396.04	Canons Prk	0.102	S C	5.87	CLAY	2.0	CMP	78	0	0	C	48.0	92.2	48	1.92	10.9	56.5	78	90	-2	12	1.00
396.05	Canons Prk	0.102	S C	6.16	CLAY	20.0	TNS	119	0	0	C	49.3	94.0	48	1.91	10.9	57.3	79	96	2	2	0.67
396.06	Canons Prk	0.102	S C	5.92	CLAY	2.0	TNS	105	0	0	C	48.2	92.6	48	1.92	10.9	56.6	74	96	2	2	0.70
396.07	Canons Prk	0.102	S C	5.80	CLAY	2.0	TNS	105	0	0	C	47.7	91.8	48	1.92	11.0	56.2	71	96	2	2	0.68
396.08	Canons Prk	0.102	S O	5.70	CLAY	2.0	TNS	94	0	0	C	47.3	91.0	49	1.93	11.0	43.0	54	94	3	3	0.57
397.01	Canons Par	0.168	S C	6.50	CLAY	108.0	CMP	189	188	0	C	62.5	95.8	47	1.53	8.4	57.2	161	85	-1	16	0.85
397.02	Canons Par	0.168	S C	6.50	CLAY	496.0	CMP	200	188	0	C	62.5	95.8	47	1.53	8.4	57.2	161	85	-1	16	0.85
397.03	Canons Par	0.168	S C	6.50	CLAY	1130.0	CMP	231	211	0	C	62.5	95.8	47	1.53	8.4	57.2	161	85	-1	16	0.76
397.04	Canons Par	0.168	S C	6.50	CLAY	6200.0	CMP	291	249	0	C	62.5	95.8	47	1.53	8.4	57.2	161	85	-1	16	0.64

Program PILCAP Version 05 Jan 2001 Time = 00 MAY 2000 16:57:46

PILES IN CLAY CLAY DATABASE - ALL PILES IN OLD AND NEW DATABASE 09 MAY 20

SAND SKIN FRICTION BY METHOD : NGI 1999 SOIL DATA QUALITY RATING = 0 CORRECTIONS INCLUDED
CLAY SKIN FRICTION BY METHOD : NGI 1999 PILE DATA QUALITY RATING = 0 Su : Yes Time : Yes

SITE No / PILE No	LOCATION NAME	DIAM M	MAT O/C	PENTR M	TIP SOIL	TIME DAYS	CMP TNS	MEASURED (kN) TCOR:N	MEASURED (kN) TCOR:Y	SHAFT SAND%	SAND CLAY	SIGV SIGV	NqCPT Su	SPT Ip	Dr Su/SIGV	PHI OCR	CALCD TAUSKN	CALCULATED (kN) TOTAL	SKN%	WGH%	TIP%	CALC MEAS
397.05	Canons Par	0.168	S C	6.65	CLAY	74.0	CMP	194	196	0	C	63.2	96.5	47	1.53	8.4	57.5	166	85	-1	16	0.85
397.06	Canons Par	0.168	S C	6.65	CLAY	217.0	CMP	197	191	0	C	63.2	96.5	47	1.53	8.4	57.5	166	85	-1	16	0.87
397.07	Canons Par	0.168	S C	6.65	CLAY	683.0	CMP	200	186	0	C	63.2	96.5	47	1.53	8.4	57.5	166	85	-1	16	0.89
397.08	Canons Par	0.168	S C	6.65	CLAY	1312.0	CMP	221	201	0	C	63.2	96.5	47	1.53	8.4	57.5	166	85	-1	16	0.83
397.09	Canons Par	0.168	S C	6.65	CLAY	6200.0	CMP	274	235	0	C	63.2	96.5	47	1.53	8.4	57.5	166	85	-1	16	0.71
398.01	Canons Par	0.168	S C	6.63	CLAY	31.0	CMP	159	167	0	C	68.2	104.7	45	1.54	8.5	62.9	145	83	-1	18	0.87
398.02	Canons Par	0.168	S C	6.63	CLAY	134.0	CMP	161	159	0	C	68.2	104.7	45	1.54	8.5	62.9	145	83	-1	18	0.91
398.03	Canons Par	0.168	S C	6.63	CLAY	248.0	CMP	163	157	0	C	68.2	104.7	45	1.54	8.5	62.9	145	83	-1	18	0.92
398.04	Canons Par	0.168	S C	6.63	CLAY	525.0	CMP	165	155	0	C	68.2	104.7	45	1.54	8.5	62.9	145	83	-1	18	0.94
398.05	Canons Par	0.168	S C	6.63	CLAY	1154.0	CMP	184	168	0	C	68.2	104.7	45	1.54	8.5	62.9	145	83	-1	18	0.87
398.06	Canons Par	0.168	S C	6.63	CLAY	6200.0	CMP	231	198	0	C	68.2	104.7	45	1.54	8.5	62.9	145	83	-1	18	0.74
399.01	Kontich	0.610	S O	23.50	CLAY	21.0	CMP	4840	5141	0	C	124.0	164.2	52	1.32	8.2	72.2	3525	86	-6	20	0.69
399.02	Kontich	0.610	S O	23.50	CLAY	26.0	TNS	4100	4355	0	C	124.0	164.2	52	1.32	8.2	72.2	3359	91	6	3	0.77
399.03	Kontich	0.610	S O	20.10	CLAY	12.0	CMP	3380	3656	0	C	108.7	155.6	52	1.43	8.7	68.5	2897	84	-7	23	0.79
399.04	Kontich	0.610	S O	20.10	CLAY	16.0	TNS	2420	2629	0	C	108.7	155.6	52	1.43	8.7	68.5	2730	89	7	4	1.04
400.01	Long Beach	0.762	S O	80.50	CLAY	60.0	TNS	10710	11287	0	C	673.4	365.0	16	0.54	2.5	204.7	12361	90	7	3	1.10
401.01	Napoli	0.381	S C	48.50	CLAY	0.0	CMP	2348	0	0	C	179.4	84.6	33	0.47	3.1	55.3	3071	98	-6	8	1.31
402.01	Livorno	0.483	S C	50.00	CLAY	19.0	CMP	2400	2701	0	C	208.2	57.7	34	0.28	1.9	36.6	3084	90	-1	11	1.14
402.02	Livorno	0.487	S C	57.00	SAND	28.0	CMP	4200	4476	12	C	212.5	58.9	33	0.28	1.9	37.3	4351	77	-8	31	0.97

Program PILCAP Version 05 Jan 2001 Time = 00 MAY 2000 16:57:46

PILES IN CLAY CLAY DATABASE - ALL PILES IN OLD AND NEW DATABASE 09 MAY 20

SAND SKIN FRICTION BY METHOD : NGI 1999 SOIL DATA QUALITY RATING = 0 CORRECTIONS INCLUDED
CLAY SKIN FRICTION BY METHOD : NGI 1999 PILE DATA QUALITY RATING = 0 Su : Yes Time : Yes

SITE No / PILE No	LOCATION NAME	DIAM M	MAT O/C	PENTR M	TIP SOIL	TIME DAYS	CMP TNS	MEASURED (kN) TCOR:N	MEASURED (kN) TCOR:Y	SHAFT SAND%	SAND CLAY	SIGV SIGV	NqCPT Su	SPT Ip	Dr Su/SIGV	PHI OCR	CALCD TAUSKN	CALCULATED (kN) TOTAL	SKN%	WGH%	TIP%	CALC MEAS
403.01	Bothkennar	0.102	S C	6.00	CLAY	4.0	CMP	27	33	0	C	29.8	17.3	40	0.58	2.9	11.0	18	96	-9	13	0.54
403.02	Bothkennar	0.102	S C	6.01	CLAY	32.0	CMP	33	35	0	C	29.9	17.4	40	0.58	2.9	11.0	18	96	-9	13	0.51
403.03	Bothkennar	0.102	S C	6.00	CLAY	1.0	TNS	26	35	0	C	29.8	17.3	40	0.58	2.9	11.0	19	91	9	0	0.54
403.04	Bothkennar	0.102	S C	3.15	CLAY	4.0	CMP	15	19	0	C	20.8	14.9	35	0.72	3.6	9.2	6	100	-27	27	0.32
403.05	Bothkennar	0.102	S C	5.95	CLAY	2.0	CMP	26	33	0	C	29.7	17.3	40	0.58	2.9	10.9	18	96	-9	13	0.54
404.01	West Delta	0.762	S O	71.20	CLAY	116.0	TNS	5030	4986	0	C	127.9	36.7	41	0.29	2.1	30.5	5655	92	14	-6	1.13
404.02	West Delta	0.762	S O	71.30	CLAY	470.0	TNS	4850	4438	0	C	128.1	36.8	41	0.29	2.1	30.5	5669	92	14	-6	1.28
405.01	Singapore	0.331	C C	28.00	SAND	7.0	CMP	2100	2203	31	C	87.4	44.1	25	0.50	8.2	29.1	2435	49	-3	54	1.11
406.01	Aalborg ha	0.382	C C	30.80	SAND	18.0	CMP	2540	2729	17	C	164.6	149.5	25	0.91	4.9	82.0	2376	70	-4	34	0.87
406.02	Aalborg ha	0.446	C C	27.80	SAND	18.0	CMP	1800	1897	8	C	164.6	149.5	25	0.91	4.9	83.5	2668	67	-4	37	1.41
407.01	Egå Rensen	0.318	C C	23.80	CLAY	27.0	CMP	1400	1473	11	C	90.6	210.4	25	2.32	14.2	121.8	2839	91	-2	11	1.93
408.01	Egå Rensen	0.382	C C	25.20	CLAY	28.0	CMP	1671	1752	11	C	83.6	194.4	25	2.33	14.1	112.9	3680	90	-2	12	2.10
409.01	Algade, Aa	0.255	C C	13.35	CLAY	14.0	CMP	660	727	1	C	86.2	134.7	25	1.56	9.7	78.7	921	87	-2	15	1.27
409.02	Algade, Aa	0.255	C C	13.35	CLAY	9778.0	CMP	930+	765+	1	C	86.2	134.7	25	1.56	9.7	78.7	921	87	-2	15	1.20
410.01	Motorvegbr	0.813	S O	35.00	CLAY	16.0	CMP	2150	2508	15	C	239.8	65.3	25	0.27	1.1	56.4	3689	90	-9	19	1.47
410.02	Motorvegbr	0.813	S O	35.00	CLAY	140.0	CMP	2800	2729	15	C	239.8	65.3	25	0.27	1.1	56.4	3689	90	-9	19	1.35
410.03	Motorvegbr	0.400	S C	35.00	CLAY	14.0	CMP	1350	1666	16	C	239.8	65.3	25	0.27	1.1	56.9	1451	115	-26	11	0.87
410.04	Motorvegbr	0.400	S C	35.00	CLAY	141.0	CMP	2210	2141	16	C	239.8	65.3	25	0.27	1.1	56.9	1451	115	-26	11	0.68
411.01	Drammen St	0.344	C C	49.00	CLAY	21.0	CMP	1100	1322	4	C	295.2	82.0	22	0.28	1.2	70.2	2820	98	-4	6	2.13

Program PILCAP Version 05 Jan 2001 Time = 00 MAY 2000 16:57:46

PILES IN CLAY CLAY DATABASE - ALL PILES IN OLD AND NEW DATABASE 09 MAY 20

SAND SKIN FRICTION BY METHOD : NGI 1999 SOIL DATA QUALITY RATING = 0 CORRECTIONS INCLUDED
CLAY SKIN FRICTION BY METHOD : NGI 1999 PILE DATA QUALITY RATING = 0 Su : Yes Time : Yes

SITE No / PILE No	LOCATION NAME	DIAM M	MAT O/C	PENTR M	TIP SOIL	TIME DAYS	CMP TNS	MEASURED (kN) TCOR:N	MEASURED (kN) TCOR:Y	SHAFT SAND%	SAND SIGV	CLAY SIGV	NqCPT Su	SPT Ip	Dr Su/SIGV	PHI OCR	CALCD TAUSKN	CALCULATED (kN) TOTAL	SKN%	WGH%	TIP%	CALC MEAS
411.02	Drammen St	0.344	C C	49.00	CLAY	153.0	CMP	1700+	1624+	4	C	295.2	82.0	22	0.28	1.2	70.2	2820	98	-4	6	1.74
411.03	Drammen St	0.344	C C	30.00	CLAY	24.0	CMP	960	1115	11	C	210.3	66.4	22	0.32	1.3	52.6	1064	96	-7	11	0.95
412.01	Nitsund te	0.276	T C	11.70	CLAY	32.0	CMP	243	258	0	C	51.4	69.1	16	1.34	15.7	33.9	363	95	-2	7	1.41
412.02	Nitsund te	0.276	T C	11.70	CLAY	207.0	CMP	321	309	0	C	51.4	69.1	16	1.34	15.7	33.9	363	95	-2	7	1.17
412.03	Nitsund te	0.276	T C	11.70	CLAY	357.0	CMP	336	315	0	C	51.4	69.1	16	1.34	15.7	33.9	363	95	-2	7	1.15
412.04	Nitsund te	0.276	T C	11.70	CLAY	641.0	CMP	350	319	0	C	51.4	69.1	16	1.34	15.7	33.9	363	95	-2	7	1.14
412.05	Nitsund te	0.276	T C	11.70	CLAY	1043.0	CMP	350+	312+	0	C	51.4	69.1	16	1.34	15.7	33.9	363	95	-2	7	1.16
412.06	Nitsund te	0.252	T C	13.70	CLAY	34.0	CMP	228	242	0	C	61.0	66.2	16	1.09	13.5	33.5	381	95	-2	7	1.58
412.07	Nitsund te	0.252	T C	13.70	CLAY	209.0	CMP	314	302	0	C	61.0	66.2	16	1.09	13.5	33.5	381	95	-2	7	1.26
412.08	Nitsund te	0.252	T C	13.70	CLAY	357.0	CMP	343	321	0	C	61.0	66.2	16	1.09	13.5	33.5	381	95	-2	7	1.19
412.09	Nitsund te	0.252	T C	13.70	CLAY	637.0	CMP	378	344	0	C	61.0	66.2	16	1.09	13.5	33.5	381	95	-2	7	1.11
412.10	Nitsund te	0.252	T C	13.70	CLAY	1023.0	CMP	414	368	0	C	61.0	66.2	16	1.09	13.5	33.5	381	95	-2	7	1.04
413.01	Skå-Edeby,	0.127	T C	15.00	CLAY	30.0	CMP	48	51	0	C	36.7	12.1	41	0.33	4.0	9.5	60	94	-3	9	1.18
413.02	Skå-Edeby,	0.127	T C	15.00	CLAY	75.0	CMP	58	59	0	C	36.7	12.1	41	0.33	4.0	9.5	60	94	-3	9	1.02
413.03	Skå-Edeby,	0.127	T C	15.30	CLAY	42.0	CMP	34	35	0	C	37.5	12.3	40	0.33	3.9	9.7	63	94	-3	9	1.77
413.04	Skå-Edeby,	0.127	T C	15.30	CLAY	456.0	CMP	55	51	0	C	37.5	12.3	40	0.33	3.9	9.7	63	94	-3	9	1.22
413.05	Skå-Edeby,	0.127	T C	15.30	CLAY	1116.0	CMP	48	43	0	C	37.5	12.3	40	0.33	3.9	9.7	63	94	-3	9	1.45
413.06	Skå-Edeby,	0.127	T C	15.00	CLAY	39.0	CMP	52	55	0	C	36.7	12.1	41	0.33	4.0	9.5	60	94	-3	9	1.11
413.07	Skå-Edeby,	0.127	T C	15.00	CLAY	75.0	CMP	64	65	0	C	36.7	12.1	41	0.33	4.0	9.5	60	94	-3	9	0.93

Program PILCAP Version 05 Jan 2001 Time = 00 MAY 2000 16:57:46

PILES IN CLAY CLAY DATABASE - ALL PILES IN OLD AND NEW DATABASE 09 MAY 20

SAND SKIN FRICTION BY METHOD : NGI 1999 SOIL DATA QUALITY RATING = 0 CORRECTIONS INCLUDED
CLAY SKIN FRICTION BY METHOD : NGI 1999 PILE DATA QUALITY RATING = 0 Su : Yes Time : Yes

SITE No / PILE No	LOCATION NAME	DIAM M	MAT O/C	PENTR M	TIP SOIL	TIME DAYS	CMP TNS	MEASURED (kN) TCOR:N	MEASURED (kN) TCOR:Y	SHAFT SAND%	SAND CLAY	SIGV SIGV	NqCPT Su	SPT Ip	Dr Su/SIGV	PHI OCR	CALCD TAUSKN	CALCULATED (kN) TOTAL	SKN%	WGH%	TIP%	CALC MEAS
413.08	Skå-Edeby,	0.127	T C	15.30	CLAY	42.0	CMP	36	38	0	C	37.5	12.3	40	0.33	3.9	9.7	63	94	-3	9	1.67
413.09	Skå-Edeby,	0.127	T C	15.30	CLAY	456.0	CMP	56	52	0	C	37.5	12.3	40	0.33	3.9	9.7	63	94	-3	9	1.20
413.10	Skå-Edeby,	0.127	T C	15.30	CLAY	1116.0	CMP	54	48	0	C	37.5	12.3	40	0.33	3.9	9.7	63	94	-3	9	1.29
413.11	Skå-Edeby,	0.127	T C	15.00	CLAY	30.0	CMP	54	57	0	C	36.7	12.1	41	0.33	4.0	9.5	60	94	-3	9	1.05
413.12	Skå-Edeby,	0.127	T C	15.00	CLAY	75.0	CMP	70	71	0	C	36.7	12.1	41	0.33	4.0	9.5	60	94	-3	9	0.85
413.13	Skå-Edeby,	0.127	T C	15.30	CLAY	42.0	CMP	41	43	0	C	37.5	12.3	40	0.33	3.9	9.7	63	94	-3	9	1.46
413.14	Skå-Edeby,	0.127	T C	15.30	CLAY	96.0	CMP	48	48	0	C	37.5	12.3	40	0.33	3.9	9.7	63	94	-3	9	1.30
413.15	Skå-Edeby,	0.127	T C	15.30	CLAY	456.0	CMP	60	56	0	C	37.5	12.3	40	0.33	3.9	9.7	63	94	-3	9	1.12
413.16	Skå-Edeby,	0.127	T C	15.30	CLAY	1116.0	CMP	62	55	0	C	37.5	12.3	40	0.33	3.9	9.7	63	94	-3	9	1.13
413.17	Skå-Edeby,	0.127	T C	15.00	CLAY	30.0	CMP	52	55	0	C	36.7	12.1	41	0.33	4.0	9.5	60	94	-3	9	1.09
413.18	Skå-Edeby,	0.127	T C	15.00	CLAY	75.0	CMP	65	66	0	C	36.7	12.1	41	0.33	4.0	9.5	60	94	-3	9	0.91
413.19	Skå-Edeby,	0.127	T C	15.30	CLAY	96.0	CMP	42	42	0	C	37.5	12.3	40	0.33	3.9	9.7	63	94	-3	9	1.49
413.20	Skå-Edeby,	0.127	T C	15.30	CLAY	171.0	CMP	47	46	0	C	37.5	12.3	40	0.33	3.9	9.7	63	94	-3	9	1.37
413.21	Skå-Edeby,	0.127	T C	15.30	CLAY	456.0	CMP	49	46	0	C	37.5	12.3	40	0.33	3.9	9.7	63	94	-3	9	1.37
413.22	Skå-Edeby,	0.127	T C	15.30	CLAY	1116.0	CMP	51	46	0	C	37.5	12.3	40	0.33	3.9	9.7	63	94	-3	9	1.37
413.23	Skå-Edeby,	0.127	T C	14.50	CLAY	75.0	CMP	56	57	0	C	35.2	11.8	41	0.34	4.1	9.2	57	94	-3	9	0.99
413.24	Skå-Edeby,	0.127	T C	14.50	CLAY	216.0	CMP	66	64	0	C	35.2	11.8	41	0.34	4.1	9.2	57	94	-3	9	0.89
413.25	Skå-Edeby,	0.127	T C	14.50	CLAY	906.0	CMP	63	57	0	C	35.2	11.8	41	0.34	4.1	9.2	57	94	-3	9	0.99

Program PILCAP Version 05 Jan 2001 Time = 00 MAY 2000 16:57:46

PILES IN CLAY CLAY DATABASE - ALL PILES IN OLD AND NEW DATABASE 09 MAY 2005

SAND SKIN FRICTION BY : NGI 1999 SOIL DATA QUALITY RATING = 0 CORRECTIONS INCLUDED
CLAY SKIN FRICTION BY : NGI 1999 PILE DATA QUALITY RATING = 0 Su : Yes Time : Yes

GROUP	CASES	SHAFT SOIL	TIP SOIL	COMP TENS	RATIO COMPUTED/MEASURED MINIMUM	AVERAGE	MAXIMUM	STANDARD DEVIATION
1	0	SAND	BOTH	COMP	0.00	0.00	0.00	0.00
2	0	SAND	BOTH	TENS	0.00	0.00	0.00	0.00
3	5	CLAY	SAND	COMP	0.87	1.08	1.41	0.20
4	210	CLAY	CLAY	COMP	0.29	1.02	2.13	0.30
5	53	CLAY	BOTH	TENS	0.54	1.02	1.35	0.21
6	268	ALL MEASUREMENTS			0.29	1.02	2.13	0.28

Title:

Capacity of Piles in Sand.

Authors:

Augustesen, A., Andersen, L., and Sørensen, C.S.

Year of publication:

2005

Published in:

Department of Civil Engineering, Aalborg University, Denmark, Internal report, ISSN: 1398-6465 R0519.

Remarks:

The first part of the report is similar to parts of the report "Capacity of Piles in Clay".

Capacity of Piles in Sand

A. Augustesen, L. Andersen, and C.S. Sørensen

Abstract: In the literature, numerous methods are available for the prediction of the axial bearing capacity of piles in sand. However, the reliability of the various methods depends on the soil and pile properties. In this report three models are considered, namely API-RP2A (1987 to present), NGI-99, and ICM-96. The first is developed by the American Petroleum Institute, the last by Jardine and his co-workers at Imperial College in London whereas NGI-99 is a calculation method proposed by Clausen and Aas at the Norwegian Geotechnical Institute. The reliability of the methods is studied by comparison with cases from the literature and static field test performed by Danish and Norwegian companies. Further comparisons between predicted and measured capacities are made based on a number of cases from a database established by the Norwegian Geotechnical Institute. In order to make a consistent evaluation of the calculation procedures, conversions related to soil parameters such as CPT tip resistance, SPT resistance, relative density, and internal angle of friction have been employed. The study indicates that the interpretation of the field tests is of paramount importance, both with regard to the soil profile and the loading conditions. Based on analyses of 152 pile tests distributed on 59 sites it is recommended to apply NGI-99 for piles longer than 15m and ICM-96 for piles with penetrations depths less than 15m. However, API-2 provides generally the most reliable description of all the available data, piles with diameters exceeding 0.4m, and steel piles. ICM-96 provides the better estimate of concrete piles and piles with diameters less than 0.4m.

1 Introduction

Design methods for piles in sand have been a controversial matter within geotechnical engineering in many years. Calculation methods have been developed, and the issue has been elucidated through dynamic and static testing procedures. In this report, results of a case-study of the axial bearing capacity based upon measured capacities from static loading tests are presented. According to Clausen and Aas (2001a), several similar studies have been carried out during the last 30 years, see for example: Dennis and Olson (1983), Focht and O'Neill (1985), Briaud et al. (1989), Olson (1988), Toolan and Ims (1988), Tang et al. (1990), Toolan et al. (1990), Randolph et al. (1994), Jardine and Chow (1996), Lehane et al. (2005a,b) and Jardine et al. (2005a).

The capacity of driven piles cannot entirely be predicted by theoretical methods. This is due to the fact that stresses acting against the pile and the mechanical properties of the disturbed pile/soil contact zone are not known (Clausen and Aas, 2001a). Therefore, in the authors opinion a design method must be based on a semi-empirical approach and calibrated against a database containing a representative set of, for example, static loading tests. The purpose of this report is to elucidate the advantages and limitations of such well-known calculation procedures. The methods employed are NGI-99, ICM-96, and API-RP2A (API, 1993), which in the following is denoted API-2. The last is a part of the existing API (American Petroleum Institute) procedure, and it is included in this study because many off-shore piles have been designed based on the API recommendations. ICM-96 has been developed at Imperial College in London by Jardine and his co-workers (Jardine and Chow, 1996, 1997), whereas NGI-99 is proposed by Clausen and Aas (2001b) at the Norwegian Geotechnical Institute (NGI). The comparison is made by testing the methods against a database (denoted AAU after Aalborg University) based on collated loading tests, see Section 3. In addition to this, the calculation procedures have also been tested against an existing NGI database (see Section 4 and Clausen and Aas, 2001b) and against a combination of the two (Section 5). Based on an evaluation of the methods' ability to predict the measured capacities, guidelines are given for the choice of calculation method to use in different circumstances (e.g. load specifications, length of pile, pile material).

Even if a prediction method gives the correct answer for the total pile capacity, it may not give the correct distribution of skin friction with depth. In such cases, the method could be non-conservative for layered soil profiles. In this report, focus is entirely placed on the reliability of a given calculation procedure to predict the correct total pile capacity. Furthermore, the comparison of the models is based upon characteristic values of the soil parameters, so no safeties in terms of partial coefficients or total factor of safety are introduced. The guidelines given are not based on conservative reasons for design but instead sober facts concerning which model that provides the better description of the data available. If the calculation procedures are applied in limit state design, safety should be employed through partial coefficients or a reasonable total factor of safety.

The starting point of this study is the studies done at Norwegian Geotechnical Institute during the last deca-

Figure 1 Flow diagram of PILCAP. The parameter *n* indicates the number of cases. *C*, *TC*, and *SF* denote total capacity, toe capacity, and shaft resistance, respectively. They are all calculated by means of NGI-99, API-2 or ICM-96.

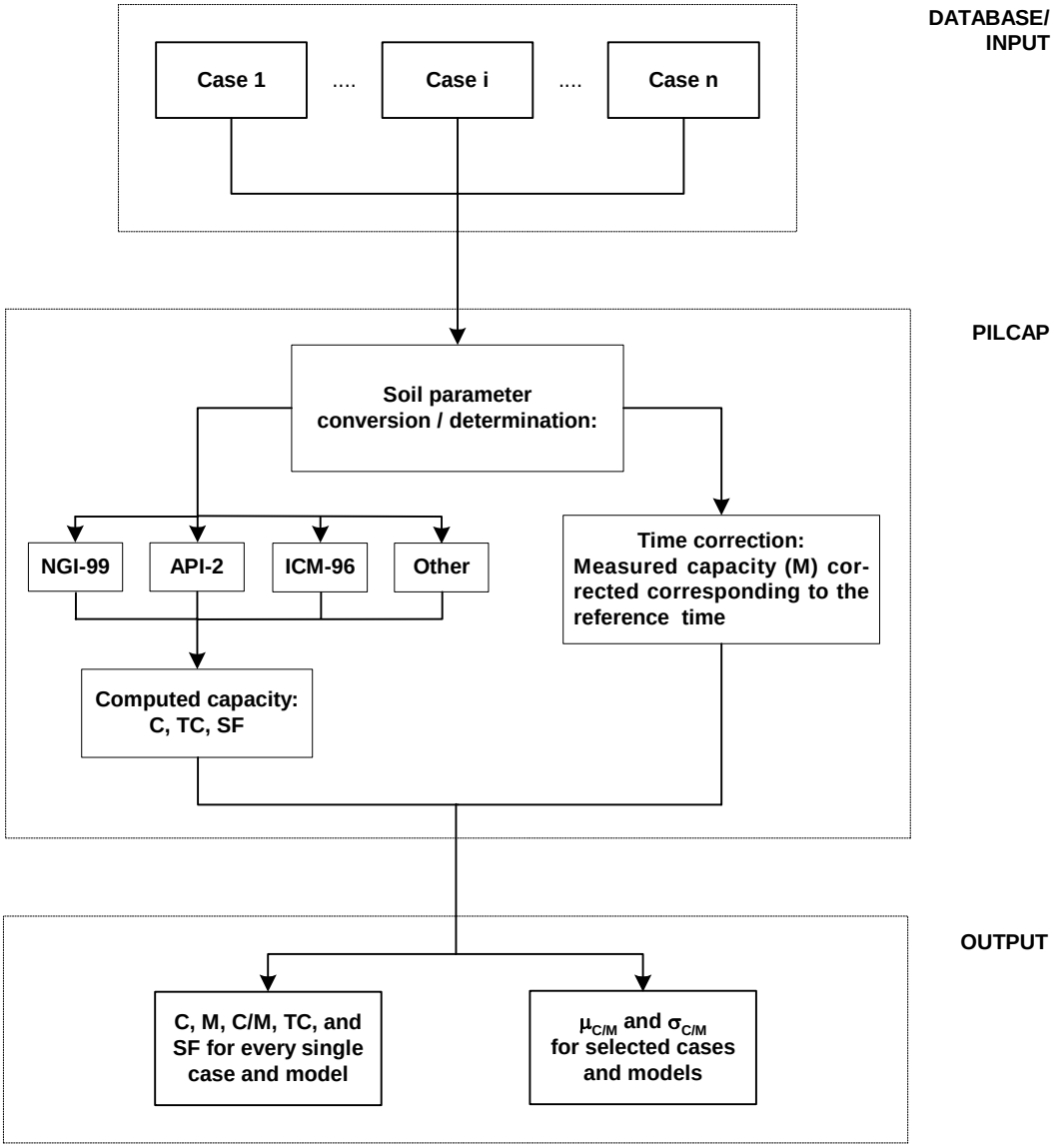

de. Further, this report is supplementary to the work performed by NGI (Clausen and Aas, 2001a,b). A significant number of cases (the AAU database) are added to the NGI database and the conclusions drawn are the results of impartially investigations of the three methods capability to predict measured pile capacities. The database should not be considered to be exhaustive and the study reported herein is therefore preliminary of nature. Recent studies, cf. for example Lehane et al. (2005a,b) and Jardine et al. (2005a) have revealed that more well-document cases are available in the literature. These are not included in the analyses due to limited time. In the future, the references will be thoroughly examined and the cases will be employed in the AAU database.

2 Background

The analyses described in this report are performed by means of the database processing program PILCAP (Figure 1) developed by the Norwegian Geotechnical Institute, see Clausen and Aas (2000, 2001b). In principle, from every single analysed case, PILCAP reads soil and pile data as well as measured capacities based on loading tests and returns quantities of interests,

e.g. the *C/M*-ratio, which is the calculated capacity, *C*, divided by the measured capacity, *M*, at a given reference time. That is, the *C/M*-value is a good parameter to use when investigating a certain method's ability to estimate the measured capacities correctly and when comparing the different calculation procedures. Though numerous other parameters are returned by PILCAP, see Clausen and Aas (2000, 2001b) and Appendix G, focus in this report is paid to the average *C/M*-ratio, $\mu_{C/M}$, and the corresponding standard deviation, $\sigma_{C/M}$, when testing the calculation methods against the data being considered. A mean value, $\mu_{C/M}$, equal to unity represents that, on the average, the predicted capacity equals the measured capacity. For $\mu_{C/M} < 0$, the method under consideration tends to underestimate the capacity, and for $\mu_{C/M} > 0$, the method has a tendency to overpredict the capacity. A measure for scatter exhibited by a predictive method is quantified by the standard deviation, $\sigma_{C/M}$. If $\sigma_{C/M} = 0$ there is no scatter in the results.

Uncertainty is introduced in several ways when comparing measured and calculated capacities:

1. Interpretation of soil conditions,
2. Conversion/determination of soil parameters,
3. Interpretation of loading tests,
4. Calculation procedures,
5. Time correction,
6. Pre-shearing and group effects.

As mentioned, the purpose of this report is to estimate the reliability of the calculation procedures NGI-99, API-2, and ICM-96. Except for pre-shearing effects, group effects and time correction, items 1-3 have been carefully taken care of in order to obtain a consistent treatment of the data and thereby to reach a reliable validation of the methods (item 4). In the remaining part of this section, the most important corrections and assumptions related to PILCAP and this study will be discussed. The subsections refer to Figure 1:

1. **Definition of failure.** All loading tests represented in the databases are analysed based on the same failure criterion, see Section 2.1.
2. **Soil parameter determination**. The different design methods depend on different soil parameters, see Section 2.3 and Appendices B to D. Further, these are not all established in every case considered in this study. In order to obtain a consistent treatment of the available data, PILCAP includes a unique set of rules relating one parameter to another. For each sand layer at least one of the following input parameters that relate to sand strength must be given; 1) CPT tip resistance, q_c, 2) SPT resistance, N, 3) Relative density, D_r, or 4) Angle of internal friction, φ. If one of the mentioned parameters is known, q_c, D_r, and φ can be determined. This is only done if the parameter in consideration is not given as input. For example, if D_r is not given it is determined from other measurements, e.g. cone penetrometer or standard penetration tests. The conversion rules adapted in this study are explained in Appendix A and it is a controversial matter within geotechnical engineering, i.e. the equations are associated with some uncertainty. Other conversion rules may advantageously be adapted. Default values of the mean particle size, d_{50}, and the overconsolidation ratio, *OCR*, are 0.15 mm and 1.0, respectively, if they are not given. Procedures used by PILCAP to generate/convert soil parameters, if they are not given, for the parts of a given pile that is located in clay can be studied in Clausen and Aas (2000) or Augustesen et al. (2005a).
3. **Time correction**. The measured capacities are compared to the calculated capacities, which are based on the design methods and correspond to a given reference time. Since pile capacities vary with time, and since all the loading tests represented in the database are performed at different times after initial driving, PILCAP should in principle include a time function that extrapolate the measured capacity at a given time to the capacity corresponding to the reference time. At the moment no time correction formula is implemented in PILCAP for the parts of the pile located in sand because it is not developed, see Section 2.2. Further, in many of the cases associated with this study the time duration between installation and testing is not known. Therefore, no time correction and no specific reference time have been employed in this study. However, Jardine et al. (2005b) indicate that the Imperial College design method matches the capacity about 10 days after installation.
4. **Prediction methods**. A brief introduction to the calculation procedures NGI-99, API-2 and ICM-96 is given in Section 2.3.

2.1 Failure criterion

The measured capacities associated with each case in the database are based on failure loads corresponding to settlements equal to 0.1*d*, where *d* is the equivalent pile diameter. It is chosen to make use of this definition because both the toe and shaft resistance are fully mobilised for displacements equal to approximately 10% of the equivalent pile diameter for piles in both sand and clayey soils (Vijayvergiya, 1977; API, 2000).

In addition to the failure criterion, the loading test results, and thereby the magnitudes of the measured capacities, may also be influenced by group effects and

Figure 2 Schematic illustration of a) Zones created during driving and b) Relative density in the soil surrounding the pile and arching mechanisms around the pile shaft due to driving.

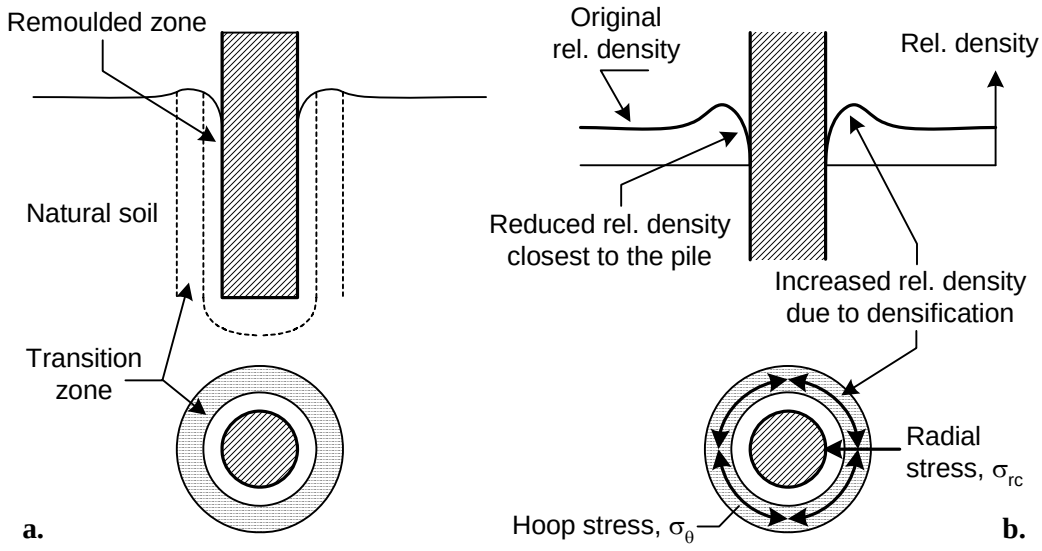

pre-shearing effects. That is, if a pile has been tested more than one time the effects of previous loading tests may influence the capacity. Bergdahl and Hult (1979) and Jardine et al. (2005b) report that pre-shearing effects can be substantial for piles in sand. Jardine and his co-workers found that any aged pile loses a substantial part of its capacity as it undergoes first time failure and relaxation to zero load. If the pile is allowed to rest, it develops a degree of capacity recovery. But pre-tested piles appear to always fall short of their "intact equivalents" over the age ranged investigated. In contrast, for piles in clay it is observed that pre-shearing results in higher capacities compared to the "intact equivalents", see for example Karlsrud and Haugen (1986) and Bullock et al. (2005a,b). However, Bergdahl and Hult (1981) postulate in the light of their tests that it is not possible to show any change in capacity as a result of previous load tests for piles in clay.

Pre-shearing effects have not been taken into consideration even though some of the piles represented in the databases have been subjected to several loading tests. Group effects are also not considered here.

2.2 Time correction

At the moment no time correction formula is implemented in PILCAP for the parts of the pile located in sand because it is not developed. However, in many of the cases associated with this study the time duration between installation and testing is unfortunately not known. According to Jardine et al. (2005b) pile capacity calculations that take no account of time will be subjected to considerable error unless they consider only a tightly specified range. Therefore, one of the goals of the future is to develop a time function, which relates capacity with time. This requires well-documented pile load tests.

The starting point of future studies into time effects and capacity for piles in sand could be Jardine et al. (2005b), Chow et al. (1997, 1998), and Axelsson (1998a, 2002). In the literature long-term set-up of piles in non-cohesive soil can roughly be divided into two main time-dependent causes, based on Schmertmann (1991) and Chow et al. (1996):

1. Stress relaxation (creep) in the surrounding soil arch, which leads to an increase in horizontal effective stress acting against the pile shaft, see Figure 2, i.e. long-term changes in the stress regime surrounding the piles influence set-up magnitudes.
2. Soil ageing leading to an increase in dilatancy and stiffness of the soil, which implies large horizontal effective stresses acting against the shaft during loading.

Both these mechanisms start directly after pile installation and are, to a certain degree, also a part of the short-term set-up that takes place during the dissipation of excess pore pressures (Axelsson, 1998a).

Chow et al. (1998) postulate that changes in stress regime controls set-up magnitudes. This is discussed in the following. Lehane et al. (1993) conclude that the

local shear stresses, τ_f, acting against the pile shaft at failure follow the simple Coulomb failure criterion:

$$\tau_f = \left(\sigma_{rc} + \Delta\sigma_{rd}\right) \cdot \tan\left(\delta\right) \quad (1)$$

where σ_{rc} is the radial effective stress after installation; $\Delta\sigma_{rd}$ is the dilatant increase in local effective stress during pile loading; and δ is the ultimate interface shear friction angle. Equation (1) is the combination of eqs. (D.2) and (D.3) employed in connection with the ICM-96 method, see Appendix D. According to Chow et al. (1998), changes in σ_{rc} with time controls the magnitude of set-up and is therefore the dominant factor when considering set-up. How σ_{rc} can increase over time can be explained by investigating Figure 2. Robinsky and Morrison (1964) have among others shown by laboratory model pile tests that the degree of sand compaction at the pile tip during driving can create a thin "sleeve" of very loose sand around the pile shaft. That is, during driving or immediately after, a remoulded zone of soil arise near the pile surface (Figure 2.a). The relative density is very low and the radial effective stresses acting against the pile are also low. Between the remoulded zone and the natural undisturbed soil a so-called transition zone arises. The relative density of the sand in that zone is very large and high tangential stresses, σ_θ (hoop stresses), can be sustained in the sand due to arching (Figure 2.b). The transition zone is unstable and over time, the tangential hoop stresses, σ_θ, relax whereby the soil grains rearrange themselves into a more compact form around the pile. This implies that the radial stress, σ_{rc}, and thereby the pile capacity increase over time.

In contrast to Chow et al. (1997, 1998), Axelsson (1998a, 2002) indicate that the most probably ruling mechanism is soil ageing and especially the effects of increasing dilatant behaviour with time. The dilation tendency is to some extent constrained during loading by the surrounding soil resulting in horizontal effective stresses, $\Delta\sigma_{rd}$, see eq. (1), and thereby capacities, increasing with the time between pile driving and testing. Lehane and Jardine (1996) indicate, based on Boulon and Foray (1986), that sand stiffness, G, and pile/soil dilation affect the magnitude of $\Delta\sigma_{rd}$ during loading and that $\Delta\sigma_{rd}$ is inversely proportional to pile radius, see eq. (D.5) in Appendix D. Therefore, increases in G and pile/soil dilation due to ageing may increase the capacity significantly (Axelsson, 1998a, 2002). Increased dilatancy with time is related to rearrangement of sand particles into a more compact configuration as suggested by Mesri et al. (1990) and Schmertmann (1991). The reorientation depends on pile/soil interaction and the interaction between sand grains. Therefore, surface roughness, interlocking between the surface and grains and between grains are important parameters (Mesri et al., 1990). That the surface roughness has a strong effect on dilation of the soil has been observed in interface tests by Uesugi et al. (1988). In contrast, Åstedt et al. (1992) did not find any correlation between angularity of sand grains and an increase in bearing capacity. Joshi et al. (1995) postulate that dissolution and precipitation of mainly salts and possibly silica at particle contacts and interspaces may also contribute to increased dilatant behaviour. Mitchell and Solymar (1984) support these conclusions.

The governing mechanism behind soil ageing and stress relaxation is to some extent rearrangement of sand grains. In order to change the sand properties in the sense of increasing dilatancy the sand particles must be more compactly packed around the pile, which implies that the tangential hoop stresses must deteriorate with time. This further implies that the horizontal effective stresses acting against the pile surface increase with time resulting in changes in the stress regime. That is, the two processes leading to set-up are interrelated. Axelsson (1998a, 2002) postulates that changes in sand properties are predominant whereas Chow et al. (1998) propose that changes in the stress regime is the major factor. In the literature, the interrelated processes of rearrangement of sand particles and deterioration of hoop stresses with time are both called creep and stress relaxation but in reality it is probably a combination of the phenomena. It should be mentioned that chemical processes (including corrosion) which might bond sand particles to the pile surface, forcing the principal displacement shear band into the sand mass, influence set-up (Chow et al., 1997).

2.3 Prediction methods

Characteristics, of the calculation procedures employed, are brief listed below and some of the dominant parameters related hereto are indicated in Figure 3.

1. **API-2.** The method assumes that the shaft resistance is a function of the horizontal effective stress acting against the pile wall, σ_h, and the soil/pile friction angle, δ. σ_h is taken as the effective overburden pressure, p_0, times the coefficient of lateral earth pressure, K. The end bearing capacity depends on the vertical effective stress at the pile toe and a dimensionless bearing capacity factor, N_q. Where detailed information such as in situ cone tests, strength tests on high quality samples, model tests, or pile driving performance is not available, design parameters can be estimated based on the density of the sand. The density is divided into five groups; very loose, loose, medium, dense, and very dense, but they are not quantified in terms of, for example, relative density, D_r. Therefore, API-2

Figure 3 Factors influencing shaft and toe resistance for piles sand.

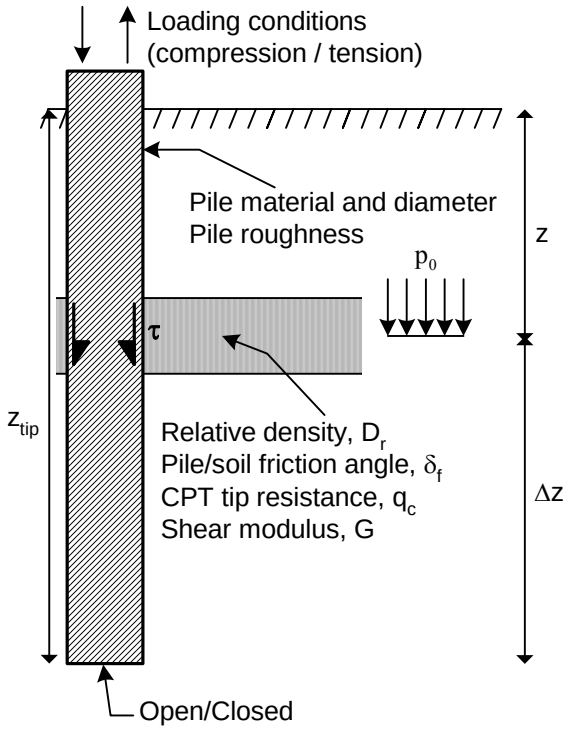

gives the designer considerable freedom to choose parameters. More information on API-2 can be found in API (1993) and Appendix C.

2. **NGI-99.** The key soil parameter when determining the unit shaft resistance at a given depth, z, is the relative density, D_r. It should be mentioned that if D_r is not given as input, the value of D_r can be determined based on the CPT tip resistance, q_c, the SPT resistance, N, or the internal angle of friction, φ (Appendix A). NGI-99 takes effects such as loading conditions and whether the pile is driven open-ended or closed-ended into consideration when estimating the shaft resistance. In addition to this, "friction fatigue effects" are taken care of by the implementation of a length factor. The unit toe resistance for closed-ended piles or piles driven open-ended behaving in a plugged way is a function of primarily the CPT tip resistance, q_c, and the relative density, D_r. Scale effects due to difference in size between a pile and a cone penetrometer are taken into consideration by the factor, F_{Diam}. Furthermore, a sand strength factor, F_{Dr}, depending on D_r and a stress level correction factor, F_{Sigz}, depending on the vertical effective stress, p_0, are included. For unplugging open-ended piles two methods are employed for evaluation of the toe resistance. One of these methods is based upon theoretical arching considerations (Murff et al., 1990) combined with the observation that piles with $D_r < 0.3$ do not plug (Chow, 1996). The other method is based upon the full scale dowel penetration resistance measurements carried out at the Condeep Beryl A platform (Clausen, 1976; Lunne and Kvalstad, 1982). The method to employ can be chosen freely. More information on NGI-99 can be found in Appendix B.
3. **ICM-96.** The local shaft resistance at failure, τ_f, is described by Coloumbs failure criterion, i.e. τ_f is a function of the radial effective stress, σ_{rf}, acting against the pile wall and the pile/soil friction angle, δ. σ_{rf} is divided into two parts; a contribution from the radial effective stresses, σ_{rc}, once equilibrium has been reached after installation and a contribution from the dilatant increase in local effective stress, $\Delta\sigma_{rd}$, during pile loading. σ_{rc} is a function of the CPT tip resistance, q_c, the vertical effective stress, p_0, and the ratio between the distance from point considered to the toe, Δz, and the pile radius (Figure 3). That is, ICM-96 takes "friction fatigue effects" into consideration. $\Delta\sigma_{rd}$ depends on the shear modulus of the soil, G, the pile roughness, and the radius of the pile. ICM-96 takes effects such as loading conditions and whether the pile is driven open-ended or closed-ended into consideration when estimating the shaft resistance. For example, ICM-96 incorporates that piles loaded in compression experience greater shaft resistances than piles loaded in tension and that piles driven

Table 1 Specification of AAU data. For more information on the AAU database, see Appendix E.

ID	Site, Reference	No. of piles	With time [a]	No time [b]	$Q_{r,soil}$ / $Q_{r,pile}$ [c]	Soil conditions			Depth [m] [g]
						q_c [MPa] [d]	D_r [-] [e]	φ [°] [f]	
01	Aalborg Østhavn [h]	1	-	1	2 / 4	13.3 [l]	0.8	39.1	17.7
02	Hanstholm-Århus vej [i]	1	-	1	3 / 3	10.2 [l]	0.77	38.8	16.8
03	Dunkirk Chow et al. (1998) [j]	3	2	1	4 / 4	17.5 – 20.1 [l]	0.89 – 0.9	40.4 – 40.6	11.6, 22.1
04	Motorvejbru Drammen Tvedt and Fredriksen (2003)	4	-	4	4 / 4	5.5 [l]	0.52 [l]	36.0 [l]	11, 17
05	Motorvegbru Drammen Tvedt and Fredriksen (2003)	4	2	2	4 / 4	3.8 – 5.2 [l]	0.39 – 0.43 [l]	34.2 – 34.3 [l]	15, 25
06	Vårby Axelsson (1998a,b,2000,2002)	1	1	-	4 / 4	3.3 [l]	0.28	31.9	12.8
07	Aalborg Værft [k]	1	-	1	2 / 3	9.2	0.64	37.0 [l]	17.5
08	Kolding forrenseanlæg [h]	1	-	1	1 / 4	10.5 [l]	0.71	37.9	18.6
09	Kolding forrenseanlæg [h]	1	-	1	1 / 4	12.5 [l]	0.72	38.1	19
	Total	17	5	12	-			-	-

a) Piles have been tested more than one time.
b) Piles have only been subjected to one static test.
c) Quality ranking of soil and pile data: 0 = not known, 1 = low, 2 = average, 3 = high, 4 = very high (super piles).
d) Average CPT tip resistance along the pile shaft.
e) Average relative density along the pile shaft.
f) Average angle of internal friction along the pile shaft.
g) Pile penetration depth.
h) Material provided by Per Aarsleff A/S, Denmark.
i) Material provided by COWI A/S, Denmark.
j) In addition: Chow et al. (1996, 1997), Brucy and Menuier (1992), Brucy et al. (1991)
k) Material provided by Geoteknisk Institut, Denmark (GEO – Danish Geotechnical Institute).
l) Parameter given in the case considered.

closed-ended obtain shaft resistances that are greater than the capacities obtained for piles driven open-ended. The unit toe resistance is a function of primarily the CPT tip resistance, q_c. For closed-ended piles or piles driven open-ended behaving in a plugged way scale effects due to difference in size between a pile and a cone penetrometer are also employed in the model. Further, ICM-96 incorporates that piles driven closed-ended experience toe capacities that are 50% greater compared to piles driven open-ended behaving in a plugged manner. More information on ICM-96 can be found in Jardine and Chow (1996, 1997) and Jardine et al. (1998) as well as Appendix D.

In some of the cases associated with this study, the shaft of the pile is partly embedded in clay and the toe may also be located in clay. How the three models tackle this can be studied in API (1993), Clausen and Aas (2000), and Jardine and Chow (1996).

Norwegian Geotechnical Institute and Imperial College, London, have modified their calculation procedures for piles in sand upon the final completion of the research reported in this document. For more details on the modified versions of the Imperial college model and the NGI approach, see Jardine et al. (2005a,c) and Clausen et al. (2005). According to Jardine et al. (2005c), the new sections of the model include pile ageing; cyclic loading; group action; pile shape and seismic effects, as well as applications in calcareous and micaceous sand. Further, more detailed recommendations are made on parameter selection and practical implementation. So fundamentally, the governing static equations remain more or less unchanged. In the modified NGI-model the relative density, D_r, and CPT tip resistance, q_c, are still the important soil parameters. The fundamental equations are modified compared to NGI-99 and importantly, the modified version includes a term that is pile material dependent, i.e. the calculated shaft resistance depends on whether the pile material is concrete or steel.

According to Clausen et al. (2005) and Lehane et al. (2005c) Fugro Engineers has also proposed a new design method for piles in sand (Fugro, 2004). At the moment, the authors have no information on this method. Lehane and his co-workers at University of Western Australia (UWA) have also developed a calculation procedure for piles in sand, see Lehane et al.

Figure 4 Range covered by the AAU database in terms of penetration depth and average relative density, D_r, along the pile shaft. Numbers associated with each point refer to site identification numbers (see Table 1).

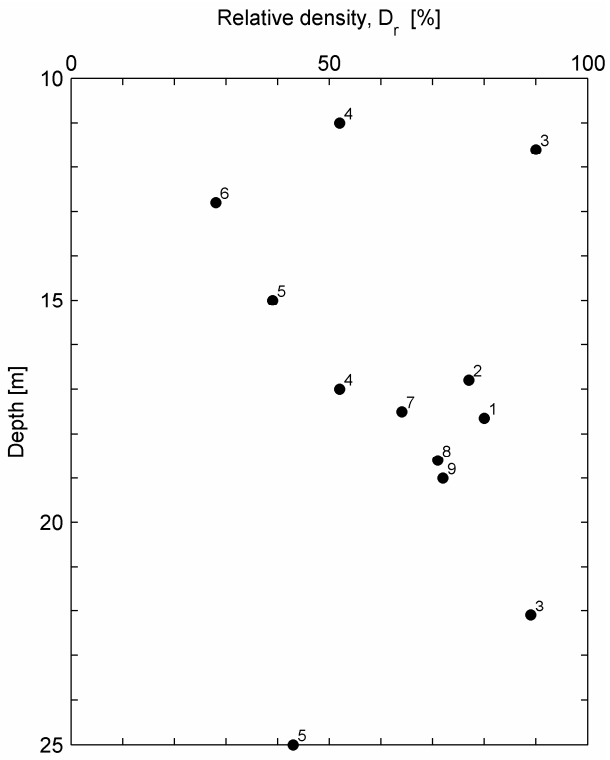

(2005a,b,c). At first sight, the UWA-model is based on the same fundamental considerations regarding pile behaviour as ICM-96, see Appendix D. Neither the Fugro nor UWA-model is taken into consideration in this study.

3 AAU data

An overview of the data initially collated in connection with this study (AAU database) is presented. The cases have been found in the literature and provided by Norwegian and Danish companies. The data were collected based on the following criteria:

1. Only loading tests in which failure occurs are included. In this case failure is reached when the movements equal 10% of the pile diameter.
2. Only cases with reasonably good information regarding soil, pile, and testing conditions have been employed. Both offshore and onshore piles are included and the different cases are divided into five groups, i.e. Group 0 to 4, depending on the quality of the soil and pile data available. Cases belonging to Group 4 ($Q_{r,soil}$ = 4 and $Q_{r,pile}$ = 4 as indicated in Table 1) are especially well-described in terms of pile, soil, and test information, whereas Group 0 contains the cases of particularly poor quality.

Details regarding the available data are presented in Table 1. In summary:

1. If a pile is driven to a given depth and then tested and hereafter driven further down and tested, the pile will be counted as "two" piles and included in the "no time" category in Table 1.
2. The average strength parameters along the pile shaft are weighted in terms of surface area. That is, a unique average relative density, D_r, an average CPT tip resistance, q_c, and an average internal angle of friction, φ, are associated with every single pile. For more information on average strength parameters, see Augustesen et al. (2005b).
3. 17 piles distributed on nine sites have been included in the analyses.
4. 12 piles have been subjected to loading tests one time whereas five piles are tested more than once. In total, 32 tests on piles in sand have been included.
5. Three piles are loaded in tension, 12 in compression, and two piles are both tested in compression and tension.
6. The embedded lengths of the piles vary between 11 and 25 m.

Figure 5 NGI-99, API-2, and ICM-96 tested on AAU data. Ratios, *C/M*, of calculated capacities, *C*, divided by associated measured capacities, *M*, are plotted as function of pile penetration depth and average relative density, D_r. ● and ○ refer to piles driven closed-ended and open-ended, respectively, and loaded in compression. Δ represents piles driven open-ended but loaded in tension. The plot labels refer to site IDs (see Table 1).

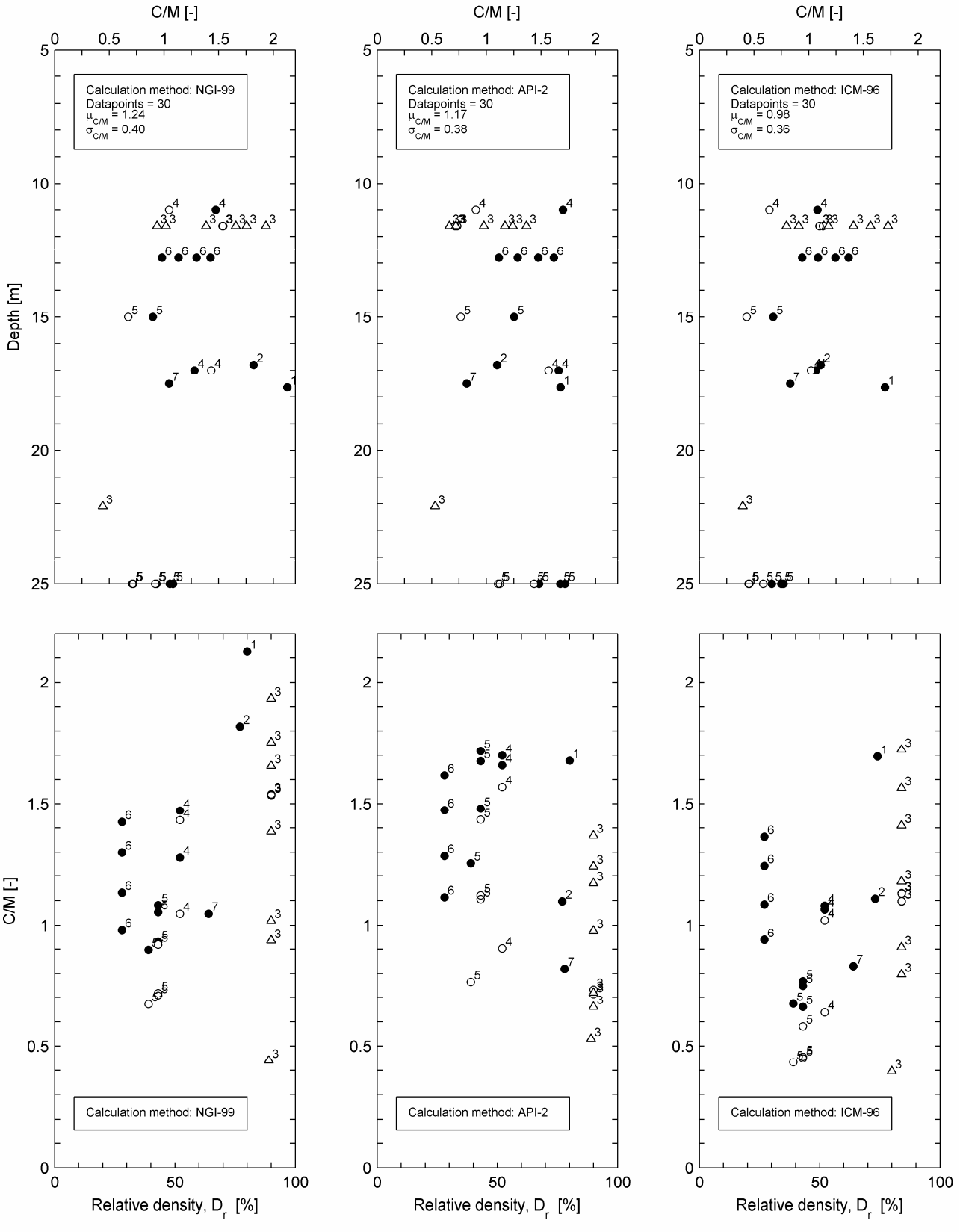

Table 2 NGI-99, API-2, and ICM-96 tested against the AAU data.

	No. of piles / No. of sites	NGI-99 $\mu_{C/M}$ / $\sigma_{C/M}$ [a)]	API-2 $\mu_{C/M}$ / $\sigma_{C/M}$ [a)]	ICM-96 $\mu_{C/M}$ / $\sigma_{C/M}$ [a)]
All piles[b)]:				
All piles in category	32 / 9	1.39 / 0.70	1.25 / 0.50	1.06 / 0.48
All piles:				
All piles in category	30 / 7	1.24 / 0.40	1.17 / 0.38	0.98 / 0.36
Piles loaded in compression	23 / 7	1.23 / 0.37	1.23 / 0.37	0.93 / 0.32
Piles loaded in tension	7 / 1	1.30 / 0.53	0.95 / 0.32	1.14 / 0.47
Piles driven open-ended	17 / 3	1.22 / 0.44	0.97 / 0.31	0.94 / 0.41
Piles driven closed-ended	13 / 6	1.27 / 0.36	1.43 / 0.29	1.02 / 0.30
Steel:				
All piles in category	23 / 3	1.19 / 0.39	1.13 / 0.39	0.91 / 0.36
Piles loaded in compression	16 / 3	1.15 / 0.33	1.21 / 0.40	0.81 / 0.27
Piles loaded in tension	7 / 1	1.30 / 0.53	0.95 / 0.32	1.14 / 0.47
Piles driven open-ended	17 / 3	1.22 / 0.44	0.97 / 0.31	0.94 / 0.41
Piles driven closed-ended	6 / 2	1.12 / 0.22	1.58 / 0.18	0.83 / 0.19
Concrete:				
All piles in category	7 / 4	1.40 / 0.43	1.30 / 0.31	1.18 / 0.29
Piles loaded in compression	7 / 4	1.40 / 0.43	1.30 / 0.31	1.18 / 0.29
Piles loaded in tension	- / -	- / -	- / -	- / -
Piles driven open-ended	- / -	- / -	- / -	- / -
Piles driven closed-ended	7 / 4	1.40 / 0.43	1.30 / 0.31	1.18 / 0.29
Group 4 [c)]:				
All piles in category	27 / 4	1.20 / 0.37	1.16 / 0.38	0.95 / 0.35
Piles loaded in compression	20 / 4	1.16 / 0.30	1.24 / 0.37	0.88 / 0.29
Piles loaded in tension	7 / 1	1.30 / 0.53	0.95 / 0.32	1.14 / 0.47
Piles driven open-ended	17 / 3	1.22 / 0.44	0.97 / 0.31	0.94 / 0.41
Piles driven closed-ended	10 / 3	1.15 / 0.20	1.50 / 0.21	0.96 / 0.24

a) μ and σ are the mean value and the standard deviation of the *C/M*-ratios.
b) Cases with IDs 8 and 9, Kolding forrenseanlæg, are only included in these investigations.
c) This category includes all cases, where soil and pile data belong to Group 4 ($Q_{r,soil} = Q_{r,pile} = 4$, cf. Table 1), i.e. cases, where soil and pile data are especially well-described.

7. Seven piles are driven open-ended whereas 10 are driven closed-ended.
8. Seven piles have circular cross sections whereas six piles have rectangular cross sections. The remaining four piles are H-profiles, which are equated with "solid/closed" circular profiles.
9. Of the 17 piles, 11 are made of steel and six of concrete. Hence, no timber piles are included in the database.

The range covered by the data in terms of penetration depth and average relative density, D_r, is sketched in Figure 4. Soil and pile data for the different sites are shown in Appendix E.

3.1 Results of analyses

In Figure 5, *C/M*-ratios (calculated capacity, *C*, divided by the measured capacity, *M*) are plotted as function of pile penetration depth and average relative density, D_r, for every single pile depending on calculation method. Results of more detailed analyses are shown in Table 2 and Table 3. It can be summarised that:

1. ICM-96 provides a better description of the data compared to NGI-99 and API-2 regarding the magnitude of the average *C/M*-ratio. Generally, NGI-99 and API-2 overestimate the measured capacities whereas ICM-96 provides an underestimate.
2. Figure 5 indicates that there is a skew distribution of *C*/*M*-ratios with penetration depth especially when applying NGI-99 and ICM-96 to the available data. This is confirmed by the results shown in Table 3. For both NGI-99 and ICM-96 the average *C/M*-ratios for piles longer than 15m are significantly lower than the average *C/M*-ratios obtained when applying NGI-99 and ICM-96 to piles shorter than 15m. The skew distribution of data points is mainly due to the low *C/M*-ratios associated with the case with ID 5, Motorvegbru Drammen. Opposite tendencies are observed when testing the three calculation methods to piles in clay, see Augustesen et al. (2005a).
3. On the average, API-2 overestimates the capacity of piles installed in depths greater than 15m more than the capacity of piles installed in depths less than 15m, see Table 3. The reason might be that API-2 does not include a length factor accounting

Table 3 NGI-99, API-2, and ICM-96 tested against piles with penetration depths greater or less than 15m.

Depth [a]	No. of piles	NGI-99 $\mu_{C/M}$ / $\sigma_{C/M}$ [b]	API-2 $\mu_{C/M}$ / $\sigma_{C/M}$ [b]	ICM-96 $\mu_{C/M}$ / $\sigma_{C/M}$ [b]
< 15	16	1.39 / 0.29	1.07 / 0.35	1.15 / 0.27
> 15	14	1.08 / 0.46	1.28 / 0.39	0.78 / 0.35

a) Penetration depth, [m].
b) μ and σ are the mean value and the standard deviation of the *C/M*-ratios.

for "friction fatigue effects". In contrast, as noted in item 2 ICM-96 and NGI-99 experience the opposite tendencies but they also take "friction fatigue effects" into consideration, cf. Section 2.3 and Appendices A and D.

4. Piles driven open-ended or closed-ended but loaded in compression as well as piles driven open-ended and loaded in tension have been investigated. It should be noticed that the number of piles in each group are relatively small implying that the conclusions drawn are encumbered with great uncertainty.
5. Generally, API-2 provides a more reliable estimate of the capacity of piles loaded in tension compared to NGI-99 and ICM-96. In contrast, the capacity of piles loaded in compression is best predicted by ICM-96.
6. On the average, API-2 describes piles driven open-ended better than NGI-99 and ICM-96.
7. The accuracy in the prediction of steel piles is greater compared to concrete piles. In continuation of this, it should be noted that that all the steel piles belong to Group 4, which are characterized by well-described soil and pile data.
8. ICM-96 generally provides the better description of the piles belonging to Group 4. It should be noted that the pile tests associated with the case with ID 3, Dunkirk, constitute approximately 40% of the piles belonging to this group. Further, the case is a part of the cases forming the basis of ICM-96. This may contribute to the fact that ICM-96 provides a better estimate of the capacities of piles belonging to Group 4 compared to the two other methods.
9. In general, the *C/M*-ratios decrease with increasing time between driving and testing. For example, for Pile D associated with the case with ID 6, Vårby, *C/M*-ratios equal 1.42, 1.30, 1.13, and 0.98, see Figure 5 and Appendix G, when the given pile has been situated 1, 8, 122, and 667 days in the ground, respectively. The calculation method employed is NGI-99. The calculated capacity, *C*, is assumed constant for a given pile located at a given depth in given soil conditions. Therefore, if *C/M* decreases with increasing time between installation and testing, *M* must increase with time after driving. In addition to time between driving and testing, pre-shearing effects may also have a significant effect on the measured capacities, *M*, see Section 2.1. The above-mentioned indicates that a time function, which relates time and capacity, is needed in order to obtain a consistent evaluation of the different calculation methods. As mentioned in Section 2.2, Jardine et al. (2005b) also postulate that pile capacity calculations that take no account of time will be subjected to considerable error unless they consider only a tightly specified range. One of the goals of the future is to develop a time function for piles in sand.
10. Some results deviate more than others, e.g. the case with ID 1, Aalborg Østhavn, and the case with ID 2, Hanstholm-Århus vej. This can be due to uncertainty in the determination of the CPT tip resistance, q_c. For the case with ID 3, Dunkirk, there is some uncertainty in the determination of failure loads, plug ratios and soil conditions. Furthermore, dynamic tests have also been performed on the test site. For the cases with IDs 4 and 5, Motorvegbru Drammen, dynamic tests may influence the measured capacities from static tests. In addition, information regarding plug ratios is sparse. For the case with ID 6, Vårby, reaction piles and dynamic tests may play an important role on the measured capacities and in connection with the case with ID 7, Aalborg Værft, failure was not reach and the soil profile is not well defined. The above mentioned listed reasons are not comprehensive. For further details, Appendix E can be studied for every single case.
11. Cases with IDs 8 and 9, Kolding forrenseanlæg (see Table 1 and Appendix E) are omitted in the rest of this report because they are statistical deviants (*C/M* $\approx$ 3.5). For example, if NGI-99 is tested on the AAU data, the average *C/M*-ratio is 1.39 if Kolding forrenseanlæg is included and 1.24 if it is omitted. The *C/M*-ratios may be affected by the fact that uncertainty is associated with the determination of the CPT based strengths of the sand layers. Furthermore, the deepest located sand layers associated with the soil profile are virtually extended approximately 5m because no information regarding the soil associated with the lower 5m of the pile is available. Even though the cases are excluded in the analyses reported herein they are a part of the database.

4 NGI data

Most offshore piles have been designed based on API recommendations. Therefore, the motivation of the work done by Clausen and Aas (2001b) is:

Table 4 Calculation methods tested against the NGI database.

	Sand-I [a] $\mu_{C/M}$ / $\sigma_{C/M}$ [g]	Sand-II [b] $\mu_{C/M}$ / $\sigma_{C/M}$ [g]	Sand-III [c] $\mu_{C/M}$ / $\sigma_{C/M}$ [g]	Sand-IV [d] $\mu_{C/M}$ / $\sigma_{C/M}$ [g]	Group 4 [e] $\mu_{C/M}$ / $\sigma_{C/M}$ [g]	All piles [f] $\mu_{C/M}$ / $\sigma_{C/M}$ [g]
Number of pile tests	28	36	64	80	34	122
API-1	0.62 / 0.20	0.55 / 0.28	0.59 / 0.36	0.74 / 0.35	0.65 / 0.35	0.70 / 0.35
API-2	0.85 / 0.22	0.76 / 0.38	0.86 / 0.48	0.98 / 0.45	0.88 / 0.56	0.93 / 0.43
ICM-96	0.79 / 0.24	0.81 / 0.29	0.88 / 0.29	0.88 / 0.26	0.93 / 0.21	0.87 / 0.27
NGI-99	0.93 / 0.31	0.76 / 0.18	1.08 / 0.44	1.09 / 0.35	1.00 / 0.21	1.08 / 0.41

a) Data taken directly from Olson (1988).
b) Data taken directly from Randolph et al. (1994).
c) Data taken directly from Chow (1996).
d) Pile test source data collected and interpreted as part of the study presented in Clausen and Aas (2001b).
e) A subset of Sand-IV. NGI-99 is calibrated based on these cases.
f) Total number of different pile tests in the NGI database. Combination of Sand-I, Sand-II, Sand-III, and Sand-IV.
g) μ and σ are the mean value and standard deviation of *C/M*-ratios.

1. To check how well the API-RP2A method (API, 1993) predicts well-documented pile tests compared to other calculation methods.
2. To develop a revised calculation procedure, denoted NGI-99, which better predicts the actual load test data compared to other existing methods.

In case of piles located in sand, API-2 was compared to:

1. NGI-99 (Clausen and Aas, 2001b and Appendix B).
2. API-1 (API-RP2A, 1972 to 1984), which is replaced by API-2 (API, 1993 and Appendix C).
3. ICM-96 (Jardine and Chow, 1996; Jardine et al., 1998 and Appendix D).

In Clausen and Aas (2001b) and also in this report, most effort is put into the comparison of API-2, ICM-96 and NGI-99 because:

1. API-2 has replaced API-1. Therefore, API-1 has mainly a historical interest. Further, API-1 gives the designer too much freedom to choose key soil parameters.
2. API-2 produces a skew distribution of *C/M*-values when plotted against for example the depth. That is, for piles shorter than 10-15m, API-2 underestimates the capacity, whereas it overpredicts the capacity of longer piles. This is also observed when testing API-2 against the AAU data, see Section 3.1.
3. API-2 is sensitive towards the designer's judgement. Small changes in D_r and silt content may produce important changes in the calculated capacity, see Appendix C.
4. ICM-96 gives capacities that on the average are approximately 10% too low.
5. NGI-99 is a new design method.

The calculation procedures are compared based on a database established by the Norwegian Geotechnical Institute (NGI) over the last decade. Static load tests and matching soil and pile data, which quality are of a more or less high standard, are included in the database. Both off- and onshore piles are included and the database is mainly based on published data. In Section 5 the AAU and NGI data are collated and API-2, ICM-96 and NGI-99 are tested, by means of PILCAP, against all data.

Facts concerning the NGI database are as follows:

1. The database consists in total of 122 pile tests.
2. 52 sites have been investigated and the piles range from few meters to above 50m.
3. Piles loaded in tension and compression as well as piles driven open-ended and closed-ended are included.
4. A subset consisting of 34 piles denoted "super piles" are used to calibrate and develop the NGI-99 method (Clausen and Aas, 2001b). These cases belong to Group 4 ($Q_{r,soil}$ = 4 and $Q_{r,pile}$ = 4 as explained in Section 3). They are especially well-described in terms of pile, soil, and test information. Therefore, they have been carefully checked against the data presented in the original publications.
5. As indicated in Table 4, the NGI database is divided into primarily four groups denoted Sand-I, Sand-II, Sand-III, and Sand-IV. Some cases are included in more than one group, which is the reason why the total number of pile tests (122) does not match the sum of all pile tests related to Sand-I, Sand-II, Sand-III, and Sand-IV (Table 4).

4.1 Results and recommendations

In Table 4, average *C/M*-ratios obtained by applying the calculation methods to the NGI data are shown. The methods for piles in sand generally underestimate the measured capacities. Table 4 indicates that NGI-99

generally provides the best fit. Further, NGI-99 is calibrated against pile tests belonging to Group 4, which of course implies a low standard deviation, $\sigma_{C/M}$, and a mean value, $\mu_{C/M}$, equal to unity. There is no particular reason why NGI-99 on the average underestimates the capacities of Sand-II piles significantly with low scatter.

Generally, API-1 fails to match the measured capacities, which might be due to the fact that the method gives the designer freedom to choose the key soil parameters. In addition to this, it is notably that when applying ICM-96 to the Sand-III piles from which it is calibrated, a relatively low average *C/M*-ratio ($\mu_{C/M}$ = 0.88) is obtained. For detailed comments concerning the results presented in Table 4, see Clausen and Aas (2001b). It should be mentioned that the calculation methods for piles in sand generally are more unreliable in predicting piles capacities compared to the models for piles in clay (Augustesen et al., 2005a).

Clausen and Aas (2001b) conclude and recommend the following for piles in sand:

1. Capacities of piles longer than 15-20m in loose to dense sands loaded in tension are likely to be over-predicted by API-2. The same tendency is also seen for ICM-96 but to a lesser extent. That is, API-2 should not be used for such kinds of piles.
2. For piles loaded in compression, API-1 and API-2 seem to overpredict the capacity in loose to medium dense sand.
3. For piles loaded in tension the conservative NGI-99 method should be used.
4. For piles loaded in compression it is proposed to calculate the capacity by both ICM-96 and NGI-99. If the two methods differ significantly, the designer should find out why and then select the method to use.
5. NGI-99 and ICM-96 seem to correctly account for the effects caused by the pile tip condition, i.e. whether the piles are driven open- or closed-ended. In contrast, API-2 does not.
6. For the piles belonging to Group 4, the pile diameter does not have a significant influence on the *C/M*-ratios. Anyway, NGI-99 works better for large piles compared to the other suggested methods.
7. It is recommended to include more high quality cases in the database, to investigate the implemented conversion procedures (for example the conversion from SPT/CPT-values to relative densities D_r) because the results are very sensitive towards these correction methods, to investigate the effects of layered soil profiles and to study the development of pile capacity with time. Furthermore, it should be checked that the models for piles in clay and sand produce a smooth transition as the soil changes from sand to silt to clay.

As mentioned, the NGI database consists, in total, of 122 different pile tests distributed on 52 sites. Results of testing NGI-99, API-2, and ICM-96 against these data are shown in Table 4. It can be concluded that NGI-99 and API-2 provide the better description of the data in terms of average *C/M*-ratio.

5 Combination of AAU and NGI

In this section, the three calculation procedures are tested against a combination of the AAU and NGI data. Initially, it should be mentioned that the total number of pile tests analysed are 152. 59 sites constitute the cases. The input file for the combined AAU and NGI database is shown in Appendix F. The corresponding output file can be seen in Appendix G.

5.1 Results and recommendations

Average *C/M*-ratios, $\mu_{C/M}$, and standard deviations, $\sigma_{C/M}$, obtained when applying NGI-99, ICM-96, and API-2 to a combination of the AAU and NGI data are shown in Table 5. The following comments and conclusions can be drawn:

1. In terms of average *C/M*-ratio, API-2 provides a better description of the measured capacities compared to NGI-99 and ICM-96, which are equally precise. NGI-99 overpredicts whereas ICM-96 underestimates the capacities.
2. NGI-99 and API-2 describe steel piles and Group 4 piles better than concrete piles, whereas the opposite tendencies are observed for ICM-96. That is, ICM-96 should apply for concrete piles. Even though the number of pile tests is few, it is worth noting that the capacity of concrete piles driven open-ended is markedly underpredicted by all methods. More effort could advantageously be put into investigations of such piles.
3. Capacities of piles loaded in compression are best predicted by API-2 in terms of average *C/M*-ratio.
4. On the average, API-2 overestimates the capacity of piles installed in depths greater than 15m more than the capacity of piles installed in depths less than 15m, see Table 6. That is, API-2 produces a skew distribution of *C*/*M*-values with penetration depth. ICM-96 and NGI-99 also produce a skew distribution of *C*/*M*-ratios with penetration depth but it is not as distinct. $\mu_{C/M}$ for piles longer than 15m is less compared to $\mu_{C/M}$ for piles shorter than 15m when applying ICM-96 and NGI-99 to the

Table 5 NGI-99, API-2, and ICM-96 tested against all available data for piles in sand.

	No. of piles / No. of sites	NGI-99 $\mu_{C/M}$ / $\sigma_{C/M}$ [a]	API-2 $\mu_{C/M}$ / $\sigma_{C/M}$ [a]	ICM-96 $\mu_{C/M}$ / $\sigma_{C/M}$ [a]
All piles [b]:				
All piles in category	154 / 61	1.14 / 0.50	1.00 / 0.46	0.91 / 0.34
All piles:				
All piles in category	152 / 59	1.11 / 0.41	0.98 / 0.43	0.89 / 0.30
Piles loaded in compression	98	1.11 / 0.38	0.98 / 0.40	0.85 / 0.28
Piles loaded in tension	54	1.12 / 0.48	1.01 / 0.48	0.95 / 0.32
Piles driven open-ended	54	1.06 / 0.44	0.97 / 0.45	0.82 / 0.36
Piles driven closed-ended	98	1.14 / 0.40	0.98 / 0.42	0.92 / 0.25
Steel:				
All piles in category	115 / 46	1.10 / 0.43	0.94 / 0.41	0.87 / 0.30
Piles loaded in compression	68	1.08 / 0.39	0.92 / 0.43	0.81 / 0.28
Piles loaded in tension	47	1.14 / 0.49	0.95 / 0.38	0.95 / 0.32
Piles driven open-ended	50	1.09 / 0.44	0.99 / 0.46	0.84 / 0.36
Piles driven closed-ended	65	1.11 / 0.43	0.89 / 0.36	0.89 / 0.25
Concrete:				
All piles in category	37 / 13	1.15 / 0.36	1.11 / 0.46	0.95 / 0.28
Piles loaded in compression	30	1.18 / 0.34	1.03 / 0.30	0.95 / 0.26
Piles loaded in tension	7	1.00 / 0.43	1.41 / 0.84	0.96 / 0.37
Piles driven open-ended	4	0.71 / 0.16	0.75 / 0.16	0.57 / 0.26
Piles driven closed-ended	33	1.20 / 0.34	1.15 / 0.47	1.00 / 0.25
Group 4 [c]:				
All piles in category	61 / 15	1.09 / 0.30	1.01 / 0.50	0.94 / 0.28
Piles loaded in compression	43	1.08 / 0.25	0.98 / 0.43	0.88 / 0.23
Piles loaded in tension	18	1.10 / 0.40	1.07 / 0.66	1.09 / 0.34
Piles driven open-ended	23	1.15 / 0.40	0.88 / 0.39	0.97 / 0.36
Piles driven closed-ended	38	1.05 / 0.22	1.08 / 0.55	0.92 / 0.22

a) μ and σ are the mean value and the standard deviation of the *C/M*-ratios.
b) Cases with IDs 8 and 9, Kolding forrenseanlæg, are only included in these investigations.
c) This category includes all cases, where soil and pile data belong to Group 4 ($Q_{r,soil} = Q_{r,pile} = 4$), i.e. cases, where soil and pile data are especially well-described.

Table 6 NGI-99, API-2, and ICM-96 tested against piles with penetration depths greater or less than 15m [a].

Depth [b]	No. of piles	NGI-99 $\mu_{C/M}$ / $\sigma_{C/M}$ [c]	API-2 $\mu_{C/M}$ / $\sigma_{C/M}$ [c]	ICM-96 $\mu_{C/M}$ / $\sigma_{C/M}$ [c]
< 15	59	1.23 / 0.41	0.76 / 0.35	1.00 / 0.26
> 15	93	1.04 / 0.40	1.12 / 0.41	0.81 / 0.30

a) Both piles driven open-ended and closed-ended.
b) Penetration depth, [m].
c) μ and σ are the mean value and the standard deviation of the *C/M*-ratios.

Table 7 Effect of pile diameter.

Diameter [m] [a]	No. of piles	NGI-99 $\mu_{C/M}$ / $\sigma_{C/M}$ [b]	API-2 $\mu_{C/M}$ / $\sigma_{C/M}$ [b]	ICM-96 $\mu_{C/M}$ / $\sigma_{C/M}$ [b]
0 – 0.3	26	1.14 / 0.24	1.03 / 0.60	1.02 / 0.19
0.3 – 0.4	48	1.16 / 0.50	0.89 / 0.40	0.93 / 0.33
> 0.4	78	1.07 / 0.41	1.01 / 0.36	0.82 / 0.29

a) Equivalent pile diameter.
b) μ and σ are the mean value and the standard deviation of the *C/M*-ratios.

available data. A possible reason for the observed tendencies is that API-2 does not include a length factor accounting for "friction fatigue effects" whereas NGI-99 and ICM-96 do. Similar observations have been made by testing the calculation procedures against the AAU database, cf. Section 3.

5. Based on Table 6 it is recommended to use NGI-99 for piles longer than 15m and ICM-96 for piles with penetration depths less than 15m independent on driving conditions (open-ended or closed-ended). Detailed studies indicate that similar conclusions can be drawn if either piles driven open-ended or piles driven closed-ended are investigated.
6. In Table 7 the effect of pile diameter on the average *C/M*-ratios, $\mu_{C/M}$, is shown. ICM-96 provides the better description of piles with equivalent diameters less than 0.4m. API-2 is the most reliable method for piles with diameters exceeding 0.4m.

6 Summary and recommendations

The purpose of this report is to elucidate which calculation procedure (NGI-99, API-2, or ICM-96) that provides the better description of the axial capacity of piles in sand. This is done by comparing measured and calculated capacities based on relatively well-documented cases. Facts regarding the established data (denoted AAU after Aalborg University) have been introduced. The database is based on static loading tests reported in the literature and provided by Danish and Norwegian companies. 32 tests on piles in sand constitute the AAU data. The piles are distributed on nine sites. Two cases - including two pile tests - are omitted in the analyses because they are statistical deviants.

The methods have been tested against the AAU data and also an existing NGI database by means of the database processing program PILCAP, which has been developed at the Norwegian Geotechnical Institute. Results of applying the calculation procedures to the AAU data and the NGI data are presented in Section 3 and 4, respectively, and will not be repeated here. Instead, recommendations based on testing the models on all available tests will be emphasized.

For piles in sand, the following is concluded and recommended based on analyses of 152 static loading tests distributed on 59 sites:

1. Time correction has not been introduced because at the moment no time function – relating time after driving and capacity - is available for piles in sand.
2. Overall, API-2 provides the better description of the available data.
3. Capacities of piles loaded in compression are best predicted by API-2 in terms of average *C/M*-ratio.
4. ICM-96 can profitably be applied to concrete piles whereas API-2 and NGI-99 work best for piles of steel.
5. Especially API-2 provides a skew distribution of *C/M*-ratios with penetration depth. Therefore, the effect of pile length on the average *C/M*-ratios has been investigated. Based on this study it is recommended to use NGI-99 for piles longer than 15m and ICM-96 for piles with penetration depths less than 15m independent on whether the piles are driven open-ended or closed-ended.
6. The effect of pile diameter on the average *C/M*-ratios has also been elucidated. ICM-96 provides the most reliable description of piles with equivalent diameters less than 0.4m. API-2 is the most reliable method for piles with diameters exceeding 0.4m.
7. Generally, the calculation methods are very sensitive towards the way the soil profile and pile tests are interpreted.

Uncertainty is introduced in several ways when comparing measured and calculated capacities. Uncertainty is associated with:

1. Interpretation of soil conditions,
2. Conversion/determination of soil parameters,
3. Interpretation of loading tests,
4. Calculation procedures,
5. Time correction,
6. Pre-shearing and group effects.

As mentioned, the purpose of this report is to elucidate the reliability of the calculation procedures NGI-99, API-2, and ICM-96. Except for pre-shearing effects, group effects, and time corrections items 1-3 have been carefully taken care of in order to obtain a consistent treatment of the data and thereby reaching a reliable validation of the methods.

Finally, it is noted that the choice of calculation method should rely on local test data if such data are available. Thus, if a number of piles have been tested in similar ground, the choice of calculation method should be based on *C/M*-ratios obtained for the given site.

7 Acknowledgement

The authors would like to thank the Norwegian Geotechnical Institute for kindly providing the FORTRAN code PILCAP and numerous pile test data.

8 References

API (1993), Recommended practice for planning, designing and constructing fixed offshore platforms- working stress design, API RP 2A-WSD, *American Petroleum Institute*, 20th edition, July 1, 1993.

API (2000), Recommended practice for planning, designing and constructing fixed offshore platforms- working stress design. API recommended practice 2A-WSD, American Petroleum Institute, 21th edition, December, 2000.

Augustesen, A, Andersen, L. and Sørensen, C.S. (2005a), Capacity of piles in clay, A*vailable from the Department of Civil Engineering, Aalborg University, Denmark*, *Internal report,* ISSN: 1398-6465 R0502.

Augustesen, A, Andersen, L. and Sørensen, C.S. (2005b), Time function for driven piles in clay, A*vailable from the Department of Civil Engineering, Aalborg University, Denmark*, *Internal report,* ISSN: 1398-6465 R0501.

Axelsson, G. (1998a), Long-term increase in shaft capacity of driven piles in sand, *Proceedings of the 4th International Conference on Case Histories in Geotechnical Engineering*, St. Louis, Missouri, Paper no. 1.25, pp.301-308.

Axelsson, G. (1998b), Long-term set-up of driven piles in non-cohesive soils evaluated from dynamic tests on penetration rods,

Proc. 1st International conference on Geotechnical Site Chracterization (eds. Robertson and Mayne), Atlanta, pp.895-900.

Axelsson, G. (2000), Long-term set-up of driven piles in sand, *Ph.D. Thesis, Kungl Tekniska Högskolan (Royal Insitute of Technology), Stockholm, Sweden*.

Axelsson, G. (2002), A conceptual model of pile set-up for driven piles in non-cohesive soil, *Proceedings of the International deep foundations congress*, Orlando, Florida, Vol.1, (Geotechnical Special Technical Publication, ASCE, Vol.116), pp.64-79.

Baldi, G., Bellotti, R., Ghionna, V., Jamiolkowski, M., and Pasqualini, E. (1986), Interpretation of CPT's and CPTU's; 2nd part: Drained penetration of sands, *4th International Geotechnical Seminar*, Singapore, pp.143-156.

Bergdahl, U., and Hult, G. (1979), Load tests on friction piles in sand – Field tests with different test procedures. *Swedish Commission on Pile Research*, Stockholm, In Swedish with English summary.

Bergdahl, U. and Hult, G. (1981), Load tests on friction piles in clay, *Proc. 10th International conference on soil mechanics and foundation engineering*, Stockholm, Sweden, Vol.2, pp.625-630.

Boulon, M. and Foray, P. (1986), Physical and numerical simulation of lateral shaft friction along offshore piles in sand, *Proceedings of 3rd International Conference on Numerical Methods in Offshore Piling*, France, pp.127-148.

Briaud, J-L., Tucker, L-M. and Ng, E. (1989), Axially loaded 5 pile group and single pile in sand, *Proceedings of the 12th ICSMFE*, Rio de Janeiro, Vol.2, p.1121.

Brucy, F. and Meunier, J. (1992), Pile restances at a dense site, *Proceedings of the 4th Application of Stress-Wave Theory to Piles, The Hague, The Netherlands*, (Ed. Barends, F.B.J.), pp.69-76.

Brucy, F., Meunier, J. and Nauroy, J.F. (1991), Behavior of pile plug in sandy soils during and after driving, *Offshore technology conference, 23rd Annual OTC in Houston, Texas, May 6-9, 1991*, OTC paper 6514, pp.145-154.

Bullock, P.J., Schmertmann, J.H., McVay, M.C. and Townsend, F.C. (2005a), Side shear setup. I: Test piles driven in Florida. *Journal of Geotechnical and Geoenvironmental Engineering*, 131(3), pp.292-300.

Bullock, P.J., Schmertmann, J.H., McVay, M.C. and Townsend, F.C. (2005b), Side shear setup. II: Results from Florida test piles. *Journal of Geotechnical and Geoenvironmental Engineering*, 131(3), pp.301-310.

Chow, F.C. (1996), Investigations into displacement pile behaviour for offshore foundations, *Ph.D. Thesis, University of London (Imperial College)*.

Chow, F.C., Jardine, R.J., Brucy, F. and Nauroy, J.F. (1996), The effects of time on the capacity of pipe piles in dense marine sand, *Offshore Technology Conference*, Houston, May 1996, Vol.1, Paper OTC 7972, pp.147-160.

Chow, F.C., Jardine, R.J., Nauroy, J.F. and Brucy, F. (1997), Time-related increases in the shaft capacities of driven piles in sand, *Géotechnique*, 47(2), pp.353-361.

Chow, F.C., Jardine, R.J., Brucy, F. and Nauroy, J.F. (1998), Effects of Time on Capacity of Pipe Piles in Dense Marine Sand, *Journal of Geotechnical and Environmental Engineering*, 124(3), pp.254-264.

Clausen, C.J.F. (1976), The condeep story, Proceedings of Offshore Soil Mechanics (eds. George and Wood), Cambridge university Engineering Department and Lloyd's Register of shipping.

Clausen, C.J.F. and Aas, P.M. (2000), Bearing capacity of driven piles – Piles in clay, *NGI report 525211-1*, Norwegian Geotechnical Institute.

Clausen, C.J.F. and Aas, P.M. (2001a), Capacity of driven piles in clays and sands on the basis of pile load tests. *ISOPE conference*.

Clausen, C.J.F. and Aas, P.M. (2001b), Bearing capacity of driven piles – Piles in sand, *NGI report 525211-2*, Norwegian Geotechnical Institute.

Clausen, C.J.F., Aas, P.M. and Karlsrud, K. (2005), Bearing capacity of driven piles in sand, the NGI approach, *Proceedings of Frontiers in Offshore Geotechnics: ISFOG 2005*, (eds. Gourvenec and Cassidy), Perth, © 2005 Taylor & Francis Group, London.

Dennis, N.D. and Olson, R.E. (1983), Axial capacity of steel pipe piles in sand, *Proceedings of Geotechnical Practice in Offshore Engineering*, Austin, Texas (1983).

Focht, J.A. and O'Neill, M.W. (1985), Piles and other deep foundations, *Proceedings of the 11th ICSMFE*, San Francisco, Vol.1, pp.187-209.

Fugro Engineers B.V. (Fugro) (2004), Axial pile capacity design method for offshore driven piles in sand, *Report P1003 presented to the American Petroleum Institute, issue 3*, August, 2004.

Jardine, R.J. and Chow, F.C. (1996), New design methods for offshore piles, *Marine technology directorate Ltd., publication MTD 96/103*, London, ISBN 1 870553 31 4.

Jardine, R.J. and Chow (1997). Improved pile design methods from field testing research. *In* proceedings of the ERTC3 (The ISSMFE European Regional Technical Committee 3 "Piles"), Design of Axially Loaded Piles – European Practice (eds. De Cock and Legrand), Belgium, Balkema, Rotterdam. pp.27-38.

Jardine, R.J., Overy, R.F. and Chow, F.C. (1998), Axial capacity of offshore piles in dense North Sea sands, *Journal of Geotechnical and Geoenvironmental Engineering*, 124(2), pp.171-178.

Jardine, R.J., Chow, F.C., Overy, R.F. and Standing, J.R. (2005a), ICP design methods for driven piles in sand and clay. *Thomas Telford, London*.

Jardine, R.J., Standing, J.R. and Chow, F.C. (2005b), Field research into the effects of time on the shaft capacity of piles driven in sand. *Proccedings of Frontiers in Offshore Geotechnics: ISFOG 2005* (eds. Gourvenec and Cassidy), Perth, © 2005 Taylor & Francis Group, London.

Jardine, R.J., Chow, F.C., Standing, J.R., Overy, R.F., Saldivar-Moguel, E. Strick van Linschoten, C. and Ridgway, A. (2005c), An updated assessment of the ICP pile capacity procedures. *Proccedings of Frontiers in Offshore Geotechnics: ISFOG 2005* (eds. Gourvenec and Cassidy), Perth, © 2005 Taylor & Francis Group, London.

Joshi, R.C., Achari, G., Kaniraj, S.R. and Wijeweera, H. (1995), Effect of aging on the penetration resistance of sands, *Canadian Geotechnical Journal*, 32, pp.767-782.

Karlsrud, K. and Haugen, T. (1986), Axial static capacity of steel model piles in overconsolidated clay, *NGI Publication No.163*, Norwegian Geotechnical Institute. Also *Proc. 11th International Conference on Soil Mechanics and Foundation Engineering*, San Francisco, 1985, Vol.3, pp.1401-1406.

Kulhawy, F.H. and Mayne, P.W. (1990), Manual on estimating soil properties for foundation design, *Electric Power Research Institute, EPRI*, August 1990.

Lehane, B.M. and Jardine, J.R. (1996), Shaft capacity of driven piles in sand: a new design approach, *7th International Conference on the Behavior of Offshore Structures, BOSS'94*, (Eds. Chryssostomidis, Triantafyllou, Whittle, Hoo Fatt,), Vol.1 Geotechnics, pp.23-36.

Lehane, B.M., Jardine, R.J., Bond, A.J. and Frank, R. (1993), Mechanisms of shaft friction in sand from instrumented pile tests, *Journal of Geotechnical Engineering*, 119(1), pp.19-35.

Lehane, B.M., Schneider, J.A. and Xu, X. (2005a), Evaluation of design methods for displacement piles in sand, *University of Western Australia*, UWA Report, GEO: 05341.1.

Lehane, B.M., Schneider, J.A. and Xu, X. (2005b), CPT based design of driven piles in sand for offshore structures, *University of Western Australia*, UWA Report, GEO: 05345.

Lehane, B.M., Schneider, J.A. and Xu, X. (2005c), The UWA-05 method for prediction of axial capacity of driven piles in sand, *Proccedings of Frontiers in Offshore Geotechnics: ISFOG 2005* (eds. Gourvenec and Cassidy), Perth, © 2005 Taylor & Francis Group, London.

Lunne, T. and Kvalstad, T.J. (1982), Analysis of full scale measurements on gravity platforms, Final report, Foundation Performance During Installation and Operation of North Sea Concrete Platforms. *Norwegian Geotechnical Institute and Det Norske Veritas*, Oslo.

Lunne, T. and Christoffersen, H.P. (1983), Interpretation of cone penetrometer data for offshore sands, *Offshore Technology Conference*, Houston, May 1983. Also NGI publication No.156, Norwegian Geotechnical Institute.

Lunne, T., Robertson, P.K. and Powell, J.J.M. (1997), Cone penetration testing in geotechnical engineering, *Blackie Academic & Professional*, London, ISBN 0 751 40393 8.

Mayne, P.W. (1992), Tentative method for estimating σ_{ho} from q_c data in sands, *Proceedings of the International Symposium on Calibration Chamber Testing*, Potsdam, New York.

Mesri, G., Feng, T.W. and Benak, J.M. (1990), Postdensification penetration resistance of clean sands, *Journal of Geotechnical Engineering*, 116(7), pp.1095-1115.

Mitchell, J.K. and Solymar, Z.V. (1984), Time-dependent strength gain in freshly deposited or densified Sand, *Journal of Geotechnical Engineering*, 110(11), pp.1559-1576.

Murff, J.D., Raines, R.D., and Randolph, M.F. (1990), Soil plug behavior piles in sand, *Offshore Technology Conference*, Houston, May 1990, Paper OTC 6421.

Olson, R.E. (1988), Comparison of measured axial load capacities of steel piles in sand with capacities calculated using 1986 API recommended practice (RP2A), *Final report to the American Petroleum institute, Project PRAC 86-294*, Austin, Texas.

Randolph, M.F., Dolwin, J. and Beck, P. (1994), Design of driven piles in sand, *Geotechnique*, 44(3), p.427.

Robinsky, E.I. and Morrison, C.F. (1964), Sand displacement and compaction around model friction piles, *Canadian Geotechnical Journal*, 1(2), pp.81-93.

Schmertmann, J.H. (1978), Guidelines for cone penetration tests, performance and design, *Federal Highway Administration*, Report FHWA-TS-78-209, Washington, July 1978.

Schmertmann, J.H. (1991), The mechanical aging of soils, *Journal of Geotechnical Engineering*, 117(9), pp.1288-1330.

Tang, W.H., Woodford, D.L. and Pelletier, J.H. (1990), Performance reliability of offshore piles, *Offshore Technology Conference*, Houston, May 1990, Paper OTC 6379.

Toolan, F.E. and Ims, B.W. (1988), Impact of recent changes in the API recommended practice for offshore piles in sand and clays, *Preprint, Oceanology international 1988*.

Toolan, F.E., Lings, M.L. and Mirza, U.A. (1990), An appraisal of API RP2A recommendations for determining skin friction of piles in sand, *Offshore Technology Conference*, Houston, May 1990, Paper OTC 6422.

Tvedt, G. and Fredriksen, F. (2003), E18 Ny motorvegbru i Drammen. Prøvebelastning av Peler, *Proceedings from the conference on Rock Blasting and Geotechnics*, Oslo, 2003.

Uesugi, M., Kishida, H. and Tsubakihara, Y. (1988), Behaviour of sand particles in sand steel friction, *Soils and Foundations*, 28(1), pp.107-118.

Vijayvergiya, V.N. (1977), Load-movement characteristics of piles, *Ports '77, Proc. 4th Annual Symposium of the Waterways, Ports, Coastal and Ocean Division of American Society of Civil Engineers*, 2, pp.269-284.

Åstedt, B., Weiner, L. and Holm, G. (1992), Increase in bearing capacity with time for friction piles in silt and sand, *Proceedings of the 11th Nordic Geotechnical Meeting*, NGM-92, Vol.2/3, session 5-8, pp.411-416.

Appendix

The following appendices are included in the report:

1. Appendix A: Conversion procedures
2. Appendix B: NGI-99
3. Appendix C: API-2
4. Appendix D: ICM-96
5. Appendix E: AAU sand database
6. Appendix F: AAU and NGI data
7. Appendix G: Calculated results

Appendix A:
Conversion procedures

The different design methods depend on different soil parameters, see Appendices B to D. Further, these are not all established in every case considered in this study. In order to obtain a consistent treatment of the available data, conversion rules relating one parameter to another are employed. For each sand layer at least one of the following input parameters that relate to sand strength must be given:

1. CPT tip resistance, q_c [kPa].
2. SPT resistance, N [blows/foot].
3. Relative density, D_r.
4. Angle of internal friction, φ [°].

If one of the above mentioned parameters is known, q_c, D_r, and φ can be determined. This is only done if the parameter in consideration is not given as input. For example, if D_r is not given it is determined from other measurements, e.g. cone penetrometer or standard penetration tests. The conversion rules adapted in this study are explained below and it is a controversial matter within geotechnical engineering, i.e. the equations are associated with some uncertainty. The formulae are taken directly from Clausen and Aas (2001b).

It should be noticed that the determination of the relevant parameters are carried out in the sequence indicated in Figure A.1.

Figure A.1 Sequence in which the CPT tip resistance, q_c, the relative density, D_r, and the friction angle, φ, are determined if they are not given as input.

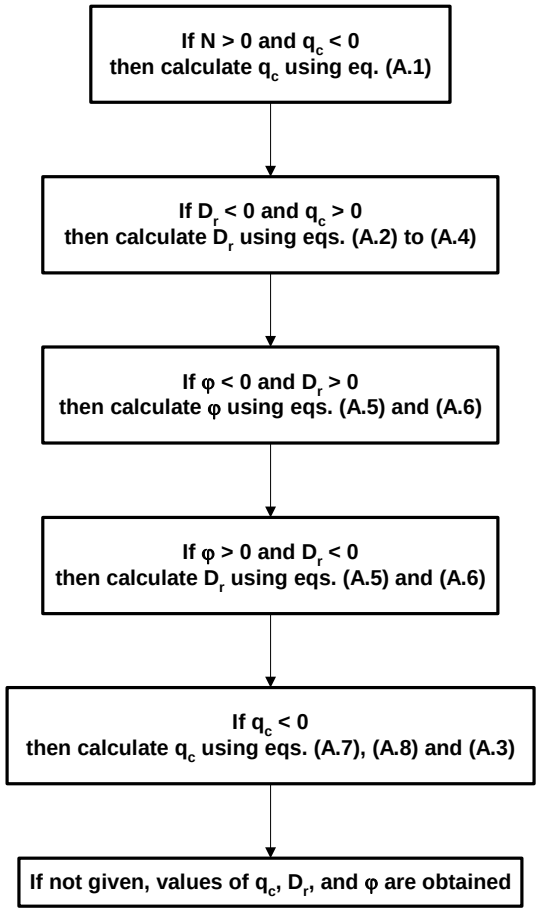

- **Determination of q_c from N**

If the CPT resistance, q_c, is not given as input, the calculated q_c-value that corresponds to a given SPT N-value based upon Kulhawy and Mayne (1990) is:

$$q_c = 5.44 \cdot d_{50}^{0.26} \cdot N \cdot p_a \quad \text{(A.1)}$$

where d_{50} is the average grain size diameter [mm] and p_a is the atmospheric pressure, which equals 100 kPa. If d_{50} is not given it is assumed that $d_{50} = 0.15$ mm

- **Determination of D_r from q_c**

If the relative density, D_r, is not given as input, it is calculated from q_c (provided that q_c is given or has been calculated from N). The calculation is based upon Baldi et al. (1986) and reproduced in Lunne et al. (1997):

$$D_r = \frac{\ln\left(\frac{q_c}{181 \cdot \sigma_m^{0.55}}\right)}{2.61}, \quad 0.01 < D_r < 1.0 \quad \text{(A.2)}$$

where

$$\sigma_m = p_0 \frac{1 + 2 \cdot K_0}{3} \text{ [kPa]} \quad \text{(A.3)}$$
$$K_0 = 0.35 \cdot OCR^{0.65}$$

Here p_0 is the vertical effective stress and OCR is the overconsolidation ratio. K_0 is the ratio of horizontal to vertical effective stress. The OCR/K_0 relationship is proposed by Mayne (1992).

If pile capacities are calculated based on ICM-96, eq. (A.2) is replaced by eq. (A.4) with *OCR* taken as 1.0:

$$D_r = \frac{\ln\left(\frac{q_c}{61 \cdot p_0^{0.71}}\right)}{2.91}, \quad 0.01 < D_r < 1.0 \tag{A.4}$$

Equation (A.4) is based upon Lunne and Christoffersen (1983). ICM-96 was established using eq. (A.4), which is the reason eq. (A.4) is used when applying this method instead of eq. (A.2).

- **Determination of φ from D_r**

If the friction angle, φ, is not given as input, it is calculated from D_r (provided that D_r is given or has been calculated). Equation (A.5) is used if the pile capacity is calculated based on API-2. Otherwise eq. (A.6) is applied.

$$\varphi = 17.5 + 25.0 \cdot D_r \quad \text{API} \tag{A.5}$$

$$\varphi = 28.0 + 14.0 \cdot D_r \quad \text{Non} - \text{API} \tag{A.6}$$

Equation (A.6) is the relationship between D_r and the drained peak triaxial angle for uniform sand. Equation (A.6) is based on Schmertmann (1978).

- **Determination of D_r from φ**

If D_r is not given as input, and not calculated from CPT or SPT results, its value is determined from eqs. (A.5) and (A.6) depending on the calculation procedure to be employed. In this case φ must be given.

- **Determination of q_c from D_r**

If the CPT tip resistance, q_c, is still zero after running through the above procedure, its value is determined using eqs. (A.7), (A.8) and (A.3), which follows directly from eqs. (A.2) to (A.4):

$$q_c = 181 \cdot \sigma_m^{0.55} \cdot \exp\left(2.61 \cdot D_r\right) \tag{A.7}$$

$$q_c = 61 \cdot p_0^{0.71} \cdot \exp\left(2.91 \cdot D_r\right) \tag{A.8}$$

The unit of q_c is kPa. Equation (A.8) should only be applied in connection with ICM-96.

Appendix B: NGI-99

The method assumes that the values of the following parameters are known:

- Depth to the considered point, z.
- Initial vertical effective stress, p_0.
- Sand relative density, D_r.
- Cone penetrometer tip resistance, q_c.
- Outside diameter of the pile, D_o.
- Inside diameter of the pile, D_i.
- Pile tip depth, z_{tip}.
- Pile tip condition during driving, open- or closed ended.
- Soil plug length, L_1.
- Loading conditions, compression or tension.
- The vertical stress acting against the top of the sand plug, σ_{top}.
- The submerged unit weight, γ.
- The cross section area of the pile and plug, A.
- Pile wall cross section area, A_{wall}.
- Soil plug side area, A_s.
- Soil plug cross section area, A_{plug}.

Notation and parameters related to the calculation of shaft resistance and pile tip capacity for piles in sand are depicted in Figure B.1.

This appendix is entirely based on Clausen and Aas (2001b).

Unit shaft resistance

The following algorithm is used to calculate the skin friction, τ:

$$\tau(z) = 2.5 \cdot \tau_{avr} \left(\frac{z}{z_{tip}} \right)^{1.5}, \quad \tau(z) \geq 0.1 \cdot p_0 \tag{B.1}$$

where:

$$\tau_{avr} = 1.25 \cdot F \cdot (D_r - 0.2) \cdot \sigma_{atm} \cdot F_{Length} \tag{B.2}$$

$$\sigma_{atm} = 100\text{kPa} \tag{B.3}$$

$$F_{Length} = \frac{z_{tip} + 10}{1.6 \cdot z_{tip} + 10} \tag{B.4}$$

Values of F as functions of loading and pile conditions can be seen in Table B.1.

Table B.1 F as function of loading and pile conditions.

	Compression	Tension
Open-ended	1.5	1.0
Closed-ended	$1.5 \cdot \left(1.0 + 0.75 \cdot D_r^3\right)$	$1.0 + 0.75 \cdot D_r^3$

Pile tip capacity

The resulting pile tip resistance, Q_{tip}, is determined by:

$$Q_{tip} = \min \begin{pmatrix} Q_{plugged} \\ Q_{coring,\,method1} \\ Q_{coring,\,method2} \end{pmatrix} \tag{B.5}$$

where $Q_{plugged}$ is the end bearing capacity for plugged piles or piles driven closed-ended. $Q_{coring,method1}$ and $Q_{coring,method2}$ are the tip resistances for piles driven open-ended based on two different methods.

The pile tip resistance for closed-ended or plugged piles loaded in compression can be calculated as follows:

$$Q_{plugged} = F_{tip} \cdot q_c \cdot A \tag{B.6}$$

$$F_{Tip} = F_{Diam} \cdot F_{Dr} \cdot F_{Sigz}, \quad 0.2 < F_{Tip} < 1.0 \tag{B.7}$$

$$F_{Diam} = 1.0 - 0.35 \log_{10} \left(\frac{D_o}{0.036} \right), \quad F_{Diam} > 0.2 \tag{B.8}$$

$$F_{Dr} = \frac{2.2}{1.0 + 4 \cdot D_r}, \quad F_{Dr} < 1.0 \tag{B.9}$$

$$F_{Sigz} = \left(\frac{p_0}{100} \right)^{0.5}, \quad F_{Sigz} < 2.0 \tag{B.10}$$

For open-ended piles the end bearing capacity can be determined based on one of the following methods:

- Method 1 is based upon Murff et al. (1990) and Chow (1996).
- Method 2 is based upon a simple procedure tested against the measured axial forces on the OD=2.34m

Beryl A platform (Clausen, 1976; Lunne and Kvalstad, 1982).

According to method 1, the tip resistance can be calculated as:

$$Q_{\text{coring, method1}} = A_{\text{plug}} \cdot \sigma_{\text{plug}} + A_{\text{wall}} \cdot \sigma_{\text{wall}} \tag{B.11}$$

$$\sigma_{\text{wall}} = 0.5 \cdot q_{\text{c}} \tag{B.12}$$

$$\sigma_{\text{plug}} = \left(\sigma_{\text{top}} + \frac{\gamma \cdot D_{\text{i}}}{4\beta} \right) \cdot \exp\left(\frac{4\beta}{D_{\text{i}}} \cdot L \right) - \frac{\gamma \cdot D_{\text{i}}}{4\beta} \tag{B.13}$$

$$\begin{aligned} &\beta = D_{\text{r}} - 0.3, \\ &\beta > 0.0 \end{aligned} \tag{B.14}$$

$$\begin{aligned} &L = \min\left(L_1, L_2\right), \\ &L_1 = \text{Actual soil plug length}, \\ &L_2 = 3 \cdot D_{\text{i}} \end{aligned} \tag{B.15}$$

According to method 2, the tip resistance can be calculated as:

$$Q_{\text{coring, method2}} = A_{\text{s}} \cdot \tau + A_{\text{wall}} \cdot \sigma_{\text{wall}} \tag{B.16}$$

$$\sigma_{\text{wall}} = q_{\text{c}} \tag{B.17}$$

where τ is the inside skin friction calculated by means of NGI-99 for an open-ended pile loaded in compression, cf. eqs. (B.1) to (B.4).

Figure B.1 Parameters associated with calculation of pile capacity for piles in sand. After Clausen and Aas (2001b).

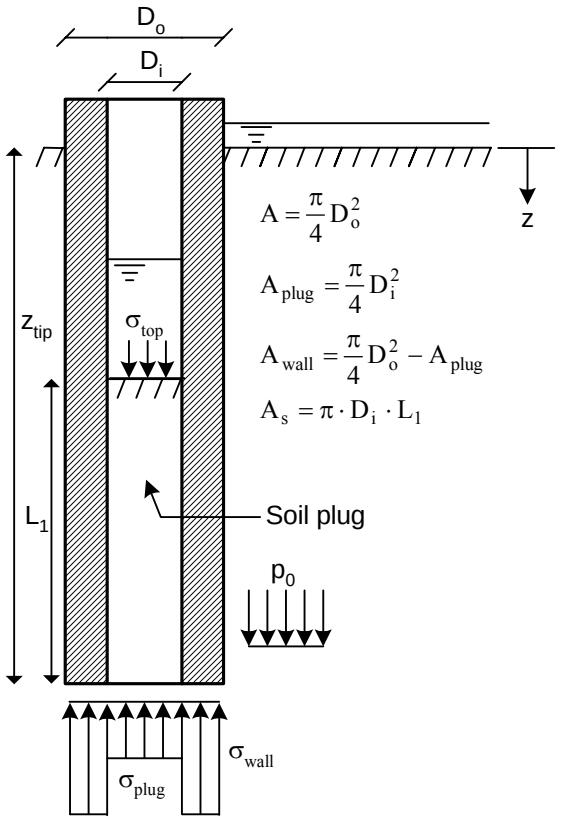

Appendix C:
API-2

The method assumes that the values of the following parameters are known:

- Coefficient of lateral earth pressure (ratio of horizontal to vertical effective stress), K.
- The vertical effective stress, p_0, at a given depth, z.
- Friction angle between soil and pile wall, δ.
- Dimensionless bearing capacity factor, N_q.

This appendix is based on API (1993) and Clausen and Aas (2001b).

The ultimate bearing capacity of a pile, Q_d, should be determined by the equation:

(C.1) $$Q_d = f \cdot A_s + q \cdot A_p$$

where f is the unit friction capacity [kPa], A_s is the side surface of the pile [m^2], q is the unit end bearing capacity [kPa], and A_p is the gross end area of a pile [m^2].

The total end bearing capacity, $q \cdot A_p$, should not exceed the capacity of the internal plug.

Unit shaft resistance

The following equation is used to calculate the skin friction:

(C.2) $$f = K \cdot p_0 \cdot \tan(\delta)$$

For open-ended piles driven unplugged, it is usually appropriate to assume K as 0.8 for both tension and compression loadings. Values of K for full displacement piles may be assumed to be 1.0. Table C.1 may be used for the selection of δ if other data are not available. For long piles f may not indefinitely increase with p_0 as implied by eq. (C.2). In such cases it may be appropriate to limit f to the values in Table C.1.

Pile tip capacity

For piles end bearing in non-cohesive soils, the unit end bearing, q, can be calculated as:

(C.3) $$q = N_q \cdot p_0$$

In this case p_0 is the vertical free field effective stress at the pile toe. Recommended values of N_q are presented in Table C.1. For piles considered to be plugged the bearing pressure may be assumed to act over the entire cross section of the pile. For unplugged piles the bearing pressure acts on the pile annulus only.

Table C.1 Design parameters for cohesionless siliceous soil [a]. Reproduced from API (1993).

Density [b]	Soil description	δ [c]	Limits on f [kPa]	N_q [d]	Limits on q [MPa]
Very Loose Loose Medium	Sand Sand-Silt [e] Silt	15	47.8	8	1.9
Loose Medium Dense	Sand Sand-Silt [e] Silt	20	67	12	2.9
Medium Dense	Sand Sand-Silt [e]	25	81.3	20	4.8
Dense Very Dense	Sand Sand-Silt [e]	30	95.7	40	9.6
Dense Very dense	Gravel Sand	35	114.8	50	12

a) The parameters listed are intended as guidelines only. Where detailed information is available, other values may be justified.
b) Descriptive terms used for the sand relative density may vary from author to author.
c) Soil-pile friction angle.
d) Dimensionless bearing capacity factor.
e) Sand-Silt includes those soils with significant fractions of both sand and silt. Strength values generally increase with increasing sand fractions and decrease with increasing silt fractions.

Miscellaneous

In order to make use of Table C.1 in practice the relative density, D_r, and the silt content should be known. If D_r is not known it can be determined based on the procedure described in Appendix A. For a given (or calculated) D_r the corresponding friction angle, φ, (if not given as input) is calculated based on eq. (C.4):

$$\varphi = 17.5° + 25.0 \cdot D_r \qquad 20° < \varphi < 40° \tag{C.4}$$

With known friction angle it is assumed that:

$$\delta = \varphi - 5° \tag{C.5}$$

where δ is the soil-pile friction angle. Instead of using the limiting skin friction values, f_{limit}, given in Table C.1, PILCAP calculates f_{limit} according to:

$$f_{limit} = 3.35 \cdot \varphi - 19.0 \tag{C.6}$$

For API-2 it is required that:

$$47.8 < f_{limit} < 114.8 \tag{C.7}$$

Instead of employing the N_q-factors given in Table C.1, N_q is calculated according to:

$$\begin{array}{ll} \varphi < 30 & N_q = 11.6 \tan^2\left(45 + \varphi/2\right)\tan\left(\varphi\right) \\ 30 < \varphi < 35 & N_q = 4 \cdot \varphi - 100 \\ \varphi > 35 & N_q = 2 \cdot \varphi - 30 \end{array} \tag{C.8}$$

The following limitations apply for the API-2 method, cf. Table C.1:

$$N_q < 50 \wedge q < 12 \tag{C.9}$$

It should be noticed that PILCAP makes use of eqs. (C.4) to (C.9) instead of Table C.1 directly. This implies that the API-2 implementation in PILCAP leads to a continueous increase in skin friction and end bearing capacity as the relative density, D_r, increases whereas the actual code (Table C.1) operates with five soil groups with constant parameter values within each group. In addition, the implemented version of API-2 does not include the silt content, only indirectly through the selected D_r or φ values.

Appendix D: ICM-96

This appendix is based on Jardine and Chow (1997), Jardine et al. (1998) and Clausen and Aas (2001b). The ICM-96 method is originally described in Jardine and Chow (1996). Notation and some of the parameters related to the calculation of skin friction and pile tip capacity for piles in sand are depicted in Figure D.1.

Figure D.1 Parameters associated with calculation of skin friction and end bearing capacity.

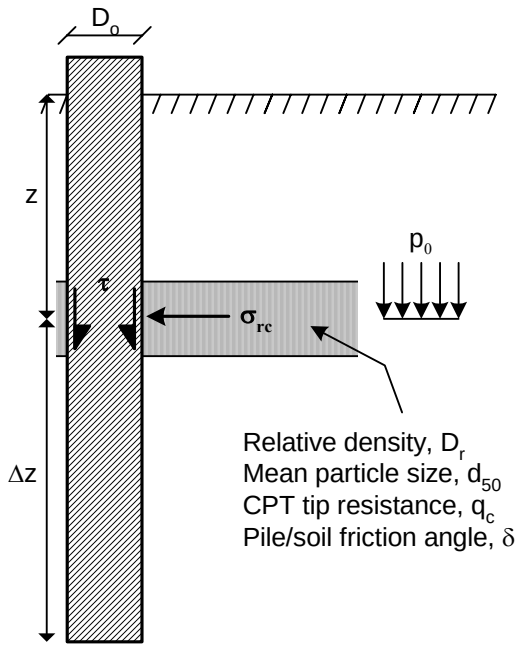

Shaft resistance

The shaft capacity, Q_s, of closed-ended piles can be calculated as:

$$Q_s = \pi \cdot D_o \int \tau_f dz \quad \text{(D.1)}$$

where

- D_o is the outer diameter of the pile.
- τ_f is the local skin friction at failure in a given depth, z.

The local shaft resistance, τ_f, is given by Coloumb's failure criterion:

$$\tau_f = \sigma_{rf} \cdot \tan\delta \quad \text{(D.2)}$$

where

- σ_{rf} is the local radial effective stress at failure.
- δ is the ultimative interface shear friction angle. δ is measured in appropriate laboratory tests or evaluated from the charts given by Jardine and Chow (1996).

For closed-ended piles loaded in compression, the radial effective stress at failure, σ_{rf}, is given by

$$\sigma_{rf} = \sigma_{rc} + \Delta\sigma_{rd} \quad \text{(D.3)}$$

σ_{rc} is the radial effective stress after installation, see Figure D.1, and it is given by

$$\sigma_{rc} = 0.029 \cdot q_c \left(\frac{p_0}{100}\right)^{0.13} \cdot \left(\frac{\Delta z}{R_o}\right)^{-0.38} \quad \text{(D.4)}$$

where:

- q_c is the CPT tip resistance.
- p_0 is the free field vertical effective stress at a given depth.
- Δz is the distance from the point considered to the toe, see Figure D.1, and R_o is the outer radius of the pile, i.e. $\Delta z / R_o$ is an expression for friction fatigue effects.

$\Delta\sigma_{rd}$ is the dilatant increase in local effective stress during pile loading given by:

$$\Delta\sigma_{rd} = \frac{4 \cdot G \cdot R_{cla}}{R_o} \quad \text{(D.5)}$$

R_{cla} is the pile roughness, which typically is 10μm for steel piles. G is the shear modulus and can be calculated as follows, cf. Baldi et al. (1986):

$$G = \frac{q_c}{A + B \cdot \eta - C \cdot \eta^2}$$

$$\eta = \frac{q_c}{\sqrt{100 \cdot p_0}} \quad \text{(D.6)}$$

$$A = 0.0203$$

$$B = 0.00125$$

$$C = 1.216 \cdot 10^{-6}$$

For closed-ended piles loaded in tension, eq. (D.3) yields:

$$\sigma_{rf} = 0.8 \cdot \sigma_{rc} + \Delta\sigma_{rd} \tag{D.7}$$

For open-ended piles loaded in compression, eqs. (D.1) to (D.6) can also be applied if the outer pile radius, R_o, in eq. (D.4) is replaced by the modified pile radius, R, according to:

$$R = \sqrt{R_o^2 - R_i^2} \tag{D.8}$$

where R_i is the inner pile radius of a tubular pile. If $\Delta z/R > 8$ the equation should be evaluated with $\Delta z/R = 8$. Further, if the pile is loaded in tension, eq. (D.3) yields:

$$\sigma_{rf} = 0.9 \cdot \left(0.8 \cdot \sigma_{rc} + \Delta\sigma_{rd}\right) \tag{D.9}$$

By comparing eq. (D.7) and eq. (D.9) it is seen that the radial effective stresses at failure, σ_{rf}, for open-ended piles loaded in tension are 10% less than the corresponding σ_{rf} for closed-ended piles loaded in tension.

Pile tip capacity

For closed-ended piles the base resistance, Q_b, can be calculated according to:

$$\begin{aligned} Q_b &= q_b \cdot \frac{\pi \cdot D_0^2}{4} \\ q_b &= q_{c,avr}\left[1 - 0.5 \cdot \log_{10}\left(\frac{D_0}{D_{CPT}}\right)\right] \end{aligned} \tag{D.10}$$

where $q_{c,avr}$ is the averaged CPT resistance. $q_{c,avr}$ is averaged 1.5 pile diameters above and below the pile toe. A lower bound $q_b = 0.13 \cdot q_{c,avr}$ applies for $D_o > 2$m and $D_{CPT} = 0.036$m. Due to the second expression in eq. (D.10) differences in scale between the CPT probe and the pile are taken into account.

The toe capacity, Q_b, of piles driven open-ended but behaving in a plugged manner can be calculated as:

$$\begin{aligned} Q_b &= q_b \cdot \frac{\pi \cdot D_0^2}{4} \\ q_b &= q_{c,avr}\left[0.5 - 0.25 \cdot \log_{10}\left(\frac{D_0}{D_{CPT}}\right)\right] \end{aligned} \tag{D.11}$$

By comparing eq. (D.10) and eq. (D.11) it is seen that fully plugged piles develop 50% lower toe capacity compared to closed-ended piles. A plug can only develop if $D_o < 0.02 \cdot (D_r - 30)$ in which D_o is in metres and D_r is in %.

For unplugged piles and large open-ended piles the base resistance which acts on the pile annulus only can be determined according to eq. (D.12):

$$\begin{aligned} Q_b &= q_b \cdot \pi\left(R_0^2 - R_i^2\right) \\ q_b &= q_{c,avr} \end{aligned} \tag{D.12}$$

Again, R_o and R_i are the outer and inner radii of a tubular pile, respectively.

Appendix E:
AAU sand database

```
PILES IN SAND    TILLÆGSCASES TIL NGI DATABASE                    18 MAR 2006

     9   NUMSIT   Number of different sites
     0   INTER    Run program in interactive mode (0=no 1=yes)

     6   ICSAND   Code for method to calculate sand skin friction, see below
     6   ICCLAY   Code for method to calculate clay skin friction, see below

   100   ATMPRS   Atmospheric pressure    (100 kPa  in S.I. units)
    10   GAMWAT   Unit weight of water    (10 kN/m3 in S.I. units)
    78   GAMSTL   Unit weight of steel    (78 kN/m3 in S.I. units)
    25   GAMCON   Unit weight of concrete (25 kN/m3 in S.I. units)
     9   GAMWOD   Unit weight of wood     ( 9 kN/m3 in S.I. units)

     1   MODFSU   Code for change of Su values to Su.UU or Su.DSS (0=No 1=Yes)
     0   TIMEFC   Time needed for development of full pile clay capacity, days
   .00   DELT10   Pile capacity increase for 10-fold time increase
  1.00   PLGFCT   Plug factor, ratio inside/outside friction force

  0  0   INCQRC   Include sites with same or higher soil and pile quality rating code
 1 1 1   INCMAT   Include piles with material code STEEL/CONCRETE/WOOD (0=No 1=Yes)
  1  1   INCMTN   Include piles loaded in compression/tension (0=No 1=Yes)
 0 100   DIAINC   Include piles with diameter within given range
 0 200   PENINC   Include piles with penetration within given range
 0 99999 CAPINC   Include piles with measured capacity within given range
 0 10000 TIMINC   Include piles with time from driving to testing within given range
 0 10.0  SUPINC   Include piles with average Su/po' ratio within given range

  4.5   65  3.0  0.05 0.2   SAND 1-5    Parameters used to calculate pile skin
  .40  .75  .30  2.0  .125  SAND 6-10   friction in sand by NGI-1999 method

 1 1 0            Codes for plotting, 0=NO 1=YES (SAND/CMP  SAND/TNS  CLAY/CMP&TNS)

  ================================    ======================================
  SAND SKIN FRICTION CODES            CLAY SKIN FRICTION CODES
  ================================    ======================================
  1 = API 1972 to 1984 (K=0.5/0.7)    1 = API 1979 to 1987 (24-72 kPa)
  2 = API 1984 to now  (K=0.8/0.8)    2 = API 1987 to now  (ALPHA=f(Su/SIGZ))
  3 = API 1984 to now  (K=0.5/0.7)    3 = API/NGI 1992
  4 = Not used                        4 = NGI 1990
  5 = Imperial College 1996           5 = Imperial College 1996
  6 = NGI 1999                        6 = NGI 1999
  7 = Not used                        7 = Not used
  ================================    ======================================

Data given below for each location and pile include :

  NUMLAY        Number of soil layers
  NUMPIL        Number of different piles or penetration depths
  GWT           Depth from soil surface to ground water table, neg. if submerged site
  GAMPWP        Water unit weight to calculate pore water pressure at pile tip
  SIGSRF        Vertical stress at soil surface
  ZHOLE         Depth below surface of open or cased hole
  QR.SOIL       Quality rating for soil and pile data :
  QR.PILE       0 = Not known  1 = Low  2 = Average  3 = High

  DEPTH BOTTM   Depth to bottom of layer
  GAMMA EFF     Effective unit weight
  TYPE          Soil type indicator (1=Clay 2=Silt 3=Sand)
  Q.CPT         Cone Penetrometer Test tip resistance qc
  SPT           Standard Penetration Test, blows/foot
  OCR           Over-consolidation ratio for CPT to Dr conversion
  SuTop         Undrained shear strength at top of layer
  SuBot         Undrained shear strength at bottom of layer
  TYP           Type of undrained shear strength measurement, see below
  St            Clay sensitivity
  Ip            Clay plasticity index = Wl - Wp
  D50           Sand grain average diameter, mm
  Dr            Sand relative density
  PHI           Sand angle of internal friction
  CLC.FLG       Flag for calcareous soils
  MISC 1-3      MISC(1) is Delta.Sig.PC, used to find OCR.  2-3 not used.

  OPN.CLS       Pile driven open ended (=1) or closed ended (=2)
  MAT.TYP       Pile material type id (1=steel 2=concrete 3=wood)
  DIAM.TIP      Pile tip diameter
  TAPER         Pile wall taper, degrees
  WALL.TIP      Wall thickness at pile tip
  TOTAL.LNGTH   Total pile length from pile but to pile tip
  TIP.PENTR     Depth of pile tip penetration
  PLUG.RATIO    Ratio soil plug length to tip penetration
  WATER.RATIO   Ratio water plug length to tip penetration
  COMPRSSN      Measured pile capacity in compression
  TENSION       Measured pile capacity in tension
  DAYS          Number of days between pile driving and pile testing
  TBF           Value 1 flags that the pile has been tested before
  MISC(1)=  1   Value 1 flags that failure was not reached
  MISC(2)= -1   No correction for time between driving and testing
```

MISC(3)= -1 Skip plug capacity control
MISC(3)= 0 Clay tip tensile force : Undrained conditions
MISC(3)= 1 Clay tip tensile force : Drained conditions
MISC(3)= 2 Clay tip tensile force : Zero force at pile tip

Undrained shear strength codes :

-1 = Estimated value 0 = Not known

1 = Torvane, pocket pentr. 8 = Field vane test
2 = Unconfined compr. test 9 = Field cone penetrometer test
3 = UU triaxial test 10 = Other field test
4 = CIU/CAU triaxial test
5 = Direct simple shear
6 = Lab vane
7 = Other lab test

001
Aarsleff (1998)
Aalborg østhavn kranfundament, P382

NUMLAY	NUMPIL	GWT	GAMPWP	SIGSRF	ZHOLE	QR.SOIL	QR.PILE
4	1	1.9	10	0.0	0.0	2	4

LAYER	DEPTH BOTTM	GAMMA EFF	TYPE ClSiSa	Q.CPT TIP	SPT N	OCR	CLAY SuTop	CLAY SuBot	CLAY TYP	CLAY St	CLAY Ip	SAND D50	SAND Dr	SAND PHI	CLC FLG	MISCELLANEOUS 1	2	3
1	2.9	20.0	3	13000	0	0	0	0	0	0	0	0	0	0	0	0	0	0
2	6.9	8.0	1	0	0	0	60	80	8	0	0	0	0	0	0	0	0	0
3	10.9	9.4	1	0	0	0	120	210	8	0	0	0	0	0	0	0	0	0
4	17.9	8.0	3	13500	0	0	0	0	0	0	0	0	0	0	0	0	0	0

PILE NO	OPN CLS	MAT TYP	DIAM TIP	TAPER degr	WALL TIP	TOTAL LNGTH	TIP PENTR	PLUG RATIO	WATER RATIO	-- MEASURED CAPACITIES -- COMPRSSN	TENSION	DAYS	TBF	MISCELLANEOUS 1 2 3
1	2	2	.382	0	.191	18.0	17.65	0.0	0.0	1320	0	26	0	0 0 0

Pile is a squared prec. concrete pile (sidelength 30cm). Diameter calculation based on surface area.
Exact location of test pile is not given.
Swedish ram sounding used to determine the strength of the sand layers. CPT-value based on correlation.

002
Hanstholm-Århus vej (1995) Site 1 Pile(s) 1 - 1 Precast concrete
Hanstholm-Århus vej. P47

NUMLAY	NUMPIL	GWT	GAMPWP	SIGSRF	ZHOLE	QR.SOIL	QR.PILE
4	1	-0.2	10	0.0	0.0	3	3

LAYER	DEPTH BOTTM	GAMMA EFF	TYPE ClSiSa	Q.CPT TIP	SPT N	OCR	CLAY SuTop	CLAY SuBot	CLAY TYP	CLAY St	CLAY Ip	SAND D50	SAND Dr	SAND PHI	CLC FLG	MISCELLANEOUS 1	2	3
1	4.4	9.0	3	5530	0	0	0	0	0	0	0	.39	0	0	0	0	0	0
2	8.1	9.0	3	11920	0	0	0	0	0	0	0	1.1	0	0	0	0	0	0
3	12.6	9.0	3	11920	0	0	0	0	0	0	0	.36	0	0	0	0	0	0
4	21.6	9.0	3	11920	0	0	0	0	0	0	0	.41	0	0	0	0	0	0

PILE NO	OPN CLS	MAT TYP	DIAM TIP	TAPER degr	WALL TIP	TOTAL LNGTH	TIP PENTR	PLUG RATIO	WATER RATIO	-- MEASURED CAPACITIES -- COMPRSSN	TENSION	DAYS	TBF	MISCELLANEOUS 1 2 3
1	2	2	.382	.00	.191	17.0	16.8	0.0	0.0	1400	0	0	0	0 0 0

Days between driving and testing are unknown.
Pile is a squared prec. concrete pile (sidelength 30cm). Diameter calculation based on surface area.
Swedish ram sounding used to determine the strength of the sand layers. CPT-value based on correlation.
Load test for another pile is presented. It is not included in the database because failure was not reached due to the definition: Load corresponding to total deformations equal 10% of pile diameter.
Artesian water pressure may be present. Not included in this database.

003
Chow et al. (1996,1997,1998), Brucy and Meunier (1992) and Brucy et al. (1991)
Dunkirk, France, pæle CS, CL, LL

NUMLAY	NUMPIL	GWT	GAMPWP	SIGSRF	ZHOLE	QR.SOIL	QR.PILE
4	11	4.0	10	0.0	0.0	4	4

LAYER	DEPTH BOTTM	GAMMA EFF	TYPE ClSiSa	Q.CPT TIP	SPT N	OCR	CLAY SuTop	CLAY SuBot	CLAY TYP	CLAY St	CLAY Ip	SAND D50	SAND Dr	SAND PHI	CLC FLG	MISCELLANEOUS 1	2	3
1	2.0	17.1	3	23000	0	0	0	0	0	0	0	0	0	0	1	0	0	0
2	4.0	17.1	3	15000	0	0	0	0	0	0	0	.25	0	0	1	0	0	0
3	10.0	9.9	3	15000	0	0	0	0	0	0	0	.25	0	0	1	0	0	0
4	22.5	9.9	3	23000	0	0	0	0	0	0	0	.25	0	0	1	0	0	0

PILE NO	OPN CLS	MAT TYP	DIAM TIP	TAPER degr	WALL TIP	TOTAL LNGTH	TIP PENTR	PLUG RATIO	WATER RATIO	-- MEASURED CAPACITIES -- COMPRSSN	TENSION	DAYS	TBF	MISCELLANEOUS 1 2 3
1	1	1	.324	.00	.0191	11.7	11.6	0.55	0.64	0	395	188	1	0 0 0
2	1	1	.324	.00	.0191	11.7	11.6	0.55	0.64	1200	0	189	1	0 0 0
3	1	1	.324	.00	.0191	11.7	11.6	0.55	0.64	0	435	272	1	0 0 0
4	1	1	.324	.00	.0191	11.7	11.6	0.55	0.64	1199	0	273	1	0 0 0
5	1	1	.324	.00	.0191	11.7	11.6	0.55	0.64	0	750	1990	1	1 0 0
6	1	1	.324	.00	.0127	11.7	11.6	0.55	0.64	0	458	176	0	0 0 0

7	1	1	.324	.00	.0127	11.7	11.6	0.55	0.64	1199	0	177	1	0	0	0
8	1	1	.324	.00	.0127	11.7	11.6	0.55	0.64	0	548	289	1	0	0	0
9	1	1	.324	.00	.0127	11.7	11.6	0.55	0.64	1200	0	290	1	0	0	0
10	1	1	.324	.00	.0127	11.7	11.6	0.55	0.64	0	810	2086	1	0	0	0
11	1	1	.324	.00	.0127	22.4	22.1	0.45	0.82	0	3100	1924	0	0	0	0

The water level inside the pile is assumed to correspond to the level of the ground water table.
Soil plugs were removed app.250 days after installation. This is not taken into account but it is postulated that the plug do not influence the overall load-settlement curve.
For pile 2 (CL) and 4(LL), the tension capacities after 2086 and 1924days, respectively are the extraction loads.
CPT ended app. 21m below ground surface. The 4th soil layer is extended to 22,5m below ground surface.
One static test and other dynamic tests have been performed on the test site.
No movement of soil plug in connection with static tests.
Addition to #613 and 614 in existing database. The soil profile has been corrected based on the above-mentioned papers.

004
Motorvegbru Drammen Site 1 Pile(s) 1 - 2 Steel tube and HP-profile
Motorvegbru Drammen, Pæle P1 og P2 (Akse 16), Tvedt and Fredriksen (2003)

NUMLAY	NUMPIL	GWT	GAMPWP	SIGSRF	ZHOLE	QR.SOIL	QR.PILE
6	4	2.8	10	0.0	0.0	4	4

LAYER	DEPTH	GAMMA	TYPE	Q.CPT	SPT	OCR	CLAY					SAND			CLC	MISCELLANEOUS		
	BOTTM	EFF	ClSiSa	TIP	N		SuTop	SuBot	TYP	St	Ip	D50	Dr	PHI	FLG	1	2	3
1	2.8	18.0	3	5500	0	0	0	0	0	0	0	0	.52	36	0	0	0	0
2	15.5	8.0	3	5500	0	0	0	0	0	0	0	0	.52	36	0	0	0	0
3	30.0	9.0	1	0	0	0	40	110	9	0	0	0	0	0	0	0	0	0
4	32.5	9.0	1	0	0	0	110	110	9	0	0	0	0	0	0	0	0	0
5	36.0	9.0	1	0	0	0	85	85	9	0	0	0	0	0	0	0	0	0
6	40.0	9.0	1	0	0	0	110	110	9	0	0	0	0	0	0	0	0	0

PILE NO	OPN CLS	MAT TYP	DIAM TIP	TAPER degr	WALL TIP	TOTAL LNGTH	TIP PENTR	PLUG RATIO	WATER RATIO	-- MEASURED CAPACITIES -- COMPRSSN	TENSION	DAYS	TBF	MISCELLANEOUS 1	2	3	
1	1	1	.813	.00	.0125	12.0	11.0	0.14	0.75	1300	0	1	1	0	0	0	P1-16
2	1	1	.813	.00	.0125	24.0	17.0	0.15	1.0	1300	0	1	1	0	0	0	P1-16
3	2	1	.400	.00	.200	12.0	11.0	0.0	0.0	640	0	1	1	0	0	0	P2-16
4	2	1	.400	.00	.200	27.0	17.0	0.0	0.0	560	0	1	1	0	0	0	P2-16

The piles have also been dynamic tested and tested in various depths.
Pile no.2 is a steel pile with H-profile. This profile is equated with a "solid/closed" circular profile.
The water level inside the pile is assumed to correspond to the level of the ground water table.
Some uncertainty associated with the determination of the plug ratio.

005
Motorvegbru Drammen Site 2 Pile(s) 3 - 4 Steel tube and HP-profile
Motorvegbru Drammen, Pæle P1 og P2 (Akse 25), Tvedt and Fredriksen (2003)

NUMLAY	NUMPIL	GWT	GAMPWP	SIGSRF	ZHOLE	QR.SOIL	QR.PILE
5	8	1.5	10	0.0	0.0	4	4

LAYER	DEPTH	GAMMA	TYPE	Q.CPT	SPT	OCR	CLAY					SAND			CLC	MISCELLANEOUS		
	BOTTM	EFF	ClSiSa	TIP	N		SuTop	SuBot	TYP	St	Ip	D50	Dr	PHI	FLG	1	2	3
1	1.5	18.0	3	3000	0	0	0	0	0	0	0	0	.35	34	0	0	0	0
2	11.0	7.5	3	3000	0	0	0	0	0	0	0	0	.35	34	0	0	0	0
3	15.0	8.0	3	6000	0	0	0	0	0	0	0	0	.50	35	0	0	0	0
4	17.0	9.0	3	9000	0	0	0	0	0	0	0	0	.58	35	0	0	0	0
5	27.4	8.0	3	7000	0	0	0	0	0	0	0	0	.48	34	0	0	0	0

PILE NO	OPN CLS	MAT TYP	DIAM TIP	TAPER degr	WALL TIP	TOTAL LNGTH	TIP PENTR	PLUG RATIO	WATER RATIO	-- MEASURED CAPACITIES -- COMPRSSN	TENSION	DAYS	TBF	MISCELLANEOUS 1	2	3	
1	1	1	.813	.00	.0125	24.0	15.0	0.09	0.90	1890	0	2	1	0	0	0	P1-25
2	1	1	.813	.00	.0125	25.0	25.0	0.16	0.94	2700	0	2	1	0	0	0	P1-25
3	1	1	.813	.00	.0125	25.0	25.0	0.16	0.94	3450	0	16	1	0	0	0	P1-25
4	1	1	.813	.00	.0125	25.0	25.0	0.16	0.94	3500	0	171	1	0	0	0	P1-25
5	2	1	.400	.00	.200	16.0	15.0	0.0	0.0	1030	0	3	1	0	0	0	P2-25
6	2	1	.400	.00	.200	25.0	25.0	0.0	0.0	1550	0	3	1	0	0	0	P2-25
7	2	1	.400	.00	.200	25.0	25.0	0.0	0.0	1590	0	16	1	0	0	0	P2-25
8	2	1	.400	.00	.200	25.0	25.0	0.0	0.0	1800	0	172	1	0	0	0	P2-25

The piles have also been dynamic tested and tested in various depths.
Pile no.2 is a steel pile with H-profile. This profile is equated with a "solid/closed" circular profile.
The water level inside the pile is assumed to correspond to the level of the ground water table.
Some uncertainty associated with the determination of the plug ratio.

006
Axelsson (1998a,1998b,2000,2002)
Vårby, Sverige, Pæl D

NUMLAY	NUMPIL	GWT	GAMPWP	SIGSRF	ZHOLE	QR.SOIL	QR.PILE
4	4	2.5	10	0.0	0.0	4	4

LAYER	DEPTH	GAMMA	TYPE	Q.CPT	SPT	OCR	CLAY					SAND			CLC	MISCELLANEOUS		
	BOTTM	EFF	ClSiSa	TIP	N		SuTop	SuBot	TYP	St	Ip	D50	Dr	PHI	FLG	1	2	3
1	2.5	19.0	1	1000	0	0	0	0	0	0	0	0	0	0	0	0	0	0
2	5.0	9.0	3	2500	0	0	0	0	0	0	0	0	0	0	0	0	0	0
3	8.0	9.0	3	3000	0	0	0	0	0	0	0	.16	0	0	0	0	0	0
4	13.4	9.0	3	4000	0	0	0	0	0	0	0	.2	0	0	0	0	0	0

PILE NO	OPN CLS	MAT TYP	DIAM TIP	TAPER degr	WALL TIP	TOTAL LNGTH	TIP PENTR	PLUG RATIO	WATER RATIO	-- MEASURED CAPACITIES -- COMPRSSN	TENSION	DAYS	TBF	MISCELLANEOUS 1 2 3
1	2	2	.299	.00	.1495	12.8	12.8	0.0	0.0	310	0	1	0	0 0 0
2	2	2	.299	.00	.1495	12.8	12.8	0.0	0.0	340	0	8	1	0 0 0
3	2	2	.299	.00	.1495	12.8	12.8	0.0	0.0	390	0	122	1	0 0 0
4	2	2	.299	.00	.1495	12.8	12.8	0.0	0.0	450	0	667	1	0 0 0

Unit weight of the soil is estimated.
Piles are sq. prec. concrete pile (sidelength 23,5cm). Diameter calculation based on surface area.
The total length of the pile is unknown.
The capacity of the pile is influenced by the "reaction piles".
Many dynamic tests have been performed in the area.

007
Aalborg værft Site 1 Pile(s) 1 - 1 Precast concrete
Aalborg Værft, P3

NUMLAY	NUMPIL	GWT	GAMPWP	SIGSRF	ZHOLE	QR.SOIL	QR.PILE
5	1	3.5	10	0.0	0.0	2	3

LAYER	DEPTH	GAMMA	TYPE	Q.CPT	SPT	OCR	CLAY					SAND			CLC	MISCELLANEOUS		
	BOTTM	EFF	ClSiSa	TIP	N		SuTop	SuBot	TYP	St	Ip	D50	Dr	PHI	FLG	1	2	3
1	3.5	15.0	1	0	0	0	15	15	8	0	0	0	0	0	0	0	0	0
2	6.0	5.0	1	0	0	0	15	15	8	0	0	0	0	0	0	0	0	0
3	7.0	5.0	1	0	0	0	110	110	8	2.2	0	0	0	0	0	0	0	0
4	15.0	9.0	3	0	0	0	0	0	0	0	0	0	0	37	0	0	0	0
5	17.6	9.7	1	0	0	0	170	250	8	3.0	0	0	0	0	0	0	0	0

PILE NO	OPN CLS	MAT TYP	DIAM TIP	TAPER degr	WALL TIP	TOTAL LNGTH	TIP PENTR	PLUG RATIO	WATER RATIO	-- MEASURED CAPACITIES -- COMPRSSN	TENSION	DAYS	TBF	MISCELLANEOUS 1 2 3
1	2	2	.318	.00	.159	17.5	17.5	0.0	0.0	1380	0	21	0	0 0 0

The third clay layer is really an organic layer. It is categorized as clay.
The unit weight of some of the soil layers is estimated. The unit weight of the third layer is changed from 3 to 5 (15-12-2003).
The triaxial friction angle is estimated.
Pile is a squared prec. concrete pile (sidelength 25cm). Diameter calculation based on surface area.
The total length is not given.
Failure was not reached due to the definition: Load corresponding to total deformations equal 10% of the pile diameter. The load-settlement curve is so flat that it is assumed that failure has occured.
Other static tests have also been performed. Not included due to the fact that they not failed nor is the soil profile well-defined.

008
Aarsleff (1998) Site 1
Kolding Forrense anlæg, TPP1

NUMLAY	NUMPIL	GWT	GAMPWP	SIGSRF	ZHOLE	QR.SOIL	QR.PILE
3	1	1.1	10	0.0	6.6	1	4

LAYER	DEPTH	GAMMA	TYPE	Q.CPT	SPT	OCR	CLAY					SAND			CLC	MISCELLANEOUS		
	BOTTM	EFF	ClSiSa	TIP	N		SuTop	SuBot	TYP	St	Ip	D50	Dr	PHI	FLG	1	2	3
1	1.1	10.0	3	6500	0	0	0	0	0	0	0	0	0	0	0	0	0	0
2	8.1	5.0	1	0	0	0	55	85	8	0	0	0	0	0	0	0	0	0
3	20.1	9.0	3	10500	0	0	0	0	0	0	0	0	0	0	0	0	0	0

PILE NO	OPN CLS	MAT TYP	DIAM TIP	TAPER degr	WALL TIP	TOTAL LNGTH	TIP PENTR	PLUG RATIO	WATER RATIO	-- MEASURED CAPACITIES -- COMPRSSN	TENSION	DAYS	TBF	MISCELLANEOUS 1 2 3
1	2	2	.382	0	.191	20.0	18.6	0.0	0.0	0	360	14	0	0 0 0 TPP1

Pile is a squared prec. concrete pile (sidelength 30cm). Diameter calculation based on surface area.
The clay layer is really an organic layer. Here it is categorized as clay.
Assumed sand from end of the boring to the pile tip.
Swedish ram sounding used to determine the strength of the sand layers. CPT-value based on correlation.
Based on Boring B/RS16 and B4.

009
Aarsleff (1998) Site 2
Kolding Forrense anlæg, TPP2

NUMLAY	NUMPIL	GWT	GAMPWP	SIGSRF	ZHOLE	QR.SOIL	QR.PILE
4	1	1.0	10	0.0	7.0	1	4

LAYER	DEPTH BOTTM	GAMMA EFF	TYPE ClSiSa	Q.CPT TIP	SPT N	OCR	CLAY SuTop	CLAY SuBot	CLAY TYP	CLAY St	CLAY Ip	SAND D50	SAND Dr	SAND PHI	CLC FLG	MISCELLANEOUS 1	MISCELLANEOUS 2	MISCELLANEOUS 3
1	1.0	18.0	3	9500	0	0	0	0	0	0	0	0	0	0	0	0	0	0
2	2.5	10.0	3	2000	0	0	0	0	0	0	0	0	0	0	0	0	0	0
3	8.5	7.0	1	0	0	0	40	80	8	0	0	0	0	0	0	0	0	0
4	20.0	9.0	3	12500	0	0	0	0	0	0	0	0	0	0	0	0	0	0

PILE NO	OPN CLS	MAT TYP	DIAM TIP	TAPER degr	WALL TIP	TOTAL LNGTH	TIP PENTR	PLUG RATIO	WATER RATIO	-- MEASURED CAPACITIES -- COMPRSSN	TENSION	DAYS	TBF	MISCELLANEOUS 1 2 3
1	2	2	.382	0	.191	20.0	19.0	0.0	0.0	0	355	14	0	0 0 0 TPP2

Pile is a squared prec. concrete pile (sidelength 30cm). Diameter calculation based on surface area.
The clay layer is really an organic layer. Here it is categorized as clay.
Assumed sand from end of the boring to the pile tip.
Swedish ram sounding used to determine the strength of the sand layers. CPT-value based on correlation.
Based on Boring B/RS17.

****
DATA BASE: TILLÆGSCASES TIL NGI-DATABASE - PILES IN SAND LOG
****

Date	By	Description
10 Dec 2003	AA	Cases approved by CJFC/NGI and PMA/NGI.
15 Dec 2003	AA	Case Aalborg værft is included in this database. Case Gudenåen is removed. Piles with non-circular cross-sections are equated with circular cross-sections. Equivalent diameter based on surface area instead of cross-section area. Soil and pile quality rating.
16 Dec 2003	AA	The sequence of the cases is changed.
07 Mar 2005	AA	PSG Domicil Kbh. included in this database.
08 MAR 2005	AA	PSG Domicil Kbh. excluded from database.
18 MAR 2006	AA	Quality rating for both pile and soil for case no. 6 changed to 4.

Appendix F:
AAU and NGI data

The following pages present the PILCAP input file for the combination of the AAU and NGI data. It should be mentioned that the references in the database cannot be found in the list of references.

```
PILES IN SAND    AAU and NGI database                                11 AUG 2004

    62   NUMSIT   Number of different sites
     0   INTER    Run program in interactive mode (0=no 1=yes)

     6   ICSAND   Code for method to calculate sand skin friction, see below
     6   ICCLAY   Code for method to calculate clay skin friction, see below

   100   ATMPRS   Atmospheric pressure    (100 kPa  in S.I. units)
    10   GAMWAT   Unit weight of water    (10 kN/m3 in S.I. units)
    78   GAMSTL   Unit weight of steel    (78 kN/m3 in S.I. units)
    25   GAMCON   Unit weight of concrete (25 kN/m3 in S.I. units)
     9   GAMWOD   Unit weight of wood     ( 9 kN/m3 in S.I. units)

     1   MODFSU   Code for change of Su values to Su.UU or Su.DSS (0=No 1=Yes)
     0   TIMEFC   Time needed for development of full pile clay capacity, days
   .00   DELT10   Pile capacity increase for 10-fold time increase
  1.00   PLGFCT   Plug factor, ratio inside/outside friction force

  0  0   INCQRC   Include sites with same or higher soil and pile quality rating code
 1 1 1   INCMAT   Include piles with material code STEEL/CONCRETE/WOOD (0=No 1=Yes)
  1  1   INCMTN   Include piles loaded in compression/tension (0=No 1=Yes)
 0 100   DIAINC   Include piles with diameter within given range
 0 200   PENINC   Include piles with penetration within given range
 0 99999 CAPINC   Include piles with measured capacity within given range
 0 10000 TIMINC   Include piles with time from driving to testing within given range
 0 10.0  SUPINC   Include piles with average Su/po' ratio within given range

  0.0  0.0  0.0  0.0  0.0   SAND 1-5    Parameters used to calculate pile skin
  0.0  0.0  0.0  0.0  0.0   SAND 6-10   friction in sand by NGI-1999 method

 1 1 0            Codes for plotting, 0=NO 1=YES (SAND/CMP  SAND/TNS  CLAY/CMP&TNS)

  ================================    ======================================
  SAND SKIN FRICTION CODES            CLAY SKIN FRICTION CODES
  ================================    ======================================
  1 = API 1972 to 1984 (K=0.5/0.7)    1 = API 1979 to 1987 (24-72 kPa)
  2 = API 1984 to now  (K=0.8/0.8)    2 = API 1987 to now  (ALPHA=f(Su/SIGZ))
  3 = API 1984 to now  (K=0.5/0.7)    3 = API/NGI 1992
  4 = Not used                        4 = NGI 1990
  5 = Imperial College 1996           5 = Imperial College 1996
  6 = NGI 1999                        6 = NGI 1999
  7 = Not used                        7 = Not used
  ================================    ======================================

Data given below for each location and pile include :

  NUMLAY        Number of soil layers
  NUMPIL        Number of different piles or penetration depths
  GWT           Depth from soil surface to ground water table, neg. if submerged site
  GAMPWP        Water unit weight to calculate pore water pressure at pile tip
  SIGSRF        Vertical stress at soil surface
  ZHOLE         Depth below surface of open or cased hole
  QR.SOIL       Quality rating for soil and pile data :
  QR.PILE       0 = Not known  1 = Low  2 = Average  3 = High

  DEPTH BOTTM   Depth to bottom of layer
  GAMMA EFF     Effective unit weight
  TYPE          Soil type indicator (1=Clay 2=Silt 3=Sand)
  Q.CPT         Cone Penetrometer Test tip resistance qc
  SPT           Standard Penetration Test, blows/foot
  OCR           Over-consolidation ratio for CPT to Dr conversion
  SuTop         Undrained shear strength at top of layer
  SuBot         Undrained shear strength at bottom of layer
  TYP           Type of undrained shear strength measurement, see below
  St            Clay sensitivity
  Ip            Clay plasticity index = Wl - Wp
  D50           Sand grain average diameter, mm
  Dr            Sand relative density
  PHI           Sand angle of internal friction
  CLC.FLG       Flag for calcareous soils
  MISC 1-3      MISC(1) is Delta.Sig.PC, used to find OCR.  2-3 not used.

  OPN.CLS       Pile driven open ended (=1) or closed ended (=2)
  MAT.TYP       Pile material type id (1=steel 2=concrete 3=wood)
  DIAM.TIP      Pile tip diameter
  TAPER         Pile wall taper, degrees
  WALL.TIP      Wall thickness at pile tip
  TOTAL.LNGTH   Total pile length from pile but to pile tip
  TIP.PENTR     Depth of pile tip penetration
  PLUG.RATIO    Ratio soil plug length to tip penetration
  WATER.RATIO   Ratio water plug length to tip penetration
  COMPRSSN      Measured pile capacity in compression
  TENSION       Measured pile capacity in tension
  DAYS          Number of days between pile driving and pile testing
  TBF           Value 1 flags that the pile has been tested before
  MISC(1)=  1   Value 1 flags that failure was not reached
  MISC(2)= -1   No correction for time between driving and testing
  MISC(3)= -1   Skip plug capacity control
  MISC(3)=  0   Clay tip tensile force : Undrained conditions
  MISC(3)=  1   Clay tip tensile force : Drained conditions
  MISC(3)=  2   Clay tip tensile force : Zero force at pile tip

Undrained shear strength codes :

  -1 = Estimated value              0 = Not known

   1 = Torvane, pocket pentr.       8 = Field vane test
```

```
   2 = Unconfined compr. test        9 = Field cone penetrometer test
   3 = UU triaxial test             10 = Other field test
   4 = CIU/CAU triaxial test
   5 = Direct simple shear
   6 = Lab vane
   7 = Other lab test


#  001
Olson (1988)  Report to API :  Comparison of Measured Axial Load Capacities
Arkansas River                 of Steel Pipe Piles in Sand ......

 NUMLAY   NUMPIL   GWT   GAMPWP    SIGSRF   ZHOLE   QR.SOIL   QR.PILE
    8       8      0.0     10        0.0     0.0       0         0

 LAYER  DEPTH  GAMMA TYPE  Q.CPT  SPT  OCR  -------- CLAY -------   ----SAND----  CLC  MISCELLANEOUS
        BOTTM   EFF ClSiSa  TIP    N        SuTop SuBot TYP St Ip   D50  Dr  PHI  FLG    1   2   3
   1     5.2   11.2   3      0   -17    3     0     0    0  0  0    0   0    0    0     0   0   0
   2     6.1    8.9   3      0   -32    2     0     0    0  0  0    0   0    0    0     0   0   0
   3     7.9   11.1   1      0     0    0    35?   35?  -1  0  0    0   0    0    0     0   0   0
   4     9.1   10.0   3      0   -23   1.5    0     0    0  0  0    0   0    0    0     0   0   0
   5     9.8    8.6   3      0   -21   1.5    0     0    0  0  0    0   0    0    0     0   0   0
   6    13.4   10.0   3      0   -30    0     0     0    0  0  0    0   0    0    0     0   0   0
   7    15.5   10.5   3      0   -36    0     0     0    0  0  0    0   0    0    0     0   0   0
   8    16.3    8.6   3      0   -41    0     0     0    0  0  0    0   0    0    0     0   0   0

 PILE OPN MAT  DIAM TAPER  WALL  TOTAL  TIP   PLUG  WATER   -- MEASURED CAPACITIES --  MISCELLANEOUS
  NO  CLS TYP   TIP degr   TIP   LNGTH PENTR  RATIO RATIO   COMPRSSN TENSION DAYS TBF  1 2 3
   1   2   1   .356  0    .010?  16.2  16.2   0.0   0.0       1561        0    0   0   0 0 0  API 089
   2   2   1   .356  0    .010?  16.2  16.2   0.0   0.0          0      876    0   0   0 0 0  API 090
   3   2   1   .533  0    .010?  16.2  16.2   0.0   0.0       2575        0    0   0   0 0 0  API 095
   4   2   1   .533  0    .010?  16.2  16.2   0.0   0.0          0     1076    0   0   0 0 0  API 096
   5   2   1   .432  0    .010?  16.2  16.2   0.0   0.0       2233        0    0   0   0 0 0  API 100
   6   2   1   .432  0    .010?  16.2  16.2   0.0   0.0          0     1027    0   0   0 0 0  API 101
   7   2   1   .432  0    .010?  16.2  16.2   0.0   0.0       2215        0    0   0   0 0 0  API 102
   8   2   1   .432  0    .010?  16.2  16.2   0.0   0.0          0     1054    0   0   0 0 0  API 103

The SPT N-values have been depth corrected as proposed by Olson in the report
24 Sep 2000 : CMP/TNS on same pile included as two tests


#  002
Olson (1988)  Report to API :  Comparison of Measured Axial Load Capacities
Florida                        of Steel Pipe Piles in Sand ......

 NUMLAY   NUMPIL   GWT   GAMPWP    SIGSRF   ZHOLE   QR.SOIL   QR.PILE
    6       1      0.0     10        0.0     0.0       0         0

 LAYER  DEPTH  GAMMA TYPE  Q.CPT  SPT  OCR  -------- CLAY -------   ----SAND----  CLC  MISCELLANEOUS
        BOTTM   EFF ClSiSa  TIP    N        SuTop SuBot TYP St Ip   D50  Dr  PHI  FLG    1   2   3
   1     2.7   12.6   3      0   -16    0     0     0    0  0  0    0   0    0    0     0   0   0
   2     7.6   10.2   3      0    -6    0     0     0    0  0  0    0   0    0    0     0   0   0
   3    10.7   10.3   3      0   -18    0     0     0    0  0  0    0   0    0    0     0   0   0
   4    16.8   10.2   3      0    -9    0     0     0    0  0  0    0   0    0    0     0   0   0
   5    18.3    9.3   3      0   -13    0     0     0    0  0  0    0   0    0    0     0   0   0
   6    18.4   10.0   3      0   -17    0     0     0    0  0  0    0   0    0    0     0   0   0

 PILE OPN MAT  DIAM TAPER  WALL  TOTAL  TIP   PLUG  WATER   -- MEASURED CAPACITIES --  MISCELLANEOUS
  NO  CLS TYP   TIP degr   TIP   LNGTH PENTR  RATIO RATIO   COMPRSSN TENSION DAYS TBF  1 2 3
   1   1   1   .914  0    .015?  18.3  18.3   0.5?  0.0       3069        0    0   0   0 0 0  API 553

The SPT N-values have been depth corrected as proposed by Olson in the report.
This pile has very low measured tip resistance, plug removed and pile concreted.


#  003
Olson (1988)  Report to API :  Comparison of Measured Axial Load Capacities
Kansas City                    of Steel Pipe Piles in Sand ......

 NUMLAY   NUMPIL   GWT   GAMPWP    SIGSRF   ZHOLE   QR.SOIL   QR.PILE
    6       2      3.0     10        0.0     0.0       0         0

 LAYER  DEPTH  GAMMA TYPE  Q.CPT  SPT  OCR  -------- CLAY -------   ----SAND----  CLC  MISCELLANEOUS
        BOTTM   EFF ClSiSa  TIP    N        SuTop SuBot TYP St Ip   D50  Dr  PHI  FLG    1   2   3
   1     4.0   17.0  2.5     0    -9    2     0     0    0  0  0    0   0    0    0     0   0   0
   2     5.3   10.2  2.0     0    -4    0     0     0    0  0  0    0   0    0    0     0   0   0
   3     7.0   10.2  2.5     0    -5    0     0     0    0  0  0    0   0    0    0     0   0   0
   4    11.4   10.2  2.5     0   -13    0     0     0    0  0  0    0   0    0    0     0   0   0
   5    16.8   10.2   3      0   -11    0     0     0    0  0  0    0   0    0    0     0   0   0
   6    16.9   10.2   3      0   -16    0     0     0    0  0  0    0   0    0    0     0   0   0

 PILE OPN MAT  DIAM TAPER  WALL  TOTAL  TIP   PLUG  WATER   -- MEASURED CAPACITIES --  MISCELLANEOUS
  NO  CLS TYP   TIP degr   TIP   LNGTH PENTR  RATIO RATIO   COMPRSSN TENSION DAYS TBF  1 2 3
   1   2   1   .330  0    .010?  16.8  16.8   1.0   0.0        836        0    0   0   0 0 0  API 341
   2   2   1   .356  0    .010?  16.8  16.8   1.0   0.0        970        0    0   0   0 0 0  API 342

The SPT N-values have been depth corrected as proposed by Olson in the report
Piles are concrete filled.

#  004
Olson (1988)  Report to API :  Comparison of Measured Axial Load Capacities
Muskegon                       of Steel Pipe Piles in Sand ......

 NUMLAY   NUMPIL   GWT   GAMPWP    SIGSRF   ZHOLE   QR.SOIL   QR.PILE
    4       2      1.0?    10        0.0     0.0       0         0

 LAYER  DEPTH  GAMMA TYPE  Q.CPT  SPT  OCR  -------- CLAY -------   ----SAND----  CLC  MISCELLANEOUS
        BOTTM   EFF ClSiSa  TIP    N        SuTop SuBot TYP St Ip   D50  Dr  PHI  FLG    1   2   3
   1     6.1   11.1   3      0    -8    0     0     0    0  0  0    0   0    0    0     0   0   0
   2    10.7   10.4   3      0   -13    0     0     0    0  0  0    0   0    0    0     0   0   0
   3    17.7   10.0   3      0    -5    0     0     0    0  0  0    0   0    0    0     0   0   0
   4    17.8   10.0   3      0    -5    0     0     0    0  0  0    0   0    0    0     0   0   0

 PILE OPN MAT  DIAM TAPER  WALL  TOTAL  TIP   PLUG  WATER   -- MEASURED CAPACITIES --  MISCELLANEOUS
  NO  CLS TYP   TIP degr   TIP   LNGTH PENTR  RATIO RATIO   COMPRSSN TENSION DAYS TBF  1 2 3
   1   2   1   .305  0    .006   17.7  17.7   0.0   0.0       1068        0    0   0   0 0 0  API 796
   2   1   1   .305  0    .006   17.7  17.7   0.0   0.9        489        0    0   0   0 0 0  API 798

The SPT N-values have been depth corrected as proposed by Olson in the report
Pile 2 had its plug removed by jetting.
```

```
#  005
Olson (1988)  Report to API :  Comparison of Measured Axial Load Capacities
Mustang Island Pile 1          of Steel Pipe Piles in Sand ......

 NUMLAY   NUMPIL   GWT   GAMPWP    SIGSRF   ZHOLE   QR.SOIL   QR.PILE
    5       1      0.0     10        0.0     0.0       0         0

 LAYER  DEPTH  GAMMA TYPE  Q.CPT  SPT  OCR  -------- CLAY -------   ----SAND----  CLC  MISCELLANEOUS
        BOTTM   EFF ClSiSa  TIP    N        SuTop SuBot TYP St Ip   D50  Dr  PHI  FLG    1   2   3
   1     4.6   10.0   3      0   -34    0     0     0    0   0  0    0   0    0    0     0   0   0
   2    11.3   10.4   3      0   -58    0     0     0    0   0  0    0   0    0    0     0   0   0
   3    14.9    8.3   1      0     0    0    14    14    1   0  0    0   0    0    0     0   0   0
   4    20.7   10.3  2.8     0   -61    0     0     0    0   0  0    0   0    0    0     0   0   0
   5    21.1   10.0   1      0     0    0    28    28    1   0  0    0   0    0    0     0   0   0

 PILE OPN MAT  DIAM TAPER  WALL  TOTAL  TIP   PLUG  WATER   -- MEASURED CAPACITIES --  MISCELLANEOUS
  NO  CLS TYP   TIP degr   TIP   LNGTH PENTR  RATIO RATIO   COMPRSSN TENSION DAYS TBF  1 2 3
   1   1   1   .610  0    .010   21.0  21.0   0.5?  1.0?        0     2024    0   0   0 0 0  API 353

The SPT N-values have been depth corrected as proposed by Olson in the report

#  006
Olson (1988)  Report to API :  Comparison of Measured Axial Load Capacities
Mustang Island Pile 2          of Steel Pipe Piles in Sand ......

 NUMLAY   NUMPIL   GWT   GAMPWP    SIGSRF   ZHOLE   QR.SOIL   QR.PILE
    5       1      0.0     10        0.0     0.0       0         0

 LAYER  DEPTH  GAMMA TYPE  Q.CPT  SPT  OCR  -------- CLAY -------   ----SAND----  CLC  MISCELLANEOUS
        BOTTM   EFF ClSiSa  TIP    N        SuTop SuBot TYP St Ip   D50  Dr  PHI  FLG    1   2   3
   1     0.6   10.0   1      0     0    0    10    10    1   0  0    0   0    0    0     0   0   0
   2    10.7    9.9  2.8     0   -33    0     0     0    0   0  0    0   0    0    0     0   0   0
   3    14.3   10.0   1      0     0    0    14    14    1   0  0    0   0    0    0     0   0   0
   4    20.1    9.3  2.8     0   -32    0     0     0    0   0  0    0   0    0    0     0   0   0
   5    21.1   10.0   1      0     0    0    28    28    1   0  0    0   0    0    0     0   0   0

 PILE OPN MAT  DIAM TAPER  WALL  TOTAL  TIP   PLUG  WATER   -- MEASURED CAPACITIES --  MISCELLANEOUS
  NO  CLS TYP   TIP degr   TIP   LNGTH PENTR  RATIO RATIO   COMPRSSN TENSION DAYS TBF  1 2 3
   1   1   1   .610  0    .010   21.0  21.0   0.5?  1.0?        0     1801    0   0   0 0 0  API 353

The SPT N-values have been depth corrected as proposed by Olson in the report

#  007
Mey et al (1985)          Data taken directly from Randolph et al (1994)
Los Barrios

 NUMLAY   NUMPIL   GWT   GAMPWP    SIGSRF   ZHOLE   QR.SOIL   QR.PILE
    1       2      0.0     10        0.0     0.0       0         0

 LAYER  DEPTH  GAMMA TYPE  Q.CPT  SPT  OCR  -------- CLAY -------   ----SAND----  CLC  MISCELLANEOUS
        BOTTM   EFF ClSiSa  TIP    N        SuTop SuBot TYP St Ip   D50  Dr  PHI  FLG    1   2   3
   1    18.1   10.0   3      0     0    0     0     0    0   0  0    0   .50  0    0     0   0   0

 PILE OPN MAT  DIAM TAPER  WALL  TOTAL  TIP   PLUG  WATER   -- MEASURED CAPACITIES --  MISCELLANEOUS
  NO  CLS TYP   TIP degr   TIP   LNGTH PENTR  RATIO RATIO   COMPRSSN TENSION DAYS TBF  1 2 3
   1   1   2   .914  0    .010   18.0  18.0   0.5   1.0       5080        0    0   0   0 0 0   1-c
   2   1   2   .914  0    .010   18.0  18.0   0.5   1.0          0     2500    0   0   0 0 0   1-t

24 Sep 2000 : CMP/TNS on same pile included as two tests

#  008
Yen et al (1989)          Data taken directly from Randolph et al (1994)
Hsin-Ta

 NUMLAY   NUMPIL   GWT   GAMPWP    SIGSRF   ZHOLE   QR.SOIL   QR.PILE
    1       3      0.0     10        0.0     0.0       0         0

 LAYER  DEPTH  GAMMA TYPE  Q.CPT  SPT  OCR  -------- CLAY -------   ----SAND----  CLC  MISCELLANEOUS
        BOTTM   EFF ClSiSa  TIP    N        SuTop SuBot TYP St Ip   D50  Dr  PHI  FLG    1   2   3
   1    34.4    9.4   3    8000    0    0     0     0    0   0  0    0   .50  0    0     0   0   0

 PILE OPN MAT  DIAM TAPER  WALL  TOTAL  TIP   PLUG  WATER   -- MEASURED CAPACITIES --  MISCELLANEOUS
  NO  CLS TYP   TIP degr   TIP   LNGTH PENTR  RATIO RATIO   COMPRSSN TENSION DAYS TBF  1 2 3
   1   2   1   .610  0    .010   34.3  34.3   0.5   1.0       4330        0    0   0   0 0 0   4-c
   2   2   1   .610  0    .010   34.3  34.3   0.5   1.0          0     2500    0   0   0 0 0   5-t
   3   2   1   .610  0    .010   34.3  34.3   0.5   1.0       4460        0    0   0   0 0 0   6-c

Remark :      Interlayered clay and sand
24 Sep 2000 : CMP/TNS on same pile included as two tests

#  009
Mansur & Kaufman (1958)    Data taken directly from Chow (1996)
Low Sill A (Old River)

 NUMLAY   NUMPIL   GWT   GAMPWP    SIGSRF   ZHOLE   QR.SOIL   QR.PILE
    1       3      0.0     10        0.0     0.0       0         0

 LAYER  DEPTH  GAMMA TYPE  Q.CPT  SPT  OCR  -------- CLAY -------   ----SAND----  CLC  MISCELLANEOUS
        BOTTM   EFF ClSiSa  TIP    N        SuTop SuBot TYP St Ip   D50  Dr  PHI  FLG    1  2  3
   1    21.0    8.05  3      0     0    0     0     0    0   0  0    0   .66  0    0     0  0  0

 PILE OPN MAT  DIAM TAPER  WALL  TOTAL  TIP   PLUG  WATER   -- MEASURED CAPACITIES --  MISCELLANEOUS
  NO  CLS TYP   TIP degr   TIP   LNGTH PENTR  RATIO RATIO   COMPRSSN TENSION DAYS TBF  1 2 3
   1   2   1   .518  0    .010   19.81 19.81  0.0   0.0         0     1664    18   0   0 0 0   2-t
   2   2   1   .419  0    .010   20.12 20.12  0.0   0.0         0     1779    18   0   0 0 0   4-t
   3   2   1   .468  0    .010   19.81 19.81  0.0   0.0         0     1646    18   0   0 0 0   6-t

#  010
Mansur & Kaufman (1958)    Data taken directly from Chow (1996)
Low Sill B (Old River)

 NUMLAY   NUMPIL   GWT   GAMPWP    SIGSRF   ZHOLE   QR.SOIL   QR.PILE
    1       1      0.0     10        0.0     0.0       0         0

 LAYER  DEPTH  GAMMA TYPE  Q.CPT  SPT  OCR  -------- CLAY -------   ----SAND----  CLC  MISCELLANEOUS
        BOTTM   EFF ClSiSa  TIP    N        SuTop SuBot TYP St Ip   D50  Dr  PHI  FLG    1  2  3
   1    21.0    7.86  3      0     0    0     0     0    0   0  0    0   .57  0    0     0  0  0

 PILE OPN MAT  DIAM TAPER  WALL  TOTAL  TIP   PLUG  WATER   -- MEASURED CAPACITIES --  MISCELLANEOUS
  NO  CLS TYP   TIP degr   TIP   LNGTH PENTR  RATIO RATIO   COMPRSSN TENSION DAYS TBF  1 2 3
   1   2   1   .419  0    .010   13.72 13.72  0.0   0.0         0      712    18   0   0 0 0   5-t
```

```
#  011
Chow (1996)              Data taken directly from Chow (1996)
Dunkirk ICP A

 NUMLAY   NUMPIL   GWT   GAMPWP    SIGSRF   ZHOLE   QR.SOIL   QR.PILE
    2       2      0.0     10       20.0     0.0       0         0

 LAYER  DEPTH  GAMMA TYPE  Q.CPT  SPT  OCR  -------- CLAY -------   ----SAND----  CLC  MISCELLANEOUS
        BOTTM   EFF ClSiSa  TIP    N        SuTop SuBot TYP St Ip   D50  Dr  PHI  FLG   1  2  3
   1     7.3    10.0  3      0     0    0     0     0    0   0  0    0   .85  0    0    0  0  0
   2     7.5    10.0  3    14250   0    0     0     0    0   0  0    0   .77  0    0    0  0  0

 PILE OPN MAT  DIAM TAPER  WALL  TOTAL  TIP   PLUG  WATER   -- MEASURED CAPACITIES --  MISCELLANEOUS
  NO  CLS TYP   TIP degr   TIP   LNGTH PENTR  RATIO RATIO   COMPRSSN TENSION DAYS TBF  1 2 3
   1   2   1   .102  0    .010    7.40  7.40  0.0   0.0       309        0   0.55  0   0 0 0  DK1/L1C
   2   2   1   .102  0    .010    7.40  7.40  0.0   0.0         0      186   0.61  0   0 0 0  DK3/L1T

#  012
Chow (1996)              Data taken directly from Chow (1996)
Dunkirk ICP B

 NUMLAY   NUMPIL   GWT   GAMPWP    SIGSRF   ZHOLE   QR.SOIL   QR.PILE
    2       1      0.0     10       18.0     0.0       0         0

 LAYER  DEPTH  GAMMA TYPE  Q.CPT  SPT  OCR  -------- CLAY -------   ----SAND----  CLC  MISCELLANEOUS
        BOTTM   EFF ClSiSa  TIP    N        SuTop SuBot TYP St Ip   D50  Dr  PHI  FLG   1  2  3
   1     5.9    10.0  3      0     0    0     0     0    0   0  0    0   .89  0    0    0  0  0
   2     6.0    10.0  3    15000   0    0     0     0    0   0  0    0   .63  0    0    0  0  0

 PILE OPN MAT  DIAM TAPER  WALL  TOTAL  TIP   PLUG  WATER   -- MEASURED CAPACITIES --  MISCELLANEOUS
  NO  CLS TYP   TIP degr   TIP   LNGTH PENTR  RATIO RATIO   COMPRSSN TENSION DAYS TBF  1 2 3
   1   2   1   .102  0    .010    5.96  5.96  0.0   0.0       231        0   0.63  0   0 0 0  DK2/L1C

#  013
Brucy et al (1991)       Data taken directly from Chow (1996)
Dunkirk Clarom B

 NUMLAY   NUMPIL   GWT   GAMPWP    SIGSRF   ZHOLE   QR.SOIL   QR.PILE
    2       1      0.0     10       26.0     0.0       0         0

 LAYER  DEPTH  GAMMA TYPE  Q.CPT  SPT  OCR  -------- CLAY -------   ----SAND----  CLC  MISCELLANEOUS
        BOTTM   EFF ClSiSa  TIP    N        SuTop SuBot TYP St Ip   D50  Dr  PHI  FLG   1  2  3
   1    21.9    10.0  3      0     0    0     0     0    0   0  0    0   .75  0    0    0  0  0
   2    22.1    10.0  3    26000   0    0     0     0    0   0  0    0   .87  0    0    0  0  0

 PILE OPN MAT  DIAM TAPER  WALL  TOTAL  TIP   PLUG  WATER   -- MEASURED CAPACITIES --  MISCELLANEOUS
  NO  CLS TYP   TIP degr   TIP   LNGTH PENTR  RATIO RATIO   COMPRSSN TENSION DAYS TBF  1 2 3
   1   1   1   .324  0    .020   22.00 22.00  0.61  0.0         0     1730    188  0   0 0 0  LS/T'89a

#  014
Briaud et al (1989)      Data taken directly from Chow (1996)
Hunter's Point

 NUMLAY   NUMPIL   GWT   GAMPWP    SIGSRF   ZHOLE   QR.SOIL   QR.PILE
    2       1      0.0     10       0.0      0.0       0         0

 LAYER  DEPTH  GAMMA TYPE  Q.CPT  SPT  OCR  -------- CLAY -------   ----SAND----  CLC  MISCELLANEOUS
        BOTTM   EFF ClSiSa  TIP    N        SuTop SuBot TYP St Ip   D50  Dr  PHI  FLG   1  2  3
   1     7.7    9.51  3      0     0    0     0     0    0   0  0    0   .60  0    0    0  0  0
   2     7.8    9.51  3    7200    0    0     0     0    0   0  0    0   .57  0    0    0  0  0

 PILE OPN MAT  DIAM TAPER  WALL  TOTAL  TIP   PLUG  WATER   -- MEASURED CAPACITIES --  MISCELLANEOUS
  NO  CLS TYP   TIP degr   TIP   LNGTH PENTR  RATIO RATIO   COMPRSSN TENSION DAYS TBF  1 2 3
   1   2   1   .273  0    .010    7.78  7.78  0.0   0.0       440        0    24   0   0 0 0   S

#  015
Helfrich et al (1985)    Data taken directly from Chow (1996)
Ras Tanajib

 NUMLAY   NUMPIL   GWT   GAMPWP    SIGSRF   ZHOLE   QR.SOIL   QR.PILE
    1       1      0.0     10       30.0     0.0       0         0

 LAYER  DEPTH  GAMMA TYPE  Q.CPT  SPT  OCR  -------- CLAY -------   ----SAND----  CLC  MISCELLANEOUS
        BOTTM   EFF ClSiSa  TIP    N        SuTop SuBot TYP St Ip   D50  Dr  PHI  FLG   1  2  3
   1    18.1    10.0  3      0     0    0     0     0    0   0  0    0   1.0  0    0    0  0  0

 PILE OPN MAT  DIAM TAPER  WALL  TOTAL  TIP   PLUG  WATER   -- MEASURED CAPACITIES --  MISCELLANEOUS
  NO  CLS TYP   TIP degr   TIP   LNGTH PENTR  RATIO RATIO   COMPRSSN TENSION DAYS TBF  1 2 3
   1   1   1   .610  0    .037   18.00 18.00  0.0   0.0         0    12700    30   0   0 0 0   C/L2T

#  016
BCP Committee (1971)     Data taken directly from Chow (1996)
Akasaka A

 NUMLAY   NUMPIL   GWT   GAMPWP    SIGSRF   ZHOLE   QR.SOIL   QR.PILE
    2       1      0.0     10       65.0     0.0       0         0

 LAYER  DEPTH  GAMMA TYPE  Q.CPT  SPT  OCR  -------- CLAY -------   ----SAND----  CLC  MISCELLANEOUS
        BOTTM   EFF ClSiSa  TIP    N        SuTop SuBot TYP St Ip   D50  Dr  PHI  FLG   1  2  3
   1     6.9    10.0  3      0     0    0     0     0    0   0  0    0   .80  0    0    0  0  0
   2     7.1    10.0  3    30000   0    0     0     0    0   0  0    0   .86  0    0    0  0  0

 PILE OPN MAT  DIAM TAPER  WALL  TOTAL  TIP   PLUG  WATER   -- MEASURED CAPACITIES --  MISCELLANEOUS
  NO  CLS TYP   TIP degr   TIP   LNGTH PENTR  RATIO RATIO   COMPRSSN TENSION DAYS TBF  1 2 3
   1   2   1   .200  0    .010    7.00  7.00  0.0   0.0       1139       0    0    0   0 0 0   1C

#  017
BCP Committee (1971)     Data taken directly from Chow (1996)
Akasaka B

 NUMLAY   NUMPIL   GWT   GAMPWP    SIGSRF   ZHOLE   QR.SOIL   QR.PILE
    2       1      0.0     10       7.0      0.0       0         0

 LAYER  DEPTH  GAMMA TYPE  Q.CPT  SPT  OCR  -------- CLAY -------   ----SAND----  CLC  MISCELLANEOUS
        BOTTM   EFF ClSiSa  TIP    N        SuTop SuBot TYP St Ip   D50  Dr  PHI  FLG   1  2  3
   1     3.9    10.0  3      0     0    0     0     0    0   0  0    0   .48  0    0    0  0  0
   2     4.1    10.0  3    7850    0    0     0     0    0   0  0    0   .70  0    0    0  0  0

 PILE OPN MAT  DIAM TAPER  WALL  TOTAL  TIP   PLUG  WATER   -- MEASURED CAPACITIES --  MISCELLANEOUS
  NO  CLS TYP   TIP degr   TIP   LNGTH PENTR  RATIO RATIO   COMPRSSN TENSION DAYS TBF  1 2 3
   1   2   1   .200  0    .010    4.00  4.00  0.0   0.0       156        0    0    0   0 0 0   6B
```

018
BCP Committee (1971) Data taken directly from Chow (1996)
Akasaka C

NUMLAY	NUMPIL	GWT	GAMPWP	SIGSRF	ZHOLE	QR.SOIL	QR.PILE
2	1	0.0	10	19.0	0.0	0	0

LAYER	DEPTH BOTTM	GAMMA EFF	TYPE ClSiSa	Q.CPT TIP	SPT N	OCR	CLAY SuTop	CLAY SuBot	TYP	St	Ip	SAND D50	SAND Dr	PHI	CLC FLG	MISCELLANEOUS 1	2	3
1	10.9	10.0	3	0	0	0	0	0	0	0	0	0	.69	0	0	0	0	0
2	11.1	10.0	3	30000	0	0	0	0	0	0	0	0	.86	0	0	0	0	0

PILE NO	OPN CLS	MAT TYP	DIAM TIP	TAPER degr	WALL TIP	TOTAL LNGTH	TIP PENTR	PLUG RATIO	WATER RATIO	-- MEASURED CAPACITIES -- COMPRSSN	TENSION	DAYS	TBF	MISCELLANEOUS 1 2 3
1	2	1	.200	0	.010	11.00	11.00	0.0	0.0	1122	0	0	0	0 0 0 6C

019
De Beer & Wallays (1969) Data taken directly from Chow (1996)
Anvers

NUMLAY	NUMPIL	GWT	GAMPWP	SIGSRF	ZHOLE	QR.SOIL	QR.PILE
1	1	0.0	10	27.0	0.0	0	0

LAYER	DEPTH BOTTM	GAMMA EFF	TYPE ClSiSa	Q.CPT TIP	SPT N	OCR	CLAY SuTop	CLAY SuBot	TYP	St	Ip	SAND D50	SAND Dr	PHI	CLC FLG	MISCELLANEOUS 1	2	3
1	8.4	10.0	3	0	0	0	0	0	0	0	0	0	.67	0	0	0	0	0

PILE NO	OPN CLS	MAT TYP	DIAM TIP	TAPER degr	WALL TIP	TOTAL LNGTH	TIP PENTR	PLUG RATIO	WATER RATIO	-- MEASURED CAPACITIES -- COMPRSSN	TENSION	DAYS	TBF	MISCELLANEOUS 1 2 3
1	1	1	.318	0	.005	8.30	8.30	0.0	0.0	0	883	0	0	0 0 0 G/T

020
Briaud et al (1989) Data taken directly from Chow (1996)
Lock & Dam 26

NUMLAY	NUMPIL	GWT	GAMPWP	SIGSRF	ZHOLE	QR.SOIL	QR.PILE
1	3	0.0	10	0.0	0.0	0	0

LAYER	DEPTH BOTTM	GAMMA EFF	TYPE ClSiSa	Q.CPT TIP	SPT N	OCR	CLAY SuTop	CLAY SuBot	TYP	St	Ip	SAND D50	SAND Dr	PHI	CLC FLG	MISCELLANEOUS 1	2	3
1	11.2	9.42	3	0	0	0	0	0	0	0	0	0	.97	0	0	0	0	0

PILE NO	OPN CLS	MAT TYP	DIAM TIP	TAPER degr	WALL TIP	TOTAL LNGTH	TIP PENTR	PLUG RATIO	WATER RATIO	-- MEASURED CAPACITIES -- COMPRSSN	TENSION	DAYS	TBF	MISCELLANEOUS 1 2 3
1	2	1	.305	0	.010	10.97	10.97	0.0	0.0	0	543	23	0	0 0 0 3-2
2	2	1	.356	0	.010	11.13	11.13	0.0	0.0	0	605	16	0	0 0 0 3-5
3	2	1	.406	0	.010	11.13	11.13	0.0	0.0	0	881	17	0	0 0 0 3-8

021
Ishihara et al (1977) Data taken directly from Chow (1996)
Kimitsu

NUMLAY	NUMPIL	GWT	GAMPWP	SIGSRF	ZHOLE	QR.SOIL	QR.PILE
2	1	0.0	10	0.0	0.0	0	0

LAYER	DEPTH BOTTM	GAMMA EFF	TYPE ClSiSa	Q.CPT TIP	SPT N	OCR	CLAY SuTop	CLAY SuBot	TYP	St	Ip	SAND D50	SAND Dr	PHI	CLC FLG	MISCELLANEOUS 1	2	3
1	19.7	7.22	3	0	0	0	0	0	0	0	0	0	.67	0	0	0	0	0
2	19.9	7.22	3	39000	0	0	0	0	0	0	0	0	.93	0	0	0	0	0

PILE NO	OPN CLS	MAT TYP	DIAM TIP	TAPER degr	WALL TIP	TOTAL LNGTH	TIP PENTR	PLUG RATIO	WATER RATIO	-- MEASURED CAPACITIES -- COMPRSSN	TENSION	DAYS	TBF	MISCELLANEOUS 1 2 3
1	1	1	1.20	0	.015	19.80	19.80	0.52	0.0	15000	0	0	0	0 0 0 H27

022
Shioi et al (1992) Data taken directly from Chow (1996)
Trans-Tokyo Bay

NUMLAY	NUMPIL	GWT	GAMPWP	SIGSRF	ZHOLE	QR.SOIL	QR.PILE
2	1	0.0	10	0.0	0.0	0	0

LAYER	DEPTH BOTTM	GAMMA EFF	TYPE ClSiSa	Q.CPT TIP	SPT N	OCR	CLAY SuTop	CLAY SuBot	TYP	St	Ip	SAND D50	SAND Dr	PHI	CLC FLG	MISCELLANEOUS 1	2	3
1	30.5	9.80	3	0	0	0	0	0	0	0	0	0	.76	0	0	0	0	0
2	30.7	9.80	3	35000	0	0	0	0	0	0	0	0	.96	0	0	0	0	0

PILE NO	OPN CLS	MAT TYP	DIAM TIP	TAPER degr	WALL TIP	TOTAL LNGTH	TIP PENTR	PLUG RATIO	WATER RATIO	-- MEASURED CAPACITIES -- COMPRSSN	TENSION	DAYS	TBF	MISCELLANEOUS 1 2 3
1	1	1	2.00	0	.042	30.60	30.60	0.99	0.0	34335	0	52	0	0 0 0 BD

023
GCG (1988) and Tomlinson (1994) Data taken directly from Chow (1996)
Cromarty Firth A

NUMLAY	NUMPIL	GWT	GAMPWP	SIGSRF	ZHOLE	QR.SOIL	QR.PILE
2	1	0.0	10	0.0	0.0	0	0

LAYER	DEPTH BOTTM	GAMMA EFF	TYPE ClSiSa	Q.CPT TIP	SPT N	OCR	CLAY SuTop	CLAY SuBot	TYP	St	Ip	SAND D50	SAND Dr	PHI	CLC FLG	MISCELLANEOUS 1	2	3
1	13.0	9.00	3	0	0	0	0	0	0	0	0	0	.59	0	0	0	0	0
2	13.2	9.00	3	16000	0	0	0	0	0	0	0	0	.92	0	0	0	0	0

PILE NO	OPN CLS	MAT TYP	DIAM TIP	TAPER degr	WALL TIP	TOTAL LNGTH	TIP PENTR	PLUG RATIO	WATER RATIO	-- MEASURED CAPACITIES -- COMPRSSN	TENSION	DAYS	TBF	MISCELLANEOUS 1 2 3
1	1	1	.610	0	.024	13.10	13.10	0.95	0.0	1960	0	0	0	0 0 0 1

024
GCG (1988) and Tomlinson (1994) Data taken directly from Chow (1996)
Cromarty Firth B

NUMLAY	NUMPIL	GWT	GAMPWP	SIGSRF	ZHOLE	QR.SOIL	QR.PILE
2	2	0.0	10	0.0	0.0	0	0

LAYER	DEPTH BOTTM	GAMMA EFF	TYPE ClSiSa	Q.CPT TIP	SPT N	OCR	CLAY SuTop	CLAY SuBot	TYP	St	Ip	SAND D50	SAND Dr	PHI	CLC FLG	MISCELLANEOUS 1	2	3
1	19.3	9.00	3	0	0	0	0	0	0	0	0	0	.64	0	0	0	0	0
2	19.5	9.00	3	23000	0	0	0	0	0	0	0	0	.74	0	0	0	0	0

PILE NO	OPN CLS	MAT TYP	DIAM TIP	TAPER degr	WALL TIP	TOTAL LNGTH	TIP PENTR	PLUG RATIO	WATER RATIO	-- MEASURED CAPACITIES -- COMPRSSN	TENSION	DAYS	TBF	MISCELLANEOUS 1 2 3	
1	1	1	.610	0	.024	19.40	19.40	0.82	0.0	2400	0	0	0	0 0 0	2
2	1	1	.610	0	.024	19.40	19.40	0.82	0.0	0	1220	0	0	0 0 0	2

\# 025
GCG (1988) and Tomlinson (1994) Data taken directly from Chow (1996)
Cromarty Firth C

NUMLAY	NUMPIL	GWT	GAMPWP	SIGSRF	ZHOLE	QR.SOIL	QR.PILE
2	2	0.0	10	0.0	0.0	0	0

LAYER	DEPTH BOTTM	GAMMA EFF	TYPE ClSiSa	Q.CPT TIP	SPT N	OCR	CLAY SuTop	CLAY SuBot	CLAY TYP	CLAY St	CLAY Ip	SAND D50	SAND Dr	SAND PHI	CLC FLG	MISCELLANEOUS 1	2	3
1	28.0	9.00	3	0	0	0	0	0	0	0	0	0	.63	0	0	0	0	0
2	28.3	9.00	3	23000	0	0	0	0	0	0	0	0	.57	0	0	0	0	0

PILE NO	OPN CLS	MAT TYP	DIAM TIP	TAPER degr	WALL TIP	TOTAL LNGTH	TIP PENTR	PLUG RATIO	WATER RATIO	-- MEASURED CAPACITIES -- COMPRSSN	TENSION	DAYS	TBF	MISCELLANEOUS 1 2 3	
1	1	1	.762	0	.024	28.10	28.10	0.30	0.0	3150	0	0	0	0 0 0	3
2	1	1	.762	0	.024	28.10	28.10	0.30	0.0	0	1800	0	0	0 0 0	3

\# 026
Mansur & Hunter (1970) ASCE JSMFD Sept 1970 Boring 200
Arkansas River

NUMLAY	NUMPIL	GWT	GAMPWP	SIGSRF	ZHOLE	QR.SOIL	QR.PILE
4	14	0.8	10	0.0	0.0	3	3

LAYER	DEPTH BOTTM	GAMMA EFF	TYPE ClSiSa	Q.CPT TIP	SPT N	OCR	CLAY SuTop	CLAY SuBot	CLAY TYP	CLAY St	CLAY Ip	SAND D50	SAND Dr	SAND PHI	CLC FLG	MISCELLANEOUS 1	2	3
1	3.5	11.5	3	0	20	0	0	0	0	0	0	.30	0	0	0	0	0	0
2	7.0	9.7	3	0	25	0	0	0	0	0	0	.30	0	0	0	0	0	0
3	11.6	9.7	3	0	32	0	0	0	0	0	0	.15	0	0	0	0	0	0
4	16.3	9.7	3	0	41	0	0	0	0	0	0	.25	0	0	0	0	0	0

PILE NO	OPN CLS	MAT TYP	DIAM TIP	TAPER degr	WALL TIP	TOTAL LNGTH	TIP PENTR	PLUG RATIO	WATER RATIO	-- MEASURED CAPACITIES -- COMPRSSN	TENSION	DAYS	TBF	MISCELLANEOUS 1 2 3	
1	2	1	.361	0	.011	16.8	16.2	0.0	0.0	1486	0	0	0	0 0 0	P1-c
2	2	1	.361	0	.011	16.8	16.2	0.0	0.0	0	846	0	0	0 0 0	P1-t
3	2	1	.477	0	.012	16.8	16.1	0.0	0.0	2092	0	0	1	0 0 0	P2-c
4	2	1	.477	0	.012	16.8	16.1	0.0	0.0	0	1068	0	1	0 0 0	P2-t
5	2	1	.542	0	.011	16.8	16.2	0.0	0.0	2278	0	0	0	0 0 0	P3-c
6	2	1	.542	0	.011	16.8	16.2	0.0	0.0	0	1086	0	0	0 0 0	P3-t
7	2	2	.488	0	.244	13.7	12.3	0.0	0.0	1780	0	0	0	0 0 0	P4-c
8	2	2	.488	0	.244	13.7	12.3	0.0	0.0	0	872	0	0	0 0 0	P4-t
9	2	2	.488	0	.244	16.8	15.5	0.0	0.0	2545	0	0	0	0 0 0	P5
-10	2	3	.272	.27	.136	12.2	11.8	0.0	0.0	1024	0	0	0	0 0 0	P8-c
-11	2	3	.272	.27	.136	12.2	11.8	0.0	0.0	0	312	0	0	0 0 0	P8-t
12	2	1	.477	0	.012	16.8	16.2	0.0	0.0	2047	0	0	0	0 0 0	P10-c
13	2	1	.477	0	.012	16.8	16.2	0.0	0.0	0	1041	0	0	0 0 0	P10-t
14	2	2	.488	0	.244	16.8	11.8	0.0	0.0	1593	0	0	0	0 0 0	P11

25 Sep 2000 : CMP/TNS on same pile included as two tests

\# 027
Vesic (1970) ASCE JSMFD March 1970
Ogeechee River Pile 1

NUMLAY	NUMPIL	GWT	GAMPWP	SIGSRF	ZHOLE	QR.SOIL	QR.PILE
11	6	2.1	10	0.0	0.0	4	4

LAYER	DEPTH BOTTM	GAMMA EFF	TYPE ClSiSa	Q.CPT TIP	SPT N	OCR	CLAY SuTop	CLAY SuBot	CLAY TYP	CLAY St	CLAY Ip	SAND D50	SAND Dr	SAND PHI	CLC FLG	MISCELLANEOUS 1	2	3
1	2.1	20.0	3	2500	0	0	0	0	0	0	0	.30	0	0	0	0	0	0
2	2.4	10.0	3	2500	0	0	0	0	0	0	0	.30	0	0	0	0	0	0
3	3.7	10.0	3	7500	0	0	0	0	0	0	0	.30	0	0	0	0	0	0
4	5.2	10.0	3	15000	0	0	0	0	0	0	0	.30	0	0	0	0	0	0
5	6.7	10.0	3	11500	0	0	0	0	0	0	0	.30	0	0	0	0	0	0
6	8.2	10.0	3	13500	0	0	0	0	0	0	0	.30	0	0	0	0	0	0
7	9.8	10.0	3	15000	0	0	0	0	0	0	0	.30	0	0	0	0	0	0
8	12.2	10.0	3	14000	0	0	0	0	0	0	0	.30	0	0	0	0	0	0
9	13.4	10.0	3	19000	0	0	0	0	0	0	0	.30	0	0	0	0	0	0
10	14.9	10.0	3	15000	0	0	0	0	0	0	0	.30	0	0	0	0	0	0
11	15.3	10.0	3	17500	0	0	0	0	0	0	0	.30	0	0	0	0	0	0

PILE NO	OPN CLS	MAT TYP	DIAM TIP	TAPER degr	WALL TIP	TOTAL LNGTH	TIP PENTR	PLUG RATIO	WATER RATIO	-- MEASURED CAPACITIES -- COMPRSSN	TENSION	DAYS	TBF	MISCELLANEOUS 1 2 3	Name
1	2	1	.457	0	.0127	3.7	3.0	0.0	0.0	676	0	.75	0	0 0 0	H11
2	2	1	.457	0	.0127	6.8	6.1	0.0	0.0	2065	0	.75	0	0 0 0	H12
3	2	1	.457	0	.0127	9.7	8.9	0.0	0.0	2643	0	.75	0	0 0 0	H13
4	2	1	.457	0	.0127	12.7	12.0	0.0	0.0	3088	0	.75	0	0 0 0	H14
5	2	1	.457	0	.0127	15.7	15.0	0.0	0.0	3747	0	.75	0	0 0 0	H15
6	2	1	.457	0	.0127	15.7	15.0	0.0	0.0	0	1540	.75	0	0 0 0	H16

18 Nov 2000 : Pile 7 diameter changed from 0.458 m to 0.475 m (square concrete pile, 50/50 skin/tip)
04 Dec 2000 : Pile 7 moved to site 731. Finer layer division, CPTs P-1 & P-4 used

\# 028
McCammon & Golder (1970) Geotechnique June 1970 p. 171 Pile 1
Lower Arrow Lake, BC, Canada

NUMLAY	NUMPIL	GWT	GAMPWP	SIGSRF	ZHOLE	QR.SOIL	QR.PILE
5	2	0.0	11	0.0	0.0	3	3

LAYER	DEPTH BOTTM	GAMMA EFF	TYPE ClSiSa	Q.CPT TIP	SPT N	OCR	CLAY SuTop	CLAY SuBot	CLAY TYP	CLAY St	CLAY Ip	SAND D50	SAND Dr	SAND PHI	CLC FLG	MISCELLANEOUS 1	2	3
1	18.9	7.8	3	0	6	0	0	0	0	0	0	0.2	0	0	0	0	0	0
2	21.9	7.8	1.5	0	0	0	47	47	-1	0	18	0	0	0	0	0	0	0
3	41.8	7.8	3	0	14	0	0	0	0	0	0	0.2	0	0	0	0	0	0
4	43.9	7.8	1.5	0	0	0	100	100	-1	0	20	0	0	0	0	0	0	0
5	50.0	7.8	3	0	47	0	0	0	0	0	0	0.2	0	0	0	0	0	0

PILE NO	OPN CLS	MAT TYP	DIAM TIP	TAPER degr	WALL TIP	TOTAL LNGTH	TIP PENTR	PLUG RATIO	WATER RATIO	-- MEASURED CAPACITIES -- COMPRSSN	TENSION	DAYS	TBF	MISCELLANEOUS 1 2 3	Name
1	1	1	.610	0	.0127	47.4	45.4	0.0	1.0	1560	0	0	0	0 0 0	1A
2	1	1	.610	0	.0127	49.2	47.2	0.34	1.0	4360	0	0	0	1 0 -1	1B

Remarks : Soil plug cleaned out during driving. Test 1B has concrete plug.
18 Nov 2000 : Set N-values to zero for clay layers, change 1B failure load from 4520 to 4360 kN

029
Gregersen et al (1973) NGI Publ. 99 p. 19
Holmen, Drammen

NUMLAY	NUMPIL	GWT	GAMPWP	SIGSRF	ZHOLE	QR.SOIL	QR.PILE
8	15	2.0	10	0.0	0.0	4	4

LAYER	DEPTH	GAMMA	TYPE	Q.CPT	SPT	OCR	CLAY					SAND			CLC	MISCELLANEOUS		
	BOTTM	EFF	ClSiSa	TIP	N		SuTop	SuBot	TYP	St	Ip	D50	Dr	PHI	FLG	1	2	3
1	2.0	18.0	3	2000	0	0	0	0	0	0	0	0.2	.3	0	0	0	0	0
2	4.0	9.0	3	4500	0	0	0	0	0	0	0	0.2	0	0	0	0	0	0
3	6.0	9.5	3	5000	0	0	0	0	0	0	0	0.5	0	0	0	0	0	0
4	10.0	9.0	3	2700	0	0	0	0	0	0	0	0.5	0	0	0	0	0	0
5	15.0	10.0	3	3500	0	0	0	0	0	0	0	0.5	0	0	0	0	0	0
6	18.0	11.0	3	5000	0	0	0	0	0	0	0	0.5	0	0	0	0	0	0
7	22.0	11.0	3	8000	0	0	0	0	0	0	0	0.5	0	0	0	0	0	0
8	25.0	11.0	3	9000	0	0	0	0	0	0	0	0.5	0	0	0	0	0	0

PILE NO	OPN CLS	MAT TYP	DIAM TIP	TAPER degr	WALL TIP	TOTAL LNGTH	TIP PENTR	PLUG RATIO	WATER RATIO	-- MEASURED CAPACITIES -- COMPRSSN	TENSION	DAYS	TBF	MISCELLANEOUS 1 2 3	Name
1	2	2	.280	0	.140	8.0	8.0	0.0	0.0	275	0	0	0	0 0 0	A-c
2	2	2	.280	0	.140	8.0	8.0	0.0	0.0	0	101	0	0	0 0 0	A-t
3	2	2	.280	0	.140	16.0	16.0	0.0	0.0	500	0	0	0	0 0 0	D/A-c
4	2	2	.280	0	.140	16.0	16.0	0.0	0.0	0	269	0	0	0 0 0	D/A-t
-5	2	2	.200	.29	.100	8.0	8.0	0.0	0.0	296	0	0	0	0 0 0	C-c
-6	2	2	.200	.29	.100	8.0	8.0	0.0	0.0	0	127	0	0	0 0 0	C-t
-7	2	2	.200	.19	.100	16.0	16.0	0.0	0.0	479	0	0	0	0 0 0	B/C-c
-8	2	2	.200	.19	.100	16.0	16.0	0.0	0.0	0	240	0	0	0 0 0	B/C-t
9	2	2	.280	0	.140	4.0	3.5	0.0	0.0	219	0	0	0	0 0 0	E
10	2	2	.280	0	.140	8.0	7.5	0.0	0.0	210	0	0	0	0 0 0	E
11	2	2	.280	0	.140	12.0	11.5	0.0	0.0	330	0	0	0	0 0 0	E
12	2	2	.280	0	.140	16.0	15.5	0.0	0.0	471	0	0	0	0 0 0	E
13	2	2	.280	0	.140	20.0	19.5	0.0	0.0	636	0	0	0	0 0 0	E
14	2	2	.280	0	.140	24.0	23.5	0.0	0.0	838	0	0	0	0 0 0	E-c
15	2	2	.280	0	.140	24.0	23.5	0.0	0.0	0	308	0	0	0 0 0	E-t

25 Sep 2000 : CMP/TNS on same pile included as two tests
29 Oct 2000 : Remove the tapered piles 5-6-7-8
06 Nov 2000 : Modified soil profile in upper part to better model actual CPT results.
18 Nov 2000 : Modified CPT profile below 18 m, increase from 7.5 MPa to 8.0-9.0 MPa.

030
Reese & Cox (1976) OTC Paper 2472
Mustang Island

NUMLAY	NUMPIL	GWT	GAMPWP	SIGSRF	ZHOLE	QR.SOIL	QR.PILE
6	2	0.0	10	0.0	0.0	3	3

LAYER	DEPTH	GAMMA	TYPE	Q.CPT	SPT	OCR	CLAY					SAND			CLC	MISCELLANEOUS		
	BOTTM	EFF	ClSiSa	TIP	N		SuTop	SuBot	TYP	St	Ip	D50	Dr	PHI	FLG	1	2	3
1	3.05	10.0	3	0	14	0	0	0	0	0	0	.13	0	0	0	0	0	0
2	6.10	10.0	3	0	22	0	0	0	0	0	0	.13	0	0	0	0	0	0
3	9.15	10.0	3	0	30	0	0	0	0	0	0	.13	0	0	0	0	0	0
4	12.20	10.0	3	0	49	0	0	0	0	0	0	.13	0	0	0	0	0	0
5	15.80	10.0	1	0	0	0	44	44	-1	0	0	0	0	0	0	0	0	0
6	21.60	10.0	3	0	59	0	0	0	0	0	0	.13	0	0	0	0	0	0

PILE NO	OPN CLS	MAT TYP	DIAM TIP	TAPER degr	WALL TIP	TOTAL LNGTH	TIP PENTR	PLUG RATIO	WATER RATIO	-- MEASURED CAPACITIES -- COMPRSSN	TENSION	DAYS	TBF	MISCELLANEOUS 1 2 3	Name
1	1	1	.610	0	.0095	21.3	21.0	0.50	0.50	0	2029	0	0	0 0 0	P1
2	1	1	.610	0	.0095	21.3	21.0	0.50	0.50	0	1793	0	0	0 0 0	P2

031
Beringen et al (1979) ICE : Recent Developments .... London Conf. p. 213
Hoogzand

NUMLAY	NUMPIL	GWT	GAMPWP	SIGSRF	ZHOLE	QR.SOIL	QR.PILE
6	6	3.1	10	0.0	0.0	4	4

LAYER	DEPTH	GAMMA	TYPE	Q.CPT	SPT	OCR	CLAY					SAND			CLC	MISCELLANEOUS		
	BOTTM	EFF	ClSiSa	TIP	N		SuTop	SuBot	TYP	St	Ip	D50	Dr	PHI	FLG	1	2	3
1	1.9	22.0	3	6000	0	0	0	0	0	0	0	.10	0	0	0	0	0	0
2	2.5	24.0	1	2000	0	0	0	0	0	0	15	0	0	0	0	0	0	0
3	3.1	24.0	3	12000	0	0	0	0	0	0	0	.15	0	0	0	0	0	0
4	4.0	12.0	3	28000	0	0	0	0	0	0	0	.15	0	0	0	0	0	0
5	6.0	12.0	3	45000	0	0	0	0	0	0	0	.15	0	0	0	0	0	0
6	8.0	12.0	3	40000	0	0	0	0	0	0	0	.15	0	0	0	0	0	0

PILE NO	OPN CLS	MAT TYP	DIAM TIP	TAPER degr	WALL TIP	TOTAL LNGTH	TIP PENTR	PLUG RATIO	WATER RATIO	-- MEASURED CAPACITIES -- COMPRSSN	TENSION	DAYS	TBF	MISCELLANEOUS 1 2 3	Name
1	1	1	.356	0	.016	7.0	7.0	0.66	0.56	2318	0	0	0	0 0 0	I-c
2	1	1	.356	0	.016	7.0	7.0	0.66	0.56	0	830	0	0	0 0 0	I-t
3	2	1	.356	0	.025	6.75	6.75	0.00	0.00	2850	0	0	0	0 0 0	II-c
4	2	1	.356	0	.025	6.75	6.75	0.00	0.00	0	1098	0	0	0 0 0	II-t
5	1	1	.356	0	.016	5.25	5.25	0.83	0.56	1853	0	0	0	0 0 0	III-c
6	1	1	.356	0	.016	5.25	5.25	0.83	0.56	0	550	0	0	0 0 0	III-t

Remark : Soil unit weights increased by 20 % to include weight on surface
Failure loads corrected to 10 % displacement
25 Sep 2000 : CMP/TNS on same pile included as two tests

032
Fujita (1989) Rio Conference Proc. Session 14 Steel pile no. 1
Hokkaido

NUMLAY	NUMPIL	GWT	GAMPWP	SIGSRF	ZHOLE	QR.SOIL	QR.PILE
6	1	2.5	10	0.0	0.0	2	3

LAYER	DEPTH	GAMMA	TYPE	Q.CPT	SPT	OCR	CLAY					SAND			CLC	MISCELLANEOUS		
	BOTTM	EFF	ClSiSa	TIP	N		SuTop	SuBot	TYP	St	Ip	D50	Dr	PHI	FLG	1	2	3
1	2.5	18.0	4	0	20	0	0	0	0	0	0	.15?	0	0	0	0	0	Fill
2	15.0	10.0	3	0	44	0	0	0	0	0	0	.15?	0	0	0	0	0	0
3	21.0	8.0	2.7	0	10	0	0	0	0	0	0	.10?	0	0	0	0	0	0
4	26.0	8.0	3	0	12	0	0	0	0	0	0	.10?	0	0	0	0	0	0
5	32.0	10.0	2.3	0	50	0	0	0	0	0	0	.10?	0	0	0	0	0	0
6	40.1	10.0	4	0	95	0	0	0	0	0	0	.10?	0	0	0	0	0	Ash

PILE NO	OPN CLS	MAT TYP	DIAM TIP	TAPER degr	WALL TIP	TOTAL LNGTH	TIP PENTR	PLUG RATIO	WATER RATIO	-- MEASURED CAPACITIES -- COMPRSSN	TENSION	DAYS	TBF	MISCELLANEOUS 1	2	3
1	1	1	1.016	0	.022	41.0	40.0	0.85	0.94	15700	0	15	0	0	0	0

Remark : Pile tip located in "volcanic ash". SPT values given by author have been multiplied by 2

033
Fujita (1989) Rio Conference Proc. Session 14 Steel pile no. 3
Chiba-3

NUMLAY	NUMPIL	GWT	GAMPWP	SIGSRF	ZHOLE	QR.SOIL	QR.PILE
6	1	1.2	10	0.0	0.0	2	3

LAYER	DEPTH BOTTM	GAMMA EFF	TYPE ClSiSa	Q.CPT TIP	SPT N	OCR	-------- CLAY ------- SuTop	SuBot	TYP	St	Ip	----SAND---- D50	Dr	PHI	CLC FLG	MISCELLANEOUS 1	2	3
1	1.2	20.0	3	0	10	0	0	0	0	0	0	.30?	0	0	0	0	0	0
2	1.9	10.0	3	0	20	0	0	0	0	0	0	.30?	0	0	0	0	0	0
3	2.8	10.0	3.5	0	24	0	0	0	0	0	0	2.0?	0	0	0	0	0	0
4	7.2	9.0	3	0	18	0	0	0	0	0	0	.10?	0	0	0	0	0	0
5	8.6	10.0	3	0	24	0	0	0	0	0	0	.30?	0	0	0	0	0	0
6	14.0	11.0	3	0	120	0	0	0	0	0	0	.10?	0	0	0	0	0	0

PILE NO	OPN CLS	MAT TYP	DIAM TIP	TAPER degr	WALL TIP	TOTAL LNGTH	TIP PENTR	PLUG RATIO	WATER RATIO	-- MEASURED CAPACITIES -- COMPRSSN	TENSION	DAYS	TBF	MISCELLANEOUS 1	2	3
1	1	1	.356	0	.0111	15.0	13.5	0.75	0.91	2940	0	0	0	0	0	0

Remark : SPT values given by author have been multiplied by 2

034
Appendino (1981) Int. Conf. Stockholm Vol. 2 p. 593 Pile Sermide
Sermide

NUMLAY	NUMPIL	GWT	GAMPWP	SIGSRF	ZHOLE	QR.SOIL	QR.PILE
5	1	0.0	10	10.0	0.0	4	4

LAYER	DEPTH BOTTM	GAMMA EFF	TYPE ClSiSa	Q.CPT TIP	SPT N	OCR	-------- CLAY ------- SuTop	SuBot	TYP	St	Ip	----SAND---- D50	Dr	PHI	CLC FLG	MISCELLANEOUS 1	2	3
1	10.0	8.0	1.8	0	0	0	10	20	-1	0	10?	0	0	0	0	0	0	0
2	20.0	9.0	2.8	10000	0	0	0	0	0	0	0	0	0	0	0	0	0	0
3	29.0	8.5	2.2	5000	0	0	0	0	0	0	0	0	0	0	0	0	0	0
4	35.0	10.0	3	14000	0	0	0	0	0	0	0	0	0	0	0	0	0	0
5	36.0	10.0	3	17000	0	0	0	0	0	0	0	0	0	0	0	0	0	0

PILE NO	OPN CLS	MAT TYP	DIAM TIP	TAPER degr	WALL TIP	TOTAL LNGTH	TIP PENTR	PLUG RATIO	WATER RATIO	-- MEASURED CAPACITIES -- COMPRSSN	TENSION	DAYS	TBF	MISCELLANEOUS 1	2	3
1	2	1	.508	0	.046	35.9	35.9	0.0	0.0	5300	0	0	0	0	0	0

Remark : Thin-walled steel pipe pile filled with concrete
18 Nov 2000 : Pile length changed from 35.9 m to 35.4 m (average of different values quoted in paper)

035
Mey et al (1985) San Francisco Conf. Vol. 3 p.1559
Cadiz

NUMLAY	NUMPIL	GWT	GAMPWP	SIGSRF	ZHOLE	QR.SOIL	QR.PILE
2	2	-21.0	10	0.0	0.0	3	3

LAYER	DEPTH BOTTM	GAMMA EFF	TYPE ClSiSa	Q.CPT TIP	SPT N	OCR	-------- CLAY ------- SuTop	SuBot	TYP	St	Ip	----SAND---- D50	Dr	PHI	CLC FLG	MISCELLANEOUS 1	2	3
1	10.0	10.0	3	0	15	0	0	0	0	0	0	.10	0	0	0	0	0	0
2	20.0	10.0	3	0	33	0	0	0	0	0	0	.10	0	0	0	0	0	0

PILE NO	OPN CLS	MAT TYP	DIAM TIP	TAPER degr	WALL TIP	TOTAL LNGTH	TIP PENTR	PLUG RATIO	WATER RATIO	-- MEASURED CAPACITIES -- COMPRSSN	TENSION	DAYS	TBF	MISCELLANEOUS 1	2	3
1	1?	2	.914	0	.100	49.0	18.0	1.0?	2.0?	5000	0	0	0	1	0	0
2	1?	2	.914	0	.100	49.0	18.0	1.0?	2.0?	0	2500	0	0	0	0	0

Remark : Compression test did not fail, head displ. = 30 mm

036
Gurtowski & Wu (1984) ASCE : "Analysis and Design ..." p. 138 Test Site A
Seattle

NUMLAY	NUMPIL	GWT	GAMPWP	SIGSRF	ZHOLE	QR.SOIL	QR.PILE
5	1	3.0	10	0.0	0.0	3	3

LAYER	DEPTH BOTTM	GAMMA EFF	TYPE ClSiSa	Q.CPT TIP	SPT N	OCR	-------- CLAY ------- SuTop	SuBot	TYP	St	Ip	----SAND---- D50	Dr	PHI	CLC FLG	MISCELLANEOUS 1	2	3
1	3.0	18.0	4	0	20	0	0	0	0	0	0	.10?	0	0	0	0	0	0 Fill
2	10.7	9.5	3	0	18	0	0	0	0	0	0	.10?	0	0	0	0	0	0
3	21.3	9.5	3	0	40	0	0	0	0	0	0	.10?	0	0	0	0	0	0
4	27.4	9.5	2.6	0	25	0	0	0	0	0	0	.10?	0	0	0	0	0	0
5	30.5	9.5	3	0	70	0	0	0	0	0	0	.10?	0	0	0	0	0	0

PILE NO	OPN CLS	MAT TYP	DIAM TIP	TAPER degr	WALL TIP	TOTAL LNGTH	TIP PENTR	PLUG RATIO	WATER RATIO	-- MEASURED CAPACITIES -- COMPRSSN	TENSION	DAYS	TBF	MISCELLANEOUS 1	2	3
1	2	2	.610	0	.305	29.9	29.9	0.0	0.0	4670	0	0	0	0	0	0

037
Gurtowski & Wu (1984) ASCE : "Analysis and Design ..." p. 138 Test Site B
Seattle

NUMLAY	NUMPIL	GWT	GAMPWP	SIGSRF	ZHOLE	QR.SOIL	QR.PILE
4	1	3.0	10	0.0	0.0	3	3

LAYER	DEPTH BOTTM	GAMMA EFF	TYPE ClSiSa	Q.CPT TIP	SPT N	OCR	-------- CLAY ------- SuTop	SuBot	TYP	St	Ip	----SAND---- D50	Dr	PHI	CLC FLG	MISCELLANEOUS 1	2	3
1	3.0	18.0	4	0	10	0	0	0	0	0	0	.10?	0	0	0	0	0	0 Fill
2	7.6	9.5	3	0	12	0	0	0	0	0	0	.10?	0	0	0	0	0	0
3	18.3	9.5	3	0	45	0	0	0	0	0	0	.10?	0	0	0	0	0	0
4	27.4	9.5	2.6	0	50	0	0	0	0	0	0	.10?	0	0	0	0	0	0

PILE NO	OPN CLS	MAT TYP	DIAM TIP	TAPER degr	WALL TIP	TOTAL LNGTH	TIP PENTR	PLUG RATIO	WATER RATIO	-- MEASURED CAPACITIES -- COMPRSSN	TENSION	DAYS	TBF	MISCELLANEOUS 1	2	3
1	2	2	.610	0	.305	25.6	25.6	0.0	0.0	4005	0	0	0	0	0	0

038
Briaud et al (1989) Single pile test in hydraulic sand fill
San Francisco

NUMLAY	NUMPIL	GWT	GAMPWP	SIGSRF	ZHOLE	QR.SOIL	QR.PILE
7	1	2.4	10	0.0	1.4	4	4

LAYER	DEPTH	GAMMA	TYPE	Q.CPT	SPT	OCR	CLAY					SAND			CLC	MISCELLANEOUS		
	BOTTM	EFF	ClSiSa	TIP	N		SuTop	SuBot	TYP	St	Ip	D50	Dr	PHI	FLG	1	2	3
1	1.4	19.0	3	0	0	0	0	0	0	0	0	0	0	35	0	0	0	0
2	2.4	18.5	3	0	0	0	0	0	0	0	0	0	0	35	0	0	0	0
3	4.6	10.1	3	4700	0	0	0	0	0	0	0	0	0	0	0	0	0	0
4	6.1	10.1	3	4700	0	0	0	0	0	0	0	0	0	0	0	0	0	0
5	7.6	10.1	3	5200	0	0	0	0	0	0	0	0	0	0	0	0	0	0
6	9.0	10.1	3	7700	0	0	0	0	0	0	0	0	0	0	0	0	0	0
7	10.7	10.1	3	7700	0	0	0	0	0	0	0	0	0	0	0	0	0	0

PILE NO	OPN CLS	MAT TYP	DIAM TIP	TAPER degr	WALL TIP	TOTAL LNGTH	TIP PENTR	PLUG RATIO	WATER RATIO	-- MEASURED CAPACITIES -- COMPRSSN	TENSION	DAYS	TBF	MISCELLANEOUS 1	2	3
1	2	1	.273	.0	.0093	10.7	9.15	0.0	0.0	441	0	24	0	0	0	0

18 Nov 2000 : CPT resistance below 9.0 m increased from 7400 to 7700 kPa.

039
Lehane et al (1993) Model pile test in loose sand
Labenne France

NUMLAY	NUMPIL	GWT	GAMPWP	SIGSRF	ZHOLE	QR.SOIL	QR.PILE
6	2	3.0	10	0.0	0.0	4	4

LAYER	DEPTH	GAMMA	TYPE	Q.CPT	SPT	OCR	CLAY					SAND			CLC	MISCELLANEOUS		
	BOTTM	EFF	ClSiSa	TIP	N		SuTop	SuBot	TYP	St	Ip	D50	Dr	PHI	FLG	1	2	3
1	1.0	16.9	3	2000	0	0	0	0	0	0	0	0	.0	0	0	0	0	0
2	2.2	16.9	3	5500	0	0	0	0	0	0	0	0	.0	0	0	0	0	0
3	3.0	16.0	3	3500	0	0	0	0	0	0	0	0	.0	0	0	0	0	0
4	4.0	9.2	3	1400	0	0	0	0	0	0	0	0	0	0	0	0	0	0
5	5.9	9.5	3	4100	0	0	0	0	0	0	0	0	0	0	0	0	0	0
6	6.0	9.5	3	4700	0	0	0	0	0	0	0	0	0	0	0	0	0	0

PILE NO	OPN CLS	MAT TYP	DIAM TIP	TAPER degr	WALL TIP	TOTAL LNGTH	TIP PENTR	PLUG RATIO	WATER RATIO	-- MEASURED CAPACITIES -- COMPRSSN	TENSION	DAYS	TBF	MISCELLANEOUS 1	2	3
1	2	1	.102	.0	.008?	6.5	5.95	0.0	0.0	97	0	0.6	0	0	0	0
2	2	1	.102	.0	.008?	6.5	5.95	0.0	0.0	0	50	0.6	0	0	0	0

18 Nov 2000 : Include an extra layer in the top of the profile, include CPT values, delete Dr values

040
Mansur & Kaufman (1956) Data taken directly from Randolph et al (1994)
Old River A

NUMLAY	NUMPIL	GWT	GAMPWP	SIGSRF	ZHOLE	QR.SOIL	QR.PILE
1	7	0.0	10	0.0	0.0	3	3

LAYER	DEPTH	GAMMA	TYPE	Q.CPT	SPT	OCR	CLAY					SAND			CLC	MISCELLANEOUS		
	BOTTM	EFF	ClSiSa	TIP	N		SuTop	SuBot	TYP	St	Ip	D50	Dr	PHI	FLG	1	2	3
1	20.2	10.0	3	0	0	0	0	0	0	0	0	0	.50	0	0	0	0	0

PILE NO	OPN CLS	MAT TYP	DIAM TIP	TAPER degr	WALL TIP	TOTAL LNGTH	TIP PENTR	PLUG RATIO	WATER RATIO	-- MEASURED CAPACITIES -- COMPRSSN	TENSION	DAYS	TBF	MISCELLANEOUS 1 2 3	
1	2	1	.533	0	.010	19.8	19.8	0.5	1.0	3290	0	0	0	0 0 0	2-c
2	2	1	.533	0	.010	19.8	19.8	0.5	1.0	0	1324	0	0	0 0 0	2-t
3	2	1	.433	0	.010	20.1	20.1	0.5	1.0	3420	0	0	0	0 0 0	4-c
4	2	1	.433	0	.010	20.1	20.1	0.5	1.0	0	1589	0	0	0 0 0	4-t
5	2	1	.482	0	.010	19.8	19.8	0.5	1.0	3470	0	0	0	0 0 0	6-c
6	2	1	.482	0	.010	19.8	19.8	0.5	1.0	0	1373	0	0	0 0 0	6-t
7	2	1	.457	0	.010	19.8	19.8	0.5	1.0	3109	0	0	0	0 0 0	7-c

25 Sep 2000 : CMP/TNS on same pile included as two tests

041
Mansur & Kaufman (1956) Data taken directly from Randolph et al (1994)
Old River B

NUMLAY	NUMPIL	GWT	GAMPWP	SIGSRF	ZHOLE	QR.SOIL	QR.PILE
1	2	0.0	10	0.0	0.0	3	3

LAYER	DEPTH	GAMMA	TYPE	Q.CPT	SPT	OCR	CLAY					SAND			CLC	MISCELLANEOUS		
	BOTTM	EFF	ClSiSa	TIP	N		SuTop	SuBot	TYP	St	Ip	D50	Dr	PHI	FLG	1	2	3
1	20.2	10.0	3	0	0	0	0	0	0	0	0	0	.40	0	0	0	0	0

PILE NO	OPN CLS	MAT TYP	DIAM TIP	TAPER degr	WALL TIP	TOTAL LNGTH	TIP PENTR	PLUG RATIO	WATER RATIO	-- MEASURED CAPACITIES -- COMPRSSN	TENSION	DAYS	TBF	MISCELLANEOUS 1 2 3	
1	2	1	.433	0	.010	13.7	13.7	0.5	1.0	1470	0	0	0	0 0 0	5-c
2	2	1	.433	0	.010	13.7	13.7	0.5	1.0	0	540	0	0	0 0 0	5-t

25 Sep 2000 : CMP/TNS on same pile included as two tests

042
Toolan et al (1990) and Jardine & Overy (1996) Case H, Southern North Sea, Leman AD
North Sea

NUMLAY	NUMPIL	GWT	GAMPWP	SIGSRF	ZHOLE	QR.SOIL	QR.PILE
6	1	0.0	10	0.0	0.0	4	4

LAYER	DEPTH	GAMMA	TYPE	Q.CPT	SPT	OCR	CLAY					SAND			CLC	MISCELLANEOUS		
	BOTTM	EFF	ClSiSa	TIP	N		SuTop	SuBot	TYP	St	Ip	D50	Dr	PHI	FLG	1	2	3
1	5.0	9.5	3	4500	0	6	0	0	0	0	0	0	0	0	0	0	0	0
2	10.0	9.5	3	7200	0	4	0	0	0	0	0	0	0	0	0	0	0	0
3	15.0	9.5	3	4500	0	3.5	0	0	0	0	0	0	0	0	0	0	0	0
4	20.0	10.0	3	9000	0	2.5	0	0	0	0	0	0	0	0	0	0	0	0
5	25.0	10.0	3	18000	0	2	0	0	0	0	0	0	0	0	0	0	0	0
6	31.0	10.0	3	31500	0	2	0	0	0	0	0	0	0	0	0	0	0	0

PILE NO	OPN CLS	MAT TYP	DIAM TIP	TAPER degr	WALL TIP	TOTAL LNGTH	TIP PENTR	PLUG RATIO	WATER RATIO	-- MEASURED CAPACITIES -- COMPRSSN	TENSION	DAYS	TBF	MISCELLANEOUS 1	2	3
1	1	1	.610	.0	.019?	30.5	30.5	0.24	1.0	0	2620	0	0	0	0	0

Note : Pile installation included drilling of pilot hole in front of tip below 18 m pentr.
Gas blow-out created 10 m deep crater under jacket, partly re-filled.
29 Oct 2000 : CPT values reduced by 10 % because of possible compaction during conductor driving.

043
Jardine & Overy (1996), Toolan et al (1990) Case I, Southern North Sea, Leman BD
North Sea

NUMLAY	NUMPIL	GWT	GAMPWP	SIGSRF	ZHOLE	QR.SOIL	QR.PILE
7	1	0.0	10	0.0	0.0	4	4

LAYER	DEPTH	GAMMA	TYPE	Q.CPT	SPT	OCR	-------- CLAY -------					----SAND----				CLC	MISCELLANEOUS		
	BOTTM	EFF	ClSiSa	TIP	N		SuTop	SuBot	TYP	St	Ip	D50	Dr	PHI	FLG		1	2	3
1	5.0	9.5	3	9000	0	6	0	0	0	0	0	0	0	0	0		0	0	0
2	8.0	9.0	1	0	0	0	80	80	-1	0	0	0	0	0	0		0	0	0
3	15.0	9.5	3	20000	0	3.5	0	0	0	0	0	0	0	0	0		0	0	0
4	20.0	10.0	3	24500	0	2.5	0	0	0	0	0	0	0	0	0		0	0	0
5	25.0	10.0	3	20000	0	2.0	0	0	0	0	0	0	0	0	0		0	0	0
6	30.0	10.0	3	36000	0	1.9	0	0	0	0	0	0	0	0	0		0	0	0
7	40.0	10.0	3	54000	0	1.8	0	0	0	0	0	0	0	0	0		0	0	0

PILE NO	OPN CLS	MAT TYP	DIAM TIP	TAPER degr	WALL TIP	TOTAL LNGTH	TIP PENTR	PLUG RATIO	WATER RATIO	-- MEASURED CAPACITIES -- COMPRSSN	TENSION	DAYS	TBF	MISCELLANEOUS 1	2	3
1	1	1	.660	.0	.019	38.1	38.1	0.91	1.0	0	5030	80	0	0	0	0

29 Oct 2000 : CPT values reduced by 10 % because of possible compaction during conductor driving.

044
McClelland Engineers Inc. (1958)   Data taken from Toolan et al (1990)
Padre Isld

NUMLAY	NUMPIL	GWT	GAMPWP	SIGSRF	ZHOLE	QR.SOIL	QR.PILE
1	2	0.0	10	5.0	0.0	3	3

LAYER	DEPTH	GAMMA	TYPE	Q.CPT	SPT	OCR	-------- CLAY -------					----SAND----				CLC	MISCELLANEOUS		
	BOTTM	EFF	ClSiSa	TIP	N		SuTop	SuBot	TYP	St	Ip	D50	Dr	PHI	FLG		1	2	3
1	20.0	10.0	3	0	0	0	0	0	0	0	0	0	.62	0	0		0	0	0

PILE NO	OPN CLS	MAT TYP	DIAM TIP	TAPER degr	WALL TIP	TOTAL LNGTH	TIP PENTR	PLUG RATIO	WATER RATIO	-- MEASURED CAPACITIES -- COMPRSSN	TENSION	DAYS	TBF	MISCELLANEOUS 1	2	3
1	1	1	.508	.0	.010?	14.6	14.6	0.5?	1.0	0	525	0	0	0	0	0
2	1	1	.508	.0	.010?	17.1	17.1	0.5?	1.0	0	694	0	0	0	0	0

045
Nottingham (1975)   Data taken from Toolan et al (1990)
Blount Isl

NUMLAY	NUMPIL	GWT	GAMPWP	SIGSRF	ZHOLE	QR.SOIL	QR.PILE
1	1	0.0	10	0.0	0.0	3	3

LAYER	DEPTH	GAMMA	TYPE	Q.CPT	SPT	OCR	-------- CLAY -------					----SAND----				CLC	MISCELLANEOUS		
	BOTTM	EFF	ClSiSa	TIP	N		SuTop	SuBot	TYP	St	Ip	D50	Dr	PHI	FLG		1	2	3
1	25.0	8.5	3	0	0	0	0	0	0	0	0	0	.59	0	0		0	0	0

PILE NO	OPN CLS	MAT TYP	DIAM TIP	TAPER degr	WALL TIP	TOTAL LNGTH	TIP PENTR	PLUG RATIO	WATER RATIO	-- MEASURED CAPACITIES -- COMPRSSN	TENSION	DAYS	TBF	MISCELLANEOUS 1	2	3
1	1	1	.273	.0	.008?	22.6	22.6	0.5?	1.0	0	721	0	0	0	0	0

-046
Martin (1987) Concrete piles in silty soils, piles T-4 and T-18-2
Virginia

NUMLAY	NUMPIL	GWT	GAMPWP	SIGSRF	ZHOLE	QR.SOIL	QR.PILE
3	2	0.0	10	0.0	1.2	2	3

LAYER	DEPTH	GAMMA	TYPE	Q.CPT	SPT	OCR	-------- CLAY -------					----SAND----				CLC	MISCELLANEOUS		
	BOTTM	EFF	ClSiSa	TIP	N		SuTop	SuBot	TYP	St	Ip	D50	Dr	PHI	FLG		1	2	3
1	3.6	9.1	2.1	0	3	0	0	0	0	0	0	0	0	0	0		0	0	0
2	15.0	9.1	2.1	0	7	0	0	0	0	0	0	0	0	0	0		0	0	0
3	21.0	9.1	2.1	0	9	0	0	0	0	0	0	0	0	0	0		0	0	0

PILE NO	OPN CLS	MAT TYP	DIAM TIP	TAPER degr	WALL TIP	TOTAL LNGTH	TIP PENTR	PLUG RATIO	WATER RATIO	-- MEASURED CAPACITIES -- COMPRSSN	TENSION	DAYS	TBF	MISCELLANEOUS 1	2	3
1	2	2	.450	.0	.225	17.2	17.2	0.0	0.0	1958	0	0	0	0	0	0
2	2	2	.570	.0	.285	20.1	20.1	0.0	0.0	4183	0	0	0	0	0	0

25 Sep 2000 : Removed from data set, difficult soils, SPT only

047
Altaee et al (1992) Concrete piles in sand
Baghdad

NUMLAY	NUMPIL	GWT	GAMPWP	SIGSRF	ZHOLE	QR.SOIL	QR.PILE
5	3	6.5	10	0.0	0.0	4	4

LAYER	DEPTH	GAMMA	TYPE	Q.CPT	SPT	OCR	-------- CLAY -------					----SAND----				CLC	MISCELLANEOUS		
	BOTTM	EFF	ClSiSa	TIP	N		SuTop	SuBot	TYP	St	Ip	D50	Dr	PHI	FLG		1	2	3
1	3.0	15.7	2.1	4000	0	0	0	0	0	0	0	0	0	0	0		0	0	0
2	6.5	17.8	3	5000	0	0	0	0	0	0	0	0	0	0	0		0	0	0
3	9.0	9.8	3	7100	0	0	0	0	0	0	0	0	0	0	0		0	0	0
4	12.0	9.8	3	5500	0	0	0	0	0	0	0	0	0	0	0		0	0	0
5	16.0	9.8	3	7000	0	0	0	0	0	0	0	0	0	0	0		0	0	0

PILE NO	OPN CLS	MAT TYP	DIAM TIP	TAPER degr	WALL TIP	TOTAL LNGTH	TIP PENTR	PLUG RATIO	WATER RATIO	-- MEASURED CAPACITIES -- COMPRSSN	TENSION	DAYS	TBF	MISCELLANEOUS 1	2	3
1	2	2	.348	.0	.174	12.0	11.0	0.0	0.0	1050	0	60	0	0	0	0
2	2	2	.363	.0	.1815	12.0	11.0	0.0	0.0	0	560	220	0	0	0	0
3	2	2	.348	.0	.174	16.0	15.0	0.0	0.0	1600	0	60	0	0	0	0

18 Nov 2000 : CPT profile modified, time for pile 2 changed from 190 to 220 days

048
Thorburn & MacVicar (1970)   "Pile load tets to failure in the Clyde alluvium"
Glasgow   Pile test 1   ICE, London

NUMLAY	NUMPIL	GWT	GAMPWP	SIGSRF	ZHOLE	QR.SOIL	QR.PILE
5	1	1.5	10	0.0	6.1	4	4

LAYER	DEPTH	GAMMA	TYPE	Q.CPT	SPT	OCR	-------- CLAY -------					----SAND----				CLC	MISCELLANEOUS			
	BOTTM	EFF	ClSiSa	TIP	N		SuTop	SuBot	TYP	St	Ip	D50	Dr	PHI	FLG		1	2	3	
1	2.7	12.0	4	0	0	0	0	0	0	0	0	0	0	33?	0		0	0	0	Fill
2	5.5	7.0?	1	0	0	0	25	25	-1	0	0	0	0	0	0		0	0	0	
3	8.8	9.0?	3	1400	0	0	0	0	0	0	0	0	0	0	0		0	0	0	
4	11.9	9.5?	3	5800	0	0	0	0	0	0	0	0	0	0	0		0	0	0	
5	13.7	9.5?	3	8200	0	0	0	0	0	0	0	0	0	0	0		0	0	0	

PILE NO	OPN CLS	MAT TYP	DIAM TIP	TAPER degr	WALL TIP	TOTAL LNGTH	TIP PENTR	PLUG RATIO	WATER RATIO	-- MEASURED CAPACITIES -- COMPRSSN	TENSION	DAYS	TBF	MISCELLANEOUS 1	2	3
1	2	1	.381	.0	.010?	12.5	12.5	0.0	0.0	819	0	10	0	0	0	0

-049
Thorburn & MacVicar (1970) "Pile load tets to failure in the Clyde alluvium"
Glasgow Pile test 2 ICE, London

NUMLAY	NUMPIL	GWT	GAMPWP	SIGSRF	ZHOLE	QR.SOIL	QR.PILE
3	1	1.5	10	0.0	0.0	3	3

LAYER	DEPTH BOTTM	GAMMA EFF	TYPE ClSiSa	Q.CPT TIP	SPT N	OCR	-------- CLAY ------- SuTop	SuBot	TYP	St	Ip	----SAND---- D50	Dr	PHI	CLC FLG	MISCELLANEOUS 1	2	3
1	3.0	15.0	3	0	0	0	0	0	0	0	0	0	0	33?	0	0	0	0
2	14.0	7.0?	1	0	0	0	24	24	8	0	0	0	0	0	0	0	0	0
3	22.0	9.5?	3	0	13	0	0	0	0	0	0	.35	0	0	0	0	0	0

PILE NO	OPN CLS	MAT TYP	DIAM TIP	TAPER degr	WALL TIP	TOTAL LNGTH	TIP PENTR	PLUG RATIO	WATER RATIO	-- MEASURED CAPACITIES -- COMPRSSN	TENSION	DAYS	TBF	MISCELLANEOUS 1	2	3
1	2	2	.444	.0	.222	21.5	21.5	0.0	0.0	1600	0	25	0	0	0	0

02 Nov 2000 : Site 725 removed, 50 % of skin friction comes from clay

050
Thorburn & MacVicar (1970) "Pile load tets to failure in the Clyde alluvium"
Glasgow Pile test 3 ICE, London

NUMLAY	NUMPIL	GWT	GAMPWP	SIGSRF	ZHOLE	QR.SOIL	QR.PILE
2	1	1.5	10	0.0	0.0	3	3

LAYER	DEPTH BOTTM	GAMMA EFF	TYPE ClSiSa	Q.CPT TIP	SPT N	OCR	-------- CLAY ------- SuTop	SuBot	TYP	St	Ip	----SAND---- D50	Dr	PHI	CLC FLG	MISCELLANEOUS 1	2	3	
1	3.0	12.0	4	0	0	0	0	0	0	0	0	0	0	33?	0	0	0	0	Fill
2	10.0	9.5?	3	0	15	0	0	0	0	0	0	.3	0	0	0	0	0	0	

PILE NO	OPN CLS	MAT TYP	DIAM TIP	TAPER degr	WALL TIP	TOTAL LNGTH	TIP PENTR	PLUG RATIO	WATER RATIO	-- MEASURED CAPACITIES -- COMPRSSN	TENSION	DAYS	TBF	MISCELLANEOUS 1	2	3
1	2	1	.406	.0	.010?	9.1	9.1	0.0	0.0	668	0	14	0	0	0	0

051
Tavenas (1971)
St. Charles River Canada

NUMLAY	NUMPIL	GWT	GAMPWP	SIGSRF	ZHOLE	QR.SOIL	QR.PILE
2	5	2.0	10	0.0	0.0	3	3

LAYER	DEPTH BOTTM	GAMMA EFF	TYPE ClSiSa	Q.CPT TIP	SPT N	OCR	-------- CLAY ------- SuTop	SuBot	TYP	St	Ip	----SAND---- D50	Dr	PHI	CLC FLG	MISCELLANEOUS 1	2	3	
1	4.9	13.0	4	0	0	0	0	0	0	0	0	0	0	33?	0	0	0	0	Fill
2	22.0	9.6	3	0	25	0	0	0	0	0	0	.3	.59	0	0	0	0	0	

PILE NO	OPN CLS	MAT TYP	DIAM TIP	TAPER degr	WALL TIP	TOTAL LNGTH	TIP PENTR	PLUG RATIO	WATER RATIO	-- MEASURED CAPACITIES -- COMPRSSN	TENSION	DAYS	TBF	MISCELLANEOUS 1	2	3
1	2	2	.33	.0	.165	8.9	8.9	0.0	0.0	680	0	0.5	0	0	0	0
2	2	2	.33	.0	.165	11.9	11.9	0.0	0.0	980	0	0.5	0	0	0	0
3	2	2	.33	.0	.165	15.0	15.0	0.0	0.0	1200	0	0.5	0	0	0	0
4	2	2	.33	.0	.165	18.0	18.0	0.0	0.0	1380	0	0.5	0	0	0	0
5	2	2	.33	.0	.165	21.1	21.1	0.0	0.0	1420	0	0.5	0	0	0	0

26 Sep 2000 : The given failure loads are for 10 % displ, they are higher than those quoted by Tavenas.

052
Fujita (1989) Rio Conference Proc. Session 14 Steel pile no. 2
Chiba-2

NUMLAY	NUMPIL	GWT	GAMPWP	SIGSRF	ZHOLE	QR.SOIL	QR.PILE
6	1	0.5	10	0.0	0.0	2	3

LAYER	DEPTH BOTTM	GAMMA EFF	TYPE ClSiSa	Q.CPT TIP	SPT N	OCR	-------- CLAY ------- SuTop	SuBot	TYP	St	Ip	----SAND---- D50	Dr	PHI	CLC FLG	MISCELLANEOUS 1	2	3
1	0.5	18.0	3	0	10	0	0	0	0	0	0	.15?	0	0	0	0	0	0
2	16.6	9.0	3	0	20	0	0	0	0	0	0	.15?	0	0	0	0	0	0
3	21.9	9.0	2	0	6	0	0	0	0	0	0	.15?	0	0	0	0	0	0
4	27.5	11.0	3	0	60	0	0	0	0	0	0	.15?	0	0	0	0	0	0
5	36.2	9.0	1	0	10	0	80	80	-1	0	0	0	0	0	0	0	0	0
6	40.7	12.0	3.5	0	120	0	0	0	0	0	0	1.0?	0	0	0	0	0	0

PILE NO	OPN CLS	MAT TYP	DIAM TIP	TAPER degr	WALL TIP	TOTAL LNGTH	TIP PENTR	PLUG RATIO	WATER RATIO	-- MEASURED CAPACITIES -- COMPRSSN	TENSION	DAYS	TBF	MISCELLANEOUS 1	2	3
1	1	1	.800	0	.012	48.0	40.6	0.99	0.99	8300	0	22	0	1	0	0

Remarks : Pile not loaded to failure, top displ. = 45 mm
SPT values given by author have been multiplied by 2

-053
Appendino (1981) Int. Conf. Stockholm Vol. 2 p. 593 Pile PT-361
Porto Tolle

NUMLAY	NUMPIL	GWT	GAMPWP	SIGSRF	ZHOLE	QR.SOIL	QR.PILE
7	1	0.0	10	10.0	0.0	2	3

LAYER	DEPTH BOTTM	GAMMA EFF	TYPE ClSiSa	Q.CPT TIP	SPT N	OCR	-------- CLAY ------- SuTop	SuBot	TYP	St	Ip	----SAND---- D50	Dr	PHI	CLC FLG	MISCELLANEOUS 1	2	3
1	8.0	10.0	2.7	4000	0	0	0	0	0	0	0	.15	0	0	0	0	0	0
2	31.0	8.0	1	0	0	0	25	70	-1	0	20?	0	0	0	0	0	0	0
3	33.5	10.0	3	10000	0	0	0	0	0	0	0	.15	0	0	0	0	0	0
4	35.0	8.0	1	0	0	0	77	77	-1	0	20?	0	0	0	0	0	0	0
5	36.5	10.0	3	6000	0	0	0	0	0	0	0	.15	0	0	0	0	0	0
6	39.0	8.0	1	0	0	0	83	83	-1	0	20?	0	0	0	0	0	0	0
7	43.0	10.0	3	20000	0	0	0	0	0	0	0	.15	0	0	0	0	0	0

PILE NO	OPN CLS	MAT TYP	DIAM TIP	TAPER degr	WALL TIP	TOTAL LNGTH	TIP PENTR	PLUG RATIO	WATER RATIO	-- MEASURED CAPACITIES -- COMPRSSN	TENSION	DAYS	TBF	MISCELLANEOUS 1	2	3
1	2	1	.508	0	.046	42.0	42.0	0.0	0.0	6000	0	0	0	0	0	0

Remark : Thin-walled steel pipe pile filled with concrete
27 Sep 2000 : Remove this site, only 35 % of shaft resistance comes from sand

054
Robertson et al (1985) Full scale test on large steel pile, only CPT data
Vancouver

NUMLAY	NUMPIL	GWT	GAMPWP	SIGSRF	ZHOLE	QR.SOIL	QR.PILE
6	3	4.0	10	0.0	4.0	3	3

LAYER	DEPTH	GAMMA	TYPE	Q.CPT	SPT	OCR	CLAY					SAND			CLC	MISCELLANEOUS		
	BOTTM	EFF	ClSiSa	TIP	N		SuTop	SuBot	TYP	St	Ip	D50	Dr	PHI	FLG	1	2	3
1	4.0	18	3	0	0	0	0	0	0	0	0	0	0.5	0	0	0	0	0
2	16.0	7.0	1.5	0	0	0	14	21	9	0	30?	0	0	0	0	0	0	0
3	30.0	9.5	3	11600	0	0	0	0	0	0	0	0	0	0	0	0	0	0
4	67.1	9.0	2.1	2600	0	0	0	0	0	0	0	0	0	0	0	0	0	0
5	78.1	9.0	2.1	3000	0	0	0	0	0	0	0	0	0	0	0	0	0	0
6	94.1	9.0	2.1	3600	0	0	0	0	0	0	0	0	0	0	0	0	0	0

PILE NO	OPN CLS	MAT TYP	DIAM TIP	TAPER degr	WALL TIP	TOTAL LNGTH	TIP PENTR	PLUG RATIO	WATER RATIO	-- MEASURED CAPACITIES -- COMPRSSN	TENSION	DAYS	TBF	MISCELLANEOUS 1	2	3
1	1	1	.915	.0	.019	67.0	67.0	0.83	0.94	7460	0	21	0	0	0	0
2	1	1	.915	.0	.019	78.0	78.0	0.83	0.95	7020	0	21	0	0	0	0
3	1	1	.915	.0	.019	94.0	94.0	0.83	0.96	7980	0	21	0	0	0	0

Remark : The above soil properties assume soils below 30 m to be sandy silt. In the paper the soils below 30 m are described as "normally consolidated clayey silt".

02 Dec 2000 : Super pile statuts removed for these piles

055
Vesic (1970) ASCE JSMFD March 1970
Ogeechee River Pile 2

NUMLAY	NUMPIL	GWT	GAMPWP	SIGSRF	ZHOLE	QR.SOIL	QR.PILE
11	1	2.1	10	0.0	0.0	4	4

LAYER	DEPTH	GAMMA	TYPE	Q.CPT	SPT	OCR	CLAY					SAND			CLC	MISCELLANEOUS		
	BOTTM	EFF	ClSiSa	TIP	N		SuTop	SuBot	TYP	St	Ip	D50	Dr	PHI	FLG	1	2	3
1	2.1	20.0	3	2500	0	0	0	0	0	0	0	.30	0	0	0	0	0	0
2	2.4	10.0	3	2500	0	0	0	0	0	0	0	.30	0	0	0	0	0	0
3	3.7	10.0	3	6000	0	0	0	0	0	0	0	.30	0	0	0	0	0	0
4	5.2	10.0	3	12000	0	0	0	0	0	0	0	.30	0	0	0	0	0	0
5	6.7	10.0	3	14500	0	0	0	0	0	0	0	.30	0	0	0	0	0	0
6	8.2	10.0	3	15000	0	0	0	0	0	0	0	.30	0	0	0	0	0	0
7	9.8	10.0	3	17000	0	0	0	0	0	0	0	.30	0	0	0	0	0	0
8	12.2	10.0	3	6500	0	0	0	0	0	0	0	.30	0	0	0	0	0	0
9	13.4	10.0	3	11000	0	0	0	0	0	0	0	.30	0	0	0	0	0	0
10	14.9	10.0	3	15000	0	0	0	0	0	0	0	.30	0	0	0	0	0	0
11	15.3	10.0	3	17500	0	0	0	0	0	0	0	.30	0	0	0	0	0	0

PILE NO	OPN CLS	MAT TYP	DIAM TIP	TAPER degr	WALL TIP	TOTAL LNGTH	TIP PENTR	PLUG RATIO	WATER RATIO	-- MEASURED CAPACITIES -- COMPRSSN	TENSION	DAYS	TBF	MISCELLANEOUS 1 2 3	Name
1	2	2	.475	0	.229	16.8	15.2	0.0	0.0	2697	0	0	0	0 0 0	H2

04 Dec 2000 : New site for Pile 2. CPTs P-2 & P-3 used for this location.

056
Aarsleff (1998)
Aalborg østhavn kranfundament, P382

NUMLAY	NUMPIL	GWT	GAMPWP	SIGSRF	ZHOLE	QR.SOIL	QR.PILE
4	1	1.9	10	0.0	0.0	2	4

LAYER	DEPTH	GAMMA	TYPE	Q.CPT	SPT	OCR	CLAY					SAND			CLC	MISCELLANEOUS		
	BOTTM	EFF	ClSiSa	TIP	N		SuTop	SuBot	TYP	St	Ip	D50	Dr	PHI	FLG	1	2	3
1	2.9	20.0	3	13000	0	0	0	0	0	0	0	0	0	0	0	0	0	0
2	6.9	8.0	1	0	0	0	60	80	8	0	0	0	0	0	0	0	0	0
3	10.9	9.4	1	0	0	0	120	210	8	0	0	0	0	0	0	0	0	0
4	17.9	8.0	3	13500	0	0	0	0	0	0	0	0	0	0	0	0	0	0

PILE NO	OPN CLS	MAT TYP	DIAM TIP	TAPER degr	WALL TIP	TOTAL LNGTH	TIP PENTR	PLUG RATIO	WATER RATIO	-- MEASURED CAPACITIES -- COMPRSSN	TENSION	DAYS	TBF	MISCELLANEOUS 1 2 3
1	2	2	.382	0	.191	18.0	17.65	0.0	0.0	1320	0	26	0	0 0 0

Pile is a squared prec. concrete pile (sidelength 30cm). Diameter calculation based on surface area.
Exact location of test pile is not given.
Swedish ram sounding used to determine the strength of the sand layers. CPT-value based on correlation.

057
Hanstholm-Århus vej (1995) Site 1 Pile(s) 1 - 1 Precast concrete
Hanstholm-Århus vej. P47

NUMLAY	NUMPIL	GWT	GAMPWP	SIGSRF	ZHOLE	QR.SOIL	QR.PILE
4	1	-0.2	10	0.0	0.0	3	3

LAYER	DEPTH	GAMMA	TYPE	Q.CPT	SPT	OCR	CLAY					SAND			CLC	MISCELLANEOUS		
	BOTTM	EFF	ClSiSa	TIP	N		SuTop	SuBot	TYP	St	Ip	D50	Dr	PHI	FLG	1	2	3
1	4.4	9.0	3	5530	0	0	0	0	0	0	0	.39	0	0	0	0	0	0
2	8.1	9.0	3	11920	0	0	0	0	0	0	0	1.1	0	0	0	0	0	0
3	12.6	9.0	3	11920	0	0	0	0	0	0	0	.36	0	0	0	0	0	0
4	21.6	9.0	3	11920	0	0	0	0	0	0	0	.41	0	0	0	0	0	0

PILE NO	OPN CLS	MAT TYP	DIAM TIP	TAPER degr	WALL TIP	TOTAL LNGTH	TIP PENTR	PLUG RATIO	WATER RATIO	-- MEASURED CAPACITIES -- COMPRSSN	TENSION	DAYS	TBF	MISCELLANEOUS 1 2 3
1	2	2	.382	.00	.191	17.0	16.8	0.0	0.0	1400	0	0	0	0 0 0

Days between driving and testing are unknown.
Pile is a squared prec. concrete pile (sidelength 30cm). Diameter calculation based on surface area.
Swedish ram sounding used to determine the strength of the sand layers. CPT-value based on correlation.
Load test for another pile is presented. It is not included in the database because failure was not reached due to the definition: Load corresponding to total deformations equal 10% of pile diameter.
Artesian water pressure may be present. Not included in this database.

058
Chow et al. (1996,1997,1998), Brucy and Meunier (1992) and Brucy et al. (1991)
Dunkirk, France, pæle CS, CL, LL

NUMLAY	NUMPIL	GWT	GAMPWP	SIGSRF	ZHOLE	QR.SOIL	QR.PILE
4	11	4.0	10	0.0	0.0	4	4

LAYER	DEPTH	GAMMA	TYPE	Q.CPT	SPT	OCR	CLAY					SAND			CLC	MISCELLANEOUS		
	BOTTM	EFF	ClSiSa	TIP	N		SuTop	SuBot	TYP	St	Ip	D50	Dr	PHI	FLG	1	2	3
1	2.0	17.1	3	23000	0	0	0	0	0	0	0	0	0	0	1	0	0	0
2	4.0	17.1	3	15000	0	0	0	0	0	0	0	.25	0	0	1	0	0	0
3	10.0	9.9	3	15000	0	0	0	0	0	0	0	.25	0	0	1	0	0	0
4	22.5	9.9	3	23000	0	0	0	0	0	0	0	.25	0	0	1	0	0	0

PILE NO	OPN CLS	MAT TYP	DIAM TIP	TAPER degr	WALL TIP	TOTAL LNGTH	TIP PENTR	PLUG RATIO	WATER RATIO	-- MEASURED CAPACITIES -- COMPRSSN	TENSION	DAYS	TBF	MISCELLANEOUS 1 2 3
1	1	1	.324	.00	.0191	11.7	11.6	0.55	0.64	0	395	188	1	0 0 0
2	1	1	.324	.00	.0191	11.7	11.6	0.55	0.64	1200	0	189	1	0 0 0
3	1	1	.324	.00	.0191	11.7	11.6	0.55	0.64	0	435	272	1	0 0 0
4	1	1	.324	.00	.0191	11.7	11.6	0.55	0.64	1199	0	273	1	0 0 0
5	1	1	.324	.00	.0191	11.7	11.6	0.55	0.64	0	750	1990	1	1 0 0
6	1	1	.324	.00	.0127	11.7	11.6	0.55	0.64	0	458	176	0	0 0 0
7	1	1	.324	.00	.0127	11.7	11.6	0.55	0.64	1199	0	177	1	0 0 0
8	1	1	.324	.00	.0127	11.7	11.6	0.55	0.64	0	548	289	1	0 0 0
9	1	1	.324	.00	.0127	11.7	11.6	0.55	0.64	1200	0	290	1	0 0 0
10	1	1	.324	.00	.0127	11.7	11.6	0.55	0.64	0	810	2086	1	0 0 0
11	1	1	.324	.00	.0127	22.4	22.1	0.45	0.82	0	3100	1924	0	0 0 0

The water level inside the pile is assumed to correspond to the level of the ground water table.
Soil plugs were removed app.250 days after installation. This is not taken into account but it is postulated that the plug do not influence the overall load-settlement curve.
For pile 2 (CL) and 4(LL), the tension capacities after 2086 and 1924days, respectively are the extraction loads.
CPT ended app. 21m below ground surface. The 4th soil layer is extended to 22,5m below ground surface.
One static test and other dynamic tests have been performed on the test site.
No movement of soil plug in connection with static tests.
Addition to #613 and 614 in existing database (this case sunstitutes the old #613).
The soil profile has been corrected based on the above-mentioned papers.

059
Motorvegbru Drammen Site 1 Pile(s) 1 - 2 Steel tube and HP-profile
Motorvegbru Drammen, Pæle P1 og P2 (Akse 16), Tvedt and Fredriksen (2003)

NUMLAY	NUMPIL	GWT	GAMPWP	SIGSRF	ZHOLE	QR.SOIL	QR.PILE
6	4	2.8	10	0.0	0.0	4	4

LAYER	DEPTH	GAMMA	TYPE	Q.CPT	SPT	OCR	CLAY					SAND			CLC	MISCELLANEOUS		
	BOTTM	EFF	ClSiSa	TIP	N		SuTop	SuBot	TYP	St	Ip	D50	Dr	PHI	FLG	1	2	3
1	2.8	18.0	3	5500	0	0	0	0	0	0	0	0	.52	36	0	0	0	0
2	15.5	8.0	3	5500	0	0	0	0	0	0	0	0	.52	36	0	0	0	0
3	30.0	9.0	1	0	0	0	40	110	9	0	0	0	0	0	0	0	0	0
4	32.5	9.0	1	0	0	0	110	110	9	0	0	0	0	0	0	0	0	0
5	36.0	9.0	1	0	0	0	85	85	9	0	0	0	0	0	0	0	0	0
6	40.0	9.0	1	0	0	0	110	110	9	0	0	0	0	0	0	0	0	0

PILE NO	OPN CLS	MAT TYP	DIAM TIP	TAPER degr	WALL TIP	TOTAL LNGTH	TIP PENTR	PLUG RATIO	WATER RATIO	-- MEASURED CAPACITIES -- COMPRSSN	TENSION	DAYS	TBF	MISCELLANEOUS 1 2 3
1	1	1	.813	.00	.0125	12.0	11.0	0.14	0.75	1300	0	1	1	0 0 0 P1-16
2	1	1	.813	.00	.0125	24.0	17.0	0.15	1.0	1300	0	1	1	0 0 0 P1-16
3	2	1	.400	.00	.200	12.0	11.0	0.0	0.0	640	0	1	1	0 0 0 P2-16
4	2	1	.400	.00	.200	27.0	17.0	0.0	0.0	560	0	1	1	0 0 0 P2-16

The piles have also been dynamic tested and tested in various depths.
Pile no.2 is a steel pile with H-profile. This profile is equated with a "solid/closed" circular profile.
The water level inside the pile is assumed to correspond to the level of the ground water table.
Some uncertainty associated with the determination of the plug ratio.

060
Motorvegbru Drammen Site 2 Pile(s) 3 - 4 Steel tube and HP-profile
Motorvegbru Drammen, Pæle P1 og P2 (Akse 25), Tvedt and fredriksen (2003)

NUMLAY	NUMPIL	GWT	GAMPWP	SIGSRF	ZHOLE	QR.SOIL	QR.PILE
5	8	1.5	10	0.0	0.0	4	4

LAYER	DEPTH	GAMMA	TYPE	Q.CPT	SPT	OCR	CLAY					SAND			CLC	MISCELLANEOUS		
	BOTTM	EFF	ClSiSa	TIP	N		SuTop	SuBot	TYP	St	Ip	D50	Dr	PHI	FLG	1	2	3
1	1.5	18.0	3	3000	0	0	0	0	0	0	0	0	.35	34	0	0	0	0
2	11.0	7.5	3	3000	0	0	0	0	0	0	0	0	.35	34	0	0	0	0
3	15.0	8.0	3	6000	0	0	0	0	0	0	0	0	.50	35	0	0	0	0
4	17.0	9.0	3	9000	0	0	0	0	0	0	0	0	.58	35	0	0	0	0
5	27.4	8.0	3	7000	0	0	0	0	0	0	0	0	.48	34	0	0	0	0

PILE NO	OPN CLS	MAT TYP	DIAM TIP	TAPER degr	WALL TIP	TOTAL LNGTH	TIP PENTR	PLUG RATIO	WATER RATIO	-- MEASURED CAPACITIES -- COMPRSSN	TENSION	DAYS	TBF	MISCELLANEOUS 1 2 3
1	1	1	.813	.00	.0125	24.0	15.0	0.09	0.90	1890	0	2	1	0 0 0 P1-25
2	1	1	.813	.00	.0125	25.0	25.0	0.16	0.94	2700	0	2	1	0 0 0 P1-25
3	1	1	.813	.00	.0125	25.0	25.0	0.16	0.94	3450	0	16	1	0 0 0 P1-25
4	1	1	.813	.00	.0125	25.0	25.0	0.16	0.94	3500	0	171	1	0 0 0 P1-25
5	2	1	.400	.00	.200	16.0	15.0	0.0	0.0	1030	0	3	1	0 0 0 P2-25
6	2	1	.400	.00	.200	25.0	25.0	0.0	0.0	1550	0	3	1	0 0 0 P2-25
7	2	1	.400	.00	.200	25.0	25.0	0.0	0.0	1590	0	16	1	0 0 0 P2-25
8	2	1	.400	.00	.200	25.0	25.0	0.0	0.0	1800	0	172	1	0 0 0 P2-25

The piles have also been dynamic tested and tested in various depths.
Pile no.2 is a steel pile with H-profile. This profile is equated with a "solid/closed" circular profile.
The water level inside the pile is assumed to correspond to the level of the ground water table.
Some uncertainty associated with the determination of the plug ratio.

061
Axelsson (1998a,1998b,2000,2002)
Vårby, Sverige, Pæl D

NUMLAY	NUMPIL	GWT	GAMPWP	SIGSRF	ZHOLE	QR.SOIL	QR.PILE
4	4	2.5	10	0.0	0.0	4	4

LAYER	DEPTH	GAMMA	TYPE	Q.CPT	SPT	OCR	CLAY					SAND			CLC	MISCELLANEOUS		
	BOTTM	EFF	ClSiSa	TIP	N		SuTop	SuBot	TYP	St	Ip	D50	Dr	PHI	FLG	1	2	3
1	2.5	19.0	1	1000	0	0	0	0	0	0	0	0	0	0	0	0	0	0
2	5.0	9.0	3	2500	0	0	0	0	0	0	0	0	0	0	0	0	0	0
3	8.0	9.0	3	3000	0	0	0	0	0	0	0	.16	0	0	0	0	0	0
4	13.4	9.0	3	4000	0	0	0	0	0	0	0	.2	0	0	0	0	0	0

PILE NO	OPN CLS	MAT TYP	DIAM TIP	TAPER degr	WALL TIP	TOTAL LNGTH	TIP PENTR	PLUG RATIO	WATER RATIO	-- MEASURED CAPACITIES -- COMPRSSN	TENSION	DAYS	TBF	MISCELLANEOUS 1 2 3
1	2	2	.299	.00	.1495	12.8	12.8	0.0	0.0	310	0	1	0	0 0 0
2	2	2	.299	.00	.1495	12.8	12.8	0.0	0.0	340	0	8	1	0 0 0
3	2	2	.299	.00	.1495	12.8	12.8	0.0	0.0	390	0	122	1	0 0 0
4	2	2	.299	.00	.1495	12.8	12.8	0.0	0.0	450	0	667	1	0 0 0

Unit weight of the soil is estimated.
Piles are sq. prec. concrete pile (sidelength 23,5cm). Diameter calculation based on surface area.
The total length of the pile is unknown.
The capacity of the pile is influenced by the "reaction piles".
Many dynamic tests have been performed in the area.

062
Aalborg værft Site 1 Pile(s) 1 - 1 Precast concrete
Aalborg Værft, P3

NUMLAY	NUMPIL	GWT	GAMPWP	SIGSRF	ZHOLE	QR.SOIL	QR.PILE
5	1	3.5	10	0.0	0.0	2	3

LAYER	DEPTH	GAMMA	TYPE	Q.CPT	SPT	OCR	CLAY					SAND			CLC	MISCELLANEOUS		
	BOTTM	EFF	ClSiSa	TIP	N		SuTop	SuBot	TYP	St	Ip	D50	Dr	PHI	FLG	1	2	3
1	3.5	15.0	1	0	0	0	15	15	8	0	0	0	0	0	0	0	0	0
2	6.0	5.0	1	0	0	0	15	15	8	0	0	0	0	0	0	0	0	0
3	7.0	5.0	1	0	0	0	110	110	8	2.2	0	0	0	0	0	0	0	0
4	15.0	9.0	3	0	0	0	0	0	0	0	0	0	0	37	0	0	0	0
5	17.6	9.7	1	0	0	0	170	250	8	3.0	0	0	0	0	0	0	0	0

PILE NO	OPN CLS	MAT TYP	DIAM TIP	TAPER degr	WALL TIP	TOTAL LNGTH	TIP PENTR	PLUG RATIO	WATER RATIO	-- MEASURED CAPACITIES -- COMPRSSN	TENSION	DAYS	TBF	MISCELLANEOUS 1 2 3
1	2	2	.318	.00	.159	17.5	17.5	0.0	0.0	1380	0	21	0	0 0 0

The third clay layer is really an organic layer. It is categorized as clay.
The unit weight of some of the soil layers is estimated. The unit weight of the third layer is changed from 3 to 5 (15-12-2003).
The triaxial friction angle is estimated.
Pile is a squared prec. concrete pile (sidelength 25cm). Diameter calculation based on surface area.
The total length is not given.
Failure was not reached due to the definition: Load corresponding to total deformations equal 10% of the pile diameter. The load-settlement curve is so flat that it is assumed that failure has occured.
Other static tests have also been performed. Not included due to the fact that they not failed nor is the soil profile well-defined.

063
Aarsleff (1998) Site 1
Kolding Forrense anlæg, TPP1

NUMLAY	NUMPIL	GWT	GAMPWP	SIGSRF	ZHOLE	QR.SOIL	QR.PILE
3	1	1.1	10	0.0	6.6	1	4

LAYER	DEPTH	GAMMA	TYPE	Q.CPT	SPT	OCR	CLAY					SAND			CLC	MISCELLANEOUS		
	BOTTM	EFF	ClSiSa	TIP	N		SuTop	SuBot	TYP	St	Ip	D50	Dr	PHI	FLG	1	2	3
1	1.1	10.0	3	6500	0	0	0	0	0	0	0	0	0	0	0	0	0	0
2	8.1	5.0	1	0	0	0	55	85	8	0	0	0	0	0	0	0	0	0
3	20.1	9.0	3	10500	0	0	0	0	0	0	0	0	0	0	0	0	0	0

PILE NO	OPN CLS	MAT TYP	DIAM TIP	TAPER degr	WALL TIP	TOTAL LNGTH	TIP PENTR	PLUG RATIO	WATER RATIO	-- MEASURED CAPACITIES -- COMPRSSN	TENSION	DAYS	TBF	MISCELLANEOUS 1 2 3
1	2	2	.382	0	.191	20.0	18.6	0.0	0.0	0	360	14	0	0 0 0 TPP1

Pile is a squared prec. concrete pile (sidelength 30cm). Diameter calculation based on surface area.
The clay layer is really an organic layer. Here it is categorized as clay.
Assumed sand from end of the boring to the pile tip.
Swedish ram sounding used to determine the strength of the sand layers. CPT-value based on correlation.
Based on Boring B/RS16 and B4.

064
Aarsleff (1998) Site 2
Kolding Forrense anlæg, TPP2

NUMLAY	NUMPIL	GWT	GAMPWP	SIGSRF	ZHOLE	QR.SOIL	QR.PILE
4	1	1.0	10	0.0	7.0	1	4

LAYER	DEPTH	GAMMA	TYPE	Q.CPT	SPT	OCR	CLAY					SAND			CLC	MISCELLANEOUS		
	BOTTM	EFF	ClSiSa	TIP	N		SuTop	SuBot	TYP	St	Ip	D50	Dr	PHI	FLG	1	2	3
1	1.0	18.0	3	9500	0	0	0	0	0	0	0	0	0	0	0	0	0	0
2	2.5	10.0	3	2000	0	0	0	0	0	0	0	0	0	0	0	0	0	0
3	8.5	7.0	1	0	0	0	40	80	8	0	0	0	0	0	0	0	0	0
4	20.0	9.0	3	12500	0	0	0	0	0	0	0	0	0	0	0	0	0	0

PILE NO	OPN CLS	MAT TYP	DIAM TIP	TAPER degr	WALL TIP	TOTAL LNGTH	TIP PENTR	PLUG RATIO	WATER RATIO	-- MEASURED CAPACITIES -- COMPRSSN	TENSION	DAYS	TBF	MISCELLANEOUS 1 2 3
1	2	2	.382	0	.191	20.0	19.0	0.0	0.0	0	355	14	0	0 0 0 TPP2

Pile is a squared prec. concrete pile (sidelength 30cm). Diameter calculation based on surface area.
The clay layer is really an organic layer. Here it is categorized as clay.
Assumed sand from end of the boring to the pile tip.
Swedish ram sounding used to determine the strength of the sand layers. CPT-value based on correlation.
Based on Boring B/RS17.

****
DATA BASE SAND-1 LOG
****

Date	By	Description
11.08.2004	AA	All piles from the different old databases collected. Taken from Clausen and Aas (2001b).
07.03.2005	AA	PSG Domicil Kbh. included in this database.
08.03.2005	AA	PSG Domicil excluded from the database.
18.03.2006	AA	Quality rating for both pile and soil for case no. 61 changed to 4.

Appendix G:
Calculated results

The following pages present an output file generated by the program PILCAP based on the input file shown in Appendix F: AAU and NGI data.

In the output file the text shown on the top of each column should be interpreted in the following way (based on Clausen and Aas, 2001b):

SITE NO PILE NO	Site number and pile number in the database.
LOCATION NAME	Short mnemonic name taken from the input file for each different site.
DIAM M	Pile outer diameter, m.
MAT O/C	Pile material type (steel, concrete or timber) and code for pile driven open-ended (o) or closed-ended (c).
TIP SOIL	Type of soil at the pile tip, sand or clay.
TIME DAYS	Number of days between end of pile driving and testing.
CMP TNS	Indicator for pile tested in compression or tension. When both a compression and a tension test was carried out on the same pile, and at the same depth, this is included as two pile tests in the database.
MEASURED (kN) TCOR:N TCOR:Y	Measured pile capacity in kN. TCOR:N value has not been time corrected, the TCOR:Y value has been time corrected. A "+" symbol after the value flags that this pile test did not reach failure, i.e. the actual capacity is higher than the value given.
SHAFT SAND%	Length of pile located in sand layers / total length times 100.
SAND CLAY	Codes "s" and "c" flag that the skin friction mainly comes from sand and clay layers, respectively.
SIGV SIGV	Average vertical stress, same value for sand and clay.
CPT Su	Average CPT tip resistance, q_{CPT}, along the shaft for piles in sand and average undrained shear strength along the shaft for piles in clay.
SPT Ip	Average SPT (blows/ft) along the shaft for sand, average plasticity index for clay.
Dr Su/SIGV	Average relative density for sand, average S_u / σ'_z ratio for clay.
PHI OCR	Average angle of internal friction for sand, average overconsolidation ratio for clay.

CALCD TAUSK	Calculated average skin friction (kPa) along pile shaft.
CALCULATED (kN) TOTAL SKN% WGH% TIP%	Calculated total pile capacity (kN) followed by skin friction, pile/plug weight and tip resistance in % of the total capacity. A positive value acts in the same direction as the skin friction force. Total stresses are used. A "*" symbol after the tip value flags the pile tip is coring according to the calculated results.
CALC MEAS	Ratio between calculated and measured pile capacity.

PILES IN SAND DATA BASE SAND NEW AND OLD DATA 11 AUG 2004

SAND SKIN FRICTION BY METHOD : NGI 1999 SOIL DATA QUALITY RATING = 0 CORRECTIONS INCLUDED
CLAY SKIN FRICTION BY METHOD : NGI 1999 PILE DATA QUALITY RATING = 0 Su : Yes Time : No

SITE No / PILE No	LOCATION NAME	DIAM M	MAT O/C	PENTR M	TIP SOIL	TIME DAYS	CMP TNS	MEASURED (kN) TCOR:N	TCOR:Y	SHAFT SAND%	SAND CLAY	SIGV SIGV	CPT Su	SPT Ip	Dr Su/SIGV	PHI OCR	CALCD TAUSKN	CALCULATED (kN) TOTAL	SKN%	WGH%	TIP%	CALC MEAS
1.01	Arkansas R	0.356	S C	16.20	SAND	0.0	CMP	1561	0	96	S	87.7	-8.6	26	0.65	37.1	77.2	1974	65	-1	36	1.26
1.02	Arkansas R	0.356	S C	16.20	SAND	0.0	TNS	876	0	96	S	87.7	-8.6	26	0.65	37.1	51.5	873	100	2	-2	1.00
1.03	Arkansas R	0.533	S C	16.20	SAND	0.0	CMP	2575	0	96	S	87.7	-8.6	26	0.65	37.1	77.2	3334	58	-1	43	1.29
1.04	Arkansas R	0.533	S C	16.20	SAND	0.0	TNS	1076	0	96	S	87.7	-8.6	26	0.65	37.1	51.5	1295	101	2	-3	1.20
1.05	Arkansas R	0.432	S C	16.20	SAND	0.0	CMP	2233	0	96	S	87.7	-8.6	26	0.65	37.1	77.2	2531	62	-1	39	1.13
1.06	Arkansas R	0.432	S C	16.20	SAND	0.0	TNS	1027	0	96	S	87.7	-8.6	26	0.65	37.1	51.5	1055	101	2	-3	1.03
1.07	Arkansas R	0.432	S C	16.20	SAND	0.0	CMP	2215	0	96	S	87.7	-8.6	26	0.65	37.1	77.2	2531	62	-1	39	1.14
1.08	Arkansas R	0.432	S C	16.20	SAND	0.0	TNS	1054	0	96	S	87.7	-8.6	26	0.65	37.1	51.5	1055	101	2	-3	1.00
2.01	Florida	0.914	S O	18.30	SAND	0.0	CMP	3069	0	100	S	99.4	-3.7	11	0.32	32.5	14.6	856	89	-7	18*	0.28
3.01	Kansas Cit	0.330	S C	16.80	SAND	0.0	CMP	836	0	100	S	109.6	-3.3	10	0.24	31.4	12.5	500	44	-8	64	0.60
3.02	Kansas Cit	0.356	S C	16.80	SAND	0.0	CMP	970	0	100	S	109.6	-3.3	10	0.24	31.4	12.5	559	42	-8	66	0.58
4.01	Muskegon	0.305	S C	17.70	SAND	0.0	CMP	1068	0	100	S	95.0	-2.7	8	0.24	31.4	13.6	360	64	-2	38	0.34
4.02	Muskegon	0.305	S O	17.70	SAND	0.0	CMP	489	0	100	S	95.0	-2.7	8	0.24	31.4	13.2	221	101	-4	3*	0.45
5.01	Mustang Is	0.610	S O	21.00	CLAY	0.0	TNS	2024	0	92	S	97.4	-17.5	53	0.94	41.1	55.9	2219	93	7	0	1.10
6.01	Mustang Is	0.610	S O	21.00	CLAY	0.0	TNS	1801	0	86	S	97.2	-10.8	33	0.75	38.6	38.1	1593	90	9	1	0.88
7.01	Los Barrio	0.914	C O	18.00	SAND	0.0	CMP	5080	0	100	S	90.0	-5.8	0	0.50	35.0	40.6	2675	78	0	22*	0.53
7.02	Los Barrio	0.914	C O	18.00	SAND	0.0	TNS	2500	0	100	S	90.0	-5.8	0	0.50	35.0	27.1	1520	92	16	-8	0.61
8.01	Hsin-Ta	0.610	S C	34.30	SAND	0.0	CMP	4330	0	100	S	161.2	8.0	0	0.50	35.0	42.0	4477	62	-5	43	1.03
8.02	Hsin-Ta	0.610	S C	34.30	SAND	0.0	TNS	2500	0	100	S	161.2	8.0	0	0.50	35.0	28.2	1985	93	12	-5	0.79

PILES IN SAND DATA BASE SAND NEW AND OLD DATA 11 AUG 2004

SAND SKIN FRICTION BY METHOD : NGI 1999 SOIL DATA QUALITY RATING = 0 CORRECTIONS INCLUDED
CLAY SKIN FRICTION BY METHOD : NGI 1999 PILE DATA QUALITY RATING = 0 Su : Yes Time : No

SITE No / PILE No	LOCATION NAME	DIAM M	MAT O/C	PENTR M	TIP SOIL	TIME DAYS	CMP TNS	MEASURED (kN) TCOR:N	TCOR:Y	SHAFT SAND%	SAND CLAY	SIGV SIGV	CPT Su	SPT Ip	Dr Su/SIGV	PHI OCR	CALCD TAUSKN	CALCULATED (kN) TOTAL	SKN%	WGH%	TIP%	CALC MEAS
8.03	Hsin-Ta	0.610	S C	34.30	SAND	0.0	CMP	4460	0	100	S	161.2	8.0	0	0.50	35.0	42.0	4477	62	-5	43	1.00
9.01	Low Sill A	0.518	S C	19.81	SAND	18.0	TNS	1664	0	100	S	79.7	-8.5	0	0.66	37.2	50.0	1594	101	2	-3	0.96
9.02	Low Sill A	0.419	S C	20.12	SAND	18.0	TNS	1779	0	100	S	81.0	-8.5	0	0.66	37.2	49.9	1314	101	2	-3	0.74
9.03	Low Sill A	0.468	S C	19.81	SAND	18.0	TNS	1646	0	100	S	79.7	-8.5	0	0.66	37.2	50.0	1444	101	2	-3	0.88
10.01	Low Sill B	0.419	S C	13.72	SAND	18.0	TNS	712	0	100	S	53.9	-6.6	0	0.57	36.0	39.1	701	101	2	-3	0.98
11.01	Dunkirk IC	0.102	S C	7.40	SAND	0.6	CMP	309	0	100	S	57.0	-10.9	0	0.85	39.9	140.9	385	87	0	13	1.25
11.02	Dunkirk IC	0.102	S C	7.40	SAND	0.6	TNS	186	0	100	S	57.0	-10.9	0	0.85	39.9	94.0	224	100	1	-1	1.20
12.01	Dunkirk IC	0.102	S C	5.96	SAND	0.6	CMP	231	0	100	S	47.8	-11.0	0	0.89	40.4	159.5	361	84	0	16	1.56
13.01	Dunkirk Cl	0.324	S O	22.00	SAND	188.0	TNS	1730	0	100	S	136.0	-13.8	0	0.75	38.5	49.0	1130	97	4	-1	0.65
14.01	Hunter's P	0.273	S C	7.78	SAND	24.0	CMP	440	0	100	S	37.0	-4.5	0	0.60	36.4	68.9	632	73	-1	28	1.44
15.01	Ras Tanaji	0.610	S O	18.00	SAND	30.0	TNS	12700	0	100	S	120.0	-25.1	0	1.00	42.0	72.3	2536	98	4	-2	0.20
16.01	Akasaka A	0.200	S C	7.00	SAND	0.0	CMP	1139	0	100	S	100.0	-12.8	0	0.80	39.2	125.9	958	58	0	42	0.84
17.01	Akasaka B	0.200	S C	4.00	SAND	0.0	CMP	156	0	100	S	27.0	-2.5	0	0.49	34.8	51.7	203	64	-1	37	1.30
18.01	Akasaka C	0.200	S C	11.00	SAND	0.0	CMP	1122	0	100	S	74.0	-8.2	0	0.69	37.7	88.4	1005	61	-1	40	0.90
19.01	Anvers	0.318	S O	8.30	SAND	0.0	TNS	883	0	100	S	68.5	-7.8	0	0.67	37.4	46.3	381	101	1	-2	0.43
20.01	Lock & Dam	0.305	S C	10.97	SAND	23.0	TNS	543	0	100	S	51.7	-14.7	0	0.97	41.6	123.4	1297	100	1	-1	2.39
20.02	Lock & Dam	0.356	S C	11.13	SAND	16.0	TNS	605	0	100	S	52.4	-14.7	0	0.97	41.6	123.2	1532	100	1	-1	2.53
20.03	Lock & Dam	0.406	S C	11.13	SAND	17.0	TNS	881	0	100	S	52.4	-14.7	0	0.97	41.6	123.2	1745	100	1	-1	1.98
21.01	Kimitsu	1.200	S O	19.80	SAND	0.0	CMP	15000	0	100	S	71.5	-7.7	0	0.67	37.4	63.4	9228	51	-1	50*	0.62

PILES IN SAND DATA BASE SAND NEW AND OLD DATA 11 AUG 2004

SAND SKIN FRICTION BY METHOD : NGI 1999 SOIL DATA QUALITY RATING = 0 CORRECTIONS INCLUDED
CLAY SKIN FRICTION BY METHOD : NGI 1999 PILE DATA QUALITY RATING = 0 Su : Yes Time : No

SITE No / PILE No	LOCATION NAME	DIAM M	MAT O/C	PENTR M	TIP SOIL	TIME DAYS	CMP TNS	MEASURED (kN) TCOR:N	TCOR:Y	SHAFT SAND%	SAND CLAY	SIGV SIGV	CPT Su	SPT Ip	Dr Su/SIGV	PHI OCR	CALCD TAUSKN	CALCULATED (kN) TOTAL	SKN%	WGH%	TIP%	CALC MEAS
22.01	Trans-Toky	2.000	S O	30.60	SAND	52.0	CMP	34335	0	100	S	149.9	-15.0	0	0.76	38.6	72.5	35588	39	-2	63*	1.04
23.01	Cromarty F	0.610	S O	13.10	SAND	0.0	CMP	1960	0	100	S	59.0	-5.6	0	0.59	36.3	55.4	2721	51	-4	53	1.39
24.01	Cromarty F	0.610	S O	19.40	SAND	0.0	CMP	2400	0	100	S	87.3	-8.0	0	0.64	37.0	59.3	4818	46	-1	55*	2.01
24.02	Cromarty F	0.610	S O	19.40	SAND	0.0	TNS	1220	0	100	S	87.3	-8.0	0	0.64	37.0	39.5	1554	95	9	-4	1.27
25.01	Cromarty F	0.762	S O	28.10	SAND	0.0	CMP	3150	0	100	S	126.5	-9.7	0	0.63	36.8	55.8	4910	76	-2	26*	1.56
25.02	Cromarty F	0.762	S O	28.10	SAND	0.0	TNS	1800	0	100	S	126.5	-9.7	0	0.63	36.8	37.2	2562	98	7	-5	1.42
26.01	Arkansas R	0.361	S C	16.20	SAND	0.0	CMP	1486	0	100	S	84.2	-12.0	32	0.81	39.4	98.7	2477	73	-1	28	1.67
26.02	Arkansas R	0.361	S C	16.20	SAND	0.0	TNS	846	0	100	S	84.2	-12.0	32	0.81	39.4	65.8	1209	100	1	-1	1.43
26.03	Arkansas R	0.477	S C	16.10	SAND	0.0	CMP	2092	0	100	S	83.7	-12.0	32	0.81	39.4	98.9	3471	69	-1	32	1.66
26.04	Arkansas R	0.477	S C	16.10	SAND	0.0	TNS	1068	0	100	S	83.7	-12.0	32	0.81	39.4	65.9	1586	100	1	-1	1.48
26.05	Arkansas R	0.542	S C	16.20	SAND	0.0	CMP	2278	0	100	S	84.2	-12.0	32	0.81	39.4	98.7	4091	67	-1	34	1.80
26.06	Arkansas R	0.542	S C	16.20	SAND	0.0	TNS	1086	0	100	S	84.2	-12.0	32	0.81	39.4	65.8	1804	101	1	-2	1.66
26.07	Arkansas R	0.488	C C	12.30	SAND	0.0	CMP	1780	0	100	S	65.1	-11.5	31	0.84	39.8	107.1	2963	68	-2	34	1.66
26.08	Arkansas R	0.488	C C	12.30	SAND	0.0	TNS	872	0	100	S	65.1	-11.5	31	0.84	39.8	71.4	1389	97	5	-2	1.59
26.09	Arkansas R	0.488	C C	15.50	SAND	0.0	CMP	2545	0	100	S	80.8	-11.9	32	0.82	39.4	99.8	3425	69	-2	33	1.35
26.12	Arkansas R	0.477	S C	16.20	SAND	0.0	CMP	2047	0	100	S	84.2	-12.0	32	0.81	39.4	98.7	3486	69	-1	32	1.70
26.13	Arkansas R	0.477	S C	16.20	SAND	0.0	TNS	1041	0	100	S	84.2	-12.0	32	0.81	39.4	65.8	1593	100	1	-1	1.53
26.14	Arkansas R	0.488	C C	11.80	SAND	0.0	CMP	1593	0	100	S	62.6	-11.4	31	0.84	39.8	108.7	2876	68	-3	35	1.81
27.01	Ogeechee R	0.457	S C	3.00	SAND	0.8	CMP	676	0	100	S	28.6	3.5	0	0.52	35.2	70.7	616	49	-1	52	0.91

PILES IN SAND DATA BASE SAND NEW AND OLD DATA 11 AUG 2004

SAND SKIN FRICTION BY METHOD : NGI 1999 SOIL DATA QUALITY RATING = 0 CORRECTIONS INCLUDED
CLAY SKIN FRICTION BY METHOD : NGI 1999 PILE DATA QUALITY RATING = 0 Su : Yes Time : No

SITE No PILE No	LOCATION NAME	DIAM M	MAT O/C	PENTR M	TIP SOIL	TIME DAYS	CMP TNS	MEASURED (kN) TCOR:N	TCOR:Y	SHAFT SAND%	SAND CLAY	SIGV SIGV	CPT Su	SPT Ip	Dr Su/SIGV	PHI OCR	CALCD TAUSKN	CALCULATED (kN) TOTAL	SKN%	WGH%	TIP%	CALC MEAS
27.02	Ogeechee R	0.457	S C	6.10	SAND	0.8	CMP	2065	0	100	S	47.9	8.0	0	0.68	37.5	131.9	1723	67	-1	34	0.83
27.03	Ogeechee R	0.457	S C	8.90	SAND	0.8	CMP	2643	0	100	S	63.0	9.7	0	0.72	38.1	125.2	2430	66	-1	35	0.92
27.04	Ogeechee R	0.457	S C	12.00	SAND	0.8	CMP	3088	0	100	S	79.2	10.9	0	0.73	38.3	114.9	2914	68	-1	33	0.94
27.05	Ogeechee R	0.457	S C	15.00	SAND	0.8	CMP	3747	0	100	S	94.5	12.0	0	0.75	38.4	111.3	3646	66	-1	35	0.97
27.06	Ogeechee R	0.457	S C	15.00	SAND	0.8	TNS	1540	0	100	S	94.5	12.0	0	0.75	38.4	74.3	1600	100	1	-1	1.04
28.01	Lower Arro	0.610	S O	45.40	SAND	0.0	CMP	1560	0	72	S	170.2	-3.1	9	0.15	30.1	17.8	1937	99	-5	6*	1.24
28.02	Lower Arro	0.610	S O	47.20	SAND	0.0	CMP	4360+	0	74	S	178.4	-3.4	9	0.16	30.2	19.4	2208	95	-4	9*	0.51
29.01	Holmen, Dr	0.280	C C	8.00	SAND	0.0	CMP	275	0	100	S	52.1	3.5	0	0.39	33.5	27.0	296	64	-4	40	1.08
29.02	Holmen, Dr	0.280	C C	8.00	SAND	0.0	TNS	101	0	100	S	52.1	3.5	0	0.39	33.5	18.8	141	94	9	-3	1.40
29.03	Holmen, Dr	0.280	C C	16.00	SAND	0.0	CMP	500	0	100	S	90.7	3.5	0	0.31	32.3	12.8	450	40	-5	65	0.90
29.04	Holmen, Dr	0.280	C C	16.00	SAND	0.0	TNS	269	0	100	S	90.7	3.5	0	0.31	32.3	10.8	168	90	15	-5	0.62
29.09	Holmen, Dr	0.280	C C	3.50	SAND	0.0	CMP	219	0	100	S	28.6	3.1	0	0.41	33.7	52.0	250	64	-2	38	1.14
29.10	Holmen, Dr	0.280	C C	7.50	SAND	0.0	CMP	210	0	100	S	49.7	3.6	0	0.40	33.7	31.2	308	67	-4	37	1.47
29.11	Holmen, Dr	0.280	C C	11.50	SAND	0.0	CMP	330	0	100	S	68.8	3.4	0	0.34	32.7	14.5	307	48	-6	58	0.93
29.12	Holmen, Dr	0.280	C C	15.50	SAND	0.0	CMP	471	0	100	S	88.3	3.5	0	0.31	32.3	12.4	433	39	-6	67	0.92
29.13	Holmen, Dr	0.280	C C	19.50	SAND	0.0	CMP	636	0	100	S	108.4	4.0	0	0.32	32.5	18.3	697	45	-4	59	1.10
29.14	Holmen, Dr	0.280	C C	23.50	SAND	0.0	CMP	838	0	100	S	129.2	4.8	0	0.34	32.8	25.3	990	53	-4	51	1.18
29.15	Holmen, Dr	0.280	C C	23.50	SAND	0.0	TNS	308	0	100	S	129.2	4.8	0	0.34	32.8	18.9	415	94	9	-3	1.35
30.01	Mustang Is	0.610	S O	21.00	SAND	0.0	TNS	2029	0	90	S	97.8	-11.7	36	0.80	39.2	44.2	1765	97	7	-4	0.87

PILES IN SAND DATA BASE SAND NEW AND OLD DATA 11 AUG 2004

SAND SKIN FRICTION BY METHOD : NGI 1999 SOIL DATA QUALITY RATING = 0 CORRECTIONS INCLUDED
CLAY SKIN FRICTION BY METHOD : NGI 1999 PILE DATA QUALITY RATING = 0 Su : Yes Time : No

SITE No / PILE No	LOCATION NAME	DIAM M	MAT O/C	PENTR M	TIP SOIL	TIME DAYS	CMP TNS	MEASURED (kN) TCOR:N	TCOR:Y	SHAFT SAND%	SAND CLAY	SIGV SIGV	CPT Su	SPT Ip	Dr Su/SIGV	PHI OCR	CALCD TAUSKN	CALCULATED (kN) TOTAL	SKN%	WGH%	TIP%	CALC MEAS
30.02	Mustang Is	0.610	S O	21.00	SAND	0.0	TNS	1793	0	90	S	97.8	-11.7	36	0.80	39.2	44.2	1765	97	7	-4	0.98
31.01	Hoogzand	0.356	S O	7.00	SAND	0.0	CMP	2318	0	96	S	69.4	27.2	0	0.93	41.1	124.1	2161	43	-1	58	0.93
31.02	Hoogzand	0.356	S O	7.00	SAND	0.0	TNS	830	0	96	S	69.4	27.2	0	0.93	41.1	82.7	650	97	3	0	0.78
31.03	Hoogzand	0.356	S C	6.75	SAND	0.0	CMP	2850	0	96	S	67.5	26.6	0	0.93	41.0	214.4	2751	56	0	44	0.97
31.04	Hoogzand	0.356	S C	6.75	SAND	0.0	TNS	1098	0	96	S	67.5	26.6	0	0.93	41.0	142.9	1047	99	1	0	0.95
31.05	Hoogzand	0.356	S O	5.25	SAND	0.0	CMP	1853	0	94	S	55.3	21.5	0	0.91	40.7	124.1	1943	35	-1	66	1.05
31.06	Hoogzand	0.356	S O	5.25	SAND	0.0	TNS	550	0	94	S	55.3	21.5	0	0.91	40.7	82.7	487	97	4	-1	0.89
32.01	Hokkaido	1.016	S O	40.00	SAND	15.0	CMP	15700	0	100	S	208.6	-10.3	33	0.50	35.0	41.1	10385	51	-2	51*	0.66
33.01	Chiba-3	0.356	S O	13.50	SAND	0.0	CMP	2940	0	100	S	77.1	-17.6	54	0.84	39.8	96.8	2586	56	-2	46	0.88
34.01	Sermide	0.508	S C	35.90	SAND	0.0	CMP	5300	0	97	S	205.5	9.4	0	0.49	34.9	58.6	4741	53	-4	51	0.89
35.01	Cadiz	0.914	C O	18.00	SAND	0.0	CMP	5000+	0	100	S	90.0	-6.8	23	0.57	36.0	47.3	4308	57	-7	50*	0.86
35.02	Cadiz	0.914	C O	18.00	SAND	0.0	TNS	2500	0	100	S	90.0	-6.8	23	0.57	36.0	31.5	2060	79	33	-12	0.82
36.01	Seattle	0.610	C C	29.90	SAND	0.0	CMP	4670	0	100	S	166.2	-7.7	26	0.50	35.0	36.4	4637	45	-5	60	0.99
37.01	Seattle	0.610	C C	25.60	SAND	0.0	CMP	4005	0	100	S	145.6	-8.9	30	0.56	35.9	55.1	4696	58	-4	46	1.17
38.01	San Franci	0.273	S C	9.15	SAND	24.0	CMP	441	0	100	S	73.6	4.3	0	0.50	35.1	58.8	624	63	-1	38	1.41
39.01	Labenne	0.102	S C	5.95	SAND	0.6	CMP	97	0	100	S	44.3	3.5	0	0.46	34.4	36.5	92	76	-1	25	0.95
39.02	Labenne	0.102	S C	5.95	SAND	0.6	TNS	50	0	100	S	44.3	3.5	0	0.46	34.4	24.6	48	98	2	0	0.96
40.01	Old River	0.533	S C	19.80	SAND	0.0	CMP	3290	0	100	S	99.0	-6.2	0	0.50	35.0	44.0	2280	64	-5	41	0.69
40.02	Old River	0.533	S C	19.80	SAND	0.0	TNS	1324	0	100	S	99.0	-6.2	0	0.50	35.0	29.3	1036	94	10	-4	0.78

PILES IN SAND DATA BASE SAND NEW AND OLD DATA 11 AUG 2004

SAND SKIN FRICTION BY METHOD : NGI 1999 SOIL DATA QUALITY RATING = 0 CORRECTIONS INCLUDED
CLAY SKIN FRICTION BY METHOD : NGI 1999 PILE DATA QUALITY RATING = 0 Su : Yes Time : No

SITE No PILE No	LOCATION NAME	DIAM M	MAT O/C	PENTR M	TIP SOIL	TIME DAYS	CMP TNS	MEASURED (kN) TCOR:N	TCOR:Y	SHAFT SAND%	SAND CLAY	SIGV SIGV	CPT Su	SPT Ip	Dr Su/SIGV	PHI OCR	CALCD TAUSKN	CALCULATED (kN) TOTAL	SKN%	WGH%	TIP%	CALC MEAS
40.03	Old River	0.433	S C	20.10	SAND	0.0	CMP	3420	0	100	S	100.5	-6.2	0	0.50	35.0	43.9	1774	68	-4	36	0.52
40.04	Old River	0.433	S C	20.10	SAND	0.0	TNS	1589	0	100	S	100.5	-6.2	0	0.50	35.0	29.3	846	95	9	-4	0.53
40.05	Old River	0.482	S C	19.80	SAND	0.0	CMP	3470	0	100	S	99.0	-6.2	0	0.50	35.0	44.0	2007	66	-4	38	0.58
40.06	Old River	0.482	S C	19.80	SAND	0.0	TNS	1373	0	100	S	99.0	-6.2	0	0.50	35.0	29.3	933	94	10	-4	0.68
40.07	Old River	0.457	S C	19.80	SAND	0.0	CMP	3109	0	100	S	99.0	-6.2	0	0.50	35.0	44.0	1877	67	-4	37	0.60
41.01	Old River	0.433	S C	13.70	SAND	0.0	CMP	1470	0	100	S	68.5	-4.8	0	0.40	33.6	29.2	965	56	-5	49	0.66
41.02	Old River	0.433	S C	13.70	SAND	0.0	TNS	540	0	100	S	68.5	-4.8	0	0.40	33.6	19.5	393	92	13	-5	0.73
42.01	North Sea	0.610	S O	30.50	SAND	0.0	TNS	2620	0	100	S	146.8	12.8	0	0.57	36.0	41.9	2560	96	8	-4	0.98
43.01	North Sea	0.660	S O	38.10	SAND	80.0	TNS	5030	0	97	S	193.7	29.2	0	0.88	40.3	65.3	5256	94	8	-2	1.04
44.01	Padre Isld	0.508	S O	14.60	SAND	0.0	TNS	525	0	100	S	78.0	-8.6	0	0.62	36.7	38.7	946	95	8	-3	1.80
44.02	Padre Isld	0.508	S O	17.10	SAND	0.0	TNS	694	0	100	S	90.5	-8.6	0	0.62	36.7	38.1	1091	95	8	-3	1.57
45.01	Blount Isl	0.273	S O	22.60	SAND	0.0	TNS	721	0	100	S	96.1	-8.0	0	0.59	36.3	34.4	689	97	5	-2	0.95
47.01	Baghdad	0.348	C C	11.00	SAND	60.0	CMP	1050	0	100	S	85.1	5.3	0	0.51	35.1	39.3	838	56	-3	47	0.80
47.02	Baghdad	0.363	C C	11.00	SAND	220.0	TNS	560	0	100	S	85.1	5.3	0	0.51	35.1	26.2	355	93	9	-2	0.63
47.03	Baghdad	0.348	C C	15.00	SAND	60.0	CMP	1600	0	100	S	108.6	5.6	0	0.48	34.8	34.2	1044	54	-4	50	0.65
48.01	Glasgow	0.381	S C	12.50	SAND	10.0	CMP	819	0	100	S	86.7	4.2	0	0.30	32.1	56.3	879	49	-1	52	1.07
50.01	Glasgow	0.406	S C	9.10	SAND	14.0	CMP	668	0	100	S	49.5	-5.0	17	0.52	35.3	66.2	1119	69	-1	32	1.68
51.01	St. Charle	0.330	C C	8.90	SAND	0.5	CMP	680	0	100	S	54.8	-5.1	22	0.46	34.5	56.3	837	62	-2	40	1.23
51.02	St. Charle	0.330	C C	11.90	SAND	0.5	CMP	980	0	100	S	70.3	-6.0	22	0.49	34.9	59.2	1089	67	-2	35	1.11

PILES IN SAND DATA BASE SAND NEW AND OLD DATA 11 AUG 2004

SAND SKIN FRICTION BY METHOD : NGI 1999 SOIL DATA QUALITY RATING = 0 CORRECTIONS INCLUDED
CLAY SKIN FRICTION BY METHOD : NGI 1999 PILE DATA QUALITY RATING = 0 Su : Yes Time : No

SITE No PILE No	LOCATION NAME	DIAM M	MAT O/C	PENTR M	TIP SOIL	TIME DAYS	CMP TNS	MEASURED (kN) TCOR:N	TCOR:Y	SHAFT SAND%	SAND CLAY	SIGV SIGV	CPT Su	SPT Ip	Dr Su/SIGV	PHI OCR	CALCD TAUSKN	CALCULATED (kN) TOTAL	SKN%	WGH%	TIP%	CALC MEAS
51.03	St. Charle	0.330	C C	15.00	SAND	0.5	CMP	1200	0	100	S	85.9	-6.5	22	0.51	35.2	59.7	1324	70	-2	32	1.10
51.04	St. Charle	0.330	C C	18.00	SAND	0.5	CMP	1380	0	100	S	100.8	-6.8	22	0.53	35.4	59.5	1539	72	-3	31	1.12
51.05	St. Charle	0.330	C C	21.10	SAND	0.5	CMP	1420	0	100	S	116.0	-7.1	22	0.54	35.5	59.2	1755	74	-3	29	1.24
52.01	Chiba-2	0.800	S O	40.60	SAND	22.0	CMP	8300+	0	72	S	162.3	-11.3	28	0.55	35.8	49.6	11799	47	-1	54*	1.42
54.01	Vancouver	0.915	S O	67.00	SAND	21.0	CMP	7460	0	87	S	391.5	5.1	0	0.17	30.3	39.6	6817	98	-4	6*	0.91
54.02	Vancouver	0.915	S O	78.00	SAND	21.0	CMP	7020	0	90	S	441.2	4.7	0	0.14	29.9	44.1	8888	99	-4	5*	1.27
54.03	Vancouver	0.915	S O	94.00	SAND	21.0	CMP	7980	0	93	S	513.4	4.5	0	0.11	29.6	51.3	12558	99	-3	4*	1.57
55.01	Ogeechee R	0.475	C C	15.20	SAND	0.0	CMP	2697	0	100	S	95.5	10.5	0	0.68	37.6	90.2	3341	61	-2	41	1.24
56.01	Aalborg øs	0.382	C C	17.65	SAND	26.0	CMP	1320	0	65	S	116.9	13.3	0	0.80	39.1	115.5	2808	73	-2	29	2.13
57.01	Hanstholm-	0.382	C C	16.80	SAND	0.0	CMP	1400	0	100	S	75.6	10.2	0	0.77	38.8	94.7	2545	75	-2	27	1.82
58.01	Dunkirk, F	0.324	S O	11.60	SAND	188.0	TNS	395	0	100	S	81.3	17.5	0	0.90	40.6	62.7	763	97	4	-1	1.93
58.02	Dunkirk, F	0.324	S O	11.60	SAND	189.0	CMP	1200	0	100	S	81.3	17.5	0	0.90	40.6	94.0	1842	60	-2	42	1.54
58.03	Dunkirk, F	0.324	S O	11.60	SAND	272.0	TNS	435	0	100	S	81.3	17.5	0	0.90	40.6	62.7	763	97	4	-1	1.75
58.04	Dunkirk, F	0.324	S O	11.60	SAND	273.0	CMP	1199	0	100	S	81.3	17.5	0	0.90	40.6	94.0	1842	60	-2	42	1.54
58.05	Dunkirk, F	0.324	S O	11.60	SAND	1990.0	TNS	750+	0	100	S	81.3	17.5	0	0.90	40.6	62.7	763	97	4	-1	1.02
58.06	Dunkirk, F	0.324	S O	11.60	SAND	176.0	TNS	458	0	100	S	81.3	17.5	0	0.90	40.6	62.7	759	98	3	-1	1.66
58.07	Dunkirk, F	0.324	S O	11.60	SAND	177.0	CMP	1199	0	100	S	81.3	17.5	0	0.90	40.6	94.0	1846	60	-1	41	1.54
58.08	Dunkirk, F	0.324	S O	11.60	SAND	289.0	TNS	548	0	100	S	81.3	17.5	0	0.90	40.6	62.7	759	98	3	-1	1.39
58.09	Dunkirk, F	0.324	S O	11.60	SAND	290.0	CMP	1200	0	100	S	81.3	17.5	0	0.90	40.6	94.0	1846	60	-1	41	1.54

PILES IN SAND DATA BASE SAND NEW AND OLD DATA 11 AUG 2004

SAND SKIN FRICTION BY METHOD : NGI 1999 SOIL DATA QUALITY RATING = 0 CORRECTIONS INCLUDED
CLAY SKIN FRICTION BY METHOD : NGI 1999 PILE DATA QUALITY RATING = 0 Su : Yes Time : No

SITE No PILE No	LOCATION NAME	DIAM M	MAT O/C	PENTR M	TIP SOIL	TIME DAYS	CMP TNS	MEASURED (kN) TCOR:N	TCOR:Y	SHAFT SAND%	SAND CLAY	SIGV SIGV	CPT Su	SPT Ip	Dr Su/SIGV	PHI OCR	CALCD TAUSKN	CALCULATED (kN) TOTAL	SKN%	WGH%	TIP%	CALC MEAS
58.10	Dunkirk, F	0.324	S O	11.60	SAND	2086.0	TNS	810	0	100	S	81.3	17.5	0	0.90	40.6	62.7	759	98	3	-1	0.94
58.11	Dunkirk, F	0.324	S O	22.10	SAND	1924.0	TNS	3100	0	100	S	135.6	20.1	0	0.89	40.4	59.2	1365	98	4	-2	0.44
59.01	Motorvegbr	0.813	S O	11.00	SAND	1.0	CMP	1300	0	100	S	68.4	5.5	0	0.52	36.0	45.6	1361	94	-2	8*	1.05
59.02	Motorvegbr	0.813	S O	17.00	CLAY	1.0	CMP	1300	0	91	S	87.5	5.5	0	0.52	36.0	37.9	1861	88	-9	21	1.43
59.03	Motorvegbr	0.400	S C	11.00	SAND	1.0	CMP	640	0	100	S	68.4	5.5	0	0.52	36.0	50.5	942	74	-12	38	1.47
59.04	Motorvegbr	0.400	S C	17.00	CLAY	1.0	CMP	560	0	92	S	87.5	5.5	0	0.52	36.0	41.9	715	124	-37	13	1.28
60.01	Motorvegbr	0.813	S O	15.00	SAND	2.0	CMP	1890	0	100	S	71.5	3.8	0	0.39	34.3	31.9	1271	96	-5	9*	0.67
60.02	Motorvegbr	0.813	S O	25.00	SAND	2.0	CMP	2700	0	100	S	111.7	5.2	0	0.43	34.2	36.6	2480	94	-2	8*	0.92
60.03	Motorvegbr	0.813	S O	25.00	SAND	16.0	CMP	3450	0	100	S	111.7	5.2	0	0.43	34.2	36.6	2480	94	-2	8*	0.72
60.04	Motorvegbr	0.813	S O	25.00	SAND	171.0	CMP	3500	0	100	S	111.7	5.2	0	0.43	34.2	36.6	2480	94	-2	8*	0.71
60.05	Motorvegbr	0.400	S C	15.00	SAND	3.0	CMP	1030	0	100	S	71.5	3.8	0	0.39	34.3	34.3	924	70	-17	47	0.90
60.06	Motorvegbr	0.400	S C	25.00	SAND	3.0	CMP	1550	0	100	S	111.7	5.2	0	0.43	34.2	39.9	1676	75	-15	40	1.08
60.07	Motorvegbr	0.400	S C	25.00	SAND	16.0	CMP	1590	0	100	S	111.7	5.2	0	0.43	34.2	39.9	1676	75	-15	40	1.05
60.08	Motorvegbr	0.400	S C	25.00	SAND	172.0	CMP	1800	0	100	S	111.7	5.2	0	0.43	34.2	39.9	1676	75	-15	40	0.93
61.01	Vårby, Sve	0.299	C C	12.80	SAND	1.0	CMP	310	0	68	S	93.8	3.3	0	0.28	31.9	15.6	442	50	-5	55	1.42
61.02	Vårby, Sve	0.299	C C	12.80	SAND	8.0	CMP	340	0	68	S	93.8	3.3	0	0.28	31.9	15.6	442	50	-5	55	1.30
61.03	Vårby, Sve	0.299	C C	12.80	SAND	122.0	CMP	390	0	68	S	93.8	3.3	0	0.28	31.9	15.6	442	50	-5	55	1.13
61.04	Vårby, Sve	0.299	C C	12.80	SAND	667.0	CMP	450	0	68	S	93.8	3.3	0	0.28	31.9	15.6	442	50	-5	55	0.98
62.01	Aalborg Væ	0.318	C C	17.50	CLAY	21.0	CMP	1380	0	59	S	106.0	-9.2	0	0.64	37.0	91.3	1444	86	-2	16	1.05

PILES IN SAND DATA BASE SAND NEW AND OLD DATA 11 AUG 2004

SAND SKIN FRICTION BY : NGI 1999 SOIL DATA QUALITY RATING = 0 CORRECTIONS INCLUDED
CLAY SKIN FRICTION BY : NGI 1999 PILE DATA QUALITY RATING = 0 Su : Yes Time : No

GROUP	CASES	SHAFT SOIL	TIP SOIL	COMP TENS	RATIO COMPUTED/MEASURED MINIMUM	AVERAGE	MAXIMUM	STANDARD DEVIATION
1	98	SAND	BOTH	COMP	0.28	1.11	2.13	0.38
2	54	SAND	BOTH	TENS	0.20	1.12	2.53	0.48
3	0	CLAY	SAND	COMP	0.00	0.00	0.00	0.00
4	0	CLAY	CLAY	COMP	0.00	0.00	0.00	0.00
5	0	CLAY	BOTH	TENS	0.00	0.00	0.00	0.00
6	152	ALL MEASUREMENTS			0.20	1.11	2.53	0.41

Title:

Evaluation of Time-Dependent Behavior of Soils.

Authors:

Augustesen, A., Liingaard, M. and Lade, P.V.

Year of publication:

2004

Published in:

International Journal of Geomechanics, 4(3), pp.137-156.

Remarks:

Evaluation of Time-Dependent Behavior of Soils

Anders Augustesen[1]; Morten Liingaard[2]; and Poul V. Lade, M.ASCE[3]

Abstract: The time-dependent behavior of soils has been investigated extensively through one-dimensional and triaxial test conditions. Most of the observations in literature have focused on the determination of the time-dependent behavior of clayey soils, whereas the reported experimental studies of granular materials are few. This paper presents an up-to-date review of the various observed time- and rate-dependent phenomena that are known to exist for both clay and sand. The description is carried out separately for creep, stress relaxation, rate dependency, and structuration in laboratory experiments. All of the above-mentioned phenomena are present in both sand and clay. The time-dependent phenomena are more pronounced in clay than sand. However, sand exhibits relatively large deformations at high confining pressures because of grain crushing. Furthermore, the review revealed an essential characteristic situation for soils. That is whether the time-dependent behavior can be characterized as isotach or nonisotach. It seems that the isotach behavior is adequate for describing the time effects in clays in most situations. But for sand, the isotach description is inadequate. Further, the phenomenon of structuration plays a role in both clay and sand.

DOI: 10.1061/(ASCE)1532-3641(2004)4:3(137)

CE Database subject headings: Clays; Creep; Sand; Time dependence; Soil properties.

Introduction

From real construction projects, it is well known that clay exhibits rheological behavior, see, e.g., Crawford and Morrison (1996), but it is not widely accepted that sand shows considerable amounts of time-dependent behavior as well (Komornik et al. 1972; Hannink 1994; Leung et al. 1996). To model the observed time-dependent behavior of sand and clay, constitutive models must be developed based on laboratory tests.

Most of the past laboratory studies of the rheological behavior of soils have been focused on the characteristics of clayey soils. This is especially true for the studies of confined conditions where the tests have been entirely based on cohesive soils, such as clay and peat. The studies of rheological behavior of soils in connection with triaxial test conditions are usually carried out on clays, but in the last few years increasing attention has been paid to experimental research into the behavior of granular materials. Sand, which is generally considered as nonviscous, exhibits time-dependent behavior. Experimental results show that the creep strains are not negligible and can reach 10% of the monotonic loading strain (usually understood as the elastoplastic strain). In addition, when loading after creep and relaxation periods, the response is much more rigid than if the time-dependent processes had not occurred (Tatsuoka et al. 2000).

[1]Graduate Student, Dept. of Civil Engineering, Aalborg Univ., Sohngaardsholmsvej 57, 9000 Aalborg, Denmark.

[2]Graduate Student, Dept. of Civil Engineering, Aalborg Univ., Sohngaardsholmsvej 57, 9000 Aalborg, Denmark.

[3]Professor, Dept. of Civil Engineering, Catholic Univ. of America, Washington, D.C. 20064 (corresponding author). E-mail: lade@cua.edu

Note. Discussion open until February 1, 2005. Separate discussions must be submitted for individual papers. To extend the closing date by one month, a written request must be filed with the ASCE Managing Editor. The manuscript for this paper was submitted for review and possible publication on October 24, 2003; approved on November 5, 2003. This paper is part of the ***International Journal of Geomechanics***, Vol. 4, No. 3, September 1, 2004. ©ASCE, ISSN 1532-3641/2004/3-137–156/$18.00.

The main purpose of this paper is to present the different time-related effects observed in soils and to remove the confusion regarding definitions, which are found in literature, i.e., a concise review is presented, which describes the observed trends within the field of time-dependent behavior of soil. To keep the review within manageable limits, the following assumptions have been made:

- The descriptions are restricted to factors that concern the macromechanical properties, such as stress, time, and strain.
- Temperature dependence has not been considered. For further studies, see Leroueil and Marques (1996).
- Only observations obtained from laboratory tests in one-dimensional oedometer tests and triaxial test conditions are considered. Tests under in situ conditions are not taken into account, see, e.g., Leroueil and Marques (1996) for other types of tests.

In this paper, the description of time-dependent observations in one-dimensional tests and triaxial tests are divided into the following subsections: Creep, relaxation, rate dependency, and accumulated effects. The characteristics of the observed behavior of clay and sand are explained separately within the four subsections. Definitions of creep, stress relaxation, and rate dependency are also presented in the section next.

It should be noticed that there are several ways in which the word ''time'' can be understood. In this paper, time has nothing to do with dynamic effects where inertial forces are involved. Instead, time and time dependency is here assumed to be related to viscous effects in the soil skeleton, such as creep, stress relaxation, and strain-rate effects. Therefore, the process of consolidation is not regarded as a true time effect either.

Basic Descriptions of Time Effects

There are three standard tests used to identify the time-dependent response of soil: creep tests, stress relaxation tests, and constant rate of strain tests (CRS tests). In the following, these tests and the soil response will be discussed because some confusion is found in literature, especially regarding the definition of creep.

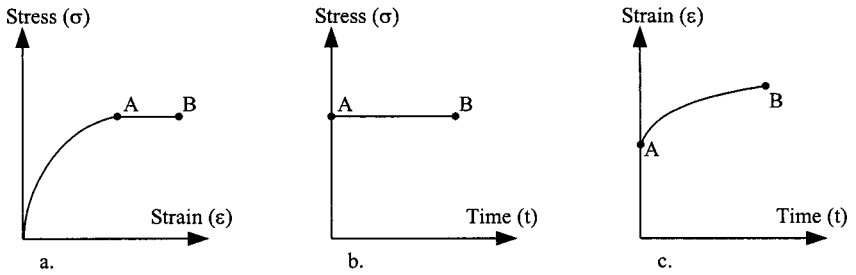

Fig. 1. Creep test performed at a low stress level: (a) Stress–strain relationship; (b) stress history; and (c) strain history

Creep

A creep test (strain path $A \rightarrow B$) is illustrated in Fig. 1. Consider a soil sheared to the stress–strain state at point A [Fig. 1(a)]. At this point, a creep process is initiated by letting the stress be constant over time [Fig. 1(b)]. As times advances, the strain state moves toward B. During this process, the strain is gradually increasing, i.e., the soil exhibits creep behavior [Fig. 1(c)]. Therefore, it can be concluded that during a creep test, which is characterized by constant stress, the strain increases.

Definition of Creep Stages

The results of a creep process performed at constant stress in a triaxial apparatus may be plotted in a strain–time diagram with arithmetic axes, as shown in Fig. 2. The process can be divided into three parts: (1) Primary creep or transient creep, (2) secondary creep or stationary creep, and (3) tertiary creep or acceleration creep.

A decreasing, a constant, and an increasing strain rate characterize the primary, secondary, and tertiary phases, respectively. This fact is further demonstrated in Fig. 2(b) where the logarithm of the strain rate is plotted against the logarithm of time. It should be noted that tertiary creep eventually leads to failure of the soil. This kind of failure is denoted as creep failure or creep rupture. The above mentioned is only valid for a creep test performed by means of a triaxial device.

Some confusion exists regarding primary, secondary, and tertiary creep defined in connection with creep tests performed in a triaxial apparatus on the one hand, and primary, secondary, and tertiary compression defined in connection with step load tests performed in an oedometer apparatus on the other hand. For oedometer tests, primary, secondary, and tertiary compression can be defined by plotting strains versus the logarithm of time, see Fig. 3(a). The primary phase is identical to the primary consolidation, i.e., the primary phase is the phase where excess pore pressure dissipates. The secondary phase is also denoted as secondary consolidation and, in oedometer tests, this phase corresponds to pure creep, i.e., deformations occur due to deformations in the soil skeleton (in this paper, there is no distinction between ''secondary consolidation'' and ''secondary compression''). Tertiary compression corresponds to pure creep, too. The tertiary compression phase is subsequent to the secondary compression phase and it is characterized by a nonlinear relationship between log (time) and strain [see Fig. 3(a)].

By comparing Figs. 2(a) and 3(a), it can be concluded that there are clear differences between primary, secondary, and tertiary creep and compression. By inspecting Fig. 3, nothing can be stated about the changes in strain rate with time ($d^2\varepsilon/dt^2$ or $\ddot{\varepsilon}$), because strain or strain rate is plotted against logarithm of time. It can be shown from elementary definitions of $\ln(t)$ and differentiation that (den Haan 1994):

$$\frac{d^2\varepsilon}{dt^2} = \frac{1}{t^2}\left(\frac{d^2\varepsilon}{d(\ln t)^2} - \frac{d\varepsilon}{d(\ln t)}\right) \tag{1}$$

where t = time and ε = strain. From Eq. (1), it can be concluded that the strain rate is increases if the second derivative of strain with regard to the logarithm of time is larger than the first derivative. The rate remains constant when both derivatives with regard to the logarithm of time are equal. The normal case will be that the rate continues to decrease, for which the second derivative with regard to the logarithm of time is smaller than the first derivative (den Haan 1994). Thus, a steepening strain versus logarithmic of time curve (tertiary compression) corresponds to a decreasing strain rate. In Fig. 3(b), the logarithm of strain rate versus logarithm of time is depicted for a single load increment in an oedometer test. It can be noted that the strain rate decreases with time. Therefore, it can be concluded that in oedometer tests,

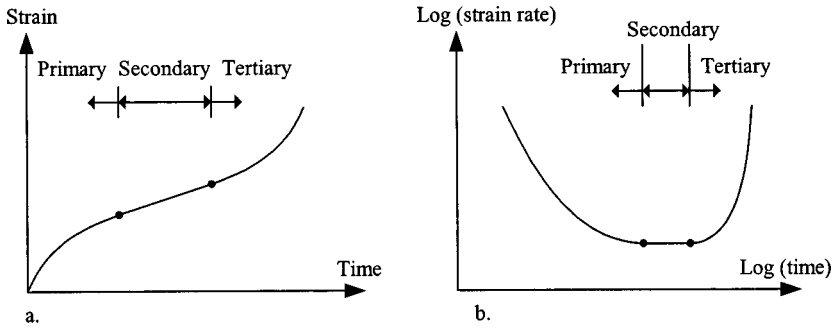

Fig. 2. Definition of creep stages when considering a creep test at constant stress performed in a triaxial apparatus: (a) Strain versus time and (b) log(strain rate) versus log(time)

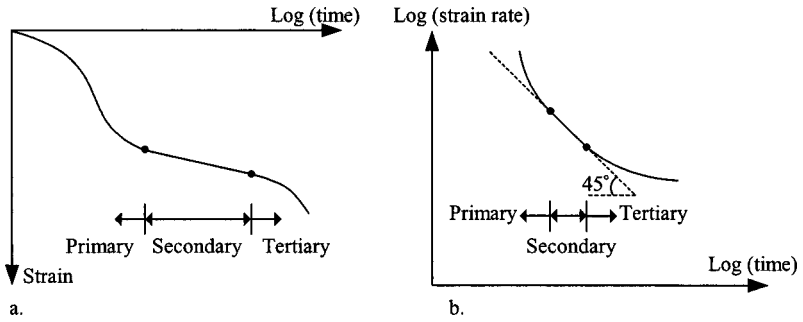

Fig. 3. Definition of primary, secondary, and tertiary compression: (a) Strain versus log(time) and (b) log(strain rate) versus log(time)

only primary creep (decreasing strain rate) can be observed whereas secondary (constant strain rate) and tertiary creep (increasing strain rate) cannot be observed.

From the above discussion, it can be concluded that primary, secondary, and tertiary creep are associated with a decreasing, constant, and increasing strain rate over time, whereas primary, secondary, and tertiary compression are in all situations associated with a decreasing strain rate over time.

Problem of Reference Time

It should be noted that the problem of defining the end of primary consolidation (EOP) is a contentious issue. It is closely related to the problem of similitude—meaning similarity or equivalence—(problem of reference time) that plays an important role with respect to determining the magnitude of creep in clayey soils. The problem of similitude does not change the fact that secondary compression exists. In other words the problem of similitude concerns the magnitude of the creep strains but not the rate or evolution of the creep strains. The concern is deciding when creep deformation starts, i.e., determining the reference time t_i. There are two aspects when evaluating the reference time:

- The reference time is taken as the time at the EOP. This implies that the value of t_i should vary with the drainage length or the thickness of the soil.
- The reference time is taken as an intrinsic parameter for a given soil. It means that t_i is independent of drainage conditions and soil thickness.

Much attention has been paid to the evaluation of reference time in literature, because it is crucial for estimating creep settlements in low permeability soils such as clay. The two aforementioned aspects express the two well-known approaches that have been adopted in the estimation of secondary compression, i.e., hypotheses A and B (Ladd et al. 1977). These approaches are as follows.

- Hypothesis A assumes that sample thickness has no effect on the location of the EOP curve and hence on the value of preconsolidation pressure. This hypothesis gives unique values of strain at the EOP, which corresponds to the fact that the soil does not show any time-dependent creep behavior during pore pressure dissipation in a manner that affects the strains at EOP. The main assumption of this hypothesis is that the secondary compression (creep) occurs only after primary consolidation. This method has been suggested by Mesri and Choi (Ladd et al. 1977; Leonards 1977; Mesri and Choi 1985a,b).
- Hypothesis B assumes that creep occurs during the whole consolidation process, which means that the strain at the EOP is not unique. This hypothesis, in which the time-dependent strains take place during the primary consolidation, is suggested by Suklje (1957), Wahls (1962), Barden (1969), Bjerrum (1967), Leroueil et al. (1985), Crawford (1986), Kabbaj et al. (1986), and Yin (1999) among others.

The predicted strain–time curves in connection with hypotheses A and B are illustrated in Fig. 4. There is still no general agreement on whether there is a combination of primary and secondary compression during the process of pore pressure dissipation (Duncan et al. 1986). The disagreements appear clearly by following the formulation from Leroueil et al. (1985):

> " . . . the experimental evidence is almost non-existent or not convincing: the consolidation test results obtained by Berre and Iversen (1972) on specimens of different heights which are often used to validate method B were also used by Leonards (1977) to justify theory A."

The conclusion of this discussion is that the real soil behavior is somewhere in the middle since the two hypotheses correspond to two extreme cases. This has been confirmed by, e.g., Aboshi (1973) who made an experimental investigation of the problem of similitude in normally consolidated clays. In all approaches by the different writers mentioned above, whether hypothesis A or B is adopted, a logarithmic function is used to fit the oedometer test data of vertical strain (or void ratio) against time after the primary (method A) or instantaneous (method B) compression (Liingaard et al. 2004). It should be noted that there is no distinction between methods A and B in permeable soil, such as sand.

Drained and Undrained Creep

In connection with a creep process performed in a triaxial apparatus, two definitions of creep are found in literature. In drained creep, the effective stresses (i.e., the mean effective stress p' and the deviatoric stress q) are kept constant, i.e., the creep process corresponds to a single stress point. In undrained creep, the drains are closed, and this causes a pore pressure buildup, and the mean effective stress p' decreases, while the deviatoric stress q, which is independent of pore pressure, remains constant. According to the definition of creep (development of strains over time at con-

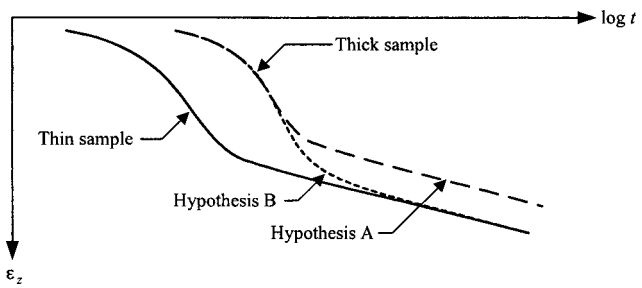

Fig. 4. Predicted strain–time curves for hypotheses A and B

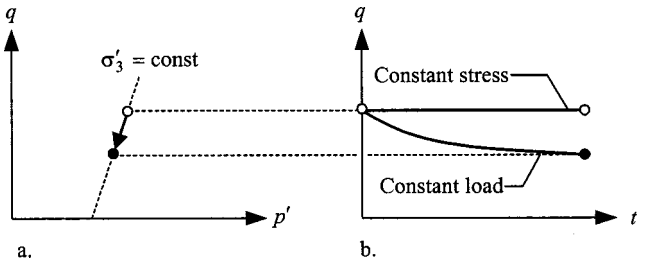

Fig. 5. Difference between creep at constant stress and constant load: (a) Triaxial plane and (b) time history for deviator stress during creep at constant stress and constant load. t is creep time.

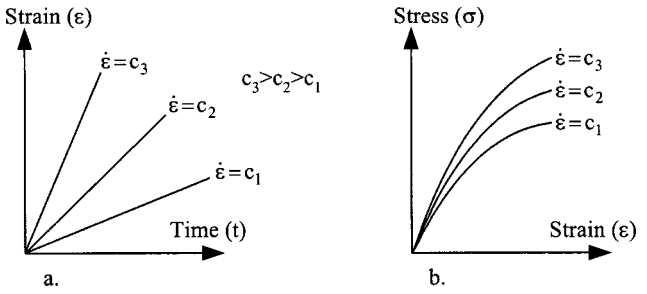

Fig. 7. Constant rate of strain tests: (CRS tests): (a) Strain history—during a CRS test, the total strain rate $\dot{\varepsilon}$ is kept constant and (b) stress–strain response. c_1, c_2 and c_3 are constants

stant effective stresses), it can be concluded that undrained creep does not represent a pure creep process, whereas drained creep does. In undrained creep deformations consist of plastic (due to changes in effective stresses) and inelastic (creep) deformations. However, in the literature, both processes are described as creep and, in the following, the processes will be denoted as drained and undrained creep.

Creep at Constant Load or Constant Stress

The requirement of constant effective stresses during a creep test is not fulfilled, in general. There are several occasions in literature where the authors refer to triaxial creep tests without explaining whether or not the effective stresses were kept constant. It is not always clear whether the writers refer to a triaxial creep test as a one where the effective stresses are kept constant or a one where the load is kept constant. There are clear differences. This is illustrated in Fig. 5.

Creep at constant stress corresponds to a point in the triaxial plane, as illustrated in Fig. 5. On the other hand, the constant load creep represents creep under stresses decreasing with time. This is due to the fact that the sample area increases, thereby resulting in a continuous decrease in creep stress. In fact, it is only the constant stress creep that can be taken as true creep, because the effective state of stress is maintained constant.

Stress Relaxation

A stress relaxation test (stress path $A \rightarrow B$) is illustrated in Fig. 6. Consider a soil sheared to the stress–strain state at point A. At this point, a stress relaxation process is initiated by letting the total strain be constant over time. As times goes by, the stress–strain state moves toward B. During this process, the stress is gradually decreasing—it relaxes. Therefore, it can be concluded that during a stress relaxation test, which is characterized by constant total strain, the stress decreases.

Constant Rate of Strain

In the CRS test, a total strain rate $\dot{\varepsilon} = d\varepsilon/dt$ is enforced and kept constant throughout the experiment. The stress response is then measured in order to obtain a stress–strain relationship.

In Fig. 7, the results of three CRS tests are shown. It appears that the larger the strain rate, the stiffer the soil. In connection with rate-independent elastoplasticity, the three curves will coincide.

Observations from One-Dimensional Tests

Creep

The observed behavior of creep in clays and sands is described in the following section. The descriptions are focused on the creep behavior with relation to factors, such as stress dependency and strain–time relations.

Clay

It is commonly accepted that clayey soils exhibit creep at constant effective stresses, especially normally consolidated clays. The phenomenon of drained creep of clays has been investigated extensively under one-dimensional conditions, where it is referred to as secondary compression. Secondary compression is often depicted as an approximately linear relationship between the vertical strain ε_z or void ratio e and the logarithm of time t. This relation is given by the coefficient of secondary compression, as seen in Fig. 8. This coefficient can be defined in different ways, with the most commonly used definitions given by

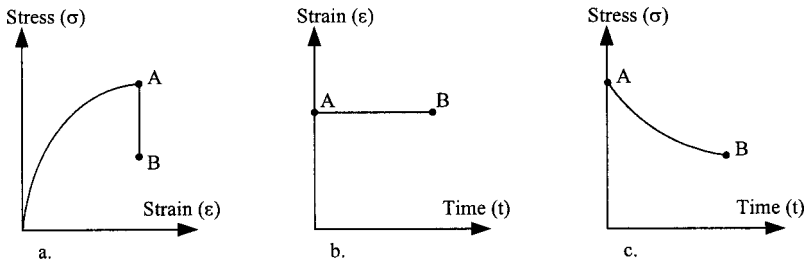

Fig. 6. Relaxation test (A→B): (a) Stress-strain relationship; (b) strain history; and (c) stress history

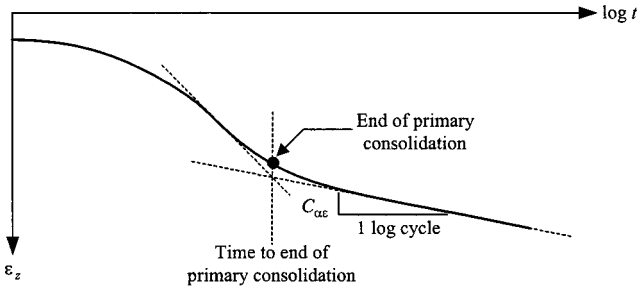

Fig. 8. Coefficient of secondary compression $C_{\alpha\varepsilon}$ is defined as the creep deformation over one log cycle of time t following the end of primary consolidation. $C_{\alpha\varepsilon}$ is given in terms of strains, hence the subscript ε. The time at which primary consolidation ends may be determined as the time when the pore water pressure is zero.

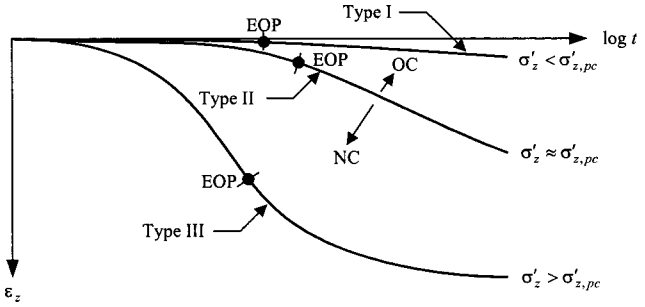

Fig. 9. Types of strain–time curves reported by Leroueil et al. (1985). Type I corresponds to a overconsolidated sample. Type II corresponds to a sample where the stress is close to the preconsolidation stress. Type III is a normally consolidated sample. (OC is overconsolidated, NC is normally consolidated, and EOP denotes end of primary consolidation.)

$$C_{\alpha e}=\frac{\Delta e}{\Delta \log(t)}; \quad C_{\alpha\varepsilon}=\frac{\Delta e}{(1+e_i)\Delta \log(t)}=\frac{\varepsilon_z}{\Delta \log(t)}=\frac{C_{\alpha e}}{1+e_i} \tag{2}$$

in which e = void ratio; ε_z = vertical strain; t = time; e_i = initial void ratio; and $C_{\alpha e}$ and $C_{\alpha\varepsilon}$ = coefficients of secondary compression with respect to e and ε. It should be noticed that C_α may appear by other notations in literature, e.g., α for both $C_{\alpha e}$ and $C_{\alpha\varepsilon}$. If Eq. (2) is rewritten with respect to ε_z, the logarithmic relation which is used to model the secondary compression appears:

$$\varepsilon_z = C_{\alpha\varepsilon} \log\left(1+\frac{t}{t_i}\right) \tag{3}$$

where t_i = some reference time. One of the major difficulties when using the logarithmic relation in Eq. (3) is deciding when the creep deformation starts, i.e., determining the reference time t_i. The problem of reference time (or problem of similitude) is discussed in the subsection "*Creep*" of the section entitled "Basic Descriptions of Time Effects."

In the following the parameter $C_{\alpha\varepsilon}$ is used as a reference for describing the one-dimensional creep characteristics of clay, because the concept is well known and widely used in geotechnical practice. Based on $C_{\alpha\varepsilon}$, the factors of effective stress dependency and strain–time relation, which influence the one-dimensional creep behavior of clay, are described.

***Stress Dependency*.** The effects of the effective vertical stress on $C_{\alpha\varepsilon}$ have been subjected to numerous investigations presented in literature. Walker and Raymond (1968) found that the secondary compression rates in the laboratory tests on sensitive Leda Clay appeared to be linearly related to the compression index $C_{c\varepsilon}$ ($C_{c\varepsilon}=\Delta\varepsilon/\Delta \log \sigma'_z$) over the entire applied stress range with an average ratio $C_{\alpha\varepsilon}/C_{c\varepsilon}$ of about 0.025.

Mesri (1973) considered the relationship between $C_{\alpha\varepsilon}$ and $C_{c\varepsilon}$ and concluded that soils that are highly compressible in the primary phase would show high compressibility in the secondary phase as well. This led to extensive studies of the relationship between $C_{\alpha\varepsilon}$ and $C_{c\varepsilon}$. Mesri and Godlewski (1977) computed the ratio of $C_{\alpha\varepsilon}/C_{c\varepsilon}$ for 22 natural soil deposits and found a range of values from 0.025 to 0.10 with the higher values applying to highly organic soils. The values of $C_{\alpha\varepsilon}/C_{c\varepsilon}$ were in general high for peats, somewhat less for organic clays, medium for clays and organic silts, and small for some clays and silts. Mesri and Castro (1987) reported that the value of $C_{\alpha\varepsilon}/C_{c\varepsilon}$ is equal to 0.04 ± 0.01 for a majority of inorganic soft clays and 0.05 ± 0.01 for the highly organic plastic clays. Upon these observations it was concluded that $C_{\alpha\varepsilon}$ is dependent on the applied effective stress σ'_z and its relation to the preconsolidation stress $\sigma'_{z,pc}$. It was shown that both $C_{c\varepsilon}$ and $C_{\alpha\varepsilon}$ increase as the effective stress σ'_z approaches the preconsolidation stress $\sigma'_{z,pc}$, reach a maximum at or just beyond the preconsolidation, and then decrease and finally remain reasonably constant. Throughout these effective stress changes the ratio $C_{\alpha\varepsilon}/C_{c\varepsilon}$ also remains reasonably constant. This marked stress dependency has also been observed by, e.g., Ladd and Preston (1965), Tavenas et al. (1978), Graham et al. (1983), and Länsivaara and Nordal (2000).

Several authors, including Mesri and Godlewski (1977), questioned the uniqueness of the $C_{\alpha\varepsilon}/C_{c\varepsilon}$ = constant concept in which $C_{\alpha\varepsilon}$ and $C_{c\varepsilon}$ are assumed to be time independent. They concluded that not only $C_{\alpha\varepsilon}$ but also $C_{c\varepsilon}$ changes with time. Furthermore, they reported that the changes in $C_{\alpha\varepsilon}$ with time might reflect the changes in $C_{c\varepsilon}$ with time, which means that the relationship between $C_{\alpha\varepsilon}$ and $C_{c\varepsilon}$ holds true for any time, effective stress, and deformation. Feda (1992) suggested that this kind of generalization should be used with utmost care and many reservations.

***Strain-Time Behavior*.** The traditional understanding of the strain–time relation during creep of clays corresponds to the behavior sketched in Fig. 8. That is, the secondary compression or creep follows a linear relation in a ε_z–log(t) diagram. This observation may be valid for several log cycles of time, but it does not hold true in general.

A general nonlinear strain–time behavior with respect to an ε_z–log(t) diagram has been observed by Leonards and Girault (1961), Bjerrum (1967), Berre and Iversen (1972), Leroueil et al. (1985), and Yin (1999). Leroueil et al. (1985) reported a general nonlinear strain–time behavior based on long-term creep tests (duration of 140 days). The strain-time curves for overconsolidated specimens, type I in Fig. 9, showed a continuously increasing slope with the logarithm of time after end of primary consolidation (EOP). On the other hand, specimens in the normally consolidated range, type III in Fig. 9, showed a continuously decreasing slope with the logarithm of time. The above states that the logarithmic relation does not hold true, in general.

When dealing with clays it is important to remember that the excess pore pressure during consolidation may hide the actual viscous effects in the soil. This is the fact for oedometer creep tests performed on samples in the vicinity of the preconsolidation

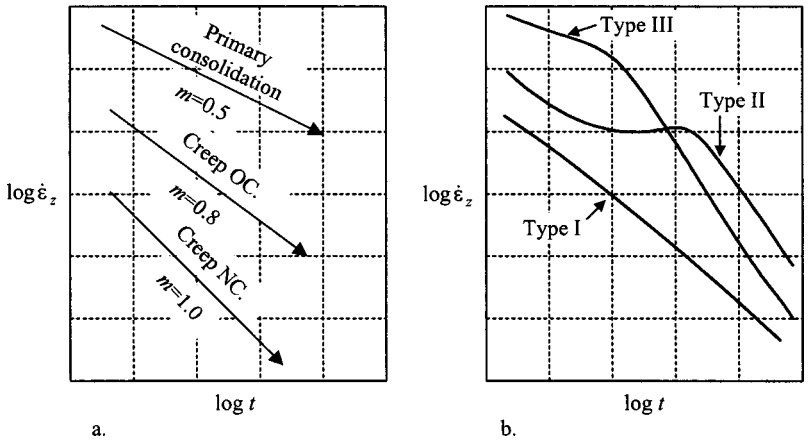

Fig. 10. (a) Illustration of the characteristic m values in $\log \dot{\varepsilon}_z$–$\log t$ diagram and (b) Types I, II, and III visualized in $\log \dot{\varepsilon}_z$–$\log t$ diagram

stress, type II in Fig. 9. At first, the specimen reacts as an overconsolidated soil, but after a certain time the strain rate remains momentarily constant. Finally, the sample reacts as a normally consolidated soil. This indicates some kind of creep delay when the sample passes from the overconsolidated range into the normally consolidated state. This behavior does not become obvious in Fig. 9. To visualize this kind of behavior, the creep test data are plotted in a $\log \dot{\varepsilon}_z$–$\log t$ diagram, as shown in Fig. 10. The main feature of this figure is that the slope of the straight line in the $\log \dot{\varepsilon}_z$–$\log t$ diagram is characterized by the m parameter by Singh and Mitchell (1968):

$$m = -\frac{\Delta \log \dot{\varepsilon}}{\Delta \log t} \tag{4}$$

In one-dimensional tests, $\dot{\varepsilon}$ should be taken as the vertical strain rate $\dot{\varepsilon}_z$. In the $\log \dot{\varepsilon}_z$–$\log t$ diagram in Fig. 10(a), a straight line with a downward slope $m = 0.5$ corresponds to Terzaghi's solution for primary consolidation. This slope is observed in the beginning of the type III curve that corresponds to a normally consolidated soil. Later, the type III soil shows a slope that corresponds to an m value greater than 1.0. The type I soil that is overconsolidated throughout the test shows an m value below 1.0 during the test period. The type II soil starts out with an m value corresponding to the overconsolidated soil (type I), but then the strain rate stops decreasing for a while. Thereafter, the type II soil shows the behavior of a normally consolidated soil. In the $\log \dot{\varepsilon}_z$–$\log t$ diagram in Fig. 10(b), the creep delay becomes clear. The S-shaped curve in Fig. 10(b) (type II) was observed by Bishop and Lovenbury (1969) and Tavenas et al. (1978), but no explanations were provided. Kabbaj et al. (1986) suggest that the S-shape corresponds to the creep delay, i.e., the transition from overly consolidated to normally consolidated creep state.

The above discussion only concerns the evolution of strains during secondary compression. As mentioned in the section entitled, ''Basic Descriptions of Time Effects,'' there is a third oedometer phase, tertiary compression, which has been observed after secondary compression. This phenomenon has been reported by Fodil et al. (1997) for oedometer creep tests on soft natural clay. The strain–time relation for creep started out as a linear relation in an e-$\log t$ diagram. After several log cycles of time, the creep behavior for the normally consolidated specimens showed a tendency for tertiary compression. Similar observations have been reported by den Haan and Edil (1994). They reported steepening of the compression—$\log t$ curves in oedometer tests on Portage (Wisconsin) peat, and defined a tertiary compression phase after the secondary compression phase. The tertiary compression occurred at all stress levels.

The phase of tertiary compression is not well documented in literature. It appears that it is only a well-accepted phenomenon in literature concerning peat.

Sand

There are only a few reported laboratory studies of one-dimensional creep tests performed on sand. For that reason, relevant observations from triaxial tests under isotropic stress states are included in this section, in order to support the few investigations performed in connection with oedometer tests on sand. To model the creep behavior of sand in confined conditions, there are two important observation aspects that will be described: Stress dependency and strain–time behavior.

Stress dependency. The deformations of granular soils occur almost instantaneously upon load application at low confining stresses but may continue, at a decreasing rate, for long periods of time at high confining stresses. The behavior of granular soils at high confining pressures is qualitatively similar to the behavior of normally consolidated clays. Thus, time-dependent behavior of granular materials can be divided into: (1) Behavior at low confining stresses (analogous to overconsolidated clay) where the deformations are caused by rearrangement over time due to sliding and rolling between the sand particles and (2) behavior at high confining stresses (analogous to normally consolidated clay) where the deformations are associated with continuous fracturing (crushing) and deformation of the grains.

The transition between the low stress and high stress regime depends on the mineralogical composition of the particles and the initial void ratio. The transition is referred to as the ''critical pressure.'' For detailed studies of the critical pressure and breakage of grains, see Yamamuro et al. (1996). The two regimes seem to have different creep characteristics. At low stresses, the creep strains are generally of small magnitudes but not negligible. Creep strains in one-dimensional conditions at low confining stresses have been reported by Mejia et al. (1988). They performed oedometer tests on two types of loose sands (Ottawa sand and Brenda Mine Tailings sand) at different vertical effective stresses. The time-dependent creep strains observed by Mejia et al. (1988) seem to be caused by sliding and rolling and not

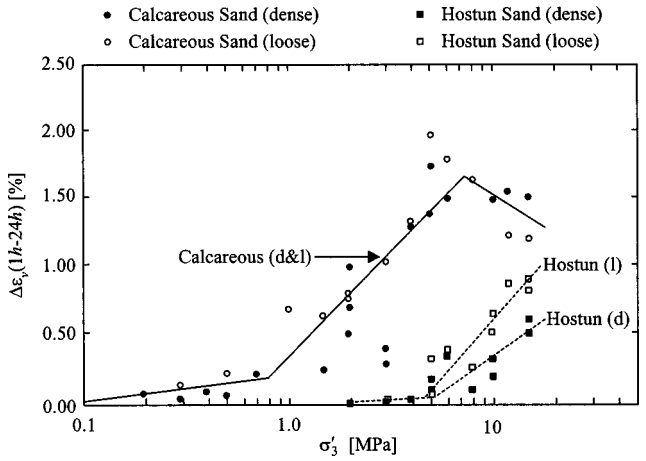

Fig. 11. Increase in volumetric creep strains between 1 and 24 h for different confining pressures (after Colliat-Dangus et al. 1988)

crushing because the stress levels were relatively low (<800 kPa).

Similar tests have been reported by Colliat-Dangus et al. (1988). They performed isotropic creep tests at both low stresses and high stresses. They found that the compression of sand is not instantaneous but continues at an ever-decreasing rate over a long period of time, in a way similar to the phenomenon of secondary compression observed in clays. The results are shown in Fig. 11.

Despite some scatter in the test results, it is observed that the volumetric creep strains increase with the confining stress. For the Hostun sand (siliceous) the compression may be considered instantaneous as long as the confining stress is lower than 2 MPa, whereas the time effects are visible for the calcareous sand even at very low confining stresses. When the stresses reach a certain level, a sharp increase in the volumetric creep strain is observed. For the calcareous sand, it occurs at about 0.8 MPa, while the sudden increase for the Hostun sand occurs at 5–6 MPa. Colliat-Dangus et al. (1988) define this threshold as a ''creep stress'' below which the strains due to creep are insignificant. They analyzed the grain size distributions before and after each test, and the analyses showed that the time effects were correlated to grain crushing. This implies that the propagation of rupture of particles may be the physical factor responsible for the effects of compression of granular materials under high confining stresses. The creep stress is closely related to the ''critical pressure'' that describes the transition between low and high stress domain.

Strain-Time Behavior. The evolution of creep strains over time is described with respect to the observations at low stresses and high stresses. In the low stress regime, the strain–time relation seems to be linear when plotted as strain versus logarithm of time. This is observed by Colliat-Dangus et al. (1988). The same tendency is observed by Mejia et al. (1988). They reported that the strain–time behavior for sand under K_0 conditions far from failure converged toward a logarithmic relation after some high initial strain rates in the first few seconds of the creep tests.

In the high stress regime, the evolution of creep strains over time is approximately linear when plotted in strain–log (time) diagrams as well. This has been observed by Leung et al. (1996) who performed one-dimensional oedometer creep tests on sands at high stresses.

The creep test at high stresses performed by Colliat-Dangus et al. (1988) showed the same tendency. The creep behavior of the Hostun sand showed a linear relation between creep strain and log (time) in the range of confining stress from 2 MPa to 10 MPa. The calcareous sand showed the same behavior but after approximately one hour of creep. The creep behavior in the initial stage was characterized by high initial strain rates that converged toward the logarithmic relation in about an hour. This suggests that a power relation between the creep strain and time in the initial creep stage may be more appropriate. The bilinear creep behavior (power relation followed by logarithmic relation) at high stresses has also been observed by Lagioia (1998) in isotropic creep tests (2–5 MPa). The isotropic creep tests were part of an investigation of time-dependent behavior of carbonate sands.

Relaxation

It appears that there are few reported investigations that treat relaxation of clay or sand in one-dimensional conditions. The only relaxation investigations on sand in one-dimensional test conditions are uniaxial relaxation tests performed on frozen sand by Ladanyi and Benyamina (1995).

Rate Dependency

The rate dependency has been investigated extensively in the past 30–40 years and several writers have confirmed that rate effects have great influence on the stress–strain behavior of clay. There are no known CRS investigations concerning rate-dependent behavior of sand in one-dimensional tests.

Clay

Increasing attention has been paid to investigation of rate dependency of clays since the introduction of various continuous loading oedometer testing procedures. These testing methods have been used in order to reduce the time involved in performing a consolidation test and to obtain continuous stress–strain curves. Among these testing methods are CRS, constant rate of load and controlled hydraulic gradient tests. The testing methods are explained in detail by Hamilton and Crawford (1959), Smith and Wahls (1969), Lowe et al. (1969), Wissa et al. (1971), Gorman et al. (1978), and Janbu et al. (1981). To show the rate dependency of clays under one-dimensional testing conditions, two different situations are explained, constant rate of strain and change of rate of strain.

Constant Rate of Strain Tests. The characteristics of CRS tests are indicated by the influence of strain rate on the preconsolidation pressure and the stress–strain behavior. The general observation is that the faster the loading rate, the higher the effective stresses for a certain strain. A typical example showing the strain-rate dependency of natural clay is illustrated in Fig. 12. It is seen that the compression curves move to the right for higher strain rates. However, it should be noted that the compression curve for the slowest rate ($\dot{\varepsilon}_{z6}$) deviates from the other tests. This deviation is explained in the section entitled, ''Observations from Triaxial Tests.''

After analyzing results from a variety of oedometer tests on different natural clays, Leroueil et al. (1985) suggested that the behavior was controlled by a unique relationship between the vertical effective stress, strain, and strain rate ($\sigma'_z - \varepsilon_z - \dot{\varepsilon}_z$). This unique relation is denoted ''isotach behavior'' and will be further discussed in the subsection entitled, ''Strain-Rate Dependency.'' Leroueil et al. (1985) showed that this unique relation could be described by two curves, one giving the normalized effective

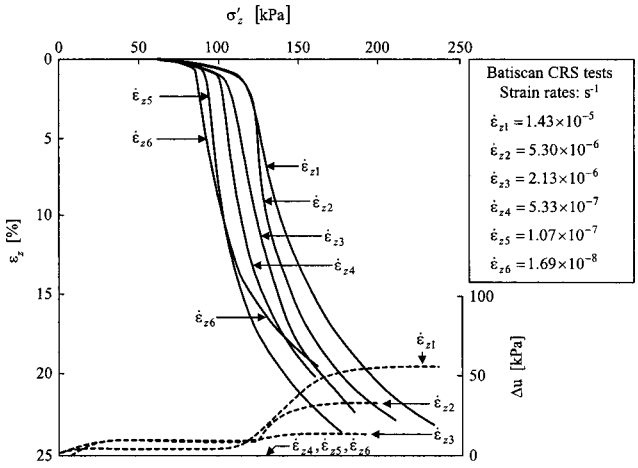

Fig. 12. Typical constant rate of strain oedometer tests on Batiscan clay. The solid lines are compression curves for different strain rates. The dotted curves are excess pore pressure during the tests (after Leroueil et al. 1985).

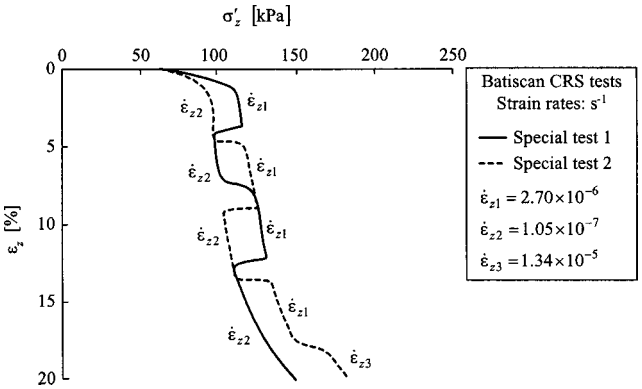

Fig. 14. Special constant rate of strain oedometer tests on Batiscan clay (after Leroueil et al. 1985)

stress–strain relationship and the other the variation of the preconsolidation pressure with strain rate. The normalized stress–strain relationship and the variation of preconsolidation with strain rate for Batiscan clay are shown in Figs. 13(a and b).

From Fig. 13, it is observed that the normalized stress–strain curves coincide for different rates of strain. Furthermore, the variation of the preconsolidation pressure with the strain rate becomes clear. The experimental data for several other types of natural clays presented by Leroueil et al. (1985) are consistent with the tendencies shown in Fig. 13.

It should be noted that most of the investigations of rate dependency are based on data obtained in the normally consolidated range; the rate-dependent behavior in the overconsolidated range is not as clear. However, creep tests in the overconsolidated range indicate different constant rate of strain curves (Tavenas et al. 1978).

Change of Rate of Strain. The existence of the unique relationship between the vertical effective stress, strain, and strain rate has been confirmed by special CRS tests in which the strain rates were changed at various strains. Leroueil et al. (1985) performed two such tests on Batiscan clay, Fig. 14. Länsivaara and Nordal (2000) have confirmed these special tests.

The results in Fig. 14 clearly show the unique stress–strain–strain-rate relationship (isotach behavior). An important feature is that the effects of change in rate are continuous, that is the soil ''stays'' on the same stress–strain curve until the strain rate is changed again. This isotach behavior is not observed for sand, as will be shown in the subsection entitled, ''Strain-Rate Dependency.''

Sand

It appears that there are no reported investigations that deal with the rate dependency of sand in one-dimensional conditions.

Accumulated Effects

The apparent preconsolidation pressure increases during secondary compression. When a soil is subjected to a constant effective

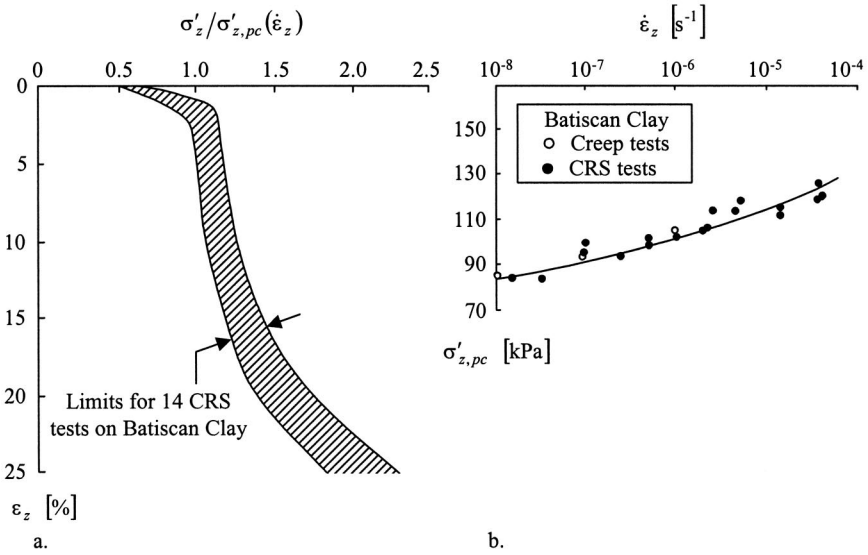

Fig. 13. (a) Normalized effective stress–strain relationship deduced from constant rate of strain oedometer tests on Batiscan clay and (b) variation of preconsolidation pressure with strain rate for Batiscan clay (after Leroueil et al. 1985).

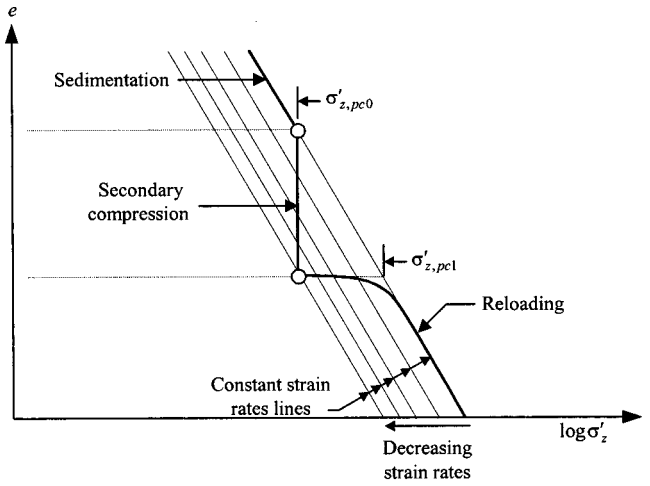

Fig. 15. Development of quasipreconsolidation pressure due to secondary compression. The preconsolidation pressure increases from $\sigma'_{z,pc0}$ to $\sigma'_{z,pc1}$. It should be noted that the lines of constant strain rate are approximately equal to the lines of constant time (after Bjerrum 1967).

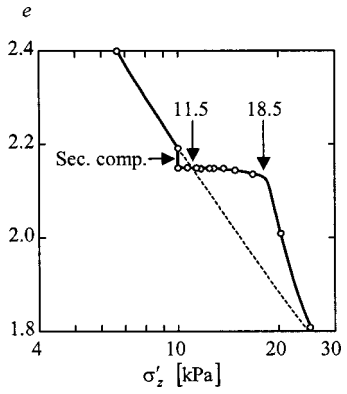

Fig. 16. Compression curve with structuration

stress for a long period of time, the void ratio and strain rate progressively decrease as shown in Fig. 15. If the soil is reloaded, there is an increase in strain rate and the compression curve moves to the curve of constant strain rate corresponding to the new strain rate. The compression curve then shows a preconsolidation pressure $\sigma_{z,pc1}$ associated with this new strain rate. The development of this ''quasipreconsolidation pressure'' was first observed by Leonards and Ramiah (1960) and explained in detail by Bjerrum (1967).

Oedometer tests performed by Leonards and Altshaeffl (1964) showed otherwise. They reported that the tested soil exhibited a preconsolidation pressure much higher than that due to its new void ratio only (after 90 days of secondary compression). Such a behavior is associated with the development of bonds between particles and aggregates and is referred to as ''structuration.'' The phenomenon of structuration has been reported by Leroueil et al. (1996) for oedometer tests on an artificially sedimented clay. In one of the tests, the soil was consolidated for 120 days under an applied vertical effective stress of 10 kPa. If the increase in the apparent preconsolidation pressure were to be determined from the concept of Bjerrum, as shown in Fig. 15, the preconsolidation pressure would have increased from 10 kPa to 11.5 kPa. However, due to the structuration effects, the preconsolidation pressure increased to 18.5 kPa during reloading. The compression curve for the oedometer test reported by Leroueil et al. (1996) is reproduced in Fig. 16.

Further investigations of structuration effects were performed by Leroueil et al. (1996). They made a comparison between the following three kinds of tests, see Fig. 17: (1) Conventional oedometer test (the applied load was increased in steps every 24 h), (2) CRS oedometer test performed at a strain rate of 1.27×10^{-5} s^{-1}, and (3) CRS oedometer test performed at a strain rate of 1.00×10^{-7} s^{-1}.

The three tests were compared and a unique relationship between the effective stress, strain, and strain rate ($\sigma'_z-\varepsilon_z-\dot{\varepsilon}_z$) was presumed. Good agreement was observed between the results from the conventional test and the ''rapid'' CRS test performed at a strain rate of 1.27×10^{-5} s^{-1}. The compression curve constructed from the conventional oedometer test data corresponded to a strain rate of approximately 1×10^{-7} s^{-1}, i.e., two orders of magnitude slower than the rapid CRS test at 1.27×10^{-5} s^{-1}. It was expected that the compression curve for the ''slow'' CRS test at a strain rate of 1.00×10^{-7} s^{-1} should coincide, or at least be close to the compression curve obtained by the conventional oedometer test.

The slow CRS test turned out to be very different from the conventional oedometer test. Furthermore, the compression curve for the slow CRS test was located above the rapid CRS test as shown in Fig. 17. This behavior did not agree with the unique $\sigma'_z-\varepsilon_z-\dot{\varepsilon}_z$ relation and the disagreement was explained by the effects of structuration developing with time. It should be noted that the deviation of the compression curve for the slowest rate ($\dot{\varepsilon}_{z6}$) in Fig. 12 might be due to structuration effects as well.

The agreement between the conventional test and the rapid CRS test was explained as follows: In the rapid CRS test, the strain rate was so high that the structuration had no time to develop; in the conventional oedometer test, the structure which might have developed during the previous loading step was destroyed when the new load was applied. In other words, the structuration in the rapid CRS test and the conventional oedometer test did not develop and the difference between the compression curves could be explained by rate dependency alone. On the other hand, the slow CRS test allowed structuration to develop resulting

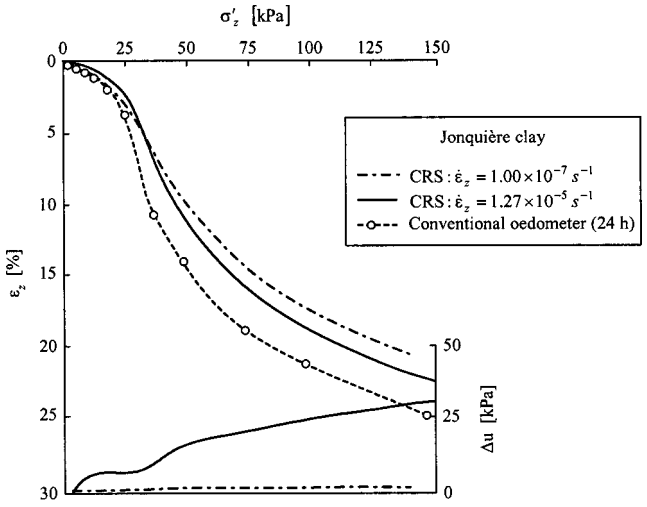

Fig. 17. Constant rate of strain and conventional 24 h oedometer tests on resedimented Jonquière clay (after Leroueil et al. 1996)

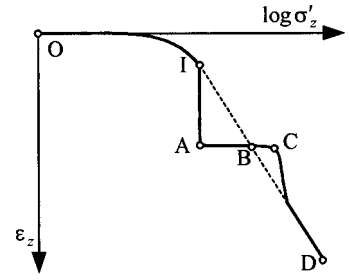

Fig. 18. Observed and expected structuration of sand due to creep (after Lagioia 1998)

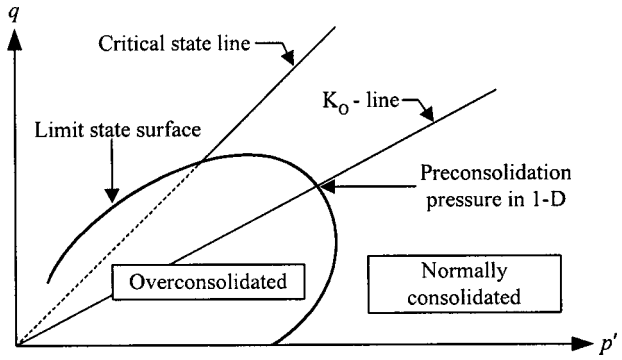

Fig. 19. Limit state surface in the triaxial plane. Inside the soil is overconsolidated and outside the soil is normally consolidated. The preconsolidation pressure in one-dimensional conditions corresponds to the intersection between the K_0 line and the limit state surface.

in a continuous strengthening. This strengthening over time is the reason that the compression curve for the slow CRS test is stiffer that the curve for the rapid CRS test.

The final comments are that the findings above show that the structuration phenomenon can be related to both time (the duration of secondary compression) and strain rates. The latter can be explained by the fact that structuration develops at slow rates. The distinction of slow and rapid rates has not yet been defined clearly but slow rates correspond to rates below 10^{-7} s^{-1} (Leroueil et al. 1996). Furthermore, Leroueil et al. (1996) suggest that structuration in clays can be explained by strengthening of contacts between particles or aggregates due to thixotropy or cementation and may be influenced by the age of the clay.

Sand

Effects of apparent preconsolidation in sand in confined conditions have been reported by Lagioia (1998), as shown in Fig. 18. Carbonate sand specimens were isotropically or one-dimensionally compressed at a constant loading rate (100 kPa/h) and then left to creep under a constant effective stress (800 kPa). Upon further loading, the specimens exhibited a considerable increase in stiffness that appeared to depend on the creep time. This behavior is similar to the concept of apparent preconsolidation observed in normally consolidated clays by Bjerrum (1967). However, the compression curve during reloading was expected to rejoin the normal compression line obtained by continuous loading (point B in Fig. 18), but Lagioia (1998) observed that the yield point moved to the right of the normal compression line (point C in Fig. 18). When the yield point was reached, the compression increased and the compression curve rejoined the normal compression line. Lagioia (1998) suggested that the structuration effects are due to complex interparticle cementation.

Observations from Triaxial Tests

Creep

In the one-dimensional case the description of creep behavior was focused on the influence of vertical stress and strain evolution over time. The creep behavior in triaxial conditions will be focused on the stress-level dependency, i.e., proximity to failure.

Clay

There are relatively few reports of drained creep tests on clay, compared with the number of undrained tests. In the following, emphasis will be placed on the observations from drained conditions whenever it is possible. The observations from undrained conditions will also be mentioned. In light of the information in the section entitled ''Basic Descriptions of Time Effects,'' undrained creep is not a true time effect. The influence of shear stress will be shown for creep in the normally and overconsolidated range (Fig. 19). The term ''limit state surface'' is equivalent to the preconsolidation pressure in one-dimensional conditions, and it corresponds to the plastic yield surface under two- and three-dimensional conditions. Inside the limit state surface, the soil is overconsolidated and ''outside'' the soil is normally consolidated.

Creep in the Normally Consolidated Range. In order to visualize the observed creep behavior in triaxial conditions, the creep test data are again plotted in $\log \dot{\varepsilon}$–$\log t$ diagrams. When the data are presented in such diagrams, the creep behavior can be analyzed by the parameter m, which is the slope of a straight line in the $\log \dot{\varepsilon}$–$\log t$ diagram. However, at first sight, it may be quite complex to imagine the consequences of varying m values. For that reason, the characteristics of three different m values are illustrated in Fig. 20. m is given by Eq. (4) and $\dot{\varepsilon}$ is taken as the axial strain rate $\dot{\varepsilon}_1$ in this section concerning triaxial conditions. In the section entitled, ''Basic Descriptions of Time Effects,'' $\dot{\varepsilon}$ is taken as the vertical strain rate $\dot{\varepsilon}_z$.

In one of the first studies of creep under drained and undrained triaxial conditions on various normally consolidated clays, Singh and Mitchell (1968) found that the parameter m varied between 0.75 and a value slightly greater than 1.0, with most values less than 1.0. They also suggested that the value of m was independent of the deviatoric stress level for a given soil. In other words, the creep lines for different deviatoric stress levels have the same slope in the $\log \dot{\varepsilon}_1$–$\log t$ diagram. Singh and Mitchell (1968) also found that the creep strain rate increases with the applied deviator stress.

In Fig. 21, a graph from Bishop and Lowenbury (1969) depicts the strain rate against time for drained triaxial tests and two oedometer tests on normally consolidated Pancone clay. Consider the part of the graph between 1 and 20 days. It is seen that $m \approx 1$ for the oedometer tests, thus the strain is more or less logarithmic with time. In the triaxial tests, m increases with deviator stress level S ($S = q/q_{\text{failure}}$) from $m = 0.8$ at $S = 50\%$ to $m > 1.2$ for $S = 85\%$. The graph in Fig. 21 illustrates that m is not always

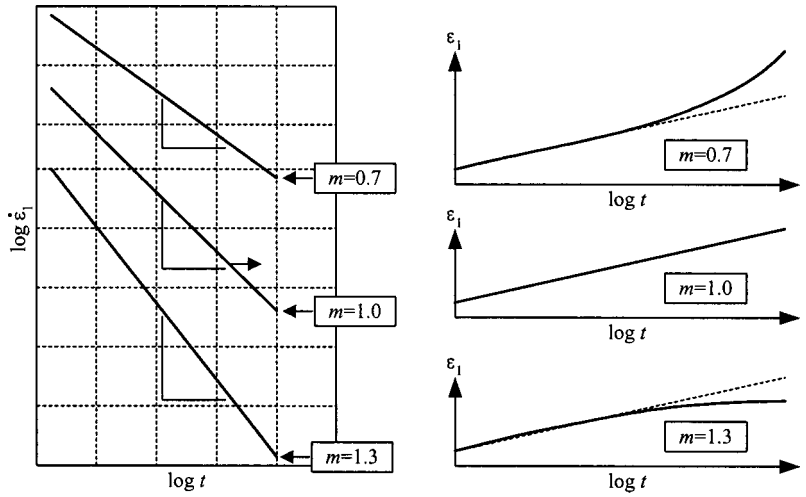

Fig. 20. Creep characteristics for three different m values. The strain–time curves for the m values are shown to the right. $m=1$ is corresponds to a straight line in the $\varepsilon_1-\log t$ diagram. $m\neq 1$ corresponds to curved lines in $\varepsilon_1-\log t$ diagrams.

constant in time and independent of deviator stress level as assumed by Singh and Mitchell (1968). But, in general, the graph shows that the strain rates increase with increasing stress levels. In the part of Fig. 21 between 20 and 100 days, the ''abrupt'' change in strain rate was interpreted as a limited instability that reflects a fundamental modification in soil structure. Bishop and Lovenbury (1969) provided no further explanations. As mentioned in the section entitled, ''Observations from One-Dimensional Tests,'' Kabbaj et al. (1986) suggested that the S-shape corresponds to a creep delay, occurring at the transition from an overconsolidated to normally consolidated creep state.

Tian et al. (1994) also reported that the m value appeared to be a function of the deviator stress level. Their analyses were based on drained triaxial creep tests on undisturbed marine sedimented clays from the Gulf of Mexico and the North-Central Pacific. The tests showed that the m value increased with increasing deviatoric stress levels for high-plasticity clay specimens from the Gulf of Mexico. The tests on clay specimens from the North-Central Pacific showed no significant variation in the m value. Variations in the m value as the deviator stress increases have also been reported by Feda (1992).

Furthermore, Zhu et al. (1999) acknowledged the change of m

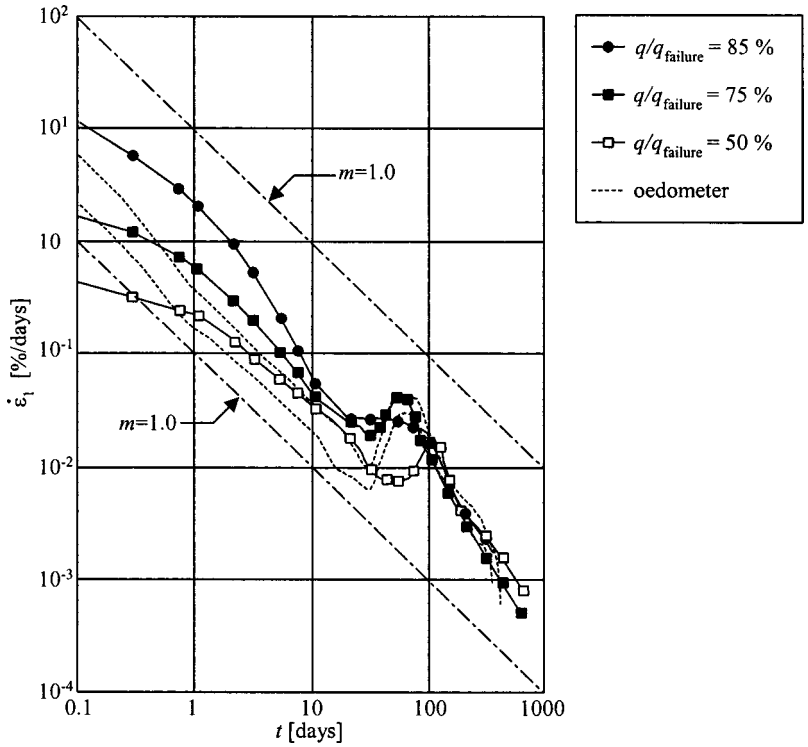

Fig. 21. Axial strain rate as a function of time for various stress levels (given as a percentage of deviator stress at failure). Results obtained from drained triaxial tests and oedometer tests on Pancone clay. Reproduced from Bishop and Lovenbury (1969). Guidelines showing $m=1.0$ are inserted.

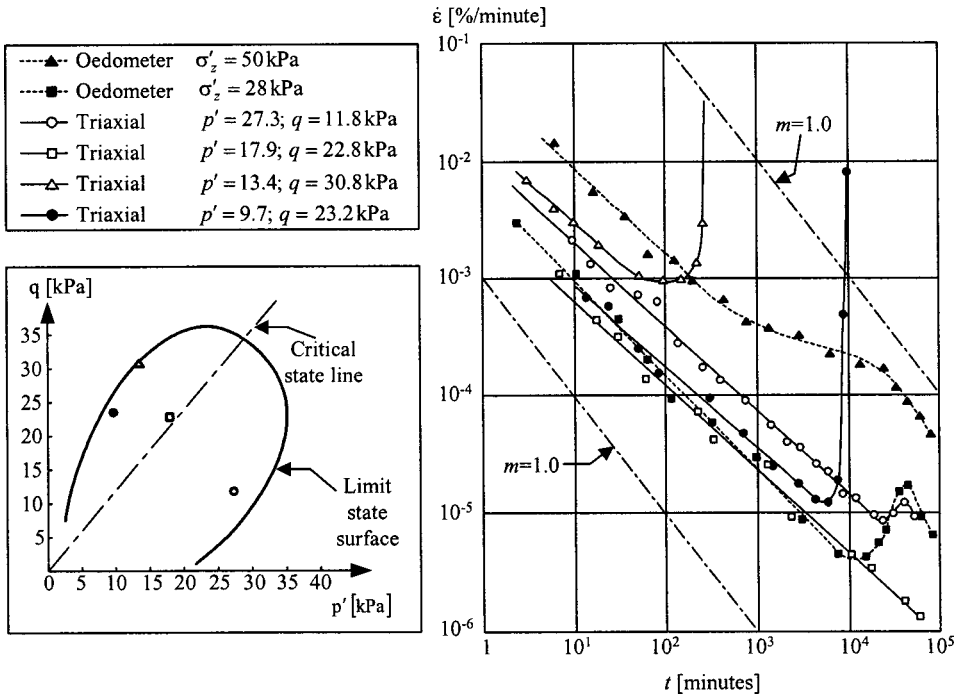

Fig. 22. (a) Stress levels at which the creep tests are carried out. Furthermore, stress levels are plotted in relation to the limit state surface and critical state line. (b) Axial strain rate–time relationship for drained tests under various stress conditions. The tests are carried out on undisturbed Saint-Alban clay (after Tavenas et al. 1978).

values with deviator stress in undrained triaxial creep tests. But they found that m decreased with an increasing stress level (m decreased from 0.91 to 0.57 for $q = 14$ kPa to 121 kPa). This tendency is opposite that observed by Tian et al. (1994). The work was based on soft Hong Kong Marine Deposits. Zhu et al. (1999) showed that the observed creep behavior in triaxial extension was somewhat similar to that in compression.

The m parameter has also been studied for other low permeability soils. den Haan (1994) reported that when drained or undrained triaxial tests are performed on peat and clays, it is common to find values of $m \approx 0.7-0.9$, largely independent of deviator stress level. In particular, it is found that $m \approx 0.84-0.90$ for peat and $m \approx 0.81-0.96$ for organic mud. Such values are also found when the applied shear stress level is close to K_0 (one-dimensional) conditions.

Creep in the Overconsolidated Range. Tavenas et al. (1978) made a detailed study of the volumetric and shear creep behavior of a lightly overconsolidated natural clay. With reference to the work of Singh and Mitchell (1968) they concluded that the development of both volumetric and shear strains with time can be represented by means of the m parameter given in Eq. (4).

Their triaxial creep tests were performed for several stress conditions inside the limit state surface of undisturbed Saint-Alban clay. The stress levels at which the creep processes were observed are shown in Fig. 22(a). Parallel to the triaxial tests, a series of long-term oedometer tests was performed.

The axial strain rates $\dot{\varepsilon}_1$ are plotted against the time t in a log–log diagram in Fig. 22(b) for triaxial and oedometer tests at various stress conditions. Note that two triaxial test specimen failed: One test corresponding to the stress state: $p' = 9.7$; $q = 23.2$ kPa and another one corresponding to the stress state: $p' = 13.4$; $q = 30.8$ kPa. The specimens failed after approximately 300 and 8000 min, respectively. The failure mode was creep rupture. The failures are probably due to the fact that the stress states are close to the strength envelope, which is representing the limit state surface for the overconsolidated soil. Fig. 22 also shows that there is a temporary increase in $\dot{\varepsilon}$ for the oedometer tests. It appears to be the same phenomenon as observed by Bishop and Lovenbury (1969).

Fig. 22(b) shows a linear decrease of $\log \dot{\varepsilon}_1$ with $\log t$. The m parameter with respect to the axial strains varies between 0.6 and 0.95 for all the triaxial creep tests. Tavenas et al. (1978) reported that the m parameter increased slightly with the deviator stress, but if m should be taken as a constant, the value would be of the order of 0.76 ± 0.16. Furthermore, there is a clear increase in axial strain rate as the deviator stress increases.

Tavenas et al. (1978) found that development of volumetric strain over time could be shown as a linear decrease of $\log \dot{\varepsilon}_v$ with $\log t$, even for the triaxial test that exhibited dilation. The m parameter with respect to the volumetric strains varied between 0.52 and 0.93 for all the triaxial creep tests, and was of the order of 0.8 for the oedometer tests. It was suggested that a constant m of the order of 0.7–0.8 could be considered representative of both the axial and volumetric behavior of the overconsolidated clay. Further, it was observed that the volumetric strain rates increase slightly with the effective mean stress p'.

The observations of linear decrease of the logarithm of strain rate with the logarithm of time for overconsolidated clay have been confirmed in tests performed by, e.g., Bishop and Lovenbury (1969) and D'Elia (1991).

Summary of the m-Parameter for Clay. The reported values of m in triaxial creep tests show that the strain–time relation, in general, differs from the classical logarithmic relation, discussed in the "*Creep*" subsection of the section entitled "Observations from One-Dimensional Tests." Within the normally consolidated range, m varies between 0.7 and 1.2 with most values less than

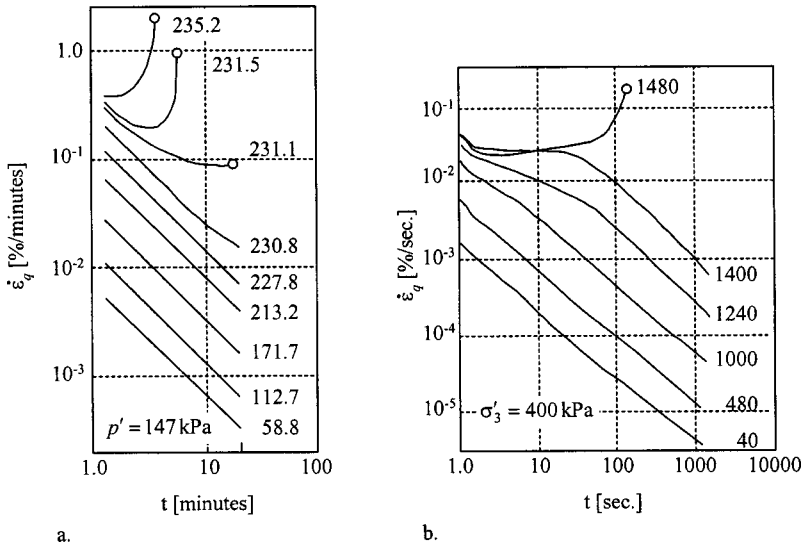

Fig. 23. (a) Shear strain rate–time response for Toyoura sand at different deviator stresses (after Muruyama et al. 1984). (b) Shear strain rate–time response for Tailings sand at different deviator stresses (after Mejia et al. 1988). Circles denote creep rupture in tests. The values are deviator stress, $q=\sigma_1-\sigma_3$ (kPa).

1.0. In the overconsolidated range the *m* values seem to be less than 1.0.

Several writers report that *m* is not always independent of deviator stress level as assumed by Singh and Mitchell (1968). In some cases, *m* decreases with increasing deviator stress; other cases show the opposite. It is a general observation that the strain rate increases with increasing deviator stress or stress level.

Most of the reported studies of creep under triaxial conditions involve determination of *m* for axial strains only. Some studies mention the *m* value for the volumetric strains. In the work of Tavenas et al. (1978), it is suggested that *m* may be taken as a constant, i.e., the same value for the volumetric and axial strain development. This is not the general opinion. Feda (1992) and Tian et al. (1994) found different values of *m* for the axial and volumetric parts of the creep tests. Note that the determination of *m* for the volumetric part is associated with some uncertainty compared with determination of *m* for the axial part.

Sand

The general opinion is that the creep behavior in sand for various stress levels is similar to that of clay. For that reason some writers investigate the creep behavior by means of the *m* parameter (defined in the section entitled, ''Basic Descriptions of Time Effects''). Fig. 23(a) shows the creep behavior of Toyoura sand at different stress levels, as reported by Murayama et al. (1984), while Fig. 23(b) shows creep tests on Tailings sand for various stress levels, as presented by Mejia et al. (1988).

In the tests by Murayama et al. (1984), the axial effective stress was applied by a loading lever, which corresponds to constant load creep, while Mejia et al. (1988) applied a static load that was periodically adjusted to maintain constant stress. However, creep was allowed for only 20 min at each stress level in both test series.

Both tests series show that the strain rates increase with the applied deviator stress as expected. The strain–time relation in Fig. 23(a) seems to be semilogarithmic at low stress levels, indicated by *m* values approximately equal to 1.0. The *m* values at low stresses in Fig. 23(b) are approximately 0.9. The results by Mejia et al. (1988) indicate an initial low slope for deviator stresses at $q=1{,}240$ kPa and 1,400 kPa. After approximately 10 s, the slopes increase and become similar to the slopes for creep at lower stress levels. In both test series, creep failure is observed at high stress levels. Mejia et al. (1988) and Murayama et al. (1984) reported that the stress levels at which creep failure occurred corresponds to the stress level at failure for the usual triaxial compression tests at the same confining pressure, i.e., creep rupture was therefore inevitable.

Only few long-term creep tests on sand have been presented in literature. The above-mentioned tests series involved creep periods of only 20 min, which is relatively short to capture the strain–time evolution. On the other hand, Lade and Liu (1998) performed long-term creep tests on Antelope Valley Sand for different stress levels. Their tests results showed more or less logarithmic strain–time relations for creep periods up to 10,000 minutes (7 days).

Stress Relaxation

Relatively few investigators have studied stress relaxation in soils under triaxial conditions. Most of the relaxation tests have been performed on clays. That is, there are only few reports of relaxation in sands, but the section is still divided into descriptions of clay and sand.

Clay

There appears to be a kind of ''reference relaxation behavior'' presented by Lacerda and Houston (1973), which acts as a basis for other investigations of relaxation. They reviewed the few previous investigations, performed several stress relaxation tests (on N.C. San Francisco Bay Mud, kaolinite, Monterey sand, and Ygnacio Valley Clay), and made contributions to the modeling aspect of time-dependent behavior. Some of the important aspects of the work of Lacerda and Houston (1973) are as follows:

- As illustrated in Fig. 24(b), the ratio between the deviator stress q at time t and the deviator stress at the beginning of stress relaxation q_0 was found to be linear with the logarithm of time after an initial time period. Previous studies performed by Murayama and Shibata (1961) and Vialov and Skibitsky

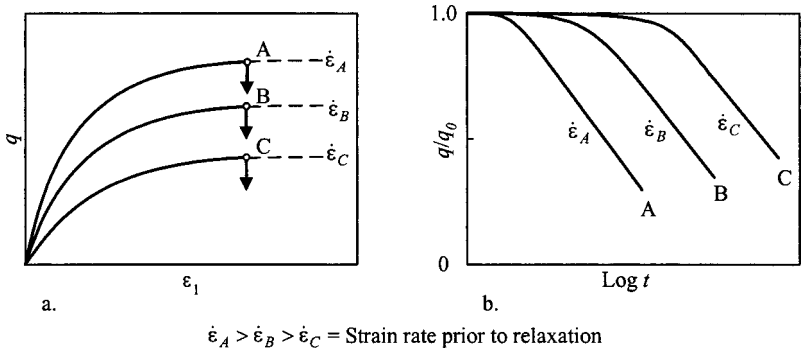

Fig. 24. Stress relaxation: (a) Stress–strain diagram showing three different relaxation tests (A, B, and C) where the strain rate prior to relaxation varies and (b) stress decay versus log time for the three relaxation tests. q is the deviator stress and q_0 is the stress at the beginning of relaxation.

(1961) showed similar patterns. However, Vialov and Skibitsky (1961) reported the existence of a final relaxed stress level. This was not observed by Lacerda and Houston (1973) for test durations up to 10,000 minutes (7 days).

- The strain rate prior to the relaxation phase influences the time at which stress relaxation begins. Lacerda and Houston (1973) observed that when slow strain rates were used to reach the relaxation strains, there was a time delay prior to the initiation of deviator stress decay. This is illustrated in Fig. 24.
- The test results were obtained in undrained stress relaxation tests. However, Lacerda and Houston (1973) observed that the variation of excess pore pressure during the undrained stress relaxation tests was practically zero, and Murayama and Shibata (1961) reported similar observations.

More recently, relaxation behavior has been investigated by Silvestri et al. (1988), Sheahan et al. (1994), and Zhu et al. (1999). Silvestri et al. (1988) performed undrained triaxial relaxation tests on a soft overconsolidated structured clay (Louiseville clay). They observed that the deviator stress reached a final relaxed level after a period of time of less than one day. Furthermore, they suggest that a curve joining these relaxed stress states would represent a ''static'' effective stress state curve. It is noteworthy that the ''static stress curve'' is similar to the term ''static yield surface,'' which is used in connection with modeling time-dependent behavior of soils by means of Perzyna's overstress theory (Perzyna 1963, 1966). The static stress curve is illustrated in Fig. 25. Reaching final relaxed stress states after relaxation were reported by Sheahan et al. (1994), while Zhu et al. (1999) reported no relaxed level when the relaxation tests were stopped after approximately 1,000 minutes. In the investigations by Silvestri et al. (1988), Sheahan et al. (1994), and Zhu et al. (1999) only small pore-pressure developments were observed during undrained relaxation.

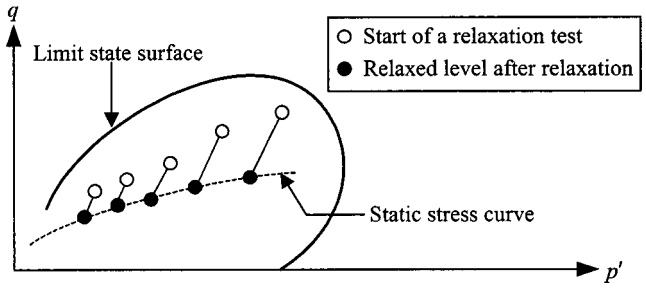

Fig. 25. Illustration of the static stress curve obtained from several relaxation tests on an overconsolidated clay.

Finally, the time delay of initiation of deviator stress decay shown in Fig. 24(b) seems to be inversely proportional to the strain rate prior to the relaxation phase. This implies that there is a relation between shearing at different strain rates and the relaxation behavior, and this suggests a correspondence between relaxation and rate dependency of clays.

Sand

Only few studies of stress relaxation in sand have been reported. Stress relaxation for Monterey sand has been reported by Lacerda and Houston (1973). Matsushita et al. (1999) reported that a considerable amount of stress relaxation was observed in triaxial tests on Hostun and Toyoura sands. Mitchell (1993) states that the relaxation behavior of clays and sands are generally the same. Most of the observations of relaxation on sand under triaxial test conditions are relaxation tests performed on frozen sand by Ladanyi and Benyamina (1995).

Strain-Rate Dependency

Clay

The description of creep phenomena in clays in the ''*Creep*'' subsection of the section entitled ''Observations from Triaxial Tests'' was divided into those observed for over and normally consolidated clays. This is also convenient for describing the rate dependency of the strength envelope for clays. The strength envelope for clays is sketched in Fig. 26.

In Fig. 19 the limit state surface is taken purely as a generalization of the preconsolidation pressure in one-dimensional conditions. It turns out that the upper part of the limit state surface corresponds to the peak strength envelope of an overconsolidated soil (from A to B in Fig. 26). The strength envelope in the normally consolidated range coincides with the critical state line (from B to C in Fig. 26). In the following, the effect of strain rate on the peak strength and the strength in the normally consolidated range will be evaluated.

Tavenas and Lereoueil (1977) indicated that the effects of time and strain rate on the preconsolidation pressure can be generalized to the entire limit state surface of the soil. Based on this statement, the rate dependency of the peak strength envelope can be explained by the rate dependency of the preconsolidation pressure obtained from one-dimensional conditions. In other words,

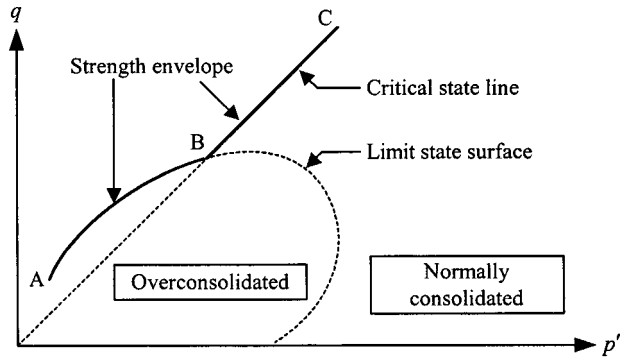

Fig. 26. Strength envelope for clays. AB is the peak strength envelope of an overconsolidated soil. BC is the strength envelope in the normally consolidated range.

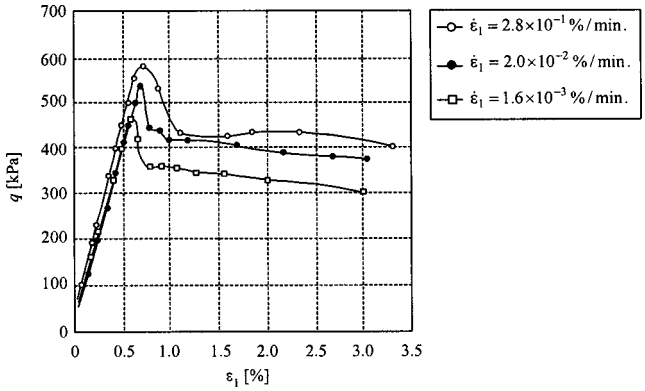

Fig. 27. Stress–strain behavior of Saint-Jean-Vianny clay in undrained constant rate of strain tests (after Vaid et al. 1979)

this means that the strain-rate effects on the strength envelope and thus the entire limit state surface are similar to the strain rate effects on the preconsolidation pressure shown in Fig. 13(b).

Fig. 27 shows the effect of strain rate on the stress–strain relation for overconsolidated Leda (Saint-Jean-Vianney) clay. The tests were performed as undrained CRS tests by Vaid et al. (1979). The results are obvious: The greater the strain rates, the greater the peak strength. Otherwise, the stress–strain relations are similar in nature. Similar observations have been reported by Tavenas et al. (1978) for overconsolidated Saint-Alban clay, Lefebvre and Leboeuf (1987) for structured Grande-Baleine clay, and Zhu et al. (1999) for soft Hong Kong marine deposits. Fig. 28 shows schematically the influence of strain rate on peak strength and thereby the limit state surface.

Fig. 28(a) also shows a stress–strain curve obtained by a hypothetical test performed at a strain rate approximating zero. The peak strength is denoted q_0. The corresponding limit state surface in Fig. 28(b) is denoted ''static yield surface,'' also see the subsection entitled ''Stress Relaxation.'' The existence of this surface has been debated in literature because several constitutive models based on Perzyna's overstress theory rely on the existence of a static yield surface (Perzyna 1963). Vaid and Campanella (1977) reported that there are indications of the existence of the static yield surface.

The part of the strength envelope denoted ''critical state line'' in Fig. 28 seems to be independent of rate effects. Several tests performed at different strain rates on normally consolidated clays did not show any significant effects of strain rate on the friction angle in the normally consolidated range (Vaid and Campanella 1977; Lefebvre and Leboeuf 1987; Sheahan et al. 1996).

Sand

Casagrande and Shannon (1948) and Lee et al. (1969) were among the first to study the strain rate effects on the strength of cohesionless soil. Yamamuro and Lade (1993) investigated the strain rate effects on dense Cambria sand in drained as well as undrained conditions performed at high pressure. The tests were performed at various constant strain rates but showed no significant rate effects on the stress–strain relations.

Matsushita et al. (1999) studied the rate dependency on the stress and strain behavior by performing drained plane strain compression tests and triaxial compression tests on Hostun sand and Toyoura sand. The rate dependency was investigated in two loading situations: (1) Tests where the strain rate for each test was kept constant, and (2) Tests where the strain rate was changed stepwise.

In tests where the axial strain rate was kept constant, the stress–strain relationships were essentially independent of the constant strain rates, which differed by a factor up to 500. This is illustrated in Fig. 29(a). In contrast, when the constant shear strain rate was changed stepwise, the shear stress increased and decreased temporarily, Fig. 29(b). The stress–strain relationship temporarily overshoots the unique relationship for the constant rate of strain curve when the strain rate is increased stepwise.

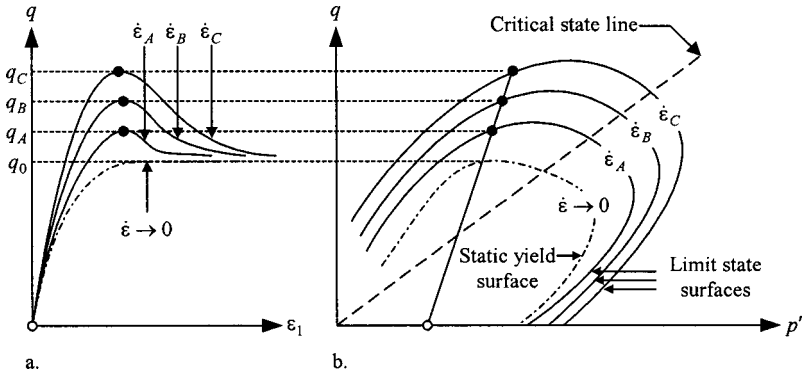

Fig. 28. Schematics of strain rate effects on limit state surface: (a) drained stress–strain curves for different constant rates of strain. q_A, q_B, and q_C are peak strengths, and (b) location of limit state surface for the different strain rates. The broken stress–strain curve in (a) corresponds to a test performed at a rate close to zero. The corresponding surface in (b) is denoted as static yield surface.

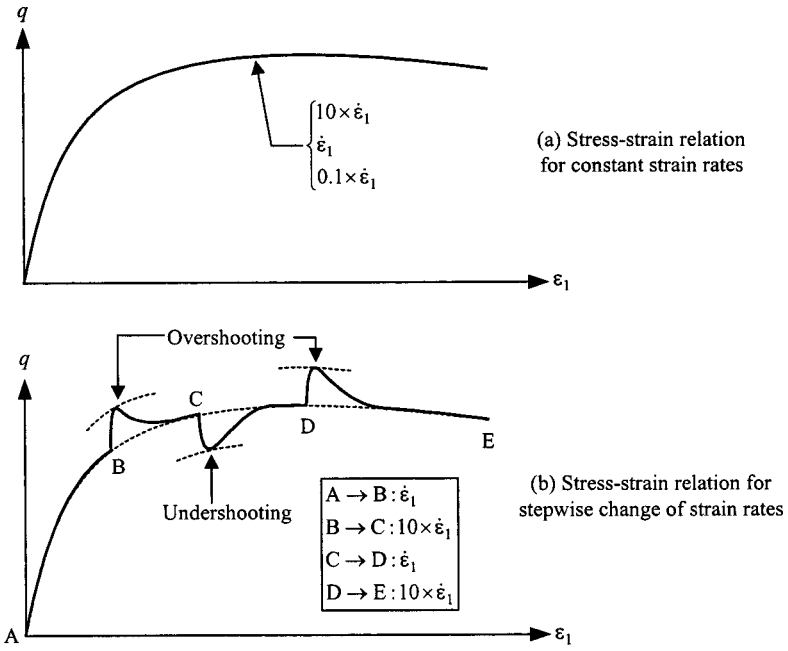

Fig. 29. Schematic diagrams illustrating the rate dependency observed for sand by Matsushita et al. (1999): (a) The stress–strain relation for different constant strain rates coincide for the three strain rates and (b) temporary over- and undershooting due to stepwise change in strain rate

After having exhibited clear yielding, the stress–strain relationship gradually rejoins the unique relationship for the constant rate of strain curve. On the other hand, when the strain rate is decreased stepwise, the stress–strain relation undershoots temporarily and eventually rejoins the unique relationship for the constant rate of strain curve. Similar observations of the phenomena of temporary over-and undershooting have been reported by Tatsouka et al. (2000) and Santucci de Magistris and Tatsouka (1999).

Comparison of Rate Effects in Sand and Clay

The fact that the phenomena of creep, relaxation, and strain-rate effects are governed by the same basic time mechanism is denoted isotach behavior, i.e., there is a unique stress–strain–strain-rate relation for a given soil as shown to the left in Fig. 30. The isotach behavior corresponds to some extent to the observed behavior of clay. This means that creep and relaxation properties can be obtained by means of CRS tests and vice versa (Leroueil and Marques 1996). This kind of mechanism where creep, relaxation, and rate dependency are considered to be due to the same basic mechanism is also denoted the ''correspondence principle'' according to Sheahan and Kaliakin (1999).

The sand tested by Matsushita et al. (1999) exhibited noticeable amounts of creep and relaxation but no strain-rate effects. This led to one of the main conclusions: The phenomena of creep and relaxation cannot be predicted from results obtained in CRS loading tests on sand. This is because the changes of strain rate

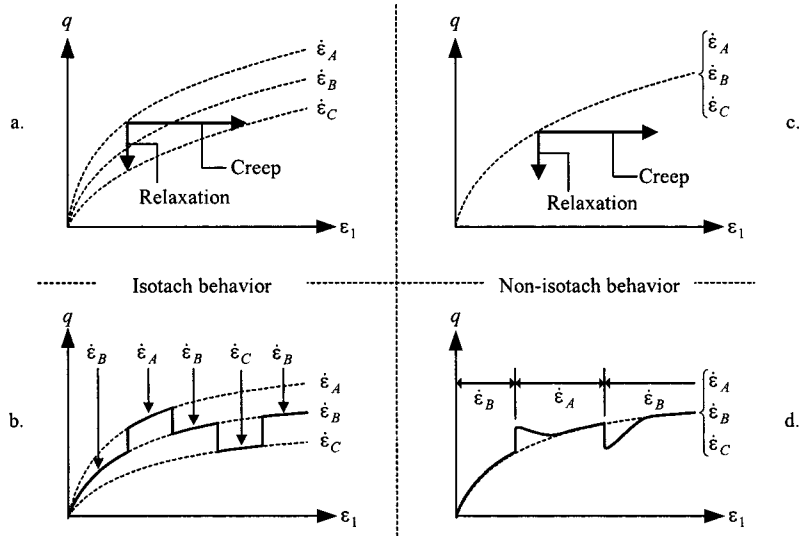

Fig. 30. Isotach behavior is observed in clay for (a) creep and relaxation and (b) stepwise change in rate. Nonisotach behavior is observed in sand for (c) creep and relaxation and (d) stepwise change in rate.

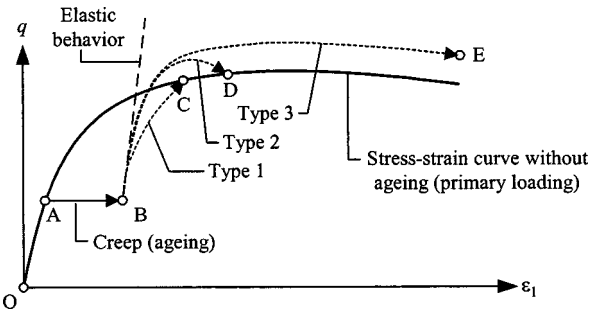

Fig. 31. The three types of postaging stress–strain relationships. The aging phase is the creep stage from A to B. The three types of postaging stress–strain relationships are from B to C, D, and E, respectively (after Tatsouka et al. 2000).

are temporary, as shown in Fig. 29. This behavior of sand does not correspond to the observed rate effects in clays. For sand, this behavior is labeled as ''nonisotach.'' The nonisotach behavior is illustrated to the right in Fig. 30.

Accumulated Effects

As mentioned in the one-dimensional cases there are several observations of aging effects in both clay and sand. These effects are observed in the stress–strain relation subsequent to long periods of aging, due to drained or undrained creep. Patterns similar to the observations in one-dimensional conditions have been reported in triaxial tests. The phenomena have been summarized by Tatsuoka et al. (2000). They consider with three types of postaging stress–strain relationships, as shown in Fig. 31:

- Type 1, aging without structuration: The stress–strain relationship after aging rejoins the original primary loading relationship without exhibiting overshooting (B to C).
- Type 2, temporary structuration effects: The stress–strain relationship after ageing rejoins the original primary loading relationship after having exhibited a temporary overshooting (B to D).
- Type 3, persistent structuration effects: The stress–strain relationship after aging does not rejoin the original primary loading relationship. There is a persistent overshooting with a noticeably larger peak strength than that obtained by the original primary loading (B to E).

Clay

The type 3 behavior has been observed for some clays, e.g. by Vaid and Campanella (1977) for undisturbed Haney clay and by Tatsouka et al. (2000) for Fujinomori clay. In Fig. 32, the observation by Vaid and Campanella (1977) is shown. The persistent overshooting is distinct.

As mentioned, it is assumed that the isotach behavior is adequate for describing time effects in clays. At first sight, it seems reasonable to confirm the isotach behavior for clays, but this holds true only with certain exceptions. When the soil is reloaded after periods of aging, structuration effects have been observed. The additional stiffness due to structuration cannot be explained by isotach behavior.

Sand

It appears that the type 2 behavior corresponds to the observations reported for sands. This type of behavior have been reported by Mejia et al. (1988) for Tailings and Ottawa sand and by Tatsouka et al. (2000) for Hostun sand. The movement of the yield surface during drained creep was investigated by Lade (1994) on Sacramento River sand. The yield surface location was calculated by means of the single hardening model (Lade and Kim 1988) and compared with experiments. The type 1 behavior was expected but a considerable amount of structuration was observed, corresponding to type 3 behavior. The stress–strain behavior subsequent to various creep periods is shown in Fig. 33. It is seen that

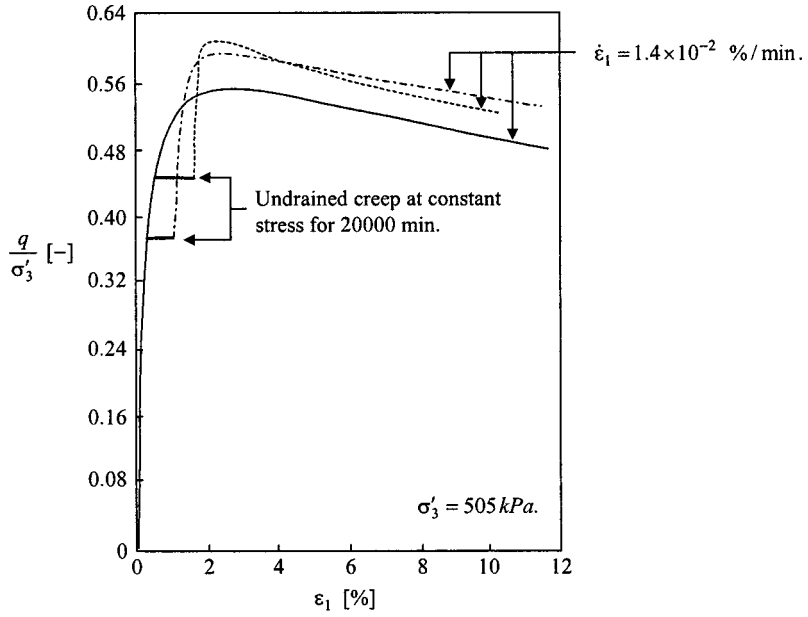

Fig. 32. Effects of undrained creep on the relationship between deviator stress and axial strain in undrained triaxial compression tests on undisturbed Haney clay. The cell pressure σ_3' is 505 kPa (after Vaid and Campanella 1977).

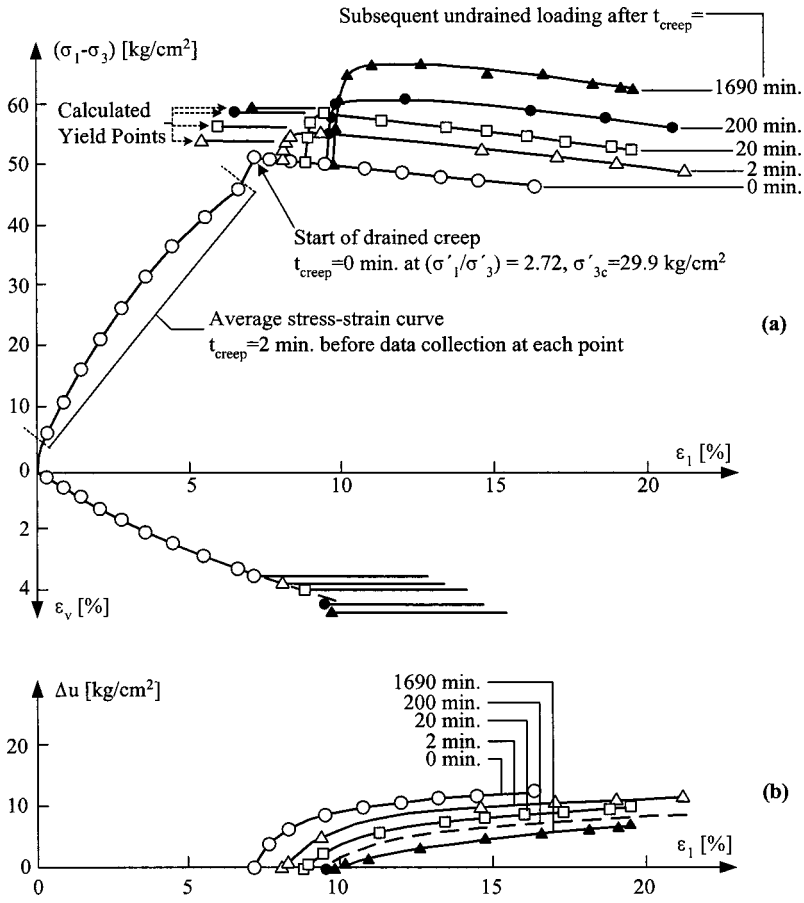

Fig. 33. (a) Stress–strain and volume change and (b) pore pressure relations for five creep tests on loose Sacramento River sand (after Lade 1994)

the stress–strain relation after creep shows structuration effects. The calculated yield points are below the observed yield points.

The disagreement with the isotach behavior for sand became evident in the previous section where the rate effects corresponded to nonisotach behavior. The nonisotach property is also observed on the stress–strain relationship after periods of aging. As for clay, there are structuration effects that cannot be explained by isotach behavior.

Conclusion

The observed time-dependent soil behavior found in literature is described. The review has focused on the observed time-dependent behavior obtained from laboratory tests in one-dimensional oedometer tests and triaxial test conditions. The description has been separated into reported characteristics of creep, stress relaxation, rate dependency, and accumulated effects. The latter have been focused on the occurrence of the phenomenon of structuration. It has been shown that all of the above-mentioned phenomena are present in both sand and clay. The time-dependent phenomena are more pronounced in clay than sand; however, sand exhibits relatively large deformations at high confining pressures because of grain crushing.

The review revealed essential characteristic situations for different types of soils. That is, whether the time-dependent behavior can be characterized as isotach or nonisotach. It seems reasonable that the isotach behavior is adequate for describing the time effects in clays in most situations. However, there are exceptions, such as the time-dependent behavior at very low strain rates, where the effects of structuration play a role. The structuration effects cannot be explained by isotach behavior.

The isotach behavior is not valid for sands. The disagreement with the isotach behavior becomes evident in several situations. The rate dependency in sand appears to be small and follows different patterns of behavior than in clays. However, when a step change is made in the CSR in tests on sand, the stress–strain state deviates temporarily from the unique strain rate-independent reference stress-strain relationship. This behavior is the so-called over- and undershooting. It appears that rate dependency in sand is of a temporary nature, which does not fit into the framework of isotach behavior. This leads to the fact that the phenomena of creep and relaxation cannot be directly related and predicted based on results obtained by CRS loading tests with respect to sand. However, it should be noted that the reported investigations of time-related phenomena for sand are few compared to the investigations of clay. The above conclusions have been made on the basis of available experimental results.

References

Aboshi, H. (1973). "An experimental investigation on the similitude in the consolidation of a soft clay, including the secondary creep settlement." *Proc., 8th Int. Conf. on Soil Mechanics and Foundation Engineering, Moscow*, Specialty Session 2, 4.3, 88.

Barden, L. (1969). "Time-dependent deformation of normally consolidated clays and peats." *J. Soil Mech. Found. Div.*, 95(SM1), 1–31.

Berre, T., and Iversen, K. (1972). ''Oedometer tests with different specimen heights on a clay exhibiting large secondary compression.'' *Geotechnique*, 17(1), 53–70.

Bishop, A. W., and Lovenbury, H. T. (1969). ''Creep characteristics of two undisturbed clays.'' *Proc., 7th ICSMFE*, Mexico, 1, 29–37.

Bjerrum, L. (1967). ''Engineering geology of Norwegian normally-consolidated marine clays as related to the settlements of buildings.'' *Geotechnique*, 17(2), 83–119.

Casagrande, A., and Shannon, W. L. (1948). ''Strength of soils under dynamic loads.'' *Proc. Am. Soc. Civ. Eng.*, 74(4), 591–632.

Colliat-Dangus, J. L., Desrues, J., and Foray, P. (1988). ''Triaxial testing of granular soil under elevated cell pressure.'' *Advanced triaxial testing of soil and rock*, ASTM, Philadelphia, 290–310.

Crawford, C. B. (1986). ''State of the art: Evaluation and interpretation of soil consolidation tests.'' *Consolidation of soils: Testing and evaluation*, R. N. Young and F. C. Townsend, eds., *ASTM Special Technical Publ., 892*, ASTM, Philadephia, 71–103.

Crawford, C. B., and Morrison, K. I. (1996). ''Case histories illustrate the importance of secondary-type consolidation settlements in the Frazer River Delta.'' *Can. Geotech. J.*, 33, 866–878.

D'Elia, B. (1991). ''Deformation problems in the Italian structurally complex clay soils.'' *10th European Conf. On Soil Mech. and Found. Engrg.*, 4, 1159–1170.

den Haan, E. J. (1994). ''Summary of session 1: One-dimensional behaviour.'' *Proc., Int. Workshop on Advances in Understanding and Modelling the Mechanical Behaviour of Peat.*, E. J. den Haan, R. Termaat, and T. B. Edil, eds., Balkema, Rotterdam, The Netherlands, 131–140.

den Haan, E. J., and Edil, T. B. (1994). ''Secondary and tertiary compression of peat.'' *Proc., Int. Workshop on Advances in Understanding and Modelling the Mechanical Behaviour of Peat*, E. J. den Haan et al., eds., Delft, The Netherlands, 16–18 June 1993, Balkema, Rotterdam, The Netherlands, 49–60.

Duncan, J. M., Rajot, J. P., and Perrone, V. J. (1996). ''Coupled analysis of consolidation and secondary compression.'' *2nd Int. Conf. On Soft Soil Engineering, Nanjing*, 3–27.

Feda, J., (1992). *Creep of soils and related phenomena, Development in geotechnical engineering*, Elsevier Science, North–Holland, Amsterdam, The Netherlands, Vol. 68.

Fodil, A., Aloulou, W., and Hicher, P. Y. (1997). ''Viscoplastic behaviour of soft clay.'' *Geotechnique*, 47(3), 581–591.

Gorman, C. T., Hopkins, T. C., Deen, R. C., and Drnevich, V. P. (1978). ''Constant-rate-of-strain and controlled-gradient consolidation testing.'' *Geotech. Test. J.*, 1, 3–15.

Graham, J., Crooks, J. H. A., and Bell, A. L. (1983). ''Time effects on the stress–strain behavior of natural soft clays.'' *Geotechnique*, 33(3), 327–340.

Hamilton, J. J., and Crawford, C. B. (1959). ''Improved determination of preconsolidation pressure of a sensitive clay.'' *Papers on soils, ASTM STP 254*, 254–271, Philadelphia.

Hannink, G., (1994). ''Settlement of high-rise buildings in Rotterdam.'' *Proc., 13th ICSMFE*, 2, 441–444.

Janbu, N., Tokheim, O., and Senneset, K. (1981). ''Consolidation tests with continuous loading.'' *Proc., 10th ICSMFE*, 1, 645–654.

Kabbaj, M., Oka, F., Leroueil, S., and Tavenas, F. (1986). ''Consolidation of natural clays and laboratory testing.'' *Consolidation of soils: Testing and evaluation, ASTM Special Technical Publ., 892*, R. N. Young and F. C. Townsend, eds., ASTM, Philadelphia, 378–404.

Komornik, A., Wiseman, G., and Zeitlen, J. G. (1972). ''Building settlement on end-bearing driven piles,'' *ASCE Specialty Conference on performance of earth and earth-supported structures*, ASCE, New York, 1135–1153, Vol. 1.

Lacerda, W. A., and Houston, W. N. (1973). ''Stress relaxation in soils.'' *Proc., 8th ICSMFE*, 1/34, 221–227.

Ladanyi, B., and Benyamina, M. B. (1995). ''Triaxial relaxation testing of a frozen sand.'' *Can. Geotech. J.*, 32, 496–511.

Ladd, C. C., Foott, R., Ishihara, K., Schlosser, F., and Poulos, H. J. (1977). ''Stress-deformation and strength characteristics.'' *Proc., 2, 9th ICSMFE*, Japan, 421–494.

Ladd, C. C., and Preston, W. B. (1965). ''On the secondary compression of saturated clays.'' *MIT Research Rep. No. R65-59*, Massachusetts Institute of Technology, Cambridge, Mass.

Lade, P. V. (1994). ''Creep effects on static and cyclic instability of granular soils.'' *J. Geotech. Eng.*, 120(2), 404–419.

Lade, P. V., and Kim, M. K. (1988). ''Single hardening constitutive model for frictional materials. II: Yield criterion and plastic work contours.'' *Comput. Geotech.*, 6(1), 13–29.

Lade, P. V., and Liu, C. T. (1998). ''Experimental study of drained creep behavior of sand.'' *J. Eng. Mech.*, 124(8), 912–920.

Lagioia, R., (1998). ''Creep and apparent preconsolidation in carbonate soils.'' *The geotechnics of hard soil—Soft rocks*, A. Evangelista and L. Picarelli, eds., Balkema, Rotterdam, The Netherlands.

Lee, K. L., Seed, H. B., and Dunlop, P. (1969). ''Effects of transient loading on the strength of sand.'' *Proc. 7th ICSMFE*, 1, 239–247.

Lefebvre, G., and Leboeuf, D. (1987). ''Rate effects and cyclic loading of sensitive clays.'' *J. Geotech. Eng.*, 113(5), 476–489.

Leonards, G. A. (1977). *Proc., 9th ICSMFE*, 384–386.

Leonards, G. A., and Altschaeffl, A. G. (1964). ''Compressibility of clays.'' *J. Soil Mech. Found. Div.*, 90(SM5), 133–155.

Leonards, G. A., and Girault, P. (1961). ''A study of one-dimensional consolidation test.'' *Proc., 5th* ICSMFE, 213–218, Vol. 1.

Leonards, G. A., and Ramiah, B. K. (1960). ''Time effects in the consolidation of clays.'' *ASTM STP 254*, ASTM, Philadelphia, 116–130.

Leroueil, S., Kabbaj, M., Tavenas, F., and Bouchard, R. (1985). ''Stress–strain–strain-rate relation for the compressibility of sensitive natural clays.'' *Geotechnique*, 35(2), 159–180.

Leroueil, S., and Marques, M. E. S. (1996). ''Importance of strain rate and temperature effects in geotechnical engineering.'' *Proc., Measuring and Modeling Time Dependent Soil Behavior, Geotechnical Special Publication No. 61*, T. C. Sheahan, and V. N. Kaliakin, eds., ASCE, Reston, Va., 1–60.

Leroueil, S., Perret, D., and Locat, J. (1996). ''Strain rate and structuring effects on compressibility of a young clay.'' *Proc., Measuring and Modeling Time Dependent Soil Behavior, Geotechnical Special Publication No. 61*, T. C. Sheahan, and V. N. Kaliakin, eds., ASCE, Reston, Va., 137–150.

Leung, C. F., Lee, F. H., and Yet, N. S. (1996). ''The role of particle breakage in pile creep in sand.'' *Can. Geotech. J.*, 33, 888–898.

Liingaard, M., Augustesen, A., and Lade, P. V. (2004). ''Characterization of models for time-dependent behavior of soils.'' *Int. J. Geomech.*, 4(3), 157–177. .

Lowe, J., Jonas, E., and Obrician, V. (1969). ''Controlled gradient consolidation test.'' *J. Soil Mech. Found. Div.*, 95(SM1), 77–97.

Länsivaara, T., and Nordal, S. (2000). ''Strain rate approach to creep evaluations.'' *13th Nordic Geotechnical Conference NGM-2000*, 25–32.

Matsushita, M., et al. (1999). ''Time effects on the prepeak deformation properties of sands.'' *Prefailure Deformation Characteristics of geomaterials*, M. Jamiolkowski, R. Lancellotta, and D. LoPresti, eds., Balkema, Rotterdam, The Netherlands, 681–689.

Mejia, C. A., Vaid, Y. P., and Negussey, D., (1988). ''Time dependent behaviour of sand.'' *Int. Conf. on Rheology and Soil Mechanics*, Coventry, England.

Mesri, G. (1973). ''Coefficient of secondary compression.'' *J. Soil Mech. Found. Div.*, 99(1), 123–137.

Mesri, G., and Castro, A. (1987). ''$C\backslash Ga/C_c$ concept and K_0 during secondary compression.'' *J. Geotech. Eng.*, 113(3), 230–247.

Mesri, G., and Choi, Y. K. (1985a). ''The uniqueness of end-of-primary (EOP) void ratio-effective stress relationship.'' *Proc., 11th ICSMFE*, 587–590, Vol. 2.

Mesri, G., and Choi, Y. K. (1985b). ''Settlement analysis of embankments on soft clays.'' *J. Geotech. Eng.*, 111, 441–464.

Mesri, G., and Godlewski, P. M. (1977). ''Time and stress-compressibility interrelationship.'' *J. Geotech. Eng.*, 103(5), 417–430.

Mitchell, J. K. (1993). *Fundamentals of soil behavior*, 2nd Ed., Wiley, New York.

Murayama, S., Michihiro, K., and Sakagami, T. (1984). ''Creep characteristics of sands.'' *Soils Found.*, 24(2), 1–15.

Murayama, S., and Shibata, T. (1961). ''Rheological properties of clays.'' *Proc., 5th Int. Conf. on Soil Mechanics and Foundation Engineering*, 269–274, Vol. 1.

Perzyna, P. (1963). ''The constitutive equations for work-hardening and rate sensitive plastic materials.'' *Proc., Vibration Problems*, 281–290, Vol. 3.

Perzyna, P. (1966). ''Fundamental problems in viscoplasticity.'' *Adv. Appl. Mech.*, 9, 244–377.

Santucci de Magistris, F., and Tatsouka, F. (1999). ''Time effects on the stress–strain behavior of Metramo silty sand.'' *Prefailure deformation characteristics of geomaterials*, M. Jamiolkowski, R. Lancellotta, and D. LoPresti, eds., Balkema, Rotterdam, The Netherlands, 681–689.

Sheahan, T. C., and Kaliakin, V. N. (1999). ''Microstructural considerations and validity of the correspondence principle for cohesive soils.'' *Engineering Mechanics, Proc., 13th Conf.*, N. Jones and R. Ghanem, eds., ASCE, Baltimore, Md.

Sheahan, T. C., Ladd, C. C., and Germaine, J. T. (1994). ''Time-dependent triaxial relaxation behavior of a resedimented clay.'' *Geotech. Test. J.*, 17(4), 444–452.

Sheahan, T. C., Ladd, C. C., and Germaine, J. T. (1996). ''Rate dependent undrained behavior of saturated clay.'' *J. Geotech. Eng.*, 122(2), 99–108.

Silvestri, V., Soulié, M., Touchan, Z., and Fay, B. (1988). ''Triaxial relaxation tests on a soft clay.'' *Advanced triaxial testing of soil and rock*, ASTM, Philadelphia, 321–337.

Singh, A., and Mitchell, J. K. (1968). ''General stress–strain–time function for soils.'' *J. Soil Mech. Found. Div.*, 94(1), 21–46.

Smith, R. E., and Wahls, H. E. (1969). ''Consolidation under constant rates of strain.'' *J. Soil Mech. Found. Div.*, 95(SM2), 519–539.

Suklje, L. (1957). ''The analysis of the consolidation process by the isotaches method.'' *Proc., 4th ICSMFE*, 200–206, Vol. 1.

Tatsuoka, F., Santucci de Magistris, F., Hayano, K. Momoya, Y., and Koseki J. (2000). ''Some new aspects of time effects on the stress–strain behaviour of stiff geomaterials.'' *The geotechnics of hard soils–soft rocks, 1998*, R. Evangelista and L. Picarelli, eds., Balkema, Rotterdam, The Netherlands, 1285–1371, Vol. 2.

Tavenas, F., and Lereoueil, S. (1977). ''Effects of stresses and time on yielding of clays.'' *Proc., 9th ICSMFE*, 319–326, Vol. 1.

Tavenas, F., Leroueil, S., La Rochelle, P., and Roy, M. (1978). ''Creep behavior of an undisturbed lightly overconsolidated clay.'' *Can. Geotech. J.*, 15(3), 402–423.

Tian, W.-M., Silva, A. J., Veyera, G. E., and Sadd, M. H. (1994). ''Drained creep of undisturbed cohesive marine sediments.'' *Can. Geotech. J.*, 31, 841–855.

Vaid, Y. P., and Campanella, R. G. (1977). ''Time-dependent behavior of undisturbed clay.'' *J. Geotech. Eng.*, 103(7), 693–709.

Vaid, Y. P., Robertson, P. K., and Campanella, R. G. (1979). ''Strain rate behavior of Saint-Jean-Vianney clay.'' *Can. Geotech. J.*, 16, 34–42.

Vialov, S. S., and Skibitsky, A. M. (1961). ''Problems of the rheology of soils.'' *Proc., 5th Int. Conf. on Soil Mechanics and Foundation Engineering*, 387–392, Vol. 1.

Wahls, H. E. (1962). ''Analysis of primary and secondary consolidation.'' *J. Soil Mech. Found. Div.*, 88(SM6), 207–231.

Walker, L. K., and Raymond, G. P. (1968). ''The prediction of consolidation rates in a cemented clay.'' *Can. Geotech. J.*, 5(4), 192–216.

Wissa, A. E. Z., Christian, J. T., Davis, E. H., and Heiberg, S. (1971). ''Consolidation at constant rate of strain.'' *J. Soil Mech. Found. Div.*, 97(10), 1393–1413.

Yamamuro, J. A., Bopp, P. A., and Lade, P. V. (1996). ''One-dimensional compression of sands at high pressures.'' *J. Geotech. Eng.*, 122(2), 147–154.

Yamamuro, J. A., and Lade, P. V. (1993). ''Effects of strain rate on instability of granular soils.'' *Geotechn. Testing J. GTJODJ*, 16(3), 304–313.

Yin, J. H. (1999). ''Nonlinear creep of soils in oedometer tests.'' *Geotechnique*, 49(2), 699–707.

Zhu, J. G., Yin, J. H., and Luk, S. T. (1999). ''Time-dependent stress-strain behavior of soft Hong Kong marine deposits.'' *Geotechn. Testing J. GTJODJ*, 22(2), 112–120.

Title:

Characterization of Models for Time-Dependent Behavior of Soils.

Authors:

Liingaard, M., Augustesen, A. and Lade, P.V.

Year of publication:

2004

Published in:

International Journal of Geomechanics, 4(3), pp.157-177.

Remarks:

Characterization of Models for Time-Dependent Behavior of Soils

Morten Liingaard[1]; Anders Augustesen[2]; and Poul V. Lade, M.ASCE[3]

Abstract: Different classes of constitutive models have been developed to capture the time-dependent viscous phenomena (creep, stress relaxation, and rate effects) observed in soils. Models based on empirical, rheological, and general stress-strain-time concepts have been studied. The first part is a review of the empirical relations, which apply only to problems of specific boundary conditions and frequently involve natural time alone. The second part deals with different rheological models used for describing the viscous effects in the field of solid mechanics. The rheological models are typically developed for metals and steel but are, to some extent, used to characterize time effects in geomaterials. The third part is a review of constitutive laws that describe not only viscous effects but also the inviscid (rate-independent) behavior of soils, in principle, under any possible loading condition. Special attention is paid to elastoviscoplastic models that combine inviscid elastic and time-dependent plastic behavior. Various general elastoviscoplastic models can roughly be divided into two categories: Models based on the concept of overstress and models based on nonstationary flow surface theory. Although general in structure, both have shortcomings when used for modeling of soils.

DOI: 10.1061/(ASCE)1532-3641(2004)4:3(157)

CE Database subject headings: Clays; Sand; Time dependence; Soil properties; Constitutive models.

Introduction

To obtain realistic solutions for time-dependent engineering problems, it is essential to use a constitutive model that account for time dependency of the stress–strain–strength properties of soils. A great number of constitutive models have been proposed in literature. The main purpose of this paper is to present a concise review, which categorizes and describes the basic features of existing models as well as their advantages and limitations. The different models are classified in an attempt to clarify the disorder and confusion, which occur in literature. ''Time'' and time dependency are assumed to be related to viscous effects in the soil skeleton, such as creep, stress relaxation, and strain-rate effects. Therefore, the process of consolidation is not regarded as a true time effect. Furthermore, time, in connection with dynamic effects where inertial forces are involved, is not treated. In this paper, the following categories are considered:

- Empirical models are mainly obtained by fitting experimental results from creep, stress relaxation, and constant rate of strain tests, and the constitutive relations are generally given by closed-form solutions or differential equations. In addition, they are strictly limited to specific boundary and loading conditions. That is, the relations are not general. The models may be used as a base for developing three-dimensional constitutive relations.
- Rheological models describe uniaxial conditions and they are given as closed-form solutions or in a differential form. Often, they are used to obtain a conceptual understanding of time effects in soil.
- General stress–strain–time models are, in principle, three-dimensional models. Furthermore, they are often given in incremental form. Therefore, they are readily adaptable to numerical implementation suitable for a finite element procedure. The models are not limited to the boundary conditions from which they are calibrated, i.e., in principle, all possible stress paths can be simulated.

In connection with the description of the above-mentioned categories of models, the following assumptions have been made: (1) The descriptions are restricted to models that concern the macromechanical properties. Models, which use terms such as stress, time, and strain, are described whereas models based on the concept of micromechanics are omitted. (2) Emphasis is placed on the description of the overall structure of the three groups, i.e., no details on specific models are presented. Furthermore, focus is placed on the comparison of the different groups of models. The observed time-dependent behavior of soils to be modeled was reviewed by Augustesen et al. (2004).

Empirical Models

Empirical constitutive relations apply only to problems of specific boundary conditions (e.g., one specific model for creep and another for relaxation) and frequently involve natural time. On the other hand, these models are quite useful in several ways. They often reflect the real behavior of the soils, and, in spite of their limited applicability and sometimes theoretical inconsistency, they provide a basis for developing more sophisticated constitu-

[1]Graduate Student, Dept. of Civil Engineering, Aalborg Univ., Sohngaardsholmsvej 57, 9000 Aalborg, Denmark.

[2]Graduate Student, Dept. of Civil Engineering, Aalborg Univ., Sohngaardsholmsvej 57, 9000 Aalborg, Denmark.

[3]Professor, Dept. of Civil Engineering, Catholic Univ. of America, Washington, D.C. 20064 (corresponding author). E-mail: lade@cua.edu

Note. Discussion open until February 1, 2005. Separate discussions must be submitted for individual papers. To extend the closing date by one month, a written request must be filed with the ASCE Managing Editor. The manuscript for this paper was submitted for review and possible publication on October 24, 2003; approved on November 5, 2003. This paper is part of the ***International Journal of Geomechanics***, Vol. 4, No. 3, September 1, 2004. ©ASCE, ISSN 1532-3641/2004/3-157–177/$18.00.

tive models. They may also provide practical solutions to engineering problems, as far as the boundary conditions comply with the laboratory experiments. The empirical models are categorized as follows:

- "Primary" empirical relations are obtained by directly fitting the observed test data with simple mathematical functions. They reflect actual observed soil behavior and are often restricted to specific phenomena, such as relations for predicting creep and others for predicting relaxation (Yin 1999).
- "Secondary" semiempirical models are classified as models obtained by combining one or more of the primary models. The models can to some extent be used as stress–strain–time or stress–strain–strain-rate models that yield solutions for creep as well as relaxation within one particular model. These models are recognized as closed-form solutions for the different phenomena, such as creep and relaxation, contrary to the elastic/viscoplastic models reviewed herein, which are presented as rate formulations in incremental form.

Empirical Primary Relations

The empirical models described below are: (1) The semilogarithmic law for creep, (2) Singh and Mitchell's creep model, (3) Lacerda and Houston's relaxation model, (4) Prevost's model, and (5) Strain-rate approach.

Semilogarithmic Creep Law

Numerous investigations have shown that it is convenient to plot the secondary compression observed in oedometer tests against the logarithm of time. The coefficient of secondary compression is used to describe the magnitude the creep strains. This coefficient can be defined in different ways, see Augustesen et al. (2004):

$$C_{\alpha e}=\frac{\Delta e}{\Delta \log(t)}$$

or

$$C_{\alpha\varepsilon}=\frac{\Delta e}{(1+e_i)\cdot\Delta \log(t)}=\frac{\varepsilon_z}{\Delta \log(t)}=\frac{C_{\alpha e}}{1+e_i} \tag{1}$$

in which e_i = initial void ratio; t = time; and $C_{\alpha e}$ and $C_{\alpha\varepsilon}$ = coefficient of secondary compression with respect to e and ε. In the simplest form, the coefficient of secondary compression is assumed constant for one specific soil. This is an oversimplification of the volumetric confined creep of any soil. Several studies of the factors influencing $C_{\alpha\varepsilon}$ have shown that the vertical effective stress in oedometer tests σ_z', time t, and other factors affect the secondary compression. Within the framework of the logarithmic law there are three concepts: (1) The concept of constant C_α, (2) the concept of constant C_α/C_c, and (3) the concept by Yin (1999) where C_α is a function of time.

Concept of Constant C_α. The simplest approach in the framework of the logarithmic law is the assumption that C_α is constant for a given soil. If this is evaluated in terms of vertical creep strains, the increase in secondary compression for a given soil can be written as

$$\varepsilon_z=C_{\alpha\varepsilon}\log\left(1+\frac{t}{t_i}\right) \tag{2}$$

where ε_z = vertical strain; t = time; and t_i = some reference time. One of the major difficulties when using the logarithmic relation in Eq. (2) is deciding when the creep deformation starts, i.e., determining the reference time t_i. The discussion of the problem of reference time is left out, but see Augustesen et al. (2004) for further details.

The model in Eq. (2) is only able to describe the behavior of primary creep (Augustesen et al. 2004), because the logarithmic function predicts a gradual continuous reduction in the rate of compression. The assumption of $C_{\alpha\varepsilon}$ = constant for one specific soil is too simple, in general, but if only the normally consolidated range is considered, then the approach may be acceptable. The variation of $C_{\alpha\varepsilon}$ with the effective stress decreases considerably when the effective stress state is above the preconsolidation pressure, see Mesri (1973).

Concept of Constant C_α/C_c. Walker and Raymond (1968) reported that the secondary compression rates in laboratory tests on sensitive Leda Clay appeared to be linearly dependent on the compression index C_c over the entire effective stress range, with an average value of C_α/C_c of about 0.025. The compression index is defined as

$$C_{ce}=\frac{\Delta e}{\Delta \log(\sigma_z')} \quad \text{or} \quad C_{c\varepsilon}=\frac{C_{ce}}{1+e_i} \tag{3}$$

in which e_i = initial void ratio; σ_z' = vertical effective stress, and C_{ce} and $C_{c\varepsilon}$ = compression indices with respect to e and ε, respectively.

Mesri (1973) concluded that soils that are highly compressible in the primary phase would show high compressibility in the secondary phase as well. This led to extensive studies of the relationship between C_α and C_c. Mesri and Godlewski (1977) found that C_α is dependent on the applied effective stress σ_z' and is related to the preconsolidation pressure. It was shown that both C_c and C_α increase as the effective stress approaches the preconsolidation pressure, then reach a maximum at or just beyond the preconsolidation, and then remain reasonably constant. Throughout these effective stress changes, the ratio C_α/C_c remains approximately constant. Combining the logarithmic law with the concept of constant C_α/C_c, Eq. (2) can be written as

$$\varepsilon_z=\frac{1}{m'}C_{c\varepsilon}\log\left(1+\frac{t}{t_i}\right), \quad m'=\frac{C_{c\varepsilon}}{C_{\alpha\varepsilon}} \tag{4}$$

where $C_{c\varepsilon}$ = compression index with respect to ε_z corresponding to the stress state for which the value of $C_{\alpha\varepsilon}$ has been determined; and m' = rate parameter that defines the unique relationship between compression and secondary compression. The main advantage of Eq. (4) compared with Eq. (2) is that the influence of the vertical effective stress σ_z' is taken into account by $C_{c\varepsilon}$.

Concept by Yin. Several authors, including Mesri and Godlewski (1977), questioned the uniqueness of the "C_α/C_c = constant" concept in which C_α and C_c are assumed to be time independent. In general, C_α does not remain constant with time. A concept where the creep parameter varies with time has been presented by Yin (1999). The motivation is that the logarithmic law has a limitation that may cause a serious error in the estimation of long-term settlement. The limitation is that when time tends toward infinity, the strains tend toward infinity as well. Thus, the logarithmic law may overestimate the long-term creep settlements. Yin (1999) presented a new creep function that is capable of describing the nonlinear creep behavior as a function of time, all within the framework of the logarithmic law:

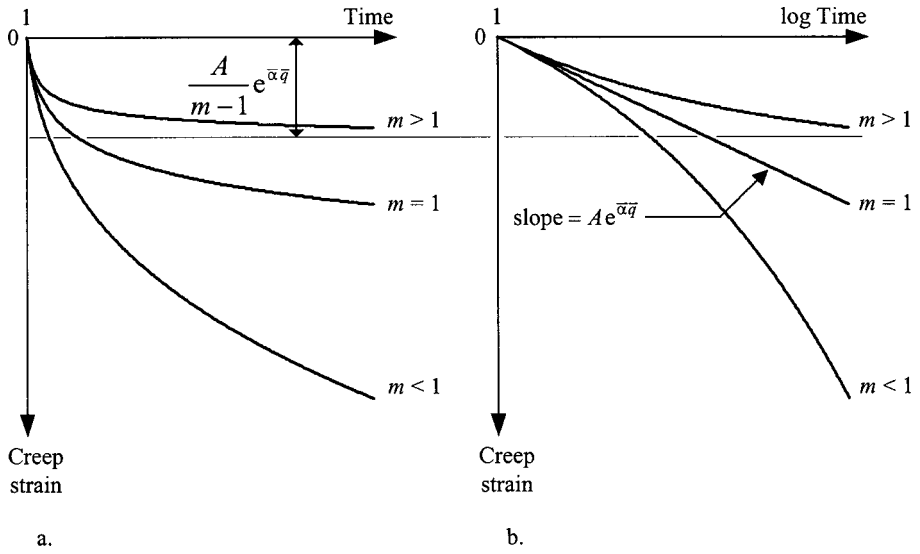

Fig. 1. Creep curves predicted by the stress–strain–time functions for $m=1$, $m<1$, and $m>1$ for $t_i=1$: (a) Strain versus time and (b) strain versus logarithm of time

$$\varepsilon_z = \frac{\Psi}{\nu}\ln\left(\frac{t+t_0}{t_0}\right) \tag{5}$$

where ψ/ν is identified as

$$\frac{\psi}{\nu} = \frac{\psi_0'}{1+(\psi_0'/\varepsilon_\infty)\ln[(t+t_0)/t_0]} \tag{6}$$

where $\nu = 1+e =$ specific volume. If the ratio ψ/ν is a constant, then Eq. (5) simplifies to the traditional logarithmic law. The ratio ψ/ν is then equal to $C_{\alpha\varepsilon}/\ln(10)$, but in this case, ψ/ν is no longer a constant but decreases with time and is likely to be dependent on time, which can be seen from Eq. (6). When the time t is infinite, the creep strain $\varepsilon_z = \varepsilon_\infty$. Thus, ε_∞ is the limiting strain and it is a model parameter like t_0 and ψ_0.

Discussion. One of the basic limitations of the logarithmic law is that it is strictly valid only for conditions that are identical to those of the test from which they have been derived, i.e., one-dimensional conditions. In the above expressions, the strains vary with logarithm of time. That is, the soil hardens with time. This implies that any application of the expressions requires the definition of an origin for the time scale. To overcome the difficulties of defining the time origin, Suklje (1957) introduced the strain-rate approach.

Singh and Mitchell's Creep Model

Based on the analysis of drained and undrained triaxial creep tests on various of clays, Singh and Mitchell (1968) suggested that a simple three-parameter phenomenological equation may be used to describe the strain-rate–time relation of clayey soils when subjected to constant stress. The model describes the creep behavior of clayey soils over the range of engineering interest, that is stresses from about 30% to as high as 90% or more of the initial strength. In this domain, the writers observed a general relationship between the logarithm of the axial strain rate and the logarithm of time, irrespective of whether the strain versus logarithm of time is linear or nonlinear:

$$\dot{\varepsilon}_1 = A\exp(\overline{\alpha q})\left(\frac{t_i}{t}\right)^m \tag{7}$$

where $\overline{\alpha} = \alpha q_{\max}$ and $\overline{q} = q/q_{\max}$. The parameter $A =$ soil property that reflects composition, structure, and stress history, α indicates the stress intensity effect on the creep rate, and the m parameter controls the rate at which the axial strain rate decreases with time. The three parameters A, α, and m can be determined by a few ordinary creep tests for any given soil, see Singh and Mitchell (1968). $\overline{q}$ is the deviator stress level expressed as the ratio of the creep stress q with respect to the strength $q_{\max}$ at the beginning of the creep process.

Integration of the creep rate function in Eq. (7) produces a general relationship between time, and axial strain may be obtained. Integration yields two solutions, one for m equal to 1 and one for m different from 1. When $m=1$, the integration yields a solution where the axial strain varies linearly with logarithm of time. In the more general case where $m \neq 1$, there is a nonlinear relationship between the axial strain and the logarithm of time. Then, the axial creep is described by a power function. The creep curves for $m=1$ and $m \neq 1$ are shown in Fig. 1.

Discussion. The Singh and Mitchell model is capable of describing either fading creep or nonfading creep. Whether the creep is fading (the strains have an asymptotic value) or nonfading (strains increase to infinity as time tend towards infinity) depends on the value of the m parameter, see Fig. 1. The values of m generally fall in the range of 0.7 to 1.3 for geomaterials, see Augustesen et al. (2004). The model has the following limitations: (1) The model describes the creep behavior at a constant level of stress in one-dimensional conditions. Furthermore, the model is only valid for first time loading, (2) for a particular soil, m is assumed to be constant. Other creep curves at different stress levels may involve different values of m for the same soil.

Lacerda and Houston's Relaxation Model

The purpose of the study of Lacerda and Houston (1973) was to correlate the parameters describing stress relaxation behavior with

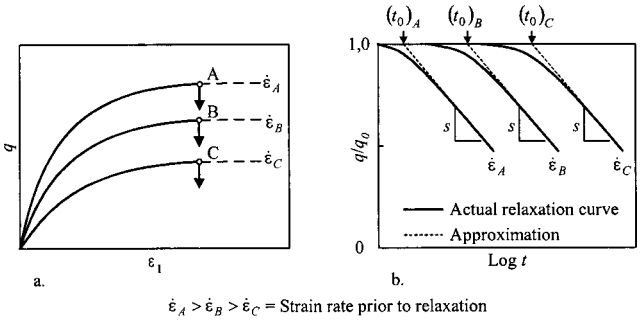

Fig. 2. (a) Stress–strain curves for different strain rates. Relaxation starts at point A, B and C. (b) Stress relaxation curves for varying strain rates prior to relaxation. The actual curves are solid and the approximations are dotted straight lines. The parameters s, t_0 are shown (after Lacerda and Houston 1973).

creep parameters obtained in traditional creep tests on clay and sand. To describe the relationship between stress relaxation and creep parameters, the three-parameter creep equation of Singh and Mitchell (1968) given in Eq. (7), was applied. Lacerda and Houston (1973) showed that when a relaxation test is started after straining a soil under constant strain rate up to a deviatoric stress q_0, a decrease of the deviatoric stress q is observed with time. The decrease varies linearly with the logarithm of time after an initial time period t_0 has been exceeded

$$\frac{q}{q_0}=\frac{\overline{q}}{\overline{q_0}}=1-s\log\left(\frac{t}{t_0}\right), \quad \text{for } t>t_0 \tag{8}$$

where $\overline{q}$=deviator stress level; $\overline{q_0}$=deviator stress level at time t_0; t=time since beginning of relaxation; t_0=initial time period at the beginning of relaxation; and s=slope of the relaxation curve in a $q/q_0-\log(t)$ diagram shown in Fig. 2(b). The slope s is related to the parameters $\overline{\alpha}$ and m of Eq. (7) in the following way:

$$s=\frac{\Phi}{\overline{q_0}} \text{ where } \Phi=\frac{2{,}3(1-m)}{\overline{\alpha}} \tag{9}$$

It should be noted that Eq. (9) is established for $m<1.0$, which corresponds to the case of nonfading creep, see Fig. 1. Eqs. (8) and (9) are derived by inverting the creep equation Eq. (7), as shown by Lacerda and Houston (1973).

Eq. (8) is an approximation to the actual stress relaxation behavior of a soil and describes the phenomenon by a straight line in a $q/q_0-\log(t)$ by two parameters, namely s and t_0. The time t_0 at the beginning of stress relaxation is also termed the ''delay time,'' since the stresses may not begin to relax immediately after the strain rate $\dot{\varepsilon}_1$ is reduced to zero. The time t_0 is a variable that depends on soil type and strain rate, as illustrated in Fig. 2.

Discussion. The model is limited to prediction for one-dimensional conditions. This is due to the fact that the expression in Eq. (8) is derived from the uniaxial Singh and Mitchell model. It should be noted that the work of Lacerda and Houston (1973) is based on results obtained in undrained stress relaxation tests. Furthermore, Lacerda and Houston (1973) observed that the variation of excess pore pressure during the undrained stress relaxation tests was practically zero. Murayama and Shibata (1961) also reported similar observations for clay.

The expression in Eq. (8) predicts a nonfading stress relaxation behavior because the logarithmic function tends toward infinity with the time t. This means the model is limited in application to a finite value of time t.

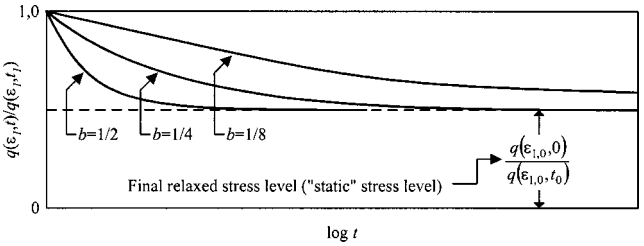

Fig. 3. Deviatoric stress level versus the logarithm of time during stress relaxation. Eq. (10) is plotted for different values of the parameter b (after Prevost 1976).

Prevost's Relaxation Model

Prevost (1976) developed a phenomenological approach to describe saturated clays under undrained triaxial conditions. In the case of stress relaxation where the initial state prior to stress relaxation is reached by shearing at a constant rate of strain, the relationship proposed is

$$q(\varepsilon_{1,0},t)=q(\varepsilon_{1,0},t_0)-[q(\varepsilon_{1,0},t_0)-q(\varepsilon_{1,0},0)]\tanh\left[b\ln\left(\frac{t}{t_0}\right)\right] \tag{10}$$

where $q(\varepsilon_{1,0},t)$=deviatoric stress acting at a fixed axial strain $\varepsilon_{1,0}$ and time $t>t_0$. $q(\varepsilon_{1,0},t_0)$=deviatoric stress acting at the beginning of stress relaxation and reached by shearing with a constant rate of strain $\dot{\varepsilon}_1=a$ (a is constant) up to a strain level $\varepsilon_{1,0}$ in a time t_0, that is $\varepsilon_{1,0}=at_0$. $q(\varepsilon_{1,0},0)$=deviatoric stress at a strain $\varepsilon_{1,0}$ in a ''static'' undrained test ($\dot{\varepsilon}_1$ close to zero). b =experimental constant. t_0=time at which relaxation starts. Therefore, the input parameters are a, t_0, t_1, b, $q(\varepsilon_{1,0},0)$, $q(\varepsilon_{1,0},t_0)$ and the contours of Eq. (10) are illustrated in Fig. 3.

Discussion. The Prevost model is also restricted to one-dimensional conditions, and it is capable of describing nonlinear stress relaxation relations in q-log(t) space. This is in contrast to the model of Lacerda and Houston (1973), in which the stress relaxation relation in q-log(t) space is linear, see Eq. (8) and Fig. 2. Another distinction is that the Prevost model operates with a final relaxed state of deviator stress (or static state of stress) when the time tends toward infinity. This relaxed state is given by $q(\varepsilon_{1,0},0)/q(\varepsilon_{1,0},t_0)$, and this is therefore an input parameter to the model, see Fig. 3. In contrast, the deviator stress level never reaches any final level of stress in the model of Lacerda and Houston (1973), see Fig. 2.

The expression in Eq. (10) was successfully applied by Silvestri et al. (1988) for interpreting the results of undrained stress relaxations tests on a soft sensitive clay.

Strain Rate Approach

This approach is based on the existence of a unique relationship between the current state of stress σ_z' and strain (ε_z or e) for a given constant strain rate ($\dot{\varepsilon}_z$ or $\dot{e}$), irrespective of the previous stress–strain–time history. Such behavior is in agreement with the findings presented by Vaid and Campanella (1977).

Concept of Model. The original model proposed by Sukjle (1957) has been investigated in detail by Leroueil et al. (1985), who confirmed it by multiple stage loading tests, constant rate of strain tests, controlled hydraulic gradient tests, and long-term creep tests. Based on experimental investigations of various types of clays, they reported that the effective stress rate $\dot{\sigma}_z$ had no

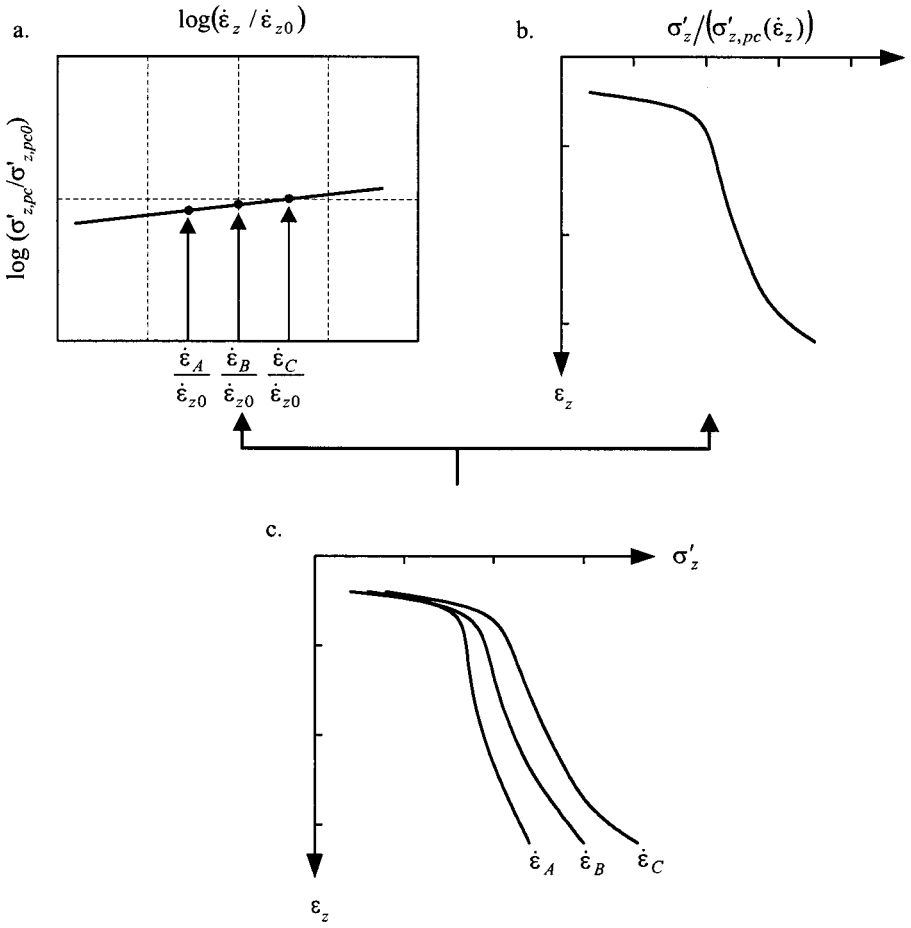

Fig. 4. Stress–strain–strain-rate relationship for the strain rate approach: (a) Normalized variation of the preconsolidation pressure with the strain rate, Eq. (14); (b) normalized effective stress–strain relation, Eq. (12); and (c) experimental curves obtained at different strain rates (after Leroueil et al. 1985)

significant influence on the rheological behavior of clays. This is the reason why $\dot{\sigma}_z$ is abandoned in the unique relationship. They suggested that the $(\sigma'_z, \varepsilon_z, \dot{\varepsilon}_z)$ relationship could be described completely by two equations, one giving the variation of the preconsolidation pressure with the strain rate

$$\sigma'_{z,pc} = f(\dot{\varepsilon}_z) \tag{11}$$

and the other presenting the normalized effective stress–strain relation:

$$\frac{\sigma'_z}{\sigma'_{z,pc}} = g(\varepsilon_z) \tag{12}$$

Once the two relationships are known for a given soil, any stress–strain–strain rate relationship for the soil may easily be reconstructed.

The relations indicated by Eqs. (11) and (12) are sketched in Fig. 4. The normalized stress–strain curve represents the reaction of the structure of the clay and it usually varies from clay to clay. The curve in Fig. 4(a) shows the capability of the clay to creep. Leroueil et al. (1985) do not recommend any closed-form expressions for f and g in Eqs. (11) and (12), but by combining Eqs. (11) and (12) the general form of any solution should be given by the following relation:

$$\dot{\varepsilon}_z = f^{-1}\left(\frac{\sigma'_z}{g(\varepsilon_z)}\right) \tag{13}$$

Discussion. The model proposed by Leroueil et al. (1985), given by Eqs. (11) and (12), has been established on the basis of tests in which the strains were always increasing, and it has been proven valid only under such conditions. It should not be used when the clay rebounds during unloading stages or relaxes under constant strain. In relaxation tests, the strain is constant, the strain rate is thus equal to zero and, for such conditions, the uniqueness of an effective stress–strain–strain rate relationship implies a constant effective stress. However, it is well known that the effective stress decreases during relaxation. This shortcoming is due to the fact that the concept was developed with respect to total strains. To capture the relaxation phenomenon, the model should be decomposed into elastic and plastic components. Another limitation is that the concept is developed mainly from observations in the normally consolidated range, which gives poor predictions in the heavily overconsolidated range where the elastic strains are relatively significant.

One of the features of the model is that the viscous properties of the clay are directly related to the primary deformation properties. This is realized when Eq. (11) is approximated by a linear relation in a log–log diagram Leroueil and Marques (1996):

$$\log\frac{\sigma'_{z,pc}}{\sigma'_{z,pc0}} = A + \frac{1}{m'}\log\frac{\dot{\varepsilon}_z}{\dot{\varepsilon}_{z0}} \tag{14}$$

where A and m' = constants. $\sigma'_{z,pc0}$ and $\dot{\varepsilon}_{z0}$ = reference values.

Leroueil and Marques (1996) showed that the relation in Eq. (14) holds for numerous inorganic clays and that the corresponding m' value is related to C_α/C_c as follows:

$$\frac{1}{m'}=\frac{C_c}{C_\alpha} \tag{15}$$

This implies that the concept of C_α/C_c = constant and the strain-rate approach are equivalent when describing the viscous behavior during secondary consolidation.

Discussion of Primary Empirical Relations

The empirical relations for soils are heavily influenced by the classical understanding of the rheology of materials. That is, creep, relaxation, and rate dependency are considered to be due to the same basic mechanism, which according to Sheahan and Kaliakin (1999) is denoted, the ''correspondence principle.'' The principle states that one of the phenomena, relaxation, for instance, can be derived from the observed creep behavior and vice versa. The following indicates the validity of the correspondence principle: (1) There are no stand-alone models for relaxation. The model by Lacerda and Houston (1973) is actually based on a creep law adopted a priori, and (2) the parameter m' obtained from constant rate of strain tests is assumed to be equal to the ratio C_c/C_α where C_α is obtained from creep tests.

The fundamental distinction between the primary models is whether they are time or strain hardening. The time-hardening models are characterized by relations in which time t enters as the hardening parameter, whereas the strain-hardening models include the strain as the hardening parameter. The time-hardening relations can be written as

$$\varepsilon^c=f(\sigma)g(t) \quad \text{or} \quad \dot{\varepsilon}^c=f(\sigma)g(t) \tag{16}$$

where ε^c = creep strain; $\dot{\varepsilon}^c$ = creep strain rate; and f and g = functions of stress and time, respectively. Both of the equations in Eq. (16) incorporate time as hardening parameter, but the equation to the right in Eq. (16) is usually referred to as the ''time-hardening model'' whereas the equation to the left is denoted the ''total strain model.'' This is further discussed in the section entitled ''Rheological Models.'' According to Eq. (16), the logarithmic law and the model by Singh and Mitchell (1968) can be categorized as time-hardening models.

The functional relation for a strain-hardening model can be written as

$$\dot{\varepsilon}^c=f(\sigma)g(\varepsilon^c) \tag{17}$$

where ε^c = creep strain; $\dot{\varepsilon}^c$ = creep strain rate; and f and g = functions of stress and creep strain, respectively. It is recognized that the general form of the strain-rate approach, that gives a unique relation between the stress, strain, and strain rate, is equivalent to the functional expression for a strain-hardening model.

Semiempirical Secondary Relations

The semiempirical models explained below are: (1) Kavazanjian and Mitchell's approach, (2) Tavenas' approach, (3) Bjerrum's model, and (4) Yin and Graham's model.

Kavazanjian and Mitchell' Approach

One of the first attempts to develop a multiaxial stress–strain–time constitutive relationship was proposed by Kavazanjian and Mitchell (1977). They presented a model for the general stress–strain–time behavior of fine-grained soils, formulated on the basis of separate volumetric and deviatoric components. The volumetric and deviatoric models are assumed to have an instantaneous and delayed component of the strains.

The volumetric part is based on the logarithmic law for secondary compression with the assumption that $C_{\alpha\varepsilon}$ is approximately constant under normally consolidated conditions, see the subsection entitled ''Empirical Primary Relations.'' Thus, the delayed volumetric component can be written as

$$\dot{\varepsilon}_v\cong\frac{C_{\alpha\varepsilon}}{\ln(10)}\frac{1}{t} \tag{18}$$

where $\dot{\varepsilon}_v$ = delayed volumetric strain rate; and $C_{\alpha\varepsilon}$ = coefficient of secondary consolidation. The deviatoric model is based on Singh and Mitchell's model, described in the subsection entitled ''Empirical Primary Relations'' as well. When the axial strain rate in Eq. (7) is taken as the strain rate along the first principal axis, Eq. (7) can be written as

$$\dot{\varepsilon}_1=A\exp(\overline{\alpha q})\left(\frac{t_i}{t}\right)^m \tag{19}$$

The deviatoric strain rates can be calculated indirectly from the axial strains in triaxial conditions Tavenas et al. (1978):

$$\dot{\varepsilon}_q=\dot{\varepsilon}_1-\dot{\varepsilon}_v/3 \tag{20}$$

where $\dot{\varepsilon}_v$ and $\dot{\varepsilon}_1$ are given by Eqs. (18) and (19), respectively. The combination of shear and volumetric creep rates has also been proposed by Poulos et al. (1976). It is noteworthy that the work of Kavazanjian and Mitchell (1977) has been developed into a general viscoplastic model, see the section entitled ''General Stress–Strain–Time Models'' for references.

Tavenas' Approach

Tavenas et al. (1978) also divided creep deformations into volumetric and deviatoric components. Based on test results of creep behavior of lightly overconsolidated clay, they concluded that the development with time of both volumetric and shear strains can be represented by the phenomenological Eq. (7):

$$\dot{\varepsilon}_v=Bf(\sigma'_{ij})\left(\frac{t_i}{t}\right)^m \tag{21}$$

$$\dot{\varepsilon}_q=Ag(\sigma'_{ij})\left(\frac{t_i}{t}\right)^m \tag{22}$$

where $f(\sigma'_{ij})$ and $g(\sigma'_{ij})$ = functions of the current state of effective stress σ'_{ij}; the parameters A and B = soil properties that reflect composition, structure, and stress history; and m = parameter that controls the rate at which the strain rates decrease with time. Based on the shapes of the contour lines for equal strain rates at $t=100$ min, Tavenas et al. (1978) suggested that the stress functions $f(\sigma'_{ij})$ and $g(\sigma'_{ij})$ should be expressed in terms of the limit state surface, also denoted yield surface.

To put this in perspective, Sekiguchi (1985) indicated that the ratio between the volumetric and the deviatoric creep rates might be a function of the current stress state σ'_{ij} only. With respect to Eqs. (21) and (22) this can be written as

$$\frac{\dot{\varepsilon}_v}{\dot{\varepsilon}_q}=\frac{f(\sigma'_{ij})}{g(\sigma'_{ij})}=h(\sigma'_{ij}) \tag{23}$$

in which $h(\sigma'_{ij})$ is a material function. Eq. (23) is actually a flow rule for creep deformation. According to Eq. (23), the volumetric strains plotted against the deviatoric strains during a creep test should form a straight line, irrespective of the time elapsed. How-

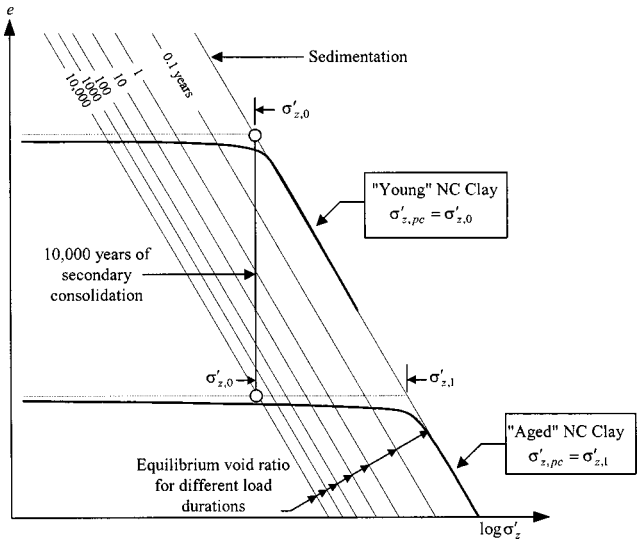

Fig. 5. Geological history and compressibility of a young and an aged normally consolidated clay (after Bjerrum 1973).

ever, Eq. (23) is only valid if the value of m for deviatoric creep coincides with the m value for volumetric creep, which is not likely to be the general pattern. This has been studied recently by several investigators (Feda 1992; Lade and Liu 1998; Tatsuoka et al. 2000). Nevertheless, the flow rule in Eq. (23) has been used extensively in the viscoplastic constitutive models described in the section entitled ''General Stress–Strain–Time Models.''

Bjerrum's Model

Bjerrum presented a concept for settlement analysis of normally and lightly overconsolidated clay that included the logarithmic law. The concept is often denoted Bjerrum's model or Bjerrum's theory of time dependent compression.

Definition of Time Lines. Buisman (1936) first formulated the effects of time on the compressibility of clay in terms of secondary compression. Later, Taylor (1942) reported that, as a result of the secondary compression, there is not a single stress–strain curve for one-dimensional compression of clay, but a family of curves, called ''time lines,'' each curve corresponding to a different duration of the applied load in a standard oedometer test. One of the characteristics of the time lines is that the magnitude of the preconsolidation pressure $\sigma'_{z,\mathrm{pc}}$ is different for each line. Bjerrum (1967) confirmed the observations by Taylor (1942), and proposed that the delayed compression could be described by parallel lines in an $e-\log \sigma'_z$ diagram representing a series of equilibrium relationships after different time periods of sustained loading. Bjerrum's and Taylor's definition of the time lines is:

> ''Time lines are lines of constant duration of loading. They may be determined as a 1-day time line by applied stress increments at intervals of 24 h, or by interpretation of other loading intervals in classical oedometer tests.''

Concept of Bjerrum's Model. Bjerrum's model is illustrated in Fig. 5 for ''young'' and ''aged'' normally consolidated (NC) clays. Young NC clays are recently deposited and at equilibrium under their own weight but have not experienced delayed compression, whereas aged NC clays have undergone significant delayed compression at constant effective stress.

The two bold curves in Fig. 5 correspond to the compression of undisturbed specimens of young and aged NC clays when subjected to uniaxial consolidation. The young NC clay would follow the upper curve and the preconsolidation pressure $\sigma'_{z,\mathrm{pc}}=\sigma'_{z,0}$ is equal to the present vertical effective stress. If the young NC clay is left intact for, e.g., several thousand years, it will continue to compress with time under constant effective stress, which is denoted delayed compression. This aged NC clay will follow the lower curve and the measured preconsolidation pressure has increased to $\sigma'_{z,\mathrm{pc}}=\sigma'_{z,1}$. This means that the reduction in the void ratio that occurs during delayed compression leads to a more stable clay structure and therefore a higher preconsolidation pressure. This is seen when stresses are again increased after a period of delayed compression at constant effective stresses. This accounts for the small amounts of overconsolidation found in natural clays that have never experienced the usual causes of overconsolidation (erosion of overlying layers, melting of ice in glaciers, groundwater level changes, weathering, and cementation).

Model Formulation. Garlanger (1972) has modeled the characteristics of Bjerrum's concept in terms of the well-known recompression, compression, and secondary compression indices C_{re}, C_{ce}, and $C_{\alpha e}$, respectively. The model was formulated in terms of logarithmic functions:

$$e=e_0-e^e-e^{ep}-e^c \Rightarrow e=e_0-C_{re}\log\frac{\sigma'_{z,pc}}{\sigma'_{z,0}} - C_{ce}\log\frac{\sigma'_z}{\sigma'_{z,\mathrm{pc}}}-C_{\alpha e}\log\frac{t_i+t}{t_i} \tag{24}$$

where e = void ratio; e_0 = initial void ratio; $\sigma'_{z,\mathrm{pc}}$ = vertical preconsolidation stress; $\sigma'_{z,0}$ = initial vertical effective in situ stress; σ'_z = current vertical effective stress; t_i = reference time; and t = elapsed time. The superscript e, ep, and c denote elastic, elastic–plastic, and creep, respectively. Eq. (24) is based on the assumption that the change in void ratio $\Delta e=e-e_0$ in a soil element is composed of three components; one, (e^e) due to elastic change; the second, (e^{ep}) due to time-independent elastic–plastic reaction of the soil skeleton to effective stress changes; and the third, (e^c) due to time-dependent change at constant effective stress.

Age Dependency. One of the key features of Bjerrum's model is that the observed overconsolidation of aged normally consolidated natural clays is taken into account. A relation for the amount of overconsolidation due to aging can be derived by means of Eq. (24).

The principle in determining the age dependency is illustrated in Fig. 6. The initial condition is a young NC clay defined by an initial void ratio e_0, an initial age t_0 and an initial stress state $\sigma'_{z,0}$ (equal to the preconsolidation pressure). The result is an aged NC clay defined by e_t and $\sigma'_{z,t}$ for a given time t of aging. The idea is to determine the magnitude of $\sigma'_{z,t}$ as a function of the time of aging. The relation is obtained by equating the expressions for path AA' and ABA', shown in Fig. 6, and solving with respect to the stress ratio. The relation for age dependency is then given by

$$\frac{\sigma'_{z,t}}{\sigma'_{z,0}}=\left(\frac{t}{t_0}\right)^{C_{\alpha e}/(C_{ce}-C_{re})} \tag{25}$$

The ratio $C_{\alpha e}/(C_{ce}-C_{re})$ is similar to the parameter m'. The

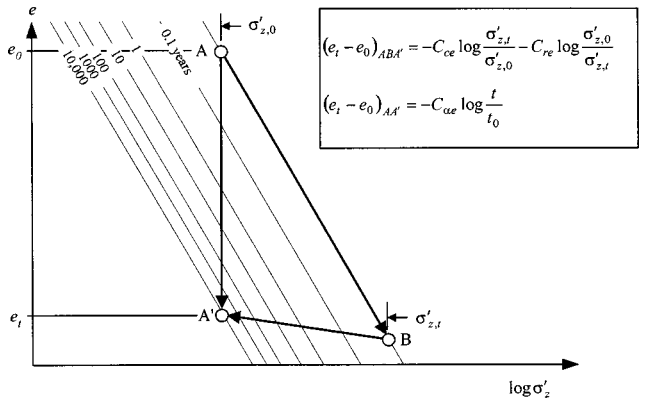

Fig. 6. Visualization of the solution for age dependency. The amount of compression from A to A′ can be determined by pure creep at a constant effective stress (line AA′) or by instant plastic loading from A to B followed by unloading from B to A′. The equations for AA′ and ABA′ are shown in the upper right corner.

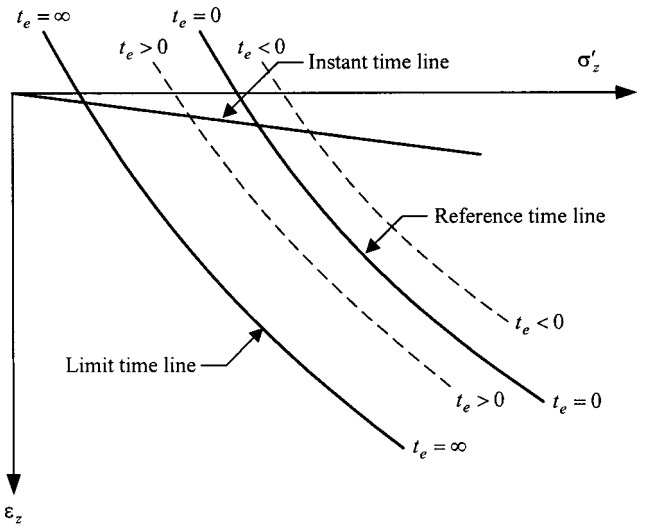

Fig. 7. Illustration of instant time line, reference time line, limit time line, and time lines for positive and negative equivalent times

only exception is that m' is defined as $C_{\alpha e}/C_{ce}$ without taking C_{re} into account. It is noteworthy that Eq. (25) is similar in structure to the relation in Eq. (14) except for the fact that Eq. (14) is based on findings from strain-rate tests where the strain-rate $\dot{\varepsilon}_z$ is involved instead of the time t.

Yin and Graham's Model

Yin and Graham (1989a,b, 1994) developed a series of models describing one-dimensional time-dependent behavior of clays. Additional studies were presented Yin et al. (1994) and Yin and Graham (1996) in which coupled equations for pore–water dissipation were developed. The concepts of Yin and Graham represent further developments of: (1) Bjerrum's model described above and (2) the strain rate approach described in the subsection entitled ''Empirical Primary Relations.''

An important new concept in the work of Yin and Graham is the concept of ''equivalent time,'' which is used to model creep behavior of normally consolidated and overconsolidated clays as a function of σ'_z, σ'_z, ε_z, and $\dot{\varepsilon}_z$. This allows clay behavior to be predicted in a variety of test conditions, e.g., relaxation tests, tests with constant rate of strain or constant rate of stress. It is emphasized that the ability to model the difference between NC and overconsolidation ratio (OCR) clays and relaxation are important improvements with respect to Bjerrum's model and the strain-rate approach.

Concept of the Model. Important concepts in connection with the model are: (1) Equivalent time, (2) reference time line, (3) instant time line, and (4) limit time line. These are illustrated on the diagram in Fig. 7.

- Equivalent time: Yin and Graham (1989b) reported that Bjerrum's time lines from constant duration of loading are not unique in all cases. They defined time lines as lines having equal values of equivalent times t_e. The equivalent time t_e is defined as the time needed to creep from a reference time line, where $t_e = 0$ (see below) to the current value of the vertical strain ε_z and the vertical effective stress σ'_z = constant (Yin and Graham 1994). In the normally consolidated range of a traditional multistage loading test with constant load increment ratio and constant load durations, the equivalent time t_e is equal to the duration of the load increments. However, in the overconsolidated range, equivalent time t_e and load duration t are quite different, depending on the OCR. The equivalent time is related to a unique creep strain rate with larger equivalent times being associated with smaller creep strain rates.
- The reference time line: is the reference state for calculating the equivalent time t_e. The reference time line is defined as a line, at which the equivalent time t_e is equal to zero (Yin and Graham 1994). Equivalent times below the reference time line are positive in the range $0 < t_e < \infty$ whereas the equivalent time is negative in the range $-t_0 < t_e < 0$ where t_0 is a material parameter. The location of the reference time line in $\varepsilon_z - \sigma'_z$ space is illustrated in Fig. 7.
- The instant time line: It is used to define instantaneous strains. These lines are assumed to be purely elastic, contrary to the elastic–plastic instant time line defined by Bjerrum (1967). The instant time line is defined as a line describing the instant elastic response of a soil skeleton due to effective stress changes (Yin and Graham 1989b, 1994). [It should be noted that the instant time line in Yin and Graham (1989a) is defined in the same way as Bjerrum (1967), i.e., the instant time line corresponds to elastic–plastic deformations.] The location of the instant time line in $\varepsilon_z - \sigma'_z$ space is illustrated in Fig. 7.
- The limit time line: Yin and Graham (1994) suggest that a unique limit line exists in $\varepsilon_z - \sigma'_z$ space, beyond which the behavior is time independent. The limit time line is defined as a time line that has an equivalent time $t_e = \infty$ and a corresponding creep rate equal to zero. The location of the limit time line in $\varepsilon_z - \sigma'_z$ space is illustrated in Fig. 7.

Model Formulation. Yin and Graham presented two types of general elastic–viscous–plastic models, one formulated by means of logarithmic functions and one by means of power functions.

The general equation for any one-dimensional loading of the logarithmic approach is established in two steps. The first step is to derive an expression for the equivalent time as a function of any state point $(\varepsilon_z, \sigma'_z)$. The second step is to determine a general relationship based on incremental strain components. The derivations of the equations are shown in Yin and Graham (1994). The general stress–strain relationship for any one-dimensional loading has been derived as follows:

$$\dot{\varepsilon}_z = \frac{\kappa}{\nu}\frac{1}{\sigma'_z}\dot{\sigma}'_z + \frac{\psi}{\nu t_0}\exp\left[-(\varepsilon_z - \varepsilon_{z0})\frac{\nu}{\psi}\right]\left(\frac{\sigma'_z}{\sigma'_{z0}}\right)^{\lambda/\psi} \tag{26}$$

where ε_{z0} = initial strain corresponding to the initial effective stress σ'_{z0}; ν = specific volume; κ = material parameter that describes the elastic stiffness of the soil; λ = elastic–plastic material parameter; ψ = creep parameter that is constant for a given soil; and t_0 = intrinsic time parameter.

The strains and stresses for the load conditions can be obtained by solving the general differential equation in Eq. (26). This implies that Eq. (26) can be solved in order to obtain solutions for creep, relaxation, constant rate of strain, and constant rate of stress. The solutions and the derivations of the solutions are rather complicated and are not shown here, for details see Yin and Graham (1994).

The resulting general stress–strain relationship for any one-dimensional loading in the framework of power functions is

$$\dot{\varepsilon}_z = a_2 n_1 \left(\frac{\sigma'_z}{\sigma'_u} - \frac{\sigma'_{z0e}}{\sigma'_u} \right)^{n_1 - 1} \dot{\sigma}'_z + (f_\infty^{ep} - f_0^{ep}) \frac{n_3}{t_0} \times \left(1 - \frac{\varepsilon_z - f_0^{ep}}{f_\infty^{ep} - f_0^{ep}} \right)^{(n_3+1)/n_3} \tag{27}$$

where the first part on the right-hand side = elastic or instant component of the total strain rate; and the second term = the viscous creep component of the total strain rate. f_0^{ep} indicates the function of the reference time line; f_∞^{ep} indicates the function of the limit time line; σ'_u = unit stress; $a_2, n_1, n_3, \sigma'_{z0e}$ = model parameters; and t_0 = intrinsic time parameter.

The general differential equation in Eq. (27) is equivalent to Eq. (26), that is, the equation can be solved in order to obtain solutions for creep, relaxation, constant rate of strain, and constant rate of stress. For details about the power-function formulation, see Yin and Graham (1989b).

Discussion. The predictions of one-dimensional viscous behavior such as creep and strain rate effects are generally in good agreement with experiments on soft soils. The best agreements are obtained by the use of the power function approach, which is due to improved options for calibrating the model as compared with the logarithmic model (Yin and Graham 1989b). To this end, it is worth noticing that the power-function approach involves the determination of 11 parameters, whereas the logarithmic model involves only 5 parameters.

Discussion of Semiempirical Secondary Relations

The correspondence principle holds true for the semiempirical models. This can be seen directly from the models of Bjerrum and Yin and Graham: A creep law is added to a basic time-independent model, and this means that the time enters the model. Now, the model contains a time-dependent component, and the solutions, e.g., for relaxation and constant rate of strain response, can be obtained by solving the expressions for appropriate boundary conditions. It should be noticed that the secondary semiempirical models rely on the same hardening methods as the primary empirical models, as discussed in the last part of the subsection entitled ''Empirical Primary Relations'' regarding the time-hardening and strain-hardening concepts.

Rheological Models

The rheological models were typically developed for metals, steel, and fluids, but they are to some extent used in the study of time effects in geomaterials. The terminology ''rheological models'' is often used when describing linear viscoelastic behavior of materials. However, in rheology of soils the term ''rheological models'' includes plastic behavior as well. The rheological models are usually divided into three categories:

- The differential approach is also referred to as the method of mechanical rheological models. The constitutive relations are constructed by combining different elementary material models, such as Hookean, Saint-Vernant's, and Newtonian materials.
- Engineering theories of creep. General theories for determining inelastic creep response of solids are widely applied in mechanics of concrete and metal. The mathematical structures of empirical models are varieties of this approach.
- The hereditary approach, also known as the method of integral representation. In this approach, the time-dependent creep strain or stress is defined by a ''creep'' or ''relaxation'' function, which is a hereditary (memory) function describing the historic dependence of strains or stresses.

The basic principles of the three above-mentioned approaches are briefly introduced in the following. The discussions of the three approaches are simplified to uniaxial conditions.

Differential Approach

The differential representation of a material may be visualized by the elementary mechanical models composed of elastic springs, plastic sliders, and viscous dashpots (Feda 1992). The characteristics of the three idealized materials are illustrated in Fig. 8.

Three well-known models used in geomechanics are: (1) The Maxwell model, (2) the Kelvin–Voigt model, and (3) the Bingham model. Special attention is paid to the Bingham model, because the concept coincides with the overstress model presented in the section entitled ''General Stress–Strain–Time Models.'' The Maxwell model consists of a spring and a dashpot in series, whereas the Kelvin–Voigt model consists of a spring and a dashpot in parallel. For further details on Maxwell and Kelvin–Voigt models, see Feda (1992) and Meschyan (1995).

Bingham Model

The Bingham model is a three-parameter model that consists of a parallel unit composed of a linear dashpot with a plastic slider, and a linear spring connected in series, as shown in Fig. 9. [Some authors refer to a ''Bingham body'' or ''Bingham model'' as a two-parameter rheological model that consists of a slider and a dashpot in parallel (Mitchell 1993; Meschyan 1995). In this paper, the Bingham model is defined as a three-parameter model, in which the spring is connected in series, too.] The model shows pure elastic response below the yield stress σ_y. Above the threshold stress, the model exhibits viscous flow of the Maxwell type.

The model can be characterized by two groups of components, which are combined in series: One is the group of time-independent components and the other is the group of time-dependent components. The time-independent group consists of the spring with spring constant E, denoted the elastic element. The time-dependent group consists of the dashpot with coefficient of viscosity η and the slider with a threshold stress σ_y combined in parallel, denoted the viscoplastic element. Since the elastic and viscoplastic element are connected in series, the total strain rate $\dot{\varepsilon}$ may be additively decomposed with respect to the two groups. The slider and with it the viscoplastic element are inactive as long as $\sigma < \sigma_y$. Therefore, it is only the difference $\sigma - \sigma_y$ that gives rise to viscoplastic strains ε^{vp}. Consider now the Bingham model subjected to the following assumptions: (1) The yield stress σ_y is zero and the material is nonhardening, and (2) the difference

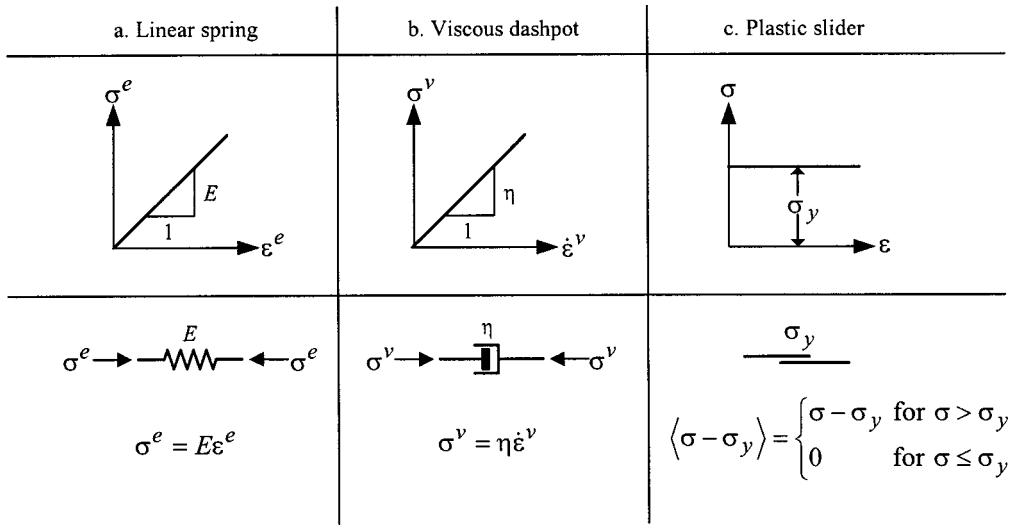

Fig. 8. Schematic representation of elementary material models: (a) Hookean spring, (b) Newtonian dashpot, and (c) Saint Vernant's slider. The subscripts e and v denotes elastic and viscous, respectively. E is the spring constant and η is the viscosity constant. The slider should be understood as an ideal plastic element that is inactive (locked) below a sudden threshold (yield) stress σ_y. If the stress σ exceeds σ_y the slider is ''unlocked'' and plastic deformations are allowed. The stress difference $\sigma-\sigma_y$ is often termed the overstress.

$\sigma-\sigma_y$ is constant and the material is nonhardening.

In the first case, the Bingham model is identical to the well-known Maxwell model, which describes a material that deforms at a constant rate, i.e., secondary creep (Meschyan 1995). In the second case, the constitutive equation in connection with a Maxwell model can be used to describe a material obeying the Bingham law if the imposed stress σ is replaced by $\sigma-\sigma_y$. In this case, the strain rate is constant too.

Differential Equation. By means of additive decomposition of strains and the material equations in Fig. 8, the constitutive equation for a nonhardening Bingham material can be described by

$$\dot{\varepsilon} = \begin{cases} \dot{\varepsilon}^e + \dot{\varepsilon}^{\text{vp}} = \dfrac{\dot{\sigma}}{E} + \dfrac{(\sigma-\sigma_y)}{\eta} & \text{for } \sigma > \sigma_y \\ \dot{\varepsilon}^e = \dfrac{\dot{\sigma}}{E} & \text{for } \sigma \leqslant \sigma_y \end{cases} \tag{28}$$

where $\dot{\varepsilon}$ = total strain rate; and $\dot{\varepsilon}^e$ and $\dot{\varepsilon}^{\text{vp}}$ = strain rates in the elastic and viscoplastic elements, respectively. The top part of Eq. (28) is analogous to the constitutive equation of the Maxwell model. The only difference is that the stress in the Maxwell model is replaced by the difference $\sigma-\sigma_y$. The constitutive equation for a Bingham model equals the equation for an elastic spring if $\sigma \leqslant \sigma_y$, asindicated in the lower part of Eq. (28). The creep, relaxation, and strain-rate response of the Bingham model are shown in Fig. 10.

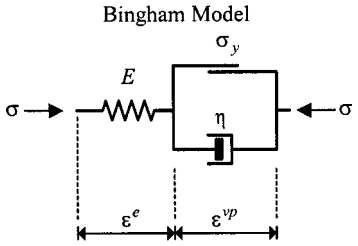

Fig. 9. Conceptual structure of the Bingham model. ε^e and ε^{vp} are the elastic and the viscoplastic strains, respectively.

Discussion of the Differential Approach

The differential approaches have some shortcomings. The Maxwell model seems to reflect the behavior in relaxation, whereas the Kelvin–Voigt model depicts creep reasonably well. The fact that the Maxwell model predicts relaxation reasonably well and is inadequate for predicting creep—and vice versa for the Kelvin–Voigt model—means that the two models are referred to as ''inverse'' models. This conclusion is only relevant when the material is known to be viscoelastic. In the case where plastic behavior is present as well, neither the Maxwell and Kelvin–Voigt models, nor the Bingham model can be used. There are several reasons for this: (1) The constitutive material relations are too simple. The spring, the dashpot, and the slider are assumed to describe linear constitutive relations. These are apparently not correct assumptions for soils. It is well known that soils show highly nonlinear elastic and plastic behavior. The linear viscous assumption is also inadequate. The above models predict either primary creep or secondary creep (flow) only, but soils may exhibit both primary and secondary creep stages during a creep process. (2) The constitutive relations for the rheological models are formulated for uniaxial compression conditions. The generalization of rheological models from one into three dimensions is possible, but practical calibration and application seems to be difficult (Singh and Mitchell 1968).

It must be emphasized that the resulting models are only geometrical pictures of the materials. However, material visualization in graphical form serves as a useful tool to explain the fundamental rheological terms and mechanisms in real materials, such as soils. Furthermore, the models within the differential approach rely on the existence of the correspondence principle. For references about the use of the differential approach in soil mechanics, see, e.g., Murayama and Shibata (1961), Barden (1965), and Murayama et al. (1984).

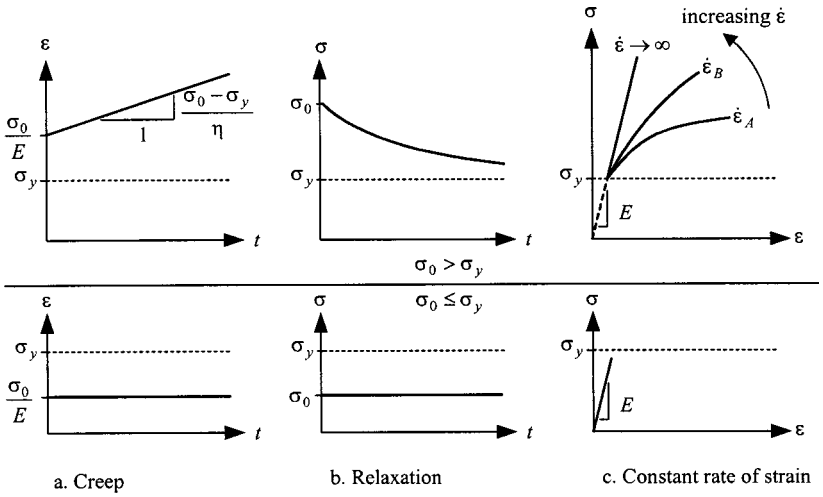

Fig. 10. Response of a Bingham model. The upper curves correspond to viscoplastic conditions where the stress state is above σ_y. The lower curves show the response in the elastic region below σ_y: (a) Response for creep; (b) response for relaxation; and (c) response for constant rate of strain. $\dot{\varepsilon}_A$ and $\dot{\varepsilon}_B$ are different constant strain rates where $\dot{\varepsilon}_B > \dot{\varepsilon}_A$.

Engineering Theories of Creep

Most of the work within the engineering theories of creep has been concentrated in the fields of metals, concrete, and ice, where the loading is below the initial yield stress. For a comprehensive review of the engineering theories of creep applied to steels and other metals, see Rabotnov (1969), and Skrzypek (1993). For reviews concerning frozen soil and ice, see Meschyan (1995), Ladanyi and Melouki (1993), Ladanyi and Benyamina (1995), and Zaretskiy and Yu (1993).

The engineering theories of creep do not represent unique methods for describing the phenomenon of creep. They are still phenomenological laws based on experimental observations, and there are obvious similarities between the structures of the empirical models mentioned in the section entitled ''Empirical Models'' and the models of the engineering theories of creep. However, the engineering theories of creep differ conceptually from the traditional way of dealing with creep in soils, because they are seen as creep theories for materials where the stress states are below the yield limit. For soils, the phenomenon of creep was originally developed for plastic, normally consolidated clays. The engineering theories of creep are represented by Skrzypek (1993): (1) The total strain model, (2) the time-hardening model, and (3) the strain-hardening model.

The descriptions in the following are based on uniaxial conditions. The uniaxial strain, strain rate, and effective stress are denoted ε, $\dot{\varepsilon}$, and σ, respectively. The elapsed time since start of creep is t. Superscripts e and c correspond to elastic and creep components.

Total Strain Model

It is assumed that the total strain consists of an instantaneous elastic and a viscous creep component:

$$\varepsilon = \varepsilon^e + \varepsilon^c \tag{29}$$

For a standard creep test where the stress σ is applied instantaneously, the creep strain component is given as a function of the applied stress σ and the loading history. In the functional relationship of the model, the loading history is uniquely related to the loading time t. This gives a straightforward relationship between creep strain, stress, and time:

$$\varepsilon^c = f(\sigma)g(t) \tag{30}$$

where f and g = functions. The relation between the creep strains and the stress is often modeled by a power function, i.e., the creep strains depend nonlinearly on the stress in contrast to the differential approach in the previous section where the stress–strain relation was approximated by a linear function. A power-law relation often models the influence of the loading time, too. Several other expressions are available, for instance exponential or hyperbolic functions.

In the total strain model, the viscous strain at constant stress σ is related directly to the time t. This yields a simple straightforward model that is easily adopted in creep predictions. In literature, it is recommended that the theory should be used for constant or slowly varying stresses only Rabotnov (1969).

Time-Hardening Model

To take the arbitrary stress changes into account, the constitutive relation should be of incremental nature, i.e., formulated with respect to the creep strain rate instead of the creep strain. In the time-hardening model, the functional relation is established between the creep strain rate, the stress and time:

$$\dot{\varepsilon}^c = f(\sigma)g(t) \tag{31}$$

where f and g = nonlinear functions. In Eq. (31), time can be identified as the hardening parameter, hence the name ''time hardening.'' One of the shortcomings of this model, as well as the total strain model, is that the governing equations are not invariant with respect to the origin of time, because time is introduced in explicit form.

Model of Strain-Hardening

In the strain-hardening model, the hardening is governed by the creep strain. The model is based on the accumulation of plastic strains or work as the hardening mechanism. The generalized model of strain-hardening is established between the creep strain rate, creep strain, and applied stress, that is

$$\dot{\varepsilon}^c = f(\sigma)g(\varepsilon^c). \tag{32}$$

Table 1. Correspondence Between the Engineering Creep Theories and the Empirical Models

Creep theory	Relation	Corresponding empirical model
Total strain model	$\varepsilon^c = f(\sigma)g(t)$	Logarithmic law. The stress function f is either constant, C_α approach, or varies with the confining stress, C_c/C_α approach. The time function g is the logarithmic function.
Time-hardening model	$\dot{\varepsilon}^c = f(\sigma)g(t)$	Singh and Mitchell model. The stress function f is an exponential function, and the time function g is a power function with the exponent m.
Strain-hardening model	$\dot{\varepsilon} = f(\sigma)g(\varepsilon^c)$	Strain rate approach. The general form of the strain rate approach states a unique relation between the stress, strain, and strain rate.

where f and g = nonlinear functions. The creep strain ε^c characterizes the state of the material and may therefore be viewed as an internal variable.

Discussion. The concept of hardening in the engineering theories of creep, whether it is time or strain hardening, is analogous to the traditional ideas when considering time-dependent behavior of soils. This is seen by the obvious similarities between the mathematical structures of the empirical models mentioned in the section entitled ''Empirical Models'' and the models of the engineering theories of creep. The empirical models that are related, in structure, to the time- and strain-hardening models are listed in Table 1.

The similarities described in Table 1 concern the empirical models only but the engineering theories of creep can be related to other concepts as well. For instance, the time- and strain-hardening models are actually Maxwell models with nonlinear creep components. The linear viscous element in the original Maxwell model may be replaced with either Eq. (31) or Eq. (32), which means that the viscous component becomes time or strain hardening, respectively. The nonlinear Maxwell model can formally be written as

$$\dot{\varepsilon} = \dot{\varepsilon}^e + \dot{\varepsilon}^c = \frac{\dot{\sigma}}{E} + \frac{\sigma}{\eta(\sigma,t)} \quad \text{for time hardening}$$
$$\dot{\varepsilon} = \dot{\varepsilon}^e + \dot{\varepsilon}^c = \frac{\dot{\sigma}}{E} + \frac{\sigma}{\eta(\sigma,\varepsilon^c)} \quad \text{for strain hardening} \tag{33}$$

In Eq. (33), it is observed that the viscosity parameter η is no longer constant but hardens with either stress and time or stress and strain.

In the above, it is seen that the engineering theories of creep are based upon a priori adopted creep relations, i.e., the primary concern is creep predictions. The ability to predict relaxation or constant rate of strain conditions are secondary and rely on the existence of the correspondence principle. The solutions for the time-hardening model are relatively simple, whereas the solutions for the strain-hardening model are rather complex. Solutions for relaxation based on the creep theories of time and strain hardening are given by Rabotnov (1969), Ladanyi and Melouki (1993), Ladanyi and Benyamina (1995), Borm and Haupt (1988), and Huneault (1992).

Hereditary Approach

The principle of the hereditary approach is that the current strain $\varepsilon(t)$ is obtained by integration over the entire loading history, i.e., integration over all infinitesimal stress changes until the current time t, hence, the name hereditary approach. The theory is developed for two cases. The simplest case is the hereditary approach based on linear viscoelasticity, which is a generalization of the differential approach. It is also possible to adopt the hereditary approach to nonlinear material behavior corresponding to a generalization of the engineering theories of creep. The general opinion is that the hereditary approach is too complex to incorporate in soil mechanics. This is due to the fact that the approach pays for its generality by a great number of experiments needed for calibration. Feda (1992) reported that 28 tests are needed to describe a uniaxial stress experiment by nonlinear hereditary theory, and for a triaxial state of stress about six times as many are required. However, it may be possible to reduce the number of tests for simple boundary conditions. For further studies of the hereditary approach, see Feda (1992), Mechyan (1995), Rabotnov (1969), Skrzypek (1993), and Ter-Martirosyan (1992).

General Stress–Strain–Time Models

This section is devoted exclusively to general constitutive laws, which describe not only viscous effects but also the inviscid (rate-independent) behavior of soils, in principle, under any possible loading condition. Special attention is paid to elastoviscoplastic models, which combine inviscid elastic and time-dependent plastic behavior. Viscoelastic–viscoplastic models are not considered here. For completeness, it should be mentioned that viscoelastic–viscoplastic models have been developed, e.g., Naghdi and Murch (1963), Murayama (1983), and Murayama et al. (1984).

Elastic–viscoplastic models can be divided into three classes [Sekiguchi (1985)]: (1) Elastoviscoplastic models based on the concept of overstress—they are denoted overstress models and the theory is called the overstress theory, (2) elastoviscoplastic models based on the concept of a nonstationary flow surface—they are denoted nonstationary flow surface (NSFS) models and the theory is called the NSFS theory, and (3) others.

Overstress Theory

The concept of overstress theory was introduced and developed by Ludwick (1922), Prandtl (1928), Hohenemser and Prager (1932), Sokolovsky (1948), and Malvern (1951) as reported by Satake (1989). Perzyna's overstress theory is a three-dimensional version of Malvern's one-dimensional constitutive model. The following description of Perzyna's overstress theory is based on Perzyna (1963a,b,c, 1966), Olszak and Perzyna (1966a, 1970), and Sekiguchi (1985).

A key assumption in connection with Perzyna's overstress theory is that viscous effects are negligible in the elastic region, i.e., no viscous strains occur within the static yield surface, which corresponds to the traditional yield surface associated with time-independent plasticity. In other words, the elastic strains are time

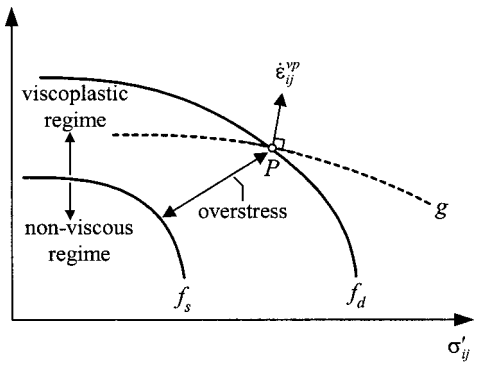

Fig. 11. Stress state P is part of the dynamic yield surface f_d and overstress F is defined as the distance between P and the static yield surface f_s. Furthermore, the viscoplastic strain rate vector is perpendicular to the plastic potential surface g.

independent whereas the inelastic strains are time dependent. The total strain rate is additively composed of the elastic and viscoplastic strain rates:

$$\dot{\varepsilon}_{ij} = \dot{\varepsilon}_{ij}^{e} + \dot{\varepsilon}_{ij}^{\mathrm{vp}} \tag{34}$$

where $\dot{\varepsilon}_{ij}$ denotes the (i,j) component of the total strain rate tensor; and the superscripts e and vp stand for the elastic and the inelastic components, respectively. In the theory of elastoviscoplasticity, the inelastic strain rate represents combined viscous and plastic effects. The elastic strain rate $\dot{\varepsilon}_{ij}^{e}$ in Eq. (34) is assumed to obey the generalized Hooke's law, while the viscoplastic strain-rate $\dot{\varepsilon}_{ij}^{\mathrm{vp}}$ is assumed to obey the following nonassociated flow rule;

$$\dot{\varepsilon}_{ij}^{\mathrm{vp}} = \gamma \phi(F) \frac{\partial g}{\partial \sigma'_{ij}} \tag{35}$$

where γ = fluidity parameter; ϕ = viscous nucleus; F = overstress function; g = potential function; and σ'_{ij} = effective stress state. The overstress function can be expressed as:

$$F(\sigma'_{ij}, W^{\mathrm{vp}}) = \frac{f_d(\sigma'_{ij}, W^{\mathrm{vp}})}{\kappa_s(W^{\mathrm{vp}})} - 1 \quad \text{where} \quad \kappa_s = \kappa_s\left(\int_0^{\varepsilon_{ij}^{\mathrm{vp}}} \sigma'_{ij} \dot{\varepsilon}_{ij}^{\mathrm{vp}} \right) \tag{36}$$

In Eq. (36), the function f_d depends on the stress state and the viscoplastic work W^{vp}. The function f_d describes the dynamic loading surface on which the current stress state P is located, as shown in Fig. 11. κ_s is the hardening parameter. $F=0$ when $f_d(\sigma'_{ij}, W^{\mathrm{vp}}) = \kappa_s(W^{\mathrm{vp}})$ which implies that κ_s must be an expression for the static yield surface f_s. The overstress theory differs from general elastoplasticity in the sense that the consistency rule is not used in the derivation of the theory. This implies that inelastic strains in the overstress model are not related to the stress history but to the current stress point only, while inelastic strains are related to the stress rate in elastoplasticity. Furthermore, by assuming the invalidity of the consistency rule, the stress state is allowed to be on, within or outside the static yield surface. This is used in the definition of overstress F. F is defined as the distance in stress space between the current stress state P and the static yield surface f_s, as illustrated in Fig. 11. $F>0$, $F<0$, and $F=0$ when the state of stress P is outside, within, or on f_s. Therefore, according to the key assumption and the flow rule, the following constraints apply to the viscous nucleus ϕ:

$$\langle \phi(F) \rangle = \begin{cases} 0 & \text{for } F \leqslant 0 \\ \phi(F) & \text{for } F > 0 \end{cases} \tag{37}$$

Eq. (37) can be considered as the loading criterion for inelastic deformations. The direction of $\dot{\varepsilon}_{ij}^{\mathrm{vp}}$ in Eq. (35) is normal to the potential surface g at the current stress point P, as shown in Fig. 11. The magnitude of $\dot{\varepsilon}_{ij}^{\mathrm{vp}}$ is given by γ and the viscous nucleus $\langle \phi(F) \rangle$. The determination of the viscous nucleus $\phi(F)$ is based on tests (Phillips and Wu 1973; Adachi and Okano 1974, 1982a; Oka et al. 1986; di Prisco and Imposimato 1996). Determination of $\phi(F)$ from tests is not widely presented, but Akai et al. (1977) and Adachi and Okano (1974) suggest procedures. Two of the most used forms are

$$\phi(F) = aF^6 \quad \text{and} \quad \phi(F) = c \exp(jF^k) - 1 \tag{38}$$

where a, b, c, j, and k = constants. As indicated in Eq. (38), the viscous nucleus $\phi(F)$ = monotonically increasing function of overstress F.

While overstress F is defined as a difference between the static and dynamic yield surfaces, the position of f_s in stress space is not easy to determine. Wood (1990), Eisenberg and Yen (1981), and Hinchberger and Rowe (1998) claim that the static yield surface is obtained by performing extremely slow tests. A method to determine an appropriate strain rate is mentioned by Sheahan (1995).

Consequences of the Overstress Theory

Creep. Consider a creep process initiated at a stress point lying outside the static yield surface. When a constant state of stress is imposed such that $F>0$, viscoplastic flow will occur and continue to occur at a constant rate if f_s is a nonhardening perfectly plastic yield surface [Fig. 12(a)], i.e., the distance between the static and the dynamic yield surface is constant with time.

If f_s is a hardening yield function, viscoplastic flow occurs at a decreasing rate, because as viscoplastic strain and consequent viscoplastic work W^{vp} accumulates, the static yield surface f_s changes in such way that $F \to 0$, thus $\dot{\varepsilon}_{ij}^{\mathrm{vp}} \to 0$. That is, the distance between f_s and f_d decreases with time, and the distance is reduced with decreasing rate. In other words, the static yield surface f_s moves out with time, and finally, after infinite time $t=\infty$ it coincides with the dynamic yield surface f_d, as indicated in Fig. 12(b). Once the new static yield surface has stabilized, $\dot{\varepsilon}_{ij}^{\mathrm{vp}} = 0$. According to di Prisco and Imposimato (1996), the viscoplastic strains accumulated during movement of the static yield surface f_s will be identical to the corresponding inviscid plasticity solution, i.e.

$$\int_0^{+\infty} d\varepsilon_{ij}^{\mathrm{vp}}(t, dt) = \delta \varepsilon_{ij}^{p} \tag{39}$$

where $\delta \varepsilon_{ij}^{p}$ = corresponding plastic strain increment tensor.

Consider now a creep process initiated from a state of stress, which lies inside f_s. In this case, the overstress $F<0$. According to Eqs. (35) and (37), no viscoplastic strains occur, and this is physically incorrect because the nature of creep strains is similar to that of plastic strains as postulated by Lade and Liu (1998).

Another consequence of the overstress theory is that it lacks the capability to model tertiary creep. Katona (1984), Oka (1985), and Mimura and Sekiguchi (1985) (as referenced by Adachi et al. 1987) have shown that because of its theoretical structure, the overstress-type model cannot describe the acceleration creep process.

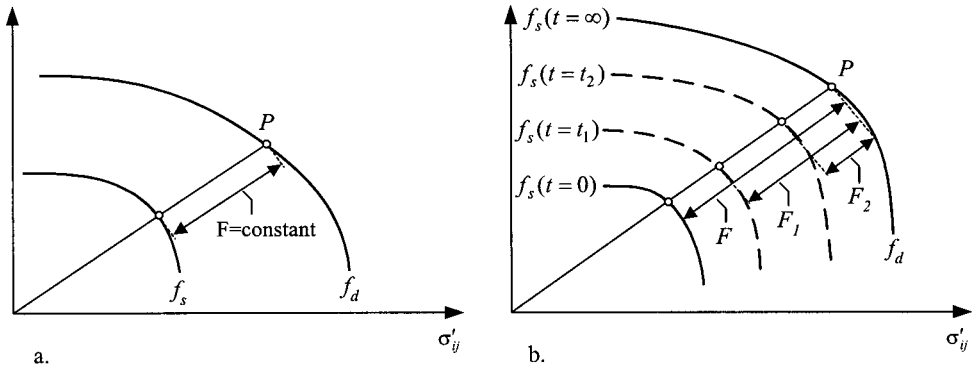

Fig. 12. (a) Creep process for a nonhardening material, and (b) Creep for a hardening material. As time goes by ($t=0<t_1<t_2<t=\infty$), the magnitude of overstress F decreases ($F>F_1>F_2$). This implies that $\phi(F)$ is a monotonically increasing function of F. F, P, t, f_s, and f_d are overstress, the current stress point, time, static yield surface, and dynamic yield surface, respectively.

Relaxation. Consider now a stress state that lies outside the current static yield surface f_s (i.e., the overstress $F>0$) and a total strain rate that is zero. This corresponds to a stress relaxation process. This implies according to Eq. (34) that time-independent elastic strains are equal in magnitude to the viscoplastic strains, but they are directed in the opposite direction. The stresses decrease during a stress relaxation process. This implies that the dynamic yield surface f_d contracts at a decreasing rate and the static yield surface f_s hardens. After an infinitely long time, f_d coincides with the static yield surface f_s. When $f_s=f_d$, the overstress $F=0$ and no further movement of the surfaces occur because the viscoplastic strain rate is zero, cf. Eqs. (35) and (37). Consider now a hypothetical stress relaxation process initiated from a stress state inside the static yield surface f_s. In this case, the viscoplastic strains are zero because the overstress $F<0$, cf. Eqs. (35) and (37). This implies, according to Eq. (34), that elastic strains must be zero too, and this is impossible during a stress relaxation process characterized by a stress decrease. In summary, a consequence of the overstress theory is that it is possible to model stress relaxation only in the case where the process is initiated from a stress state that lies outside the current static yield surface f_s.

Constant Rate of Strain. In a constant rate of strain test, the total strain rate must be constant, i.e., the sum of the elastic and viscoplastic strains must be constant according to Eq. (34). Consider now loading from a stress state inside the static yield surface f_s at a constant rate of strain. When the current state of stress is inside f_s, the total strain rate is equal to the elastic strain rate. As soon as the current state of stress moves outside f_s, viscoplastic strains will be produced, cf. Eqs. (35) and (37), and the sum of the viscoplastic and elastic strain rate must now be equal to the total constant strain rate. In this case, the amount of overstress F must all the time be updated and adjusted in the numerical algorithms in such a way that the total strain rate is constant. In contrast, when an unloading process takes place from a stress point outside the static yield surface, elastoviscoplastic strains are generated until the static yield surface is reached. In summary, it is possible to model constant rate of strain tests.

Static Yield Surface versus Classical Yield Surface. In the above discussion of the overstress theory, it has been stated that the static yield surface f_s may be understood as the classical yield surface in rate independent plasticity. This analogy has been suggested by, e.g., Zienkiewicz and Cormeau (1974), Katona and Mulert (1984), and di Prisco and Imposimato (1996). They postulated that the integration of the viscoplastic strains over time eventually gives the elastoplastic solution. Hashiguchi and Okayasu (2000) have questioned the fact that overstress theory can be used to obtain classical plastic solutions. They report that the viscoplastic overstress model is fundamentally different from elastoplasticity. This is due to the fact that plastic straining in the overstress model is not related to the stress rate but to stress, while plastic straining is related to the stress rate in elastoplasticity.

Perzyna's Overstress Theory as a Three-Dimensional Generalization of Bingham's Model

The overstress theory is a three-dimensional expansion of the one-dimensional Bingham model discussed in the section entitled ''Rheological Models.'' For simplicity, this will be shown in a case of nonhardening plasticity. The constitutive equations for a Bingham material are given by Eq. (27) and the constitutive equations for a material that is based on the concept of overstress theory are obtained by combining Eqs. (34), (35), (37), and Hooke's generalized law:

$$\dot{\varepsilon}=\begin{cases}\dot{\varepsilon}^e+\dot{\varepsilon}^{\mathrm{vp}}=C_{ijkl}\dot{\sigma}'_{ij}+\gamma\phi(F)\dfrac{\partial g}{\partial\sigma'_{ij}} & \text{for } \sigma'_{ij}>f(\sigma'_{ij})\\ \dot{\varepsilon}^e=C_{ijkl}\dot{\sigma}'_{ij} & \text{for } \sigma'_{ij}\leqslant f(\sigma'_{ij})\end{cases} \tag{40}$$

By comparing Eqs. (28) and (40), it is seen that the elastic matrix C_{ijkl} can be looked upon as a three-dimensional version of the elastic modulus E. The direction of the viscoplastic strain-rate $\partial g/\partial\sigma'_{ij}$ is omitted in Eq. (28) because the Bingham model is valid only in one-dimensional cases. The overstress function F is the excess stress above the yield surface. In the one-dimensional case, the overstress F can be interpreted as the distance between the current stress and the yield stress, i.e., $\sigma'-\sigma'_y$. In other words, $\phi(F)$ is the three-dimensional version of $\sigma'-\sigma'_y$. The fluidity parameter γ is the inverse of the coefficient of viscosity η.

Overstress Models

Many elastoviscoplastic models based on the concept of overstress are found in literature:

- The Adachi/Okano model, which models fully saturated normally consolidated clay (Adachi and Okano 1974).
- Different versions of the model proposed by Adachi and Oka

(Adachi and Oka 1982a,b; Adachi et al. 1987, 1996). As a matter of fact, the Adachi/Oka model is a consequence of further development of the Adachi/Okano model and the work of Oka (1981). Therefore, the model is capable of describing more time-related phenomena associated with fully saturated normally consolidated clay than the Adachi/Okano model.

- A viscoplastic cap model proposed by Katona (1984) and Katona and Mulert (1984). The objective of the Katona model is to model a wide range of geological materials, especially soils and rocks.
- Models proposed by di Prisco and his co-workers (di Prisco and Imposimato 1996; de Prisco et al. 2000). The objective of the models is to describe time effects in loose sand.
- A model proposed by Oka and his co-workers to describe the behavior of overconsolidated clay (Oka et al. 1988).
- The Zienkiewicz-model (Zienkiewicz and Cormeau 1974; Zienkiewicz et al. 1975). The papers focus attention on both associated and nonassociated behavior of soils. Furthermore, the papers attach some importance to numerical algorithms and examples solved numerically.
- The Akai/Adachi/Nishi model (Akai et al. 1977). The objective of the model is to obtain a stress–strain–time relationship for soft rock.
- The Desai/Zhang model (Desai and Zhang 1987). The purpose of the model is to describe the viscoplastic behavior of geologic material such as sand and rock salt.

Nonstationary Flow Surface Theory

The concept of the NSFS theory has been introduced and developed by Naghdi and Murch (1963) and Olszak and Perzyna (1966b, 1970) as reported by Matsui and Abe (1985a,b). The following description is based on Olszak and Perzyna (1966b, 1970), Sekiguchi (1985), and Satake (1989).

The NSFS theory is a result of the further development of the inviscid theory of elastoplasticity. That is, the NSFS theory is based on the basic concepts of inviscid elastoplasticity. Therefore, in the following, only the differences between the theories will be discussed.

The major difference between the NSFS theory and classical elastoplasticity lies in the definition of the yield condition. According to the latter, the yield condition for an isotropic hardening material is given by

$$f(\sigma'_{ij}, \varepsilon^{p}_{ij}) = 0 \tag{41}$$

where σ'_{ij} and ε^{p}_{ij} = effective stress state and plastic strains, respectively. According to Eq. (41), the yield condition does not change with time when the plastic strains are held constant. In that sense, the yield surface can be denoted as ''stationary.'' In contrast, the yield condition associated with the NSFS theory depends on time:

$$f(\sigma'_{ij}, \varepsilon^{\mathrm{vp}}_{ij}, \beta) = 0 \tag{42}$$

where $\varepsilon^{\mathrm{vp}}_{ij}$ and β = viscoplastic strains and a time-dependent function, respectively. It can be concluded from Eq. (42) that the yield surface changes every moment even though the viscoplastic strains are held constant. In that sense, the flow surface can be denoted ''nonstationary.'' The difference between the yield surface defined in connection with classical elastoplasticity and NSFS theory is illustrated in Fig. 13.

The nonstationary yield condition $f=0$ defines a surface in stress space and all possible stress states lie on or within this surface. In the case of $f<0$, the current stress state lies inside the flow surface and the soil is therefore in the elastic state and only elastic strains occur. When $f=0$ and a loading condition is considered, the soil is said to be in an elastoviscoplastic state and both elastic and viscoplastic strains occur.

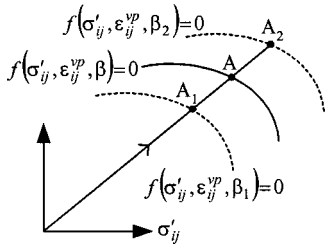

Fig. 13. Loading path and yield surfaces. For an elastoviscoplastic material, the yield surface corresponding to a given viscoplastic strain will be reached at different points A, A_1, or A_2 dependent on time β. For an elastoplastic material, the yield surface corresponding to a given viscoplastic strain will for a given load path be reached at the same point (for example A) independently of time β.

Like the overstress theory, the total strain rate $\dot{\varepsilon}$ associated with the NSFS theory can be decomposed into an elastic $\dot{\varepsilon}^{e}$ and a viscoplastic $\dot{\varepsilon}^{\mathrm{vp}}$ part in the following way:

$$\dot{\varepsilon}_{ij} = \dot{\varepsilon}^{e}_{ij} + \dot{\varepsilon}^{\mathrm{vp}}_{ij} \tag{43}$$

The elastic strain rate is determined by Hooke's generalized law and the viscoplastic strain rate is defined according to the flow rule:

$$\dot{\varepsilon}^{\mathrm{vp}}_{ij} = \langle \Lambda \rangle \frac{\partial g}{\partial \sigma'_{ij}} \tag{44}$$

where Λ = non-negative multiplier; and g = viscoplastic potential. $\langle\ \rangle$ = MacCauley's brackets. That is, MacCauley's brackets ensure that viscoplastic strains occur when loading from a plastic state and, in all other cases, the viscoplastic strains are zero. The multiplier Λ can be determined by using the consistency rule, which says that loading from a stress state lying on the current yield surface must again lead to a stress state lying on another yield surface, which constitutes the new current yield surface (Prager 1949). The expression for Λ yields

$$\Lambda = -\frac{\dfrac{\partial f}{\partial \sigma'_{ij}}\dot{\sigma}'_{ij} + \dfrac{\partial f}{\partial \beta}\dot{\beta}}{\dfrac{\partial f}{\partial \varepsilon^{\mathrm{vp}}_{kl}}\dfrac{\partial g}{\partial \sigma'_{ij}}} \tag{45}$$

where Λ, defined in Eq. (45), may be viewed as the sum of two contributions Λ_1 and Λ_2:

$$\Lambda = \Lambda_1 + \Lambda_2,\quad \Lambda_1 = -\frac{\dfrac{\partial f}{\partial \sigma'_{ij}}\dot{\sigma}'_{ij}}{\dfrac{\partial f}{\partial \varepsilon^{\mathrm{vp}}_{kl}}\dfrac{\partial g}{\partial \sigma'_{ij}}}\ \text{and}\ \Lambda_2 = -\frac{\dfrac{\partial f}{\partial \beta}\dot{\beta}}{\dfrac{\partial f}{\partial \varepsilon^{\mathrm{vp}}_{kl}}\dfrac{\partial g}{\partial \sigma'_{ij}}} \tag{46}$$

The parameter Λ_1 is identical to the plastic multiplier λ defined in connection with classical elastoplasticity. Therefore, it can be concluded from Eq. (46), that the only difference between the plastic multiplier λ and the viscoplastic multiplier Λ is that the latter includes an additional term $\dot{\beta}(\partial f/\partial \beta)$ in the numerator.

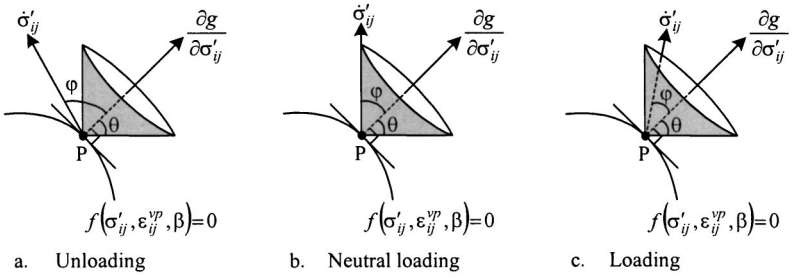

Fig. 14. Complete loading criteria for an elastoviscoplastic material based on the concept of nonstationary flow surface theory

This ''additional'' term implies that elastoviscoplastic strains occur even though the stresses are held constant, which corresponds to a creep process.

The constitutive equations in connection with the NSFS theory can, by use of Eqs. (43)–(45), and Hooke's generalized law, be described as

$$\dot{\varepsilon} = \frac{\dot{\sigma}'}{E} + \left\langle \frac{\frac{\partial f}{\partial \sigma'_{ij}} + \frac{\partial f}{\partial \beta}\dot{\beta}}{-\frac{\partial f}{\partial \varepsilon^{vp}_{kl}}\frac{\partial g}{\partial \sigma'_{ij}}} \right\rangle \frac{\partial g}{\partial \sigma'_{ij}} \tag{47}$$

According to Naghdi and Murch (1963) and Perzyna (1996a,b,c), criteria for unloading, neutral loading, and loading can be described as

$$\begin{aligned} f=0 \quad L(\dot{\sigma}'_{ij}, \beta) < 0 \quad \text{(unloading)} \\ f=0 \quad L(\dot{\sigma}'_{ij}, \dot{\beta}) = 0 \quad \text{(neutral loading)} \\ f=0 \quad L(\dot{\sigma}'_{ij}, \dot{\beta}) > 0 \quad \text{(loading)} \end{aligned} \tag{48}$$

where the operator $L(\dot{\sigma}'_{ij}, \dot{\beta})$ is defined as

$$L(\dot{\sigma}'_{ij}, \dot{\beta}) = \frac{\partial f}{\partial \dot{\sigma}'_{ij}}\dot{\sigma}'_{ij} + \frac{\partial f}{\partial \beta}\dot{\beta} \tag{49}$$

Since time now influences the loading criterion, loading at one rate may be unloading for another, and nontangent directions to the yield surface may also result in neutral loading. This can be illustrated by use of a geometrical interpretation of the loading conditions, which is discussed in the following. Assume now that the yield condition for an isotropic hardening material in Eq. (42) can be expressed as

$$\begin{aligned} f(\sigma'_{ij}, \varepsilon^{vp}_{ij}, \beta) = f'(\sigma'_{ij}, \varepsilon^{vp}_{ij}) - \kappa(\varepsilon^{vp}_{ij}, \beta) = 0 \\ \Rightarrow f'(\sigma'_{ij}, \varepsilon^{vp}_{ij}) = \kappa(\varepsilon^{vp}_{ij}, \beta), \end{aligned} \tag{50}$$

where κ = hardening function. Differentiating Eq. (50) and introducing it into Eqs. (48) and (49) for the neutral loading case yields

$$\begin{aligned} \frac{\partial f}{\partial \sigma'_{ij}}\dot{\sigma}'_{ij} - \frac{\partial \kappa}{\partial \beta}\frac{\partial \beta}{\partial t} = 0 \Leftrightarrow \cos\theta = \left(\frac{\frac{\partial \kappa}{\partial \beta}\frac{\partial \beta}{\partial t}}{\left|\frac{\partial f}{\partial \sigma'_{ij}}\right| |\dot{\sigma}'_{ij}|} \right) \\ \Rightarrow \theta = \arccos\left(\frac{\frac{\partial \kappa}{\partial \beta}\frac{\partial \beta}{\partial t}}{\left|\frac{\partial f}{\partial \sigma'_{ij}}\right| |\dot{\sigma}'_{ij}|} \right) \end{aligned} \tag{51}$$

where θ = angle between the stress rate $\dot{\sigma}'_{ij}$ and the normal to the yield surface $\partial f/\partial \sigma'_{ij}$ in the case of neutral loading. That is, neutral loading can geometrically be symbolized as a cone in stress space with the opening angle θ as illustrated in Fig. 14.

Now let the angle between the stress rate vector $\dot{\sigma}'_{ij}$ and the normal to yield surface $\partial f/\partial \sigma'_{ij}$ in an arbitrary loading condition (unloading, neutral, and loading) be denoted as φ. It can be shown that the complete loading criteria is defined as (Naghdi and Murch 1963):

$$\begin{aligned} \varphi > \theta \quad \text{(unloading)} \\ \varphi = \theta \quad \text{(neutral loading)} \\ \varphi < \theta \quad \text{(loading)} \end{aligned} \tag{52}$$

This is illustrated in Fig. 14. It should be noted that specification of the physical nature of the time-dependent parameter β is a key for the NSFS theory.

Consequences of the Nonstationary Flow Surface Theory

Relaxation. Consider a relaxation process initiated from a stress state within the yield surface. In this case, the total strain rate has to be zero, which implies that the elastic strain rate has to be equal to the viscoplastic strain rate but in the opposite direction as indicated in Eq. (43). The effective stresses decrease during a relaxation process and the NSFS theory will, because of its theoretical structure, only predict elastic strains, i.e., no viscoplastic strains are assumed to occur. Therefore, the NSFS theory is not able to describe a relaxation process when it is initiated from a stress state inside the yield surface. It appears that it is not described in the literature whether or not the NSFS theory is capable of describing a relaxation process initiated from a point on the yield surface. In principle, it is possible.

Creep. Consider a creep process initiated at a stress state located within the yield surface. Again, the NSFS theory will not predict any inelastic strains. According to Nova (1982), creep strains developed during a creep process are inelastic. That is, the NSFS theory cannot describe a creep process initiated from a state of stress inside the yield surface satisfactorily. Does this imply that the theory is incapable of describing a creep process? As a matter of fact, the theory is able to predict creep strains when the process is started from a state on the current yield surface. This will be discussed in the following.

Consider a creep process initiated at a point Q on the current yield surface f at a given time t as illustrated in Fig. 15. Viscoplastic deformations are triggered because the stress state Q is on the flow surface f and the ''loading criterion'' corresponds to a point, which coincides with the apex P of the cone describing the

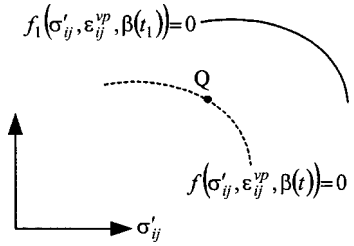

Fig. 15. According to the nonstationary flow surface theory if a creep process is initiated at stress state Q lying on the current yield surface, viscoplastic strains occur, and the yield surface expands with time even though the stress state Q is held constant

loading criterion as illustrated in Fig. 14. Viscoplastic strains ε^{vp}_{ij} occur according to Eqs. (44) and (45), but the term that includes the stress rate $\dot{\sigma}'_{ij}$ vanishes. The development of viscoplastic strains implies that the yield surface expands in stress space indicated in Eq. (42) and at a subsequent time t_1 the imposed constant stress state Q will be inside the new current yield surface f_1 as illustrated in Fig. 15. Therefore, no further viscoplastic deformation should develop during the remaining part of the creep process because the stress state Q is interior to the yield surface f_1. But in association with the NSFS theory, it is assumed that if a viscoplastic deformation process is first triggered in connection with a creep process initiated at a point Q on the yield surface f, the creep process will continue to occur even though the stress state Q at a subsequent time t_1 will be inside the new current yield surface f_1.

Consider normally consolidated clay under the assumption that the primary consolidation is instantaneous. The clay is subjected to the stress path *origin*→A→B→C→D. The stress path is illustrated in Fig. 16. From the *origin* to A, only elastic strains occur because the stress state is inside the current yield surface f. Point A lies on the yield surface f and, at this state, a creep process is initiated. During a creep process, the stress state is constant and this implies that A and B coincide. As discussed above, viscoplastic strains develop during a creep process initiated from a stress state lying on the current yield surface f and this implies that the flow surface expands with time even though the stresses are constant. During the creep process, the yield surface expands in such way that $f_1=0$ constitutes the new current yield surface and point C is located on f_1. The clay appears then to be overconsolidated although the history of effective stresses is such that the soil is in fact normally consolidated. Therefore, when loading from B to C occurs, the stiffness is the elastic stiffness until point C is reached and the response is instantaneous. From C to D, the stress state is always on the current yield surface and the response is elastoviscoplastic. From this example it can be concluded that during a creep process the yield surface expands. If the soil is loaded afterward, the response is elastic until the stress state reaches the current yield surface and, hereafter, the response is elastoviscoplastic. This is consistent with Bjerrum's description (see subsection entitled, ''semiempirical secondary relations'' and Bjerrum 1973).

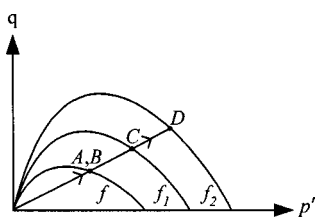

Fig. 16. Normally consolidated clay subjected to the stress path origin→A→B→C→D

Constant Rate of Strain. The NSFS theory is able to describe the behavior of soil in a range of deformations rates. The slowest rate corresponds to a total strain rate approximating zero. The fastest strain rate corresponds to the rate at which the time term in Eq. (47) can be neglected. If the time term vanishes in Eq. (47), the constitutive equations for an elastoviscoplastic material are equivalent to the equations for an elastoplastic material.

Nonstationary Flow Surface Models

Many elastoviscoplastic models based on the NSFS theory are found in literature:

- The Sekiguchi model is proposed and validated by Sekiguchi (1977)—it is further developed to include anisotropy by Sekiguchi and Ohta (1977), and the model's capability to describe creep rupture under undrained conditions is discussed by Sekiguchi (1984). The Sekiguchi model is an extension of Murayama and Shibata's model (1961) as reported by Sekiguchi and Ohta (1977). The objective of the Sekiguchi model is to model normally consolidated clay.
- The Dragon/Mroz model (1979)—the objective of the model is to describe creep behavior of rocklike materials. The model differs from other elastoviscoplastic models based on the concept of NSFS theory in the way that time-dependent microcracking is responsible for the macroscopic behavior. In other words, micromechanics is used in the description of time-dependent macroscopic behavior.
- An elastoviscoplastic model developed by Nova (1982)—it is an extension of the elastoplastic model proposed by Nova and Wood (1979). The objective of the Nova model is to model normally consolidated clay.
- The Matsui/Abe-model (Matsui and Abe 1985a,b)—the model is valid for normally consolidated clay. Furthermore, the Matsui/Abe model includes the Sekiguchi model as a special case as reported by Satake (1989).

Comparison of Structures of Overstress and Nonstationary Flow Surface Theories

Both overstress theory and NSFS theory make use of reference lines when defining the domain in which they are applicable. This is illustrated in Fig. 17 where q is the deviator stress, ε_1 is the principal strain, and $\dot{\varepsilon}$ is the strain rate. The instant time line defines the instant response, i.e., the response predicted by the theories when deformation is induced at an infinitely high rate. The limit state line defines the transition from the nonviscous region to the viscoplastic domain. The limit state line and the instant time line have been defined by Yin and Graham, see the section entitled ''Empirical Models.'' Differences and similarities between the overstress theory and NSFS theory are summarized in Table 2 and illustrated in Fig. 17.

As indicated in Table 2, the instant time line in connection with the overstress theory is the elastic limit. This can be realized by considering the following loading case: Suppose that an infinite strain rate is imposed, i.e., the loading occurs instantaneously. The plastic strains that require time to develop are therefore suppressed. According to Eq. (34), the total response predicted by the theory is therefore elastic. Consider now the same loading case in

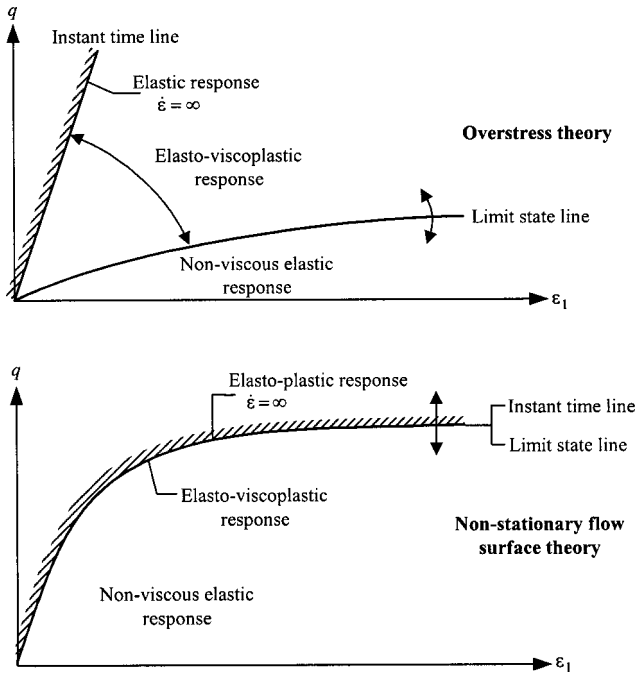

Fig. 17. Domains and reference lines used in connection with overstress and nonstationary flow surface theory

connection with NSFS theory. If the duration of the loading process is infinitely small, the time-dependent term β vanishes in Eq. (47) and the total strains correspond to a time-independent elastoplastic response.

According to Eqs. (34) and (43), the viscoplastic part $\dot{\varepsilon}^{vp}$ of the total strain rate tensor $\dot{\varepsilon}$ is treated as a single quantity. In literature, there are conflicting opinions as to whether or not the viscoplastic strain-rate tensor can be decomposed into a plastic and a viscous part. According to Tatsuoka et al. (2000), the decomposition is not possible whereas Hashiguchi and Okayasu (2000) argued that plastic and viscous strain rate tensors have to be formulated as independent quantities.

Correspondence Principle

Like empirical and rheological models, models based on the concepts of the overstress and NSFS theories also make use of the correspondence principle. The same fundamental equation, Eq. (34) or Eq. (43), is used when predicting creep, stress relaxation, and constant rate of strain behavior. It is only the boundary conditions that are changed when modeling the different time-dependent behaviors. Therefore, the overstress and NSFS theories make use of the correspondence principle.

Other Contributions

Elastoviscoplastic models other than those based on the concepts of the overstress and the NSFS theories also exist. These models will be briefly mentioned to complete the review.

- The Borja model—a stress–strain–time relation for cohesive soils in the ''wet'' region is proposed by Hsieh et al. (1990) and the model's capability to describe time effects is verified by Borja et al. (1990). The model predicts the behavior of normally and lightly overconsolidated clay. The Borja model is an extension of the single yield surface model proposed by Borja and Kavazanjian (1985), and Borja (1992) describes another formulation of the model incorporating a single yield surface.
- A time-dependent constitutive model for cohesive soils is described by Dafalias (1982), and Kaliakin and Dafalias (1990a, 1991). The model's capability to describe time effects is verified by Kaliakin and Dafalias (1990b). The model is denoted as the bounding surface model. It predicts the behavior of overconsolidated soils.
- The endochronic model is proposed by Valanis (1971). The prominent feature of this model is that no yield surface is incorporated in the theory. Furthermore, time is included in the equations by means of an intrinsic time scale, which is a material property.
- The subloading surface model is developed by Hashiguchi and his co-workers, see for example (Hashiguchi and Ueno 1977). Hashiguchi and Okayasu (2000) extend this elastoplastic model for the purpose of predicting time-dependent behavior. The subloading surface model is substantially identical to the bounding surface model but, in connection with the former, the loading surface can be outside the normal yield surface surrounding the elastic region, which corresponds to the bounding surface in connection with the bounding surface model.
- A model proposed by Tian and his co-workers (Tian et al. 1994). This isotropic hardening model is a variety of the bounding surface model in the sense that it is based on a nonassociated flow rule.
- Another model is proposed by Adachi and his co-workers (Adachi et al. 1990). The model deals with memory and internal variables in the sense that a strain measure is introduced in the constitutive equations instead of real time (Oka and Adachi

Table 2. Comparison of the Structure of Overstress Theory and Nonstationary Flow Surface Theory

Overstress theory	Nonstationary flow surface theory
The instant time line is a line describing the elastic response.	The instant time line is a line describing the elasto-plastic response when loaded from a plastic state.
The limit state line is the static yield surface.	The limit state line is the normal yield surface and it coincides with the instant time line.
The limit state line can harden.	The limit state line can harden.
Elastoviscoplastic behavior occurs in the domain between the current instant time line and the current limit state line. That is, time effects take place in the elasto-viscoplastic domain.	Elastoviscoplastic behavior occurs if the process in question is triggered from a stress state located on the limit state line. That is, time effects take place if a given time-dependent process is initiated from a point on the limit state line.
A creep or relaxation process stops when the current state of stress coincides with the limit state line.	A creep process can in principle continue in eternity. In principle, a stress relaxation process stops when the effective stress state becomes negative.

1985). The strain measure is similar to the concept proposed by Valanis (1971). Adachi et al. (1997) introduced another time measure and a nonassociated flow rule.
- A model proposed by Lade and Liu (2001), includes time effects. The model is an extension of the ''single hardening model'' (Lade and Kim 1988a,b; Kim and Lade 1988), and time is introduced in the plastic multiplier.
- A model proposed by Cristescu (1991) has the purpose of describing sand behavior.

Discussion

The purpose of this review is to give a survey of the types of models that exist for modeling time effects and their limitations. Existing constitutive models used in connection with prediction of time-dependent behavior of soils can roughly be categorized as one of the following types: (1) Empirical models, (2) rheological models, and (3) general stress–strain–time models.

It is clear that none of the models developed so far (reviewed above) can handle all of the observed time effects in soils (Augustesen et al. 2004). Whether models are empirical, rheological, or general in nature, they all make use of the correspondence principle. That is, the same constitutive relationship can be used to predict creep, stress relaxation, and constant rate of strain behavior by imposing appropriate boundary conditions on the soil element. Furthermore, Augustensen et al. (2004) pointed out that isotach behavior is valid for clay but not for sand. Isotach behavior is characterized by a unique stress–strain–strain-rate relationship, and it implies correspondence between creep, stress relaxation, and constant rate of strain. That is, the correspondence principle can be used when modeling isotach behavior. From the above, it can be concluded that:

- Existing models and concepts can in principle be used when modeling time-dependent behavior of clay.
- Existing models and concepts cannot be used when modeling time-dependent behavior of sand.

Does this imply that time effects in clay can be fully modeled? Actually, there are still many areas within the scope of modeling of time effects in clays that the existing models are not able to describe. So, future studies concern, for example, modeling of: (1) Three-dimensional clay behavior, (2) structuration, and (3) high rate tests on low permeability clay (Augustesen et al. 2004).

New concepts and models must be developed to describe time-dependent behavior in sand. In connection with this development, it may be of interest to consider the following: (1) Is there correspondence between creep and stress relaxation? If this is the case, the development of a new model may be easier, because then it is only the constant rate of strain behavior that deviates from normal. (2) Can a modified elastoviscoplasticity concept be used in connection with new models? (3) Should the rate of strain rate, i.e., strain acceleration or deceleration, be included in the constitutive equations in order to model the temporary over- and undershoot in connection with a step increase or decrease in the constant strain rate? Furthermore, is the effect of structuration of a similar nature to the effect of changing the strain rate?

It must also be considered whether or not the constitutive relations should constitute a unified model or make use of the coupling principle. The decision influences the way in which the constitutive model is constructed. A unified model is, as the name indicates, a model that combines all time effects (and other effects) in a set of constitutive equations, which are solved by numerical methods. In connection with constitutive relations making use of the coupling principle, a set of constitutive equations are coupled depending on the problem that has to be solved. That is, if for example a creep process is predicted, the basic model, e.g., an existing elastoplastic model, is coupled with the constitutive relation that models creep and all the other constitutive components are frozen. In reality, it may be physically impossible or hard to couple the different time effects. Furthermore, in connection with the unified model, it may be impractical to make a set of equations from which all time mechanisms can be predicted. That is, the same set of equations cannot be used to describe, e.g., crushing and stress relaxation in sand. The coupling principle indirectly implies that it is not the same basic mechanisms that control different time effects.

References

Adachi, T., and Okano, M. (1974). ''A constitutive equation for normally consolidated clay.'' *Soils Found.*, 14(4), 55–73.

Adachi, T., and Oka, F. (1982a). ''Constitutive equations for normally consolidated clay based on elasto-viscoplasticity.'' *Soils Found.*, 22(4), 57–70.

Adachi, T., and Oka, F. (1982b). ''Constitutive equations for normally consolidated clays and assigned works for clay.'' *Results of the Int. Workshop on Constitutive Relations for Soils, Grenoble*, G. Gudehus et al., eds., 123–140.

Adachi, T., Oka, F., and Mimura, M. (1987). ''Mathematical structure of an overstress elasto-viscoplastic model for clay.'' *Soils Found.*, 27(3), 31–42.

Adachi, T., Oka, F., and Poorooshasb, H. B. (1990). ''A constitutive model for frozen sand.'' *Trans. ASME*, 112, 208–212.

Adachi, T., Oka, F., and Mimura, M. (1996). ''State of the art: Modeling aspects associated with time dependent behavior of soils.'' *Measuring and modeling time dependent soil behavior, Geotechnical Special Publication No. 61*, T. C. Sheahan and V. N. Kaliakin, eds. ASCE, New York, 61–95.

Adachi, T., Oka, F., and Zhang, F. (1997). ''An elasto-viscoplastic constitutive model with strain softening.'' *Numerical models in geomechanics*, S. Pietruszczak and G. Pande, eds., Balkema, Rotterdam, The Netherlands, 81–86.

Akai, K., Adachi, T., and Nishi, K. (1977). ''Mechanical properties of soft rocks.'' *Proc., 9th ICSMFE*, Tokyo, 1, 7–10.

Augustesen, A., Liingaard, M., and Lade, P. V. (2004). ''Evaluation of time-dependent behavior of soils.'' *Int. J. Geomech.*, 4(3), 137–156.

Barden, L. (1965). ''Consolidation of clay with nonlinear viscosity.'' *Geotechnique*, 15(4), 345–362.

Bjerrum, L. (1967). ''Engineering geology of Norwegian normally-consolidated marine clays as related to the settlements of buildings.'' *Geotechnique*, 17(2), 83–119.

Bjerrum, L. (1973). ''Problems of soil mechanics and construction on soft clays and structurally unstable soils.'' *Proc., 8th ICSMFE (13)*, Moscow, 111–159.

Borja, R. I. (1992). ''Generalized creep and relaxation model for clays.'' *J. Geotech. Eng.*, 118(11), 1765–1786.

Borja, R. I., and Kavazanjian, E. (1985). ''A constitutive model for the stress–strain–time behaviour ''wet'' clays.'' *Geotechnique*, 35(3), 283–298.

Borja, R. I., Kavazanjian, E., Jr., and Hsieh, H. S. (1990). ''Double-yield-surface cam-clay plasticity Model: II. Implementation and verification.'' *J. Geotech. Eng.*, 116(9), 1402–1421.

Borm, G., and Haupt, M. (1988). ''Constitutive behavior of rock salt: Power-law or hyperbolic sine creep?'' *6th Int. Conf. on Numerical Methods in Geomechanics*, G. Swoboda, ed., Balkema, Rotterdam, The Netherlands, 1883–1893.

Buisman, A. S. (1936). ''Results of long duration settlement tests.'' *Proc., 1st Int. Conf. on Soil Mechanics and Foundation Engineering*, Cambridge, Mass., 1, 103–107.

Cristescu, N. (1991). ''Nonassociated elasti/viscoplastic constitutive equations for sand.'' *Int. J. Plast.*, 6, 41–64.

Dafalias, Y. F. (1982). ''Bounding surface elastoplasticity-viscoplasticity for particulate cohesive media.'' *Int. Union of Theoretical and Applied Mechanics Conf. on Deformation and Failure of Granular Materials*, P. A. Vermeer and H. J. Luger, eds., 97–107.

Desai, C. S., and Zhang, D. (1987). ''Viscoplastic model for geological materials with generalized flow rule.'' *Int. J. Numer. Analyt. Methods Geomech.,* 11, 603–620.

di Prisco, C., and Imposimato, S. (1996). ''Time dependent mechanical behaviour of loose sands.'' *Mech. Cohesive-Frict. Mater.,* 1(1), 45–73.

di Prisco, C., Imposimato, S., and Vardoulakis, I. (2000). ''Mechanical modelling of drained creep triaxial tests on loose sand.'' *Geotechnique,* 50(1), 73–82.

Dragon, A., and Mroz, Z. (1979). ''A model for plastic creep of rock-like materials accounting for the kinetics of fracture.'' *Int. J. Rock Mech. Min. Sci. Geomech. Abstr.,* 16, 253–259.

Eisenberg, M. A., and Yen, C. F. (1981). ''A theory of multiaxial anisotropic viscoplasticity.'' *J. Appl. Mech.,* 48, 276–284.

Feda, J. (1992). *Creep of soils and related phenomena, developments in geotechnical engineering*, Elsevier Science, North–Holland, Amsterdam, The Netherlands, Vol. 68.

Garlanger, J. E. (1972). ''The consolidation of soils exhibiting creep under constant effective stress.'' *Geotechnique,* 22(1), 71–78.

Hashiguchi, K., and Ueno, M. (1977). ''Elastoplastic constitutive laws of granular materials.'' *Proc. 9th ICFSME, Spec. Session 9, JSSMFE*, Tokyo, 73–82.

Hashiguchi, K., and Okayasu, T. (2000). ''Time-dependent elastoplastic constitutive equation based on the subloading surface model and its application to soils.'' *Soils Found.,* 40(4), 19–36.

Hinchberger, S. D., and Rowe, R. K. (1998). ''Modelling the rate-sensitive characteristics of the Gloucester foundation soil.'' *Can. Geotech. J.*, 35, 769–789.

Hohenemser, K., and Prager, W. (1932). ''Über die ansätze der mechanik isotroper kontinua.'' *Z. Angew. Math. Mech.,* 12, 216–226.

Hsieh, H. S., Kavazanjian, E., and Borja, R. I. (1990). ''Double-yield-surface cam-clay plasticity model. I: Theory.'' *J. Geotech. Eng.,* 116(9), 1381–1401.

Huneault, P. A. (1992). ''Strain-hardening relaxation.'' *J. Appl. Mech.,* 59, 217–219.

Kaliakin, V. N., and Dafalias, Y. F. (1990a). ''Theoretical aspects of the elastoplastic-viscoplastic bounding surface model for cohesive soils.'' *Soils Found.,* 30(3), 11–24.

Kaliakin, V. N., and Dafalias, Y. F. (1990b). ''Verification of the elastoplastic-viscoplastic bounding surface model for cohesive soils.'' *Soils Found.,* 30(3), 25–36.

Kaliakin, V. N., and Dafalias, Y. F. (1991). ''Details regarding the elasto-viscoplastic bounding surface model for isotropic cohesive soils.'' *Civil Engineering Rep. No. 91-1*, Dept. of Civil Engineering, Univ. of Delaware, Newark, Del.

Katona, M. G. (1984). ''Evaluation of viscoplastic cap model.'' *J. Geotech. Eng.,* 110(8), 1106–1125.

Katona, M. G., and Mulert, M. A. (1984). ''A viscoplastic cap model for soils and rock.'' *Mechanics of engineering materials*, C. S. Desai and R. H. Gallagher, eds., Wiley, New York, 335–350.

Kavazanjian, E., and Mitchell, J. K. (1977). ''A general stress–strain–time formulation for soils.'' *Proc., 9th ICSMFE,* 113–120.

Kim, M. K., and Lade, P. V. (1988). ''Single hardening constitutive model for frictional materials. I: Plastic potential function.'' *Comput. Geotech.,* 5(4), 307–324.

Lacerda, W. A., and Houston, W. N. (1973). ''Stress relaxation in soils.'' *Proc., 8th ICSMFE*, 1/34, 221–227.

Ladanyi, B., and Melouki, M. (1993). ''Determination of creep properties of frozen soils by means of borehole stress relaxation tests.'' *Can. Geotech. J.*, 30, 170–186.

Ladanyi, B., and Benyamina, M. B. (1995). ''Triaxial relaxation testing of a frozen sand.'' *Can. Geotech. J.*, 32, 496–511.

Lade, P. V., and Kim, M. K. (1988a). ''Single hardening constitutive model for frictional materials. II: Yield criterion and plastic work contours.'' *Comput. Geotech.,* 6(1), 13–29.

Lade, P. V., and Kim, M. K. (1988b). ''Single hardening constitutive model for frictional materials. III: Comparisons with experimental data.'' *Comput. Geotech.,* 6(1), 31–47.

Lade, P. V., and Liu, C. T. (1998). ''Experimental study of drained creep behavior of sand.'' *J. Eng. Mech.,* 124(8), 912–920.

Lade, P. V., and Liu, C. T. (2001). ''Modeling creep behavior of granular materials.'' *Proc., 10th Int. Conf. on Computer Methods and Advances in Geomechanics*, Desai et al., eds., Tuscon, Ariz., 277–284.

Leroueil, S., Kabbaj, M., Tavenas, F., and Bouchard, R. (1985). ''Stress-strain-strain rate relation for the compressibility of sensitive natural clays.'' *Geotechnique,* 35(2), 159–180.

Leroueil, S., and Marques, M. E. S. (1996). ''Importance of strain rate and temperature effects in geotechnical engineering,'' *Measuring and Modeling Time Dependent Soil Behavior, Geotechnical Special Publication No. 61*, Sheahan, T. C. and Kaliakin, V. N., eds., ASCE, Reston, Va. 1–60.

Ludwick, P. (1922). ''Uber den Einfluss der Deformationsgeschwindigkeit bei bleibenden Deformationen mit besonderer Berucksichtigung der Nachwirkungserscheinungen.'' *Phys. Z.,* 10(12), 411–417.

Malvern, L. E. (1951). ''The propagation of longitudinal waves of plastic deformation in a bar of metal exhibiting a strain rate effect.'' *J. Appl. Mech.,* 18, 203–208.

Matsui, T., and Abe, N. (1985a). ''Elasto/viscoplastic constitutive equation of normally consolidated clays based on flow surface theory.'' *5th Int. Conf. on Numerical Methods in Geomechanics*, Nagoya, Japan, 407–413.

Matsui, T., and Abe, N. (1985b). ''Undrained creep characteristics of normally consolidated clay based on the flow surface model.'' *Proc., 11th ICSMFE,* 140–143.

Meschyan, S. R. (1995). *Experimental rheology of clayey soils, geotechnika 13 (selected translation of Russian geotechnical literature)*, A. A. Balkema, Rotterdam/Brookfield.

Mesri, G. (1973). ''Coefficient of secondary compression.'' *J. Soil Mech. Found. Div.,* 99(1), 123–137.

Mesri, G., and Godlewski, P. M. (1977). ''Time and stress-compressibility interrelationship.'' *J. Geotech. Eng.,* 103(5), 417–430.

Mimura, M., and Sekiguchi, H. (1985). ''A review of existing viscoplastic constitutive models regarding the performance of creep rupture prediction.'' *Proc., 40th Japan Nat. Conf., JSCE,* 1097–1100 (in Japanese).

Mitchell, J. K. (1993). *Fundamentals of soil behavior*, 2nd Ed., Wiley, New York.

Murayama, S. (1983). ''Formulation of stress-strain-time behavior of soils under deviatoric stress condition.'' *Soils Found.,* 23(2), 43–57.

Murayama, S., and Shibata, T. (1961). ''Rheological properties of clays.'' *Proc., 5th Int. Conf., S.M.F.E.*, 1, 269–274.

Murayama, S., Michihiro, K., and Sakagami, T. (1984). ''Creep characteristics of sands.'' *Soils Found.,* 24(2), 1–15.

Naghdi, P. M., and Murch, S. A. (1963). ''On the mechanical behavior of viscoelastic/plastic solids.'' *J. Appl. Meteorol.,* 30, 321–328.

Nova, R. (1982). ''A viscoplastic constitutive model for normally consolidated clay,'' *Int. Union of Theoretical and Applied Mechanics Conf. on Deformation and Failure of Granular Materials*, Delft, The Netherlands, 287–295.

Nova, R., and Wood, D. M. (1979). ''A constitutive model for sand in triaxial compression.'' *Int. J. Numer. Analyt. Meth. Geomech.,* 3(3), 255–278.

Oka, F. (1981). ''Prediction of time-dependent behaviour of clay.'' *Proc., 10th ICSMFE*, 1, 215–218.

Oka, F. (1985). ''Elasto-viscoplastic constitutive equations with memory and internal variables.'' *Comput. Mech.,* 1, 59–69.

Oka, F., and Adachi, T. (1985). ''An elasto-plastic Constitutive Equation of Geologic Materials with Memory.'' *Proc., 5th Int. Conf. on Numerical Methods in Geomechanics*, 293–300.

Oka, F., Adachi, T., and Okano, Y. (1986). ''Two-dimensional consolidation analysis using an elasti-viscoplastic constitutive equation.'' *Int. J. Numer. Analyt. Meth. Geomech.,* 10, 1–16.

Oka, F., Adachi, T. and Mimura M. (1988). ''Elasto-viscoplastic consti-

tutive models for clays.'' *Proc., Int. Conf. Rheology and Soil Mechanics*, Elsevier, Science, New York, 12–28.
Olszak, W., and Perzyna, P. (1966a). ''On elastic-viscoplastic soils, rheology and soil mechanics.'' *Int. Union of Theoretical and Applied Mechanics Symp., Grenoble*, Springer, Berlin.
Olszak, W., and Perzyna, P. (1966b). ''The constitutive equations of the flow theory for a nonstationary yield condition.'' *Proc., 11th Int. Congress of Applied Mechanics*, Springer, Berlin, 545–553.
Olszak, W., and Perzyna, P. (1970). *Stationary and nonstationary viscoplasticity*, McGraw-Hill, New York [Kanninen, F. (1969). ''Inelastic behavior of solids.'' Battelle Institute Materials of Science Colloquia, Columbus and Atwood Lake, Ohio, 53–75.]
Perzyna, P. (1963a). ''The constitutive equations for work-hardening and rate sensitive plastic materials.'' *Proc., Vib. Probl.*, 3(4), 281–290.
Perzyna, P. (1963b). ''The constitutive equations for rate sensitive plastic materials.'' *Q. Appl. Math.*, 20(4), 321–332.
Perzyna, P. (1963c). ''The study of the dynamical behaviour of rate sensitive plastic materials.'' *Arch. Mech. Stos.*, 1(15), 113–130.
Perzyna, P. (1966). ''Fundamental problems in viscoplasticity.'' *Adv. Appl. Mech.*, 9, 244–377.
Phillips, A., and Wu, H. C. (1973). ''A theory of viscoplasticity.'' *Int. J. Solids Struct.*, 9, 15–30.
Poulos, H. G., Davis, E. H., and Ambrosis, L. P. (1976). ''Method of calculating long-term creep settlements.'' *J. Geotech. Eng. Div., Am. Soc. Civ. Eng.*, 102(7), 787–804.
Prager, W. (1949). ''Recent developments in the mathematical theory of plasticity.'' *J. Appl. Phys.*, 20(3), 235–241.
Prandtl, L. (1928). ''Ein Gedanken model zur kinetischen Theorie der festen Korper.'' *Z. Angew. Math. Mech.*, 8, 85–106.
Prevost, J.-H. (1976). ''Undrained stress-strain-time behavior of clays.'' *J. Geotech. Eng.*, 102(12), 1245–1259.
Rabotnov, Y. N. (1969). *Creep problems in structural members*, North-Holland, Amsterdam, The Netherlands.
Satake, M. (1989). ''Mechanics of granular materials.'' *Rep., Int. Society of Soil Mechanics and Foundation Engineering, technical committee on mechanics of granular materials, 12th, ICSMFE*, M. Satake, ed., 62–79.
Sekiguchi, H. (1977). ''Rheological characteristics of clays.'' *Proc., 9th ICSMFE*, 289–292, Vol. 1.
Sekiguchi, H., and Ohta, H. (1977). ''Induced anisotropy and time dependency in clays,'' *Proc., 9th Int. Conf., Soil Mechanics and Foundation Engineering*, Tokyo, 229–238.
Sekiguchi, H. (1984). ''Theory of undrained creep rupture of normally consolidated clay based on elasto-viscoplasticity.'' *Soils Found.*, 24(1), 129–147.
Sekiguchi, H. (1985). ''Macrometric Approaches—Static—Intrinsically Time Dependent Constitutive Laws of Soils.'' *Rep., ISSMFE Subcommittee on Constitutive Laws of Soils and Proc. of Discussion Session 1A*, Int. Society of Soil Mechanics and Foundation Engineering, Subcommittee on Constitutive Laws of Soils, 11th ICFMFE, San Francisco, 66–98.
Sheahan, T. C. (1995). ''Interpretation of undrained creep tests in terms of effective stresses.'' *Can. Geotech. J.*, 32, 373–379.
Sheahan, T. C., and Kaliakin, V. N. (1999). ''Microstructural considerations and validity of the correspondence principle for cohesive soils.'' *Proc., 13th Conf., Engineering Mechanics*, N. Jones and R. Ghanem, eds., ASCE, Reston, Va.
Silvestri, V., Soulié, M., Touchan, Z., and Fay, B. (1988). ''Triaxial relaxation tests on a soft clay.'' *Advanced triaxial testing of soil and rock*, ASTM, Philadelphia, 321–337.
Singh, A., and Mitchell, J. K. (1968). ''General stress-strain-time function for soils.'' *J. Soil Mech. Found. Div.*, 94(1), 21–46.
Skrzypek, J. J. (1993). *Plasticity and creep-Theory, examples, and problems* (English edition) B. H., Richard, ed., CRC Press, London.
Sokolovsky, V. V. (1948). ''Propagation of elastic-viscoplastic waves in bar.'' *Dokl. Akad. Nauk SSSR*, 60, 775–778 (in Russian).
Suklje, L. (1957). ''The analysis of the consolidation process by the isotaches method.'' *Proc., 4th ICSMFE*, 1, 200–206.
Tatsuoka, F., Santucci de Magistris, F., Hayano, K. Momoya, Y., and Koseki J. (2000). ''Some new aspects of time effects on the stress-strain behaviour of stiff geomaterials.'' *Proc., 2nd HSSR, Napoli*, 1998, A. Evangelista and L. Picarelli, eds., Balkema, Rotterdam, The Netherlands, Vol. 2, 1285–1371.
Tavenas, F., Leroueil, S., La Rochelle, P., and Roy, M. (1978). ''Creep behavior of an undisturbed lightly overconsolidated clay.'' *Can. Geotech. J.*, 15(3), 402–423.
Taylor, D. W. (1942). ''Research on consolidation of clays.'' *Serial 85*, Massachusetts Institute of Technology, Dept. of Civil and Sanitary Engineering, Cambridge, Mass.
Ter-Martirosyan, Z. G. (1992). *Rheological parameters of soils and design of foundations*, Balkema, Rotterdam, The Netherlands.
Tian, W. M., Sadd, M. H., Silva, A. J., and Veyera, G. E. (1994). ''Modeling creep behavior of anisotropically consolidated marine clays.'' *Computer methods and advances in geomechanics*, H. J. Siriwardane and M. M. Zaman, eds., Balkema, Rotterdam, The Netherlands, 701–706.
Vaid, Y. P., and Campanella, R. G. (1977). ''Time-dependent behavior of undisturbed clay.'' *J. Geotech. Eng.*, 103(7), 693–709.
Valanis, K. C. (1971). ''A theory of viscoplasticity without a yield surface. I.'' *Arch. Mech.*, 23(4), 517–533.
Walker, L. K., and Raymond, G. P. (1968). ''The prediction of consolidation rates in a cemented clay.'' *Can. Geotech. J.*, 5(4), 192–216.
Wood, D. M. (1990). *Soil behavior and critical state soil mechanics*, Cambridge University Press, Cambridge, U.K.
Yin, J. H. (1999). ''Nonlinear creep of soils in oedometer tests.'' *Geotechnique*, 49(2), 699–707.
Yin, J. H., and Graham, J. (1989a). ''Viscous-elastic-plastic modeling of one-dimensional time-dependent behaviour of clays.'' *Can. Geotech. J.*, 26, 199–209.
Yin, J. H., and Graham, J. (1989b). ''General elastic viscous plastic constitutive relationships for 1D straining in clays.'' *Proc., 3rd Int. Symp. Numerical Models in Geomechanics*, 108–117.
Yin, J. H., and Graham, J. (1994). ''Equivalent times and one-dimensional elastic visco-plastic modelling of time-dependent stress-strain behaviour of clays.'' *Can. Geotech. J.*, 31, 45–52.
Yin, J.-H., Graham, J., Clark, J. I., and Gao, L. (1994). ''Modelling unanticipated pore-water pressures in soft clays.'' *Can. Geotech. J.*, 31, 773–778.
Yin, J. H., and Graham, J. (1996). ''Elastic visco-plastic modelling of one-dimensional consolidation.'' *Geotechnique*, 46(3), 515–527.
Zaretskiy, Y. K. (1993). *Soil viscoplasticity and design of structures*, Balkema, Rotterdam, The Netherlands.
Zienkiewicz, O. C., and Cormeau, I. C. (1974). ''Visco-plasticity-plasticity and creep in elastic solids—A unified numerical solution approach.'' *Int. J. Numer. Methods Eng.*, 8, 821–845.
Zienkiewicz, O. C., Humpheson, C., and Lewis, R. W. (1975). ''Associated and nonassociated viscoplasticity and plasticity in soil mechanics.'' *Geotechnique*, 25(4), 671–689.

The Effects of Time on Soil Behaviour and Pile Capacity

Department of Civil Engineering ♦ Aalborg University ♦ Sohngaardsholmsvej 57 ♦ DK-9000 Aalborg

ISSN 1901-7294 - DCE Thesis No. 4